frontiers | Research Topics

Overcoming resistance to systemic therapy in breast cancer

Edited by
Zhi-Gang Zhuang, Helena Chang and Chunyan Dong

Published in
Frontiers in Oncology
Frontiers in Immunology

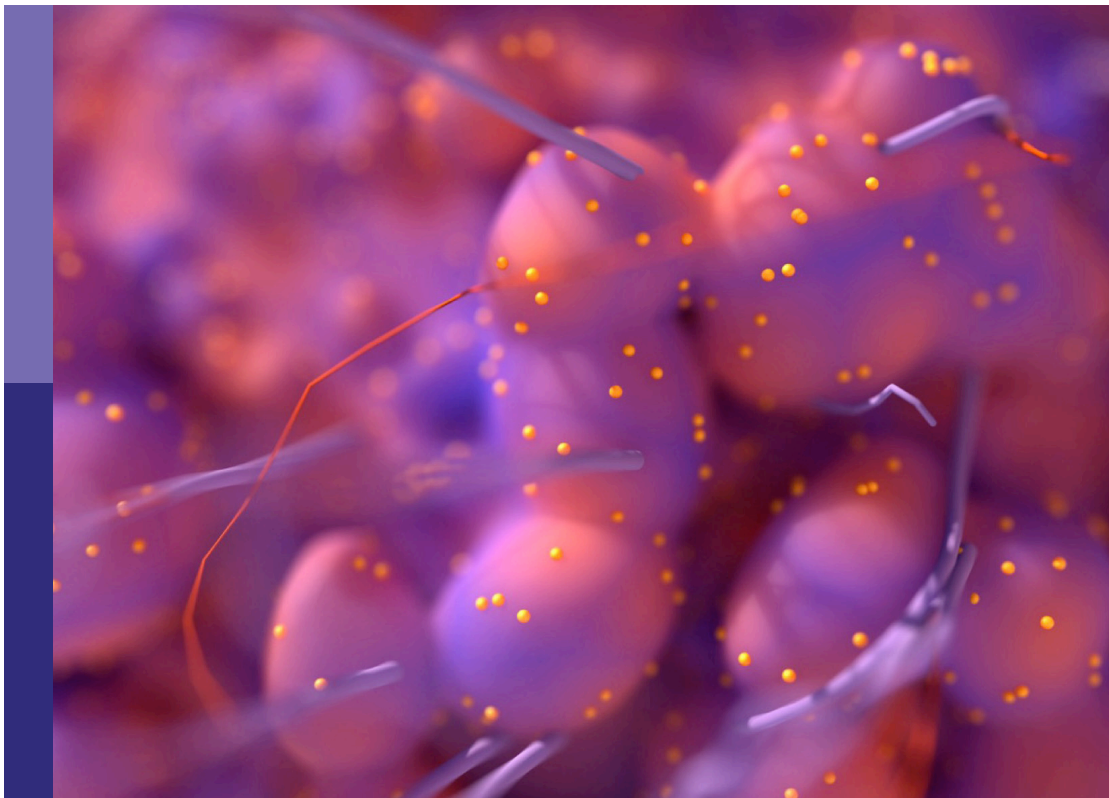

ISSN 1664-8714
ISBN 978-2-8325-4188-3
DOI 10.3389/978-2-8325-4188-3

About Frontiers

Frontiers is more than just an open access publisher of scholarly articles: it is a pioneering approach to the world of academia, radically improving the way scholarly research is managed. The grand vision of Frontiers is a world where all people have an equal opportunity to seek, share and generate knowledge. Frontiers provides immediate and permanent online open access to all its publications, but this alone is not enough to realize our grand goals.

Frontiers journal series

The Frontiers journal series is a multi-tier and interdisciplinary set of open-access, online journals, promising a paradigm shift from the current review, selection and dissemination processes in academic publishing. All Frontiers journals are driven by researchers for researchers; therefore, they constitute a service to the scholarly community. At the same time, the *Frontiers journal series* operates on a revolutionary invention, the tiered publishing system, initially addressing specific communities of scholars, and gradually climbing up to broader public understanding, thus serving the interests of the lay society, too.

Dedication to quality

Each Frontiers article is a landmark of the highest quality, thanks to genuinely collaborative interactions between authors and review editors, who include some of the world's best academicians. Research must be certified by peers before entering a stream of knowledge that may eventually reach the public - and shape society; therefore, Frontiers only applies the most rigorous and unbiased reviews. Frontiers revolutionizes research publishing by freely delivering the most outstanding research, evaluated with no bias from both the academic and social point of view. By applying the most advanced information technologies, Frontiers is catapulting scholarly publishing into a new generation.

What are Frontiers Research Topics?

Frontiers Research Topics are very popular trademarks of the *Frontiers journals series*: they are collections of at least ten articles, all centered on a particular subject. With their unique mix of varied contributions from Original Research to Review Articles, Frontiers Research Topics unify the most influential researchers, the latest key findings and historical advances in a hot research area.

Find out more on how to host your own Frontiers Research Topic or contribute to one as an author by contacting the Frontiers editorial office: frontiersin.org/about/contact

Overcoming resistance to systemic therapy in breast cancer

Topic editors

Zhi-Gang Zhuang — Shanghai First Maternity and Infant Hospital, China
Helena Chang — UCLA Health System, United States
Chunyan Dong — Tongji University, China

Citation

Zhuang, Z.-G., Chang, H., Dong, C., eds. (2024). *Overcoming resistance to systemic therapy in breast cancer*. Lausanne: Frontiers Media SA.
doi: 10.3389/978-2-8325-4188-3

Table of contents

frontiers | Frontiers in Immunology

TYPE Review
PUBLISHED 24 November 2022
DOI 10.3389/fimmu.2022.1038225

OPEN ACCESS

EDITED BY
Zhi-Gang Zhuang,
Shanghai First Maternity and Infant Hospital, China

REVIEWED BY
Sunita Keshari,
University of Texas MD Anderson Cancer Center, United States
Dipendra Khadka,
Wonkwang University School of Medicine, South Korea

*CORRESPONDENCE
Yuehua Li
liyuehua2020@stu.usc.edu.cn
Liming Xie
xlmusc@163.com

†These authors have contributed equally to this work

SPECIALTY SECTION
This article was submitted to Cancer Immunity and Immunotherapy, a section of the journal Frontiers in Immunology

RECEIVED 06 September 2022
ACCEPTED 11 November 2022
PUBLISHED 24 November 2022

CITATION
Qi X, Wan Z, Jiang B, Ouyang Y, Feng W, Zhu H, Tan Y, He R, Xie L and Li Y (2022) Inducing ferroptosis has the potential to overcome therapy resistance in breast cancer. *Front. Immunol.* 13:1038225. doi: 10.3389/fimmu.2022.1038225

Inducing ferroptosis has the potential to overcome therapy resistance in breast cancer

Xiaowen Qi[1†], Zhixing Wan[1†], Baohong Jiang[2†], Yuhan Ouyang[1], Wenjie Feng[1], Hongbo Zhu[1], Yeru Tan[1], Rongfang He[3], Liming Xie[1*] and Yuehua Li[1,4*]

[1]Department of Medical Oncology, The First Affiliated Hospital, Hengyang Medical School, University of South China, Hengyang, Hunan, China, [2]Department of Pharmacy, The First Affiliated Hospital, Hengyang Medical School, University of South China, Hengyang, Hunan, China, [3]Department of Pathology, The First Affiliated Hospital, Hengyang Medical School, University of South China, Hengyang, Hunan, China, [4]Institute of Pathogenic Biology, Hengyang Medical College, University of South China, Hengyang, China

Breast cancer is the most common type of malignancy among women. Due to the iron-dependent character of breast cancer cells, they are more sensitive to ferroptosis compared to normal cells. It is possible to reverse tumor resistance by inducing ferroptosis in breast cancer cells, thereby improving tumor treatment outcomes. Ferroptosis is highly dependent on the balance of oxidative and antioxidant status. When ferroptosis occurs, intracellular iron levels are significantly increased, leading to increased membrane lipid peroxidation and ultimately triggering ferroptosis. Ferroptotic death is a form of autophagy-associated cell death. Synergistic use of nanoparticle-loaded ferroptosis-inducer with radiotherapy and chemotherapy achieves more significant tumor suppression and inhibits the growth of breast cancer by targeting cancer tissues, enhancing the sensitivity of cells to drugs, reducing the drug resistance of cancer cells and the toxicity of drugs. In this review, we present the current status of breast cancer and the mechanisms of ferroptosis. It is hopeful for us to realize effective treatment of breast cancer through targeted ferroptosis.

KEYWORDS

ferroptosis, breast cancer, therapy resistance, autophagy, chemotherapy, radiotherapy, nanoparticles

1 Introduction

Breat cancer is the most prevalent malignancy among women (1). The current status of breast cancer treatment remains suboptimal, mainly using surgery, radiotherapy, chemotherapy, and targeted therapy. Drug resistance remains a major obstacle for

clinicians in the treatment of breast cancer (2). Ferroptosis was first proposed by Dixon, S.J in 2012, is a novel form of cell death induced by erastin and RSL3, distinct from apoptosis, autophagy and necrosis, is an iron-dependent chain reaction of destructive membrane lipid peroxidation, which leads to an imbalance of intracellular redox state (3). Altered cellular redox status has an intimate relationship with malignant transformation and metastasis of cancer cells (4, 5).

Ferroptosis is associated with many cancer types, including breast cancer (6), lung cancer (7)and pancreatic cancer (8). Effective evasion of regulated cell death is one of the most important features of cancer. It has been found that cancer cells that have evaded other forms of cell death still maintain sensitivity to ferroptosis. It seems that induction of ferroptosis in breast cells has the potential to affect tumor drug resistance (9). Tumor stem cells are highly iron-dependent and have an important role in promoting tumor cell proliferation and invasion, which are the main causes of tumor recurrence and metastasis. These cells are insensitive to conventional anticancer therapy, but can induce ferroptosis by modulating iron metabolism to exert more effective antitumor effects (10). Combined use of ferroptosis inducers during cancer radiotherapy and chemotherapy can effectively promote the sensitivity of cancer cells to ferroptosis and considerably improve the effectiveness of tumor treatment (11, 12).

Induction of ferroptosis in breast cancer cells can significantly inhibit tumor cell growth (13, 14). In breast cancer cells, the expression of transferrin receptor1 (TFR1), certain six transmembrane epithelial antigen of the prostate (STEAP) family members and Hepcidin were upregulated, while the expression of ferroportin (FPN) was downregulated. This suggests that breast cancer cells are iron-dependent and more sensitive to ferroptosis inducers (15). Long-chain acyl-coenzyme A synthetase 4 (ACSL4) is participated in lipid peroxidation formation and presents a high expression in a subpopulation of triple-negative breast cancer (TNBC) cell lines. The expression of ACSL4 positively correlates with breast cancer cell ferroptosis sensitivity (16). Glutathione (GSH) deficiency is associated with malignant transformation of breast cancer cells (17). Thioredoxin reductase 1 protein (TXNRD1), glutathione pathway and superoxide dismutase are predominantly and commonly regulated in breast cancer. High thioredoxin expression is strongly related to increased oxidative stress and poor prognosis in breast cancer. Cells with TXNRD1 knockdown (KO)are more sensitive to ferroptosis (18). GTP Cyclohydrolase (GCH) expression is associated with tumor development as well as angiogenesis. Upregulation of GCH1 expression in breast cancer cells stimulates proliferation and growth of cancer cells, results in poor prognosis of breast cancer. The use of GCH1 inhibitors suppress tumor growth and induce a switch in tumor immune response from M2 to M1 polarization of tumor associated macrophages. M2 is associated with tumor angiogenesis and metastasis (19, 20). Inhibition of GCH1 activity increases the susceptibility of drug-resistant cancer cells to ferroptosis (20, 21). Nuclear factor erythroid 2-related factor 2 (NRF2) exerts its antioxidant effects by upregulating the expression of genes related to iron and ROS metabolism and HO-1 to reduce ROS levels, increasing chemoresistance and ferroptosis resistance in breast cancer cells. The upregulated expression of heme oxygenase -1 (HO-1) in breast cancers has an inhibitory effect on cancer cell proliferation and invasion, and displays a dual role in ferroptotic cells, which depends on intracellular oxidative stress levels (22–24).

Ferroptosis offers a new direction in the treatment of breast cancer, but how to avoid its side effects is still an open question. In the presents of ferroptosis activation carries with the risk of inducing neurodegenerative disease and exacerbating ischemia-reperfusion injury (25–28). Ferroptotic damage also includes inflammatory reactions such as inflammatory bowel disease (29) and acute pancreatitis (30). In-depth understanding of ferroptosis metabolism in breast cancer is of utmost importance in searching for new breast cancer therapeutic-agents.

2 Current status of breast cancer and its treatment

Breast cancer is a major public health problem that threatens women's health and is the most prevalent malignancy among women (1). Women in the 50-64 age group are at high risk of breast cancer, and the prevalence is significantly higher in women than in men, with only about 1% of breast cancers occurring in men (31, 32). An epidemiological survey on breast cancer shows that the development of breast cancer is mainly affected by estrogen levels, with about 10% of breast cancers are associated with genetic mutations (1). Long-term exposure to estrogen, obesity, smoking, alcohol consumption, previous history of radiation therapy to the chest, and increased breast density can all increase the risk of breast cancer. Proper exercise can reduce the risk of breast cancer (1). With the improvement of medical technology as well as the early detection and interventional treatment of breast cancer, the incidence and effective cure rate of breast cancer have increased in recent years. The U.S. Preventive Services Task Force recommends that women aged 50-74 have a mammogram every two years to improve breast cancer screening rates (1, 31). Breast cancer has a distinct tumor heterogeneity, with multiple subtypes and differences in incidence, treatment options and prognosis for each subtype (33). Breast cancer can be classified into four molecular subtypes based on the expression of Estrogen receptor (ER), Progesterone receptor (PR) and human epidermal growth factor receptor type 2 (HER-2) with the use

of immunohistochemistry: luminal A, luminal B, HER-2 and TNBC (34). Current treatments for breast cancer mainly use surgery, radiotherapy, chemotherapy and targeted therapy, but a single treatment method does not achieve the expected therapeutic effect, and a combination of surgery-based treatment with other means is usually adopted (34). Breast cancer, with its many subtypes, is mainly treated with surgery and chemotherapy, supplemented by treatments based on the specificity of each subtype of receptor. Such as endocrine therapy for ER and PR receptor-positive breast cancer patients and anti-HER-2+ therapy for HER-2 positive breast cancer patients. As the most refractory type of breast cancer (33, 34), TNBC can be divided into four subtypes base on the heterogeneity of molecular characteristics, metabolomics and tumor microenvironment (35–38), which including mesenchymal-like (MES), luminal androgen receptor (LAR), basal-like and immune-activated (BLIA), basal-like and immune-suppressed (BLIS) subtypes (39, 40). Most of the current clinical trials focus on LAR in TNBC, applying an AR antagonist alone (41, 42) or in combination with a phosphatidylinositol 3-kinase (PI3K) inhibitor (43, 44), or combining immunotherapy to achieve AR inhibition with immune checkpoint blockade (45). The use of CDK4/6 inhibitors and hormone therapy in luminal B patients provides a strategy for the treatment of breast cancer without chemotherapy (46). The combination of PI3K inhibitors with aromatase inhibitors can produce positive effects, but their toxic effects are not negligible (47). HER-2-positive breast cancer patients will benefit from the dual inhibitory effect of trastuzumab and lapatinib on HER-2 (48). Estrogen receptor-positive breast cancer cells are highly susceptible to PI3K mutations, making the combination of letrozole and taselisib more effective (49). Nanoparticle albumin-bound paclitaxel (nab-Paclitaxel) in luminal A reduced the toxicity and increased the antitumor activity of paclitaxel (50). We have summarized the molecular subtype-based emerging clinical trials for breast cancer in Table 1. LAR tumors have higher fatty acid metabolic activity, ROS levels and overexpression of lipoxygenase than the other three subtypes of TNBC, all of which are evidence that LAR tumors are more vulnerable to ferroptosis (40, 51). High expression of CD44 in mesenchymal state tumor cells activates iron metabolic pathways, resulting in increased cellular susceptibility to ferroptosis (52). BLIA and BLIS were less correlated with ferroptosis (40). The combination of GPX4 inhibitors with immune checkpoint inhibitors for ferroptosis induction and enhanced immunosuppression has great potential for LAR tumor therapy (40). Discovering and developing safer and more effective drugs are warranted.

Breast cancer patients have a high rate of drug toxicity, drug resistance and recurrence during treatment (2). Tumor cell genomic instability is the main cause of tumor heterogeneity, which drives the evolution of cancer cells, affects their sensitivity to therapeutic agents, and ultimately promotes tumor drug resistance (53–55). Tumor drug resistance is also associated with the available concentration of drugs in the tumor as well as the tumor microenvironment (54). The tumor microenvironment involves complex interactions between cancer cells and stromal cells. Alterations in the tumor microenvironment can lead to changes in the properties of stromal cells and their secretion of soluble small molecules, which can lead to microenvironmental mediating tumor drug resistance (56). Ferroptosis exerts anti-tumor effects by engaging complicated crosstalk between tumor cells and immune cells to mediate tumor immunity (57, 58). KRAS is the key to macrophage polarization and its alteration leads to tumor associated macrophages formation and M2-like pro-tumor phenotype (59). A tumor-associated macrophage type is associated with immunosuppression (19). CD8+ T cells promote tumor cell ferroptosis and induce radiosensitization *via* IFN (60).

3 Mechanism of ferroptosis

Catalyzed by iron and iron-dependent enzymes, cells produce functional oxidative metabolites and promote labile

TABLE 1 Emerging therapies for breast cancer based on molecular subtypes.

Molecular subtypes	Drugs	Phase	Target
HER-2 +	trastuzumab and lapatinib	II	HER2 blockade (48)
Luminal A	Etrozole and taselisib	II	ER and PI3K (49)
	Nanoparticle albumin-bound paclitaxel	II	B tubulin (50)
Luminal B	Ribociclib and letrozole	II	CDK4/6 and hormone receptor (46)
	Buparlisib and capecitabine	I	PI3K and aromatase (47)
TNBC	abiraterone acetate and prednisone	II	AR and PI3K (43)
	Bicalutamide	II	AR (41)
	Enzalutamide	IB/II	AR and PI3K (44)
	GT0918	I	AR (42)
	Pembrolizumab and Enobosarm	II	AR and programmed death receptor (PD-1) (45)

iron pool (LIP) formation, while inevitably leading to the accumulation of some undesirable oxidative byproducts (61–63). When they accumulate to a lethal level can cause severe cellular damage and even lead to cell death. Therefore, antioxidant mechanisms have evolved in cells to remove these metabolic wastes in a timely manner, such as the glutathione peroxidase-4-GSH (GPX4-GSH) system, Coenzyme Q10 (CoQ10) (64).

Ferroptosis is an iron-dependent form of regulated cell death (3), characterized by massive accumulation of disruptive membrane lipid peroxidation (65). There are three main features of ferroptosis including imbalance of iron metabolism, massive production of lipid peroxides, and collapse of the GPX4-GSH system (58). Morphologically, ferroptotic cells show significant changes in mitochondrial morphology, with mitochondrial contraction, rupture of the outer mitochondrial membrane (OMM), and enlarged mitochondrial cristae. In the absence of swelling or contraction of cells in necrosis and apoptosis, neither nuclear changes nor chromatin condensation (3, 66, 67).

Lipid peroxidation due to massive accumulation of the iron positively regulate ferroptosis, while GSH depletion due to system xc- and GPX4 inactivation negatively regulate ferroptosis (61–63). Apart from the classical GPX4-GSH axis, there are other antioxidant mechanisms involved in the negative regulation of ferroptosis in breast cancer cells, such as the ferroptosis suppressor protein 1-NADH-CoQ10 (FSP1-NADH-CoQ10) axis (68) and the GCH1 -Tetrahydrobiopterin (GCH1-BH4) axis through the involvement of COQ10 (69), and the regulation of some antioxidant transcription factors, such as NRF2 (70). A mutant of p53 can promote ferroptosis (71, 72). Here, we summarized and mapped the ferroptosis mechanism in Figure 1. FINs in breast cancer are summarized in Table 2.

TABLE 2 FINS in breast cancer.

Target	Drugs
Increased iron	Sulfasalazine
	Lapatinib+siramsine
	Neratinib
	Artemisinin
Mitochondrial disorders	RF-A
	Nitroxide
Reduced iNOS activity	GA
Inactivation of GPX4	DT
	Metformin
	Simvastatin
	Curcumin
Inhibition of GSH synthesis	Metformin
	Sulfasalazine
	BSO+AUR
Inhibition of CoQ10 synthesis	FIN56

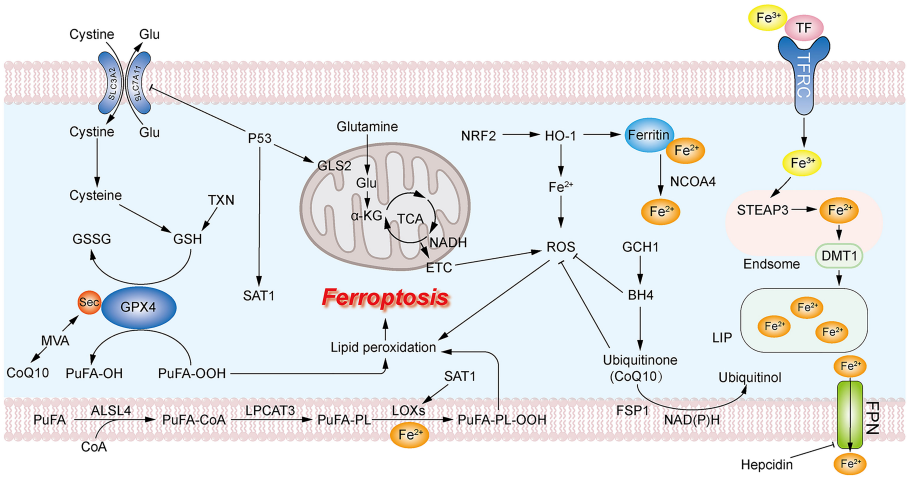

FIGURE 1
Mechanism of ferroptosis. The massive accumulation of PUFA on the cell membrane leads to excessive production of PUFA-OOH. GPX4 uses GSH as a reducing agent to reduce PUFA-OOH to PUFA-OH, reducing the production of lipid peroxides. GSH can be formed from cystine transported into the cell *via* system XC- or *via* the TXN pathway. The accumulation of intracellular ROS promotes lipid peroxidation. Mitochondrial GLS2 promotes glutamine catabolism to facilitate ROS production leading to the accumulation of lipid peroxides. Large accumulation of intracellular ferrous ions leads to overproduction of ROS. CoQ10 acts as an antioxidant to inhibit ROS production, and the MVA pathway and GCH1-BH4 are associated with the production of CoQ10.

3.1 Intracellular iron metabolism and its redox reactions

Iron is one of the most important trace elements in the human body and essential for the vital activities of the body, participating in the formation and regulation of the activity of Reactive Oxygen Species (ROS)-producing enzymes, such as Lipid oxidases (LOXs) (3). Iron homeostasis plays a key role in controlling the balance between ROS production and ROS scavenging as well as cellular redox and potential oxidative damage (73, 74). Elevated iron levels in mitochondria may lead to excessive production of ROS (65). High iron diet causes ferroptosis in mouse cardiomyocytes (75). Iron levels are significantly elevated in ferroptosis cells, suggesting that the accumulation of intracellular iron is a prerequisite for cells to undergo ferroptosis. Deferoxamine (DFO) inhibits erastin-induced cell death by chelating intracellular iron and reducing iron overload (3). Transferrin (TF) and TFR1 regulate ferroptosis by mediating cellular uptake of iron (26). Nuclear receptor coactivator 4 (NCOA4) regulates ferroptosis by mediating ferritinophagy to control iron homeostasis (76). Ferritin consists of ferritin heavy chain (FTH) and ferritin light chain (FTL), of which FTH1 has iron oxidase activity and oxidizes ferrous ion to ferric ion (77). Knockdown or inhibition of FTH1 both promote ferroptotic death (76, 78).

Sulfasalazine targeting Transferrin receptor (TFRC) and its ferroptosis-inducing effect is reduced in ER-positive breast cancer (14). The combination of lapatinib and siramsine induces ferroptosis in breast cancer cells rather their individual treatment. Promoting the expression of transferrin and degradation of FPN, causing a time-dependent increase in intracellular iron levels and ROS levels, ultimately leading to cellular ferroptosis and autophagy at different time (79). Neratinib causes iron imbalance by regulating the expression of proteins related to the iron transport system, ultimately inducing ferroptosis (80). Artemisinin mediates the degradation of ferritin, which is an elevated level of intracellular ferrous iron, leading to cellular ferroptosis (81).

Ferric ions from foods bind to TF in blood and attach to TFR1 on the cell membrane, transporting ferric ions into the cell, where STEAP3 in acidic nuclear endosome reduces ferric ions to ferrous ions. Ferrous ions are transferred *via* divalent mental transporter 1 (DMT1) to LIP. Binding to ferritin is the storage form of intracellular free irons, and NCOA4 is involved in the degradation of ferritin, releasing ferrous ions (76).

Excess Ferrous ions generate large amounts of hydroxyl radicals through Fenton and Haberweth reactions, which alter the intracellular redox state. Due to their high instability and reactivity, hydroxyl radicals can cause severe damage to lipids and proteins and intense oxidative damage to DNA (82, 83). In ferroptotic cells, hydroxyl radicals are able to attack polyunsaturated fatty acids (PUFAs) on membranes, triggering membrane lipid peroxidation (9).

3.2 Mitochondrial involvement in reactive superoxide formation

Mitochondria is important for maintaining normal cellular function, energy supply and redox homeostasis, and is a major site for intracellular ROS production. The Tricarboxylic Acid (TCA) cycle and electron transport chain (ETC) action are necessary for mitochondria to produce sufficient ROS *via* oxidative phosphorylation (OXPHOS) (84, 85). Ferroptotic cells undergo significant changes in mitochondrial morphology with mitochondrial contraction, rupture of the OMM, and enlarged mitochondrial cristae (3, 67). Robustaflavone A (RF-A) promotes Voltage-dependent anion-selective channel protein 2 (VDAC2) expression and ubiquitinated degradation, inducing the breakdown of mitochondrial functional systems, lipid peroxidation and ROS production, ultimately leading to ferroptosis in breast cancer cells. Blocking mitochondrial function contributes to ferroptosis inhibition independent of GPX4 activity (86). Nitroxide targets mitochondria as a ROS scavenger and inhibits lipid peroxidation of mitochondrial membranes thereby inhibiting ferroptosis (87). BAY87-2243 induces ferroptosis in melanoma cells through inhibition of mitochondrial respiratory chain complex 1 and induction of mitochondrial membrane potential depolarization (88). In cysteine-starved cells, mitochondrial metabolism is significantly enhanced, promoting GSH depletion, ROS production and ferroptosis. Mitochondrial GLS2 promotes glutamine catabolism to glutamate, which is then converted to α-KG *via* glutamine dehydrogenase into the TCA cycle, driving ETC and leading to mitochondrial membrane hyperpolarization and lipid peroxide accumulation, eventually ferroptosis is triggered (26, 85).

3.3 Accumulation of lipid peroxides

PUFAs are major components of membrane lipids, which are highly susceptible to oxidation and play an important role in maintaining membrane integrity and participating in trans-plasma membrane transport activity (89). Increased production of lipid peroxides occurs in both erastin- and RSL-induced ferroptosis (90). Extensive production of ROS attack PUFAs on the membrane, triggering membrane lipid peroxidation, leading to a massive accumulation of lipid peroxides and ferroptosis (9). The presence of more and longer PUFAs exacerbates ferroptosis (91). Glycyrrhetinic acid (GA) generates ROS and Reactive nitrogen species (RNS) by upregulating NADPH oxidase and iNOS activity in TNBC cells, which exacerbates intracellular oxidative stress level, leads to lipid peroxidation and ferroptosis (92). Inhibition of peroxidation of PUFAs with antioxidants inhibits ferroptoisis (3). Acyl coenzyme A (CoA) synthase ACSL4 and lysophosphatidylcholine acyltransferase 3 (LPCAT3)

are involved in the synthesis of lipid ROS and their deletion contributes to ferroptosis resistance (93). ACSL4 is engaged in the production and activation of the long-chain polyunsaturated fatty acids arachidonic acid (AA) and adrenalic acid (AdA), acylating PUFA to form PUFA-CoA (16), LPCAT3 inserts PUFA-CoA into membrane phospholipids (PL) and catalyzes the production of PUFA-PL (94). Finally, PUFAs are oxidized by iron and iron-dependent oxidase LOXs to produce PUFA-PL-OOH, which initiates ferroptosis (95).Oxidized PUFAs accumulate on the membrane, causing membrane thinning and bending to increase the accessibility of oxidants. Oxidants react with PUFAs in the membrane, forming a positive feedback loop, which further accelerates membrane instability and ultimately leads to irreversible damage to membrane integrity and promotes cellular ferroptosis (96).

3.4 XC-/GPX4-GSH system

GSH is vital in normal embryonic growth and development as well as an essential reducer. GPX4 catalyzes the reduction of harmful lipid peroxides to harmless lipid alcohols, thus protecting cell membranes from peroxidative damage by PUFA-OOH (17, 97, 98). Cystine-starved cells with reduced GSH synthesis are more sensitive to ferroptosis inducers (FINs) (26). Overexpression of SLC3A1 enhances tumor progression in breast cancer cells, while blocking SLC3A1 with specific siRNA or SLC3A1-specific inhibitor sulfasaliazine inhibits tumor growth (99). Erastin acts on system xc- to inhibit cystine uptake, and intracellular GSH synthesis is depressed (3). RSL inactivates GPX4 by binding to selenocysteine, with massive accumulation of lipid peroxides (100). When GPX4 is inhibited or knocked down, intracellular antioxidant activity is significantly diminished and lipid peroxides accumulate excessively, eventually leading to ferroptosis (101, 102). Sulfasaliazine induces ferroptosis in breast cancer cells by functioning on system xc- which is currently in a type II clinical trial. Dihydroisotanshinone I (DT) induces cellular ferroptosis and inhibits tumor growth without adverse effects through down-regulation of GPX4 expression (103). Metformin enhanced ferroptosis in breast cancer cells by altering the stability of SLC7A11, downregulating GPX4 activity and inhibiting the autophagy induced by H19. This effect is more sensitive in estrogen receptor-positive breast cancer cells. In addition, the combination of metformin with sulfasazine enhanced its ferroptosis induction and exerted more effective anti-cancer effects (104–106). MVA pathway and the activity of GPX4 is inhibited in ferroptotic death breast cancer cells induced by Simvastatin (107). Curcumin induces ferroptosis in breast cancer cells by upregulating the expression of redox target genes such as HO-1 and downregulating antioxidants such as GPX4, an effect that is more pronounced than in normal human breast epithelial cells (108). Moreover, high expression of Glycogen synthase kinase-3β (GSK-3β) was able to increase the sensitivity of erastin-induced ferroptosis by enhancing the inhibition of GPX4 (109).

System xc- is a glutamate-cystine transporter located on the plasma membrane, consisting of the heavy chain subunit SLC3A2/CD98hc and the light chain subunit xCT/SLC7A11, responsible for cellular uptake of cystine and transport of glutamate (110). Cystine is reduced to cysteine upon entry into the cell, then glutamate-cysteine ligase (Gcl) and glutathione synthetase (Gss) catalyze the production of GSH (111, 112). GSH is the most abundant and common antioxidant in cells, maintaining intracellular redox homeostasis. GPX4 is one of the glutathione peroxidases, selenocysteine is an important component of the GPX4 active center (113). Mevalonate is involved in the synthesis of selenoprotein in the GPX4 active center (114). GPX4 uses GSH as an essential reducing agent to catalyze the reduction of harmful lipid peroxides to harmless lipid alcohols, thereby protecting cell membranes from peroxidative damage by PUFAs. When the function of system xc- is inhibited, TXN pathway can be an alternative GSH synthesis pathway. TXNRD1 KO cell survival is highly dependent on intracellular GSH levels (115). Buthionine sulfoximine (BSO) can induce cell death in TXNRD1 KO cell (116). Forced expression of xCT in cells which are completely deficient in GSH production, TXN pathway increases cellular cystine uptake to rescue GSH deficiency. Overexpression of xCT in TXNRD1 KO cells not only exacerbates but also accelerates BSO-induced cell death (117). Expression of TXNRD1 are higher in Gclm(-/-) mice compared to WT mice (118). Thus, the TXN pathway is another major antioxidant approach that has been shown to support cell survival after system xc- inhibition, TXN and system xc- synergistically control intracellular GSH level (119). Due to the presence of the TXN pathway and the essential role of GPX4 in the embryo, directly targeting of GPX4 is more effective than inhibiting the activity of SLC7A11 when inducing ferroptosis (98, 120). BSO can induce ferroptosis by inhibiting GCL and thus decreasing GSH synthesis (121). However, inhibition of GSH by BSO alone can only elevate ROS at the tumor initiation stage and cannot affect established tumor growth (17). Auranofin (AUR) is an FDA-approved thioredoxin reductase inhibitor for the suppression of TNBC tumor growth (122). Combining BSO with AUR can significantly increase the mortality of breast cancer cells through combined inhibition of GSH synthesis and TXN pathway (17).

3.5 COQ10 as an endogenous membrane antioxidant inhibits ferroptosis

CoQ10 is involved in respiratory chain activities in the mitochondrial membrane and is critical for electron translocation. The non-mitochondrial CoQ10 acts as a free radical trapping

antioxidant (RTA) and prevents plasma membrane lipid damage. MVA pathway is engaged in CoQ10 skeleton generation (114, 123). A significant decrease in CoQ10 level occurs in ferroptotic cells (124). The MVA pathway is involved in CoQ10 backbone formation, and FIN56 induces ferroptosis by reducing CoQ10 production *via* the MVA pathway (125). Inhibition of CoQ10 synthesis by inhibiting CoQ10 synthase CoQ2 increases RLS-induced lipid ROS and exacerbates ferroptosis (126). CoQ10 is involved in ferroptosis resistance through the FSP1-NADH-CoQ10 axis and the GCH1-BH4 axis.

3.5.1 FSP1-NADH-CoQ10

FSP1 is the key component of the antioxidant system in ferroptotic death independent of the GPX4-GSH axis (68). FSP1 expression positively correlates with cancer cell resistance to ferroptosis induced by GSH depletion or GPX4 inhibition (98, 123). FSP1 KO leads to increased cellular phospholipid oxidation and increased sensitivity to ferroptosis inducers. NAD(P)H-quinone oxidoreductase-1 (NQO1) is a CoQ oxidoreductase that may be involved in CoQ10 reduction in synergy with FSP1 to regulate ferroptosis (123). NQO1 knockdown cells showed increased sensitivity to erastin- and sorafenib-induced ferroptosis (78). Elevated NADH/NADPH ratio indicates a weakened intracellular antioxidant capacity and a greater susceptibility to cellular ferroptosis (127). FSP1 targets the plasma membrane and converts oxidized CoQ10 (ubiquitinone) to reduced CoQ10 (ubiquitinol), NAD(P)H acts as a reducing co-substrate to provide hydrogen ions for this reaction, which inhibits lipid peroxidation and ferroptosis (68, 123).

3.5.2 GCH1-BH4-phospholipid axis

The GCH1-BH4-phospholipid axis links to ferroptosis resistance. GTP Cyclohydrolase 1 (GCH1) is the key enzyme that catalyzes the production of tetrahydrobiopterin (BH4) (69). The expression level of GCH1 determines the BH4 availability, which influence the redox balance in cancer cell. Intracellular levels of BH4 are negatively correlated with oxidized GSH and NADP (128). An increase in BH4 can lead to an increase in CoQ10 levels. Inhibition of GCH1 activity results in the sensitivity of drug-resistant cancer cells to ferroptosis. Conversely, overexpression of GCH1 effectively prevents cell death induced by deletion of RSL3, IKE and GPX4, and inhibits lipid peroxidation (69). BH4 can act directly as an antioxidant or indirectly by synthesizing CoQ10 to inhibit lipid peroxidation and attenuate oxidative damage in the presence of FSP1, protecting cells from ferroptosis (69, 128).

3.6 NRF2 involved Redox homeostasis

NRF2 is a major antioxidant transcription factor *in vivo*. NRF2 increases cellular resistance to ferroptosis, by upregulating the expression of iron, HO-1, and ROS metabolism-related gene. The expression of NRF2 was upregulated in ferroptosis, while knockdown or pharmacological inhibition of NRF2 revealed the phenomena of GSH depletion, increased iron level and lipid ROS production in erastin- and sorafenib-induced cells, promoting cellular ferroptosis and enhancing the anticancer activity (70). Moreover, there is a p62-Keap1-NRF2 pathway to regulate intracellular NRF2 levels. P62 expression positively correlates with NRF2 levels, while Keap1 negatively regulates NRF2 and mediates its degradation (78). Kelch-like ECH-associated protein 1 (Keap1) binds to Cul3 and Rbx1 to form a functional E3 ubiquitin ligase complex that ubiquitinates NRF2 for degradation. This process can be inhibited by the NRF2-dependent transcriptional chemoattractants Sulforaphane and quinone (tBHQ)-induced oxidative stress, mainly because they enable a redox-dependent alteration of multiple cysteine residues in Keap1, and NRF2 separates from Keap1 and enters the nucleus (129, 130). In nucleus, NRF2 forms a heterodimer with sMaf (131) and binds to ARE (132), protecting cancer cells from GPX4 inhibition and promoting the transcription of antioxidant enzymes, such as HMOX1, NOQ1, and GSTS (108, 133–135), reducing ROS levels, forming resistance to ferroptosis (78).

HO-1 has been shown to have anti-proliferative, antioxidant and anti-inflammatory effects. Upregulated HO-1 expression in breast cancer cells has an inhibitory effect on cancer cell proliferation and invasion (23, 136). HO-1 degrades heme to CO, ferrous ions as well as bilirubin and can induce upregulation of ferritin expression. Ferritin binds to free intracellular iron and inhibits the Fenton reaction, thereby reducing ROS production and exerting its antioxidant activity (24). HO-1 acts as an antioxidant, and HO-1 expression is upregulated in erastin- and sorafenib-induced ferroptosis. Meanwhile, inhibition of HO-1 expression or the occurrence of HO-1 deficiency exacerbates intracellular ferroptosis (22, 78). However, HO-1, a major source of intracellular iron. Under high oxidative stress, a significant rise in intracellular concentration of ferrous ions, which increases ROS levels to promote lipid peroxidation and thus lead to ferroptosis (108, 137, 138). HO-1 is important for maintaining redox homeostasis and its dual role in ferroptosis may be related to intracellular levels of oxidative stress and cellular stress. In response to induction of cellular stress, HO-1 expression is moderate upregulated and acts as an antioxidant defense mechanism to mitigate ferroptosis. In contrast, when excessive intracellular oxidative stress occurs, HOs are overactivated and overexpressed, which acts as pro-oxidant to accelerate cellular ferroptosis (22, 137). The role of HO-1 in ferroptosis remains controversial, and the mechanism underlying its role in ferroptosis remains to be identified.

3.7 P53-mediated GSH synthesis and depletion

P53 is the most frequent and susceptible gene to mutation in breast cancer. In previous studies, it has been shown that mutant

p53 has a higher mortality rate and worse prognosis than wild-type p53 (139–141). Induced restoration of the wild-type properties of mutant p53 offers a new idea for the treatment of breast cancer, and PRIMA-1MET(APR-246, Aprea AB) may be able to achieve this goal (71, 72). PRIMA-1MET increased intracellular GSH depletion and induced ROS production. Synergy with BSO increased the sensitivity of cells to PRIMA-1METm (142, 143). PRIMA-1MET can induce ferroptosis in AML cells (144). In addition, a novel ferroptosis inducer, MMRI62, with dual targeting of FTH1 and mutant p53, which induces ferroptosis in pancreatic cancer cells by inducing lysosomal degradation of FTH1 and NCOA4 as well as proteasomal degradation of mutant p53 to improve chemoresistance and control metastasis of cancer cells (145).

A P533KR (K117R + K161R + K162R) mutant, which fails to induce cell cycle arrest, senescence and apoptosis, but presence of inhibitory properties on SLC7A11 expression renders the cell incapable of cystine uptake, reduction in GSH synthesis, more susceptible to ferroptosis and can be inhibited by Fer-1. While overexpression of SLC7A11 in P533KR mutant rescues its ferroptosis. Suggesting that P53 triggers ferroptosis by mediating transcriptional repression of SLC7A11 (146). P534KR (K98R + K117R + K161R + K162R) mutant, with complete depletion of acetylation capacity compared to p533KR resulted in loss of ferroptosis induction, suggesting p53-mediated acetylation capacity plays an important role in ferroptosis induction (147). In addition, p533KR retains the transcriptional activity of glutaminase 2 (GLS2), which induces ferroptosis by promoting glutaminolysis (26, 147). P53 upregulates the expression of spermidine/spermine N1-acetyltransferase 1 (SAT1) and promotes ALOX15 activity, leading to lipid peroxidation (148). Mutant p53 also increases ferroptosis sensitivity of pancreatic cancer cells by downregulating the expression of FTH1 and NCOA4 (145).On the other hand, P53 inhibits ferroptosis by upregulating the expression of cell cycle protein-dependent kinase inhibitor 1A (CDKN1A/p21) (149) and GLS2 (26, 150), which also inhibit the formation of DPP4-NOX1 complex (151) by altering the localization and activity of DPP4 in CRC cells.

4 Correlation between autophagy and ferroptosis

Ferroptosis has an autophagic correlation (59, 76, 152, 153). Autophagy (Macroautophagy) is a form of cell death that exists within normal cells to maintain a state of intracellular homeostasis. It is a lysosomal degradation process that cells engulf cytoplasmic material to form autophagosomes, which then bind to lysosomes to form autolysosomes (154). Autophagic lysosomes can degrade protein, lipid and damaged mitochondria, etc. (152, 155, 156).

Elevated autophagic activity occurred in erastin-induced ferroptosis cells, whereas the use of the lysosomal inhibitors Bafa1 and CQ blocked ferroptotic death cells (76, 153), and this inhibition was time-differentiated, with a more pronounced inhibition effect at 12h than 24h. Autophagy genes (ATGs) were found to be involved in the positive regulation of ferroptosis by RNAi screening (76). Knockdown of ATGs or pharmacological inhibition both achieved the blocking effect of ferroptosis (76, 157).

Ferritinophagy is a NCOA4-mediated ferritin degradation exists in ferroptotic death cells, which is an elevation of ferrous ions thereby promoting the accumulation of lipid ROS, while independent of GSH depletion (76, 153). Autophagic degradation of FTH1 is also found in erastin-induced cells (76). Lipophagy promotes ferroptosis by mediating the selective autophagic degradation of lipid droplet (LD). The accumulation of neutral LD protects cells from ferroptosis by suppressing lipid peroxidation (157). LDs are involved in the redistribution of PUFAs. PUFAs are transferred from the phospholipid membrane to the core of LDs. Where PUFAs are less susceptible to ROS attack, thus inhibiting lipid peroxidation (158). Mitophagy is a process of selective autophagic degradation of damaged or redundant mitochondria to maintain intracellular mitochondrial homeostasis (155). There is a mitochondrial autophagy-associated ferroptosis in BAY87-2243-induced human melanoma cells, which exerts an inhibitory effect on tumor growth (88). Chaperone-mediated autophagy (CMA) is a cellular autophagic degradation pathway that recognizes soluble cytoplasmic proteins containing specific KEFRQ motifs through heat shock-associated proteins (HSP) and targets them directly to the lysosome for degradation (155). HSP90 upregulates the level of lysosome-associated membrane protein type 2a (Lamp-2a), promotes chaperone-mediated autophagic degradation of GPX4, and thus participates in the regulation of ferroptosis (159, 160). A graphical representation of the relationship between ferroptosis and autophagy is shown in Figure 2.

Perhaps induction of cellular autophagy could be an effective way to activate ferroptosis (76).

5 Effective ways to enhance ferroptosis

In the process of breast cancer chemotherapy and radiotherapy, it is difficult to distinguish between normal cells and cancer cells. Thus it is hard to target breast cancer cells, which will inevitably cause damage to normal tissues and lead to high toxicity and adverse effects (2). The discovery of ferroptosis emerges a new ray of light for cancer treatment. However, the poor water solubility and rapid metabolism of therapeutic drugs lead to their low bioavailability *in vivo*. Nanoparticles have the

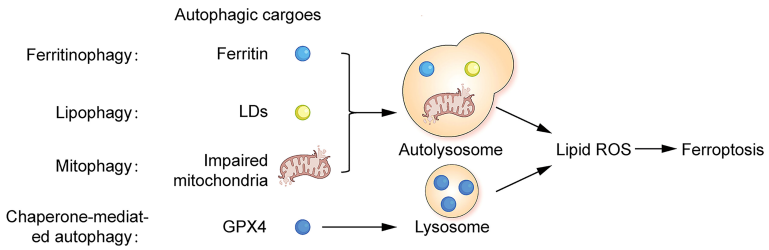

FIGURE 2
Correlation between ferroptosis and autophagy Ferritin, lipid droplets and impaired mitochondria can act as autophagic substrates for ferritinophagy, lipophagy, and mitophagy, forming autolysosomes in cells. GPX4 can act as autophagic substrates for CMA-mediated autophagy, forming lysosomes in cells. Facilitating the production of intracellular lipid ROS, leading to ferroptosis.

characteristics of small size and low toxicity, ferroptosis-inducers (FINs) can be loaded on these particles, which can help us solve these problems. Nano-FINs in breast cancer cells are summarized in Table 3. More importantly nanoparticles can target drug transport to tumor cells, reducing the toxic damage effect of drugs on normal cells. The application of Nanoparticle-loaded ferroptosis-inducer-targeted transport technology can greatly enhance the tumor suppressive effect of the drugs (161). Drug resistance of cancer cells is also a thorny issue in current cancer treatment. FINs can be used as chemotherapy and radiotherapy sensitizers enhance ferroptosis of cancer cells, achieving effective improvement in drug resistance during treatment and prolong patients' survival (11, 12).

5.1 Nanomaterial-based therapeutic drugs

TA-Fe/ART@ZIF, a ferrous nanocarrier encapsulated with ART enhanced the ferroptosis-inducing effect of ART in TNBC cells and exhibited stronger tumor suppression compared to ART alone (162). A novel nanomedicine Fe3O4@PCBMA-SIM can slow down the metabolism of the drug and increase the accumulation and duration of action at the tumor site to exert better cancer suppressive effects (107). A newly discovered folate (FA)-exosome-encapsulated erastin can help us address the low water solubility and nephrotoxicity of erastin and target erastin delivery to FA receptor overexpressing TNBC cells. This erastin@FA-exo induced ferroptosis by inhibiting the expression of GPX4, upregulating the expression of cysteine dioxygenase (CDO1), and increasing the depletion of GSH is intracellular production of excess ROS, which greatly enhanced the antitumor effect of erastin (163). A heparanase (HPSE)-driven sequential released nanoparticles, NLC/H(D + F + S) NPs, induces ferroptosis characterized by excessive ROS production and GSH depletion in mouse breast cancer cells, significantly inhibits the metastatic growth of tumors and improves anti-cancer efficiency (164).

5.2 Ferroptosis inducers as sensitizers for chemotherapy

A new nanomedicine DFHHP can inhibit tumor growth by inducing apoptosis and ferroptosis in tumor cells to overcome tumor chemoresistance. DFHHP is an integration of Fe (VI) species and Doxorubicin (DOX) into HMS nanomaterials. DOX, a common chemotherapeutic agent in tumor therapy, generates a large amount of reactive superoxide radicals by promoting tumor cell reoxidation. DFHHP provides exogenous iron, generating highly reactive ROS by Fenton reaction, leading to the depletion of GSH and exacerbating ferroptosis of tumor cells (11). HMCM nanocomposites have photothermal properties

TABLE 3 Nano-FINS in breast cancer.

Nanomedicines	Composition	Cell
TA-Fe/ART@ZIF	artemisinin +tannic acid+Fe(II)+zeolitic imidazolate framework-8	MDA-MB-231
Fe3O4@PCBMA	simvastatin+Fe3O4+zwitterionic polymer coated magnetic nanoparticles	MDA-MB-231+MCF-7
erastin@FA-exo	Folate+Erastin+Exosome	MDA-MB-231
HMCM	MnO2+HMCu2-xS+Nanoparticles	MCF-7
DFTA	Doxorubicin+FeCl3+tannic acid	MCF7

that enable PT, and the nanodrug also incorporates the autophagy promoter Rapa, which enhances the sensitivity of breast cancer cells to ferroptosis and effectively controls tumor growth (165).

A drug-organics-inorganics self-assembled nanosystem (DFTA) effectively inhibits the progression of ER+ breast cancer by using a chemotherapeutic agent DOX, a ferroptosis inducer ferric chloride (FeCl3) and a activator of superoxide dismutase (SOD) tannic acid (TA), which activates a cascade reaction generated by intracellular ROS and significantly reduces GSH levels. In addition the combination with photothermal therapy (PT) can greatly increase the efficiency of ROS production. It is expected to achieve the combination of chemotherapy, PT, and ferroptosis against ER+ breast cancer (166).

5.3 Ferroptosis inducers as sensitizers for radiotherapy

Radiotherapy mainly uses targeted delivery of ionizing radiation (IR) to cause cell death. Hypoxia is the main mechanism leading to radiotherapy resistance in tumor cells, while hypoxia-induced ROS production and massive activation of the hypoxia-inducible factors result in the induction of ferroptosis (12, 167). The use of FINs may overcome hypoxia-induced resistance to radiotherapy by promoting ferroptosis in tumor cells. Conversely, inhibition of ferroptosis leads to resistance to radiotherapy (12).

Tumor cells treated with radiotherapy showed typical ferroptotic features, with mitochondrial atrophy and its increased membrane density, enhanced lipid peroxidation, as well as increased expression of the ferroptosis marker gene prostaglandin-endoperoxide synthase-2 (PTGS2) (12). IR can promote the production of PUFA-PLs by upregulating the expression of ACSL4, while stimulating cells to produce large amounts of ROS, leading to lipid peroxidation and inducing ferroptosis in cancer cells (12, 168). Meanwhile IR may inhibit ferroptosis by inducing the expression of SLC7A11 and GPX4 as a negative feedback regulatory pathway to induce radiotherapy resistance in cancer cells. The combination of sulfasalazine, an ferroptosis inducer targeting SLC7A11, and IR enhanced the sensitivity of cancer cells to radiotherapy, synergistically induced ferroptosis, and significantly inhibited tumor growth (120, 169). Another study found that IR also antagonized the upregulation of SLC7A11 expression by activating P53, making cancer cells more sensitive to ferroptosis. The combination of FINs and radiation therapy is more effective in the treatment of P53-mutated cancers (170). CD8+ T cells promote tumor cell ferroptosis and induce radiosensitization *via* IFN. Immunotherapy-activated CD8+T cells induce tumor cell ferroptotic death by producing IFN in concert with radiotherapy -activated ATM targeting SLC7A11 to inhibit cystine uptake (60). Immunotherapy enhances the efficacy of radiotherapy, radiation and immunotherapy synergistically induce ferroptosis in tumor cells (60, 171).

6 Discussion

Ferroptosis is an iron-dependent form of lipid peroxidative cell death. With GSH as a reducing agent and CoQ10 as an endogenous membrane antioxidant to inhibit lipid peroxidation and ferroptosis (28, 69). Mitochondria are involved in ferroptosis by promoting glutaminolysis (26, 85). NRF2 and P53 have dual roles in ferroptotic cells. Whether CoQ10 could be a new target for ferroptosis? What is the role of HO-1 in ferroptosis and how does it work? Nevertheless, in-depth studies are required to clarify the mechanism of ferroptosis. However, it is clear that induction of ferroptosis in breast cancer cells inhibits tumor growth (13, 14). Given the positive role of autophagy in facilitating ferroptosis, perhaps autophagy activation can be used as a target to induce cellular ferroptosis (76, 153). FINs can be used as sensitizers for radiotherapy and chemotherapy to enhance tumor efficacy (11, 12). We are expected to realize the combination of nano-ferroptosis-inducers with chemotherapy and radiotherapy. It can not only enhance the targeting effect of drugs, but also solve the problem of drug resistance and greatly promote the tumor suppression effect. However, the toxic side effects associated with this treatment modality are elusive and require further investigation. It is imperative to develop new ferroptosis-inducing drugs that are highly effective and less toxic. In summary, induction of ferroptosis has the potential to surmount treatment resistance in breast cancer.

Author contributions

XWQ and YHL conceived the content. ZXW ,WJF and BHJ collected all data. YHO, HBZ and RYT analysed and sorted the data. WJF,YHY XWQ are response to pictureS. LMX and YHL were the major contributors in writing and modified the manuscript. All authors read and approved the final manuscript.

Funding

This study was supported by the National Natural Science Foundation of China (No.81902707, YL), the Key Research Project of Hunan Provincial Education Department (21A0270, YL), China Postdoctoral Science Foundation (2022M711541), YL the Natural Science Foundation of Hunan Province (2019JJ80036, RH, 2021SK51818, LX) and Scientific

Research Fund Project of Hunan Provincial Health Commission (B202303109577, D202303109450, 20201974, B20180052).

Conflict of interest

The authors declare that the research was conducted in the absence of any commercial or financial relationships that could be construed as a potential conflict of interest.

Publisher's note

References

1. Rojas K, Stuckey A. Breast cancer epidemiology and risk factors. *Clin Obstet Gynecol* (2016) 59:651–72. doi: 10.1097/GRF.0000000000000239

2. Burguin A, Diorio C, Durocher F. Breast cancer treatments: Updates and new challenges. *J Pers Med* (2021) 11:808. doi: 10.3390/jpm11080808

3. Dixon SJ, Lemberg KM, Lamprecht MR, Skouta R, Zaitsev EM, Gleason CE, et al. Ferroptosis: An iron-dependent form of nonapoptotic cell death. *Cell* (2012) 149:1060–72. doi: 10.1016/j.cell.2012.03.042

4. Luo M, Shang L, Brooks MD, Jiagge E, Zhu Y, Buschhaus JM, et al. Targeting breast cancer stem cell state equilibrium through modulation of redox signaling. *Cell Metab* (2018) 28:69–86. doi: 10.1016/j.cmet.2018.06.006

5. Wang Y, Qi H, Liu Y, Duan C, Liu X, Xia T, et al. The double-edged roles of ROS in cancer prevention and therapy. *Theranostics* (2021) 11:4839–57. doi: 10.7150/thno.56747

6. Ma S, Henson ES, Chen Y, Gibson SB. Ferroptosis is induced following siramesine and lapatinib treatment of breast cancer cells. *Cell Death Dis* (2016) 7: e2307. doi: 10.1038/cddis.2016.208

7. Zhang W, Sun Y, Bai L, Zhi L, Yang Y, Zhao Q, et al. RBMS1 regulates lung cancer ferroptosis through translational control of SLC7A11. *J Clin Invest* (2021) 131:e152067. doi: 10.1172/JCI152067

8. Kremer DM, Nelson BS, Lin L, Yarosz EL, Halbrook CJ, Kerk SA, et al. GOT1 inhibition promotes pancreatic cancer cell death by ferroptosis. *Nat Commun* (2021) 12:4860. doi: 10.1038/s41467-021-24859-2

9. Bebber CM, Müller F, Prieto Clemente L, Weber J, von Karstedt S. Ferroptosis in cancer cell biology. *Cancers* (2020) 12:164. doi: 10.3390/cancers12010164

10. Cosialls E, El HR, Dos SL, Gong C, Mehrpour M, Hamai A. Ferroptosis: Cancer stem cells rely on iron until "to die for" it. *Cells-Basel* (2021) 10:2981. doi: 10.3390/cells10112981

11. Fu J, Li T, Yang Y, Jiang L, Wang W, Fu L, et al. Activatable nanomedicine for overcoming hypoxia-induced resistance to chemotherapy and inhibiting tumor growth by inducing collaborative apoptosis and ferroptosis in solid tumors. *Biomaterials* (2021) 268:120537. doi: 10.1016/j.biomaterials.2020.120537

12. Lei G, Mao C, Yan Y, Zhuang L, Gan B. Ferroptosis, radiotherapy, and combination therapeutic strategies. *Protein Cell* (2021) 12:836–57. doi: 10.1007/s13238-021-00841-y

13. Torti SV, Torti FM. Iron: The cancer connection. *Mol Aspects Med* (2020) 75:100860. doi: 10.1016/j.mam.2020.100860

14. Yu H, Yang C, Jian L, Guo S, Chen R, Li K, et al. Sulfasalazineinduced ferroptosis in breast cancer cells is reduced by the inhibitory effect of estrogen receptor on the transferrin receptor. *Oncol Rep* (2019) 42:826–38. doi: 10.3892/or.2019.7189

15. Torti SV, Torti FM. Ironing out cancer. *Cancer Res* (2011) 71:1511–4. doi: 10.1158/0008-5472.CAN-10-3614

16. Doll S, Proneth B, Tyurina YY, Panzilius E, Kobayashi S, Ingold I, et al. ACSL4 dictates ferroptosis sensitivity by shaping cellular lipid composition. *Nat Chem Biol* (2017) 13:91–8. doi: 10.1038/nchembio.2239

17. Harris IS, Treloar AE, Inoue S, Sasaki M, Gorrini C, Lee KC, et al. Glutathione and thioredoxin antioxidant pathways synergize to drive cancer initiation and progression. *Cancer Cell* (2015) 27:211–22. doi: 10.1016/j.ccell.2014.11.019

18. Leone A, Roca MS, Ciardiello C, Costantini S, Budillon A. Oxidative stress gene expression profile correlates with cancer patient poor prognosis: Identification of crucial pathways might select novel therapeutic approaches. *Oxid Med Cell Longev* (2017) 2017:2597581. doi: 10.1155/2017/2597581

19. Sica A, Porta C, Riboldi E, Locati M. Convergent pathways of macrophage polarization: The role of b cells. *Eur J Immunol* (2010) 40:2131–3. doi: 10.1002/eji.201040736

20. Pickert G, Lim HY, Weigert A, Haussler A, Myrczek T, Waldner M, et al. Inhibition of GTP cyclohydrolase attenuates tumor growth by reducing angiogenesis and M2-like polarization of tumor associated macrophages. *Int J Cancer* (2013) 132:591–604. doi: 10.1002/ijc.27706

21. Chen L, Zeng X, Kleibeuker E, Buffa F, Barberis A, Leek RD, et al. Paracrine effect of GTP cyclohydrolase and angiopoietin-1 interaction in stromal fibroblasts on tumor Tie2 activation and breast cancer growth. *Oncotarget* (2016) 7:9353–67. doi: 10.18632/oncotarget.6981

22. Adedoyin O, Boddu R, Traylor A, Lever JM, Bolisetty S, George JF, et al. Heme oxygenase-1 mitigates ferroptosis in renal proximal tubule cells. *Am J Physiol Renal Physiol* (2018) 314:F702–14. doi: 10.1152/ajprenal.00044.2017

23. Hill M, Pereira V, Chauveau C, Zagani R, Remy S, Tesson L, et al. Heme oxygenase-1 inhibits rat and human breast cancer cell proliferation: mutual cross inhibition with indoleamine 2,3-dioxygenase. *FASEB J* (2005) 19:1957–68. doi: 10.1096/fj.05-3875com

24. Otterbein LE, Soares MP, Yamashita K, Bach FH. Heme oxygenase-1: Unleashing the protective properties of heme. *Trends Immunol* (2003) 24:449–55. doi: 10.1016/s1471-4906(03)00181-9

25. Fang X, Wang H, Han D, Xie E, Yang X, Wei J, et al. Ferroptosis as a target for protection against cardiomyopathy. *Proc Natl Acad Sci U S A* (2019) 116:2672–80. doi: 10.1073/pnas.1821022116

26. Gao M, Monian P, Quadri N, Ramasamy R, Jiang X. Glutaminolysis and transferrin regulate ferroptosis. *Mol Cell* (2015) 59:298–308. doi: 10.1016/j.molcel.2015.06.011

27. Yan HF, Zou T, QZ T, Xu S, Li H, AA B, et al. Ferroptosis: Mechanisms and links with diseases. *Signal Transduct Target Ther* (2021) 6:49. doi: 10.1038/s41392-020-00428-9

28. Yoo SE, Chen L, Na R, Liu Y, Rios C, Van Remmen H, et al. Gpx4 ablation in adult mice results in a lethal phenotype accompanied by neuronal loss in brain. *Free Radic Biol Med* (2012) 52:1820–7. doi: 10.1016/j.freeradbiomed.2012.02.043

29. Xu M, Tao J, Yang Y, Tan S, Liu H, Jiang J, et al. Ferroptosis involves in intestinal epithelial cell death in ulcerative colitis. *Cell Death Dis* (2020) 11:86. doi: 10.1038/s41419-020-2299-1

30. Dai E, Han L, Liu J, Xie Y, HJ Z, Kang R, et al. Ferroptotic damage promotes pancreatic tumorigenesis through a TMEM173/STING-dependent DNA sensor pathway. *Nat Commun* (2020) 11:6339. doi: 10.1038/s41467-020-20154-8

31. Ellington TD, Miller JW, Henley SJ, Wilson RJ, Wu M, Richardson LC. Trends in breast cancer incidence, by race, ethnicity, and age among women aged ≥20 years - united states, 1999-2018. *MMWR Morbidity mortality weekly Rep* (2022) 71:43–7. doi: 10.15585/mmwr.mm7102a2

32. Sopik V. International variation in breast cancer incidence and mortality in young women. *Breast Cancer Res Treat* (2021) 186:497–507. doi: 10.1007/s10549-020-06003-8

33. Polyak K. Heterogeneity in breast cancer. *J Clin Invest* (2011) 121:3786–8. doi: 10.1172/JCI60534

34. Harbeck N, Gnant M. Breast cancer. *Lancet* (2017) 389:1134–50. doi: 10.1016/S0140-6736(16)31891-8

35. Gong Y, Ji P, YS Y, Xie S, Yu TJ, Xiao Y, et al. Metabolic-Pathway-Based subtyping of triple-negative breast cancer reveals potential therapeutic targets. *Cell Metab* (2021) 33:51–64. doi: 10.1016/j.cmet.2020.10.012

36. Jiang YZ, Liu Y, Xiao Y, Hu X, Jiang L, WJ Z, et al. Molecular subtyping and genomic profiling expand precision medicine in refractory metastatic triple-negative breast cancer: The FUTURE trial. *Cell Res* (2021) 31:178–86. doi: 10.1038/s41422-020-0375-9

37. Xiao Y, Ma D, Zhao S, Suo C, Shi J, MZ X, et al. Multi-omics profiling reveals distinct microenvironment characterization and suggests immune escape mechanisms of triple-negative breast cancer. *Clin Cancer Res* (2019) 25:5002–14. doi: 10.1158/1078-0432.CCR-18-3524

38. Xiao Y, Ma D, YS Y, Yang F, JH D, Gong Y, et al. Comprehensive metabolomics expands precision medicine for triple-negative breast cancer. *Cell Res* (2022) 32:477–90. doi: 10.1038/s41422-022-00614-0

39. Asleh K, Riaz N, Nielsen TO. Heterogeneity of triple negative breast cancer: Current advances in subtyping and treatment implications. *J Exp Clin Cancer Res* (2022) 41:265. doi: 10.1186/s13046-022-02476-1

40. Yang F, Xiao Y, JH D, Jin X, Ma D, Li DQ, et al. Ferroptosis heterogeneity in triple-negative breast cancer reveals an innovative immunotherapy combination strategy. *Cell Metab* (2022) S1550–4131:00411–9. doi: 10.1016/j.cmet.2022.09.021

41. Gucalp A, Tolaney S, SJ I, JN I, MC L, LA C, et al. Phase II trial of bicalutamide in patients with androgen receptor-positive, estrogen receptor-negative metastatic breast cancer. *Clin Cancer Res* (2013) 19:5505–12. doi: 10.1158/1078-0432.CCR-12-3327

42. Li H, Song G, Zhou Q, Ran R, Jiang H, Zhang R, et al. Activity of preclinical and phase I clinical trial of a novel androgen receptor antagonist GT0918 in metastatic breast cancer. *Breast Cancer Res Treat* (2021) 189:725–36. doi: 10.1007/s10549-021-06345-x

43. Bonnefoi H, Grellety T, Tredan O, Saghatchian M, Dalenc F, Mailliez A, et al. A phase II trial of abiraterone acetate plus prednisone in patients with triple-negative androgen receptor positive locally advanced or metastatic breast cancer (UCBG 12-1). *Ann Oncol* (2016) 27:812–8. doi: 10.1093/annonc/mdw067

44. Lehmann BD, Abramson VG, Sanders ME, Mayer EL, Haddad TC, Nanda R, et al. TBCRC 032 IB/II multicenter study: Molecular insights to AR antagonist and PI3K inhibitor efficacy in patients with AR(+) metastatic triple-negative breast cancer. *Clin Cancer Res* (2020) 26:2111–23. doi: 10.1158/1078-0432.CCR-19-2170

45. Yuan Y, Lee JS, Yost SE, Frankel PH, Ruel C, Egelston CA, et al. A phase II clinical trial of pembrolizumab and enobosarm in patients with androgen receptor-positive metastatic triple-negative breast cancer. *Oncologist* (2021) 26:99–217. doi: 10.1002/onco.13583

46. Prat A, Saura C, Pascual T, Hernando C, Munoz M, Pare L, et al. Ribociclib plus letrozole versus chemotherapy for postmenopausal women with hormone receptor-positive, HER2-negative, luminal b breast cancer (CORALLEEN): An open-label, multicentre, randomised, phase 2 trial. *Lancet Oncol* (2020) 21:33–43. doi: 10.1016/S1470-2045(19)30786-7

47. McRee AJ, Marcom PK, Moore DT, Zamboni WC, Kornblum ZA, Hu Z, et al. A phase I trial of the PI3K inhibitor buparlisib combined with capecitabine in patients with metastatic breast cancer. *Clin Breast Cancer* (2018) 18:289–97. doi: 10.1016/j.clbc.2017.10.014

48. Llombart-Cussac A, Cortes J, Pare L, Galvan P, Bermejo B, Martinez N, et al. HER2-enriched subtype as a predictor of pathological complete response following trastuzumab and lapatinib without chemotherapy in early-stage HER2-positive breast cancer (PAMELA): An open-label, single-group, multicentre, phase 2 trial. *Lancet Oncol* (2017) 18:545–54. doi: 10.1016/S1470-2045(17)30021-9

49. Saura C, Hlauschek D, Oliveira M, Zardavas D, Jallitsch-Halper A, de la Pena L, et al. Neoadjuvant letrozole plus taselisib versus letrozole plus placebo in postmenopausal women with oestrogen receptor-positive, HER2-negative, early-stage breast cancer (LORELEI): A multicentre, randomised, double-blind, placebo-controlled, phase 2 trial. *Lancet Oncol* (2019) 20:1226–38. doi: 10.1016/S1470-2045(19)30334-1

50. Martin M, JI C, Anton A, Plazaola A, Garcia-Martinez E, MA S, et al. Neoadjuvant therapy with weekly nanoparticle albumin-bound paclitaxel for luminal early breast cancer patients: Results from the NABRAX study (GEICAM/2011-02), a multicenter, non-randomized, phase II trial, with a companion biomarker analysis. *Oncologist* (2017) 22:1301–8. doi: 10.1634/theoncologist.2017-0052

51. Tang D, Chen X, Kang R, Kroemer G. Ferroptosis: Molecular mechanisms and health implications. *Cell Res* (2021) 31:107–25. doi: 10.1038/s41422-020-00441-1

52. Muller S, Sindikubwabo F, Caneque T, Lafon A, Versini A, Lombard B, et al. CD44 regulates epigenetic plasticity by mediating iron endocytosis. *Nat Chem* (2020) 12:929–38. doi: 10.1038/s41557-020-0513-5

53. Dagogo-Jack I, Shaw AT. Tumour heterogeneity and resistance to cancer therapies. *Nat Rev Clin Oncol* (2018) 15:81–94. doi: 10.1038/nrclinonc.2017.166

54. Damia G, Garattini S. The pharmacological point of view of resistance to therapy in tumors. *Cancer Treat Rev* (2014) 40:909–16. doi: 10.1016/j.ctrv.2014.05.008

55. Quail DF, Joyce JA. Microenvironmental regulation of tumor progression and metastasis. *Nat Med* (2013) 19:1423–37. doi: 10.1038/nm.3394

56. Wu T, Dai Y. Tumor microenvironment and therapeutic response. *Cancer Lett* (2017) 387:61–8. doi: 10.1016/j.canlet.2016.01.043

57. Xu H, Ye D, Ren M, Zhang H, Bi F. Ferroptosis in the tumor microenvironment: Perspectives for immunotherapy. *Trends Mol Med* (2021) 27:856–67. doi: 10.1016/j.molmed.2021.06.014

58. Lei G, Zhuang L, Gan B. Targeting ferroptosis as a vulnerability in cancer. *Nat Rev Cancer* (2022) 22:381–96. doi: 10.1038/s41568-022-00459-0

59. Dai E, Han L, Liu J, Xie Y, Kroemer G, DJ K, et al. Autophagy-dependent ferroptosis drives tumor-associated macrophage polarization via release and uptake of oncogenic KRAS protein. *Autophagy* (2020) 16:2069–83. doi: 10.1080/15548627.2020.1714209

60. Wang W, Green M, JE C, Gijon M, PD K, JK J, et al. CD8(+) T cells regulate tumour ferroptosis during cancer immunotherapy. *Nature* (2019) 569:270–4. doi: 10.1038/s41586-019-1170-y

61. Han S, Lin F, Qi Y, Liu C, Zhou L, Xia Y, et al. HO-1 contributes to luteolin-triggered ferroptosis in clear cell renal cell carcinoma *via* increasing the labile iron pool and promoting lipid peroxidation. *Oxid Med Cell Longev* (2022) 2022:3846217. doi: 10.1155/2022/3846217

62. Hattori K, Ishikawa H, Sakauchi C, Takayanagi S, Naguro I, Ichijo H. Cold stress-induced ferroptosis involves the ASK1-p38 pathway. *EMBO Rep* (2017) 18:2067–78. doi: 10.15252/embr.201744228

63. Yu B, Choi B, Li W, Kim DH. Magnetic field boosted ferroptosis-like cell death and responsive MRI using hybrid vesicles for cancer immunotherapy. *Nat Commun* (2020) 11:3637. doi: 10.1038/s41467-020-17380-5

64. Rodriguez R, SL S, Conrad M. Persister cancer cells: Iron addiction and vulnerability to ferroptosis. *Mol Cell* (2021) 82:728–40. doi: 10.1016/j.molcel.2021.12.001

65. Diaz DLLM, Gallardo M, ML G-R, Izquierdo A, Herrero E, Aguilera A, et al. Zim17/Tim15 links mitochondrial iron-sulfur cluster biosynthesis to nuclear genome stability. *Nucleic Acids Res* (2011) 39:6002–15. doi: 10.1093/nar/gkr193

66. Clemente LP, Rabenau M, Tang S, Stanka J, Cors E, Stroh J, et al. Dynasore blocks ferroptosis through combined modulation of iron uptake and inhibition of mitochondrial respiration. *Cells-Basel* (2020) 9:2259. doi: 10.3390/cells9102259

67. Lin HY, Ho HW, Chang YH, Wei CJ, Chu PY. The evolving role of ferroptosis in breast cancer: Translational implications present and future. *Cancers (Basel)* (2021) 13::4576. doi: 10.3390/cancers13184576

68. Doll S, Freitas FP, Shah R, Aldrovandi M, Da SM, Ingold I, et al. FSP1 is a glutathione-independent ferroptosis suppressor. *Nature* (2019) 575:693–8. doi: 10.1038/s41586-019-1707-0

69. Kraft V, Bezjian CT, Pfeiffer S, Ringelstetter L, Muller C, Zandkarimi F, et al. GTP cyclohydrolase 1/Tetrahydrobiopterin counteract ferroptosis through lipid remodeling. *ACS Cent Sci* (2020) 6:41–53. doi: 10.1021/acscentsci.9b01063

70. Dodson M, Castro-Portuguez R, Zhang DD. NRF2 plays a critical role in mitigating lipid peroxidation and ferroptosis. *Redox Biol* (2019) 23:101107. doi: 10.1016/j.redox.2019.101107

71. Duffy MJ, Synnott NC, O'Grady S, Crown J. Targeting p53 for the treatment of cancer. *Semin Cancer Biol* (2020) 79:58–67. doi: 10.1016/j.semcancer.2020.07.005

72. Synnott NC, Murray A, McGowan PM, Kiely M, Kiely PA, O'Donovan N, et al. Mutant p53: A novel target for the treatment of patients with triple-negative breast cancer? *Int J Cancer* (2017) 140:234–46. doi: 10.1002/ijc.30425

73. Crielaard BJ, Lammers T, Rivella S. Targeting iron metabolism in drug discovery and delivery. *Nat Rev Drug Discovery* (2017) 16:400–23. doi: 10.1038/nrd.2016.248

74. Zorov DB, Juhaszova M, Sollott SJ. Mitochondrial reactive oxygen species (ROS) and ROS-induced ROS release. *Physiol Rev* (2014) 94:909–50. doi: 10.1152/physrev.00026.2013

75. Fang X, Cai Z, Wang H, Han D, Cheng Q, Zhang P, et al. Loss of cardiac ferritin h facilitates cardiomyopathy *via* Slc7a11-mediated ferroptosis. *Circ Res* (2020) 127:486–501. doi: 10.1161/CIRCRESAHA.120.316509

76. Gao M, Monian P, Pan Q, Zhang W, Xiang J, Jiang X. Ferroptosis is an autophagic cell death process. *Cell Res* (2016) 26:1021–32. doi: 10.1038/cr.2016.95

77. Gozzelino R, Soares MP. Coupling heme and iron metabolism via ferritin h chain. *Antioxid Redox Signal* (2014) 20:1754–69. doi: 10.1089/ars.2013.5666

78. Sun X, Ou Z, Chen R, Niu X, Chen D, Kang R, et al. Activation of the p62-Keap1-NRF2 pathway protects against ferroptosis in hepatocellular carcinoma cells. *Hepatology* (2016) 63:173–84. doi: 10.1002/hep.28251

79. Ma S, Dielschneider RF, Henson ES, Xiao W, Choquette TR, Blankstein AR, et al. Ferroptosis and autophagy induced cell death occur independently after siramesine and lapatinib treatment in breast cancer cells. *PloS One* (2017) 12:e182921. doi: 10.1371/journal.pone.0182921

80. Nagpal A, Redvers RP, Ling X, Ayton S, Fuentes M, Tavancheh E, et al. Neoadjuvant neratinib promotes ferroptosis and inhibits brain metastasis in a novel syngeneic model of spontaneous HER2(+ve) breast cancer metastasis. *Breast Cancer Res* (2019) 21:94. doi: 10.1186/s13058-019-1177-1

81. Chen GQ, Benthani FA, Wu J, Liang D, ZX B, Jiang X. Artemisinin compounds sensitize cancer cells to ferroptosis by regulating iron homeostasis. *Cell Death Differ* (2020) 27:242–54. doi: 10.1038/s41418-019-0352-3

82. Ayoubi M, Naserzadeh P, Hashemi MT, Reza RM, Tamjid E, Tavakoli MM, et al. Biochemical mechanisms of dose-dependent cytotoxicity and ROS-mediated apoptosis induced by lead sulfide/graphene oxide quantum dots for potential bioimaging applications. *Sci Rep* (2017) 7:12896. doi: 10.1038/s41598-017-13396-y

83. Dixon SJ, Stockwell BR. The role of iron and reactive oxygen species in cell death. *Nat Chem Biol* (2014) 10:9–17. doi: 10.1038/nchembio.1416

84. Chiang JL, Shukla P, Pagidas K, Ahmed NS, Karri S, Gunn DD, et al. Mitochondria in ovarian aging and reproductive longevity. *Ageing Res Rev* (2020) 63:101168. doi: 10.1016/j.arr.2020.101168

85. Gao M, Yi J, Zhu J, Minikes AM, Monian P, Thompson CB, et al. Role of mitochondria in ferroptosis. *Mol Cell* (2019) 73:354–63. doi: 10.1016/j.molcel.2018.10.042

86. Xie Y, Zhou X, Li J, XC Y, WL L, FH K, et al. Identification of a new natural biflavonoids against breast cancer cells induced ferroptosis via the mitochondrial pathway. *Bioorg Chem* (2021) 109:104744. doi: 10.1016/j.bioorg.2021.104744

87. Krainz T, Gaschler MM, Lim C, Sacher JR, Stockwell BR, Wipf P. A mitochondrial-targeted nitroxide is a potent inhibitor of ferroptosis. *ACS Cent Sci* (2016) 2:653–9. doi: 10.1021/acscentsci.6b00199

88. Basit F, van Oppen LM, Schockel L, Bossenbroek HM, van Emst-de VS, Hermeling JC, et al. Mitochondrial complex I inhibition triggers a mitophagy-dependent ROS increase leading to necroptosis and ferroptosis in melanoma cells. *Cell Death Dis* (2017) 8:e2716. doi: 10.1038/cddis.2017.133

89. Boylan JA, Lawrence KA, Downey JS, Gherardini FC. Borrelia burgdorferi membranes are the primary targets of reactive oxygen species. *Mol Microbiol* (2008) 68:786–99. doi: 10.1111/j.1365-2958.2008.06204.x

90. Yang WS, Stockwell BR. Ferroptosis: Death by lipid peroxidation. *Trends Cell Biol* (2016) 26:165–76. doi: 10.1016/j.tcb.2015.10.014

91. Yang WS, Kim KJ, Gaschler MM, Patel M, Shchepinov MS, Stockwell BR. Peroxidation of polyunsaturated fatty acids by lipoxygenases drives ferroptosis. *Proc Natl Acad Sci U S A* (2016) 113:E4966–75. doi: 10.1073/pnas.1603244113

92. Wen Y, Chen H, Zhang L, Wu M, Zhang F, Yang D, et al. Glycyrrhetinic acid induces oxidative/nitrative stress and drives ferroptosis through activating NADPH oxidases and iNOS, and depriving glutathione in triple-negative breast cancer cells. *Free Radic Biol Med* (2021) 173:41–51. doi: 10.1016/j.freeradbiomed.2021.07.019

93. Dixon SJ, Winter GE, Musavi LS, Lee ED, Snijder B, Rebsamen M, et al. Human haploid cell genetics reveals roles for lipid metabolism genes in nonapoptotic cell death. *ACS Chem Biol* (2015) 10:1604–9. doi: 10.1021/acschembio.5b00245

94. Kapralov AA, Yang Q, Dar HH, Tyurina YY, Anthonymuthu TS, Kim R, et al. Redox lipid reprogramming commands susceptibility of macrophages and microglia to ferroptotic death. *Nat Chem Biol* (2020) 16:278–90. doi: 10.1038/s41589-019-0462-8

95. Kagan VE, Mao G, Qu F, Angeli JP, Doll S, Croix CS, et al. Oxidized arachidonic and adrenic PEs navigate cells to ferroptosis. *Nat Chem Biol* (2017) 13:81–90. doi: 10.1038/nchembio.2238

96. Agmon E, Solon J, Bassereau P, Stockwell BR. Modeling the effects of lipid peroxidation during ferroptosis on membrane properties. *Sci Rep* (2018) 8:5155. doi: 10.1038/s41598-018-23408-0

97. Brigelius-Flohe R, Maiorino M. Glutathione peroxidases. *Biochim Biophys Acta* (2013) 1830:3289–303. doi: 10.1016/j.bbagen.2012.11.020

98. Wei Y, Lv H, Shaikh AB, Han W, Hou H, Zhang Z, et al. Directly targeting glutathione peroxidase 4 may be more effective than disrupting glutathione on ferroptosis-based cancer therapy. *Biochim Biophys Acta Gen Subj* (2020) 1864:129539. doi: 10.1016/j.bbagen.2020.129539

99. Jiang Y, Cao Y, Wang Y, Li W, Liu X, Lv Y, et al. Cysteine transporter SLC3A1 promotes breast cancer tumorigenesis. *Theranostics* (2017) 7:1036–46. doi: 10.7150/thno.18005

100. Gao J, Yang F, Che J, Han Y, Wang Y, Chen N, et al. Selenium-encoded isotopic signature targeted profiling. *ACS Cent Sci* (2018) 4:960–70. doi: 10.1021/acscentsci.8b00112

101. Hayano M, Yang WS, Corn CK, Pagano NC, Stockwell BR. Loss of cysteinyl-tRNA synthetase (CARS) induces the transsulfuration pathway and inhibits ferroptosis induced by cystine deprivation. *Cell Death Differ* (2016) 23:270–8. doi: 10.1038/cdd.2015.93

102. Eaton JK, Ruberto RA, Kramm A, Viswanathan VS, Schreiber SL. Diacylfuroxans are masked nitrile oxides that inhibit GPX4 covalently. *J Am Chem Soc* (2019) 141:20407–15. doi: 10.1021/jacs.9b10769

103. Lin YS, Shen YC, Wu CY, Tsai YY, Yang YH, Lin YY, et al. Danshen improves survival of patients with breast cancer and dihydroisotanshinone I induces ferroptosis and apoptosis of breast cancer cells. *Front Pharmacol* (2019) 10:1226. doi: 10.3389/fphar.2019.01226

104. Chen J, Qin C, Zhou Y, Chen Y, Mao M, Yang J. Metformin may induce ferroptosis by inhibiting autophagy *via* lncRNA H19 in breast cancer. *FEBS Open Bio* (2021) 12:146–153. doi: 10.1002/2211-5463.13314

105. Hou Y, Cai S, Yu S, Lin H. Metformin induces ferroptosis by targeting miR-324-3p/GPX4 axis in breast cancer. *Acta Biochim Biophys Sin (Shanghai)* (2021) 53:333–41. doi: 10.1093/abbs/gmaa180

106. Yang J, Zhou Y, Xie S, Wang J, Li Z, Chen L, et al. Metformin induces ferroptosis by inhibiting UFMylation of SLC7A11 in breast cancer. *J Exp Clin Cancer Res* (2021) 40:206. doi: 10.1186/s13046-021-02012-7

107. Yao X, Xie R, Cao Y, Tang J, Men Y, Peng H, et al. Simvastatin induced ferroptosis for triple-negative breast cancer therapy. *J Nanobiotechnol* (2021) 19:311. doi: 10.1186/s12951-021-01058-1

108. Li R, Zhang J, Zhou Y, Gao Q, Wang R, Fu Y, et al. Transcriptome investigation and *In vitro* verification of curcumin-induced HO-1 as a feature of ferroptosis in breast cancer cells. *Oxid Med Cell Longev* (2020) 2020:3469840. doi: 10.1155/2020/3469840

109. Wu X, Liu C, Li Z, Gai C, Ding D, Chen W, et al. Regulation of GSK3beta/Nrf2 signaling pathway modulated erastin-induced ferroptosis in breast cancer. *Mol Cell Biochem* (2020) 473:217–28. doi: 10.1007/s11010-020-03821-8

110. Shin CS, Mishra P, Watrous JD, Carelli V, D'Aurelio M, Jain M, et al. The glutamate/cystine xCT antiporter antagonizes glutamine metabolism and reduces nutrient flexibility. *Nat Commun* (2017) 8:15074. doi: 10.1038/ncomms15074

111. Verma N, Vinik Y, Saroha A, Nair NU, Ruppin E, Mills G, et al. Synthetic lethal combination targeting BET uncovered intrinsic susceptibility of TNBC to ferroptosis. *Sci Adv* (2020) 6:eaba8968. doi: 10.1126/sciadv.aba8968

112. Yang Y, Chen Y, Johansson E, Schneider SN, Shertzer HG, Nebert DW, et al. Interaction between the catalytic and modifier subunits of glutamate-cysteine ligase. *Biochem Pharmacol* (2007) 74:372–81. doi: 10.1016/j.bcp.2007.02.003

113. Kajarabille N, Latunde-Dada GO. Programmed cell-death by ferroptosis: Antioxidants as mitigators. *Int J Mol Sci* (2019) 20:4968. doi: 10.3390/ijms20194968

114. Santoro MM. The antioxidant role of non-mitochondrial CoQ10: Mystery solved! *Cell Metab* (2020) 31:13–5. doi: 10.1016/j.cmet.2019.12.007

115. Sahoo K, Dozmorov MG, Anant S, Awasthi V. The curcuminoid CLEFMA selectively induces cell death in H441 lung adenocarcinoma cells via oxidative stress. *Invest New Drugs* (2012) 30:558–67. doi: 10.1007/s10637-010-9610-4

116. Mandal PK, Schneider M, Kolle P, Kuhlencordt P, Forster H, Beck H, et al. Loss of thioredoxin reductase 1 renders tumors highly susceptible to pharmacologic glutathione deprivation. *Cancer Res* (2010) 70:9505–14. doi: 10.1158/0008-5472.CAN-10-1509

117. Mandal PK, Seiler A, Perisic T, Kolle P, Banjac CA, Forster H, et al. System x(c)- and thioredoxin reductase 1 cooperatively rescue glutathione deficiency. *J Biol Chem* (2010) 285:22244–53. doi: 10.1074/jbc.M110.121327

118. Haque JA, McMahan RS, Campbell JS, Shimizu-Albergine M, Wilson AM, Botta D, et al. Attenuated progression of diet-induced steatohepatitis in glutathione-deficient mice. *Lab Invest* (2010) 90:1704–17. doi: 10.1038/labinvest.2010.112

119. Gorrini C, Mak TW. Glutathione metabolism: An achilles' heel of ARID1A-deficient tumors. *Cancer Cell* (2019) 35:161–3. doi: 10.1016/j.ccell.2019.01.017

120. Ye LF, Chaudhary KR, Zandkarimi F, Harken AD, Kinslow CJ, Upadhyayula PS, et al. Radiation-induced lipid peroxidation triggers ferroptosis and synergizes with ferroptosis inducers. *ACS Chem Biol* (2020) 15:469–84. doi: 10.1021/acschembio.9b00939

121. Harris IS, Endress JE, Coloff JL, Selfors LM, McBrayer SK, Rosenbluth JM, et al. Deubiquitinases maintain protein homeostasis and survival of cancer cells upon glutathione depletion. *Cell Metab* (2019) 29:1166–81. doi: 10.1016/j.cmet.2019.01.020

122. Raninga PV, Lee AC, Sinha D, Shih YY, Mittal D, Makhale A, et al. Therapeutic cooperation between auranofin, a thioredoxin reductase inhibitor and anti-PD-L1 antibody for treatment of triple-negative breast cancer. *Int J Cancer* (2020) 146:123–36. doi: 10.1002/ijc.32410

123. Bersuker K, Hendricks JM, Li Z, Magtanong L, Ford B, Tang PH, et al. The CoQ oxidoreductase FSP1 acts parallel to GPX4 to inhibit ferroptosis. *Nature* (2019) 575:688–92. doi: 10.1038/s41586-019-1705-2

124. Tesfay L, Paul BT, Konstorum A, Deng Z, Cox AO, Lee J, et al. Stearoyl-CoA desaturase 1 protects ovarian cancer cells from ferroptotic cell death. *Cancer Res* (2019) 79:5355–66. doi: 10.1158/0008-5472.CAN-19-0369

125. Shimada K, Skouta R, Kaplan A, Yang WS, Hayano M, Dixon SJ, et al. Global survey of cell death mechanisms reveals metabolic regulation of ferroptosis. *Nat Chem Biol* (2016) 12:497–503. doi: 10.1038/nchembio.2079

126. Mugoni V, Postel R, Catanzaro V, De Luca E, Turco E, Digilio G, et al. Ubiad1 is an antioxidant enzyme that regulates eNOS activity by CoQ10 synthesis. *Cell* (2013) 152:504–18. doi: 10.1016/j.cell.2013.01.013

127. Lee J, You JH, Kim MS, Roh JL. Epigenetic reprogramming of epithelial-mesenchymal transition promotes ferroptosis of head and neck cancer. *Redox Biol* (2020) 37:101697. doi: 10.1016/j.redox.2020.101697

128. Soula M, Weber RA, Zilka O, Alwaseem H, La K, Yen F, et al. Metabolic determinants of cancer cell sensitivity to canonical ferroptosis inducers. *Nat Chem Biol* (2020) 16:1351–60. doi: 10.1038/s41589-020-0613-y

129. Baird L, Lleres D, Swift S, Dinkova-Kostova AT. Regulatory flexibility in the Nrf2-mediated stress response is conferred by conformational cycling of the Keap1-Nrf2 protein complex. *Proc Natl Acad Sci U S A* (2013) 110:15259–64. doi: 10.1073/pnas.1305687110

130. Zhang DD, Lo SC, Cross JV, Templeton DJ, Hannink M. Keap1 is a redox-regulated substrate adaptor protein for a Cul3-dependent ubiquitin ligase complex. *Mol Cell Biol* (2004) 24:10941–53. doi: 10.1128/MCB.24.24.10941-10953.2004

131. Motohashi H, Yamamoto M. Nrf2-Keap1 defines a physiologically important stress response mechanism. *Trends Mol Med* (2004) 10:549–57. doi: 10.1016/j.molmed.2004.09.003

132. Shin D, Kim EH, Lee J, Roh JL. Nrf2 inhibition reverses resistance to GPX4 inhibitor-induced ferroptosis in head and neck cancer. *Free Radic Biol Med* (2018) 129:454–62. doi: 10.1016/j.freeradbiomed.2018.10.426

133. Chen Y, Liu K, Zhang J, Hai Y, Wang P, Wang H, et al. C-jun NH2 -terminal protein kinase phosphorylates the Nrf2-ECH homology 6 domain of nuclear factor erythroid 2-related factor 2 and downregulates cytoprotective genes in acetaminophen-induced liver injury in mice. *Hepatology* (2020) 71:1787–801. doi: 10.1002/hep.31116

134. Itoh K, Mimura J, Yamamoto M. Discovery of the negative regulator of Nrf2, Keap1: A historical overview. *Antioxid Redox Signal* (2010) 13:1665–78. doi: 10.1089/ars.2010.3222

135. van Raaij S, Masereeuw R, Swinkels DW, van Swelm R. Inhibition of Nrf2 alters cell stress induced by chronic iron exposure in human proximal tubular epithelial cells. *Toxicol Lett* (2018) 295:179–86. doi: 10.1016/j.toxlet.2018.06.1218

136. Lin CW, Shen SC, Hou WC, Yang LY, Chen YC. Heme oxygenase-1 inhibits breast cancer invasion via suppressing the expression of matrix metalloproteinase-9. *Mol Cancer Ther* (2008) 7:1195–206. doi: 10.1158/1535-7163.MCT-07-2199

137. Chang LC, Chiang SK, Chen SE, Yu YL, Chou RH, Chang WC. Heme oxygenase-1 mediates BAY 11-7085 induced ferroptosis. *Cancer Lett* (2018) 416:124–37. doi: 10.1016/j.canlet.2017.12.025

138. Kwon MY, Park E, Lee SJ, Chung SW. Heme oxygenase-1 accelerates erastin-induced ferroptotic cell death. *Oncotarget* (2015) 6:24393–403. doi: 10.18632/oncotarget.5162

139. Lisboa BW, Vogtlander S, Gilster T, Riethdorf L, Milde-Langosch K, Loning T. Molecular and immunohistochemical analysis of p53 mutations in scrapings and tissue from preinvasive and invasive breast cancer. *Virchows Arch* (1997) 431:375–81. doi: 10.1007/s004280050114

140. Rossner PJ, Gammon MD, Zhang YJ, Terry MB, Hibshoosh H, Memeo L, et al. Mutations in p53, p53 protein overexpression and breast cancer survival. *J Cell Mol Med* (2009) 13:3847–57. doi: 10.1111/j.1582-4934.2008.00553.x

141. Shahbandi A, Nguyen HD, Jackson JG. TP53 mutations and outcomes in breast cancer: Reading beyond the headlines. *Trends Cancer* (2020) 6:98–110. doi: 10.1016/j.trecan.2020.01.007

142. Ceder S, Eriksson SE, Liang YY, Cheteh EH, Zhang SM, Fujihara KM, et al. Mutant p53-reactivating compound APR-246 synergizes with asparaginase in inducing growth suppression in acute lymphoblastic leukemia cells. *Cell Death Dis* (2021) 12:709. doi: 10.1038/s41419-021-03988-y

143. Tessoulin B, Descamps G, Moreau P, Maiga S, Lode L, Godon C, et al. PRIMA-1Met induces myeloma cell death independent of p53 by impairing the GSH/ROS balance. *Blood* (2014) 124:1626–36. doi: 10.1182/blood-2014-01-548800

144. Birsen R, Larrue C, Decroocq J, Johnson N, Guiraud N, Gotanegre M, et al. APR-246 induces early cell death by ferroptosis in acute myeloid leukemia. *Haematologica* (2021) 107:403–16. doi: 10.3324/haematol.2020.259531

145. Li J, Lama R, Galster SL, Inigo JR, Wu J, Chandra D, et al. Small molecule MMRi62 induces ferroptosis and inhibits metastasis in pancreatic cancer via degradation of ferritin heavy chain and mutant p53. *Mol Cancer Ther* (2022) 21:535–45. doi: 10.1158/1535-7163.MCT-21-0728

146. Li T, Kon N, Jiang L, Tan M, Ludwig T, Zhao Y, et al. Tumor suppression in the absence of p53-mediated cell-cycle arrest, apoptosis, and senescence. *Cell* (2012) 149:1269–83. doi: 10.1016/j.cell.2012.04.026

147. Wang SJ, Li D, Ou Y, Jiang L, Chen Y, Zhao Y, et al. Acetylation is crucial for p53-mediated ferroptosis and tumor suppression. *Cell Rep* (2016) 17:366–73. doi: 10.1016/j.celrep.2016.09.022

148. Ou Y, Wang SJ, Li D, Chu B, Gu W. Activation of SAT1 engages polyamine metabolism with p53-mediated ferroptotic responses. *Proc Natl Acad Sci USA* (2016) 113:E6806–12. doi: 10.1073/pnas.1607152113

149. Tarangelo A, Magtanong L, Bieging-Rolett KT, Li Y, Ye J, Attardi LD, et al. p53 suppresses metabolic stress-induced ferroptosis in cancer cells. *Cell Rep* (2018) 22:569–75. doi: 10.1016/j.celrep.2017.12.077

150. Hu W, Zhang C, Wu R, Sun Y, Levine A, Feng Z. Glutaminase 2, a novel p53 target gene regulating energy metabolism and antioxidant function. *Proc Natl Acad Sci USA* (2010) 107:7455–60. doi: 10.1073/pnas.1001006107

151. Xie Y, Zhu S, Song X, Sun X, Fan Y, Liu J, et al. The tumor suppressor p53 limits ferroptosis by blocking DPP4 activity. *Cell Rep* (2017) 20:1692–704. doi: 10.1016/j.celrep.2017.07.055

152. Chen X, Yu C, Kang R, Kroemer G, Tang D. Cellular degradation systems in ferroptosis. *Cell Death Differ* (2021) 28:1135–48. doi: 10.1038/s41418-020-00728-1

153. Hou W, Xie Y, Song X, Sun X, Lotze MT, Zeh HR, et al. Autophagy promotes ferroptosis by degradation of ferritin. *Autophagy* (2016) 12:1425–8. doi: 10.1080/15548627.2016.1187366

154. Denton D, Kumar S. Autophagy-dependent cell death. *Cell Death Differ* (2019) 26:605–16. doi: 10.1038/s41418-018-0252-y

155. Dikic I, Elazar Z. Mechanism and medical implications of mammalian autophagy. *Nat Rev Mol Cell Biol* (2018) 19:349–64. doi: 10.1038/s41580-018-0003-4

156. Singh R, Kaushik S, Wang Y, Xiang Y, Novak I, Komatsu M, et al. Autophagy regulates lipid metabolism. *Nature* (2009) 458:1131–5. doi: 10.1038/nature07976

157. Bai Y, Meng L, Han L, Jia Y, Zhao Y, Gao H, et al. Lipid storage and lipophagy regulates ferroptosis. *Biochem Biophys Res Commun* (2019) 508:997–1003. doi: 10.1016/j.bbrc.2018.12.039

158. Bailey AP, Koster G, Guillermier C, Hirst EM, MacRae JI, Lechene CP, et al. Antioxidant role for lipid droplets in a stem cell niche of drosophila. *Cell* (2015) 163:340–53. doi: 10.1016/j.cell.2015.09.020

159. Chen C, Wang D, Yu Y, Zhao T, Min N, Wu Y, et al. Legumain promotes tubular ferroptosis by facilitating chaperone-mediated autophagy of GPX4 in AKI. *Cell Death Dis* (2021) 12:65. doi: 10.1038/s41419-020-03362-4

160. Wu Z, Geng Y, Lu X, Shi Y, Wu G, Zhang M, et al. Chaperone-mediated autophagy is involved in the execution of ferroptosis. *Proc Natl Acad Sci USA* (2019) 116:2996–3005. doi: 10.1073/pnas.1819728116

161. Liyanage PY, Hettiarachchi SD, Zhou Y, Ouhtit A, Seven ES, Oztan CY, et al. Nanoparticle-mediated targeted drug delivery for breast cancer treatment. *Biochim Biophys Acta Rev Cancer* (2019) 1871:419–33. doi: 10.1016/j.bbcan.2019.04.006

162. Li Z, Wu X, Wang W, Gai C, Zhang W, Li W, et al. Fe(II) and tannic acid-cloaked MOF as carrier of artemisinin for supply of ferrous ions to enhance treatment of triple-negative breast cancer. *Nanoscale Res Lett* (2021) 16:37. doi: 10.1186/s11671-021-03497-z

163. Yu M, Gai C, Li Z, Ding D, Zheng J, Zhang W, et al. Targeted exosome-encapsulated erastin induced ferroptosis in triple negative breast cancer cells. *Cancer Sci* (2019) 110:3173–82. doi: 10.1111/cas.14181

164. Zhang J, Yang J, Zuo T, Ma S, Xokrat N, Hu Z, et al. Heparanase-driven sequential released nanoparticles for ferroptosis and tumor microenvironment modulations synergism in breast cancer therapy. *Biomaterials* (2021) 266:120429. doi: 10.1016/j.biomaterials.2020.120429

165. An P, Gao Z, Sun K, Gu D, Wu H, You C, et al. Photothermal-enhanced inactivation of glutathione peroxidase for ferroptosis sensitized by an autophagy promotor. *ACS Appl Mater Interfaces* (2019) 11:42988–97. doi: 10.1021/acsami.9b16124

166. Xiong H, Wang C, Wang Z, Jiang Z, Zhou J, Yao J. Intracellular cascade activated nanosystem for improving ER+ breast cancer therapy through attacking GSH-mediated metabolic vulnerability. *J Control Release* (2019) 309:145–57. doi: 10.1016/j.jconrel.2019.07.029

167. Lin Z, Song J, Gao Y, Huang S, Dou R, Zhong P, et al. Hypoxia-induced HIF-1alpha/lncRNA-PMAN inhibits ferroptosis by promoting the cytoplasmic translocation of ELAVL1 in peritoneal dissemination from gastric cancer. *Redox Biol* (2022) 52:102312. doi: 10.1016/j.redox.2022.102312

168. Ma S, Fu X, Liu L, Liu Y, Feng H, Jiang H, et al. Iron-dependent autophagic cell death induced by radiation in MDA-MB-231 breast cancer cells. *Front Cell Dev Biol* (2021) 9:723801. doi: 10.3389/fcell.2021.723801

169. Lei G, Zhang Y, Koppula P, Liu X, Zhang J, Lin SH, et al. The role of ferroptosis in ionizing radiation-induced cell death and tumor suppression. *Cell Res* (2020) 30:146–62. doi: 10.1038/s41422-019-0263-3

170. Lei G, Zhang Y, Hong T, Zhang X, Liu X, Mao C, et al. Ferroptosis as a mechanism to mediate p53 function in tumor radiosensitivity. *Oncogene* (2021) 40:3533–47. doi: 10.1038/s41388-021-01790-w

171. Lang X, Green MD, Wang W, Yu J, Choi JE, Jiang L, et al. Radiotherapy and immunotherapy promote tumoral lipid oxidation and ferroptosis via synergistic repression of SLC7A11. *Cancer Discovery* (2019) 9:1673–85. doi: 10.1158/2159-8290.CD-19-0338

Glossary

ACSL4	Long-chain acyl-coenzyme A synthetase
ATG	Autophagy genes
AUR	Auranofin
BH4	Tetrahydrobiopterin
BLIA	Basal-like and immune-activated
BLIS	Basal-like and immune-suppressed
BSO	Buthionine sulfoximine
CoA	Acyl coenzyme A
CoQ10	Coenzyme Q10
DOX	Doxorubicin
ER	Estrogen receptor
ETC	Electron transport chain
FINs	Ferroptosis inducers
FPN	Ferroportin
FSP1	Ferroptosis suppressor protein 1
FTH	Ferritin heavy chain
GA	Glycyrrhetinic acid
GCH1	GTP Cyclohydrolase 1
Gcl	Glutamate-cysteine ligase
GPX4	Glutathione peroxidase-4
GSH	Glutathione
HER-2	Human epidermal growth factor receptor type 2
IR	Ionizing radiation
Keap1	Kelch-like ECH-associated protein 1
KO	Knockdown
LAR	Luminal androgen receptor
LD	Lipid droplet
LIP	Labile iron pool
LOX	Lipid oxidase
LPCAT3	Lysophosphatidylcholine acyltransferase 3
NCOA4	Nuclear receptor coactivator 4
NRF2	Nuclear factor erythroid 2-related factor 2
OMM	Outer mitochondrial membrane
PI3K	Phosphatidylinositol 3-kinase
PL	Phospholipids
PR	Progesterone receptor
PUFAs	Polyunsaturated fatty acids
RF-A	Robustaflavone A
ROS	Reactive Oxygen Species
STEAP	Six-transmembrane epithelial antigen of prostate 3
TCA Cycle	Tricarboxylic Acid Cycle
TF	Transferrin
TFRC	Transferrin receptor
TFR1	Transferrin receptor1
TNBC	Triple-negative breast cancer
TXNRD1	Thioredoxin reductase 1 protein.

frontiers | Frontiers in Oncology

TYPE Original Research
PUBLISHED 17 March 2023
DOI 10.3389/fonc.2023.1125021

OPEN ACCESS

EDITED BY
Chunyan Dong,
Tongji University, China

REVIEWED BY
Federica Guffanti,
Mario Negri Institute for Pharmacological Research (IRCCS), Italy
Guang Peng,
University of Texas MD Anderson Cancer Center, United States
Yinlong Yang,
Fudan University, China
Pete Simpson,
The University of Queensland, Australia

*CORRESPONDENCE
Charles Theillet
charles.theillet@inserm.fr

†These authors have contributed equally to this work

SPECIALTY SECTION
This article was submitted to Breast Cancer, a section of the journal Frontiers in Oncology

RECEIVED 15 December 2022
ACCEPTED 03 March 2023
PUBLISHED 17 March 2023

CITATION
Velazquez C, Orhan E, Tabet I, Fenou L, Orsetti B, Adélaïde J, Guille A, Thézénas S, Crapez E, Colombo P-E, Chaffanet M, Birnbaum D, Sardet C, Jacot W and Theillet C (2023) *BRCA1*-methylated triple negative breast cancers previously exposed to neoadjuvant chemotherapy form RAD51 foci and respond poorly to olaparib. *Front. Oncol.* 13:1125021. doi: 10.3389/fonc.2023.1125021

BRCA1-methylated triple negative breast cancers previously exposed to neoadjuvant chemotherapy form RAD51 foci and respond poorly to olaparib

Carolina Velazquez[1†], Esin Orhan[1†], Imene Tabet[1], Lise Fenou[1], Béatrice Orsetti[1], José Adélaïde[2], Arnaud Guille[2], Simon Thézénas[3], Evelyne Crapez[4], Pierre-Emmanuel Colombo[1,5], Max Chaffanet[2], Daniel Birnbaum[2], Claude Sardet[1], William Jacot[1,6] and Charles Theillet[1*]

[1]Institut de Recherche en Cancérologie de Montpellier, IRCM U1194, Montpellier University, INSERM, ICM, CNRS, Montpellier, France, [2]Centre de Recherche en Cancérologie de Marseille, CRCM UMR1068, Aix-Marseille University, IPC, CNRS, Marseille, France, [3]Biometry Unit, Institut du Cancer de Montpellier, Montpellier, France, [4]Unité de Recherche Translationnelle, Institut du Cancer de Montpellier, Montpellier, France, [5]Oncological Surgery, Institut du Cancer de Montpellier, Montpellier, France, [6]Clinical Oncology, Institut du Cancer de Montpellier, Montpellier, France

Background: About 15% of Triple-Negative-Breast-Cancer (TNBC) present silencing of the *BRCA1* promoter methylation and are assumed to be Homologous Recombination Deficient (HRD). *BRCA1*-methylated (*BRCA1*-Me) TNBC could, thus, be eligible to treatment based on PARP-inhibitors or Platinum salts. However, their actual HRD status is discussed, as these tumors are suspected to develop resistance after chemotherapy exposure.

Methods: We interrogated the sensitivity to olaparib *vs*. carboplatin of 8 TNBC Patient-Derived Xenografts (PDX) models. Four PDX corresponded to *BRCA1-Me*, of which 3 were previously exposed to NeoAdjuvant-Chemotherapy (NACT). The remaining PDX models corresponded to two *BRCA1*-mutated (*BRCA1-Mut*) and two BRCA1-wild type PDX that were respectively included as positive and negative controls. The HRD status of our PDX models was assessed using both genomic signatures and the functional BRCA1 and RAD51 nuclear foci formation assay. To assess HR restoration associated with olaparib resistance, we studied pairs of *BRCA1* deficient cell lines and their resistant subclones.

Results: The 3 *BRCA1-Me* PDX that had been exposed to NACT responded poorly to olaparib, likewise *BRCA1-WT* PDX. Contrastingly, 3 treatment-naïve BRCA1-deficient PDX (1 *BRCA1*-Me and 2 *BRCA1*-mutated) responded to olaparib. Noticeably, the three olaparib-responsive PDX scored negative for BRCA1- and RAD51-foci, whereas all non-responsive PDX models, including the 3 NACT-exposed *BRCA1-Me* PDX, scored positive for RAD51-foci. This

suggested HRD in olaparib responsive PDX, while non-responsive models were HR proficient. These results were consistent with observations in cell lines showing a significant increase of RAD51-foci in olaparib-resistant subclones compared with sensitive parental cells, suggesting HR restoration in these models.

Conclusion: Our results thus support the notion that the actual HRD status of *BRCA1-Me* TNBC, especially if previously exposed to chemotherapy, may be questioned and should be verified using the BRCA1- and RAD51-foci assay.

KEYWORDS

TNBC, BRCA1 methylation, RAD51, nuclear foci, HRD (homologous recombination deficiency)

Background

Triple-negative breast cancers (TNBCs) represent 15% of all breast cancers and its most aggressive subtype (1, 2). Despite good initial chemosensitivity, these tumors show early relapse (1, 3) and, until recently, in the absence of validated drugs only a minority of TNBC were eligible for targeted therapies, thus, stressing the need to develop novel approaches (4).

Another interesting characteristic of TNBC is that this subtype comprises the largest fraction of BRCA deficient breast tumors (5, 6). BRCA deficiency was originally shown to result from coding mutations affecting the *BRCA1* or *BRCA2* genes, which are the principal determinants of genetic predisposition to breast and ovarian cancers and play central role in Homologous Recombination (HR) Repair, also called BRCA pathway (7). HR is an essential and accurate DNA repair pathway (7, 8) and, noticeably, tumors with an HR deficiency (HRD) show elevated genetic instability (9) and accrued sensitivity to DNA cross linking agents such as platinum salts (10, 11). Accordingly, it has been proposed to include platinum in the standard of care of TNBC (12). Furthermore, over the past decade, it has been demonstrated that breast tumors with germline *BRCA1* or *BRCA2* mutations are exquisitely sensitive to PARP inhibitors, as part of a synthetic lethal interaction (13–16).

While germline *BRCA1 or BRCA2* mutations have, until recently, been the only validated indications for PARPi-based therapy in breast and ovarian cancer, it has become clear that they were not the sole causes of an HRD phenotype. Indeed, HRD has also been associated with somatic mutations and/or epigenetic silencing affecting the *BRCA1* and *BRCA2* genes, as well as other genes in the pathway, such as *PALB2*, *RAD51B*, *RAD51C* or *RAD51D* (5, 6). Because of their obvious clinical implications, the questions of the actual number of TNBC presenting HRD and the best approach to detect them have drawn increasing attention. Whole Genome Sequencing of large cohorts of breast and ovarian cancers have revealed that BRCA-deficient tumors presented specific patterns of genomic rearrangements, corresponding to scars left behind in the tumor genome by faulty repair (17). Different genomic signatures (HRDetect, HRD-score, Tandem Duplicator Phenotype, copy number signatures) were established and used to stratify TNBCs and ovarian cancers (17–20). Some of these signatures showed strong association with *BRCA1/2* mutations (germline or somatic), as well as epigenetic silencing of *BRCA1* (17–19, 21). Consequently, the fraction of TNBC with an HRD phenotype, which initially was estimated to range 2.7-17.5% (22, 23), when only germline *BRCA1/2* mutations were taken into account, raised up to 35% on the basis of genomic signatures (17–19, 21). Interestingly, tumors with an HRD genomic profiles were associated with better response to therapy and a more favorable disease outcome (24–27).

Hence, the extension of current PARPi-based therapy indications in TNBC beyond patients bearing germline *BRCA1/2* mutations has become a major question. In particular, the actual sensitivity of tumors with epigenetically silenced *BRCA1* gene due to the hypermethylation of its promoter is of particular interest, as they represent an appreciable 15 to 20% of TNBC (19, 21, 28), but has led to conflicting conclusions (27, 29–32). In particular, the actual BRCA-deficiency of post-treatment residual BRCA1-hypermethylated tumors and their subsequent recurrences has been questioned (31). This point concurs with observations made in different model systems showing that BRCA-deficient tumors rapidly acquire treatment resistance and, in most cases, resistance is due to the partial or complete restoration of HRR upon exposure to either platinum or PARPi (33, 34). Thus, the actual sensitivity of TNBC showing all signs of HRD and, particularly, those with *BRCA1* hypermethylation that have been previously exposed to chemotherapy in the course of the disease could be questioned (31, 35).

To this aim, we tested in the present study the sensitivity of 8 PDX models, comprising 7 TNBC (2 *BRCA1-WT*, 4 *BRCA1*-methylated (*BRCA1-Me*), 1 *BRCA1-Mut*) and 1 *BRCA1-Mut* High Grade Ovarian Serous Ovarian Carcinoma (HGSOC), to the PARP inhibitor olaparib and to carboplatin (CBP). Of the 8 PDX models tested, 3 showed stable disease (SD), while the 5 others progressed under olaparib. PDX models that responded to olaparib were all treatment naïve and corresponded to 2 *BRCA1*-mutated and one

BRCA1-methylated PDX. The five non-responsive PDX comprised 2 *BRCA1* wild type and 3 *BRCA1*-methylated that, noticeably, were established from TNBC tumors that responded poorly to neo-adjuvant chemotherapy (NACT). We, thus, interrogated the HRD status of the tested PDX models and used BRCA1, RAD51, γH2AX and 53BP1 nuclear foci in olaparib treated PDX as read-outs of HR functionality and of DNA damage response. PDX models with reduced BRCA1 and RAD51 foci formation corresponded to olaparib responders, whereas non-responders were all RAD51-foci positive. Remarkably, the three *BRCA1-Me* PDX established from tumors that responded poorly to NACT were RAD51-foci-positive and progressed under olaparib. This suggested that, despite severely reduced BRCA1 protein expression, HR remained at least partially functional in these models, thus precluding their sensitivity to olaparib. We treated *BRCA1* deficient cell lines with olaparib and derived resistant variants. We observed increased BRCA1 and RAD51 foci formation in olaparib resistant variants. The data presented herein suggest that tumors with epigenetically silenced *BRCA1* that have been exposed to genotoxic treatment show poor response to olaparib and exhibit BRCA1 and RAD51 foci formation capacity compatible with HR proficiency. Our data, thus, suggest that olaparib may not be a good indication in tumors with epigenetically silenced *BRCA1* and supports the implementation of BRCA1 and RAD51 nuclear foci assay as functional read out of HR deficiency in TNBC.

Materials and methods

TNBC and HGSOC PDX models and in vivo treatment

TNBC and Ovarian cancer PDX models establishment was as described (36, 37). PDX models used are described in Table 1. The study was reviewed and approved by the ethics committees for animal experimentations of the University of Montpellier (CEEA-LR-12028). PDX models were established from fresh tumor fragments obtained from the Pathology Department at the Comprehensive Cancer Center of Montpellier (ICM) after informed consent of the patients. Establishment of PDX models was reviewed and approved by the institutional review board. Approximately 50 mm^3 PDX fragments were grafted subcutaneously into the flank of 3-4week old Swiss-nude female mice (Charles Rivers, Saint-Germain-sur-l'Arbresle, France). The present study comprised three experimental arms; vehicle, olaparib and Carboplatin (CBP) treatment comprising 6 to 8 mice per arm. When median tumor volume reached 100-150mm^3, mice were randomly distributed in the two arms and treatment was started. Olaparib (Lynparza, AstraZeneca) was administered orally 5 times/week for 5 weeks at 100 mg/kg. CBP (Accord Healthcare, Middlesex, UK) was administered by intra-peritoneal (IP) injection twice per week for 4 weeks at 50 mg/kg CBP. At treatment end, mice were euthanized to collect tumor samples for further biochemical (RNA and proteins) or histological analyses. Some mice were kept for tumor volume monitoring.

MS-PCR

CpG methylation patterns at the *BRCA1* promoter were determined using the MS-PCR assay as previously described (28).

Array-CGH

For each PDX sample, the genomic profile was established by using aCGH onto high-resolution 4 × 180 K CGH-microarrays (SurePrint G3-Human CGH-Microarray, Agilent Technologies). Human female DNA was used as reference (G152A, Promega, Madison, WI, USA). Both experimental and analytic methods have been previously described (38). All probes for aCGH were mapped according to the Genome Reference Consortium Human Build 37 (CGCh37/Hg19; https://www.ncbi.nlm.nih.gov/assembly/GCF_000001405.13/). We used two different threshold values (log2 ratio > 0.5 and 1.0) to distinguish low- (gain/) from high-(amplification) and (log2 ratio < -0.3 and -1) to distinguish simple loss from deletion CAN (Copy Number Alterations), respectively. Percentage of altered genome was the number of

TABLE 1 Principal bio-clinical characteristics of the patient tumors from which the PDX models were derived.

PDX ID	BRCA1 Status	Cancer type	Grade or Stage	NACT	Type of NACT	response to NACT	RFS months	OS months
b1995	WT	TNBC	SBR III	No	NA	NA	>120	>120
b3804	WT	TNBC	SBR III	yes	Taxol+ avastin	Poor response	>120	>120
b3977	Me/Me	TNBC	SBR III	yes	FEC+T	refractory	5	9
b4122	Me/Me	TNBC	SBR III	No	NA	NA	>120	>120
15b0018	Me/Me	TNBC	SBR II	yes	FEC+T	Poor response	35	>60
15b1516	U/Me	TNBC	SBR III	yes	FEC+T	refractory	7	8
Tm168	Mut pS1524fs	TNBC	SBR III	No	NA	NA	3	7
o10047	Mut Del exon 8-13	HGSOC	Stage IV	No	NA	NA	>145	>145

WT, wild type; Me/Me both alleles methylated. U/Me hemi methylation. TNBC, triple negative breast cancer; HGSOC, High grade serous ovarian carcinoma.
NC, not communicated; NA, not applicable; NACT, neoadjuvant chemotherapy; FEC, Fluorouracy. Epirubicin. Cyclophosphamide; RFS, recurrence free survival; OS, Overall Survival.

probes above the threshold divided by the total number of probes for autosomal chromosomes.

Genetic instability and HRD scores

For each tumor, to evaluate genetic instability, we quantified the activity of the 17 copy number signatures described (20) with the R package CINSignatureQuantification.

For each tumor, a HRD score (HRDaCGH score), based on losses of heterozygosity (LOH), was calculated as previously described (39). A score ≥ 10 was considered as HRD-high. The percentage of genome altered was calculated as the sum of altered probes divided by the total number of probes after removing sexual chromosomes.

Next generation sequencing

Mutation profiles were established by using targeted-NGS panel of 559 genes commonly mutated in breast cancer (40). The list of genes targeted is available in the Supplementary Information. The sequence data were aligned to the human reference genome (UCSC hg19) using Burrows–Wheeler Aligner (41). Tumor samples were sequenced at an average depth of 851× (range, 520 to 1055) for the targeted regions. Bam files were processed as described (40). Single nucleotide variants (SNVs) calling was performed with a consensus approach using 8 variants callers for the SNV (Freebayes) (42), HaplotypeCaller (43), LoFreq (44), Mutect2 (45), Pisces (46), Platypus (47), VarDict (48) and Varscan2 (49) and 10 variants callers for the indel (FreeBayes (42), HaplotypeCaller (43), LoFreq (44), Mutect2 (45), pindel (50), Pisces (46), Platypus (47), Scalpel (51), VarDict (48) and Varscan2 (49)). Variants called by less than 5 variants callers were filtered out. Then, the filtered variants were annotated with the Annotate Variation Software (ANNOVAR, version 2013-11-12). Known variants found in dbsnp129 and dbsnp137 with a variant allele frequency (VAF) superior to 1% (1000 G or ESP6500) were removed. Finally, low frequency SNVs and indels that were suspected to be false positives were systematically inspected with IGV version 2.3.32 (52, 53). Mutations were classified as "neutral" or "damaging" using the majority rule of predictor software (provided by dbnsfp: Sift, Polyphen2, LRT, MutationTaster, MutationAssesor, FATHMM, RadialSVM, LR) as previously described (54). A "recurrent" mutation, also called "hot spot", was defined as being found more than 10 times in the Catalogue of Somatic Mutations in Cancer (COSMIC V68) database (http://cancer.sanger.ac.uk/cosmic).

RT qPCR

Total RNA was isolated from cell lines lysed in TRIzol (Invitrogen, Fisher Scientific, Illkirch-Graffenstaden, France), while PDX tumors were lysed using Lysing Matrix D (MP Biomedicals™, Doornveld, France). Subsequently, the RNA was extracted using the RNeasy Kit (Qiagen, Les Ulis, France) following manufacturer instructions. cDNAs were synthesized from 1µg of total RNAs using random hexamers and SuperScript III Reverse transcription (Invitrogen, Fisher Scientific, Illkirch-Graffenstaden, France). Real-time qPCR was performed on a LightCycler 480 SW 1.5 apparatus (Roche, Meylan, France) with ONEGreen® FAST QPCR PREMIX (Ozyme, Saint Cyr l'Ecole, France) and designed human specific primers (Supplementary Table 1). Results were quantified with a standard curve generated by serial dilutions of a reference cDNA preparation. GAPDH transcripts were used for normalization. The fold change in gene expression was calculated as: Fold change = $2^{-\Delta\Delta CT}$.

Cell lines and CRISPR-Cas9 engineered mutants

SUM159 and SUM149 TNBC cell lines a generous gift from Dr S Ethier (MUSC, Charleston, SC), were maintained in Ham's F-12 medium (Gibco™, Fisher Scientific, Illkirch-Graffenstaden, France) supplemented with 5% FBS, 10 µg/ml insulin, 1µg/ml hydrocortisone and 1% Antibiotic-antimycotic (100X) (Gibco™, Fisher Scientific, Illkirch-Graffenstaden, France). UWB1.289PT cell line was obtained from the American Type Culture Collection (ATCC) and maintained in the 50% RPMI-1640 (Gibco™), 50% MEGM (MEGM Bullet Kit; CC-3150, Lonza, Basel, Switzerland) and supplemented with 3% FBS, 1% Antibiotic-antimycotic (100X) (Gibco™, Fisher Scientific, Illkirch-Graffenstaden, France). HCC38 cell line was obtained from ATCC and maintained in RPMI-1640 supplemented with 10% FBS and 1% Antibiotic-antimycotic.

For CRISPR-Cas9 generation of KO clones, SUM159PT cells were first transduced with a plasmid vector containing doxycycline inducible lentiviral expression of SpCas9. Lentiviral transduction was performed on 70% confluent cell cultures. Viral particles were added in the fresh medium containing 8µg/ml polybrene. After 16h the medium was changed and 2µg/ml puromycin added for cell selection for at least 5 days. Next, the cells were transduced as described above with two lentiviral plasmid vectors for the expression of sgBRCA1 (kind gift from Yea-Lih Lin, IGH, Montpellier). After lentiviral transduction, cells were selected with 400µg/ml G418 for 10 days and Cas9 expression was induced by treating a population of cells with 1µg/ml of doxycycline for 6 days. The cells were then cloned and clones verified for the KO by Sanger sequencing and western blot. All cell lines and selected clones were genetically typed by Eurofins Genomics cell line authentification (Eurofins Genomics, Les Ulis).

Protein extraction and Western blotting

Protein extracts were prepared by lysing either tumor tissue or cell line pellets on ice for 30 min in Tris-HCl pH7.4 50mM, NaCl 100mM, NaF 50mM, β-glycerophosphate 40mM, EDTA 5mM, Triton X100 1%, Aprotinin 10mg/ml, PMSF 100mM, Leupeptin 1mM, Pepstatin 1mM, followed by a short centrifugation to pellet debris. Protein concentrations were measured using the BCA kit (Fisher Scientific, Illkirch-Graffenstaden, France) SDS-PAGE gel

electrophoresis was done on 30µg protein samples subsequently transferred onto nitrocellulose membranes (Amersham, Velizy-Villacoublay, France) and incubated overnight at 4°C with the primary antibody. Antibodies used are listed in a separate section. Membranes were then washed and incubated with the appropriate secondary antibody in 5% non-fat dry milk in PBST for 2h at room temperature and revealed by incubation with Chemiluminescent HRP Substrate (Sigma Aldrich, Saint Quentin Fallavier, France).

Immunofluorescence

For cell lines, cells were grown on 12mm diameter slides cover slips in 24 well-plate for 24h, then drugs were added at the predetermined IC50 concentration. After 24h drugs were washed off and cells prepared as described below. For tumor tissues, 6µm cryosections were prepared from OCT embedded deep frozen tissue and mounted on Fisherbrand™ Superfrost™ Plus Microscope Slides (Fisher Scientific, Illkirch-Graffenstaden, France) and stored at -80°C until used. Cells and tumor sections were sequentially subjected to mild extraction (0.4% Triton in PBS, 5min in cold), fixation (4% PFA diluted in PBS) and blockage/permeabilization (3% BSA + 0.2% Triton in PBS, 1 hour at room temperature), incubated overnight at 4°C with the primary antibody (diluted in 3% BSA + 0.2% Triton in PBS), then with the secondary antibody (diluted in 3% BSA + 0.2% Triton in PBS, 1h at room temperature). Between each step, slides were washed 3 times with PBS. Tumor cryosections were immersed 0.1% SBB (Sigma Aldrich, Saint Quentin Fallavier, France) and 70% ethanol for 20 minutes at room temperature to reduce tissue autofluorescence and subsequently washed three times for 5 minutes PBS with 0.02% Tween 20. Stained sections or cell were counterstained with DAPI (Fisher Scientific, Illkirch-Graffenstaden, France) to stain the nuclei and cover slips were mounted with MWL4-88 (Citifluor, CliniSciences, Nanterre, France) and stored at 4°C. Antibodies used are described in the Antibody section.

Immunofluorescence images were acquired using Zeiss microscope with a 63X-immersion oil lens and generated using Zeiss Blue software. RAD51, BRCA1, 53BP1 and γH2AX nuclear foci were scored using the CellProfiler image analysis software (version 2.2.0, Broad Institute). At least three biological replicates of each model (both vehicle- and olaparib-treated) were analyzed. Cells presenting >5 foci/nucleus for RAD51, BRCA1, 53BP1 or γH2AX were considered positive and tumors presenting >10% of positive cells were scored positive for the given marker.

Antibodies

Immunofluorescence; rabbit anti-RAD51 PC130 1:300 (Merck Millipore Sigma Aldrich, Saint Quentin Fallavier, France), rabbit anti-geminin 52508 1:200 (CST OZYME, Saint Cyr l'Ecole, France), mouse anti-BRCA1 sc-6954 1:100 (SCBT, Heidelberg, Germany), mouse anti-γ-H2AX (H2-3F4, kind gift from Dr. Mustapha Oulad-Abdelghani, MAB-IGBMC Illkirch-Graffenstaden, 1:4000), rabbit anti-53BP1 NB100-304 1:500 (Bio-techne LTD, Abington, UK). Secondary antibodies; goat anti-mouse Alexa Fluor 488 (Abcam ab150113, 1:1000), goat anti-rabbit Alexa Fluor 555 ab150078 1:1000 (Abcam, Cambridge, UK).

Western blotting; BRCA1 9010 1:500 (CST OZYME, Saint Cyr l'Ecole, France), BRCA2 A303-434A 1:1000 (Bethyl OZYME, Saint Cyr l'Ecole, France), PARP1 WH0000142M1 1:1000 (Sigma Aldrich, Saint Quentin Fallavier, France), RAD51 8875, 1:1000 (CST OZYME, Saint Cyr l'Ecole, France) and alfa tubulin T9026 1:20000 (Sigma Aldrich, Saint Quentin Fallavier, France); secondary antibodies goat anti-mouse-HRP 70745 1:10000 (CST OZYME, Saint Cyr l'Ecole, France) and goat anti-rabbit-HRP 7076 1:10000 (CST OZYME, Saint Cyr l'Ecole, France).

Results

PDX models show variable response to olaparib

To test the relative sensitivity of TNBC with silenced *BRCA1* due to promoter hypermethylation (designated hereafter *BRCA1-Me*) to the PARP inhibitor olaparib and assess the impact of neoadjuvant treatment (NACT) on olaparib sensitivity, we selected 8 PDX models (7 TNBC and 1 High Grade Serous Ovarian Carcinoma) showing different *BRCA1* profiles. Our experimental PDX set comprised 2 *BRCA1* wild type (*BRCA1*-WT) TNBC (b1995, b3804), 4 *BRCA1-Me* TNBC (b3977, b4122, 15b1516, 15b0018) and 2 (1 TNBC and 1 HGSOC) *BRCA1* mutated (*BRCA1*-Mut) models (tm168, o10047) (Table 1; Supplementary Figure 1). *BRCA1*-Me PDX models 15b1516, 15b0018 and b3977 were established from post-NACT residual tumors that had shown poor response to neoadjuvant treatment (Table 1; Supplementary Figure 1). The two *BRCA1-Mut* models (tm168, o10047) and the remaining BRCA1-Me model (b4122) were established from treatment naïve tumors. Hypermethylation of the *BRCA1* promoter region was determined in both the PDX models and the patient tumors using methylation specific PCR (MS-PCR). It is of note that no pre-treatment biopsy was available for the tumors that had undergone NACT, hence, *BRCA1* promoter methylation was determined after NACT on these tumor samples. Of the four *BRCA1-Me* PDX, 3 presented homozygous (Me/Me) methylation (15b0018, b3977, b4122) and 1 hemizygous (Me/U) methylation (15b1516) (Supplementary Figure 2).

PDX were grafted subcutaneously on Swiss-nude mice and olaparib was administered orally at 100 mg/kg, 5days per week for 5 weeks. In a parallel treatment group, mice received 50mg/kg Carboplatin (CBP) by intraperitoneal injection twice a week for 4 weeks, while the control group received daily the olaparib vehicle administered orally. Tumor volumes were measured twice a week. Three (tm168, b4122, o10047) of the 8 PDX showed disease stabilization or limited tumor size reduction under olaparib treatment, while the 5 other models (b3804, 15b0018, 15b1516, b1995, b3977) progressed (Figures 1A, B; Supplementary Figure 3A). Of the 3 olaparib responders, PDX tm168 and o10047 were *BRCA1-Mut* and b4122 was *BRCA1-Me*, but established from a treatment naïve tumor. The 3 other *BRCA1-Me* models (15b0018,

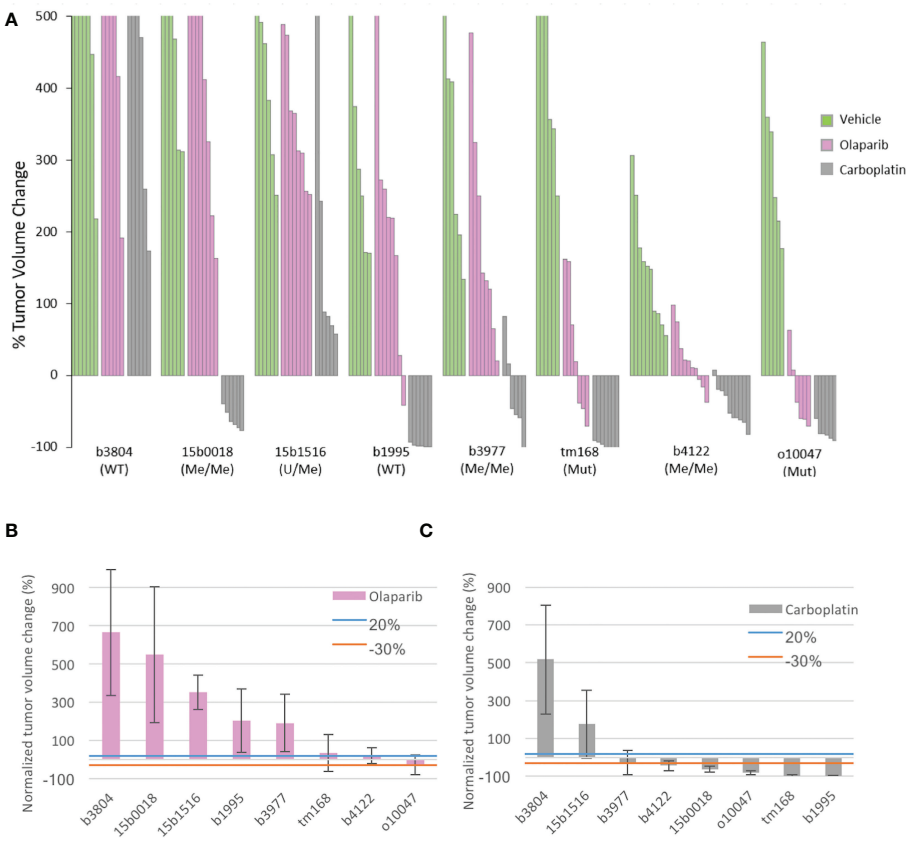

FIGURE 1
Tumor volume change of the 8 PDX models under olaparib and Carboplatin treatment and principal characteristics related to HR of the PDX models **(A)** Waterfall plot of tumor volume changes in the 3 experimental arms were computed at the end of treatment for individual tumors as the percentage of the starting volume (green vehicle; pink olaparib, grey Carboplatin) **(B)** mean tumor volume change in each PDX model treated with olaparib. **(C)** mean tumor volume change in each PDX model treated with Carboplatin. Blue an orange lines indicate the +20% and −30% thresholds for tumor response defined by the RECIST criteria; > 20% progressive (PD). < 20%- > -30% stable disease (SD). < 30% responsive (R).

15b1516 and b3977, which progressed under olaparib, were established from tumors that had received NACT. In the CBP arms we globally noted more favorable response patterns, with 6 of 8 PDX models showing partial to complete response and 2 PDX (b3804, 15b1516) progressing under treatment (Figures 1A, C; Supplementary Figure 3A). Tumor growth was monitored after treatment end in 3 PDX, 2 *BRCA1-Me* TNBC (b3977, b4122) and 1 *BRCA1-Mut* HGSOC (o10047) (Supplementary Figure 3B) Both *BRCA1-Me* TNBC resumed growth shortly after end of olaparib administration. By contrast, the *BRCA1-Mut* o10047 exhibited complete regression 25 days after treatment ended and recurred after a lull of 3 weeks. In the CBP arm, progression after treatment end was observed in 1 of 3 PDX (b4122), while the two other models did not recur during the follow up period (Supplementary Figure 3B).

Genomic profiles and genetic instability scores of the tested TNBC models

Targeted sequencing was performed on the 7 TNBC PDX to search for mutations affecting principal DNA damage response genes and targetable cancer genes. The HGSOC PDX was analyzed by exome sequencing as part of a previous study (55). Mutations were found in the *TP53*, *PTEN*, *KRAS*, *RIF1* and *STK11* genes (7, 2, 1, 1 and 1 PDX respectively) (Supplementary Table 2). No mutations were detected in further DNA repair genes such as *BRCA2*, *PALB2* or the *RAD51* orthologs *RAD51B*, *C* or *D*. The 8 PDX models were also analyzed for copy number changes by array-CGH. Genetic instability and HRD scores were determined (Figure 2A). All TNBC models, irrespective of *BRCA1* mutation or epigenetic silencing, presented elevated genetic instability scores (CX2, CX5) shown to be linked with BRCA-deficiency (20). We also noted that all tested TNBC models presented elevated HRD scores as defined by Abkevich and coworkers (39). Thus, elevated genetic instability and HRD scores suggested preexisting HR deficiency in the PDX models used in this study, including the two *BRCA1-WT* models.

We took advantage of the CGH analysis to determine copy number changes affecting key repair genes in the TNBC models. Except b3804, most PDX presented hemizygous losses affecting 3 to 4 HR genes of a list including *BRCA1*, *BRCA2, PALB2, RAD51, RAD51B* and *RAD51C* suggesting that the combined copy number reductions on these key HR genes could have contributed to a global HR attenuation and elevated genetic instability in these tumors (Supplementary Figure 4). But we cannot exclude the existence of undetected genetic or epigenetic anomalies affecting genes involved in HR maintenance.

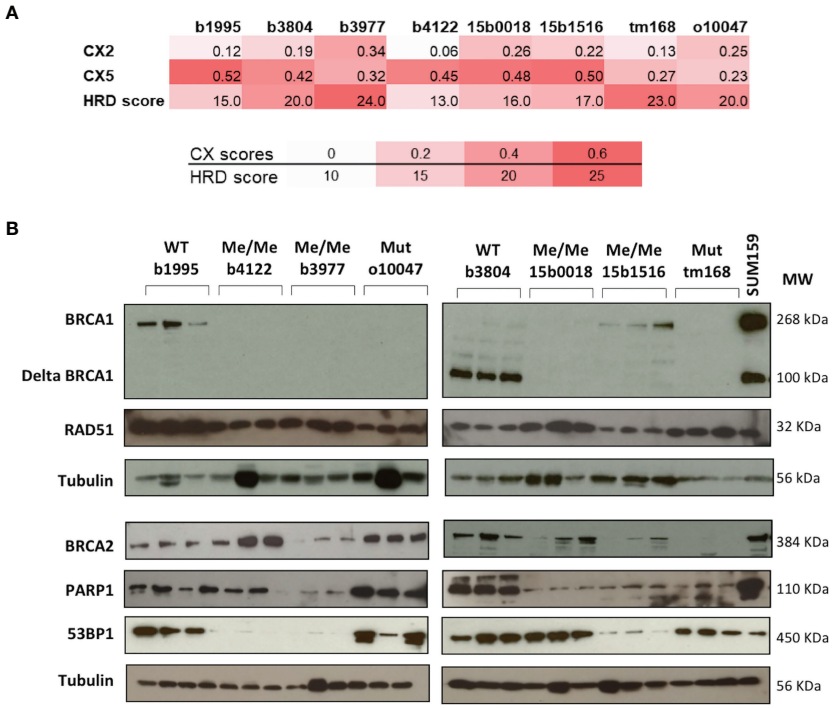

FIGURE 2
Principal characteristics related to HR of the PDX models. **(A)** CX Chromosomal instability and HRD scores of each PDX model. Color shades indicate from white to red the level of instability. **(B)** Protein expression patterns were assessed by Western blotting. The *BRCA1* status of each model is indicated on top of the autoradiograms. WT wild type. Me/Me homozygous methylation. U/Me hemizygous methylation. Mut coding mutation. For each PDX model three independent extracts from individual PDX tumors were loaded and analyzed. Proteins analyzed are indicated on the left and Molecular Weights in KDalton on the right. The protein extract of SUM159 cell line extract was added to the BRCA1 panel to illustrate the full length and the Δ11 BRCA1 protein variants.

Principal genes of the BRCA pathway showed protein expression profiles concordant with olaparib response

To determine the impact of promoter hypermethylation or coding mutations on BRCA1 protein expression, BRCA1 protein levels were measured by western blotting (WB) in the 8 PDX models. Noticeably, *BRCA1-Me* PDX b4122, b3977, 15b0018 and *BRCA1-Mut* o10047, tm168 showed no detectable BRCA1 band, suggesting a loss of BRCA1 functionality in these tumors. By contrast, the *BRCA1-WT* b1995, b3804 and the *BRCA1*-hemimethylated 15b1516 PDX presented detectable BRCA1 bands (Figure 2B). We noted that PDX b3804 expressed high levels of a short 100 kD BRCA1 protein isoform and low levels of the full length (268 kD) protein (Figure 2B). The 100 kD band is compatible with the size of the hypomorphic Δ11-BRCA1 isoform, which corresponds to a *BRCA1* splice-variant where exon 11 is excluded and that is frequently expressed in tumors bearing mutations in exon 11 (56). However, no *BRCA1* coding mutation, that could have explained the expression of the Δ11-BRCA1 isoform, was detected in PDX b3804 (Supplementary Table 1). We also analyzed expression of the BRCA2, RAD51, PARP1 and 53BP1 proteins, which are important actors of HR. Whereas RAD51 expression appeared elevated and relatively constant in the different PDX models, that of BRCA2 was more variable, with no obvious link with BRCA1 status or olaparib response, except possibly the *BRCA1-Mut* PDX tm168, which showed very low BRCA2 protein levels (Figure 2B). PARP1 protein expression was detected in all PDX models, but, interestingly, the lowest levels were detected in the 3 *BRCA1-Me* (b3977, 150018 and 15b1516) that had been exposed to NACT and responded poorly to olaparib (Figure 1A). Finally, 53BP1 protein was expressed at high levels in 5 models and at low levels in 3 other PDX (Figure 2B).

BRCA1, RAD51 and 53BP1 nuclear foci formation in treated tumors correlate with olaparib response

In HR-proficient cells, BRCA1 and RAD51 proteins cluster at DNA damage sites forming nuclear foci that can be detected by immunofluorescence labeling. Absence of BRCA1 and/or RAD51 foci is considered as a sign of HR-deficiency. We scored the fraction of cells positive for BRCA1 and RAD51 foci in cryosections of PDX models sampled at the end of olaparib and vehicle treatment and searched for an association with olaparib response. Tumors presenting >10% cells showing >5 BRCA1 or RAD51 per nucleus were scored positive. PDX sections were immunolabeled with commercial antibodies directed against BRCA1, RAD51, and the S phase marker Geminin. Because of secondary antibodies species compatibility, BRCA1 and RAD51 were co-immunolabeled (Figure 3A; Supplementary Figure 5), whereas Geminin staining

was performed separately to ascertain the presence of S phase cells in each sample. Immunolabeling scoring was performed in 3 independent PDX tumors per model on at least 100 cells per section. Geminin staining showed 10 to 30% of Geminin-positive cells, confirming that tissue section actually comprised S phase tumor cells (Supplementary Figure 6). Four (4) of the 8 olaparib treated PDX, corresponding to 2 *BRCA1-Mut* (tm168, o10047) and 2 *BRCA1-Me* (b3977, b4122), scored negative for BRCA1-foci (Figures 3B, J), in agreement with the absence of BRCA1 band in the WB analysis (Figure 2B). BRCA1-foci positive models comprised two *BRCA1-WT* (b3804, b1995) and two *BRCA1-Me* PDX (b15b1516, 15b0018). Three of the four BRCA1-foci negative PDX (tm168, o10047, b4122) scored negative for RAD51-foci (Figures 3A, C, J, K) and corresponded to the 3 models that responded to olaparib (Figures 1A, B). Noticeably, PDX b3977, which progressed under olaparib (Figures 1A, B), scored positive for RAD51-foci, despite the fact it did not show BRCA1-foci (Figures 3A, C, J, K). All other RAD51-foci-positive PDX scored also positive for BRCA1 foci and showed mediocre response to olaparib (Figures 1A, B; 3A–C, J, K). Noticeably, the 3 *BRCA1-Me* models established from NACT treated TNBC (15b0018, 15b1516, b3977) were RAD51-foci positive and showed scores similar to those observed in the 2 *BRCA1-WT* models (b1995, b3804) (Figures 3B, J). By contrast, the *BRCA1-Me* PDX b4122, which was not exposed to NACT prior PDX establishment, was both BRCA1 and RAD51-foci-negative and did not progress under olaparib. These data suggested that while b4122 was indeed HR deficient, the 3 NACT treated *BRCA1-Me* models were, at least partially, HR proficient.

We verified whether BRCA1 or RAD51 nuclear foci formation was associated with olaparib response (Figures 3F-I). We noted a significantly association of BRCA1 and RAD51 foci absence (or low levels) with olaparib response (t-test $p=0.0017$ and $p<0.0001$ respectively) (Figures 3F, G). Interestingly, the differences in foci positive cells between responsive and non-responsive cells were discernible in both tumor sections from olaparib treated (Figures 3F, G) and sections from vehicle treated tumors and showed equivalent statistical significance (Figures 3J, K).

We also scored γH2AX and 53BP1 foci, which are standard DNA damage markers, and observed that models presented 20 to 60% foci-positive cells for either marker, indicating severe DNA damage in olaparib treated PDX, to the exception of 15b1516 where only 5 to 10% cells scored positive (Figures 3D, E). Interestingly, we noted that 53BP1-foci tended to be more frequent in olaparib responsive PDX, compared with non-responsive PDX (t-test $p=0.028$) (Figure 3H). However, no difference was found with γH2AX-foci (Figure 3I).

Acquired olaparib resistance in BRCA1 deficient cell lines is associated with increased BRCA1 and RAD51 foci formation and reduced levels of DNA damage

It is well documented that BRCA-deficient tumors or cell lines rapidly acquire resistance to treatment associated with the restoration of HRR (56). We were, thus, interested to explore the restoration of RAD51-foci formation in *BRCA1*-deficient cell lines with acquired olaparib resistance. We, thus, isolated olaparib resistant clones from three cell lines; SUM159-KO1 and SUM159-KO2, two CRISPR *BRCA1* knock out clones we engineered from the TNBC SUM159 cell line, the SUM149 TNBC cell line which bears a frameshift mutation in exon 11 (2288delT) (57) and the UWB1.289 ovarian cancer cell line also showing a frameshift mutation in exon 11 (2594delC) (58). Resistance was obtained by exposing cell cultures to incremental olaparib concentrations for at least 12 weeks. Olaparib resistant cell lines were designated with the suffix Re (SUM159-KO1-Re, SUM159-KO2-Re, SUM149-Re and UWB1.289-Re). We characterized BRCA1, BRCA2, RAD51 and PARP1 protein expression by WB, as well as RNA expression changes associated with the acquisition of olaparib resistance (Figures 4A, B). In SUM159-KO1 and SUM159-KO2 no BRCA1 protein was detected. SUM159-KO1-Re reexpressed the full length BRCA1 protein and SUM159-KO2-Re showed no difference in BRCA1 protein expression compared with it clone of origin. SUM149 and UWB1.289 expressed no full length BRCA1 and variable levels of the Δ11-BRCA1 100 kD band. Interestingly, SUM149-Re expressed the BRCA1 full length and increased levels of the Δ11-BRCA1 variant, whereas UWB1.289-Re showed strongly increased Δ11-BRCA1 levels (Figure 4A). No significant difference was found for BRCA2, RAD51 and PARP1 protein expression in the different cell line models. At the RNA expression level, we noted increased gene expression of *RAD51* and *RAD51C* in SUM159-KO1, of *RAD51C* and *ABCG2* in SUM149-Re, as well as of Δ11-*BRCA1, RAD51C, RAD51D, PALB2* and *ATM* in UWB1.289-Re which could be related with their acquisition of olaparib resistance.

Next, we scored BRCA1, RAD51, 53BP1 and γH2AX foci formation in the olaparib treated cell lines (Figure 5A). Except in SUM159-KO2-Re which does not express BRCA1, nor Δ11-BRCA1, and scored BRCA1-foci-negative, BRCA1-foci scores tended to increase in olaparib resistant clones compared with cells or origin (Figure 5B). A similar trend was noticeable for RAD51-foci, whose numbers nearly doubled in olaparib resistant cells relative to cell lines of origin (Figure 5C). By contrast, 53BP1 and γH2AX foci numbers clearly decreased in olaparib resistant variants (Figures 5D, E). These differences in foci numbers between olaparib resistant cells and their original counterparts, increase for BRCA1 and RAD51, decrease for 53BP1 and γH2AX, were all statistically significant and in coherence with findings we made on PDX (Figures 5F-I). The reduction of γH2AX-foci associated with the increase of BRCA1 and RAD51-foci observed in resistant cells suggest a global decrease of DNA damage in these cells upon olaparib treatment due to restored HR capacity. We also derived olaparib resistant cells from the hemimethylated *BRCA1-Me/UM* HCC38 TNBC cell line, whose methylation status we confirmed. While BRCA1-foci scores only modestly increased in olaparib treated cells, the fraction of RAD51-foci positive cells doubled in HCC38-Re variant cells (Supplementary Figure 7). Overall, our cell line data strongly support the notion that resistance to treatment and particularly to olaparib in BRCA1-deficient cancer cells is frequently associated with restoration of RAD51 foci formation, thus, signing for restored HR capacity.

10.3389/fonc.2023.1125021

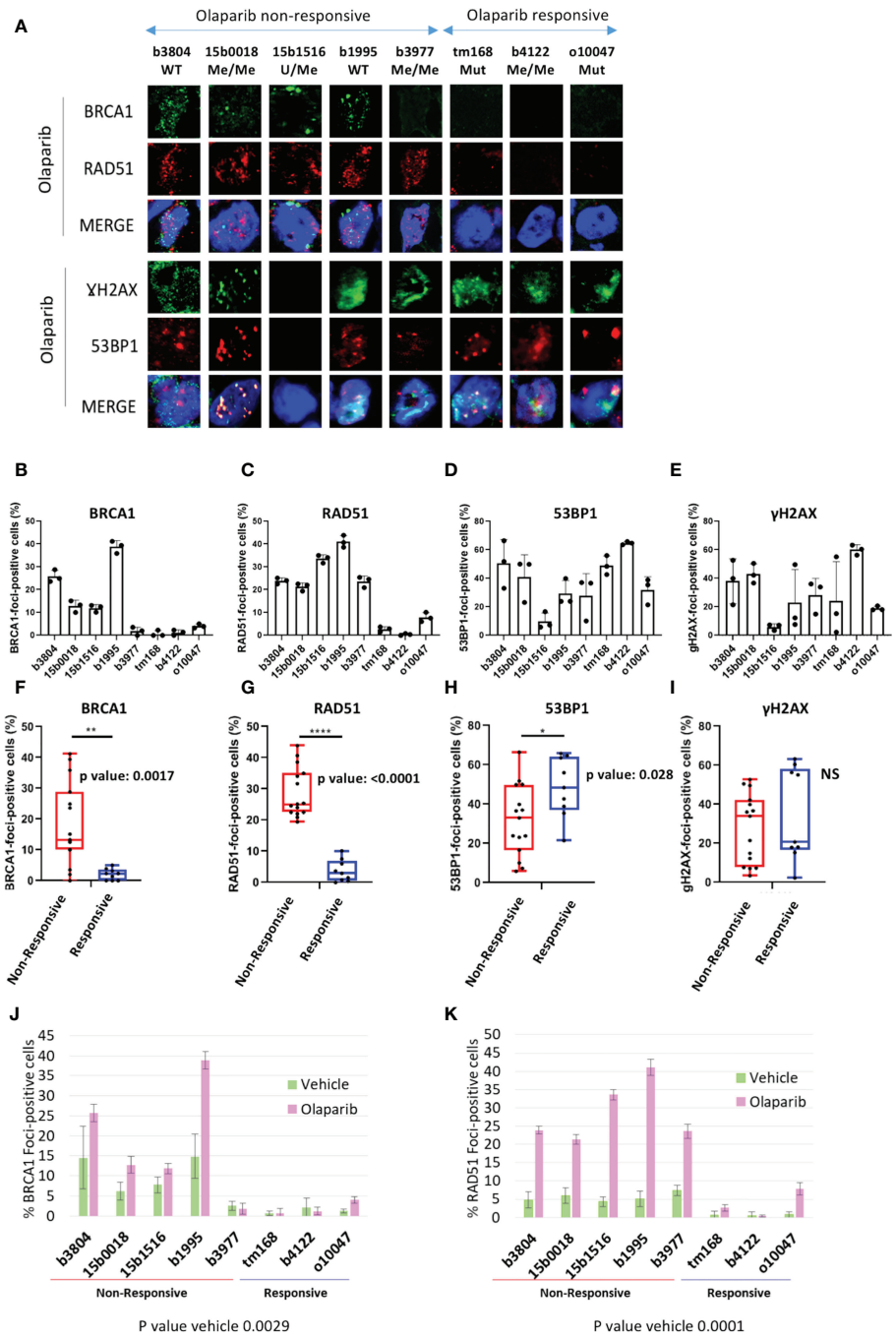

FIGURE 3
BRCA1, RAD51, γH2AX and 53BP1 nuclear foci formation in olaparib treated PDX. **(A)** Representative immunofluorescence images of frozen PDX tissue section harvested from mice sacrificed after the last administration of olaparib or before the tumor reached ethical size for vehicle treated models. PDX tumor sections were ordered from worst to best olaparib response. A complete version including vehicle treated tumors is visible in Supplementary Figure 5. **(B)** Quantification of BRCA1, **(C)** RAD51, **(D)** γH2AX, **(E)**: 53BP1 foci formation in olaparib treated PDX. Results are represented as % of foci positive cells in the analyzed tumor sections in each PDX. Cells presenting at least 5 foci/nucleus were considered positive. At least 100 cells were quantified in each tissue section. **(F–I)**: by two-tailed unpaired t-test analyses of correlation between foci numbers and olaparib response. Nuclear foci analyzed are indicated on top of each graph, as well as p-values. *, **,**** on top of the graph indicate the level of significance of the t-test **(J, K)** Histograms showing the percentage of BRCA1- **(J)** and RAD51-**(K)** foci positive cells of BRCA1 and RAD51 nuclear foci quantification in vehicle and olaparib treated PDX.

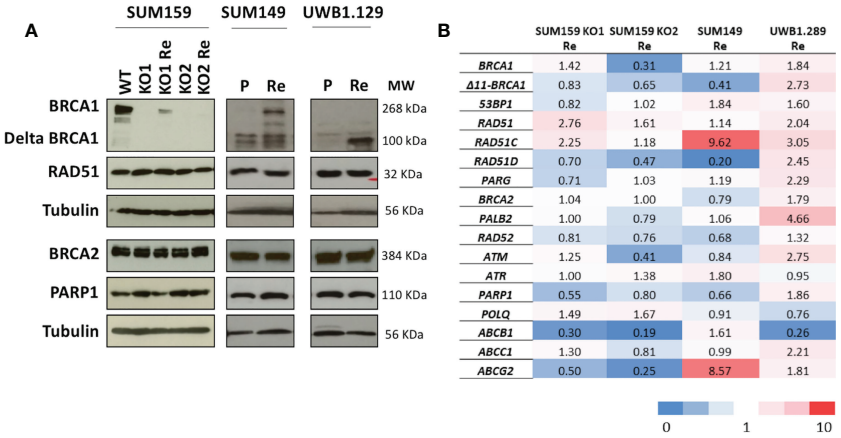

FIGURE 4
Protein and mRNA expression profiles of principal HR genes in the cell line models **(A)** Western blots showing protein expression patterns; analyzed proteins are indicated on the left and molecular weights in KDa on the right. **(B)** mRNA expression changes of genes potentially associated with olaparib resistance in cell line models selected for acquired olaparib resistance. mRNA levels are expressed as fold changes of the expression levels measured between the olaparib-resistant cell line and their parental lines used as reference (horizontal line). Reference cell lines were SUM159-KO1, SUM159-KO2 parental SUM149 and parental UWB1.289.

BRCA1, RAD51, γH2AX and 53BP1 nuclear-foci as predictors of the response to olaparib or carboplatin

As PDX responding to CBP represented twice the number of olaparib responders (6 *vs.* 3 respectively), we wanted to determine whether the response to CBP was associated with reduced RAD51 and/or BRCA1-foci formation (Figures 1B, C). Like in the olaparib arm, individual grafts that responded to CBP were predominantly BRCA1-foci-negative/RAD51-foci-negative (Figures 6A, B) and, interestingly, most grafts of the BRCA-foci-negative/RAD51-foci-positive model b3977, whose response to olaparib was mediocre, showed tumor size reduction under CBP. However, grafts of the BRCA1-positive/RAD51-positive PDX 15b0018 and b1995, respectively *BRCA1-WT* and *BRCA1-Me* and bad responders to olaparib, showed good response to CBP pointing to the fact that CBP efficacy is not solely based on the HR status, but can also rely on alternative DNA repair mechanisms (Figure 6B). Despite these two BRCA1-foci-positive/RAD51-foci-positive models, both BRCA1-foci-negativity and RAD51-foci-negativity were significantly associated (t-test p-value 0.0059 and 0.0176 respectively) with CBP response in our dataset (Figure 6D). Next, we computed the Sensitivity, Specificity and Accuracy of RAD51, BRCA1, 53BP1 and γH2AX foci in predicting the response to olaparib and CBP (Table 2). Concerning olaparib response RAD51 foci showed high sensitivity (88%), specificity (82%) and accuracy (84%), while BRCA1 foci showed excellent sensitivity (94%) but lower specificity (66%) and accuracy (74%). Interestingly, when CBP response was considered, BRCA1 foci performed globally better showing 70% sensitivity, 92% Specificity and 75% accuracy in comparison with RAD51 foci, which showed 57% sensitivity, 100% Specificity but 68% accuracy. The performances of 53BP1 and γH2AX foci were overall rather contrasted showing excellent sensitivity (100%), but poor specificity (18%) and accuracy (41%) for olaparib response, while they reached better values for CBP response with high accuracy (87%) mitigating the mediocre specificity (46%). Overall, these data support the use of RAD51 foci for olaparib response prediction, while BRCA1 foci, possibly in combination with RAD51 foci, appear interesting for CBP response. While γH2AX and 53BP1 foci do not appear as convincing it may be interesting to reevaluate their performance for CBP response on a larger dataset.

Discussion

About one TNBC in three is estimated to be HR deficient. HRD has been linked with genetic or epigenetic impairment of genes belonging to the BRCA-pathway such as *BRCA1*, *BRCA2*, *PALB2* and *RAD51B*, *RAD51C* and *RAD51D*, but *BRCA1* is the most frequently affected gene in TNBC (5, 6). Because HR deficient tumors show increased sensitivity to PARPi or Platinum salts, detection of HRD has important implications in treatment definition (59). Identification of HRD is generally based on targeted sequencing of commonly mutated HR genes, combined with the determination of patterns of genomic rearrangements typical of HRD, such as the genomic HRD score, Tandem Duplication score or CX scores (20, 27, 31). However, BRCA-deficient cancers frequently develop resistance to treatment associated with HR restoration. Involved molecular events range from reverting secondary mutations, gene rearrangements producing gene chimeras, loss or mutations of the *53BP1* gene or of one of its cofactors in the Shieldin complex (34, 35, 59). Hence, the actual status of residual HRD tumors that have previously been exposed to genotoxic treatment could be in question. This point has been specifically raised concerning TNBC with silenced *BRCA1* gene due to hypermethylation of the promoter, whose sensitivity to PARPi has been disputed (31, 34).

These questions motivated the present study, where we interrogated the sensitivity to olaparib and CBP of 4 TNBC PDX models with epigenetically silenced *BRCA1*, 3 of which had received NACT prior PDX establishment. Noticeably, despite obliterated or severely reduced BRCA1 protein expression levels, the 3 *BRCA1*-

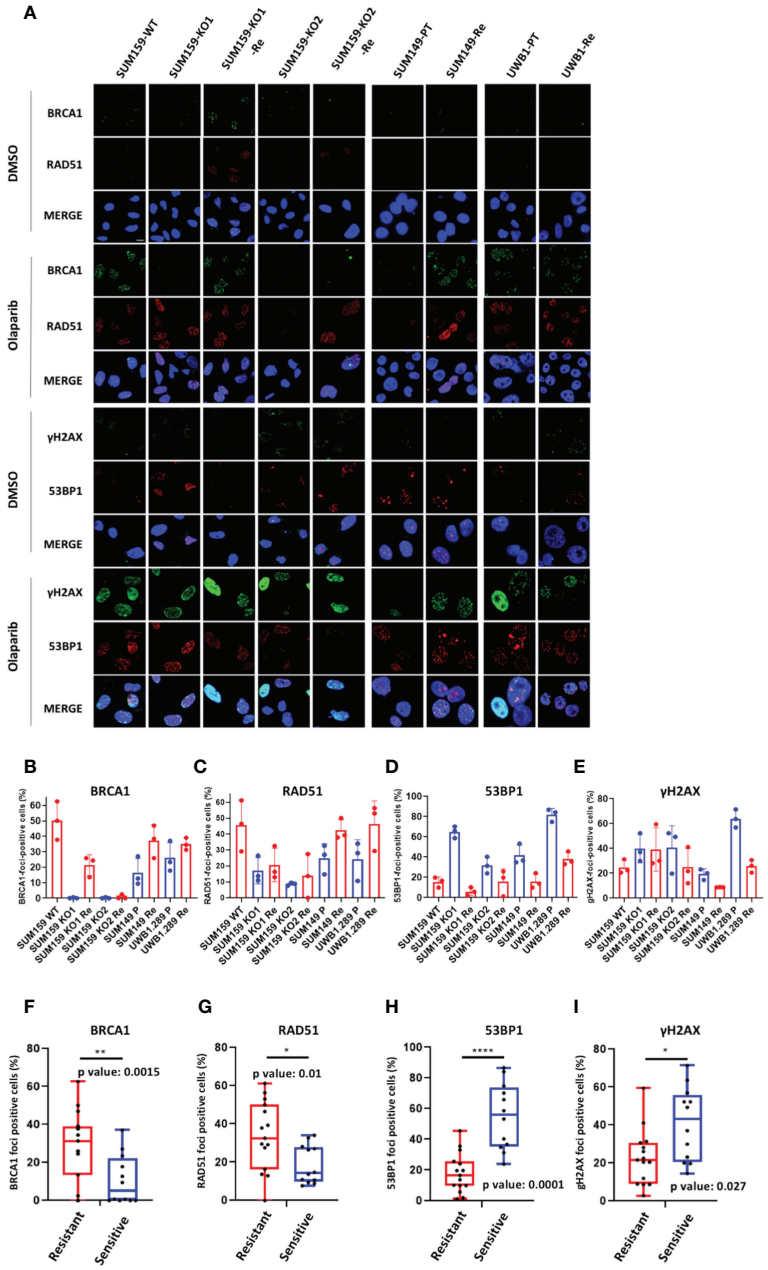

FIGURE 5
BRCA1, RAD51, γH2AX and 53BP1 nuclear foci in BRCA1 deficient cell line models **(A)** Representative immunofluorescence images of cell line models treated or not (control) with Olaparib for 24h. Cell line names are indicated on top *BRCA1*-WT (WT), BRCA1-KO (KO), BRCA1-KO-Ola-Resistant (Re), SUM149; parental (PT), Ola-Resistant (Re), UWB1.289; parental (PT), Ola-Resistant (Re) **(B)** BRCA1, **(C)** RAD51, **(D)** 53BP1, **(E)** γH2AX foci formation in the respective olaparib treated cell lines. Results are represented as % of foci positive cells in the analyzed tumor sections in each PDX. Cells presenting at least 5 foci/nucleus were considered positive. At least 150 cells were quantified in each section. Representative IF images are shown in the Supplementary Figures. **(F–I)**: Box plot presenting the difference in the number of BRCA1- **(F)**, RAD51- **(G)**, 53BP1-**(H)** and gH2AX- **(I)** foci positive cells between olaparib resistant and sensitive cell lines. p-values were calculated with two-tailed unpaired t-test. *, **,**** on top of the graph indicate the level of significance of the t-test

methylated PDX that had undergone NACT responded poorly to olaparib, showing response profiles similar to those of the two *BRCA1-WT* models used as controls. These observations, thus, questioned the actual functionality of HR in the *BRCA1-Me* PDX models included in our study, leading us to test for BRCA1 and RAD51 nuclear foci formation in tissue sections of olaparib treated PDX and use this assay as a functional read out. In HR proficient cells, the BRCA1 and RAD51 proteins cluster onto DNA lesions and these clusters can be detected as nuclear foci by immunofluorescence microscopy (60). Their presence in tumor tissues signs for HR proficiency (61). Remarkably, the three *BRCA1-Me* PDX that responded poorly to olaparib scored positive for BRCA1 and/or RAD51 foci, likewise the two *BRCA1-WT* models. By contrast, the three PDX models responding to olaparib (2 *BRCA1-Mut* and 1 *BRCA1-Me*) scored negative for BRCA1 and RAD51-foci. Noticeably, the BRCA1 and RAD51 foci

10.3389/fonc.2023.1125021

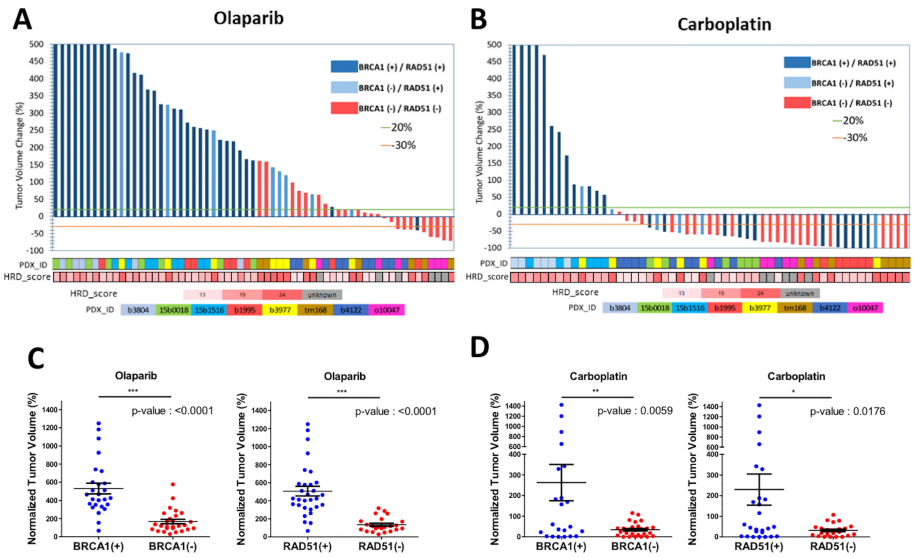

FIGURE 6
BRCA1 and RAD51 scores are good predictors of olaparib and Carboplatin response. Waterfall plots of the tumor volume change in individual PDX models (percentage of the starting volume) treated with either olaparib or Carboplatin. The status according to BRCA1 and/or RAD51 foci formation of each model is indicated by the color of the bar; dark blue BRCA1+/RAD51+; light blue BRCA1-/RAD51+; red BRCA1-/RAD51-. The identity of the PDX model is indicated by color boxes at the bottom of the graph. **(A)** olaparib treated mice. **(B)** Carboplatin treated mice. **(C)** tumor volume change under olaparib treatment stratified according to the BRCA1 foci status. **(D)** tumor volume change under olaparib treatment stratified according the RAD51 foci status. *, **,*** on top of the graph indicate the level of significance of the t-test.

negative *BRCA1-Me* model had never been exposed to chemotherapy. Thus, our data suggest that HR was, at least partially, functional in the *BRCA1-Me* PDXs established from residual TNBC previously exposed to NACT, contributing to their poor response to olaparib. These observations were consistent with the increased RAD51 foci formation and HR restoration we evidenced in *BRCA1*-deficient cell line models that we rendered olaparib-resistant. Results presented herein support the notion that the actual HRD status of *BRCA1-Me* TNBC may be in doubt, especially if they have been previously exposed to genotoxic treatment. Since we did not have access to tumor samples prior NACT, we cannot conclude on HR restoration due to treatment exposure, but our data are in line with previous reports (31, 35). This calls for the verification of the HRD status based on functional read outs such as BRCA1 and/or RAD51 foci formation (62). Indeed, genetic tests or genomic scores yield valuable information on the HRD status of a given tumor, however, they point to its natural history and may be misleading in terms of actual HR functionality. We wish, moreover, to point out that all the PDX models included in our study presented elevated HRD or genetic instability scores, irrespective of their mutational, *BRCA1* methylation status or sensitivity to olaparib.

TABLE 2 Test performance values for the indicated HRD biomarkers to predict olaparib and CBP response.

	Biomarkers	RAD51 Foci (n=61)	BRCA1 Foci (n=61)	γH2AX Foci (n=61)	53BP1 Foci (n=61)
Olaparib response	Sensitivity	88%	94%	100%	100%
	Specificity	82%	66%	18%	18%
	PPV	65%	52%	32%	32%
	NPV	95%	97%	100%	100%
	Accuracy	84%	74%	41%	41%
		(n=53)	(n=53)	(n=53)	(n=53)
CBP response	Sensitivity	57%	70%	100%	100%
	Specificity	100%	92%	46%	46%
	PPV	100%	97%	85%	85%
	NPV	43%	50%	100%	100%
	Accuracy	68%	75%	87%	87%

Response includes disease stabilization.

Genetic and genomic scores are being considered concurrently with RAD51 foci determination as biomarkers predictive of treatment in TNBC and prostate cancer (63–65). Results support the excellent correlation between low RAD51 scores and HR deficiency, as well as with increased sensitivity to olaparib or platinum based regimen (63, 65, 66). However, these works also point out the detection of tumors showing poor response to treatment, whilst presenting inactivating BRCA1 or BRCA2 mutations or elevated HRD scores and scoring positive for RAD51 foci. Our data are in perfect concordance with these observations and further support the relevance of BRCA1 and/or RAD51 foci-based tests to determine the functionality of HR in TNBC presenting all signs or HRD (63, 65, 66). Further, our data highlight the importance of verifying the actual functionality of HRR in tumors with epigenetically silenced *BRCA1*, particularly those previously exposed to chemotherapy during the course of the disease.

A number of studies highlight the exquisite sensitivity of HRD tumors to cis or carboplatin, alone or in combination with other molecules (63, 65, 66). We thus, documented the sensitivity to CBP of our models and determine their overlap with BRCA1 and RAD51 scores. PDX models responding to CBP were twice more frequent than olaparib responders and included all BRCA1-foci negative cases, as well as 2 BRCA1-foci/RAD51-foci positive PDX models, underlining the fact that CBP sensitivity is not solely determined by the HRD status. Indeed, platinum salts produces bulky adducts that must be removed by NER to avoid DNA breaks and tumors with faulty NER have been shown to be highly sensitive to platinum (59, 67, 68). Hence, while BRCA1 foci appeared a better predictor of CBP sensitivity than RAD51 in our dataset, they missed 2 out 6 CBP sensitive cases, thus calling for complementary tests.

Conclusion

Our work shows that TNBC with a silenced *BRCA1* gene, due to hypermethylation of its promoter, may be prone to HR restoration and, thus, become resistant to olaparib. Interestingly, two of the olaparib resistant and RAD51-foci positive PDX models appeared sensitive to CBP. Our data thus support the notion that the HRD status of TNBC should be systematically checked using a combination of biomarkers, among which the BRCA1 and RAD51 foci formation tests play a major role. Not only do these assays inform on HR functionality in a given tumor, they are cheap, rapid and quite easy to implement. We performed the immunofluorescence analysis on olaparib treated tumor samples to ensure a clear signal difference between foci positive and foci negative samples, but noted, in accordance with other works, that the difference was also perceptible in non-treated tumors (63). Hence, this test, which we and others have shown to reliably predict sensitivity to olaparib, and also to CBP, could be implemented on Formalin fixed tumors as part of a pathology routine in a number of cancer treating institutions.

Data availability statement

The raw data supporting the conclusions of this article will be made available by the authors, without undue reservation.

Ethics statement

The animal study was reviewed and approved by CEEA-LR-12028.

Author contributions

Conceptualization: CT. Funding acquisition: WJ and CT. Investigation: CV, EO, IT, LF, JA, and EC. Methodology and resources: BO, MC, and AG. Supervision: CT and WJ. Validation: DB, CS, WJ, and CT. Writing: CT and WJ. All authors contributed to the article and approved the submitted version.

Funding

The authors declare that this study received funding from Astra-zeneca (contract # 2018-02069). The funder was not involved in the study design, collection, analysis, interpretation of data, the writing of this article, or the decision to submit it for publication. This work also benefited from the following financial support: Institut National du Cancer PRTK-2017 MODUREPOIS, Ligue Nationale Contre le Cancer 'Comité régional Occitanie-Est' 2021-R22031FF and the SIRIC Montpellier Cancer Grant INCa-DGOS-Inserm_12553.

Acknowledgments

The authors sincerely acknowledge Dr Genevieve Rodier for fruitful discussions and help throughout this project, Dr Isabelle Jariel for critical reading and constructive comments on the manuscript, and Dr Rui-Bras Gonçalvez and Dr Stanislas du Manoir for help during the establishment of the PDX models. Furthermore, sincere thanks are due to the staffs of the animal facility at IRCM and the Centre de Ressources Biologiques at ICM for their constant support and expert help.

Conflict of interest

The authors declare that the research was conducted in the absence of any commercial or financial relationships that could be construed as a potential conflict of interest.

Publisher's note

Supplementary material

The Supplementary Material for this article can be found online at: https://www.frontiersin.org/articles/10.3389/fonc.2023.1125021/full#supplementary-material

References

1. Dent R, Trudeau M, Pritchard KI, Hanna WM, Kahn HK, Sawka CA, et al. Triple-negative breast cancer: clinical features and patterns of recurrence. *Clin Cancer Res* (2007) 13:4429–34. doi: 10.1158/1078-0432.CCR-06-3045

2. Elias AD. Triple-negative breast cancer: A short review. *Am J Clin Oncol* (2010) 33:637–45. doi: 10.1097/COC.0b013e3181b8afcf

3. Carey LA, Dees EC, Sawyer L, Gatti L, Moore DT, Collichio F, et al. The triple negative paradox: Primary tumor chemosensitivity of breast cancer subtypes. *Clin Cancer Res* (2007) 13:2329–34. doi: 10.1158/1078-0432.CCR-06-1109

4. Zagami P, Carey LA. Triple negative breast cancer: Pitfalls and progress. *NPJ Breast Cancer.* (2022) 8:95. doi: 10.1038/s41523-022-00468-0

5. Stephens PJ, Tarpey PS, Davies H, Van Loo P, Greenman C, Wedge DC, et al. The landscape of cancer genes and mutational processes in breast cancer. *Nature.* (2012) 486:400–4. doi: 10.1038/nature11017

6. Couch FJ, Hart SN, Sharma P, Toland AE, Wang X, Miron P, et al. Inherited mutations in 17 breast cancer susceptibility genes among a Large triple-negative breast cancer cohort unselected for family history of breast cancer. *JCO.* (2015) 33:304–11. doi: 10.1200/JCO.2014.57.1414

7. Lord CJ, Ashworth A. BRCAness revisited. *Nat Rev Cancer.* (2016) 16:110–20. doi: 10.1038/nrc.2015.21

8. Roy R, Chun J, Powell SN. BRCA1 and BRCA2: different roles in a common pathway of genome protection. *Nat Rev Cancer.* (2012) 12:68–78. doi: 10.1038/nrc3181

9. Helleday T, Eshtad S, Nik-Zainal S. Mechanisms underlying mutational signatures in human cancers. *Nat Rev Genet* (2014) 15:585–98. doi: 10.1038/nrg3729

10. Hastak K, Alli E, Ford JM. Synergistic chemosensitivity of triple-negative breast cancer cell lines to Poly(ADP-ribose) polymerase inhibition, gemcitabine, and cisplatin. *Cancer Res* (2010) 70:7970–80. doi: 10.1158/0008-5472.CAN-09-4521

11. Silver DP, Richardson AL, Eklund AC, Wang ZC, Szallasi Z, Li Q, et al. Efficacy of neoadjuvant cisplatin in triple-negative breast cancer. *J Clin Oncol* (2010) 28:1145–53. doi: 10.1200/JCO.2009.22.4725

12. Sikov WM, Berry DA, Perou CM, Singh B, Cirrincione CT, Tolaney SM, et al. Impact of the addition of carboplatin and/or bevacizumab to neoadjuvant once-per-week paclitaxel followed by dose-dense doxorubicin and cyclophosphamide on pathologic complete response rates in stage II to III triple-negative breast cancer: CALGB 40603 (Alliance). *J Clin Oncol* (2015) 33:13–21. doi: 10.1200/JCO.2014.57.0572

13. Fong PC, Boss DS, Yap TA, Tutt A, Wu P, Mergui-Roelvink M, et al. Inhibition of poly(ADP-ribose) polymerase in tumors from BRCA mutation carriers. *N Engl J Med* (2009) 361:123–34. doi: 10.1056/NEJMoa0900212

14. Tutt A, Robson M, Garber JE, Domchek SM, Audeh MW, Weitzel JN, et al. Oral poly(ADP-ribose) polymerase inhibitor olaparib in patients with BRCA1 or BRCA2 mutations and advanced breast cancer: a proof-of-concept trial. *Lancet* (2010) 376:235–44. doi: 10.1016/S0140-6736(10)60892-6

15. Audeh MW, Carmichael J, Penson RT, Friedlander M, Powell B, Bell-McGuinn KM, et al. Oral poly(ADP-ribose) polymerase inhibitor olaparib in patients with BRCA1 or BRCA2 mutations and recurrent ovarian cancer: a proof-of-concept trial. *Lancet* (2010) 376:245–51. doi: 10.1016/S0140-6736(10)60893-8

16. Robson M, Im S-A, Senkus E, Xu B, Domchek SM, Masuda N, et al. Olaparib for metastatic breast cancer in patients with a germline *BRCA* mutation. *N Engl J Med* (2017) 377:523–33. doi: 10.1056/NEJMoa1706450

17. Davies H, Glodzik D, Morganella S, Yates LR, Staaf J, Zou X, et al. HRDetect is a predictor of BRCA1 and BRCA2 deficiency based on mutational signatures. *Nat Med* (2017) 23:517–25. doi: 10.1038/nm.4292

18. Polak P, Kim J, Braunstein LZ, Karlic R, Haradhavala NJ, Tiao G, et al. A mutational signature reveals alterations underlying deficient homologous recombination repair in breast cancer. *Nat Genet* (2017) 49:1476–86. doi: 10.1038/ng.3934

19. Menghi F, Barthel FP, Yadav V, Tang M, Ji B, Tang Z, et al. The tandem duplicator phenotype is a prevalent genome-wide cancer configuration driven by distinct gene mutations. *Cancer Cell* (2018) 34:197–210.e5. doi: 10.1016/j.ccell.2018.06.008

20. Drews RM, Hernando B, Tarabichi M, Haase K, Lesluyes T, Smith PS, et al. A pan-cancer compendium of chromosomal instability. *Nature.* (2022) 606:976–83. doi: 10.1038/s41586-022-04789-9

21. Glodzik D, Bosch A, Hartman J, Aine M, Vallon-Christersson J, Reuterswärd C, et al. Comprehensive molecular comparison of BRCA1 hypermethylated and BRCA1 mutated triple negative breast cancers. *Nat Commun* (2020) 11:3747. doi: 10.1038/s41467-020-18098-0

22. Pujol P, Yauy K, Coffy A, Duforet-Frebourg N, Gabteni S, Daurès J-P, et al. Predominance of BRCA2 mutation and estrogen receptor positivity in unselected breast cancer with BRCA1 or BRCA2 mutation. *Cancers.* (2022) 14:3266. doi: 10.3390/cancers14133266

23. Armstrong N, Ryder S, Forbes C, Ross J, Quek RG. A systematic review of the international prevalence of BRCA mutation in breast cancer. *CLEP* (2019) 11:543–61. doi: 10.2147/CLEP.S206949

24. Telli ML, Timms KM, Reid J, Hennessy B, Mills GB, Jensen KC, et al. Homologous recombination deficiency (HRD) score predicts response to platinum-containing neoadjuvant chemotherapy in patients with triple-negative breast cancer. *Clin Cancer Res* (2016) 22:3764–73. doi: 10.1158/1078-0432.CCR-15-2477

25. Tutt A, Tovey H, Cheang MCU, Kernaghan S, Kilburn L, Gazinska P, et al. Carboplatin in BRCA1/2-mutated and triple-negative breast cancer BRCAness subgroups: the TNT trial. *Nat Med* (2018) 24:628–37. doi: 10.1038/s41591-018-0009-7

26. Staaf J, Glodzik D, Bosch A, Vallon-Christersson J, Reuterswärd C, Häkkinen J, et al. Whole-genome sequencing of triple-negative breast cancers in a population-based clinical study. *Nat Med* (2019) 25:1526–33. doi: 10.1038/s41591-019-0582-4

27. Chopra N, Tovey H, Pearson A, Cutts R, Toms C, Proszek P, et al. Homologous recombination DNA repair deficiency and PARP inhibition activity in primary triple negative breast cancer. *Nat Commun* (2020) 11:2662. doi: 10.1038/s41467-020-16142-7

28. Jacot W, Lopez-Crapez E, Mollevi C, Boissière-Michot F, Simony-Lafontaine J, Ho-Pun-Cheung A, et al. BRCA1 promoter hypermethylation is associated with good prognosis and chemosensitivity in triple-negative breast cancer. *Cancers.* (2020) 12:828. doi: 10.3390/cancers12040828

29. Drew Y, Mulligan EA, Vong W-T, Thomas HD, Kahn S, Kyle S, et al. Therapeutic potential of poly(ADP-ribose) polymerase inhibitor AG014699 in human cancers with mutated or methylated BRCA1 or BRCA2. *J Natl Cancer Inst* (2011) 103:334–46. doi: 10.1093/jnci/djq509

30. Veeck J, Ropero S, Setien F, Gonzalez-Suarez E, Osorio A, Benitez J, et al. BRCA1 CpG island hypermethylation predicts sensitivity to poly(adenosine diphosphate)-ribose polymerase inhibitors. *J Clin Oncol* (2010) 28:e563–564. doi: 10.1200/JCO.2010.30.1010

31. Menghi F, Banda K, Kumar P, Straub R, Dobrolecki L, Rodriguez IV, et al. Genomic and epigenomic BRCA alterations predict adaptive resistance and response to platinum-based therapy in patients with triple-negative breast and ovarian carcinomas. *Sci Transl Med* (2022) 14:eabn1926. doi: 10.1126/scitranslmed.abn1926

32. Eikesdal HP, Yndestad S, Elzawahry A, Llop-Guevara A, Gilje B, Blix ES, et al. Olaparib monotherapy as primary treatment in unselected triple negative breast cancer. *Ann Oncol* (2021) 32:240–9. doi: 10.1016/j.annonc.2020.11.009

33. D'Andrea AD. Mechanisms of PARP inhibitor sensitivity and resistance. *DNA Repair* (2018) 71:172–6. doi: 10.1016/j.dnarep.2018.08.021

34. Dias MP, Moser SC, Ganesan S, Jonkers J. Understanding and overcoming resistance to PARP inhibitors in cancer therapy. *Nat Rev Clin Oncol* (2021) 18:773–91. doi: 10.1038/s41571-021-00532-x

35. Ter Brugge P, Kristel P, van der Burg E, Boon U, de Maaker M, Lips E, et al. Mechanisms of therapy resistance in patient-derived xenograft models of BRCA1-deficient breast cancer. *J Natl Cancer Inst* (2016) 108:1–12. doi: 10.1093/jnci/djw148

36. du Manoir S, Orsetti B, Bras-Gonçalves R, Nguyen T-T, Lasorsa L, Boissière F, et al. Breast tumor PDXs are genetically plastic and correspond to a subset of aggressive cancers prone to relapse. *Mol Oncol* (2014) 8:431–43. doi: 10.1016/j.molonc.2013.11.010

37. Colombo P-E, du Manoir S, Orsetti B, Bras-Gonçalves R, Lambros MB, MacKay A, et al. Ovarian carcinoma patient derived xenografts reproduce their tumor of origin and preserve an oligoclonal structure. *Oncotarget.* (2015) 6:28327–40. doi: 10.18632/oncotarget.5069

38. Adélaïde J, Finetti P, Bekhouche I, Repellini L, Geneix J, Sircoulomb F, et al. Integrated profiling of basal and luminal breast cancers. *Cancer Res* (2007) 67:11565–75. doi: 10.1158/0008-5472.CAN-07-2536

39. Abkevich V, Timms KM, Hennessy BT, Potter J, Carey MS, Meyer LA, et al. Patterns of genomic loss of heterozygosity predict homologous recombination repair defects in epithelial ovarian cancer. *Br J Cancer.* (2012) 107:1776–82. doi: 10.1038/bjc.2012.451

40. Bertucci F, Finetti P, Guille A, Adélaïde J, Garnier S, Carbuccia N, et al. Comparative genomic analysis of primary tumors and metastases in breast cancer. *Oncotarget.* (2016) 7:27208–19. doi: 10.18632/oncotarget.8349

41. Li H, Durbin R. Fast and accurate short read alignment with burrows-wheeler transform. *Bioinformatics.* (2009) 25:1754–60. doi: 10.1093/bioinformatics/btp324

42. Garrison E, Marth G. *Haplotype-based variant detection from short-read sequencing* (2012). Available at: https://arxiv.org/abs/1207.3907.

43. Poplin R, Ruano-Rubio V, DePristo MA, Fennell TJ, Carneiro MO, van der Auwera GA, et al. Scaling accurate genetic variant discovery to tens of thousands of samples. *bioRxiv* (2017). doi: 10.1101/201178

44. Wilm A, Aw PPK, Bertrand D, Yeo GHT, Ong SH, Wong CH, et al. LoFreq: a sequence-quality aware, ultra-sensitive variant caller for uncovering cell-population heterogeneity from high-throughput sequencing datasets. *Nucleic Acids Res* (2012) 40:11189–201. doi: 10.1093/nar/gks918

45. Auwera GAVd, O'Connor BD. *Genomics in the cloud: Using docker, GATK, and WDL in Terra*. O'Reilly Media (2020).

46. Dunn T, Berry G, Emig-Agius D, Jiang Y, Lei S, Iyer A, et al. Pisces: an accurate and versatile variant caller for somatic and germline next-generation sequencing data. *Bioinformatics* (2019) 35:1579–81. doi: 10.1093/bioinformatics/bty849

47. Rimmer A, Phan H, Mathieson I, Iqbal Z, Twigg SRF, Wilkie AOM, et al. Integrating mapping-, assembly- and haplotype-based approaches for calling variants in clinical sequencing applications. *Nat Genet* (2014) 46:912–8. doi: 10.1038/ng.3036

48. Lai Z, Markovets A, Ahdesmaki M, Chapman B, Hofmann O, McEwen R, et al. VarDict: a novel and versatile variant caller for next-generation sequencing in cancer research. *Nucleic Acids Res* (2016) 44:e108–8. doi: 10.1093/nar/gkw227

49. Koboldt DC, Zhang Q, Larson DE, Shen D, McLellan MD, Lin L, et al. VarScan 2: Somatic mutation and copy number alteration discovery in cancer by exome sequencing. *Genome Res* (2012) 22:568–76. doi: 10.1101/gr.129684.111

50. Ye K, Schulz MH, Long Q, Apweiler R, Ning Z. Pindel: a pattern growth approach to detect break points of large deletions and medium sized insertions from paired-end short reads. *Bioinformatics*. (2009) 25:2865–71. doi: 10.1093/bioinformatics/btp394

51. Fang H, Bergmann EA, Arora K, Vacic V, Zody MC, Iossifov I, et al. Indel variant analysis of short-read sequencing data with scalpel. *Nat Protoc* (2016) 11:2529–48. doi: 10.1038/nprot.2016.150

52. Robinson JT, Thorvaldsdóttir H, Winckler W, Guttman M, Lander ES, Getz G, et al. Integrative genomics viewer. *Nat Biotechnol* (2011) 29:24–6. doi: 10.1038/nbt.1754

53. Thorvaldsdottir H, Robinson JT, Mesirov JP. Integrative genomics viewer (IGV): high-performance genomics data visualization and exploration. *Briefings Bioinf* (2013) 14:178–92. doi: 10.1093/bib/bbs017

54. Bertucci F, Rypens C, Finetti P, Guille A, Adélaïde J, Monneur A, et al. NOTCH and DNA repair pathways are more frequently targeted by genomic alterations in inflammatory than in non-inflammatory breast cancers. *Mol Oncol* (2020) 14:504–19. doi: 10.1002/1878-0261.12621

55. Manoir S, Delpech H, Orsetti B, Jacot W, Pirot N, Noel J, et al. In high-grade ovarian carcinoma, platinum-sensitive tumor recurrence and acquired-resistance derive from quiescent residual cancer cells that overexpress CRYAB , CEACAM6, and SOX2. *J Pathology*. (2022) 257:367–78. doi: 10.1002/path.5896

56. Wang Y, Bernhardy AJ, Cruz C, Krais JJ, Nacson J, Nicolas E, et al. The BRCA1-Δ11q alternative splice isoform bypasses germline mutations and promotes therapeutic resistance to PARP inhibition and cisplatin. *Cancer Res* (2016) 76:2778–90. doi: 10.1158/0008-5472.CAN-16-0186

57. Elstrodt F, Hollestelle A, Nagel JHA, Gorin M, Wasielewski M, van den Ouweland A, et al. *BRCA1* mutation analysis of 41 human breast cancer cell lines reveals three new deleterious mutants. *Cancer Res* (2006) 66:41–5. doi: 10.1158/0008-5472.CAN-05-2853

58. DelloRusso C, Welcsh PL, Wang W, Garcia RL, King M-C, Swisher EM. Functional characterization of a novel BRCA1-null ovarian cancer cell line in response to ionizing radiation. *Mol Cancer Res* (2007) 5:35–45. doi: 10.1158/1541-7786.MCR-06-0234

59. Konstantinopoulos PA, Ceccaldi R, Shapiro GI, D'Andrea AD. Homologous recombination deficiency: Exploiting the fundamental vulnerability of ovarian cancer. *Cancer Discovery*. (2015) 5:1137–54. doi: 10.1158/2159-8290.CD-15-0714

60. Willers H, Taghian AG, Luo C-M, Treszezamsky A, Sgroi DC, Powell SN. Utility of DNA repair protein foci for the detection of putative BRCA1 pathway defects in breast cancer biopsies. *Mol Cancer Res* (2009) 7:1304–9. doi: 10.1158/1541-7786.MCR-09-0149

61. Graeser M, McCarthy A, Lord CJ, Savage K, Hills M, Salter J, et al. A marker of homologous recombination predicts pathologic complete response to neoadjuvant chemotherapy in primary breast cancer. *Clin Cancer Res* (2010) 16:6159–68. doi: 10.1158/1078-0432.CCR-10-1027

62. van Wijk LM, Kramer CJH, Vermeulen S, ter Haar NT, de Jonge MM, Kroep JR, et al. The RAD51-FFPE test; calibration of a functional homologous recombination deficiency test on diagnostic endometrial and ovarian tumor blocks. *Cancers*. (2021) 13:2994. doi: 10.3390/cancers13122994

63. Castroviejo-Bermejo M, Cruz C, Llop-Guevara A, Gutiérrez-Enríquez S, Ducy M, Ibrahim YH, et al. A RAD 51 assay feasible in routine tumor samples calls PARP inhibitor response beyond BRCA mutation. *EMBO Mol Med* (2018) 10:1–16. doi: 10.15252/emmm.201809172

64. Carreira S, Porta N, Arce-Gallego S, Seed G, Llop-Guevara A, Bianchini D, et al. Biomarkers associating with PARP inhibitor benefit in prostate cancer in the TOPARP-b trial. *Cancer Discovery*. (2021) 11:2812–27. doi: 10.1158/2159-8290.CD-21-0007

65. Pellegrino B, Herencia-Ropero A, Llop-Guevara A, Pedretti F, Moles-Fernández A, Viaplana C, et al. Preclinical *In vivo* validation of the RAD51 test for identification of homologous recombination-deficient tumors and patient stratification. *Cancer Res* (2022) 82:1646–57. doi: 10.1158/0008-5472.CAN-21-2409

66. Llop-Guevara A, Loibl S, Villacampa G, Vladimirova V, Schneeweiss A, Karn T, et al. Association of RAD51 with homologous recombination deficiency (HRD) and clinical outcomes in untreated triple-negative breast cancer (TNBC): analysis of the GeparSixto randomized clinical trial. *Ann Oncol* (2021) 32:1590–6. doi: 10.1016/j.annonc.2021.09.003

67. Reardon JT, Vaisman A, Chaney SG, Sancar A. Efficient nucleotide excision repair of cisplatin, oxaliplatin, and bis-aceto-ammine-dichloro-cyclohexylamine-platinum(IV) (JM216) platinum intrastrand DNA diadducts. *Cancer Res* (1999) 59:3968–71.

68. Ceccaldi R, O'Connor KW, Mouw KW, Li AY, Matulonis UA, D'Andrea AD, et al. A unique subset of epithelial ovarian cancers with platinum sensitivity and PARP inhibitor resistance. *Cancer Res* (2015) 75:628–34. doi: 10.1158/0008-5472.CAN-14-2593

frontiers | Frontiers in Oncology

TYPE Original Research
PUBLISHED 20 March 2023
DOI 10.3389/fonc.2023.1110751

OPEN ACCESS

EDITED BY
Zhi-Gang Zhuang,
Shanghai First Maternity and Infant Hospital, China

REVIEWED BY
Dharmendra Kumar Yadav,
Gachon University, Republic of Korea
Yi Tao,
Zhejiang University of Technology, China

*CORRESPONDENCE
Tinghong Zhang
snowrabbit58@163.com
Huaqiong Li
lihq@ucas.ac.cn
Longteng Xie
xfxlt@126.com

†These authors have contributed equally to this work

SPECIALTY SECTION
This article was submitted to Breast Cancer, a section of the journal Frontiers in Oncology

RECEIVED 29 November 2022
ACCEPTED 08 March 2023
PUBLISHED 20 March 2023

CITATION
Zhang L, Tang L, Jiang Y, Wang C, Huang L, Ding T, Zhang T, Li H and Xie L (2023) GE11-antigen-loaded hepatitis B virus core antigen virus-like particles efficiently bind to TNBC tumor. *Front. Oncol.* 13:1110751. doi: 10.3389/fonc.2023.1110751

GE11-antigen-loaded hepatitis B virus core antigen virus-like particles efficiently bind to TNBC tumor

Long Zhang[1,2†], Lin Tang[3†], Yongsheng Jiang[1,2], Chenou Wang[3], Lijiang Huang[1,2], Ting Ding[1], Tinghong Zhang[2*], Huaqiong Li[2,3*] and Longteng Xie[1*]

[1]Department of Infectious Diseases, The Affiliated Xiangshan Hospital of Wenzhou Medical University, Ningbo, Zhejiang, China, [2]Zhejiang Engineering Research Center for Tissue Repair Materials, Wenzhou Institute, University of Chinese Academy of Sciences, Wenzhou, Zhejiang, China, [3]School of Biomedical Engineering, Wenzhou Medical University, Wenzhou, Zhejiang, China

Purpose: This study aimed to explore the possibility of utilizing hepatitis B core protein (HBc) virus-like particles (VLPs) encapsulate doxorubicin (Dox) to reduce the adverse effect caused by its off-target and toxic side effect.

Methods: Here, a triple-negative breast cancer (TNBC) tumor-targeting GE11-HBc VLP was constructed through genetic engineering. The GE11 peptide, a 12-amino-acid peptide targeting epidermal growth factor receptor (EGFR), was inserted into the surface protein loops of VLPs. The Dox was loaded into HBc VLPs by a thermal-triggered encapsulation strategy. The *in vitro* release, cytotoxicity, and cellular uptake of TNBC tumor-targeting GE11-HBc VLPs was then evaluated.

Results: These VLPs possessed excellent stability, DOX loading efficiency, and preferentially released drug payload at high GSH levels. The insertion of GE11 targeting peptide caused improved cellular uptake and enhanced cell viability inhibitory in EGFR high-expressed TNBC cells.

Conclusion: Together, these results highlight DOX-loaded, EGFR-targeted VLPs as a potentially useful therapeutic choice for EGFR-overexpressing TNBC.

KEYWORDS

virus-like particles, Ge11, triple-negative breast cancer, nanomedicine, drug delivery

1 Introduction

According to the statistical data from the WHO, cancer caused the leading death among all diseases in most countries and is an important barrier to increasing lifetime. In 2022, there will be approximately 4,820,000 and 2,370,000 new cancer cases and 3,210,000 and 640,000 cancer deaths in China and the USA, respectively (1). With diagnosed 2.3

million new cases in 2020, female breast cancer has exceeded lung cancer as the most commonly detected cancer (2). In the USA, breast cancer continues to be the most prevalent cancer with a number of annual cases, with 287,850 incidences in 2022 (3). The lack of ER, PR, and HER2 makes target therapy difficult to use in triple-negative breast cancer (TNBC), leaving cytotoxic chemotherapy as the main type of treatment (4, 5). Therefore, the development of a novel delivery system with enhanced target efficiency is still urgently needed (6–8).

Composed of natural biological building blocks, the VLPs exhibit great promise as an efficient targeted nanocarrier in medicine (9). Compared to synthetic nanoparticles, the VLPs as natural protein nanoparticles take the advantages of lower toxicity, easy biodegradation, and biocompatibility (10). The structure of VLPs is stable under a wide range of pH and temperature (11–13). Among a range of VLPs, HBc VLPs as the most commonly used model for basic medical research can be easily produced in all known expression systems (14). HBc VLPs take accurately defined composition, suitability for modification, capacity to self-assembly, and complete biocompatibility/biodegradability *in vivo* (15, 16). HBc VLPs can maintain structural integrity after deletions, substitutions, or insertions in its two immunodominant loop regions (MIR) and C-terminal tail (17–22). Normally, exogenous targeting epitope was most commonly inserted into the MIR region (AA 78-82) of HBc by genetic engineering (23–25).

Actually, peptides represent a suitable alternative to monoclonal antibodies as active targeting agents (26).They are studied for drug delivery systems functionalization with the goal to achieve smart drug delivery systems. They have low immunogenic potential and show good penetration into solid tumor tissues. The GE11 peptide (YHWYGYTPQNVI) is reported to bind specifically to EGFR but is significantly minus mitogenic than EGF (27). It is much smaller than EGF, and it binds only to one EGFR region. Lots of studies suggested that the GE11 peptide is suitable for targeting EGFR-expressing tumors (28–30). GE11-targeted drug delivery systems include liposomes, polymer-based polyplexes, and filamentous plant viruses based or polymeric nanoparticles for diagnostic and anticancer and gene delivery applications (31). However, utilizing GE11-targted HBc VLP for TNBC therapy is rarely attempted.

In this study, we successfully obtained hybrid HBc VLPs, which presented a GE11 peptide. We examined HBc VLPs as drug delivery carriers in a model of TNBC cancer. Modified VLPs delivered DOX to EGFR-expressing cancer cells. Our results highlight DOX-loaded, EGFR-targeted VLPs as a potentially effective therapeutic option for EGFR-overexpressing TNBC.

2 Materials and methods

2.1 Preparation of GE11-HBc monomer

HBc sequence was synthesized by the company, and the GE11 peptide was inserted into the MIR region by SphI single enzyme digestion. The GE11-HBc was attached to a His tag at the end of the C-terminus to facilitate protein purification. The GE11-HBc sequence was cloned into the pET28a vector *via Xho*I and *Nco*I restriction enzyme sites. The plasmid pET28a-GE11-HBc was transformed into *Escherichia coli* BL21 (DE3) and cultured in Luria–Bertani (LB) medium at 37°C until the OD_{600} reached approximately 0.6–0.8; then, 0.5mM isopropyl-β-d-thiogalactoside (IPTG) was added to the culture, and cells were grown at 26°C overnight to induce protein expression. The protein was purified with Nickel affinity chromatography (GE Healthcare) as the product description described.

2.2 Preparation and purification of HBc VLPs

The purified protein was heated at 70°C for 20 min, then centrifuged at 10,000 rpm for 30 min to collect the supernatant. The supernatant was filtered through a 0.45-μm filter and subjected to ion exchange chromatography purification (GE Healthcare, Sepharose 4FF). The HBc VLPs were isolated by using sucrose density gradient centrifugation. Briefly, lower-density solutions were prepared by diluting with buffer (250 mM sucrose, 10 mM Tris–HCl, 1 mM EDTA, pH 7.4) to yield final sucrose concentrations (vol/vol) of 55%, 45%, 35%, 25%, and 15%. Crude protein was added to the top of the gradient and then centrifuged for 2 h at 35,000 rpm at 4°C. After centrifugation, the fractions were collected and analyzed using sodium dodecyl sulfate–polyacrylamide gel electrophoresis (SDS-PAGE) and transmission electron microscopy (TEM) images.

2.3 Preparation of DOX-loaded HBc VLPs

The DOX-loaded HBc VLPs were prepared by a thermal-triggered encapsulation strategy (32). The Hg particles were first treated with RNase for 3 h at 37°C to remove the RNA. DOX (0.2 mg/ml) was incubated with 0.2 mg/ml Hg at 50°C, 60°C, 70°C, and 80°C for 30, 60, 90, and 120 min. The OD_{482} of each group was measured after the removal of free DOX by desalting column.

To calculate the loading capacity, 1 mg/ml DOX was diluted to 0.05, 0.1, 0.15, 0.2, 0.25, and 0.5mg/ml, and the standard curve of Dox was obtained after the measurement of the absorbance at A 482 nm.

2.4 *In vitro* release

The *in vitro* release process of DOX in VLPs under GSH conditions was analyzed according to a previously reported method (33). In brief, 20 ml of HBc-DOX VLPs (containing 0.1 mg/ml DOX) was added to a dialysis tube (MWCO of 3.5 kDa). Drug release was carried out by incubating dialysis tubing containing HBc-DOX VLP in 1 L of various PBS stoste, which contained different concentrations of GSH (0, 0.02, 5, and 10 mM). Finally, 500 μl of the test solution was withdrawn at different time intervals (0, 12, 24, 36, 48, 60, and 72 h, followed by the addition of the same volume of fresh medium, and quantitative analysis by a UV–Vis spectroscopy at A 482 nm. The accumulative release (%)

was acquired from the following equation:

$$\text{Accumulative release}(\%) = (C_t \times V_t + \Sigma_i C_i \times V_i)/W_{total} \times 100\,\%$$

where C_t and C_i are the concentration of the drug in the stoste at testing time point (t) and the concentration of the drug in the discarded medium at testing time points (i) before t, respectively; V_t is the volume of the stoste; V_i is the volume of discarded medium; and W_{total} is the total drug mass in VLPs.

2.5 Cytotoxicity assays

EGFR-positive MCF7 and MDA-MB-231 cells (1×10^4) were seeded to each well of 96-well plates. The medium in each well was removed after 24 h of incubation. Then, HBc-GE11, HBc-GE11-DOX (equal to 0.2 mg/ml free DOX), and free DOX (0.2 mg/ml) were suspended in Dulbecco's modified Eagle's medium (DMEM) and added to cells. The cells were further cultured for 12, 24, 36, or 48 h before standard CCK-8 assay testing (Dojindo).

2.6 Cellular uptake

A total of 5×10^4 MCF7, MDA-MB-231 or MDA-MB-453 cells (EGFR−) were seeded on a cover-slide system overnight. Subsequently, the cells were treated with PBS, HBc-GE11-DOX (equal to 1.086 mg/ml free DOX) and free DOX (1.086 mg/ml), respectively. After 0.5, 1, and 2 h incubation, the cells were washed three times with PBS and then fixed with cold 4% paraformaldehyde (PFA) for 1.5 h. The cell nucleus was stained with 1 μg/ml 4′,6-diamidino-2-phenylindole (DAPI) dye for 10 min. At last, a confocal laser scanning microscope was used to obtain the image.

2.7 Flow cytometry assays

For further quantification, MCF7 and MDA-MB-231 cells (1×10^5 cells/well) were seeded in 12-well plates, respectively, in fresh medium containing HBc-GE11, HBc-GE11-DOX, and free DOX (calculated on DOX at a final concentration of 2 μmol/ml) for 2, 4, 6, 8, 10, and 12 h. After this, cells were collected and suspended in a cold PBS buffer, then analyzed by CytoFLEX flow cytometry (Beckman, USA).

3 Results and discussion

3.1 Generation and characterization of HBc-GE11

The HBc-GE11 protein was induced at 26°C overnight by 0.5 mM isopropyl β-D-1-thiogalactopyranoside (IPTG), and cells were lysed and purified by Nickel affinity chromatography (GE Healthcare). The expressed protein was subjected to SDS gel electrophoresis and Western blot analysis (Figures 1A, B). The HBc-GE11 monomer was observed as a ~35 kDa band. Interestingly, the multimeric complexes were also observed as higher-molecular-mass bands. The purified HBc-GE11 monomer was further purified by Sepharose 4FF ion-exchange chromatography and then subjected to sucrose density gradient centrifugation. The SDS-PAGE results suggest that VLPs mainly existed in a 15%–25% gradient fraction (Figure 1C, line2). Negative stain TEM analysis showed the existence of 40.481 ± 0.015 nm diameter vesicles (Figure 1D).

3.2 Generation of HBc-DOX VLPs

It is reported that the thermal-triggered strategy can be applied to encapsulate the drug into VLPs in 10 min. By using thermally induced pore opening of the HBc capsid, 1,055 dye molecules could be encapsulated in each HBc VLP by simply mixing them at 60°C (34). Hence, a thermal-triggered encapsulation strategy was used for DOX encapsulation in this study. To find the optimal encapsulation condition, a fixed DOX and HBc concentration of 0.2 mg/ml was used. The initial temperature for encapsulation was set to 50°C. After being heated in a 70°C water bath for 90 min, 34.01% DOX was encapsulated into VLPs (Figure 2A). Compared to incubation at 60°C, a decreased encapsulation efficiency (EE) was observed, which was mainly due to the dissociation of the complete VLPs structure. It should be noted that some of HBc VLPs could not keep a complete structure after being heated 120 min at 70°C (Figure 2B). The optimal DOX encapsulation concentration was confirmed by incubating various concentrations of DOX (0.05, 0.1, 0.15, 0.2, and 0.25 mg/ml) with fixed HBc VLP (0.2 mg/ml) at 70°C for 90 min. The highest DOX loading capacity was observed when incubating 0.2 mg/ml DOX with 0.2 mg/ml HBc VLPs (Figure 2C). TEM result showed that DOX-loaded VLPs has a similar size to unloaded one (Figure 2D).

3.3 Release of DOX from VLPs under high GSH condition

It is well known that lots of disulfide bonds on the surface of HBc VLPs and high concentration of GSH in the tumor can reduce disulfide bonds and destroy HBc VLP structure. The concentration of GSH in the tumor site is up to 10 mM but only 0.02 mM in normal tissues (35). Thus, when HBc VLP particles enter the tumor cell, the high concentration of GSH will destroy the structure of HBc VLPs to release internal drugs. It can be seen from Figure 2E that when the GSH concentration is 0 and 0.02 mM (normal tissue cell concentration), the release of DOX in HBc-GE11-DOX is very small. When the GSH concentration is 5 mM, the release amount can reach 40.5% in 72 h, while 10 mM GSH treatment results in 95.97% drug release in 72 h. pH-dependent drug release is mostly used in anti-tumor drug design. To confirm whether pH influences VLPs drug release, HBc-DOX VLPs were exposed to different pH buffers under the same GSH concentration. There is no significant difference in the drug release of HBc-DOX under different pH

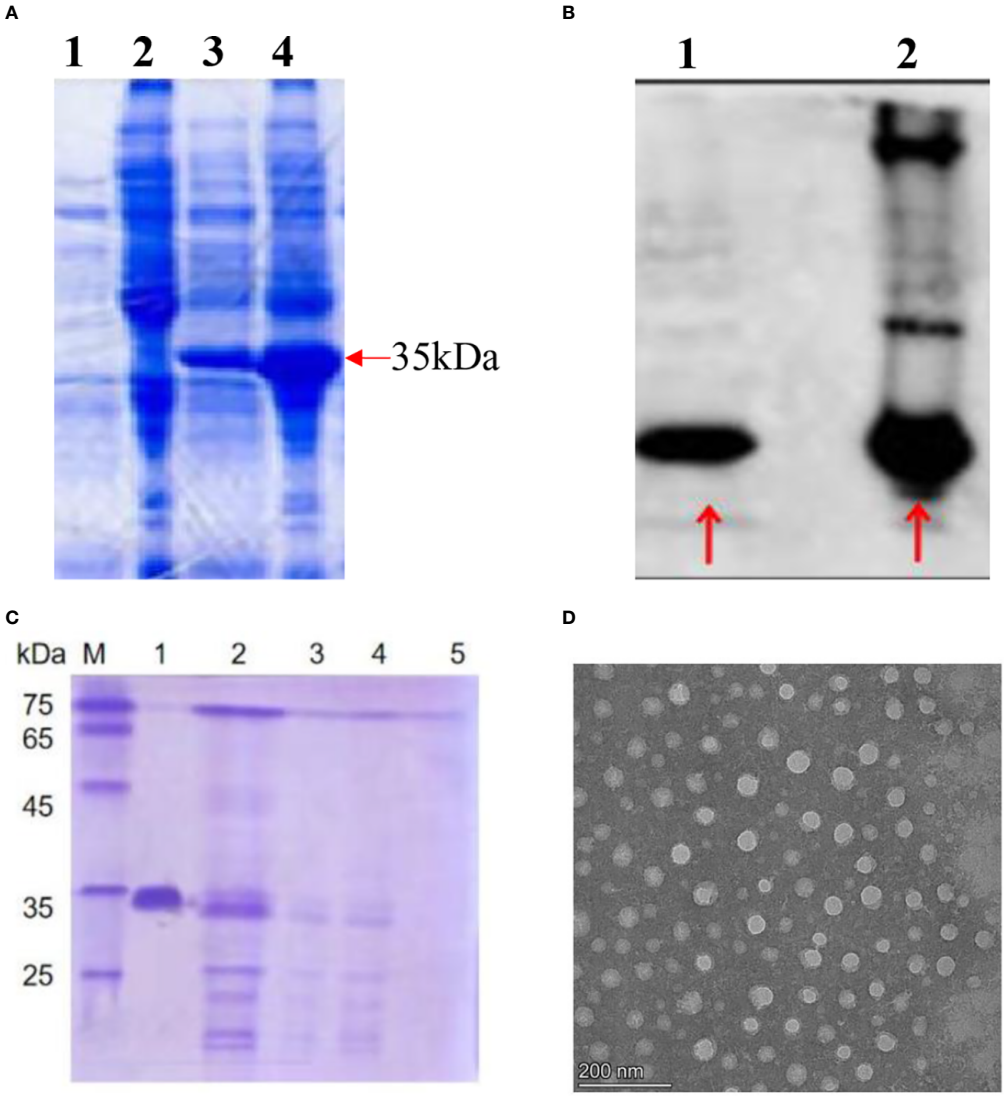

FIGURE 1
Production and morphology of the HBc-GE11 VLPs. **(A, B)** SDS-PAGE and Western blot analysis of HBc-GE11 protein expression. **(A)** Lines 1 and 2, bacterial lysate precipitation and supernatant before induction; lines 3 and 4, bacterial lysate precipitation and supernatant after induction. **(B)** Line 1, bacterial lysate precipitation after induction; line 2, bacterial lysate supernatant after induction. **(C)** Representative protein normalized SDS-PAGE of F1–F5. **(D)** Representative transmission electron micrographs of HBc-GE11 VLPs.

conditions with the same GSH concentration, which indicates that HBc VLPs are not sensitive to pH (Figure 2F).

3.4 Cellular uptake of HBc-GE11-DOX VLPs

The cellular uptake of HBc-GE11-DOX was first assessed by confocal laser scanning microscope. The breast cancer cell lines (MDA-MB-231 and MDA-MB-453) were treated with free DOX and HBc-GE11-DOX, and images were obtained at different time intervals. The free DOX and HBc-GE11-DOX entered the MDA-MB-231 cell line very fast. Even at a feeding time as short as 0.5 h, the accumulation of DOX in cells was clearly noted for both DOX and HBc-GE11-DOX (Figure 3A). As the feeding time extended (from 0.5 to 2 h), more DOX accumulated in the cells for both HBc-GE11-DOX and DOX groups. Interestingly, at the same time intervals, the DOX cannot be found in HBc-GE11-DOX but not in free DOX-treated MDA-MB-453 cell, which is an EGFR-negative cell line (Figure 3B). We also used the FCM to evaluate the cellular uptake of HBc-GE11-DOX nanoparticles in both MCF7 (Figure 3C) and MDAMB-231 cells (Figure 3D). As shown in Figures 3C, D, all the cells are DOX-positive, suggesting that HBc-GE11-DOX and free DOX can easily be uptake by tumor cells.

3.5 Effect of HBc-GE11-DOX on killing breast cancer cells *in vitro*

The cytotoxicity of HBc VLPs was valued first. No significant inhibition effect was observed on cellular viability in two different

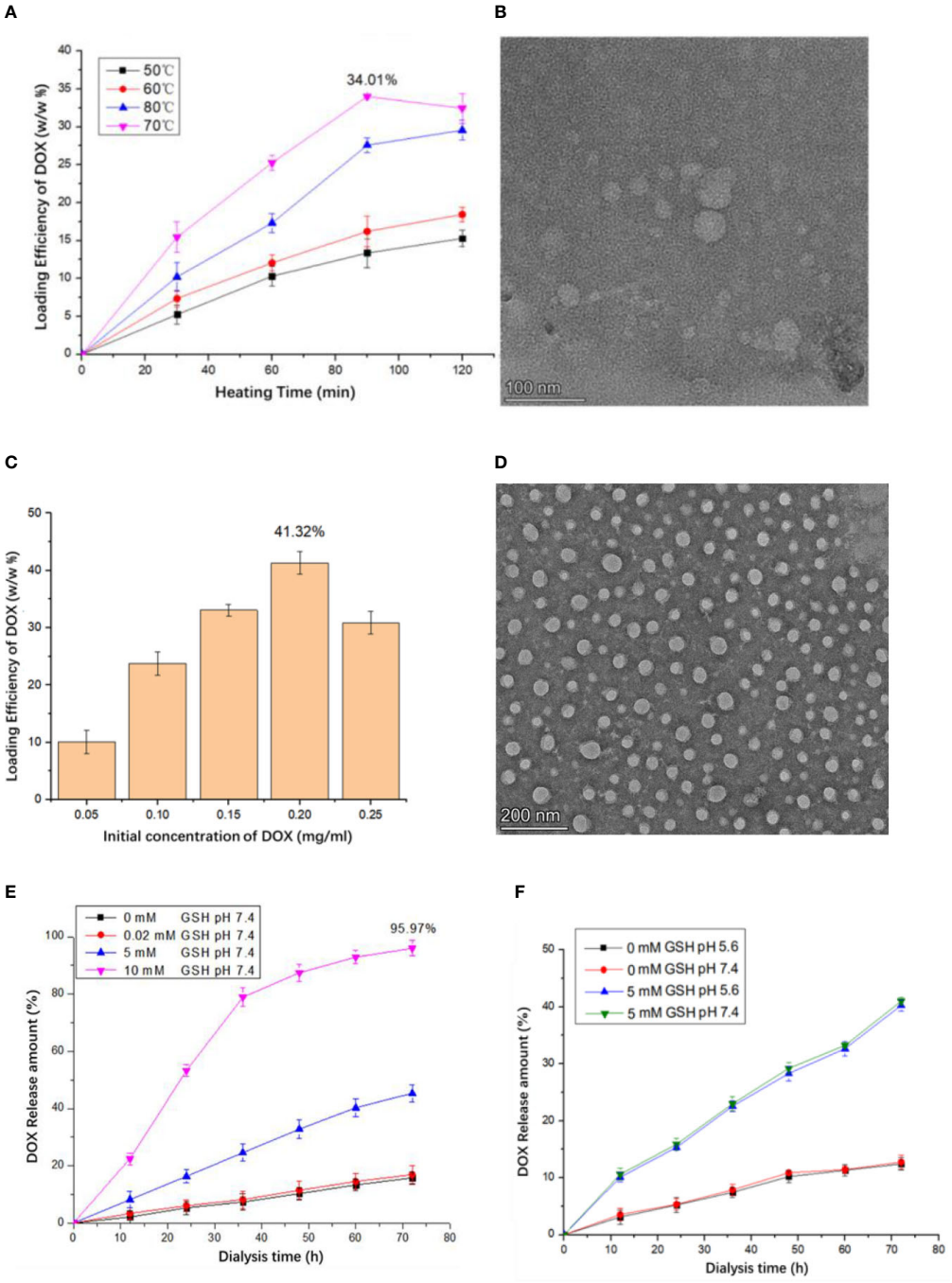

FIGURE 2
Production of the HBc-DOX VLPs and influence of different concentrations of GSH and Ph on drug release of HBc-DOX particles. **(A)** DOX loading at different heating temperatures and times. **(B)** TEM observation of HG particles heated at 70°C for 120 min. **(C)** Relationship between DOX concentration and loading rate. **(D)** HBc-DOX particles observed by TEM. **(E, F)** Influence of different concentrations of GSH **(E)** and Ph **(F)** on drug release of HBc-DOX particles.

cancer cell lines with indicated HBc VLPs concentration and incubation times from 12 to 48 h (Figure 4). It is suggested that HBc VLPs have no or minimal cytotoxicity to the breast cancer cell lines. Subsequently, the HBc-GE11-DOX was used to treat two EGFR+ cells. The cytotoxicity of the HBc-GE11- DOX to two breast cancer cell lines was evaluated by CCK-8 kits, under various intervals of treatment times (12–48 h) (Figures 4A, B). PBS and pure VLPs groups were set up as the control, and no obvious cytotoxicity was observed, while notable cytotoxicity was observed for both free DOX and HBc-GE11-DOX groups. For both cell lines

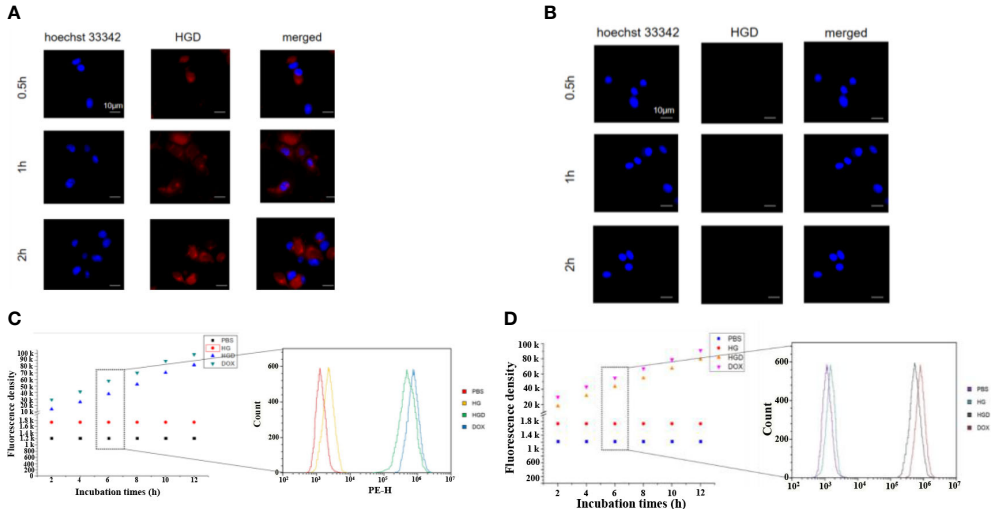

FIGURE 3
CLSM images after feeding free DOX and HBc-GE11-DOX to MDA-MB-231 **(A)** and MDA-MB-453 cells **(B)** at different time intervals. Red, DOX; blue, DAPI for cell nucleus. The scale bar is 10 μm. **(C, D)** Flow cytometry of MCF7 **(C)** and MDA-MB-231 cells **(D)** by the cellular uptake assay after feeding HBc VLPs, HBc-GE11-DOX, or free DOX for different times.

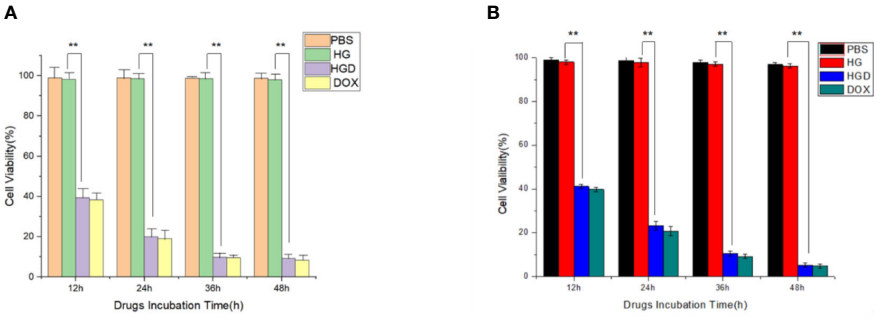

FIGURE 4
Viabilities of MCF7 **(A)** and MDA-MB-231 **(B)** after treating with 0.2 mg/ml of free DOX, HBc-GE11-DOX (equal to 0.2 mg/ml free DOX), or pure HBc VLPs for 12, 24, 36, and 48 h. **p < 0.01.

treated with different coincubation times, the cellular viability decreased with the increased incubation time (Figure 4). It should be pointed out that free DOX-treated cells exhibited lower cell viability, although no significant difference was observed.

4 Conclusion

Here, we constructed hybrid HBc-GE11 VLPs, which presented GE11 peptide to target EGFR+ breast cancer. We examined HBc VLPs as drug delivery carriers in a model of TNBC cancer. Modified VLPs delivered DOX to EGFR-expressing cancer tissues and exhibited a GSH-dependent drug release. Our results highlight DOX-loaded, EGFR-targeted VLPs as a potentially effective therapeutic option for EGFR-overexpressing TNBC.

Data availability statement

The original contributions presented in the study are included in the article/supplementary material. Further inquiries can be directed to the corresponding authors.

Author contributions

LZ and HL conceived and designed the project. LZ, TZ and HL prepared the manuscript. LT carried out the experiments and analyzed the data. CW did the materials characterization. YJ, HL and TD analyzed the data. LX and HL provided funding for this project. LZ and HL cowrote the manuscript. All authors contributed to the article and approved the submitted version.

Funding

This work was supported by grants from Wenzhou Institute, University of Chinese Academy of Sciences (WIUCASQD2019002 and WIUCASZZXF21005) and The Affiliated Xiangshan Hospital of Wenzhou Medical University.

Conflict of interest

The authors declare that the research was conducted in the absence of any commercial or financial relationships that could be construed as a potential conflict of interest.

Publisher's note

References

1. Xia C, Dong X, Li H, Cao M, Sun D, He S, et al. Cancer statistics in China and united states, 2022: profiles, trends, and determinants. *Chin Med J (Engl)* (2022) 135:584–90. doi: 10.1097/CM9.0000000000002108

2. Sung H, Ferlay J, Siegel RL, Laversanne M, Soerjomataram I, Jemal A, et al. Global cancer statistics 2020: GLOBOCAN estimates of incidence and mortality worldwide for 36 cancers in 185 countries. *CA Cancer J Clin* (2021) 71:209–49. doi: 10.3322/caac.21660

3. Siegel RL, Miller KD, Fuchs HE, Jemal A. Cancer statistics, 2022. *CA Cancer J Clin* (2022) 72:7–33. doi: 10.3322/caac.21708

4. Perou CM, Sorlie T, Eisen MB, van de Rijn M, Jeffrey SS, Rees CA, et al. Molecular portraits of human breast tumours. *Nature* (2000) 406:747–52. doi: 10.1038/35021093

5. Cancer Genome Atlas N. Comprehensive molecular portraits of human breast tumours. *Nature* (2012) 490:61–70. doi: 10.1038/nature11412

6. Dent R, Trudeau M, Pritchard KI, Hanna WM, Kahn HK, Sawka CA, et al. Triple-negative breast cancer: clinical features and patterns of recurrence. *Clin Cancer Res* (2007) 13:4429–34. doi: 10.1158/1078-0432.CCR-06-3045

7. Teo MYM, Fong JY, Lim WM, In LLA. Current advances and trends in KRAS targeted therapies for colorectal cancer. *Mol Cancer Res* (2022) 20:30–44. doi: 10.1158/1541-7786.MCR-21-0248

8. Maqbool M, Bekele F, Fekadu G. Treatment strategies against triple-negative breast cancer: An updated review. *Breast Cancer (Dove Med Press)* (2022) 14:15–24. doi: 10.2147/BCTT.S348060

9. Yoo JW, Irvine DJ, Discher DE, Mitragotri S. Bio-inspired, bioengineered and biomimetic drug delivery carriers. *Nat Rev Drug Discovery* (2011) 10:521–35. doi: 10.1038/nrd3499

10. Maham A, Tang Z, Wu H, Wang J, Lin Y. Protein-based nanomedicine platforms for drug delivery. *Small* (2009) 5:1706–21. doi: 10.1002/smll.200801602

11. Ausar SF, Foubert TR, Hudson MH, Vedvick TS, Middaugh CR. Conformational stability and disassembly of Norwalk virus-like particles. *Effect pH temperature J Biol Chem* (2006) 281:19478–88. doi: 10.1074/jbc.M603313200

12. Samandoulgou I, Hammami R, Morales Rayas R, Fliss I, Jean J. Stability of secondary and tertiary structures of virus-like particles representing noroviruses: Effects of pH, ionic strength, and temperature and implications for adhesion to surfaces. *Appl Environ Microbiol* (2015) 81:7680–6. doi: 10.1128/AEM.01278-15

13. Shan W, Chen R, Zhang Q, Zhao J, Chen B, Zhou X, et al. Improved stable indocyanine green (ICG)-mediated cancer optotheranostics with naturalized hepatitis b core particles. *Adv Mater* (2018) 30:e1707567. doi: 10.1002/adma.201707567

14. Clarke BE, Newton SE, Carroll AR, Francis MJ, Appleyard G, Syred AD, et al. Improved immunogenicity of a peptide epitope after fusion to hepatitis b core protein. *Nature* (1987) 330:381–4. doi: 10.1038/330381a0

15. Shen L, Zhou J, Wang Y, Kang N, Ke X, Bi S, et al. Efficient encapsulation of Fe (3)O(4) nanoparticles into genetically engineered hepatitis b core virus-like particles through a specific interaction for potential bioapplications. *Small* (2015) 11:1190–6. doi: 10.1002/smll.201401952

16. Lu Y, Chan W, Ko BY, VanLang CC, Swartz JR. Assessing sequence plasticity of a virus-like nanoparticle by evolution toward a versatile scaffold for vaccines and drug delivery. *Proc Natl Acad Sci U.S.A.* (2015) 112:12360–5. doi: 10.1073/pnas.1510533112

17. Koschel M, Thomssen R, Bruss V. Extensive mutagenesis of the hepatitis b virus core gene and mapping of mutations that allow capsid formation. *J Virol* (1999) 73:2153–60. doi: 10.1128/JVI.73.3.2153-2160.1999

18. Kratz PA, Bottcher B, Nassal M. Native display of complete foreign protein domains on the surface of hepatitis b virus capsids. *Proc Natl Acad Sci U.S.A.* (1999) 96:1915–20. doi: 10.1073/pnas.96.5.1915

19. Lachmann S, Meisel H, Muselmann C, Koletzki D, Gelderblom HR, Borisova G, et al. Characterization of potential insertion sites in the core antigen of hepatitis b virus by the use of a short-sized model epitope. *Intervirology* (1999) 42:51–6. doi: 10.1159/000024960

20. Milich DR, Peterson DL, Zheng J, Hughes JL, Wirtz R, Schodel F. The hepatitis nucleocapsid as a vaccine carrier moiety. *Ann N Y Acad Sci* (1995) 754:187–201. doi: 10.1111/j.1749-6632.1995.tb44451.x

21. Pumpens P, Grens E. HBV core particles as a carrier for b cell/T cell epitopes. *Intervirology* (2001) 44:98–114. doi: 10.1159/000050037

22. Pumpens P, Borisova GP, Crowther RA, Grens E. Hepatitis b virus core particles as epitope carriers. *Intervirology* (1995) 38:63–74. doi: 10.1159/000150415

23. Cheng K, Du T, Li Y, Qi Y, Min H, Wang Y, et al. Dual-Antigen-Loaded hepatitis b virus core antigen virus-like particles stimulate efficient immunotherapy against melanoma. *ACS Appl Mater Interfaces* (2020) 12:53682–90. doi: 10.1021/acsami.0c16012

24. Skamel C, Ploss M, Bottcher B, Stehle T, Wallich R, Simon MM, et al. Hepatitis b virus capsid-like particles can display the complete, dimeric outer surface protein c and stimulate production of protective antibody responses against borrelia burgdorferi infection. *J Biol Chem* (2006) 281:17474–81. doi: 10.1074/jbc.M513571200

25. Zhao Y, Li Z, Voyer J, Li Y, Chen X. Flagellin/Virus-like particle hybrid platform with high immunogenicity, safety, and versatility for vaccine development. *ACS Appl Mater Interfaces* (2022) 14:21872–85. doi: 10.1021/acsami.2c01028

26. Ruoslahti E. Peptides as targeting elements and tissue penetration devices for nanoparticles. *Adv Mater* (2012) 24:3747–56. doi: 10.1002/adma.201200454

27. Li Z, Zhao R, Wu X, Sun Y, Yao M, Li J, et al. Identification and characterization of a novel peptide ligand of epidermal growth factor receptor for targeted delivery of therapeutics. *FASEB J* (2005) 19:1978–85. doi: 10.1096/fj.05-4058com

28. Song S, Liu D, Peng J, Sun Y, Li Z, Gu JR, et al. Peptide ligand-mediated liposome distribution and targeting to EGFR expressing tumor in vivo. *Int J Pharm* (2008) 363:155–61. doi: 10.1016/j.ijpharm.2008.07.012

29. Klutz K, Schaffert D, Willhauck MJ, Grunwald GK, Haase R, Wunderlich N, et al. Epidermal growth factor receptor-targeted (131)I-therapy of liver cancer following systemic delivery of the sodium iodide symporter gene. *Mol Ther* (2011) 19:676–85. doi: 10.1038/mt.2010.296

30. Schafer A, Pahnke A, Schaffert D, van Weerden WM, de Ridder CM, Rodl W, et al. Disconnecting the yin and yang relation of epidermal growth factor receptor (EGFR)-mediated delivery: a fully synthetic, EGFR-targeted gene transfer system avoiding receptor activation. *Hum Gene Ther* (2011) 22:1463–73. doi: 10.1089/hum.2010.231

31. Genta I, Chiesa E, Colzani B, Modena T, Conti B, Dorati R. GE11 peptide as an active targeting agent in antitumor therapy: A minireview. *Pharmaceutics* (2017) 10. doi: 10.3390/pharmaceutics10010002

32. Wei J, Li Z, Yang Y, Ma X, An W, Ma G, et al. A biomimetic VLP influenza vaccine with interior NP/exterior M2e antigens constructed through a temperature shift-based encapsulation strategy. *Vaccine* (2020) 38:5987–96. doi: 10.1016/j.vaccine.2020.07.015

33. Wang Y, Uchida M, Waghwani HK, Douglas T. Synthetic virus-like particles for glutathione biosynthesis. *ACS Synth Biol* (2020) 9:3298–310. doi: 10.1021/acssynbio.0c00368

34. Lu F, Li Z, Sheng Y, Ma Y, Yang Y, Ren Y, et al. Thermal-triggered packing of lipophilic NIR dye IR780 in hepatitis b core at critical ionic strength and cargo-host ratio for improved stability and enhanced cancer phototherapy. *Biomaterials* (2021) 276:121035. doi: 10.1016/j.biomaterials.2021.121035

35. Yan L, Wang Y, Hu T, Mei X, Zhao X, Bian Y, et al. Layered double hydroxide nanosheets: towards ultrasensitive tumor microenvironment responsive synergistic therapy. *J Mater Chem B* (2020) 8:1445–55. doi: 10.1039/C9TB02591J

frontiers | Frontiers in Oncology

TYPE Original Research
PUBLISHED 27 April 2023
DOI 10.3389/fonc.2023.1146008

OPEN ACCESS

EDITED BY
Chunyan Dong,
Tongji University, China

REVIEWED BY
Gianluca Tedaldi,
Laboratory of Biosciences (IRCCS), Italy
Madan Kundu,
Daiichi Sankyo, United States

*CORRESPONDENCE
David Cantú de León
dfcantu@gmail.com
Carlos Pérez-Plasencia
carlos.pplas@gmail.com

†These authors have contributed equally to this work

RECEIVED 16 January 2023
ACCEPTED 14 April 2023
PUBLISHED 27 April 2023

CITATION
Vázquez-Romo R, Millan-Catalan O, Ruíz-García E, Martínez-Gutiérrez AD, Alvarado-Miranda A, Campos-Parra AD, López-Camarillo C, Jacobo-Herrera N, López-Urrutia E, Guardado-Estrada M, Cantú de León D and Pérez-Plasencia C (2023) Pathogenic variant profile in DNA damage response genes correlates with metastatic breast cancer progression-free survival in a Mexican-mestizo population. *Front. Oncol.* 13:1146008. doi: 10.3389/fonc.2023.1146008

Pathogenic variant profile in DNA damage response genes correlates with metastatic breast cancer progression-free survival in a Mexican-mestizo population

Rafael Vázquez-Romo[1†], Oliver Millan-Catalan[2†], Erika Ruíz-García[3], Antonio D. Martínez-Gutiérrez[2], Alberto Alvarado-Miranda[1], Alma D. Campos-Parra[4], César López-Camarillo[5], Nadia Jacobo-Herrera[6], Eduardo López-Urrutia[7], Mariano Guardado-Estrada[8], David Cantú de León[4*] and Carlos Pérez-Plasencia[2,7*]

[1]Departamento de Cirugía de Tumores Mamarios, Instituto Nacional de Cancerología (INCan), Ciudad de México, Mexico, [2]Laboratorio de Genómica, Instituto Nacional de Cancerología (INCan), Ciudad de México, Mexico, [3]Laboratorio de Medicina Traslacional y Departamento de Tumores Gastrointestinales, Instituto Nacional de Cancerología, CDMX, Mexico, [4]Dirección de Investigación, Instituto Nacional de Cancerología (INCan), Ciudad de México, Mexico, [5]Posgrado en Ciencias Genómicas, Universidad Autónoma de la Ciudad de México, Ciudad de México, Mexico, [6]Unidad de Bioquímica, Instituto Nacional de Ciencias Médicas y Nutrición, Salvador Zubirán (INCMNSZ), Ciudad de México, Mexico, [7]Laboratorio de Genómica, Unidad de Biomedicina, FES-IZTACALA, UNAM, Tlalnepantla, Mexico, [8]Laboratorio de Genética, Ciencia Forense, Facultad de Medicina, Universidad Nacional Autónoma de México, Ciudad de México, Mexico

Introduction: Metastatic breast cancer causes the most breast cancer-related deaths around the world, especially in countries where breast cancer is detected late into its development. Genetic testing for cancer susceptibility started with the BRCA 1 and 2 genes. Still, recent research has shown that variations in other members of the DNA damage response (DDR) are also associated with elevated cancer risk, opening new opportunities for enhanced genetic testing strategies.

Methods: We sequenced BRCA1/2 and twelve other DDR genes from a Mexican-mestizo population of 40 metastatic breast cancer patients through semiconductor sequencing.

Results: Overall, we found 22 variants –9 of them reported for the first time– and a strikingly high proportion of variations in ARID1A. The presence of at least one variant in the ARID1A, BRCA1, BRCA2, or FANCA genes was associated with worse progression-free survival and overall survival in our patient cohort.

Discussion: Our results reflected the unique characteristics of the Mexican-mestizo population as the proportion of variants we found differed from that of other global populations. Based on these findings, we suggest routine screening for variants in ARID1A along with BRCA1/2 in breast cancer patients from the Mexican-mestizo population.

KEYWORDS

metastatic breast cancer, DNA damage response, Latin American population, Mexican-mestizo population, Progression free survival (PFS)

1 Introduction

As the number of new breast cancer cases and fatalities continues to rise worldwide (1), detection and treatment of this disease is more of a pressing issue for researchers and health professionals. Widely adopted screening programs have proven efficient at detecting stage I-II cases before they develop further into stage III and compromise survival, effectively decreasing the fatal cases. Yet, a significant amount of these deaths occur in stage IV or metastatic patients (2, 3).

An important aspect of the screening programs that has become increasingly widespread with the advancement of technology is genetic testing for cancer susceptibility. The first surveyed genes were *BRCA 1* and *2*, where germline variants are associated with around 25% of breast cancer cases (4). But recent research has revealed that several other genes that also participate in the DNA damage response (DDR) also confer increased breast cancer risk, such as *PALB2, TP53, RAD50, RAD51D*, and *CHEK2*, among others (5, 6). For example, variants in *PALB2* (Partner and Localizer of *BRCA2*) are associated with an estimated cumulative risk of breast cancer of 14% (7). Somatic alterations, on the other hand, are associated with high-grade tumor progression; for instance, *TP53* variants correlate with metastasis spread and relapse risk (8, 9). Both germline and somatic alterations drive tumor development cooperatively and influence response to treatment (10, 11).

Variants in the DNA damage response (DDR) genes –a complex machinery encompassing several pathways that maintain the integrity of DNA within the cell (12)– produce malfunctioning proteins that restrict the ability of cells to repair DNA lesions, rendering them susceptible to genetic instability and cancer development (13); such is the case of *ARID1A*, a recently studied subunit of the SWI/SNF chromatin remodeler complex whose variants have been associated with breast cancer brain metastasis (14).The presence of these variants also influences treatment choice, as patients carrying them can benefit from treatment alternatives that target the DDR to create synthetic lethality by inhibiting the Poly ADP-ribose (PARP) –a polymerase that synthesizes DNA in the final steps of the repair process– with purpose-designed drugs (15, 16).

Our group is interested in studying the distribution of BRCA variants, particularly in the Mexican-mestizo population, where we have found unreported variants (17, 18), confirming that variation distribution can vary significantly from one geographical location to another (19, 20). So, surveying local populations looking for characteristic individual variations or patterns is an important stepping stone toward universal tailored diagnostics and treatments, especially in Latin American countries where breast cancer is mostly diagnosed in later stages (21).

In this work, we sequenced fourteen DDR genes in a Mexican cohort of 40 metastatic breast cancer patients, searching for an association between variants in DDR genes and response to treatment. The genes we sequenced belong mainly to the DNA Interstrand Crosslink Repair, a DDR pathway that has been recently associated which high tumor burden in breast carcinomas (22); the rest were DNA damage sensors (*ATM, CHK2*) and transcriptional activators (*ARID1A, TP53*) that had been recently associated with metastatic breast cancer (23–25). We found 19 unique variants, from which 9 had not been reported before, and a correlation between the combination of alterations in the *ARID1A, BRCA1, BRCA2*, and *FANCA* genes and progression-free survival. To our knowledge, the association between alterations in DDR genes other than BRCA and treatment response in metastatic breast cancer had not been surveyed yet in the Mexican-mestizo population.

2 Materials and methods

2.1 Patient cohort

This study included prospectively tumor biopsy and clinical data from forty stage-IV breast cancer patients that attended the Instituto Nacional de Cancerología (INCan, Mexico City, Mexico. The study was approved by INCan's Review Board and Ethics Committee (016/010/IBI; CEI/1001/16); all patients signed informed consent. After the surgical excision, tumor biopsies were segmented into two pieces, one for pathological confirmation and another for DNA extraction.

2.2 Patients and clinical outcome assessment

A total of 40 patients were enrolled diagnosed with metastatic breast cancer confirmed by positron emission tomography (PET) and computed tomography (CT) scans. All patients were treated according to the National Comprehensive Cancer Network (NCCN) guidelines. Clinical outcome was evaluated by The Response Evaluation Criteria in Solid Tumors (RECIST Version 1.1) at baseline and at 6 months (26). Progression-free survival (PFS) was defined as the time from the commencement of treatment until disease progression or the last visit. Overall survival (OS) was defined as the time from diagnosis until death or the last visit.

2.3 DNA extraction

Tumor DNA was extracted using the QIAamp DNA Blood Mini kit (Qiagen, cat. no. 51106). following the manufacturer's recommendations. DNA integrity was verified by agarose electrophoresis and the concentration was determined using RNase P Detection Reagent (FAM) (Applied Biosystems, cat. no. 4316831).

2.4 Targeted sequencing

Fourteen DDR genes were selected for sequencing. Two of them, *BRCA1* and *BRCA2*, were amplified using Ion Ampliseq *BRCA 1* and *2* panel (Thermo Fisher Scientific); this panel includes 167 primers pairs in three pools. The remaining genes, *ARID1A, ATM, CHK2, FANCA, FANCB, FANCC, FANCD2, PARP1, PALB2,*

RAD50, RAD51, and *TP53* were amplified with the custom panel IAD94476_197_Designed; this panel includes 440 primers in two pools. (Supplementary Table 1). Libraries were prepared from 25 ng DNA, and amplification of each patient's DDR-genes was identified using a unique Ion Xpress barcode adapter (Thermo Fisher Scientific cat. no. 4471250). For sequencing, we used the Ion PGM Hi-Q Sequencing kit (REFA25589) in the Ion torrent PGM (Personal Genome Machine) instrument (Thermo Fisher Scientific).

2.5 Data analysis

The sequences were aligned to the hg19 human reference genome (GRCh37). The.bam files were exported to the Ion Reporter version 5.18 for variation analysis. Pathogenic and probably pathogenic variants were classified according to the American College of Medical Genetics and Genomics guidelines (27)

Kaplan–Meier curves and Cox regressions were calculated using the survival package in R (R version 4.2.2, we used the survival package version 3.4.0.). Variable selection for the Multivariate Cox regressions was performed using a forward stepwise procedure. Statistical significance was defined as $p < 0.05$ (two sided).

3 Results

The 40 stage-IV screened tumor samples came from patients with a mean age of 53 years, ranging from 27 to 81 (n = 40). Most tumors were ductal (85%) and the remainder, lobular (15%). The molecular type corresponded with previously reported proportions; Luminal A and B tumors were more frequent that HER+ and TNBC. Notably, 16 of the 40 samples came from patients with a family history of cancer (Table 1). Twenty-two of the samples carried at least one variant in the sequenced genes, one had multiple variants in BRCA1, two had multiple variants in TP53, and two had variants in two genes –*ARID1A* and *ATM* or *FANCA* and *TP53* (Figure 1, Table 2)

Overall, we found 19 unique sequence variants in the 22 samples carrying them, 10 had been already identified and 9 were previously unreported. Ten (52%) of the found variants were in the TP53 gene. The most frequent alterations in this gene –c.742C>T and c.215_216insG– were only the second most frequent, while the first was c.3980_3981insC, in ARID1A. Thirteen variants were found only once in the studied population. Strikingly, no variants in the *CHK2, FANCB, FANCC, FANCD2, PALB2, RAD50*, or *RAD51* genes were present in our cohort (Figure 1, Table 3). Pathogenic or likely pathogenic variants are depicted in Supplementary Table 1.

An overall survival analysis was performed considering the patients included with a median follow-up of 5 years (1-13 years). The median PFS of all patients was 6 months (0-45) and median OS was 34 months (1-161). An univariate and multivariate Cox analysis were performed examining the association of the individual variants, with the clinical outcomes (PFS and OS), nevertheless, no significant association was observed (data not shown). So, we considered the genes with highest number of variants observed at the multivariate analysis combined (*ARID1A*, *BRCA1*, *BRCA2* and *FANC* genes*)* and regrouped the variation frequencies of these genes into a single binary variant where at least one variation needed to be

TABLE 1 Clinical characteristics of 40 unrelated metastatic breast cancer patients.

Characteristics	No. (%) (n= 40)
Age, mean (range, years)	53 (27-81)
Menopausal status	
Premenopausal	18 (45)
Postmenopausal	22 (55)
Histology	
Ductal	34 (85)
Lobular	6 (15)
Tumor size	
TX	1 (2.5)
T1	1 (2.5)
T2	4 (10)
T3	7 (17.5)
T4	27 (67.5)
Nodes	
N1	8 (20)
N2	8 (20)
N3	24 (60)
Molecular subtype	
Luminal A	18 (45)
Luminal B	10 (25)
HER+	5 (12.5)
TNBC	7 (17.5)
Cancer family history	
Breast/Ovarian cancer	6 (15)
Other cancers	10 (25)
No	24 (60)
Chemotherapy regime	
Antimitotic	14 (35)
Hormone therapy	12 (30)
Alkylating-antimitotic	10 (25)
Alkylating	4 (10)
Status	
Alive	13 (32.5)
Dead	27 (67.5)

Numbers in parenthesis express percentages.

10.3389/fonc.2023.1146008

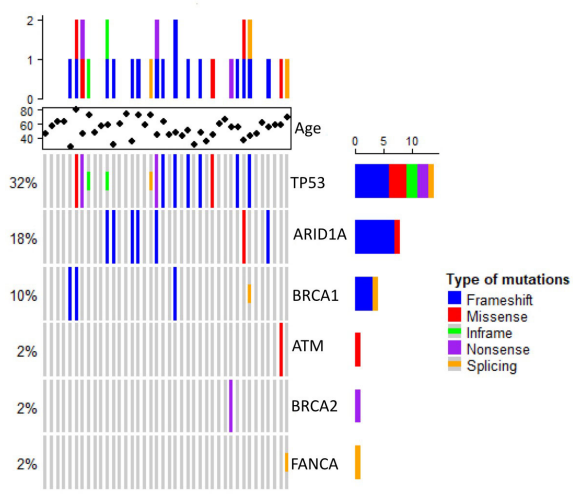

FIGURE 1
Heat map showing somatic variants profiles of metastatic breast cancer.

met. To assess the association between the combination of these variants and clinical outcome, we compared PFS and OS between patient's with or without variants in those genes. Median PFS was 8 months in patients without sequence variants in selected genes, versus 4 months in patients with at least one variant of the genes selected (p-value=0.0025) (Figure 2). Besides, the median OS in patients without variants was 51 months versus 31 months for patients with variants of the genes selected (p-value= 0.014) (Figure 3).

A univariate and multivariate analysis was performed comparing the presence/absence of pathogenic variants in at least one selected gene and clinical outcome (PFS and OS). At PFS Cox models, the presence of at least one pathogenic variant, demonstrated to be predictors of PFS (univariate, HR: 3.3 (95% CI 1.5-7.5), p-value=0.004) (multivariate, HR: 3.74 (95% CI 1.44-9.74), p-value=0.006). Additionally, at OS Cox models, the presence of at least one pathogenic variant, also demonstrated to be predictors of OS (univariate, HR: 2.7 (95% CI 1.2-6), p-value=0.017) (multivariate HR: 2.87 (95% CI 1.07-7.67), p-value=0.035) (Table 4).

TABLE 2 Genes with variants in unrelated metastatic breast cancer samples.

ARID1A	ATM	BRCA1	BRCA2	FANCA	TP53
M11	M15	M05 (3)	M31	M42	M06 (2)
M12	M33	M34			M08
M15	M40				M18 (2)
M16					M20 (3)
M19					M22
M38					M24
					M26
					M28
					M32
					M42

Numbers in parentheses indicate the different variations present in the samples.

4 Discussion

Variants in DNA damage response (DDR) genes in cancer are important biomarkers for treatment selection and are also functionally important, since malfunctioning DDR can potentially increase genomic instability, eventually leading to treatment resistance or relapse (Reviewed in 28). Here we analyzed a 40-patient cohort of metastatic breast cancer patients in search for variations in DDR genes and found 13 previously identified variants and 9 that had not been reported before. These findings contribute to the understanding of the genomic landscape of metastatic breast cancer in the Mexican-mestizo population which, due to its diverse ancestry (29), is likely to differ from the mostly Caucasian populations of North America (30) and Europe (31) where the genomic characterizations of metastatic breast cancer has been reported.

Sequence variants in *TP53* accounted for roughly half of our findings. A similar proportion was previously reported in metastatic tumors (31) but in breast tumors in general, *TP53* variants accounted for less than 10% (32), highlighting the high risk of metastasis associated with *TP53* variants. Half (5/10) of the variants that we report here had not been reported before, suggesting they are exclusive or more frequent in the Mexican-mestizo population and underlining the importance of studying local populations.

Variants in *PALB2* are usually reported in frequencies around 1%, second to the BRCA genes at 3-5% (6, 33, 34). The absence of is *PALB2* variants in our cohort is similar to the low incidence observed in a separate study where only two of 115 patients carried *PALB2* variants (35), suggesting that *PALB2* variants are scarce in the Mexican-mestizo population.

We found a significant association between the presence of at least one pathogenic variant and worse PFS and OS. Three of these genes are related to the DNA Interstrand Crosslink Repair: BRCA1 and BRCA2 are the quintessential breast cancer susceptibility genes (36). *FANCA* variations are the most frequent in Fanconi anemia (37) and, according to recent reports, it might be the only *FANC* gene involved in hereditary cancer (38). These findings bolster previous reports on the association between variations in individual genes of the DNA Interstrand Crosslink Repair pathway and breast cancer susceptibility in Iranian (39) and Chinese populations (40). Interestingly, while there is evidence that variations in the DDR pathways –particularly HR– sensitize several cancer types to chemotherapy (15), secondary variants in these genes can generate resistance to alkylating agent therapy (41, 42). These findings suggest that the variants in *BRCA1, BRCA2*, and *FANCA*, associated with worse prognosis in our sample set, might have contributed to chemotherapy resistance. The mechanisms underlying this phenomenon will undoubtedly motivate further analysis. Sequence variants in the fourth gene, *ARID1A*, have been associated with breast cancer brain metastasis, though the specific variants that we found had not been reported before (14).

TABLE 3 Variants found in 40 unrelated metastatic breast cancer samples.

Gene	Coding Sequence Position	AminoAcid Change	Significance*	dbSNP	Frequency
ARID1A	c.3977_3980delCGCA	p.Pro1326ArgfsTer154	LP	not reported	2
ARID1A	c.3980_3981insC	p.Gln1327HisfsTer11	LP	not reported	4
ATM	c.6861delA	p.Val2288SerfsTer22	LP	not reported	1
ATM	c.8124T>A	p.Asp2708Glu	LP	rs587781990	2
BRCA1	c.3759_3760delTA	p.Lys1254GlufsTer12	P	rs80357520	1
BRCA1	c.5054_5060delCTCATGT	p.Thr1685MetfsTer3	LP	not reported	2
BRCA1	c.5277 + 1delG	splice site	P	rs273901754	1
BRCA2	c.5635G>T	p.Glu1879Ter	P	rs55996097	1
FANCA	c.709 + 5G>A	splice site	P	rs759877008	1
TP53	c.1123C>T	p.Gln375Ter	LP	rs1555524156	1
TP53	c.215_216insG	p.Val73ArgfsTer76	LP	not reported	3
TP53	c.522_539delGCGCTGCCCCCACCATGA	p.Pro177_Cys182del	P	not reported	1
TP53	c.560-1G>A	splice site	P	rs1202793339	1
TP53	c.586C>T	p.Arg196Ter	P	rs397516435	1
TP53	c.626_627delGA	p.Arg209LysfsTer6	P	rs1057517840	1
TP53	c.718delA	p.Ser240ValfsTer7	LP	not reported	1
TP53	c.742C>T	p.Arg248Trp	P	rs121912651	3
TP53	c.815_817dup	p.Val272_Arg273insLeu	P	not reported	1
TP53	c.866_873delTCCGCAAG	p.Leu289GlnfsTer14	LP	not reported	1

*Clinical Significance according to stablished criteria [24]. LP, likely pathogenic; P, pathogenic.

In Latin America, breast cancer is detected late in its development (21) a trend that can only be reverted through optimized screening strategies. Since tumors with altered *ARID1A* are sensible to PARP inhibitors (43) and its variants are frequent in cohorts as small as the 40 patients that we report here, we suggest screening tumors for variants *ARID1A* in the Mexican-mestizo population. Such screening might broaden the treatment options for breast cancer patients, as these variants have been associated with enhanced effects of treatments such as ATR inhibitors and Gemcitabine in ovarian cancer (44). Further studies will confirm

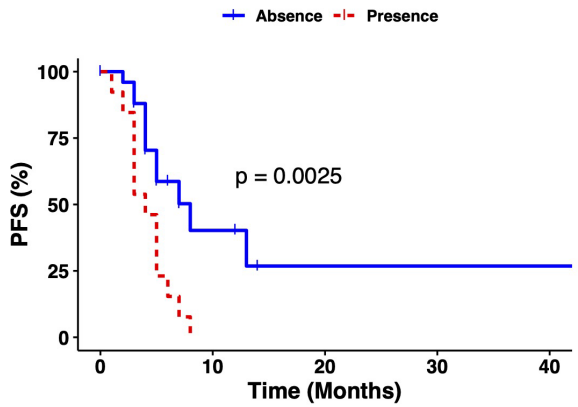

FIGURE 2
The presence of at least one variant in *ARID1A, BRCA1, BRCA2 or FANCA* genes correlates with lower PFS.

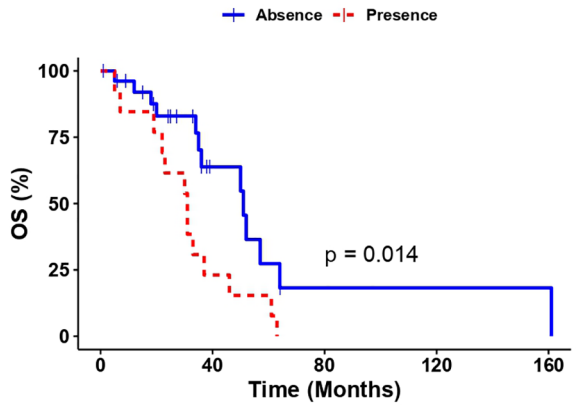

FIGURE 3
The presence of at least one variant in *ARID1A, BRCA1, BRCA2 or FANCA* genes correlates with lower OS.

TABLE 4 Univariate and Multivariate analysis of clinical characteristics and variants in grouped genes (*ARID1A + BRCA1 + BRCA2 + FANCA)* in the analyzed population.

	PFS				OS			
	Univariate		Multivariate		Univariate		Multivariate	
Characteristic	HR (IC 95%)	p-value	HR (IC 95%)	p-value	HR (IC 95%)	p-value	HR (IC 95%)	p-value
Histology (Ductual vs Lobulillar)	1.1 (0.39-3.3)	0.82			0.71 (0.24-2.1)	0.54		
Molecular classification* (Luminal A vs Luminal B vs HER enriched vs TNBC)	0.88 (0.61-1.3)	0.51	0.53 (0.03-9.18)	0.669	1.3 (0.81-2)	0.3	0.50 (0.02-9.77)	0.651
Estrogens (Negative vs Positive)	1.1 (0.47-2.7)	0.79	1.02 (0.00-106.)	0.992	0.4 (0.15-1.1)	0.067	0.29 (0.00-31.9)	0.612
Progesterone (Negative vs Positive)	0.71 (0.31-1.7)	0.43	0.23 (0.02-2.13)	0.197	0.4 (0.16-1)	0.051	0.22 (0.02-2.46)	0.223
HER2 (Negative vs Positive)	0.5 (0.19-1.3)	0.17	1.54 (0.09-24.8)	0.76	0.53 (0.18-1.5)	0.25	1.48 (0.08-27.6)	0.789
KI67 (Low vs High)	1 (0.98-1)	0.93	0.99 (0.97-1.02)	0.714	1 (0.99-1)	0.58	0.99 (0.96-1.01)	0.422
Oncologic history No vs Yes	0.7 (0.31-1.6)	0.39			0.46 (0.2-1.1)	0.076		
Chemotherapy regime* (Antimitotic vs Hormone therapy vs Alkylating-antimitotic vs Alkylating)	0.94 (0.78-1.1)	0.47	0.85 (0.69-1.04)	0.116	0.99 (0.83-1.2)	0.94	0.85 (0.68-1.07)	0.177
Radiotherapy (Negative vs Positive)	0.67 (0.29-1.5)	0.35			0.57 (0.24-1.4)	0.2		
ARID1A + BRCA1 + BRCA2 + FANCA (Absent vs Present)	3.3 (1.5-7.5)	**0.004**	3.74 (1.44-9.74)	**0.006**	2.7 (1.2-6)	**0.017**	2.87 (1.07-7.67)	**0.035**

*All mentioned characteristics were compared in the statistical analysis.
The bold values denote statistically significant P values.

whether the high prevalence of *ARID1A* variants in tumor samples is valid for other Latin American populations and whether there is a functional relationship between *ARID1A* and the DNA Interstrand Crosslink Repair genes. Additionally, whether the *ARID1A* variants we observed were acquired during tumor development or already present in the germline and thus related to cancer susceptibility besides response to treatment remains to be determines. If these variants are germline, *ARID1A* might be a better indicator of cancer risk than PALB2 in the Mexican-mestizo populations.

Our study was limited by the number of genes sequenced and the relatively low number of samples; additionally, the sequencing was performed only from tumor. A larger sample would provide a more comprehensive perspective of the variations in these and other genes; however, our sample included only metastatic breast cancer patients, which represent less than 20% of the total breast cancer cases (45, 46).

5 Conclusions

Our findings contribute to the description of the sequence variation landscape of metastatic breast cancer in the Mexican-mestizo population. We found the expected high frequency variants in TP53 and *BRCA 1* and *2*; conversely, *PALB2* variants seem scarce compared to other reported populations. The presence of at least one pathogenic variant in the *ARID1A, BRCA1, BRCA2*, or *FANCA* genes remains predictor of worse progression-free survival and overall survival.

Data availability statement

All data generated or analyzed during this study are included in this published article and are available from the corresponding author on reasonable request.

Ethics statement

The studies involving human participants were reviewed and approved by National Cancer Institute of México, Ethics and Scientific Committee. The patients/participants provided their written informed consent to participate in this study.

Author contributions

Conceptualization, CP-P, DC and RV-R; Data curation, AM-G; Formal analysis, OM-C, AC-P, RV-R and AA-M; Investigation, DC;

Methodology, ER-G, OM-C, MG-E and NJ-H; Resources, CL-C; Supervision, DC and CP-P; Writing – original draft, CP-P; Writing – review and editing, EL-U and CP-P. All authors contributed to the article and approved the submitted version.

Funding

This research was funded by Instituto Nacional de Cancerología Research funds.

Acknowledgments

OM-C is a doctoral student from Programa de Doctorado en Ciencias Biológicas, Universidad Nacional Autónoma de México (UNAM) and was supported by CONACYT (451334). We want to acknowledge administrative support from the Institutional Research Deputy.

Conflict of interest

The authors declare that the research was conducted in the absence of any commercial or financial relationships that could be construed as a potential conflict of interest.

Publisher's note

Supplementary material

The Supplementary Material for this article can be found online at: https://www.frontiersin.org/articles/10.3389/fonc.2023.1146008/full#supplementary-material

References

1. Sung H, Ferlay J, Siegel RL, Laversanne M, Soerjomataram I, Jemal A, et al. Global cancer statistics 2020: GLOBOCAN estimates of incidence and mortality worldwide for 36 cancers in 185 countries. *CA Cancer J Clin* (2021) 71:209–49. doi: 10.3322/caac.21660

2. Dillekås H, Rogers MS, Straume O. Are 90% of deaths from cancer caused by metastases? *Cancer Med-us* (2019) 8:5574–6. doi: 10.1002/cam4.2474

3. Daily K, Douglas E, Romitti PA, Thomas A. Epidemiology of *De Novo* metastatic breast cancer. *Clin Breast Cancer* (2021) 21:302–8. doi: 10.1016/j.clbc.2021.01.017

4. Mahdavi M, Nassiri M, Kooshyar MM, Vakili-Azghandi M, Avan A, Sandry R, et al. Hereditary breast cancer; genetic penetrance and current status with BRCA. *J Cell Physiol* (2019) 234:5741–50. doi: 10.1002/jcp.27464

5. Lang G-T, Shi J-X, Huang L, Cao A-Y, Zhang C-H, Song C-G, et al. Multiple cancer susceptible genes sequencing in BRCA-negative breast cancer with high hereditary risk. *Ann Transl Med* (2020) 8:1417–7. doi: 10.21037/atm-20-2999

6. Kuusisto KM, Bebel A, Vihinen M, Schleutker J, Sallinen S-L. Screening for BRCA1, BRCA2, CHEK2, PALB2, BRIP1, RAD50, and CDH1 mutations in high-risk Finnish BRCA1/2-founder mutation-negative breast and/or ovarian cancer individuals. *Breast Cancer Res* (2011) 13:R20. doi: 10.1186/bcr2832

7. Antoniou AC, Casadei S, Heikkinen T, Barrowdale D, Pylkäs K, Roberts J, et al. Breast-cancer risk in families with mutations in PALB2. *N Engl J Med* (2014) 371:497–506. doi: 10.1056/nejmoa1400382

8. Guerra E, Cimadamore A, Simeone P, Vacca G, Lattanzio R, Botti G, et al. p53, cathepsin d, bcl-2 are joint prognostic indicators of breast cancer metastatic spreading. *BMC Cancer* (2016) 16:649. doi: 10.1186/s12885-016-2713-3

9. Zhang P, Kitchen-Smith I, Xiong L, Stracquadanio G, Brown K, Richter PH, et al. Germline and somatic genetic variants in the p53 pathway interact to affect cancer risk, progression, and drug response. *Cancer Res* (2021) 81:1667–80. doi: 10.1158/0008-5472.can-20-0177

10. Grünewald TGP, Delattre O. Cooperation between somatic mutations and germline susceptibility variants in tumorigenesis – a dangerous liaison. *Mol Cell Oncol* (2016) 3:e1086853. doi: 10.1080/23723556.2015.1086853

11. Pennington KP, Walsh T, Harrell MI, Lee MK, Pennil CC, Rendi MH, et al. Germline and somatic mutations in homologous recombination genes predict platinum response and survival in ovarian, fallopian tube, and peritoneal carcinomas. *Clin Cancer Res* (2014) 20:764–75. doi: 10.1158/1078-0432.ccr-13-2287

12. Kciuk M, Bukowski K, Marciniak B, Kontek R. Advances in DNA repair–emerging players in the arena of eukaryotic DNA repair. *Int J Mol Sci* (2020) 21:3934. doi: 10.3390/ijms21113934

13. Suh KJ, Ryu HS, Lee K-H, Kim H, Min A, Kim T-Y, et al. Prognostic effects of abnormal DNA damage response protein expression in breast cancer. *Breast Cancer Res Tr* (2019) 175:117–27. doi: 10.1007/s10549-019-05128-9

14. Morgan AJ, Giannoudis A, Palmieri C. The genomic landscape of breast cancer brain metastases: a systematic review. *Lancet Oncol* (2021) 22:e7–e17. doi: 10.1016/s1470-2045(20)30556-8

15. Patel PS, Algouneh A, Hakem R. Exploiting synthetic lethality to target BRCA1/2-deficient tumors: where we stand. *Oncogene* (2021) 40:3001–14. doi: 10.1038/s41388-021-01744-2

16. Rose M, Burgess JT, O'Byrne K, Richard DJ, Bolderson E. PARP inhibitors: clinical relevance, mechanisms of action and tumor resistance. *Front Cell Dev Biol* (2020) 8:564601. doi: 10.3389/fcell.2020.564601

17. Vaca-Paniagua F, Alvarez-Gomez RM, Fragoso-Ontiveros V, Vidal-Millan S, Herrera LA, Cantú D, et al. Full-exon pyrosequencing screening of BRCA germline mutations in Mexican women with inherited breast and ovarian cancer. *PloS One* (2012) 7:e37432. doi: 10.1371/journal.pone.0037432

18. Millan-Catalan O, Campos-Parra AD, Vázquez-Romo R, de León DC, Jacobo-Herrera N, Morales-González F, et al. A multi-center study of BRCA1 and BRCA2 germline mutations in Mexican-mestizo breast cancer families reveals mutations unreported in Latin American population. *Cancers* (2019) 11:1246. doi: 10.3390/cancers11091246

19. Rebbeck TR, Friebel TM, Friedman E, Hamann U, Huo D, Kwong A, et al. Mutational spectrum in a worldwide study of 29,700 families with BRCA1 or BRCA2 mutations. *Hum Mutat* (2018) 39:593–620. doi: 10.1002/humu.23406

20. Macchini M, Centonze F, Peretti U, Orsi G, Militello AM, Valente MM, et al. Epidemiology and geographic distribution of BRCA1-2 and DNA damage response genes pathogenic variants in pancreatic ductal adenocarcinoma patients. *Cancer Treat Rev* (2022) 104:102357. doi: 10.1016/j.ctrv.2022.102357

21. Pinto JA, Pinillos L, Villarreal-Garza C, Morante Z, Villarán MV, Mejía G, et al. Barriers in Latin America for the management of locally advanced breast cancer. *Ecancermedicalscience* (2019) 13:897. doi: 10.3332/ecancer.2019.897

22. Mei P, Freitag CE, Wei L, Zhang Y, Parwani AV, Li Z. High tumor mutation burden is associated with DNA damage repair gene mutation in breast carcinomas. *Diagn Pathol* (2020) 15:50. doi: 10.1186/s13000-020-00971-7

23. Cheng X, Zhao J-X, Dong F, Cao X-C. ARID1A mutation in metastatic breast cancer: a potential therapeutic target. *Front Oncol* (2021) 11:759577. doi: 10.3389/fonc.2021.759577

24. Bai H, Yu J, Jia S, Liu X, Liang X, Li H. Prognostic value of the TP53 mutation location in metastatic breast cancer as detected by next-generation sequencing. *Cancer Manage Res* (2021) 13:3303–16. doi: 10.2147/cmar.s298729

25. Stucci LS, Internò V, Tucci M, Perrone M, Mannavola F, Palmirotta R, et al. The ATM gene in breast cancer: its relevance in clinical practice. *Genes-basel* (2021) 12:727. doi: 10.3390/genes12050727

26. Eisenhauer EA, Therasse P, Bogaerts J, Schwartz LH, Sargent D, Ford R, et al. New response evaluation criteria in solid tumours: revised RECIST guideline (version 1.1). *Eur J Cancer* (2009) 45:228–47. doi: 10.1016/j.ejca.2008.10.026

27. Hampel H, Bennett RL, Buchanan A, Pearlman R, Wiesner GLCommittee GDG American College of Medical Genetics and Genomics Professional Practice and Guidelines Committee and National Society of Genetic Counselors Practice Guidelines. A practice guideline from the American college of medical genetics and genomics and the national society of genetic counselors: referral indications for cancer predisposition assessment. *Genet Med* (2015) 17:70–87. doi: 10.1038/gim.2014.147

28. Huang R, Zhou P-K. DNA Damage repair: historical perspectives, mechanistic pathways and clinical translation for targeted cancer therapy. *Signal Transduct Target Ther* (2021) 6:254. doi: 10.1038/s41392-021-00648-7

29. Moreno-Estrada A, Gignoux CR, Fernández-López JC, Zakharia F, Sikora M, Contreras AV, et al. The genetics of Mexico recapitulates native American substructure and affects biomedical traits. *Science* (2014) 344:1280–5. doi: 10.1126/science.1251688

30. Paul MR, Pan T, Pant DK, Shih NNC, Chen Y, Harvey KL, et al. Genomic landscape of metastatic breast cancer identifies preferentially dysregulated pathways and targets. *J Clin Invest* (2020) 130:4252–65. doi: 10.1172/jci129941

31. Bertucci F, Ng CKY, Patsouris A, Droin N, Piscuoglio S, Carbuccia N, et al. Genomic characterization of metastatic breast cancers. *Nature* (2019) 569:560–4. doi: 10.1038/s41586-019-1056-z

32. Schon K, Tischkowitz M. Clinical implications of germline mutations in breast cancer: TP53. *Breast Cancer Res Tr* (2018) 167:417–23. doi: 10.1007/s10549-017-4531-y

33. Shimelis H, LaDuca H, Hu C, Hart SN, Na J, Thomas A, et al. Triple-negative breast cancer risk genes identified by multigene hereditary cancer panel testing. *Jnci J Natl Cancer Inst* (2018) 110:855–62. doi: 10.1093/jnci/djy106

34. Cragun D, Weidner A, Tezak A, Clouse K, Pal T. Cancer risk management among female BRCA1/2, PALB2, CHEK2, and ATM carriers. *Breast Cancer Res Tr* (2020) 182:421–8. doi: 10.1007/s10549-020-05699-y

35. Gómez-Flores-Ramos L, Barraza-Arellano AL, Mohar A, Trujillo-Martínez M, Grimaldo L, Ortiz-Lopez R, et al. Germline variants in cancer genes from young breast cancer Mexican patients. *Cancers* (2022) 14:1647. doi: 10.3390/cancers14071647

36. Armstrong N, Ryder S, Forbes C, Ross J, Quek RG. A systematic review of the international prevalence of BRCA mutation in breast cancer. *Clin Epidemiol* (2019) 11:543–61. doi: 10.2147/clep.s206949

37. Solomon PJ, Margaret P, Rajendran R, Ramalingam R, Menezes GA, Shirley AS, et al. A case report and literature review of fanconi anemia (FA) diagnosed by genetic testing. *Ital J Pediatr* (2015) 41:38. doi: 10.1186/s13052-015-0142-6

38. del Valle J, Rofes P, Moreno-Cabrera JM, López-Dóriga A, Belhadj S, Vargas-Parra G, et al. Exploring the role of mutations in fanconi anemia genes in hereditary cancer patients. *Cancers* (2020) 12:829. doi: 10.3390/cancers12040829

39. Abbasi S, Rasouli M. A rare FANCA gene variation as a breast cancer susceptibility allele in an Iranian population. *Mol Med Rep* (2017) 15:3983–8. doi: 10.3892/mmr.2017.6489

40. Pan Z-W, Wang X-J, Chen T, Ding X-W, Jiang X, Gao Y, et al. Deleterious mutations in DNA repair gene FANCC exist in BRCA1/2-negative Chinese familial breast and/or ovarian cancer patients. *Front Oncol* (2019) 9:169. doi: 10.3389/fonc.2019.00169

41. Edwards SL, Brough R, Lord CJ, Natrajan R, Vatcheva R, Levine DA, et al. Resistance to therapy caused by intragenic deletion in BRCA2. *Nature* (2008) 451:1111–5. doi: 10.1038/nature06548

42. Imyanitov E, Sokolenko A. Mechanisms of acquired resistance of BRCA1/2-driven tumors to platinum compounds and PARP inhibitors. *World J Clin Oncol* (2021) 12:544–56. doi: 10.5306/wjco.v12.i7.544

43. Shen J, Peng Y, Wei L, Zhang W, Yang L, Lan L, et al. ARID1A deficiency impairs the DNA damage checkpoint and sensitizes cells to PARP inhibitors. *Cancer Discovery* (2015) 5:752–67. doi: 10.1158/2159-8290.cd-14-0849

44. Mullen J, Kato S, Sicklick JK, Kurzrock R. Targeting ARID1A mutations in cancer. *Cancer Treat Rev* (2021) 100:102287. doi: 10.1016/j.ctrv.2021.102287

45. Siegel RL, Miller KD, Fuchs HE, Jemal A. Cancer statistics, 2022. *CA Cancer J Clin* (2022) 72:7–33. doi: 10.3322/caac.21708

46. Weigelt B, Peterse JL, van't Veer LJ. Breast cancer metastasis: markers and models. *Nat Rev Cancer* (2005) 5:591–602. doi: 10.1038/nrc1670

frontiers | Frontiers in Oncology

TYPE Original Research
PUBLISHED 03 May 2023
DOI 10.3389/fonc.2023.1105117

OPEN ACCESS

EDITED BY
Chunyan Dong,
Tongji University, China

REVIEWED BY
Helena Chang,
UCLA Health System, United States
Marcos Lopez,
University of Puerto Rico, Puerto Rico
Sarrah Widatalla,
Roche Diagnostics, United States

*CORRESPONDENCE
Jing Zhang
Jing_Zhang@whu.edu.cn
Qing Zhang
Qing.Zhang@UTSouthwestern.edu

RECEIVED 22 November 2022
ACCEPTED 19 April 2023
PUBLISHED 03 May 2023

CITATION
Yan C, Gao R, Gao C, Hong K, Cheng M, Liu X, Zhang Q and Zhang J (2023) FDXR drives primary and endocrine-resistant tumor cell growth in ER+ breast cancer via CPT1A-mediated fatty acid oxidation. *Front. Oncol.* 13:1105117. doi: 10.3389/fonc.2023.1105117

FDXR drives primary and endocrine-resistant tumor cell growth in ER+ breast cancer via CPT1A-mediated fatty acid oxidation

Chaojun Yan[1], Ronghui Gao[1], Chuan Gao[1], Kai Hong[2], Meng Cheng[3], Xiaojing Liu[4], Qing Zhang[5,6]* and Jing Zhang[1]*

[1]Department of Thyroid and Breast Surgery, Medical Research Institute, Frontier Science Center for Immunology and Metabolism, Zhongnan Hospital of Wuhan University, Wuhan University, Wuhan, China, [2]Department of Medical Ultrasound, Tongji Hospital, Tongji Medical College, Huazhong University of Science and Technology, Wuhan, China, [3]Lineberger Comprehensive Cancer Center, University of North Carolina School of Medicine, Chapel Hill, NC, United States, [4]Department of Pharmacology and Cancer Biology, Duke University School of Medicine, Durham, NC, United States, [5]Department of Pathology, University of Texas Southwestern Medical Center, Dallas, TX, United States, [6]Simmons Comprehensive Cancer Center, University of Texas Southwestern Medical Center, Dallas, TX, United States

Background: The majority of breast cancers (BCs) expressing estrogen receptor (ER) have shown endocrine resistance. Our previous study demonstrated that ferredoxin reductase (FDXR) promoted mitochondrial function and ER+ breast tumorigenesis. But the underlying mechanism is not clear.

Methods: Liquid chromatography (LC) tandem mass spectrometry (MS/MS)-based metabolite profiling was utilized to reveal the metabolites regulated by FDXR. RNA microarray was utilized to determine the potential downstream targets of FDXR. Seahorse XF24 analyzer was performed to analyze the FAO-mediated oxygen consumption rate (OCR). Q-PCR and western blotting assays were used to measure expression levels of FDXR and CPT1A. MTS, 2D colony formation and anchorage-independent growth assays were used to evaluate the effects of FDXR or drug treatments on tumor cell growth of primary or endocrine-resistant breast cancer cells.

Results: We found that depletion of FDXR inhibited fatty acid oxidation (FAO) by suppressing CPT1A expression. Endocrine treatment increased the expression levels of both FDXR and CPT1A. Further, we showed that depletion of FDXR or FAO inhibitor etomoxir treatment reduced primary and endocrine-resistant breast cancer cell growth. Therapeutically, combining endocrine therapy with FAO inhibitor etomoxir synergistically inhibits primary and endocrine-resistant breast cancer cell growth.

Discussion: We reveal that the FDXR-CPT1A-FAO signaling axis is essential for primary and endocrine-resistant breast cancer cell growth, thus providing a potential combinatory therapy against endocrine resistance in ER+ breast cancer.

KEYWORDS

breast cancer, endocrine resistance, ferredoxin reductase, palmitoyltransferase 1A, fatty acid oxidation, combination therapy

Introduction

Breast cancer is the leading cause of cancer death among women. Approximately 75% of breast cancer is estrogen receptor-positive (ER+), which leads to the majority of breast cancer deaths (1–3). Despite treatment with antiestrogen therapy, up to 50% of patients with ER+ breast cancer do not benefit from these treatments due to intrinsic or acquired resistance (4–9). Recently, scientists have elucidated altered molecular signal transduction pathways and genetic driver mutations involved in the development of endocrine resistance, thereby identifying novel therapeutic targets to improve patient outcomes, such as mTOR inhibitors or cyclin-dependent kinase (CDK) 4/6 inhibitors; however, there are also similar problems with intrinsic or acquired resistance in patients (10–19), highlighting the urgent need for additional effective therapies.

Altered metabolism, which tumorigenesis heavily depends on to support uncontrolled cell proliferation, is a hallmark of cancer (20, 21). Cancer metabolic programs include the reprogramming of glycolysis, glutaminolysis, oxidative phosphorylation, fatty acid metabolism, and one-carbon metabolism, which provide essential energy, biosynthesis factors and intermediates for tumor growth, division and redox homeostasis (22). Therefore, tumor cell metabolism has been considered the Achilles' heel of cancer and is a successful therapeutic target (23–25). For example, the mitochondrial complex I inhibitor metformin is approved for the treatment of type 2 diabetes and has been reported to possess anticancer activity in various investigations and clinical trials (26–30). The fatty acid oxidation inhibitor perhexiline is approved to treat angina and exhibits anticancer effects *in vitro* and *in vivo* (31–33). Although targeting cancer metabolic alterations holds promise, identifying novel predictive biomarkers is needed to lead to precision therapy (23).

Emerging evidence has shown that tumor cells derive most of their ATP from mitochondria-mediated oxidative phosphorylation that is mainly driven by glucose metabolism, glutaminolysis and fatty acid oxidation (34–38). Recent evidence has demonstrated that mitochondrial oxidative metabolism drives therapeutic resistance, suggesting an important role of mitochondrial inhibitors in preventing cancer progression (39, 40). ER+ breast cancer cells depend more on mitochondrial function to provide the essential ATP needed for survival than other subtypes of breast cancer (35, 41). Therefore, identifying the mechanisms that control mitochondrial function in ER+ breast cancer will potentially lead to the development of novel therapeutic interventions. Research from our group and others has demonstrated that the proline hydroxylase EglN2 is an estrogen-responsive gene that is highly expressed in ER+ breast cancer, including luminal A and B subtypes, and contributes to breast tumorigenesis (42, 43). We also discovered a novel function of EglN2 as a transcription coactivator that interacts with NRF1 and PGC1α to maintain mitochondrial function during hypoxia (44). FDXR, a mitochondrial flavoprotein, is known to initiate electron transport for cytochrome p450 from NADPH, leading to increased reactive oxygen species (ROS) production (45–47), and acts as a key downstream target gene of the EglN2-NRF1-PGC1α complex, which modulates mitochondrial function and cell proliferation in ER+ breast cancer cells (44). However, the mechanism by which FDXR regulates altered mitochondrial function and supports ER+ breast tumorigenesis is poorly defined.

Here, through an integrative targeted metabolomics assay and gene expression profiling, we showed that FDXR promoted fatty acid oxidation (FAO) by positively regulating CPT1A expression and illustrated that the FDXR-CPT1A-FAO axis was responsible for primary and endocrine-resistant breast cancer cell growth. Furthermore, combined endocrine therapy with FAO inhibitors exerted a synergistic effect on primary and endocrine-resistant breast tumor cell growth. We identified a new FDXR-CPT1A-FAO signaling axis as a promising target for the development of therapies against endocrine resistance in ER+ breast cancer.

Abbreviations: BCs, breast cancers; CPT1A, palmitoyltransferase 1A; ER, estrogen receptor; ER+, estrogen receptor positive; EglN2, Egl-9 family hypoxia inducible factor 2; FAO, fatty acid oxidation; FCCP, Carbonyl cyanide 4-(trifluoromethoxy) phenylhydrazone; FDXR, ferredoxin reductase; NRF1, Nuclear Respiratory Factor 1; OCR, oxygen consumption rate; PGC1α, PPARG Coactivator 1 Alpha.

Materials and methods

Cell culture and reagents

MCF7 and 293T cells were cultured in Dulbecco's modified Eagle medium (DMEM, Sigma–Aldrich) containing 10% fetal bovine serum (FBS) plus 1% penicillin–streptomycin. T47D cells were cultured in RPMI-1640 (Sigma–Aldrich) containing 10% fetal bovine serum with 1% penicillin–streptomycin. Tamoxifen- or fulvestrant-resistant T47D or MCF7 cells were developed by continuous treatment with tamoxifen (100 nM, > 6 months) or fulvestrant (100 nM, > 4 months), the resistant derivatives were selected when the initially sensitive cells resumed the comparable growth rates to the parental cells, and these cells were cultured in phenol-red free RPMI-1640 medium (Gibco) containing 10% heat-inactivated charcoal-stripped FBS, 1% penicillin–streptomycin and 100 nM 4-OH-tamoxifen or fulvestrant (48, 49). Following viral infection, the cells were maintained in the presence of G418 (100 μg/mL) or puromycin (2 μg/mL) depending on the vector. All cells were maintained in an incubator at 37°C and 5% CO_2. 4-OH-tamoxifen, fulvestrant and etomoxir were obtained from Sigma –Aldrich. DMNQ and TEMPO were purchased from Selleck.

Western blotting and antibodies

EBC buffer (50 mM Tris pH 8.0, 120 mM NaCl, 0.5% NP40, 0.1 mM EDTA and 10% glycerol) supplemented with complete protease inhibitor (Roche Applied Biosciences) was used to harvest whole cell lysates. Cell lysate concentrations were measured by the Bradford assay (ThermoFisher Scientific), and equal amounts of proteins were loaded onto an SDS-polyacrylamide gel, separated by electrophoresis and blotted onto a nitrocellulose membrane (Millipore). Rabbit FDXR (15584-1-AP) and CPT1A antibodies (15184-1-AP) were purchased from Proteintech. Mouse Vinculin (V9131) and mouse Flag (F3165) antibodies were

purchased from Sigma–Aldrich. Peroxidase-conjugated goat anti-mouse (170-6516) and peroxidase-conjugated goat anti-rabbit (1706515) secondary antibodies were purchased from Bio-Rad.

Plasmids

Full-length FLAG and HA double-tagged FDXR was amplified by PCR and cloned into the pBABE-puro vector. A KOD-Plus Mutagenesis Kit (SMK-101, TOYOBO) was used to construct FDXR mutants. All plasmids were sequenced to confirm validity.

Virus production and infection

293T packaging cell lines were used for lentiviral amplification. Lentiviral infection was carried out as previously described (50). Briefly, posttransfection with Lipofectamine 3000, viruses were collected at 48 and 72 h. After being passed through 0.45 μm filters, appropriate amounts of viruses were used to infect target cells in the presence of 8 μg/ml polybrene (Sigma–Aldrich). Subsequently, target cell lines underwent appropriate antibiotic selection.

siRNAs and lentiviral shRNA vectors

Nontargeting siRNA was obtained from Dharmacon (catalog number: D0012100220). FDXR siRNA (FDXR si434) with the targeting sequence GCUCAGCAGCAUUGGGUAUAA was obtained from Dharmacon.

Lentiviral FDXR shRNAs were obtained from the Broad Institute TRC shRNA library. The target sequences are as follows:

Ctrl shRNA: AACAGTCGCGTTTGC GACTGG;
FDXR (434): GCTCAGCAGCATTGGGTATAA;
FDXR (433): CCATTTCTCCACACAGGAGAA.

Oxygen consumption rate (OCR) measurement

Extracellular oxygen consumption was determined by measuring the OCRs using a Seahorse XF24 extracellular flux analyzer (Seahorse Bioscience). Approximately 1×10^5 of the indicated cells were seeded into an XF24 cell culture microplate 24 h before the assay. For OCR analysis, baseline mitochondrial respiration was established by recording extracellular oxygen concentrations at several time points. Respiration not linked to mitochondrial ATP synthesis was measured after adding 1 μM oligomycin through an automated injection port of the XF24. Uncoupled respiration measurements were obtained after adding 1 μM FCCP.

Metabolomics analysis

Intracellular metabolites were prepared and analyzed by LC–MS/MS as described previously (51). Briefly, cells were cultured in 6-well plates (1×10^6), and the plates were placed on dry ice immediately after the medium was aspirated. Then, 1 ml of 80% methanol/water (precooled at -80°C for at least 1 hour) was added. The plates were transferred to a -80°C freezer for 15 minutes to further inactivate enzymes. Then, the cells were scraped into 80% methanol/water on dry ice and centrifuged at 20,000×*g* for 10 minutes at 4°C. The supernatant was transferred into a new tube and dried with a speed vacuum at room temperature. Finally, the dry pellets were stored at -80°C for further LC–MS/MS analysis (Vanquish, Thermo Fisher Scientific).

Cell proliferation assays

Tamoxifen- or fulvestrant-resistant T47D or MCF7 cells were plated in triplicate in 96-well plates (3,000 cells/well) in the appropriate growth medium. At the indicated time points, the cells were placed in 90 μl of fresh growth medium supplemented with 10 μl of MTS reagents (Promega) and incubated at 37°C for 2 h. The absorbance value was measured at 490 nm using a 96-well plate reader. The experiments were repeated three times with similar results.

Colony formation assays

T47D-, MCF7-, tamoxifen- or fulvestrant-resistant cells were trypsinized and plated in triplicate in 6-well dishes (5,000 cells/well). At the indicated time points, the cells were fixed with 4% paraformaldehyde for 15 min at 37°C and then stained with 0.02% crystal violet.

Anchorage-independent growth assays

Tamoxifen- or fulvestrant-resistant T47D or MCF7 cells were plated at a density of 5,000 cells per ml in complete medium with 0.4% agarose on layers composed of medium with 1% agarose and incubated at 4°C for 10 min. Afterward, the cells were moved to a 37°C incubator. Every 4 days, three drops of complete media were added to the plate. After 2 weeks, the extra liquid on the plate was aspirated, 1 ml of medium was added to each well, and colonies were stained with 100 μg/ml iodonitrotetrazolium chloride solution. The cell culture plates were returned to the incubator overnight, after which the number of foci were counted. The experiments were repeated three times with similar results.

Bioinformatics analyses of metabolomics data

The metabolomics data were analyzed by R statistical software version 4.1.3. MSEA was performed using MetaboAnalyst (https://www.metaboanalyst.ca/). Differentially regulated metabolites were identified by the edgeR package (v3.36.0) (https://doi.org/10.1093/bioinformatics/btp616) with the thresholds of FDXRsh434/ctrl greater than 1.2 or less than 0.8 following an adjusted p value <

0.05. The heatmaps were drawn with the ComplexHeatmap package (v2.10.0) (https://doi.org/10.1093/bioinformatics/btw313).

Bioinformatics analyses of the gene expression profile

The gene expression profile was analyzed by R statistical software version 4.1.3. GSEA based on hallmarks was performed using GSEA software (v4.2.3) (https://doi.org/10.1073/pnas.0506580102). Differentially regulated genes were identified by using the limma package (v3.50.3) (https://doi.org/10.1093/nar/gkv007) with an adjusted p value < 0.05. We selected biological process (BP) of GO analysis with the clusterProfiler package (v4.2.2) (https://doi.org/10.1089/omi.2011.0118) in the study. The connection between the significantly enriched fatty acid metabolism GO terms and participating genes was analyzed by the ComplexHeatmap package (v2.10.0).

Statistical analyses of TCGA and METABRIC datasets

Statistical analyses of these clinical datasets was analyzed by R statistical software version 4.1.3. Survival analyses and Cox proportional hazards models were constructed by using the survival package (v3.5-5). The Kaplan-Meier Curves were drawn with the survminer package (v0.4.9).

Statistical analysis

The unpaired two-tailed Student's *t* test was used for experiments comparing two sets of data. The data are presented as the mean ± SEM from three independent experiments. *, **, and *** denote *P* values < 0.05, 0.01, and 0.005, respectively. NS denotes not significant.

Data availability

The gene expression microarray discussed in this paper have been deposited in NCBI's Gene Expression Omnibus (GEO) under the accession number GSE217902 and the password is ulgfqumujhkvvqn (https://www.ncbi.nlm.nih.gov/geo/query/acc.cgi?&acc=GSE217902).

The relevant code for R statistical analyses is provided online through https://github.com/whumri-grh/FDXR-Drives-Primary-and-Endocrine-Resistant-1-Tumor-Cell-Growth-in-ER-Breast-Cancer-via-CPT1A-Media.git

Results

FDXR is required for fatty acid oxidation and CPT1A expression

We previously reported that FDXR acts as a downstream target gene of the EglN2-NRF1-PGC1α complex to maintain mitochondrial function (44). To explore the mechanism by which FDXR regulates mitochondrial function in breast cancer cells, we performed liquid chromatography (LC) tandem mass spectrometry (MS/MS)-based metabolite profiling in FDXR-knockdown (KD) T47D human ER+ breast cancer cells (Supplementary Figure 1A; Supplementary Table 1). Among the identified small metabolites, 46 metabolites were significantly decreased and 35 metabolites were significantly increased by FDXR KD (Supplementary Figure 1B; Supplementary Table 2). Metabolite set enrichment analysis showed that pyrimidine metabolism, aspartate metabolism, glutathione metabolism, glutamate metabolism and fatty acid metabolism were enriched among groups that were positively regulated by FDXR (Figure 1A). Among these decreased metabolites, one-third were involved in fatty acid metabolism, and almost all of them belonged to acyl-carnitine (Figure 1B; Supplementary Table 3). Moreover, gene expression profiling of FDXR KD T47D cells showed that a set of metabolism-related genes were positively regulated by FDXR (Supplementary Figure 1C; Supplementary Table 4). Gene set enrichment analysis (GSEA) showed that fatty acid metabolism was enriched in groups that were positively regulated by FDXR (Figure 1C). Specifically, we found that CPT1A, which catalyzes acyl-CoA to acyl-carnitine to allow mitochondrial uptake of long-chain fatty acids and is a key rate-limiting enzyme for fatty acid oxidation (Supplementary Figure 1D) (52), was significantly decreased by FDXR KD in T47D lines (Figure 1D; Supplementary Table 5). Therefore, we hypothesized that the decrease in CPT1A is the main reason for the reduction in acyl-carnitine in FDXR-depleted cells.

To test this hypothesis, we specifically showed the metabolite levels related to the synthesis of palmitylcarnitine from palmitate (Figure 1E). Through LC-MS/MS, we confirmed that FDXR depletion decreased palmitylcarnitine, which is generated through CPT1-mediated catalysis of palmityl-CoA, but had no effect on palmitate or carnitine (Figure 1E). The gene expression profile showed that among the enzymes involved in the formation of palmitylcarnitine, only CPT1A was reduced by FDXR depletion (Figure 1F). Furthermore, Q-PCR and western blotting assays confirmed that FDXR depletion inhibited CPT1A expression (Figure 1G). The integrative analyses of the targeted metabolomics assay and gene expression profiling suggest that FDXR KD decreased acyl-carnitine by downregulating CPT1A expression. Since CPT1A is a key enzyme for fatty acid oxidation, we hypothesized that FDXR may consequently regulate fatty acid oxidation. We measured the oxygen consumption rate (OCR) with an XF-24 extracellular flux analyzer and found that FDXR KD inhibited basal levels of mitochondrial respiration. The decreased amount of OCR caused by etomoxir represents the amount of OCR derived from FAO pathway, therefore, we treated cells with etomoxir, an inhibitor of FAO that targets CPT1 used to measure FAO-dependent OCR in cells, and found that FDXR KD-mediated inhibition of OCR was largely mediated by FAO (Figures 1H–J). Collectively, these results suggest that FDXR positively regulates CPT1A expression and fatty acid oxidation.

FDXR regulates fatty acid oxidation and tumor cell growth through CPT1A

To verify whether FDXR KD-mediated inhibition of fatty acid oxidation occurs through the downregulation of CPT1A, we further

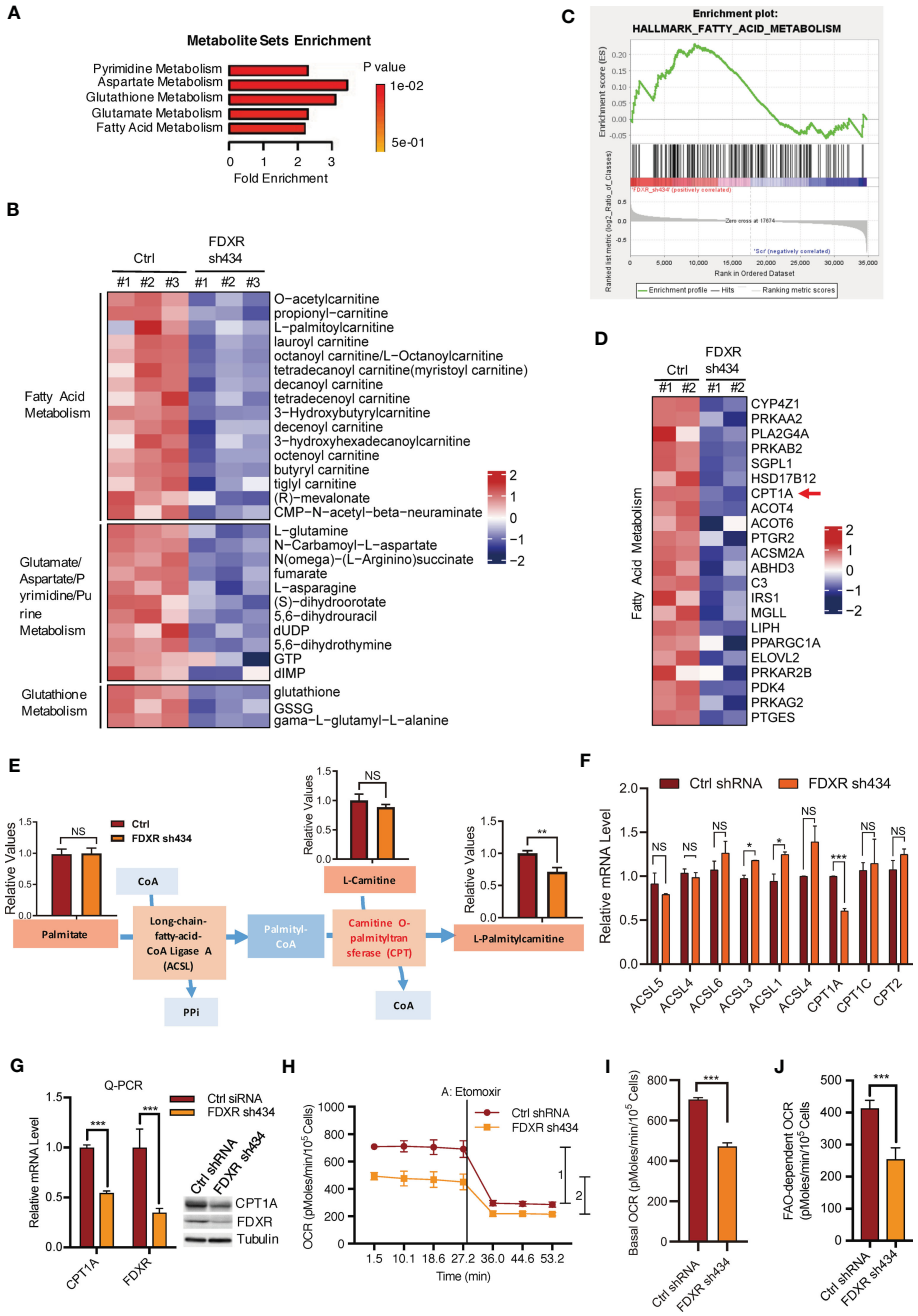

FIGURE 1
The effect of FDXR on metabolic pathways in ER+ breast cancer cells. **(A)** Metabolite sets enrichment analysis of targeted metabolomics assays in T47D cells infected with lentivirus encoding Ctrl shRNA and FDXR sh434. **(B)** Heatmaps showing the metabolites involved in the indicated metabolic pathways positively regulated by FDXR. **(C)** Gene set enrichment analysis (GSEA) of gene expression profile in T47D cells infected with lentivirus encoding Ctrl shRNA and FDXR sh434. **(D)** Heatmaps showing genes related to fatty acid metabolism positively regulated by FDXR. **(E)** The diagram for FDXR regulation on fatty acid metabolic pathway. **(F)** The relative mRNA levels of fatty acid associated genes under FDXR depletion from gene expression microarray. **(G)** Q-PCR and immunoblots assay to detect FDXR and CPT1A level from T47D cells infected with lentivirus encoding Ctrl shRNA and FDXR sh434. **(H–J)**. Seahorse assays **(H)** and their quantifications of basal OCR **(I)** and indicated 1 and 2 **(J)** for measurement of FAO-dependent OCR under the treatment of an FAO inhibitor etomoxir (40 μM) in T47D cells infected with lentivirus encoding Ctrl shRNA and FDXR sh434. *, **, and *** denote P-value of < 0.05, 0.01, and 0.005, respectively. NS denotes not significant.

examined FAO-driven OCR by adding exogenous palmitate, which served as the sole carbon source driving OXPHOS. We found that FDXR KD abrogated palmitate-derived OCR, decreased basal and maximal respiration, and inhibited ATP production (Figures 2A, B). Then, we reconstituted CPT1A in FDXR KD cells and found that CPT1A could partially rescue the decrease in OCR caused by FDXR KD (Figures 2C–E), indicating that FDXR regulates FAO at least partially through CPT1A. Our data showed that depletion of FDXR inhibited tumor cell growth in T47D and MCF7 breast cancer cell lines (44) (Supplementary Figures 2A–D), and this

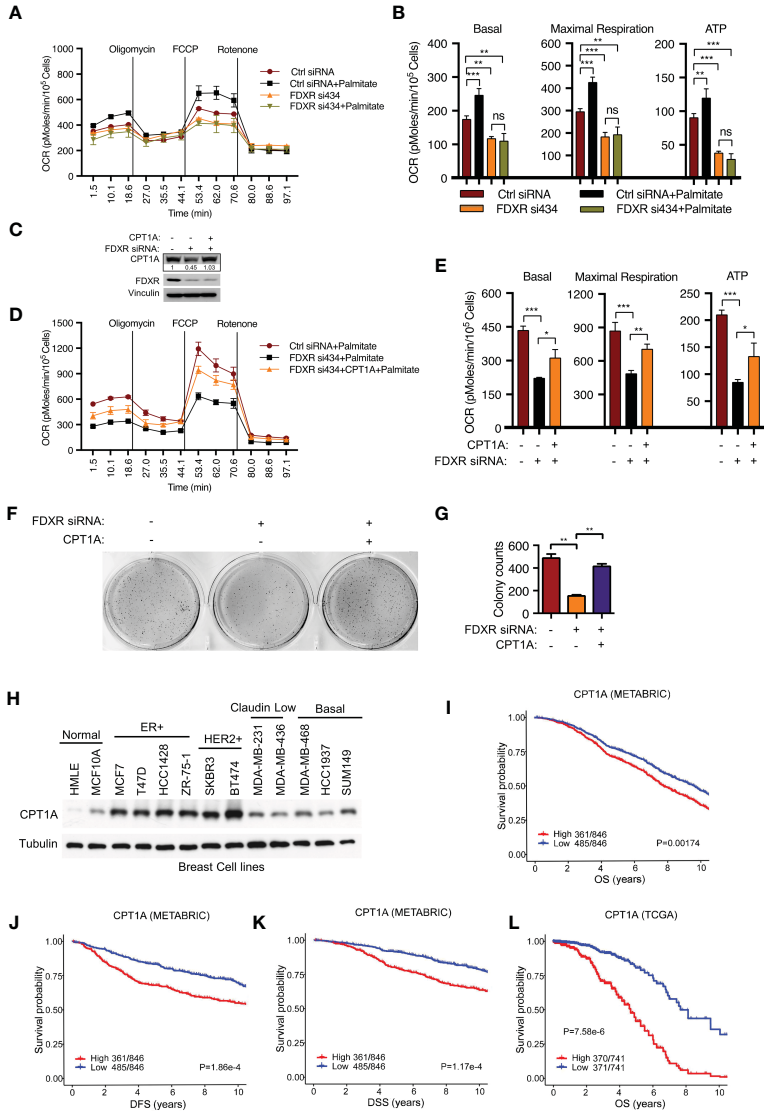

FIGURE 2
FDXR regulates fatty acid oxidation and tumor cell growth through CPT1A in ER+ breast cancer cells. **(A, B)** Seahorse assays **(A)** and their quantifications of basal, maximal respiration, or ATP production **(B)** from T47D cells transfected with Ctrl siRNA and FDXR si434. **(C–G)**. Immunoblots **(C)**, Seahorse assays **(D)** and their quantifications of basal, maximal respiration, or ATP production **(E)**, soft agar assays **(F)** and their quantifications **(G)** from T47D cells infected with vector (control) or CPT1A followed by transfection with Ctrl siRNA and FDXR si434. **(H)** Immunoblots of the breast cell lines as indicated. **(I–L)**. The Kaplan–Meier curves of overall survival (OS) **(I, L)**, disease free survival (DFS) **(J)**, and disease special survival (DSS) **(K)** based on CPT1A expression in ERα-positive patients from METABRIC **(I–K)** and TCGA **(L)** cohorts. Patients were rank-ordered and divided into two equal groups (low in blue and high in red), using the CPT1A gene expression levels. *, **, and *** denote P-value of < 0.05, 0.01, and 0.005, respectively. ns denotes not significant.

phenotype could be at least partially rescued by the reconstitution of CPT1A expression (Figures 2F, G). Thus, our data indicate that FDXR regulates tumor cell growth through CPT1A. Similar to FDXR, as we previously reported (44), CPT1A was upregulated in breast cancer cell lines compared to the human mammary epithelial cell lines HMLE and MCF10A (Figure 2H), and higher expression of CPT1A was associated with decreases in overall survival (OS) (Figures 2I, L), disease-free survival (DFS) (Figure 2J) and disease-specific survival (DSS) (Figure 2K) in the METABRIC and TCGA ER+ breast patient datasets (Supplementary Tables 6, 7). These data reveal FDXR-CPT1A-FAO axis as a potential target for breast cancer.

FDXR is required for endocrine-resistant ER+ breast tumor growth

Endocrine therapy is the first-line clinical treatment for estrogen receptor-positive (ER+) breast cancer, but long-term hormone therapy, such as tamoxifen and fulvestrant, can lead to the development of endocrine resistance (53). Increasing evidence indicates that endocrine-resistant tumor cells exhibit a high mitochondrial OXPHOS status (54). Therefore, we examined whether FDXR-CPT1A-FAO axis-driven OXPHOS was responsible for endocrine resistance in breast cancer. According to previous reports (48, 49, 55), T47D and MCF7 cells were treated

with 0.1 μM tamoxifen or fulvestrant for three weeks to induce drug resistance, and we found that long-term treatment with tamoxifen or fulvestrant increased the expression levels of FDXR and CPT1A (Figures 3A, B). Furthermore, western blotting, cell proliferation assays and anchorage-independent growth assays showed that FDXR KD in tamoxifen- or fulvestrant-resistant T47D and MCF7 cell lines inhibited CPT1A expression and decreased tumor cell growth (Figures 3C–R; Supplementary Figures 3A–D). As the endocrine-resistant cells were cultured in the presence of 100 nM tamoxifen or fulvestrant, and FDXR depletion along with this constant endocrine treatment in those cells blocked cell growth, implying that FDXR may sensitize these endocrine-resistant cells back to endocrine treatment and is essential for endocrine-resistant cell growth.

Endocrine-resistant ER+ breast cancer cells are highly dependent on fatty acid oxidation compared with primary cells

Given that both FDXR and CPT1A were upregulated by long-term treatment with tamoxifen or fulvestrant, we hypothesized that endocrine-resistant cells may rely more on the FDXR-CPT1A-FAO axis to survive the harsh environment than primary cells. To test this hypothesis, we performed MTT assays on primary and endocrine-resistant ER+ breast cancer cells treated with various concentrations of etomoxir. Our data showed that etomoxir inhibited the proliferation of primary and endocrine-resistant T47D and MCF7 cells, but endocrine-resistant breast cancer cells showed much lower IC50 values for etomoxir treatment

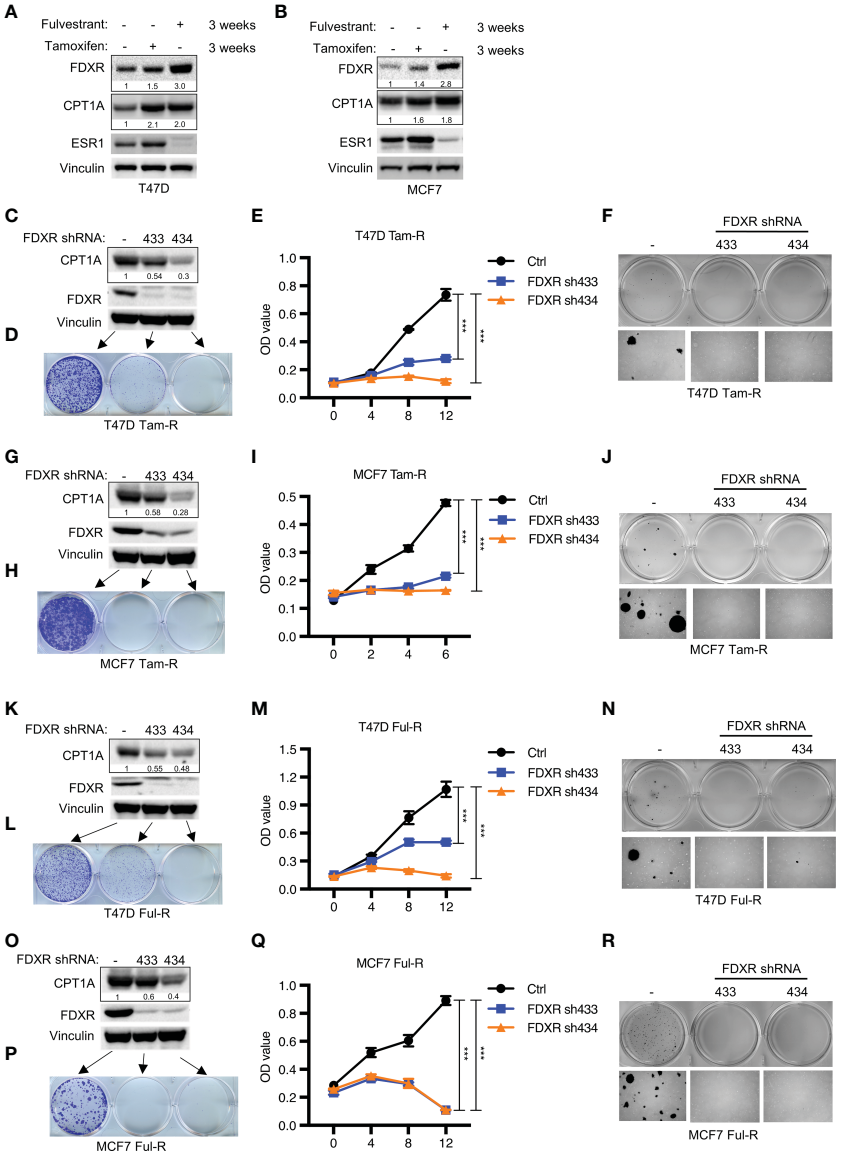

FIGURE 3
The effect of FDXR depletion on endocrine resistant ER+ breast cancer cell growth. **(A, B)** Immunoblot assays of T47D **(A)** or MCF7 **(B)** with three weeks of treatment with fulvestrant (0.1 μM) or tamoxifen (0.1 μM). **(C–R)** Immunoblot assays **(C, G, K, O)**, 2D colony formation **(D, H, L, P)**, cell proliferation **(E, I, M, Q)** and soft agar assay **(F, J, N, R)** from T47D or MCF7 tamoxifen-resistant (T47D Tam-R, MCF7 Tam-R) or fulvestrant-resistant (T47D Ful-R, MCF7 Ful-R) cells infected with lentivirus encoding Ctrl shRNA and FDXR shRNA (433 or 434). *** denote P-value of < 0.005.

(Figures 4A, B; Supplementary Figures 4A, B). In addition, 2D colony formation assays showed that endocrine-resistant breast cancer cells were more sensitive to etomoxir treatment than primary breast cancer cells (Figures 4C, D), indicating that endocrine-resistant breast cancer cells are more dependent on fatty acid oxidation. These data suggest that fatty acid oxidation is required for both primary and endocrine-resistant ER+ breast cancer cell proliferation, and endocrine-resistant cells rely highly on fatty acid oxidation compared with primary cells.

Combining a CPT1 inhibitor with fulvestrant treatment synergistically reduces primary and endocrine-resistant ER+ breast cancer cell growth

Given that long-term tamoxifen or fulvestrant treatment increased CPT1A levels, we hypothesized that inhibiting CPT1A might synergize with endocrine therapy to exert enhanced therapeutic efficacy. We firstly examined the proper concentrations of tamoxifen/fulvestrant and CPT1 inhibitor etomoxir for their combinatory treatment by using different doses, we found that combining fulvestrant with etomoxir showed synergistic effect on inhibiting endocrine-resistant cancer cell growth in a dose-dependent manner (Supplementary Figures 5A–F). Moreover, our data showed that primary cells are indeed more sensitive than endocrine-resistant cells to endocrine treatment (Supplementary Figures 5G, H). Further, we found that treatment with either fulvestrant or etomoxir alone led to differential inhibition of cell proliferation in both primary and endocrine-resistant ER+ breast cancer, and combining etomoxir with fulvestrant resulted in a synergistic decrease in cell proliferation (Figures 5A–F). However, combining etomoxir with tamoxifen showed no synergistic effect on cell growth (Supplementary Figures 5A, B; Supplementary Figure 6) (56). Thus, our data reveal that the CPT1 inhibitor etomoxir restores the sensitivity of endocrine-resistant breast cancer cells to fulvestrant and that combining etomoxir with fulvestrant synergistically reduces breast cancer cell growth.

Discussion

Endocrine therapies are the first-line treatment for early-stage ER+ breast cancers, but many patients relapse and develop drug resistance (53, 57). Understanding the factors and pathways that drive drug resistance has allowed the development of subsequent therapies and helped guide decision-making to maximize efficacious and successful treatment of cancers (58). Accumulating evidence has suggested that metabolic reprogramming is associated with drug resistance (59–61). Investigating metabolic alterations and therefore exploiting metabolic vulnerabilities in cancers are critical for precision medicine (62). Mitochondrial respiration is increased in response to endocrine resistance in ER+ breast cancer; however, the mechanism is not well understood (63). Previously, we showed that the EglN2-NRF1-PGC1α axis regulates mitochondrial function by promoting FDXR expression, but it is unclear how FDXR regulates mitochondrial function. Through an integrative targeted

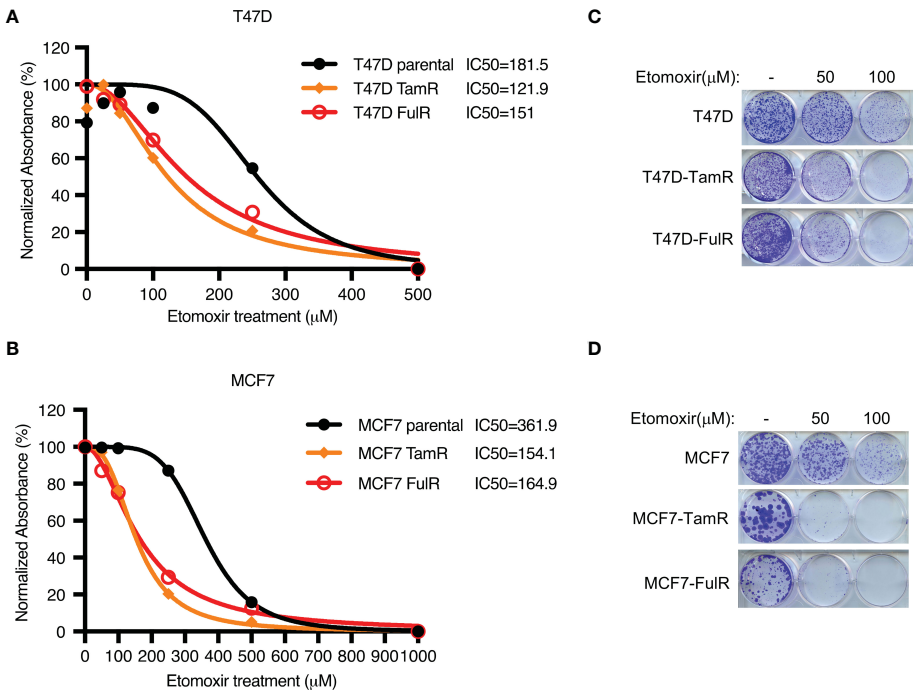

FIGURE 4
The effect of CPT1 inhibitor etomoxir on primary and endocrine resistant ER+ breast cancer cell growth. **(A–D)** Cell proliferation **(A, B)** and 2D colony formation **(C, D)** from T47D or MCF7 cells with or without the indicated doses of etomoxir treatment for 4 days and 10 days, respectively.

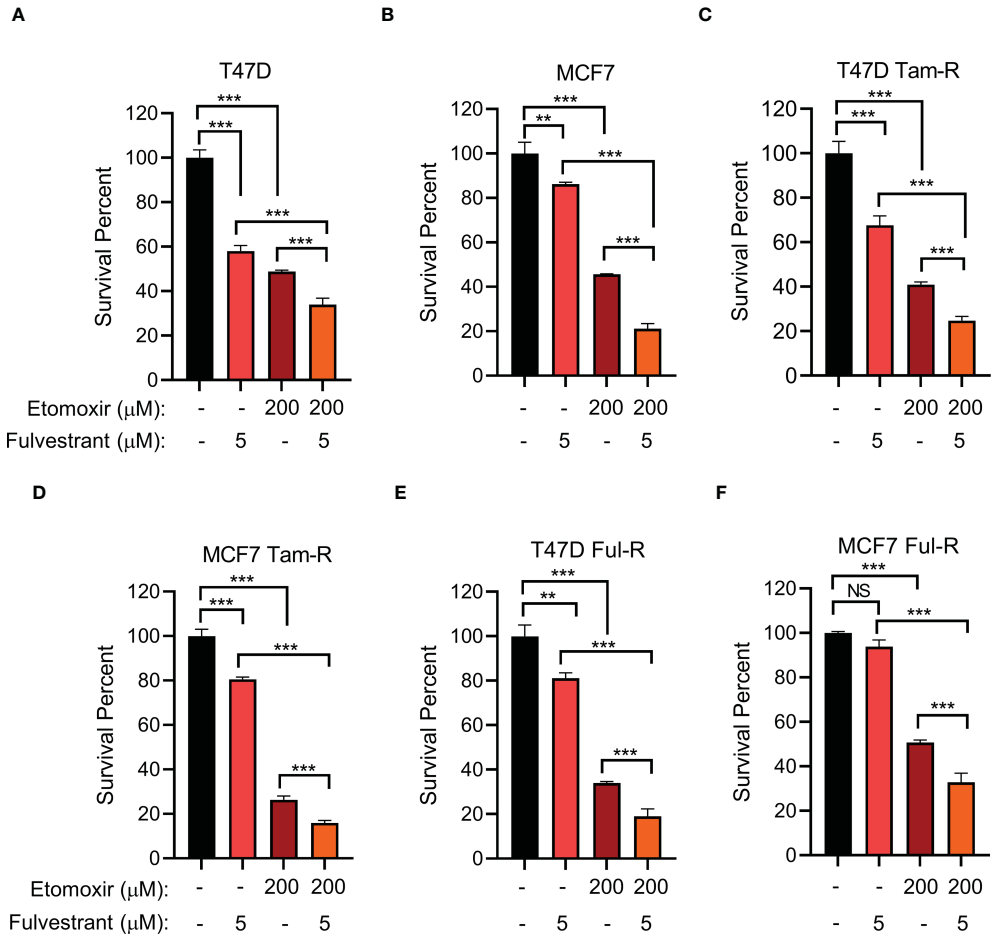

FIGURE 5
The effect of combined CPT1 inhibitor and fulvestrant treatment on primary and endocrine resistant ER+ breast tumor cell growth. **(A–F)** Cell survival analysis of the indicated T47D or MCF7 cell lines under the indicated treatments for 4 days. **, and *** denote P-value of < 0.05, 0.01, and 0.005, respectively. NS denotes not significant.

metabolomics assay and gene expression profiling approach, we found that FDXR was essential for fatty acid oxidation and mitochondrial respiration through the positive regulation of CPT1A. Furthermore, we found that endocrine-resistant breast cancer cells highly depend on the fatty acid oxidation pathway compared with primary cells, and the combination of endocrine therapy with an FAO inhibitor synergistically inhibits primary and endocrine-resistant breast cancer cell growth. Thus, we reveal an important mechanism of mitochondrial adaptation to endocrine treatment and provide a new therapeutic strategy by combining endocrine therapy with FAO inhibitors.

We found that FDXR correlated with mitochondrial OXPHOS genes in the ER+ breast cancer patients, while CPT1A did not have this correlation. Also, FDXR and CPT1A did not correlated in the ER+ breast cancer patients (Supplementary Figures 7A–C; Supplementary Table 8), the reason could be that both CPT1A and mitochondrial OXPHOS genes were downstream genes regulated by FDXR, and also other factors may co-regulate CPT1A expression. FDXR, which is a mitochondrial flavoprotein that initiates electron transport from NADPH, positively regulates ROS production (47) (Supplementary Figure 8). But whether this process contributes to mitochondrial OXPHOS and endocrine resistance requires further investigation. Also, we have been focusing on the regulatory mechanism of how FDXR regulates mitochondrial oxidative phosphorylation in this study, whether FDXR regulates the extracellular acidification rate (ECAR) and modulates oxidization of other primary mitochondrial fuels glucose and glutamine needs future study. Besides, it takes much longer time for obtaining the endocrine-resistant tumor tissues from breast cancer patients, future study will be needed to validate the roles of FDXR and CPT1A in endocrine resistance *in vivo* by patient-derived xenograft (PDX) models.

Lipid metabolism has been recognized as essential for tumor cell growth and progression (64, 65), and it has emerged as a promising target for many cancers (66, 67). Accumulating evidence suggests that alterations in lipid metabolism mediate the development of acquired drug resistance in various types of cancers, including breast cancer (60, 61). In this study, through combining different datasets derived from two separate cohorts of ER+ breast cancer patients, we show that higher expression of CPT1A is associated with worse prognosis. Further, we also find that the endocrine-resistant cell lines are highly sensitive to

CPT1A inhibitor compared with primary cell lines, and endocrine treatment leads to upregulation of CPT1A, implying that cancer cells develop CPT1A-mediated pathway for cellular adaptation to the new environment. Therefore, CPT1A could be used as a biomarker and tested at baseline and after recurrence. As such, targeting CPT1A has a potential to be used in combination therapy with endocrine treatment. Our data have showed that endocrine resistant cells highly depend on FAO compared with primary cells, and inhibition of FAO with etomoxir significantly inhibits endocrine resistant cell growth. It is well-known that metabolic reprogramming plays an important role in development of drug resistance (59), but whether cell metabolisms can be reprogrammed towards glycolysis or glutamine following endocrine or etomoxir treatment awaits future investigation. It has reported that inhibition of glycolysis results in upregulation of FAO (68), but whether inhibition of FAO leads to metabolic reprogramming towards glycolysis or glutamine needs future study. These studies may provide additional combination therapies for breast cancer.

Data availability statement

The datasets presented in this study can be found in online repositories. The names of the repository/repositories and accession number(s) can be found in the article/Supplementary Material.

Author contributions

QZ and JZ conceived and supervised the project. JZ and CY analyzed the data. JZ and CY performed most of experiments. RG and CG performed bioinformatics analyses. KH and MC performed plasmid construction. XL helped with metabolomics assays. QZ, JZ, and CY wrote the paper with critical comments from all authors. All authors contributed to the article and approved the submitted version.

Funding

This work is supported by the Fundamental Research Funds for the Central Universities 2042020kf0197 (JZ), ACS RSG-18-059-01-TBE (QZ), National Natural Science Foundation of China 31970737 (JZ) and 32100570 (CY), the Startup Funding from Wuhan University (JZ), Natural Science Foundation of Hubei Province 2020CFA071 (JZ) and the China Postdoctoral Science Foundation 2020M672408 (CY). We also sincerely thank the core facility of the Medical Research Institute at Wuhan University for their technical support.

Acknowledgments

The authors thank members of our laboratory for helpful discussions. We thank Jason Locasale laboratory for help with metabolomics assays and Rachel Schiff for providing endocrine resistant ER+ breast cancer cell lines.

Conflict of interest

The authors declare that the research was conducted in the absence of any commercial or financial relationships that could be construed as a potential conflict of interest.

Publisher's note

Supplementary material

The Supplementary Material for this article can be found online at: https://www.frontiersin.org/articles/10.3389/fonc.2023.1105117/full#supplementary-material

SUPPLEMENTARY FIGURE 1
Integrative analyses of the targeted metabolomics and gene expression prolife reveal FDXR-mediated gene regulation of cell metabolism in ER+ breast cancer. **(A)** Heatmap analysis of the targeted metabolomics assays from T47D cells infected with lentivirus encoding Ctrl shRNA and FDXR sh434. **(B)** Heatmaps showing differentially regulated metabolites affected by FDXR in T47D cells infected with lentivirus harboring either Ctrl shRNA or FDXR sh434. **(C)** Heatmaps showing metabolism-related genes positively regulated by FDXR from T47D cells infected with lentivirus encoding Ctrl shRNA and FDXR sh434. **(D)** Schematic diagram showing CPT1-mediated regulation of fatty acid oxidation pathway to feed TCA cycle for mitochondrial oxidative phosphorylation.

SUPPLEMENTARY FIGURE 2
FDXR is essential for MCF7 cells proliferation. **(A–D)** Immunoblot assays **(A)**, cell proliferation **(B)**, soft agar assay **(C)** and quantification **(D)** for MCF7 cells infected with lentivirus encoding Ctrl shRNA and FDXR shRNA (433 or 434). *** denote P-value of < 0.005.

SUPPLEMENTARY FIGURE 3
FDXR is required for the endocrine resistant ER+ breast cancer cell growth. **(A–D)** Quantification of soft agar assays described in Figures 3D, H, L, P, respectively. *** denote P-value of < 0.005.

SUPPLEMENTARY FIGURE 4
The effect of CPT1 inhibitor etomoxir on primary and endocrine resistant ER+ breast cancer cell growth. **(A, B)** Cell proliferation of primary or endocrine resistant T47D or MCF7 cells with or without the indicated doses of etomoxir treatment for 4 days. *, **, and *** denote P-value of < 0.05, 0.01, and 0.005, respectively. NS denotes not significant.

SUPPLEMENTARY FIGURE 5
The effect of CPT1 inhibitor etomoxir on primary and endocrine resistant ER+ breast cancer cell growth. **(A–F)** Cell survival analysis of the indicated primary or endocrine resistant T47D or MCF7 cell lines under the indicated treatments for 4 days. **(G, H)** MTS assays of primary or endocrine resistant T47D or MCF7 cells with

or without tamoxifen (5 μM) or fulvestrant (5 μM) treatment for 4 days. *, **, and *** denote P-value of < 0.05, 0.01, and 0.005, respectively. NS denotes not significant.

SUPPLEMENTARY FIGURE 6

The effect of combined etomoxir and tamoxifen treatment on tamoxifen-resistant ER+ breast cells. Cell survival analysis from tamoxifen-resistant T47D cells with the indicated treatments with etomoxir (200 μM) and tamoxifen (5 μM) for 4 days. *, **, and *** denote P-value of < 0.05, 0.01, and 0.005, respectively. NS denotes not significant.

SUPPLEMENTARY FIGURE 7

Correlation of FDXR with OXPHOS-related gene expression in ER+ patients. **(A, B)** Correlation analysis of FDXR or CPT1A with OXPHOS-related parameters in the ER + cohort of patients. **(C)** Correlation between FDXR and CPT1A in the ER+ cohort of patients.

SUPPLEMENTARY FIGURE 8

Silencing of FDXR reduces cellular ROS production. ROS level analysis by using DCFH-DA from T47D cells transfected with FDXR siRNA. * denote P-value of < 0.05.

References

1. Garcia-Becerra R, Santos N, Diaz L, Camacho J. Mechanisms of resistance to endocrine therapy in breast cancer: focus on signaling pathways, mirnas and genetically based resistance. *Int J Mol Sci* (2012) 14(1):108–45. doi: 10.3390/ijms14010108

2. Hanamura T, Hayashi SI. Overcoming aromatase inhibitor resistance in breast cancer: possible mechanisms and clinical applications. *Breast Cancer* (2018) 25(4):379–91. doi: 10.1007/s12282-017-0772-1

3. Ma CX, Reinert T, Chmielewska I, Ellis MJ. Mechanisms of aromatase inhibitor resistance. *Nat Rev Cancer* (2015) 15(5):261–75. doi: 10.1038/nrc3920

4. Miller WR, Larionov A, Renshaw L, Anderson TJ, Walker JR, Krause A, et al. Gene expression profiles differentiating between breast cancers clinically responsive or resistant to letrozole. *J Clin Oncol* (2009) 27(9):1382–7. doi: 10.1200/JCO.2008.16.8849

5. Colleoni M, Montagna E. Neoadjuvant therapy for er-positive breast cancers. *Ann Oncol* (2012) 23 Suppl 10:x243–8. doi: 10.1093/annonc/mds305

6. Ma CX, Sanchez CG, Ellis MJ. Predicting endocrine therapy responsiveness in breast cancer. *Oncol (Williston Park)* (2009) 23(2):133–42.

7. Selli C, Dixon JM, Sims AH. Accurate prediction of response to endocrine therapy in breast cancer patients: current and future biomarkers. *Breast Cancer Res BCR* (2016) 18(1):118. doi: 10.1186/s13058-016-0779-0

8. Hart CD, Migliaccio I, Malorni L, Guarducci C, Biganzoli L, Di Leo A. Challenges in the management of advanced, er-positive, Her2-negative breast cancer. *Nat Rev Clin Oncol* (2015) 12(9):541–52. doi: 10.1038/nrclinonc.2015.99

9. Ignatiadis M, Sotiriou C. Luminal breast cancer: from biology to treatment. *Nat Rev Clin Oncol* (2013) 10(9):494–506. doi: 10.1038/nrclinonc.2013.124

10. Bachelot T, Bourgier C, Cropet C, Ray-Coquard I, Ferrero JM, Freyer G, et al. Randomized phase ii trial of everolimus in combination with tamoxifen in patients with hormone receptor-positive, human epidermal growth factor receptor 2-negative metastatic breast cancer with prior exposure to aromatase inhibitors: a gineco study. *J Clin Oncol* (2012) 30(22):2718–24. doi: 10.1200/JCO.2011.39.0708

11. Treilleux I, Arnedos M, Cropet C, Wang Q, Ferrero JM, Abadie-Lacourtoisie S, et al. Translational studies within the tamrad randomized gineco trial: evidence for Mtorc1 activation marker as a predictive factor for everolimus efficacy in advanced breast cancer. *Ann Oncol* (2015) 26(1):120–5. doi: 10.1093/annonc/mdu497

12. Beck JT, Hortobagyi GN, Campone M, Lebrun F, Deleu I, Rugo HS, et al. Everolimus plus exemestane as first-line therapy in hr(+), Her2(-) advanced breast cancer in bolero-2. *Breast Cancer Res Treat* (2014) 143(3):459–67. doi: 10.1007/s10549-013-2814-5

13. Baselga J, Campone M, Piccart M, Burris HA3rd, Rugo HS, Sahmoud T, et al. Everolimus in postmenopausal hormone-Receptor-Positive advanced breast cancer. *N Engl J Med* (2012) 366(6):520–9. doi: 10.1056/NEJMoa1109653

14. Finn RS, Crown JP, Lang I, Boer K, Bondarenko IM, Kulyk SO, et al. The cyclin-dependent kinase 4/6 inhibitor palbociclib in combination with letrozole versus letrozole alone as first-line treatment of oestrogen receptor-positive, Her2-negative, advanced breast cancer (Paloma-1/Trio-18): a randomised phase 2 study. *Lancet Oncol* (2015) 16(1):25–35. doi: 10.1016/S1470-2045(14)71159-3

15. Finn RS, Dering J, Conklin D, Kalous O, Cohen DJ, Desai AJ, et al. Pd 0332991, a selective cyclin d kinase 4/6 inhibitor, preferentially inhibits proliferation of luminal estrogen receptor-positive human breast cancer cell lines in vitro. *Breast Cancer Res* (2009) 11(5):R77. doi: 10.1186/bcr2419

16. Corona SP, Generali D. Abemaciclib: a Cdk4/6 inhibitor for the treatment of Hr +/Her2- advanced breast cancer. *Drug Des Devel Ther* (2018) 12:321–30. doi: 10.2147/DDDT.S137783

17. Herrera-Abreu MT, Palafox M, Asghar U, Rivas MA, Cutts RJ, Garcia-Murillas I, et al. Early adaptation and acquired resistance to Cdk4/6 inhibition in estrogen receptor-positive breast cancer. *Cancer Res* (2016) 76(8):2301–13. doi: 10.1158/0008-5472.CAN-15-0728

18. Osborne CK, Schiff R. Mechanisms of endocrine resistance in breast cancer. *Annu Rev Med* (2011) 62:233–47. doi: 10.1146/annurev-med-070909-182917

19. Klein ME, Kovatcheva M, Davis LE, Tap WD, Koff A. Cdk4/6 inhibitors: the mechanism of action may not be as simple as once thought. *Cancer Cell* (2018) 34(1):9–20. doi: 10.1016/j.ccell.2018.03.023

20. Hanahan D, Weinberg RA. Hallmarks of cancer: the next generation. *Cell* (2011) 144(5):646–74. doi: 10.1016/j.cell.2011.02.013

21. Ward PS, Thompson CB. Metabolic reprogramming: a cancer hallmark even warburg did not anticipate. *Cancer Cell* (2012) 21(3):297–308. doi: 10.1016/j.ccr.2012.02.014

22. Pavlova NN, Thompson CB. The emerging hallmarks of cancer metabolism. *Cell Metab* (2016) 23(1):27–47. doi: 10.1016/j.cmet.2015.12.006

23. Martinez-Outschoorn UE, Peiris-Pages M, Pestell RG, Sotgia F, Lisanti MP. Cancer metabolism: a therapeutic perspective. *Nat Rev Clin Oncol* (2017) 14(2):113. doi: 10.1038/nrclinonc.2017.1

24. Kroemer G, Pouyssegur J. Tumor cell metabolism: cancer's achilles' heel. *Cancer Cell* (2008) 13(6):472–82. doi: 10.1016/j.ccr.2008.05.005

25. Vander Heiden MG. Targeting cancer metabolism: a therapeutic window opens. *Nat Rev Drug Discov* (2011) 10(9):671–84. doi: 10.1038/nrd3504

26. Hadad SM, Coates P, Jordan LB, Dowling RJ, Chang MC, Done SJ, et al. Evidence for biological effects of metformin in operable breast cancer: biomarker analysis in a pre-operative window of opportunity randomized trial. *Breast Cancer Res Treat* (2015) 150(1):149–55. doi: 10.1007/s10549-015-3307-5

27. Hadad S, Iwamoto T, Jordan L, Purdie C, Bray S, Baker L, et al. Evidence for biological effects of metformin in operable breast cancer: a pre-operative, window-of-Opportunity, randomized trial. *Breast Cancer Res Treat* (2011) 128(3):783–94. doi: 10.1007/s10549-011-1612-1

28. Kordes S, Pollak MN, Zwinderman AH, Mathot RA, Weterman MJ, Beeker A, et al. Metformin in patients with advanced pancreatic cancer: a double-blind, randomised, placebo-controlled phase 2 trial. *Lancet Oncol* (2015) 16(7):839–47. doi: 10.1016/S1470-2045(15)00027-3

29. Jara JA, Lopez-Munoz R. Metformin and cancer: between the bioenergetic disturbances and the antifolate activity. *Pharmacol Res* (2015) 101:102–8. doi: 10.1016/j.phrs.2015.06.014

30. Cha JH, Yang WH, Xia W, Wei Y, Chan LC, Lim SO, et al. Metformin promotes antitumor immunity via endoplasmic-Reticulum-Associated degradation of pd-L1. *Mol Cell* (2018) 71(4):606–20.e7. doi: 10.1016/j.molcel.2018.07.030

31. Schlaepfer IR, Nambiar DK, Ramteke A, Kumar R, Dhar D, Agarwal C, et al. Hypoxia induces triglycerides accumulation in prostate cancer cells and extracellular vesicles supporting growth and invasiveness following reoxygenation. *Oncotarget* (2015) 6(26):22836–56. doi: 10.18632/oncotarget.4479

32. Holubarsch CJ, Rohrbach M, Karrasch M, Boehm E, Polonski L, Ponikowski P, et al. A double-blind randomized multicentre clinical trial to evaluate the efficacy and safety of two doses of etomoxir in comparison with placebo in patients with moderate congestive heart failure: the ergo (Etomoxir for the recovery of glucose oxidation) study. *Clin Sci (Lond)* (2007) 113(4):205–12. doi: 10.1042/CS20060307

33. Wang T, Fahrmann JF, Lee H, Li YJ, Tripathi SC, Yue C, et al. Jak/Stat3-regulated fatty acid beta-oxidation is critical for breast cancer stem cell self-renewal and chemoresistance. *Cell Metab* (2018) 27(1):136–50.e5. doi: 10.1016/j.cmet.2017.11.001

34. Strohecker AM, White E. Autophagy promotes Brafv600e-driven lung tumorigenesis by preserving mitochondrial metabolism. *Autophagy* (2014) 10 (2):384–5. doi: 10.4161/auto.27320

35. Fan J, Kamphorst JJ, Mathew R, Chung MK, White E, Shlomi T, et al. Glutamine-driven oxidative phosphorylation is a major atp source in transformed mammalian cells in both normoxia and hypoxia. *Mol Syst Biol* (2013) 9:712. doi: 10.1038/msb.2013.65

36. Guo JY, Chen HY, Mathew R, Fan J, Strohecker AM, Karsli-Uzunbas G, et al. Activated ras requires autophagy to maintain oxidative metabolism and tumorigenesis. *Genes Dev* (2011) 25(5):460–70. doi: 10.1101/gad.2016311

37. Sonveaux P, Vegran F, Schroeder T, Wergin MC, Verrax J, Rabbani ZN, et al. Targeting lactate-fueled respiration selectively kills hypoxic tumor cells in mice. *J Clin Invest* (2008) 118(12):3930–42. doi: 10.1172/JCI36843

38. Viale A, Pettazzoni P, Lyssiotis CA, Ying H, Sanchez N, Marchesini M, et al. Oncogene ablation-resistant pancreatic cancer cells depend on mitochondrial function. *Nature* (2014) 514(7524):628–32. doi: 10.1038/nature13611

39. Vander Heiden MG, DeBerardinis RJ. Understanding the intersections between metabolism and cancer biology. *Cell* (2017) 168(4):657–69. doi: 10.1016/j.cell.2016.12.039

40. Roesch A, Vultur A, Bogeski I, Wang H, Zimmermann KM, Speicher D, et al. Overcoming intrinsic multidrug resistance in melanoma by blocking the mitochondrial respiratory chain of slow-cycling Jarid1b(High) cells. *Cancer Cell* (2013) 23(6):811–25. doi: 10.1016/j.ccr.2013.05.003

41. Pelicano H, Zhang W, Liu J, Hammoudi N, Dai J, Xu RH, et al. Mitochondrial dysfunction in some triple-negative breast cancer cell lines: role of mtor pathway and therapeutic potential. *Breast Cancer Res* (2014) 16(5):434. doi: 10.1186/s13058-014-0434-6

42. Zhang Q, Gu J, Li L, Liu J, Luo B, Cheung HW, et al. Control of cyclin D1 and breast tumorigenesis by the Egln2 prolyl hydroxylase. *Cancer Cell* (2009) 16(5):413–24. doi: 10.1016/j.ccr.2009.09.029

43. Seth P, Krop I, Porter D, Polyak K. Novel estrogen and tamoxifen induced genes identified by sage (Serial analysis of gene expression). *Oncogene* (2002) 21(5):836–43. doi: 10.1038/sj.onc.1205113

44. Zhang J, Wang C, Chen X, Takada M, Fan C, Zheng X, et al. Egln2 associates with the Nrf1-Pgc1alpha complex and controls mitochondrial function in breast cancer. *EMBO J* (2015) 34(23):2953–70. doi: 10.15252/embj.201591437

45. Hanukoglu I, Rapoport R, Weiner L, Sklan D. Electron leakage from the mitochondrial nadph-adrenodoxin reductase-Adrenodoxin-P450scc (Cholesterol side chain cleavage) system. *Arch Biochem Biophys* (1993) 305(2):489–98. doi: 10.1006/abbi.1993.1452

46. Hwang PM, Bunz F, Yu J, Rago C, Chan TA, Murphy MP, et al. Ferredoxin reductase affects P53-dependent, 5-Fluorouracil-Induced apoptosis in colorectal cancer cells. *Nat Med* (2001) 7(10):1111–7. doi: 10.1038/nm1001-1111

47. Bhaduri A, Ungewickell A, Boxer LD, Lopez-Pajares V, Zarnegar BJ, Khavari PA. Network analysis identifies mitochondrial regulation of epidermal differentiation by Mpzl3 and fdxr. *Dev Cell* (2015) 35(4):444–57. doi: 10.1016/j.devcel.2015.10.023

48. Fu X, Jeselsohn R, Pereira R, Hollingsworth EF, Creighton CJ, Li F, et al. Foxa1 overexpression mediates endocrine resistance by altering the er transcriptome and il-8 expression in er-positive breast cancer. *Proc Natl Acad Sci* (2016) 113(43):E6600–E9. doi: 10.1073/pnas.1612835113

49. Alves CL, Ehmsen S, Terp MG, Portman N, Tuttolomondo M, Gammelgaard OL, et al. Co-Targeting Cdk4/6 and akt with endocrine therapy prevents progression in Cdk4/6 inhibitor and endocrine therapy-resistant breast cancer. *Nat Commun* (2021) 12(1):5112. doi: 10.1038/s41467-021-25422-9

50. Zhang J, Wu T, Simon J, Takada M, Saito R, Fan C, et al. Vhl substrate transcription factor Zhx2 as an oncogenic driver in clear cell renal cell carcinoma. *Science* (2018) 361(6399):290–5. doi: 10.1126/science.aap8411

51. Liao C, Zhang Y, Fan C, Herring LE, Liu J, Locasale JW, et al. Identification of Bbox1 as a therapeutic target in triple-negative breast cancer. *Cancer Discov* (2020) 10 (11):1706–21. doi: 10.1158/2159-8290.cd-20-0288

52. Foster DW. The role of the carnitine system in human metabolism. *Ann New York Acad Sci* (2004) 1033:1–16. doi: 10.1196/annals.1320.001

53. Musgrove EA, Sutherland RL. Biological determinants of endocrine resistance in breast cancer. *Nat Rev Cancer* (2009) 9(9):631–43. doi: 10.1038/nrc2713

54. Bosc C, Selak MA, Sarry JE. Resistance is futile: targeting mitochondrial energetics and metabolism to overcome drug resistance in cancer treatment. *Cell Metab* (2017) 26(5):705–7. doi: 10.1016/j.cmet.2017.10.013

55. Giltnane JM, Hutchinson KE, Stricker TP, Formisano L, Young CD, Estrada MV, et al. Genomic profiling of er+ breast cancers after short-term estrogen suppression reveals alterations associated with endocrine resistance (Vol 9, Eaai7993, 2017). *Sci Trans Med* (2019) 11(479):eaaw7620. doi: 10.1126/scitranslmed.aaw7620

56. Loh YN, Hedditch EL, Baker LA, Jary E, Ward RL, Ford CE. The wnt signalling pathway is upregulated in an in vitro model of acquired tamoxifen resistant breast cancer. *BMC Cancer* (2013) 13(1):1–9. doi: 10.1186/1471-2407-13-174

57. Cuzick J, Sestak I, Baum M, Buzdar A, Howell A, Dowsett M, et al. Effect of anastrozole and tamoxifen as adjuvant treatment for early-stage breast cancer: 10-year analysis of the atac trial. *Lancet Oncol* (2010) 11(12):1135–41. doi: 10.1016/S1470-2045(10)70257-6

58. Palmieri C, Patten DK, Januszewski A, Zucchini G, Howell SJ. Breast cancer: current and future endocrine therapies. *Mol Cell Endocrinol* (2014) 382(1):695–723. doi: 10.1016/j.mce.2013.08.001

59. Pranzini E, Pardella E, Paoli P, Fendt SM, Taddei ML. Metabolic reprogramming in anticancer drug resistance: a focus on amino acids. *Trends Cancer* (2021) 7(8):682–99. doi: 10.1016/j.trecan.2021.02.004

60. Feng WW, Kurokawa M. Lipid metabolic reprogramming as an emerging mechanism of resistance to kinase inhibitors in breast cancer. *Cancer Drug Resist (Alhambra Calif)* (2020) 3(1):1–17. doi: 10.20517/cdr.2019.100

61. Iwamoto H, Abe M, Yang Y, Cui D, Seki T, Nakamura M, et al. Cancer lipid metabolism confers antiangiogenic drug resistance. *Cell Metab* (2018) 28(1):104–17.e5. doi: 10.1016/j.cmet.2018.05.005

62. Wolpaw AJ, Dang CV. Exploiting metabolic vulnerabilities of cancer with precision and accuracy. *Trends Cell Biol* (2018) 28(3):201–12. doi: 10.1016/j.tcb.2017.11.006

63. Kulkoyluoglu-Cotul E, Arca A, Madak-Erdogan Z. Crosstalk between estrogen signaling and breast cancer metabolism. *Trends Endocrinol Metab* (2019) 30(1):25–38. doi: 10.1016/j.tem.2018.10.006

64. Corbet C, Feron O. Emerging roles of lipid metabolism in cancer progression. *Curr Opin Clin Nutr Metab Care* (2017) 20(4):254–60. doi: 10.1097/MCO.0000000000000381

65. Dheeraj A, Agarwal C, Schlaepfer IR, Raben D, Singh R, Agarwal R, et al. A novel approach to target hypoxic cancer cells via combining beta-oxidation inhibitor etomoxir with radiation. *Hypoxia* (2018) 6:23–33. doi: 10.2147/Hp.S163115

66. Broadfield LA, Pane AA, Talebi A, Swinnen JV, Fendt SM. Lipid metabolism in cancer: new perspectives and emerging mechanisms. *Dev Cell* (2021) 56(10):1363–93. doi: 10.1016/j.devcel.2021.04.013

67. Guo D, Bell EH, Chakravarti A. Lipid metabolism emerges as a promising target for malignant glioma therapy. *CNS Oncol* (2013) 2(3):289–99. doi: 10.2217/cns.13.20

68. Patsoukis N, Bardhan K, Chatterjee P, Sari D, Liu B, Bell LN, et al. Pd-1 alters T-cell metabolic reprogramming by inhibiting glycolysis and promoting lipolysis and fatty acid oxidation. *Nat Commun* (2015) 6:6692. doi: 10.1038/ncomms7692

frontiers | Frontiers in Oncology

TYPE Original Research
PUBLISHED 26 May 2023
DOI 10.3389/fonc.2023.1141755

OPEN ACCESS

EDITED BY
Zhiyu Zhang,
Fourth Affiliated Hospital of China Medical University, China

REVIEWED BY
Tharcisio CItrangulo Tortelli Jr,
University of São Paulo, Brazil
Dr. Prem P. Kushwaha,
Western Reserve University, United States

*CORRESPONDENCE
Raghu Pandurangi
raghuaa66@yahoo.com

RECEIVED 10 January 2023
ACCEPTED 12 April 2023
PUBLISHED 26 May 2023

CITATION
Pandurangi R, Karwa A, Sagaram US, Henzler-Wildman K and Shah D (2023) *Medicago Sativa* Defensin1 as a tumor sensitizer for improving chemotherapy: translation from anti-fungal agent to a potential anti-cancer agent.
Front. Oncol. 13:1141755.
doi: 10.3389/fonc.2023.1141755

Medicago Sativa Defensin1 as a tumor sensitizer for improving chemotherapy: translation from anti-fungal agent to a potential anti-cancer agent

Raghu Pandurangi[1]*, Amol Karwa[2], Uma Shankar Sagaram[3], Katherine Henzler-Wildman[3] and Dilip Shah[4]

[1]Sci-Engi-Medco Solutions Inc (SEMCO), St Charles, MO, United States, [2]Mallinckrodt Pharmaceuticals, Hazelwood, MO, United States, [3]DeLuca Biochemistry Laboratories, University of Wisconsin, Madison, WI, United States, [4]Donald Danforth Plant Science Center, St Louis, MO, United States

Plant defensins including *Medicago Sativa* defensin 1 (MsDef1) are cysteine-rich antifungal peptides which are known for potent broad-spectrum antifungal activity against bacterial or fungal pathogens of plants. The antimicrobial activities of these cationic defensins are attributed to their capacity to bind to cell membranes to create potentially structural defects tin the cell membranes to interact with intracellular target (s) and mediates cytotoxic effects. Our earlier work identified Glucosylceramide (GlcCer) of fungus *F. graminearum* as a potential target for biological activity. Multi-drug resistant (MDR) cancer cells overexpress GlcCer on the surface of plasma membrane. Hence, MsDef1 may have a potential to bind to GlcCer of MDR cancer cells to induce cell death. We have characterized the three-dimensional structure of MsDef1 and the solution dynamics using of ^{15}N-labeled MsDef1 nuclear magnetic resonance (NMR) spectroscopy which showed that GlcCer binds MsDef1 at two specific sites on the peptide molecule. The ability of MsDef1 to permeate MDR cancer cells was demonstrated by measuring the release of apoptotic ceramide in drug resistant MCF-7R cells. It was also shown that MsDef1 activated dual cell death pathways ceramide and Apoptosis Stimulating Kinase ASK1 by disintegrating GlcCer and oxidizing tumor specific biomarker thioredoxin (Trx) respectively. As a result, MsDef1 sensitizes MDR cancer cells to evoke a better response from Doxorubicin, a front-line chemotherapy for triple negative breast cancer (TNBC) treatment. The combination of MsDef1 and Doxorubicin induced 5 to10-fold greater apoptosis *in vitro* MDR cells MDA-MB-231R compared to either MsDef1 or Doxorubicin alone. Confocal microscopy revealed that MsDef1 facilitates a) influx of Doxorubicin in MDR cancer cells, b) preferential uptake by MDR cells but not by normal fibroblasts and breast epithelial cells (MCF-10A). These results suggest that MsDef1 targets MDR cancer cells and may find utility as a neoadjuvant chemotherapy. Hence, the extension of antifungal properties of MsDef1 to cancer my result in addressing the MDR problems in cancer.

KEYWORDS

defensin, multi-drug resistance MDR, thioredoxin Trx, synergy, Doxorubicin

Introduction

The development of multidrug resistance (MDR) is a serious clinical problem that is responsible for therapy failure, relapse of cancer and making tumors refractory to future treatments (1–3). Deactivation of cell death pathways (e.g., ceramide, apoptosis stimulating kinase, ASK1) (4) and avoidance of immune surveillance (5, 6) play major roles in desensitizing cancer cells to treatments irrespective of nature of treatments. As a result, high drug dose is needed to treat the cancer which in turn induces stemness into cancer cells, increases resistance, suppresses immune function, and enhances the off-target toxicity leading to side effects and treatment failure (7–10).

Despite its moderate to low efficacy and high off-target toxicity, chemotherapy is still the front-line treatment for most cancers (11, 12). The major problem with chemotherapy is that it kills only bulk non-stem cancer cells leaving behind resistant cells. This results in high disease recurrence [13% for kidney cancer, 36% for breast and almost 100% for brain cancer (13, 14)] and makes tumors refractory to future treatments (15). Dose related side effects such as acute lymphedema and low platelets may force discontinuation of treatment altogether creating more resistant cancer cells (16) and thus, causing a vicious circle. Sensitizing resistant tumor cells is known to evoke a better response from chemotherapy (17, 18). However, sensitizing tumor cells selectively using MDR biomarkers is of prime importance in order to make chemotherapy effective in lowering the side effects. This is true particularly for TNBC patients who have no option but chemotherapy with a >90% recurrence rate and a median survival of 13 months (19, 20). The situation is worse for African Americans with recurrence rates of >95%. Current targeted treatments for TNBC patients do not work since they lack biomarkers (e.g., ER, PR and HER2 negative) for which drugs are designed (21). That leaves non-specific anthracyclines (e.g., Doxorubicin, Paclitaxel) as sole options in spite of their high side effects and suppressed immune function (5, 6).

Cancer cells desensitize themselves to chemotherapy for their survival. For example, TNBC cells circumvent Doxorubicin effect by glycosylating lethal, apoptotic ceramide using glucosylceramide synthase (GCS) enzyme to non-apoptotic GlcCer which becomes a biomarker of MDR (22). In addition, GlcCer is consistently present at high levels in drug resistant tumors and in tumors taken from patients who are non-responsive to chemotherapy (23). GlcCer was found to be low in patients who responded to chemotherapy (24). Stemness of cancer cells increases as glycosylation increases (25). In fact, ceramide glycosylation selectively maintains the properties of cancer stem cells (CSCs) which is a serious clinical issue (25). Cancer cells also overexpress Trx and deactivate ASK1 cell death pathway (26–28) resulting in immune response suppression (29–31). Tumors with low Trx levels exhibit a better prognosis than tumors with high Trx levels (poorer prognosis, $P < 0.001$) for partial free survival (PFS) and for overall survival (OS) (32, 33). GlcCer and Trx are the two tumor specific biomarkers of resistance (34, 35). Hence, tumor sensitizers targeting GlcCer and Trx which act as immunoadjuvants are presently the unmet medical need in cancer therapy.

Medicago sativa Defensin1 (MsDef1) is a natural antifungal peptide (36) consisting of 45 amino acids and containing four disulfide bonds to form a folded protein. MsDef1 overexpressed in genetically modified potato wards off a Verticillium wilt disease caused by a fungal pathogen *Verticillium dahlia* (37). Ramamoorthy et al. (38) previously reported that a knockout of the GlcCer synthase gene, *gcs1*, in a fungal pathogen *Fusarium graminearum* blocked the antifungal activity of MsDef1 revealing the involvement of GlcCer in the mode of action (MOA) of this peptide. To date, no plant defensins have been shown to bind to MDR cancer cells and synergize with chemotherapies. None of the current MDR modulators (e.g., Eliglustat) target two tumor specific MDR targets.

Here, we report 3-dimensional structure of MsDef1 and determine its binding sites for its sphingolipid receptor GlcCer. We show that MsDef1 targets dual tumor specific targets namely MDR biomarker GlcCer in cancer cells and Trx, liberating ceramide and ASK1 protein from GlcCer and Trx respectively and in the process activating dual cell death pathways. We further show that MsDef1 synergizes with Doxorubicin and makes it effective at lower doses *in vitro*.

Materials and methods

Production of MsDef1

MsDef1 was produced using two methods. 1) It was produced recombinantly in *Pichia pastoris* as described previously (39). MsDef1 expressed recombinantly in *P. pastoris* was further purified by RP-HPLC using a reverse phase C18 column (Delta Pak Wat 011793, 15063.9 mm, 5 µM, 300 A) to obtain 95% purity and characterized by mass spectrometry. The purification yielded several species of MsDef1 which was separated by RT-HPLC (See Figure S1; Supplementary Materials). MsDef1 was dissolved in sterile double distilled water and its concentration was determined by using the BCA assay kit (Pierce, Rockford, IL). 2) Linear MsDef1 was chemically synthesized by using the standard peptide synthesizer (Apex 396 Parallel Synthesizer). Folding of the peptide was achieved through controlled air oxidation of the linear peptide. A solution of linear MsDef1 was dissolved in the double-distilled water in a test tube fitted with a probe through which air was bubbled through the solution for 36-48 hrs and monitored using mass spectrometry for a molecular ion corresponding to the oxidation of four S-S bonds. For example, 0.4 mg of linear peptide was dissolved in double distilled water in 50 mM phosphate buffer containing 1M Guanidinium-HCl at pH 7.5. The peptide sample was aliquoted at different time points: 0, 4h, 18h, 24h, 36 and 48h. Each peptide sample was desalted using C18 zip tip and run on LTQ-Orbitrap Velos by direct infusion. The samples were run with high resolution (60,000, LTQ-Velos Pro Orbitrap LC-MS/MS). The characterization includes purity by HPLC (> 96%), linear MsDef1 corresponding to deconvoluted mono isotopic mass 5191.23 and the fully folded MsDef1 corresponding to deconvoluted mono isotopic mass 5183.25. The exact difference 8 is due to the formation of four S-S bonds, a loss of 8 hydrogens. MsDef1 prepared by the slow oxidation method coincides with the one by recombinant method. The oxidation protocol was necessary for the production of large quantities of MsDef1 with correct molecular mass and folding for *in vivo* studies.

Synthesis of 6-((N-(7-nitrobenz-2-oxa-1, 3-diazol-4-yl) amino) hexanoyl -MsDef1

The crude linear MsDef1 was dissolved in 20% methanol/8 M guanidinium hydrochloride and mixed with 6-((N-(7-nitrobenz-2-oxa-1, 3-diazol-4-yl) amino) hexanoyl (NBD) sphingosine in dark conditions. The mixture was stirred for 48 hrs before passing through the Sep-Pak and purified by RP-HPLC using eluents of H_2O/0.1% TFA (eluent A) and acetonitrile/0.1% TFA (eluent B). The programmed elution profile 0–1 min, 100% A; 1–80 min, B is increased from 0–75% at a flow rate of 10 mL/min on preparative column (Spirit Peptide C18, 5 µm column, 19× 100 mm). Peptide purity was determined by an analytical HPLC monitoring peptide elution by absorbance at 220 nm. The conjugated peptide was folded using the air oxidation protocol described earlier. The mass of the conjugated peptide was determined to be 5745.9 (M+H) in agreement with the expected mass of the correctly folded NBD-MsDef1 conjugate.

Structural analysis of ^{15}N-labeled MsDef1 using NMR

^{15}N-labeled MsDef1 was prepared as described previously (38). Briefly, *P. pastoris* cultures were grown overnight in buffered YNB media with no amino acids and 1.2% $^{15}NH_4Cl$ dissolved in 1M potassium phosphate (pH = 6.0), 500x biotin, 10% glycerol and then induced with 0.05% methanol every 24 h, according to the manufacturer's directions (Thermo Fisher Scientific, CA, USA). The cultures were grown for 7 d at 29^0 C, and cells were removed by centrifugation at 2,000g for 15 min. ^{15}N-labeled MsDef1 was purified from the growth medium using CM-Sephadex C-25 cation-exchange chromatography and reverse-phase HPLC. The mass spec analysis of the labeled peptide revealed a single peak at 5254.03 (M+H) corresponding to the correctly folded ^{15}N-labeled MsDef1.

NMR experiments were conducted on a Varian 700MHz spectrometer with HCN probe (backbone dynamics) and Bruker 600 MHz spectrometer with QCI cryoprobe (assignments and structure determination). Backbone (N and H_N) and side chain protons were assigned for MsDef1 in aqueous buffer (25 mM HEPES, 20 mM NaCl, pH 6) at 25°C. The backbone amides were assigned using ^{15}N-separated TOCSY and NOESY spectra with 60 ms and 150 ms mixing times, respectively. These experiments were acquired at 25°C with a 250 µM ^{15}N-labeled MsDef1 in 90% H2O/10% D_2O. Side chain protons were assigned using these spectra plus ^{1}H-^{1}H COSY, TOCSY, and NOESY spectra acquired for an otherwise identical unlabeled MsDef1 sample in 100% D_2O. Backbone amide dynamics experiments were carried out using the same ^{15}N-labeled peptide. R_1, R_2, and heteronuclear NOE experiments were performed using the standard pulse sequences. At least 8 timepoints were acquired for R_1 and R_2 measurements and heteronuclear NOEs were determined from an average of two independent experiments. Error estimates were based on the signal/noise ratio of each spectrum. Single exponential decays were fit to determine R_1 and R_2 rates using IgoPro (Wave metrics). Model free analysis was performed using fast MF and Model Free 4.15. Chemical shift changes upon interaction of MsDef1 with GlcCer were determined using the ^{15}N-labeled peptide. Sixty micromolar d25-DPC (dodecyl phosphocholine, per deuterated acyl tail) was added to 0.25 µM MsDef1 in aqueous buffer to investigate the interaction of this peptide with DPC micelles. This sample was then added to lyophilized GlcCer, allowed to equilibrate for 2 h, and returned to the NMR tube to look for additional changes reflecting specific interaction with GlcCer.

Isolation and purification of GlcCer from *F. graminearum*

Total lipids were extracted from 1g of *F. graminearum* mycelium and a glycolipid fraction containing GlcCer was purified with minor modifications as described previously (38). The mass spec analysis of the purified GlcCer showed a single peak (> 95% purity) at M+ ion 754.

Cancer cell viability assays and determination of IC_{50}

The MCF-7 cells were cultured in RPMI-1640 (Sigma, USA) while MDA-MB-231 was maintained in Dulbecco's modified eagle medium (Sigma, USA). MCF10A cells (American Type Culture Collection, Manassas, VA) were cultured in DMEM/Ham's F-12 (GIBCO-Invitrogen, Carlsbad, CA) supplemented with 100 ng/ml cholera toxin, 20 ng/ml epidermal growth factor (EGF), 0.01 mg/ml insulin, 500 ng/ml hydrocortisone, and 5% chelex-treated horse serum. The cells were cultured at 37 °C in a 90% humidified incubator with 5% CO_2. When the cells were 80% confluent, they were sub-cultured to a fresh media. The SKOV3 cell line was obtained from the American Type Culture Collection (Manassas, VA) and cultured in DMEM growth media supplemented with 10% Fetal Bovine Serum, 2 mM Glutamine, and Pen-Strep antibiotic mixture. The flask containing cells were placed in an incubator which was maintained at a temperature of 37°C and 5% concentration of carbon dioxide (CO_2) gas. Cardiomyocytes were derived from this engineered stem cell clone line as follows. Stem cell aggregates were formed from single cells and cultured in suspension in medium containing zebrafish bFGF (basic fibroblast growth factor) and fetal bovine serum. Upon observation of beating cardiac aggregates, cultures were subjected to blasticidin selection at 25 ug/ml to enrich the cardiomyocyte population. Cardiomyocyte aggregate cultures were maintained in Dulbecco's modified Eagle's medium (DMEM) containing 10% fetal bovine serum during cardiomyocyte selection through the duration of the culture prior to cryopreservation. At 30 to 32 days of culture the enriched, stem cell-derived cardiomyocytes were subjected to enzymatic.

dissociation using 0.5% trypsin to obtain single cell suspensions of purified cardiomyocytes, which were >98% cardiac troponin-T (cTNT) positive. These cells (iCell1Cardiomyocytes) were cryopreserved and stored in liquid nitrogen before delivery to

Ionic Transport Assays from Cellular Dynamics International, Madison, WI.

Doxorubicin resistant MCF-7R and MDA-MB-231R cells were grown in DMEM 10% FBS with increasing concentrations of Doxorubicin as described by Bielawski et al. (40). Cells were seeded and exposed to increasing concentrations of Doxorubicin (10 nM to 100 nM). MCF-7 or MDA-MB-231 cells were seeded in cell culture flasks and after 24 h, cells were trypsinized, counted viable cells and reseeded into a new culture flask before adding Doxorubicin again. Cells were considered chemoresistant when at a particular concentration did not cause cell death. Generally, it took 6-7 passages to get Doxorubicin resistant cells.

Cell viability was evaluated by the standard MTT (3,4,5-dimethylthiazol-2-yl)-2,5-diphenyltetrazolium bromide, Sigma) method. All cancer cells (MDA-MB-231, MCF-7, MCF-R, Hela, MCF-10A epithelial breast cells, induced pluripotent stem cells derived cardiomyocytes (iPSc) were added to the wells of 96-well flat-bottom plates at the density of 2×10^4 per well, allowed to attach overnight, and treated with different concentrations of MsDef1 (1-100 μM). After 24 h, 10 μl of MTT solution was added to each well and the plate was incubated at 37°C for 3 h. After removing the media, 200 μl of isopropanol were added to dissolve the crystals. Absorbance was read at 550 nm in an ELISA plate reader (Sunrise, Tecan, Milan, Italy), and the results are expressed as relative change with respect to the controls set as 100%. For cardiomyocytes, human iPSCs were used (Ionic Transports, St Louis).

Thioredoxin assays using western blots

The Trx Western blotting was performed as described previously, with minor modifications (39). Briefly, 3 x 10^6 cells were lysed in G-lysis buffer (50 mM Tris HCl, pH 8.3, 3 mM EDTA, 6 M guanidine–HCl, 0.5% Triton X-100) containing 50 mM iodoacetic acid (IAA; pH 8.3). For each experiment, control plates, for identifying Trx redox state bands in the Western blot, were also incubated with 2mM H_2O_2, for 10 min at room temperature, before incubation with 50 mM IAA. Subsequently, the lysates from all cells were incubated in the dark for 30 min with the IAA. The lysates were then centrifuged in G-25 micro spin columns (GE Healthcare). Protein was quantified from the eluent using the Bradford protein assay, as previously described (41–45).

Ceramide assessment

Ceramide was extracted from cancer cells using the procedure described by Bielawski et al. (40). Briefly, drug resistant MCF-7R cells were grown on 10 cm plates containing 2–5 $X10^6$ cells per plate, washed with 10 mL of phosphate buffer saline (PBS). The cells were scraped with 1 mL of methanol and transferred into a 5.5 mL glass vial with either aluminum or Teflon-sealed caps (SKS Science). Cells were sonicated for 60 min in a bath sonicator, and 100 μL of the solution was taken for protein concentration measurements. 50 μL of a 50 ng/mL C17 standard solution was added to the remaining cells in the glass vial to obtain a final concentration of 10 ng/mL of C17 as the internal standard (IS). At the end of the extraction procedure, 2 mL of chloroform was added to the cell suspension. After vortexing for 5s followed by 30 min of sonication, the cell lysates were spun for 5 min at 3000 rpm. Then, the lower layer containing chloroform was transferred to a new tube using a 1 mL glass pipette, leaving the upper layer (containing methanol) and the middle layers (containing proteins) (~75% extraction efficiency for this first extraction) and repeated twice to get > 92% extraction. The extracted solution was dried under nitrogen gas, reconstituted in acetonitrile before subjected to HPLC analysis (Agilent 1200, Agilent Technologies, Santa Clara, CA, RP column, 50 X 2.0 mm, 3 mm), Mobile phase A consisted of 0.1% formic acid and 25 mM ammonium acetate in water and mobile phase B consisted of 100% acetonitrile.

Permeability assays

Resistant TNBC cancer cells MDA-MB-231R and ovarian SKOV3 cells were incubated with 20 μg/ml, 6.6 μg/mL, or 2.2 μg/ml of NBD-MsDef1 for 15 min at 37° C in a total volume of 200 μl. The excess NBD-MsDef1 was washed off with 1xPBS and cells were fixed with 4% paraformaldehyde to be imaged using the Nikon Confocal Microscope (TE 2000-E, PES). In order to determine the specificity of NBD-MsDef1 internalization, labeled cells were washed with water 3 times before imaging them. For assessing Doxorubicin influx in resistant MDA-MB-231 TNBC cells, autofluorescence of Doxorubicin was measured using confocal microscopy at emission wavelength of 595 nm post excitation with a 470 nm laser. For enhanced uptake of Doxorubicin by MDA-MB-231R cells post MsDef1 treatment, about 35,000 cells/well were plated in 8-well chambered lab-tek 2 slides and allowed to grow overnight. Cells were treated with 20 μ M of MsDef1, 3 μM Doxorubicin and a combination of 20 μ M MsDef1 and 3 μM Doxorubicin in separate batches for 4 h before examined by confocal microscopy (Nikon A1i laser scanning confocal microscope). Images at 1-min intervals were collected and analyzed. All fluorescence images were analyzed, and the background subtracted with ImageJ software. Pearson's coefficient was quantified using the Colocalisation Analysis plugin for ImageJ.

MsDef1 stability

The Simulated Gastric Fluid (SGF) assay was performed as described by Fu et al., 2002 with some modification. Tests were performed in 500 μL of SGF (200 mg NaCl, 0.2% pepsin, pH 2) in glass tubes in a 37°C water bath with continuous stirring of the enzyme reaction. After 2 min preincubation, the assay was started by the addition of 25 μL of MsDef1 peptide (5 mg/ml) to each vial containing SGF, SGF without pepsin or ultrapure water. Five mg/ml bovine serum albumin (minimum 98%, A-7030, Sigma Aldrich) in ultrapure water was used as the positive control for pepsin digestion. Protein samples were analyzed for degradation by SDS PAGE followed by staining for 1 h and extensive washing with ultrapure water.

Synergy studies

The percentage of apoptotic cells was determined by using TUNEL assay according to the manufacturer protocol. Briefly, cells were fixed with 1% paraformaldehyde at 4^0C, followed by two washing with PBS. Cold 70% ethanol was added to the cell pellet. Cells were then incubated at −20°C for permeabilization. After washing with PBS, cells were incubated with staining solution containing TdT enzyme and fluorescein-dUTP for 60 min at 37° C. Samples were washed with rinse buffer and resuspended in 500 ml of propidium iodise/RNase solution for flow cytometry analysis.

Results

MsDef1 is a 45-amino acid cysteine-rich peptide predicted to form four disulfide bonds was identified for its antifungal activity against filamentous plant pathogens was first reported in 2000 by Gao et al (46). Some defensins bind to specific sphingolipids with high affinity that are localized in the fungal cell wall and plasma membrane of their target fungi (47–49). Sphingolipids serve as second messengers for regulating cell growth, cell survival and death (50). Mechanistic studies suggest that MsDef1 binds to GlcCer in the cell wall of the fungal pathogen *F. graminearum*. A Gcs1 knock-out mutant (Δ*Fggcs1)* lacking GlcCer synthase activity and a depleted in GlcCer displays strong resistance to MsDef1. Understanding the binding of the specific amino acid residues of MsDef1 with MDR biomarker GlcCer opens an opportunity to design small peptide based drugs for a potential to treat MDR cancer. Here, we have determined the structural basis for the engagement of GlcCer by ^{15}N labeled MsDef1 using ^{15}N longitudinal relaxation (T1) and ^{15}N-^{1}H Nuclear Overhauser Effect (NOE) in solution dynamics NMR.

Three-dimensional structure of MsDef1

The parameters characterizing the structure of MsDef1 are shown in Table 1. The structure of this peptide was derived from 981 distance constraints derived from 216 sequential, 61 short range, 38 medium range, 204 long range NOEs and 12 hydrogen bonds. Figure 1 is a superposition of the final ensemble of structures calculated for MsDef1 with a single cartoon representation of this ensemble. This ensemble of structures results from 20 lowest energy structures from 80 calculated structures. The mean rmsd is 0.99 Å for backbone heavy atoms and 0.52 Å for all heavy atoms, respectively. Not surprisingly, MsDef1 has a highly compact structure which consists of one α-helix (α1=Cys18-Thr23) and three anti-parallel β-strands (β1=Thr2-Leu6, β2=Val29-Arg32, β3=Cys39-Arg44). The structure is stabilized by the presence of four disulfide bonds with Cys3-Cys45, Cys14-Cys33, Cys18-Cys39, Cys22-Cys41 configuration. The core structure is almost identical to the homology-based structure of MsDef1 published earlier (51) and is similar to other plant defensins with regard to folding and

TABLE 1 Statistics from Structure Calculation.

Parameter	Value
Number of Restraints	
NOE (total)	981
Sequential	216
Short-range	61
Medium-range	38
Long-range	204
Dihedral angles[a]	67
H-bonds	12
Energy (kcal/mol)	
Total	-1100.8 ± 85.5
Bond lengths	2.0 ± 0.1
Bond angles	23.6 ± 0.7
Impropers	4.2 ± 0.3
Van der Waals	-260.3 ± 51.6
Dihedral angles	207.7 ± 1.6
Electrostatics	-1077.9 ± 62.2
NOEs	187.1 ± 140.0
No. of NOE violations >0.5 Å (Å)	3 ± 2.3
No. of dihedral angle violations >5° (°)	0
RMS Deviations	
NOEs (Å)	0.059 ± 0.024
Dihedral angle restraints (°)	2.11 ± 0.05
Ideal bond lengths (Å)	0.0017 ± 0.0001
Ideal bond angles (°)	0.355 ± 0.005
Ideal improper angles (°)	0.270 ± 0.011
Backbone atoms (Å)	0.26 ± 0.04
	0.15 ± 0.02[b]
Heavy atoms (Å)	0.99 ± 0.09
	0.52 ± 0.09[b]
All atoms (Å)	
Ramachandran Plot (%)	
Most favored regions	76.2
Additional allowed regions	20.9
Generously allowed regions	2.9
Disallowed regions	0.0

Results from ensemble of 20 lowest energy structures from 80 calculated structures.
[a]ϕ and ψ torsion angles restraints derived from $^{3}J_{HNH\alpha}$ couplings directly measured from COSY spectra and chemical shift index analyzed with TALOS+.
[b]values for secondary structure elements only.

10.3389/fonc.2023.1141755

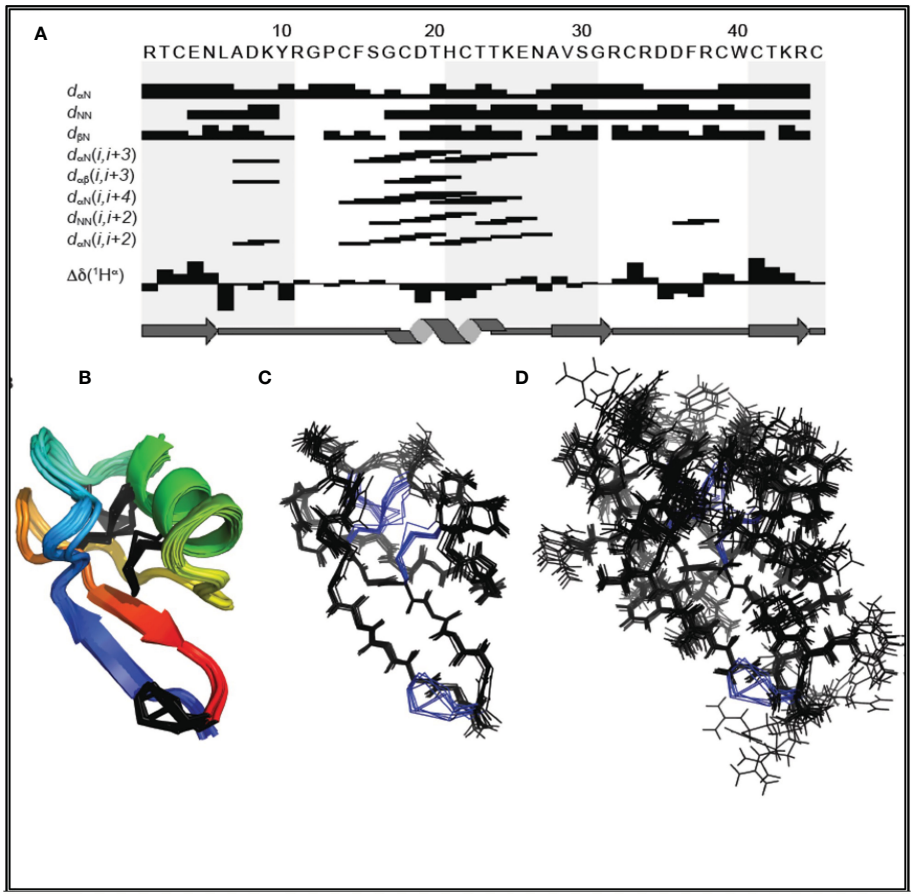

FIGURE 1
(A) Amino acid sequence of MsDef1 and survey of NMR data used to identify secondary structures. The sequential and medium range weak, medium, and strong NOEs are represented by the heights of the bars. The positions of β1, α-helix, β2 and β3 are shown relative to the amino acid sequence of MsDef1. **(B)** Backbone superposition of the 20 energy-minimized structures of MsDef1 showing the global fold and secondary structures. The disulfide bonds are shown in black. **(C)** Stereo view of the backbone atoms (N, C and O) of the structures in **(B)**. **(D)** Backbone superposition of the ensemble of structures showing the amino acid side chains.

locations of the four disulfide bonds (52). Statistics from structural calculations are tabulated in Table 1.

MsDef1 binds to GlcCer "in situ"

The solution dynamics of MsDef1 with GlcCer was assessed using chemical shift perturbation, ^{15}N longitudinal relaxation (T1) and ^{15}N-^{1}H NOE. Upon binding of ^{15}N–labeled MsDef1 with GlcCer with d25-DPC micelles, significant peak shifts occurred and upon addition of GlcCer additional chemical shift changes in a smaller subset of residues occurred (Figures 2A, B). Our results revealed that MsDef1 binds to GlcCer at two regions: amino acids between residues 12-20 and residues 33-40 (red color, Figures 2C, D). This is consistent with our earlier finding that mutation of Arg38 to Gln38 resulted in a complete loss of the antifungal activity of MsDef1 against *F. graminearum* (39). Binding of MsDef1 to GlcCer is the first premise on which MsDef1 is proposed as a targeted tumor sensitizer.

MsDef1 regenerates ceramide from GlcCer

Revamping ceramide pathway is important for those drugs which mediate the cell death through ceramide pathway (e.g., Doxorubicin). Changes in the liberation of ceramide in Doxorubicin resistant MCF-7R cells were measured at Lipidomics Shared Resource, Medical University of South Carolina (MUSC), using high performance liquid chromatography-mass spectrometry (LC-MS/MS) as previously described by Jacek et al. (40). Preliminary studies (Figure 3B) showed an enhanced accumulation of ceramide until 6 hrs of treatment with 20 μM MsDef1 in GlucCer positive MCF-7R (resistant) breast cancer cells compared to normal breast epithelial GlucCer negative control cells (MCF-10A). Ceramide is known for inducing apoptosis in cancer cells exemplified by Doxorubicin which goes through ceramide pathway mechanistically. Hence, apoptosis induced by ceramide released was also measured in MCF-7R cells which showed an order of magnitude higher than for normal cells (MCF-10A) which are GlucCer negative at 3 and 6 hrs of treatment

10.3389/fonc.2023.1141755

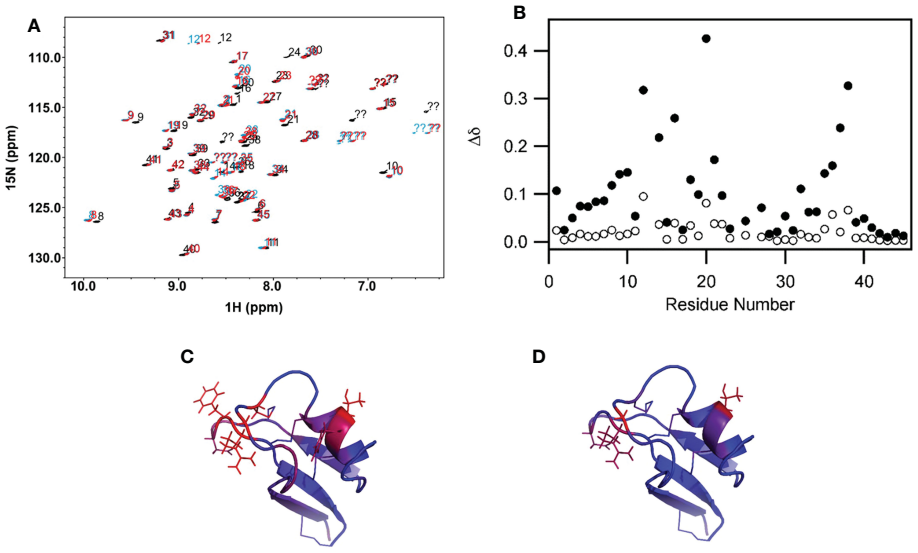

FIGURE 2
(A) Backbone region of the ^{1}H-^{15}N HSQC spectrum showing chemical shift changes in MsDef1 (black spectrum, aqueous buffer) upon addition of the DPC micelles (blue spectrum) and further addition of GlcCer (red spectrum). Significant peak shifts upon addition of the lipid-like detergent DPC indicates that MsDef1 does interact with the micelles. Addition of GlcCer causes additional chemical shift changes in a smaller subset of residues indicating that GlcCer interacts with MsDef1 in a more localized region. **(B)** Quantification of the chemical shift changes in MsDef1 upon addition of lipid. $\Delta d = (\Delta d_H^2 + 0.1{*}\Delta d_N^3)^{1/2}$. Significant chemical shift changes are observed in two regions upon addition of micelles of the lipid-like detergent, DPC (solid symbols, DPC versus aqueous buffer). Smaller additional changes are observed in a few localized sites upon further addition of GlcCer (open symbols, DPC + ceramide versus DPC only). **(C)** Chemical shift mapping of MsDef1-GlcCer interactions. **(A)** Residues with chemical shift changes upon association with DPC micelles. The color scale extends from blue (no change, $\Delta d=0$) to red (significant chemical shift change, $\Delta d \geq 0.25$). **(D)** Residues with additional chemical shift changes upon addition of GlcCer to the DPC micelles. The same color scale is used but with a narrower range ($0 \leq \Delta d \leq 0.10$). One face of the molecule has significant backbone chemical shift changes upon addition of micelles indicating that this face interacts with DPC. GlcCer interacts with a smaller, more localized subset of the residues that interact with the lipid-like detergent micelles.

(Figure 3A). The enhanced accumulation of ceramide in response to MsDef1 treatment was similar to that observed upon treatment with 20 μM α-tocopheryl succinate (TOS) (53) serving as a positive control. Reactivation of ceramide pathway is important since it is an effective sensitizing strategy in overcoming the resistance in metastatic colon and breast cancers *in vivo* (54). The enhanced accumulation of ceramide upon MsDef1 treatment in cancer cells selectively compared to normal breast cells is the second premise on which MsDef1 is proposed as a MDR targeted tumor sensitizer.

MsDef1 oxidizes tumor specific biomarker Trx

Several disulfide-linked peptide derivatives are shown to oxidize Trx, a tumor specific biomarker (54–60). Trx is known to be involved in development of Doxorubicin resistant cells by deactivating ASK1-pathway. MsDef1 was anticipated to interact with Trx due to its four disulfide bonds and availability of SH groups on Trx protein. Hence, further studies were conducted in cancer cells (e.g., TNBC, MDA-MB-231) using MsDef1.

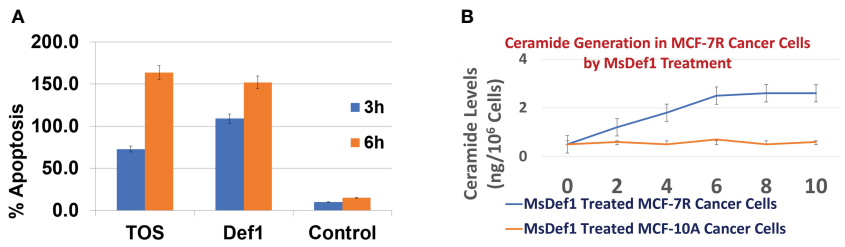

FIGURE 3
(A) Extent of apoptosis in GlucCer positive MDR MCF-7R cells treated with Def1 (20 μM) compared to positive control α-Tocopheryl succinate (TOS, 20 μM) and GlucCer negative normal MCF-10A breast epithelial cells, **(B)** Ceremide regeneration from GlucCer positive MCF-7R cells treated with Def1 (20 μM) compared to GlucCer negative normal MCF-10A breast epithelial cells.

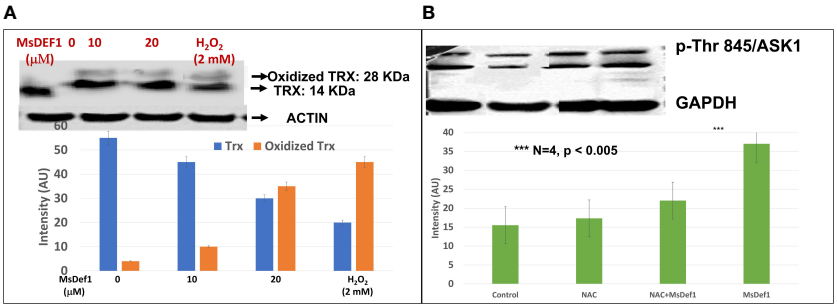

FIGURE 4
(A) MsDef1 oxidizes Trx at 20 μM dose compared to positive control H_2O_2 (2 mM) & presumably activates ASK1 cell death pathway in MDA-MB-231-R TNBC cells, N=4, $p < 0.05$, **(B)** Immunoblot analysis of phosphorylation of Threonine-845 residue of ASK1 Protein in response to the treatment of Def1 in MDA-MB-231 cells: 1. Control, 2. N-Acetyl-Cysteine (NAC, 5 mM)/60 mins, 3. NAC (5 mM) + Def1 (50 μM) for 60 min, 4. Def-1 (50 μM) alone for 60 minutes, N=4, $P < 0.005$, GAPDH: Internal Control. *** Statistically siginificant.

Doxorubicin resistant MDA-MB-231-R cells were treated with 0, 10 and 20 μM MsDef1 or 2 mM H_2O_2 (positive control). Figure 4A clearly indicates the oxidation of Trx at 20 μM MsDef1 by showing Trx peptide band at 28 KDa compared to untreated control which showed Trx band at 14 KDa. The oxidation of Trx by MsDef1 is similar to that observed with positive control 2 mM H_2O_2 (N=4, $p < 0.05$). This is the third premise on which MsDef1 is proposed as a targeted tumor sensitizer.

MsDef1 disrupts Trx-ASK1 complex to activate ASK1 cell death pathway and induces apoptosis in resistant cancer cells

The oxidation of Trx is known to release ASK1 from the Trx complex through phosphorylation of several amino acid residues (33). We corroborated Trx oxidation data (Figure 4A) by assessing the phosphorylation status of Thr845 residue of ASK1 protein using specific antibody phosphorylation kit (Santa Cruz Biotech, CA). Fas resistant triple negative MDA-MB-231R cancer cells were treated with a) 50 μM MsDef1 for 60 minutes, b) 5 mM N-acetyl cysteine (NAC) as a negative control and c) NAC treated cells plus 50 μM MsDef1. Figure 4B showed a significant increase in phosphorylation of Thr845 residue (lane 4) upon treatment with MsDef1 compared to the solvent control (lane 1) and the NAC control (lane 2, N= 4, $p < 0.005$). NAC is an FDA approved drug which inhibits phosphorylation of Thr485 of ASK1 protecting cells from death. MsDef1 induces significantly higher phosphorylation of Thr485 of ASK1 (lane 4) than it does even in presence of NAC (lane 3). These results indicate that MsDef1 might have targeted tumor specific Trx and activates ASK1 cell death pathway. Trx inhibitors with disulfide bonds are known to reactivate ASK1 pathway and sensitize cancer cells to chemotherapy similar to MsDef1 (55–60).

MsDef1 permeates resistant cancer cells

Defensins are cationic peptides known for creating irreversible structural defects on the cell membranes with pore formation similar to CPPs (61). However, the specificity of MsDef1 to MDR tumor cells needs to be tested. Optical marker 6-((N-(7-nitrobenz-2-oxa-1, 3-diazol-4-yl) amino) hexanoyl (NBD) sphingosine was modified with linear MsDef1 before it was cyclized through oxidative protocol developed by us. The modified NBD-MsDef1 showed IC_{50} (12 μM) similar to the native MsDef1 indicating that the modification of the peptide did not alter its biological activity by a large margin. Confocal microscopy studies on MsDef1-NBD incubated with resistant TNBC MDA-MB-231R and ovarian SKOV3 cells respectively showed a significant uptake of MsDef1-NBD (Figures 5A, B) compared to untreated tumor cells while, normal epithelial breast cells (MCF-10A) and fibroblasts cells (Figures 5C, D) did not take up MsDef1 even at 5-fold higher dose of MsDef1 at 200 mg/mL. Simple washing of stained cells did not reduce the fluorescence intensity originated from NBD which confirms trapping of MsDef1 inside the cancer cells. Permeation of membrane compromised fungal cells by MsDef1 was recently reported by us using optical marker DyLight 550-MsDef1 (39). The low uptake of the scrambled MsDef1-NBD by tumor cells (Figure 5E) established the potential selectivity of MsDef1 action for tumor cells. Figure 5F shows accumulation of NBD-MsDef1 with respect to concentration in cancer cells graphically.

Uptake of MsDef1 in resistant TNBC cells

MsDef1 presumably compromises MDR cell membrane integrity by disintegrating GlucCer to ceramide and allowing internalized MsDef1 to interact with the intracellular Trx. That is expected to allow a better perfusion of drugs influx into the cancer cells. The hypothesis was corroborated by measuring the influx of Doxorubicin by MsDef1 in MDR cancer cells through the intrinsic fluorescence of Doxorubicin at 488 nm using confocal microscopy. Figures 5G, H demonstrates a significant increase in the fluorescence intensity of Doxorubicin in MDA-MB-231R cells after treatment with 20 μM MsDef1 for 6-12 hr. compared to Doxorubicin alone. The increase in the fluorescence intensity showed uptake of Doxorubicin 3-fold more in presence of MsDef1 than in its absence Figure 5i. This result confirms the

10.3389/fonc.2023.1141755

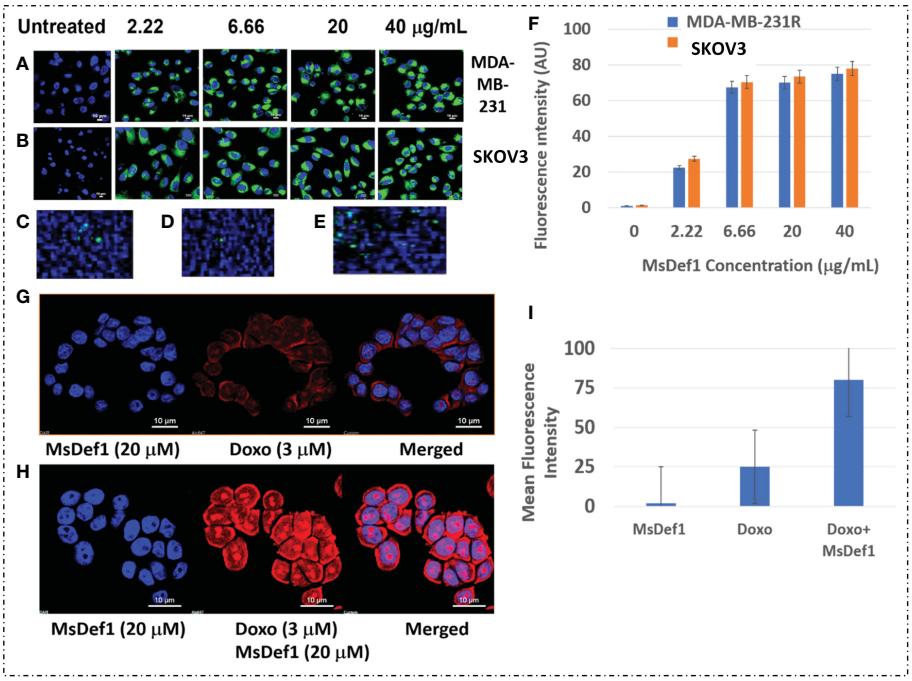

FIGURE 5
(A) NBD-Def1 permeates resistant **(A)** TNBC MDA-MB-231R Cells **(B)** SKOV3 Cells while, uptake is low for **(C)** Normal Epithelial Breast Cells **(D)** Fibroblasts & **(E)** Scrambled Def1 indicating selectivity, **(F)** Graphic representation of MsDef1Def1 uptake (N= 4, p < 001), **(G)** Effect of MsDef1Def1 on doxorubicin influx into MDR cancer cells MDA-MB-231R by confocal microscopy, N = 4, P < 0.002. Cells were stained with Hoechst 3325 and doxorubicin fluorescence was visualized at 488 nm, **(H)** Quantitative intrinsic mean fluorescence intensity of Doxorubicin. **(I)** Quantification of Uptake of Doxorubicin through Mean Fluorescence Intensity (AU).

poor tumor penetration limitation of Doxorubicin on its own and may explain a potential pore formation of cancer cell membranes and the synergistic effect of MsDef1 allowing Doxorubicin to perfuse better into the tumor cells.

MsDef1 exhibits antitumorigenic activity

Table in Figure 6A shows IC_{50} values for MsDef1 in several GlcCer and Trx positive cancer cells. These values are in the similar range as those of many chemotherapeutics (62–65). Several similar defensin type of molecules derived from natural sources also showed IC_{50} values in similar range (66, 67). However, none of them has been shown to have multiple characteristics of MsDef1 including liberation of ceramide, oxidation of Trx and synergy with chemotherapeutics. It should be noted that MsDef1 targets cancer cells *in vitro* (e.g., MDA-MB-231, MDA-MB-231R, HeLa, BT-459) while sparing normal epithelial breast cells (e.g., MCF-10A), bone marrow cells (MSC-001F) and cardiomyocytes (iPSC), an attribute important in determining the potential side effects of MsDef1 if it moves to the clinical phase. It should be noted that Doxorubicin, the first line treatment for TNBC, has IC_{50} value of 9.6 μM in iPSC cardiomyocytes compared to >180 μM for MsDef1 indicating a better safety profile for MsDef1. Figure 6A shows the tabulation of IC_{50} values for varieties of cancer cells which are GlucCer positive (e.g., MDA-MB-231, MDA-MB-231R, HeLa, BT-459) and normal cells including bone marrow cells (MSC-001F) and iPSc cardiomyocytes which are in general get severely affected by chemotherapy. It is to be noted that Doxorubicin kills normal cells at relatively lower doses (~ 9.6 μM), while MsDef1 is relatively safer even at > 200 μM (Figure 6B). On the contrary, MsDef1 kills cancer cells at lower μM similar to Doxorubicin potency. The combination of MsDef1 and Doxorubicin reduced IC_{50} values significantly from 396.6 nM for Doxorubicin to 16.5 nM indicating the synergy between MsDef1 and Doxorubicin (Figure 6C). The data is further confirmed by the measurement of combination index which was <1.00, hallmark of synergy (Figure 6D).

MsDef1 synergizes with Doxorubicin to enhance apoptosis in cancer cells

Although MsDef1 is cytotoxic to cancer cells, its activation potential to sensitize low responsive MDR cancer cells will have a major impact on improving the clinical performance of chemotherapy. Studies were conducted to determine synergy between MsDef1 and Doxorubicin drugs using cell death quantification. For example, MsDef1 (e.g., ~25 μM) and Doxorubicin (1mg/mL) showed ~30% cell death individually compared to untreated controls (Figures 7A–C or 7E–G) in both MDA-MB-231R and MCF-7R cancer cells. However, when the cancer cells were pretreated with 25 μM MsDef1 followed by treatment with 1mg/mL Doxorubicin, a synergistic increase in cell death (>75%) was observed as compared to that observed for Doxorubicin or MsDef1 treatment alone (Figures 7D–H). This is true for both MDA-MB-231R triple negative breast cancer cells and MCF-7R breast cancer cells. In viability assays, a combination of MsDef1 and Doxorubicin had IC_{50}

value ~10-fold lower than that of Doxorubicin (Figure 6C). Synergistic cell death was also verified by calculating the combination index (CI) values using Chaou-Talalay method[41]. (Figure 6D). Combination index value suggested synergy (CI <1.00) and not just additive activity (CI =1). CI values were obtained over a range of fractional cell kill levels (*i.e.*, 0.05 to 0.95; 5-95% cell kill), and demonstrated values <1 for two dose combinations of MsDef1 and Doxorubicin (Figure 6D, blue and red lines). This is the fourth premise on which MsDef1 is proposed as a targeted tumor sensitizer.

MsDef1 stability to protease digestion

The most important parameter that determines drug efficacy and safety is the stability of drug "*in vivo*". The stability of MsDef1 to digestion by proteases was assessed by incubating MsDef1 with pepsin simulated gastric fluid (SGF) to predict it's *in vivo* stability. MsDef1, in presence of SGF, remained undigested (lanes 3-6 compared to lanes 1-2 in Figure 8), while positive control BSA (lanes 9-10 in Figure 8) was completely degraded. This result suggests high stability of MsDef1 towards protease digestion *in vivo*.

Discussion

The antifungal properties of plant defensins, particularly MsDef1 are well studied by our collaborator Shah et al. (36–38) in plant science. However, their potential as anti-cancer agents remain largely underexplored. We have previously reported that the antifungal mechanism of action (MOA) of the plant defensin MsDef1 involves its potential interaction with GlcCer (38). In order to characterize the role of this interaction with cancer cells, we first determined the three-dimensional structure of MsDef1 using nuclear magnetic resonance (NMR) similar to the homology-based three-dimensional structure of MsDef1 reported earlier (51) and NMR structures of several other plant defensins (51). The structure of MsDef1 consists of one α-helix and a β-sheet consisting of three anti-parallel strands and adopts the cysteine-stabilized α/β fold. In this study, we used NMR to analyze the conformation and dynamics of MsDef1 in presence of DPC micelles and DPC micelles plus GlcCer extracted from the cell walls of *F. graminearum*. The ^{15}N longitudinal relaxation (T1), ^{15}N-^{1}H NOE and chemical shift identified amino acid residues 12-20 and 33-40 as the binding sites for this sphingolipid of the uniformly ^{15}N-labeled peptide. These two binding sites are located in the Loop1 and Loop2 regions of the MsDef1 structure, respectively. Similar interaction of the plant defensin Psd1 with GlcCer has been reported previously (66, 67). Binding of MsDef1 with GlcCer is the first step in mediating cytotoxicity in cancer cells and is the first premise on which we rationalized the utility of MsDef1 as a potential tumor sensitizer for cancer therapy. The interaction of MsDef1 with GlcCer enabled us to predict and propose the potential utility of this peptide in cancer therapeutics.

The MDR cancer cells is a major problem in the treatment of cancer. For example, Doxorubicin which is a front-line treatment for TNBC patients mediates cell death through the ceramide pathway. However, cancer cells circumvent the benefits of the therapy by GlcCer using the GCS enzyme converting lethal ceramide to innocuous GlcCer (25). GlcCer is established as a biomarker for MDR (23). Hence, targeting GlcCer may be a novel

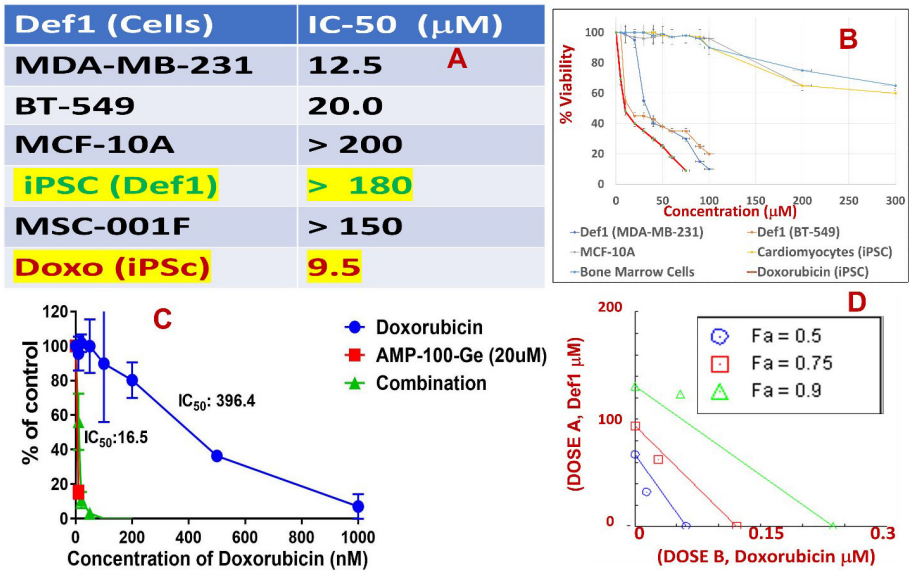

FIGURE 6
(A) Tabulated IC_{50} values of MsDef1 in MDA-MB-231, BT-549 cancer cells compared to normal cells MCF-10A, induced pluripotent stem cell derived cardiomyocytes (iPSCs), bone marrow cells (MSC-001F) and Doxorubicin. **(B)** The IC_{50} values were derived from viability assays. N=3, $p < 0.05$, Note: IC-50 values for normal cells by Def1 is ~ 10-15 times lower compared to cancer cells indicating better safety profile for Def1 *in vitro*, **(C)** IC_{50} curve for a) Def1 and b) combination of Def1 at 20 μM as a function of Doxorubicin dose in MDA-MB-231 cells, N= 4, $p< 0.002$. **(D)** Combination Index calculation for Def1 and doxorubicin in MDA-MB-231 cells: fa = fractional killing of cells. CI < 1.00 Synergistic, CI = 1.00 Additive, CI > 1.00, Antagonist.

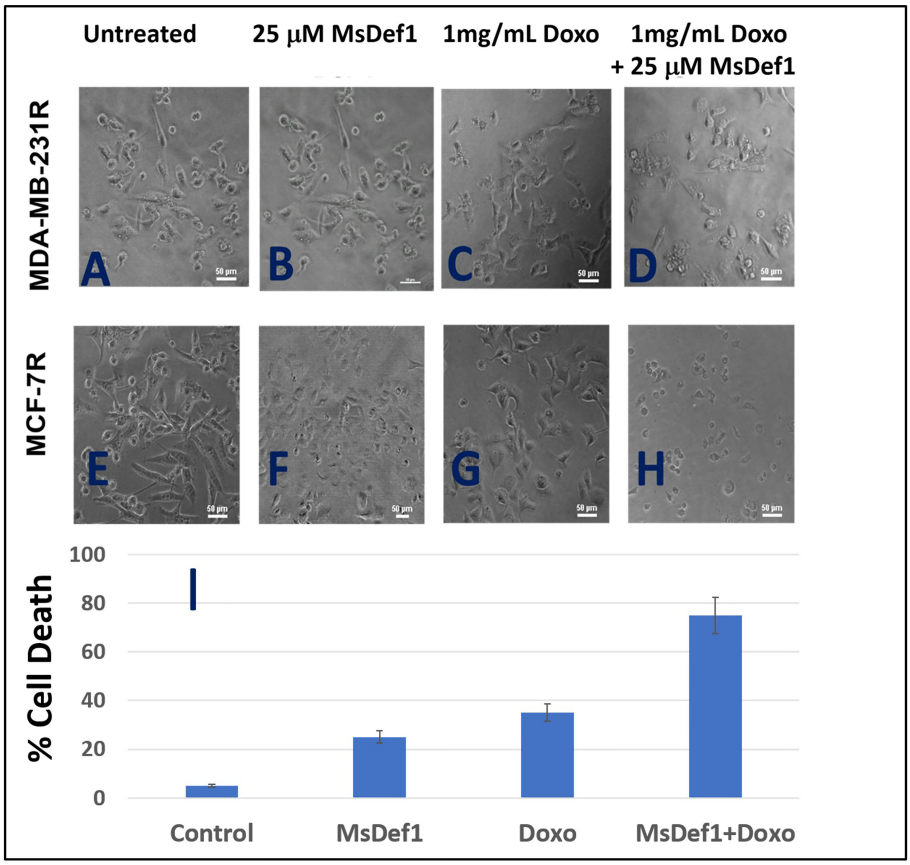

FIGURE 7
MsDef1 synergizes with doxorubicin in resistant MDA-MB-231R and MCF-7R cells **(A–D)** Micro photographs of **(A, E)** control, **(B, F)** Def1 alone, **(C, G)** Doxorubicin alone and **(D, H)** Combination followed by **(I)** quantification of apoptosis, N = 4, $p < 0.007$.

and innovative strategy for addressing clinical MDR issues. MDR cancer cells (e.g., MDA-MB-231R) are characterized by the overexpression of GlcCer on their surface. Jacek et al. (40) successfully extracted and quantified GlcCer from Doxorubicin resistant MCF-7R tumor cells using chromatography. MsDef1 has a net positive charge of +4 but has potential to carry a net charge of up to +7 at low pH conditions. The anionic character of the plasma membranes of cancer cells brought about by externalization of phosphatidylserine could facilitate high binding of cationic MsDef1. Our NMR studies (Figures 1, 2) established that specific residues of MsDef1 binding to GlcCer mediating intracellular cytotoxic effects.

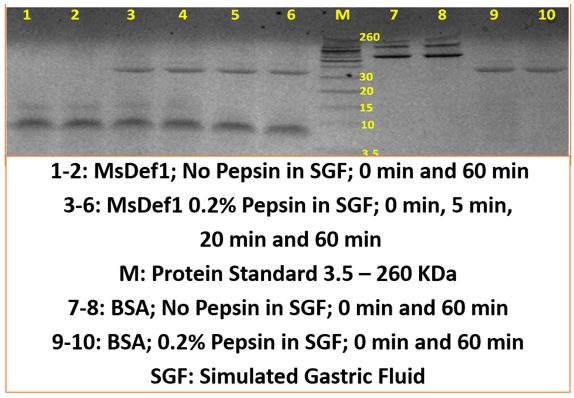

FIGURE 8
MsDef1 stability in Simulated Gastric Fluid (SGF, *in vivo* mimicking conditions) while, positive control BSA degraded, n=4, $p < 0.08$.

Ceramide pathway is involved in mediating cytotoxicity of anthracyclines. Our results on resistant TNBC cells showed the release of ceramide from GlcCer (Figure 3). This is in contrast to the conversion of apoptotic ceramide to non-apoptotic GlcCer, a biomarker of MDR by cancer cells. In other words, MsDef1 treatment could revamp the ceramide pathway inhibiting one of the resistance mechanisms. Our data showed that MsDef1 induced sphingomyelinase activity and enhanced ceramide levels in resistant MCF-7R cells (Figure 3B). Since ceramide is a powerful cell death inducer, the ceramide levels were correlated to the apoptosis (Figure 3A). The importance of the restoration of ceramide pathway lies in its ability to modulate the biochemical and cellular processes that lead to apoptosis. MsDef1 was also compared with α-Tocopheryl succinate (α-TOS) which mediates its cytotoxic effect through ceramide pathway (53). A significant increase in the ceramide release by MsDef1 in resistant cancer cells suggests that this peptide might be able to create structural defects

on the surface of cancer cell membranes by cleaving the bond between ceramide and glucose. A potential permeation mechanism is proposed based on confocal studies (see below).

Equally important in the development of MDR is the overexpression of Trx as a defense mechanism which occurs in response to oxidative stress during chemotherapy treatment. High Trx levels are directly correlated with inhibition of the endogenous ASK1 pathway making chemotherapy ineffective. Tumors with low Trx levels exhibit a better prognosis than tumors with high Trx levels (poorer prognosis, $P < 0.001$) for partial free survival (PFS) and for overall survival (OS) (32, 33). In fact, Trx is a well-studied target which lowers the response rate to specific docetaxel, cis-platin and Doxorubicin treatment while sensitizes cancer cells to Perifosin once Trx is inhibited (68). Oxidation of Trx releases ASK1 bonded to Trx. Our data clearly showed oxidation of Trx by 20 μM MsDef1 as compared to 2 mM H_2O_2 demonstrating a better oxidation potential of MsDef1 than H_2O_2. Oxidation of Trx is known to activate ASK1 cell death pathway and sensitizes tumor cells (68). The presumption that Def1 permeates MDR tumor cells is true because MsDef1 could access intracellular Trx. Similarly, creation of pores on the membrane surface of GlcCer positive MDR cancer cells by MsDef1 may also be rationalized since MsDef1 got the access of intracellular Trx in tumor cells, despite more research is needed to corroborate it. This result agrees with the finding that human β-defensin1 (hBD-1) similar to MsDef1oxidizes Trx *in situ* (69, 70) and unmasks its biological activity. For example, after reduction of disulphide-bridges hBD-1 becomes a potent antimicrobial peptide against opportunistic pathogens. Similarly, MsDef1 presumably becomes anti-tumorigenic after it got reduced to a potent form by tumor specific Trx. It is observed in our studies that all cancers cells were Trx positive while normal cells, cardiomyocytes and bone marrow cells were Trx negative. These data also indicate a potential strong selectivity of MsDef1. Similarly, Trx inhibitors (e.g.PX12) are known to oxidize Trx to reactivate ASK1 pathway and sensitize cancer cells to chemotherapy (68). Targeting ceramide and ASK1 dual cell death pathways is the hallmark of MsDef1 which may be unique compared to the other existing cancer treatments.

Interaction of MsDef1 with the tumor specific MDR biomarker Trx may have several implications for the potential trapping of MsDef1 inside cancer cells. This may be important for the continuous activation of ASK1 cell death pathway resulting in the antitumor properties and/or synergy of MsDef1 with the existing treatments. Defensins are cationic at low pH with cell penetrating properties [e.g., human β-defensin, hBD-1 (69, 70)]. In this study, we tested the cell penetrating ability of MsDef1 in MDR tumor cells using the NBD-conjugated peptide. Confocal microscopy studies performed using MsDef1-NBD incubated with TNBC MDA-MB-231R and ovarian SKOV3 cells showed the uptake of the peptide, although not linearly to different concentrations. It appears that there is a significant change in the intensity of fluorescence signal from 0 mg/mL to 2.22 mg/mL to 6.6 mg/mL and get saturated at higher concentrations. The low uptake of MsDef1-NBD by tumor cells established the selectivity of the peptide to tumor cells. BODIPY-labeled plant defensin NaD1 was also reported to localize in organelles of lymphoma U937 cells (66, 67) demonstrating the cancer cell penetrating ability of plant defensins.

We hypothesized that MsDef1 with its ability to penetrate GlcCer positive cancer cell membranes could potentially increase the diffusion of Doxorubicin into the tumor. This hypothesis was corroborated by measuring the influx of Doxorubicin by MsDef1 in MDR cancer cells through the intrinsic fluorescence of Doxorubicin at 488 nm measured using confocal microscopy (Figure 5G). The low intensity of fluorescent signal by Doxorubicin alone confirms the reported poor tumor penetrating ability of Doxorubicin. The higher influx of Doxorubicin indicated by the higher intensity of fluorescent signal by cancer cells which are pretreated with MsDef1 implies that MsDef1 may permeate MDR cancer cells making Doxorubicin diffuse better into the tumor cells.

The inhibitory activity IC_{50} of MsDef1 against several GlcCer and Trx positive cancer cells is in the 10-15 μM range which is similar for many chemotherapeutics (62–65) making MsDef1 clinically viable. The interesting part is that IC_{50} MsDef1 is 15-20-fold more in normal epithelial breast cells and more importantly in cardiomyocytes (Table in Figure 6A). In contrast, Doxorubicin has IC_{50} very low at 9.6 μM in cardiomyocytes which makes it cardiotoxic (Figures 6A, B). However, Doxorubicin combined with MsDef1 was ~25x more potent, against MDA-MB-231R cancer cells confirming the synergy between MsDef1 and Doxorubicin (Figure 6B). The data was further corroborated with the calculation of combination index (CI) using Towley method (61) which showed CI values less than 1.00 indicative of synergy and not just addition (6D). Although, several defensins (71) have been reported to be cytotoxic to cancer cells (Table in Figure 6A) they shared little sequence homology with MsDef1 and none of them were shown to bind GluCer, permeate cells, synergize with Doxorubicin, and hit the intracellular tumor specific target (Trx). This was the fourth premise on which MsDef1 is proposed as a targeted tumor sensitizer.

The risk of anthracycline related cardiomyopathy increases with a higher cumulative anthracycline dose (72, 73). About 3% of that dose persist even after the completion of therapy leading to potential heart failure and death for a dose of 400 mg/m^2, 7% for a dose of 550 mg/m^2, and 18% for a dose of 700 mg/m^2. The poor tumor penetration capacity by Doxorubicin and its off target hyperactivation of endogenous PARP in heart leads to cardiomyopathy (74). Hence, improving the clinical performance of Doxorubicin may pave the way for new combination adjunctive therapy. *A priori* activation of apoptosis pathways of tumor (AAAPT) technology developed by us (39) involves targeted natural tumor sensitizers, small molecules and defensins to sensitize specifically desensitized resistant tumor cells to evoke a better response from Doxorubicin (39). In other words, sensitizing MDR cells and making them better responsive to chemotherapy is expected to make chemotherapy work at lower doses without compromising on the efficacy on tumor regression, yet reducing the cardiotoxicity to minimum by dose reduction. This synergistic

approach may facilitate the expansion of the therapeutic index of the drug. Both Def1 (25 μM) and Doxorubicin (1mg/mL) induced cell death in resistant TNBC MDA-MB-231-R cells reasonably assessed through morphology of cell death (Figure 7). However, when combined together, the cumulative cell death was greater than just adding the two drugs. The change in IC_{50} for the combination is ~25 times higher compared to individual drugs (Figure 6C, from 394.6 nM to 16.5 nM for the combination). This translates, clinically that a combined formulation potentially may reduce the tumor burden at a lower Doxorubicin dose which in turn may reduce the dose related toxicity induced by Doxorubicin, particularly cardiotoxicity. It is to be noted that MsDef1 does not tackle the Doxorubicin toxicity directly. We infer that cardiotoxicity of Doxorubicin is tackled by making it work effectively at lower doses which automatically lowers dose related cardiotoxicity. In other words, physicians may have a larger window for fine tuning the combination dose regimen based on the potential combined lower toxicity rather than the individual toxicities. MsDef1, being natural and expressed in corn and alfalfa is presumably not expected to be toxic at the clinical dose levels, although not proved *in vivo* so far. However, FDA considers MsDef1 belongs to the GRAS (generally regarded as safe) category. It is possible to leverage this by changing MsDef1 dose in a larger window and reducing the Doxorubicin dose for potential, combinatory synergistic effects. In our recently published work (40) on small molecules we have established in a rat tumor model that the ejection fraction measured through US imaging was retained for the combination (> 65%) while it did not for Doxorubicin alone (< 45%).

Two major requirements for the translation of bench concept to clinical product are a) stability of MsDef1 and b) selectivity of MsDef1 to cancer cells. In general, MsDef1 type of molecules are quite stable in media due to the cyclization of cysteines. Stability of MsDef1 *in vivo* towards proteolytic enzymes may not be a big concern since several tetra sulfide array compounds including FDA approved products developed by Pandurangi et al. (75, 76); (e.g., NeoTect, NeoTide), human beta defensin (hBD-1) with three S-S bonds (69, 70), cyclized cyclotides (77), θ defensins (78) provide solid examples of high stable compounds similar to MsDef1. Typical concentration of defensin involved in host defense against microbial infections range ~ 10mg/mL (e.g., granules, intestine) indicates reasonable stability *in vivo* (79). Preliminary studies on the stability involved incubation of MsDef1 in simulated gastric fluid (SGF) which mimics *in vivo* conditions, and the stability was assessed through Western Blotting. MsDef1 showed no significant change in the intensity of the bands with respect to time, while positive control BSA was degraded easily (Figure 8). This implies high stability of MsDef1 towards protease digestion. The combination of a cyclic cysteine knots (CCK) and a circular backbone renders peptide impervious to enzymatic breakdown exemplified by cyclotides (77), theta defensins (78) and FDA approved drugs like AcuTect (75, 76) and NeoTect (75, 76).

MsDef1 is shown to target two tumor specific targets in this study, i.e., GlcCer and Trx. Overexpression of both GlcCer and Trx made cancer cells resistant to treatments and are considered as biomarkers of resistance. The selectivity of MsDef1 may be hypothesized as described in Scheme 1. Cells are categorized into 3 classes for understanding selectivity: Class A: Tumor cells which are anionic, low pH, GlcCer positive and Trx positive, Class B: Nontumor cells, GlucCer Positive, normal pH, and Class C: Normal cells, Normal pH, Both GlcCer and Trx negative. In Class A, tumor cells, particularly MDR cells have both GlcCer and Trx positivity and are also at low pH conditions. Under these conditions, MsDef1 is cationic with +7 charge which interacts with anionic sphingolipids strongly to liberate ceramide from GlcCer. Hence, it is reasonable to assume that MsDef1 might have created structural pore defects on the membrane of cancer cells allowing the diffuse of MsDef1 which in turn interacts with intracellular Trx through Trx. That liberates ASK1 protein from Trx activating ASK1 pathway. In Class B case, off target cells have low GlcCer positivity and low

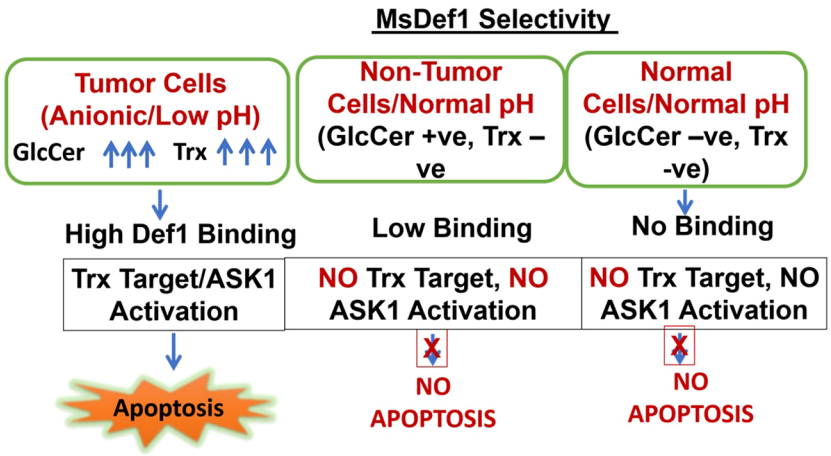

SCHEME 1
Selectivity of MsDef1.

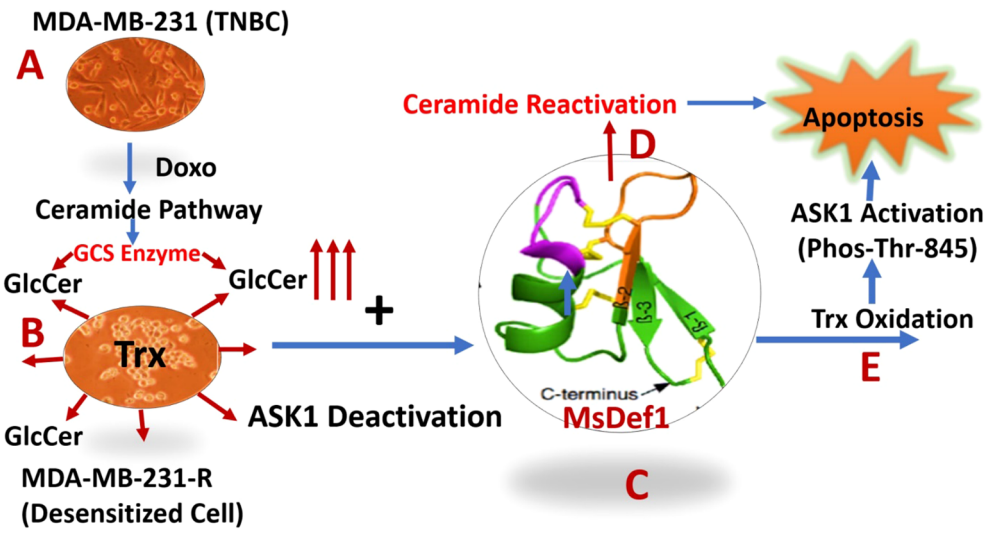

SCHEME 2
Description of dual Pathways activation by MsDef1 which sensitizes multidrug resistant (MDR) cancer cells: **(A)** Doxorubicin activates ceramide pathway in triple negative breast cancer cells (MDA-MB-231), while cancer cells circumvent it by overexpressing Glucosilceramide Synthase (GCS) which glycosylates ceramide to convert it to Glucosilceramide (GlcCer) which is MDR biomarker, **(B)** Deactivated MDR-MB-231R MDR cancer cells overexpress Thioredoxin (Trx) deactivating Apoptosis Stimulating Kinase 1 (ASK-1) pathway, **(C)** MsDef1, Upon treatment liberates ceramide by reactivating ceramide pathway, **(D)** leading to apoptosis, **(E)** MsDef1 also oxidizes Trx activating ASK1 Pathway sensitizing MDR cancer cells to Doxorubicin leading to synergistic apoptosis.

binding of MsDef1 to GlcCer positive cells is expected to trigger the release of ceramide. However, low levels of ceramide are expected to have little side effects. In Class C, it is obvious that these cells are both GlcCer and Trx negative leading to no uptake of MsDef1 (Figures 5C–E). Although, the undesired off-target expression of GlcCer and Trx (e.g., brain, kidney etc.) may be of a little concern, it is to be noted that the overexpression of GlcCer and Trx in tumor compared to other cells is the key. It is the relative target Vs. non-target expression of the biomarker which makes it better selective compared to nonspecific chemotherapy. For example, high target/non-target ratio for many FDA approved targeted imaging and therapeutic drugs (e.g., Octreoscan (80), Herceptin (81)) based on somatostatin and ErbB2 overexpression respectively, are good examples of selectivity despite low expression of the biomarker at non-target sites. It is the combination of two tumor specific targets (GlcCer & Trx) and reactivation of two pathways (ceramide and ASK) which makes MsDef1 unique (Scheme 2).

In summary, TNBC patients treated with Doxorubicin are not getting benefitted much since ceramide pathway through which Doxorubicin mediates cell death was deactivated by cancer cells (Scheme 2A). The deactivation of ceramide pathway is due to the classic glycosylation of ceramide which produces MDR cancer cells. We have clearly shown that MsDef1 reactivated ceramide pathway, liberating ceramide from GlcCer, oxidizing intracellular Trx and in turn activating ASK1 pathway. As a result, MDR cancer cells are sensitized to Doxorubicin through synergy. Our studies revealed that MsDef1 could be a natural tumor sensitizer which can be useful at neoadjuvant settings with chemotherapy. Further studies are needed to test the synergicity of MsDef1 in tumor animal models *in vivo* for a potential smooth clinical translation.

Data availability statement

The datasets presented in this study can be found in online repositories. The names of the repository/repositories and accession number(s) can be found in the article/Supplementary Material.

Author contributions

RP: conceptualization, interpretation of data, writing original draft, design of experiments. DS: expertise review on MsDef1, manuscript editing. KH-W: NMR data collection, interpretation. US and AK: data collection. All authors contributed to the article and approved the submitted version.

Funding

Funding for this research came from NIH in the form of SBIR grant to Sci-Engi-Medco Solutions Inc. (SEMCO), Grant R43CA183385. The content is solely the responsibility of the authors and does not necessarily represent the official views of the National Institutes of Health. NIH had no role in the study design, data collection and analysis, decision to publish, or preparation of the manuscript.

Acknowledgments

RP acknowledges the collaborative efforts from DS, Danforth Plant Science Center, St Louis and Professor KH-W, University of Wisconsin.

Conflict of interest

Raghu Pandurangi was employed by Sci-Engi-Medco Solutions Inc.

The remaining authors declare that the research was conducted in the absence of any commercial or financial relationships that could be construed as a potential conflict of interest.

Publisher's note

All claims expressed in this article are solely those of the authors and do not necessarily represent those of their affiliated organizations, or those of the publisher, the editors and the reviewers. Any product that may be evaluated in this article, or claim that may be made by its manufacturer, is not guaranteed or endorsed by the publisher.

Supplementary material

The Supplementary Material for this article can be found online at: https://www.frontiersin.org/articles/10.3389/fonc.2023.1141755/full#supplementary-material

SUPPLEMENTARY FIGURE S1
MsDef1 oxidizes Trx at 20 mM dose compared to positive control H_2O_2 (2 mM) in MDA-MB-231-R TNBC cells, 1. Def1 (0 mM), 2. Def1, (10 mM), 3. (20 mM), 4. H_2O_2 (10 mM) (N=4, $p < 0.05$).

SUPPLEMENTARY FIGURE S2
(A) SDS-PAGE of MsDef1 prepared using E-coli Rosetta (DE3/pET 28a). **(B)** 1-6 HPLC Fractions, Fraction 1 corresponds to molecular weight of fully folded MsDef1 (5183) which showed antifungal activity.

SUPPLEMENTARY FIGURE S3
Immunoblot analysis of phosphorylation of Threonine-845 residue of ASK1 Protein in response to the treatment of Def1 in MDA-MB-231 cells: 1. Control, 2. N-Acetyl-Cystein (NAC, 5 mM)/60 mins, 3. NAC (5 mM) + Def1 (50 μM) for 60 min, 4. Def-1 (50 μM) alone for 60 minutes, N=4, $P < 0.005$, GAPDH: Internal Control.

References

1. Szakács G, Paterson JK, Ludwig JA, Booth-Genthe C, Gottesman MM. Targeting multidrug resistance in cancer. *Nat Rev Drug Discov* (2006) 5(3):219–34. doi: 10.1038/nrd1984

2. Trédan O, Galmarini CM, Patel K, Tannock IF. Drug resistance and the solid tumor microenvironment. *J Natl Cancer Inst* (2007) 99(19):1441–54. doi: 10.1093/jnci/djm135

3. Wu Q, Yang Z, Nie Y, Shi Y, Fan D. Multi-drug resistance in cancer chemotherapeutics: mechanisms and lab approaches. *Cancer Lett* (2014) 347(2):159–66. doi: 10.1016/j.canlet.2014.03.013

4. Jin Z, El-Deiry WS. Overview of cell death signaling pathways. *Cancer Biol Ther* (2005) 4(2):139–63. doi: 10.4161/cbt.4.2.1508

5. Evans C, Dalgleish AG, Kumar D. Review article: immune suppression and colorectal cancer. *Aliment Pharmacol Ther* (2006) 24(8):1163–77. doi: 10.1111/j.1365-2036.2006.03075.x

6. Markman JL, Shiao SL. Impact of the immune system and immunotherapy in colorectal cancer. *J Gastrointest Oncol* (2015) 6(2):208–23.

7. Regnard C, Kindlen M, Regnard C, Kindlen M. Chemotherapy: side effects. In: *Supportive and palliative care in cancer* (2019).

8. Monsuez JJ, Charniot JC, Vignat N, Artigou JY. Cardiac side-effects of cancer chemotherapy. *Int J Cardiol* (2010) 144(1):3–15. doi: 10.1016/j.ijcard.2010.03.003

9. Love RR, Leventhal H, Easterling DV, Nerenz DR. Side effects and emotional distress during cancer chemotherapy. *Cancer* (1989) 63(3):604–12. doi: 10.1002/1097-0142(19890201)63:3<604::AID-CNCR2820630334>3.0.CO;2-2

10. Shapiro CL, Recht A. Side effects of adjuvant treatment of breast cancer. *New Engl J Med* (2001) 344(26):1997–2008. doi: 10.1056/nejm200106283442607

11. Bauer KR, Brown M, Cress RD, Parise CA, Caggiano V. Descriptive analysis of estrogen receptor (ER)-negative, progesterone receptor (PR)-negative, and HER2-negative invasive breast cancer, the so-called triple-negative phenotype: a population-based study from the California cancer registry. *Cancer* (2007) 109 (9):1721–8. doi: 10.1002/cncr.22618

12. Wahba HA, El-Hadaad HA. Current approaches in treatment of triple-negative breast cancer. *Cancer Biol Med* (2015) 12(2):106–16. doi: 10.7497/j.issn.2095-3941.2015.0030

13. Reddy SM, Barcenas CH, Sinha AK, Hsu L, Moulder SL, Tripathy D, et al. Long-term survival outcomes of triple-receptor negative breast cancer survivors who are disease free at 5 years and relationship with low hormone receptor positivity. *Br J Cancer.* (2017) 118(1):17–23. doi: 10.1038/bjc.2017.379

14. Alfarouk KO, Stock CM, Taylor S. Resistance to cancer chemotherapy: failure in drug response from ADME to p-gp. *Cancer Cell Int* (2015) 15:71. doi: 10.1186/s12935-015-0221-1

15. Shelley M, Harrison C, Coles B, Staffurth J, Wilt TJ, Mason MD. Chemotherapy for hormone-refractory prostate cancer. *Cochrane Database Systematic Rev* (2006) (4): CD005247. doi: 10.1002/14651858.CD005247.pub2

16. Lee M-J. Lymphedema following taxane-based chemotherapy in women with early breast cancer. *Lymphatic Res Biol* (2014) 12(4):282–8. doi: 10.1089/lrb.2014.0030

17. Duda DG, Kozin SV, Kirkpatrick ND, Xu L, Fukumura D, Jain RK. CXCL12 (SDF1α)-CXCR4/CXCR7 pathway inhibition: an emerging sensitizer for anticancer therapies? *Clin Cancer Res* (2011) 17(8):2074–80. doi: 10.1158/1078-0432.CCR-10-2636

18. Kvols LK. Radiation sensitizers: a selective review of molecules targeting DNA and non-DNA targets. *J Nucl Med* (2005) 46 Suppl 1:187S–90S.

19. Dietze EC, Sistrunk C, Miranda-Carboni G, O'Regan R, Seewaldt VL. Triple-negative breast cancer in African American women: disparities versus biology. *Nat Rev Cancer* (2015) 15(4):248–54. doi: 10.1038/nrc3896

20. Siddharth S, Sharma D. Racial disparity and triple-negative breast cancer in African American women: a multifaceted affair between obesity, biology, and socioeconomic determinants. *Cancers (Basel).* (2018) 10(12):514. doi: 10.3390/cancers10120514

21. Onitilo AA, Engel JM, Greenlee RT, Mukesh BN. Breast cancer subtypes based on ER/PR and Her2 expression: comparison of clinicopathologic features and survival. *Clin Med Res* (2009) 7(1-2):4–13. doi: 10.3121/cmr.2009.825

22. Lavie Y, Cao H, Bursten SL, Giuliano AE, Cabot MC. Accumulation of glucosylceramides in multidrug-resistant cancer cells. *J Biol Chem* (1996) 271 (32):19530–6. doi: 10.1074/jbc.271.32.19530

23. Park MA. The relationship between multidrug resistance and glucosylceramide levels: an opportunity for combined therapies. *Cancer Biol Ther* (2009) 8(12):1122–4. doi: 10.4161/cbt.8.12.8706

24. Kartal Yandım M, Apohan E, Baran Y. Therapeutic potential of targeting ceramide/glucosylceramide pathway in cancer. *Cancer Chemother Pharmacol* (2013) 71:13–20. doi: 10.1007/s00280-012-1984-x

25. Gupta V, Bhinge KN, Hosain SB, Xiong K, Gu X, Shi R, et al. Ceramide glycosylation by glucosylceramide synthase selectively maintains the properties of breast cancer stem cells. *J Biol Chem* (2012) 287(44):37195–205. doi: 10.1074/jbc.M112.396390

26. Grogan TM, Fenoglio-Prieser C, Zeheb R, Bellamy W, Frutiger Y, Vela E, et al. Thioredoxin, a putative oncogene product, is overexpressed in gastric carcinoma and associated with increased proliferation and increased cell survival. *Hum Pathol* (2000) 31(4):475–81. doi: 10.1053/hp.2000.6546

27. Kaimul AM, Nakamura H, Masutani H, Yodoi J. Thioredoxin and thioredoxin-binding protein-2 in cancer and metabolic syndrome. *Free Radical Biol Med* (2007) 43 (6):861–8. doi: 10.1016/j.freeradbiomed.2007.05.032

28. Nadeau PJ, Charette SJ, Toledano MB, Landry J. Disulfide bond-mediated multimerization of Ask1 and its reduction by thioredoxin-1 regulate H(2)O(2)-induced c-jun NH(2)-terminal kinase activation and apoptosis. *Mol Biol Cell* (2007) 18(10):3903–13. doi: 10.1091/mbc.e07-05-0491

29. Michaud M, Martins I, Sukkurwala AQ, Adjemian S, Ma Y, Pellegatti P, et al. Autophagy-dependent anticancer immune responses induced by chemotherapeutic agents in mice. *Science* (2011) 334:1573–7. doi: 10.1126/science.1208347

30. Zitvogel L, Apetoh L, Ghiringhelli F, Kroemer G. Immunological aspects of cancer chemotherapy. *Nat Rev Immunol* (2008) 8(1):59–73. doi: 10.1038/nri2216

31. Kam T, Alexander M. Drug-induced immune thrombocytopenia. *J Pharm Practice.* (2014) 27(5):430–9. doi: 10.1177/0897190014546099

32. Woolston CM, Zhang L, Storr SJ, Al-Attar A, Shehata M, Ellis IO. The prognostic and predictive power of redox protein expression for anthracycline-based chemotherapy response in locally advanced breast cancer. *Mod Pathol* (2012) 25 (8):1106–16. doi: 10.1038/modpathol.2012.60

33. Saitoh M, Nishitoh H, Fujii M, Takeda K, Tobiume K, Sawada Y, et al. Mammalian thioredoxin is a direct inhibitor of apoptosis signal-regulating kinase (ASK) 1. *EMBO J* (1998) 17(9):2596–606. doi: 10.1093/emboj/17.9.2596

34. Liu YY, Hill RA, Li YT. Ceramide glycosylation catalyzed by glucosylceramide synthase and cancer drug resistance. *Adv Cancer Res* (2013) 117:59–89. doi: 10.1016/B978-0-12-394274-6.00003-0

35. Shan W, Zhong W, Zhao R, Oberley TD. Thioredoxin 1 as a subcellular biomarker of redox imbalance in human prostate cancer progression. *Free Radical Biol Med* (2010) 49(12):2078–87. doi: 10.1016/j.freeradbiomed.2010.10.691

36. Sathoff AE, Velivelli S, Shah DM, Samac DA. Plant defensin peptides have antifungal and antibacterial activity against human and plant pathogens. *Phytopathology* (2019) 109(3):402–8. doi: 10.1094/PHYTO-09-18-0331-R

37. Shah DM, Snyder AK. Antifungal plant proteins and generation of transgenic plants that inhibit the growth of phytopathogenic fungi. (2008).

38. Ramamoorthy V, Zhao X, Snyder AK, Xu JR, Shah DM. Two mitogen-activated protein kinase signalling cascades mediate basal resistance to antifungal plant defensins in fusarium graminearum. *Cell Microbiol* (2007) 9(6):1491–506. doi: 10.1111/j.1462-5822.2006.00887.x

39. Scarbrough PM, Mapuskar KA, Mattson DM, Gius D, Watson WH, Spitz DR. Simultaneous inhibition of glutathione- and thioredoxin-dependent metabolism is necessary to potentiate 17AAG-induced cancer cell killing *via* oxidative stress. *Free Radic Biol Med* (2012) 52(2):436–43. doi: 10.1016/j.freeradbiomed.2011.10.493

40. Bielawski J, Pierce JS, Snider J, Rembiesa B, Szulc ZM, Bielawska A. Comprehensive quantitative analysis of bioactiue sphingolipids by high-performance liquid chromatography-tandem mass spectrometry. *Methods Mol Biol* (2009) 579:443–67. doi: 10.1007/978-1-60761-322-0_22

41. Sagaram US, Pandurangi R, Kaur J, Smith TJ, Shah DM. Structure-activity determinants in antifungal plant defensins MsDef1 and MtDef4 with different modes of action against *Fusarium graminearum*. *PloS One* (2011) 6(4):e18550. doi: 10.1371/journal.pone.0018550

42. Sagaram US, El-Mounadi K, Buchko GW, Berg HR, Kaur J, Pandurangi RS, et al. Structural and functional studies of a phosphatidic acid-binding antifungal plant defensin MtDef4: identification of an RGFRRR motif governing fungal cell entry. *PloS One* (2013) 8(12):e82485. doi: 10.1371/journal.pone.0082485

43. AAAPT Technology, Pandurangi R. *Compositions and methods for sensitizing low-responsive tumors to cancer therapy, PCT filed* (2016). Available at: https://patentimages.storage.googleapis.com/6d/3a/2b/2e778b81566dbc/WO2017131911A1.pdf.

44. Pandurangi RS, Tomasetti M, Verapazham ST, Paulmurugan R, Ma C, Rajput S, et al. *A Priori* Activation of apoptosis pathways of tumor (AAAPT) technology: development of targeted apoptosis initiators for cancer treatment. *PloS One* (2021) 16(2):e0225869. doi: 10.1371/journal.pone.0225869

45. Pandurangi RS, Cseh O, Luchman HA, Ma CX, Senadheera SN, Forrest ML. Rational drug design of targeted and enzyme-cleavable vitamin e analogs as a neoadjuvant to chemotherapy: in vitro and *In Vivo* evaluation on reduction of the cardiotoxicity side effect of doxorubicin. *ACS-Pharmacology Trans Sci* (2023) 6(3):372–86. doi: 10.1021/acsptsci.2c00091

46. Gao A-G, Hakimi S, Mittanck C, Wu Y, Stark D, Shah DM, et al. Fungal pathogen protection in potato by expression of a plant defensin peptide. *Nat Biotechnol* (2000) 18:1307–10. doi: 10.1038/82436

47. Thevissen K, Francois IE, Aerts AM, Cammue BP. Fungal sphingolipids as targets for the development of selective antifungal therapeutics. *Curr Drug Targets* (2005) 6:923–8. doi: 10.2174/138945005774912771

48. Thevissen K, Kristensen HH, Thomma BP, Cammue BP, Francois IE. Therapeutic potential of plant and insect defensins. *Drug Discovery Today* (2007) 12:966–71. doi: 10.1016/j.drudis.2007.07.016

49. Aerts AM, Francois IE, Cammue BP, Thevissen K. The mode of action of antifungal plant defensins. *Cell Mol Life Sci* (2008) 65:2069–79. doi: 10.1007/s00018-008-8035-0

50. Thevissen K, Francois IE, Winderickx J, Pannecouque C, Cammue BP. Ceramide involvement in apoptosis and apoptotic diseases. *Mini Rev Med Chem* (2006) 6:699–709. doi: 10.2174/138955706777435643

51. Lay FT, Schirra HJ, Scanlon MJ, Anderson MA, Craik DJ. The three-dimensional solution structure of NaD1, a new floral defensin from *Nicotiana alata* and its application to a homology model of the crop defense protein alf AFP. *J Mol Biol* (2003) 325:175–88. doi: 10.1016/S0022-2836(02)01103-8

52. Kovaleva V, Bukhteeva I, Kit OY, Nesmelova IV. Plant defensins from a structural perspective. *Int J Mol Sci* (2020) 21:5307–31. doi: 10.3390/ijms21155307

53. Gu X, Song X, Dong Y. Vitamin e succinate induces ceramide-mediated apoptosis in head and neck squamous cell carcinoma *In vitro* and *In vivo*. *Clin Cancer Res* (2008) 14:1840–8. doi: 10.1158/1078-0432.CCR-07-1811

54. Chen CL, Lin CF, Chang WT, Huang WC, Teng CF, Lin YS, et al. Ceramide induces P38 MAPK and JNK activation through a mechanism involving a thioredoxin-interacting protein-mediated pathway. *Blood* (2008) 111(8):4365–74. doi: 10.1182/blood-2007-08-106336

55. Ramanathan RK. A randomized phase II study of PX-12, an inhibitor of thioredoxin in patients with advanced cancer of the pancreas following progression after a gemcitabine-containing combination. *Cancer Chemother Pharmacol* (2011) 67 (3):503–9. doi: 10.1007/s00280-010-1343-8

56. Lin P, Wong JH, Ng TB. A defensin with highly potent antipathogenic activities from the seeds of purple pole bean. *Biosci Rep* (2010) 30:101–9. doi: 10.1042/BSR20090004

57. Joe AK. Resveratrol induces growth inhibition, s-phase arrest, apoptosis, and changes in biomarker expression in several human cancer cell lines. *Clin Cancer Res* (2002) 8:893–903.

58. Ahmad A, Aziuza S, Ahmad H. Anti-cancer activity of quercetin, Gallic acid and ellagic acid against HEPG2 and HCT116 cell lines *in vitro*. *Int J Pharm Bio Sci* (2016) 7 (4):584–92.

59. Barnes S. Anticancer effects of genistein, effect of genistein on *In Vitro* and *In Vivo* models of cancer. *J Nutr* (1995) 125:3 Suppl 777S–783S.

60. Goel A, Aggarwal BB. Curcumin, the golden spice from Indian saffron, is a chemosensitizer and radiosensitizer for tumors and chemoprotector and radioprotector for normal organs. *Nutr Cancer*. (2010) 62(7):919–30. doi: 10.1080/01635581.2010.509835

61. Chou TC. Theoretical basis, experimental design, and computerized simulation of synergism and antagonism in drug combination studies. *Pharmacol Rev* (2006) 58:621–81. doi: 10.1124/pr.58.3.10

62. Tiwary R, Yu W, Sanders BG, Kline K. α-TEA cooperates with chemotherapeutic agents to induce apoptosis of p53 mutant, triple-negative human breast cancer cells via activating p73. *Breast Cancer Res* (2011) 13(1):R1. doi: 10.1186/bcr2801

63. Kwon Y-E. *In Vitro* Histo culture drug response assay and *In Vivo* blood chemistry of a novel pt (IV) compound, K104. *Anticancer Res* (2007) 27:321–6.

64. Yamasaki F, Zhang D, Bartholomeusz C, Sudo T, Hortobagyi GN. Sensitivity of breast cancer cells to erlotinib depends on cyclin-dependent kinase 2 activity. *Mol Cancer Ther* (2007) 6:2168–77. doi: 10.1158/1535-7163.MCT-06-0514

65. Moon DO, Kim MO, Heo MS, Lee JD, Choi YH, Kim GY. Gefitinib induces apoptosis and decreases telomerase activity in MDA-MB-231 human breast cancer cells. *Arch Pharm Res* (2009) 32(10):1351–60. doi: 10.1007/s12272-009-2002-7

66. Poon I, Baxter AA, Lay FT, Mills GD, Adda CG, Payne JA, et al. Phosphoinositide-mediated oligomerization of a defensin induces cell lysis. *eLife* (2014) 3:e01808. doi: 10.7554/eLife.01808

67. Amaral VSGD, Santos SACS, de Andrade PC. *Pisum sativum* Defensin 1 eradicates mouse metastatic lung nodules from B16F10 melanoma cells. *Int J Mol Sci* (2020) 21(8):2662. doi: 10.3390/ijms21082662

68. Simons AL, Parsons AD, Foster KA, Orcutt KP, Fath MA, Spitz DR. Inhibition of glutathione and thioredoxin metabolism enhances sensitivity to perifosine in head and neck cancer cells. *J Oncol* (2009) 2009:519563. doi: 10.1155/2009/519563

69. Schroeder BO, Wu Z, Nuding S, Groscurth S, Marcinowski M, Beisner J, et al. Reduction of disulphide bonds unmasks potent antimicrobial activity of human β 2-defensin 1. *Nature* (2011) 469:419–23. doi: 10.1038/nature09674

70. Pandurangi R, Sekar TV, Paulmurugan R. Restoration of human beta defensin (hBD-1) levels *in vivo* as immunomodulate for cancer therapy, NIH report 2015. *Immunity* (2020) 115(2):155–62. doi: 10.1159/000265166

71. Tani K, Murphy WJ, Chertov O, Salcedo R, Koh CY. Utsunomiya et al.; defensins act as potent adjuvants that promote cellular and humoral immune responses in mice to a lymphoma idiotype and carrier antigens. *Int Immunol* (2000) 12(5):691–700. doi: 10.1093/intimm/12.5.691

72. Wang X, Han W, Yu Y, Zhu J, Zhang R. Doxorubicin-induced cardiomyopathy. In: *Doxorubicin: biosynthesis, clinical uses and health implications* (2014). doi: 10.1056/nejm199809243391307

73. Chatterjee K, Zhang J, Honbo N, Karliner JS. Doxorubicin cardiomyopathy. *Cardiology* (2010). doi: 10.1159/000265166

74. Renu K, V.G. A, Tirupathi TP, Arunachalam S. Molecular mechanism of doxorubicin-induced cardiomyopathy – an update. *Eur J Pharmacol* (2018) 818:241–53. doi: 10.1016/j.ejphar.2017.10.043

75. *Pandurangi, drug development reports for IND and NDA of AccuTect and NeoTect for FDA and EMEA approval, schering AG, 2001-2004.*

76. Taillefer R, Edell S, Innes G, Lister-James Jthe Multicenter Trial Investigators. Acute thromboscintigraphy with 99mTc-apcitide: results of the phase 3 multicenter clinical trial comparing 99mTc-apcitide scintigraphy with contrast venography for imaging acute DVT. *J Nucl Med* (2000) 41:1214–23.

77. Gould A, Ji Y, Aboye TL, Camarero JA. Cyclotides, a novel ultra-stable polypeptide scaffold for drug discovery. *Curr Pharm Des* (2011) 17(38):4294–307. doi: 10.2174/138161211798999438

78. Conibear AC, Rosengren KJ, Daly NL, Henriques ST, Craik DJ. The cyclic cystine ladder in θ-defensins is important for structure and stability, but not antibacterial activity. *J Biol Chem* (2013) 288(15):10830–40. doi: 10.1074/jbc.M113.451047

79. Lacerda AF, Vasconcelos ÉAR, Pelegrini PB, Grossi de Sa MF. Antifungal defensins and their role in plant defense. *Front Microbiol* (2014) 5:116. doi: 10.3389/fmicb.2014.00116

80. Squires MH, Volkan Adsay N, Schuster DM, Russell MC, Cardona K. Octreoscan versus FDG-PET for neuroendocrine tumor staging: a biological approach. *Ann Surg Oncol* (2015) 22(7):2295–301. doi: 10.1245/s10434-015-4471-x

81. Nahta R, Esteva FJ. Herceptin: mechanisms of action and resistance. *Cancer Letters.* (2006) 232(2):123–38. doi: 10.1016/j.canlet.2005.01.041

82. de Medeiros LN, Angeli R, Sarzedas CG, Barreto-Bergter E, Valente AP, Kurtenbach E, et al. Backbone dynamics of the antifungal Psd1 pea defensin and its correlation with membrane interaction by NMR spectroscopy. *Biochim Biophys Acta (BBA) - Biomembranes* (2010) 1798(2):105–13. doi: 10.1016/j.bbamem.2009.07.013

83. Droin N, Hendra JB, Ducoroy P, Solary E. Human defensins as cancer biomarkers and antitumour molecules. *J Proteomics.* (2009) 72(6):918–27. doi: 10.1016/j.jprot.2009.01.002

frontiers | Frontiers in Oncology

TYPE Original Research
PUBLISHED 15 June 2023
DOI 10.3389/fonc.2023.1135836

OPEN ACCESS

EDITED BY
Thomas J. Sferra,
Rainbow Babies & Children's Hospital,
United States

REVIEWED BY
Radka Václavíková,
National Institute of Public Health (NIPH),
Czechia
Qiuxia Cui,
Wuhan University, China

*CORRESPONDENCE
Vahid Jajarmi
v.jajarmi@gmail.com

RECEIVED 01 January 2023
ACCEPTED 30 May 2023
PUBLISHED 15 June 2023

CITATION
Miri A, Gharechahi J, Samiei Mosleh I, Sharifi K and Jajarmi V (2023) Identification of co-regulated genes associated with doxorubicin resistance in the MCF-7/ADR cancer cell line. *Front. Oncol.* 13:1135836. doi: 10.3389/fonc.2023.1135836

Identification of co-regulated genes associated with doxorubicin resistance in the MCF-7/ADR cancer cell line

Ali Miri[1], Javad Gharechahi[2], Iman Samiei Mosleh[3], Kazem Sharifi[1,4] and Vahid Jajarmi[1]*

[1]Department of Medical Biotechnology, School of Advanced Technologies in Medicine, Shahid Beheshti University of Medical Sciences, Tehran, Iran, [2]Human Genetic Research Center, Baqiyatallah University of Medical Sciences, Tehran, Iran, [3]Department of Bioinformatics, Institute of Biochemistry and Biophysics, University of Tehran, Tehran, Iran, [4]Anesthesiology Research Center, Shahid Beheshti University of Medical Sciences, Tehran, Iran

Introduction: The molecular mechanism of chemotherapy resistance in breast cancer is not well understood. The identification of genes associated with chemoresistance is critical for a better understanding of the molecular processes driving resistance.

Methods: This study used a co-expression network analysis of Adriamycin (or doxorubicin)-resistant MCF-7 (MCF-7/ADR) and its parent MCF-7 cell lines to explore the mechanisms of drug resistance in breast cancer. Genes associated with doxorubicin resistance were extracted from two microarray datasets (GSE24460 and GSE76540) obtained from the Gene Expression Omnibus (GEO) database using the GEO2R web tool. The candidate differentially expressed genes (DEGs) with the highest degree and/or betweenness in the co-expression network were selected for further analysis. The expression of major DEGs was validated experimentally using qRT–PCR.

Results: We identified twelve DEGs in MCF-7/ADR compared with its parent MCF-7 cell line, including 10 upregulated and 2 downregulated DEGs. Functional enrichment suggests a key role for RNA binding by IGF2BPs and epithelial-to-mesenchymal transition pathways in drug resistance in breast cancer.

Discussion: Our findings suggested that *MMP1*, *VIM*, *CNN3*, *LDHB*, *NEFH*, *PLS3*, *AKAP12*, *TCEAL2*, and *ABCB1* genes play an important role in doxorubicin resistance and could be targeted for developing novel therapies by chemical synthesis approaches.

KEYWORDS

breast cancer, chemoresistance, differentially expressed genes, gene co-expression network, doxorubicin (DOX)

Abbreviations: ADR, Adriamycin resistance; DEG, differentially expressed genes; GCN, gene co-expression network; GEO, gene expression omnibus; PPI, protein-protein interaction; ECM, extracellular matrix.

Introduction

Breast cancer is the most common malignancy among women worldwide and is the second cause of cancer-related mortalities after lung cancer (1). In the United States alone, 268,600 new cases and 41,760 fatalities were reported for breast cancer in 2019 (2), accounting for greater than 30% of all new cancers and 15% of all cancer-related deaths. Breast cancer is distinguished by molecular, histological, and clinical characteristics, necessitating distinct clinical management strategies (3). Based on immunohistochemistry analysis, breast cancer can be classified into three distinct molecular subtypes, including estrogen or progesterone receptor positive (ER+/PR+), human epidermal growth factor receptor positive (HER2+), and triple-negative (TNBC) (4, 5). ER+/PR+ breast tumors have distinct gene expression signatures characteristic of ductal luminal cells of the breast and are accordingly subclassified into luminal A and luminal B subgroups with very different prognoses (6, 7). The luminal A subtype, for example, is characterized by a high expression of proliferative and cell cycle-related genes and a low proliferative rate (8). A high expression of Ki-67 and proliferating cell nuclear antigen and a high mutation rate of p53 are characteristics of luminal B subtypes (9, 10). TNBC or basal-like tumors are heterogeneous in gene expression profiles and can be categorized into multiple different subgroups (11).

Endocrine hormone therapies, including ovarian function suppression, selective estrogen receptor modulators, selective estrogen receptor down regulators, and aromatase inhibitors, are commonly used as primary systemic therapies in patients with ER+/PR+ breast cancer, complementing surgery (12, 13). HER2+ breast cancer, which accounts for ~20% of all breast cancer cases, benefits from therapies targeting the epidermal growth factor 2 (ERBB2 or HER2/neu) gene, such as anti-ERBB2 antibodies and tyrosine kinase inhibitors (13). However, TNBC, which represents about 15% of all breast cancer cases and is more common in premenopausal young women under 40, lacks effective targeted therapies and is unresponsive to current endocrine therapies (14). Chemotherapy, including doxorubicin/Adriamycin, paclitaxel, docetaxel, cyclophosphamide, and carboplatin, alone or in combination, is commonly used for neoadjuvant or adjuvant treatment of breast cancer, to downstage tumors or as a standard-of-care regimen for aggressive and early-stage disease (13, 15–20). Doxorubicin, an anthracycline chemotherapeutic agent, is still a first-line therapy for early-stage breast, ovarian, lymphoma, and leukemia cancers (21–24). However, the development of chemoresistance continues to be a significant clinical obstacle in treating breast cancer (15).

Chemoresistance refers to the ability of cancer cells to survive and proliferate despite exposure to high doses of chemotherapeutic agents, resulting in a lack of response or failure of the treatment. The most common routes for chemoresistance include over-expression of membrane efflux pumps, such as ATP-binding cassette (ABC) transporters, drug sequestration in lysosomes, alterations in drug metabolism, mutations or downregulation of drug targets, upregulation of cell cycle regulators and apoptosis inhibitors, activation of survival pathways, changes to cellular metabolism, mitochondrial alteration, and changes to the tumor microenvironment (25–33). Understanding the molecular mechanisms underlying doxorubicin resistance in breast cancer is crucial for developing effective strategies to overcome this resistance and improve patient outcomes.

Despite extensive research on doxorubicin resistance in breast cancer, there are still gaps in our knowledge regarding the specific genes and pathways involved in this process. In this study, we aimed to identify co-regulated genes associated with doxorubicin resistance in the MCF-7/ADR breast cancer cell line using gene co-expression network (GCN) analysis of publicly available microarray gene expression datasets (34). GCN analysis has been extensively used for the identification of genes and molecular pathways dysregulated in various cancers (35, 36), particularly those genes with uncertain significance in biological processes (37).

Materials and methods

Breast adenocarcinoma datasets

We searched the GEO database for breast cancer mRNA expression data related to doxorubicin or Adriamycin resistance, specifically focusing on datasets that included profiling of both MCF-7/ADR and normal parent MCF-7 cell lines for downstream analysis. Four human mRNA datasets (GSE5920, GSE87864, GSE24460, and GSE76540) were identified based on these criteria. After an initial analysis, we noticed that the GSE87864 and GSE5920 datasets were unsuitable for network analysis due to high heterogeneity among replicates and inconsistent patterns of results. The remaining two datasets comprised at least two cell lines (MCF-7/ADR and parent cell line MCF-7) and two experimental conditions (doxorubicin and no doxorubicin), and both were generated by the same Affymetrix platform (Affymetrix Human Genome U133 Plus 2.0 Array). Table 1 shows detailed information about the analyzed datasets.

Identification of dysregulated genes

Primary analyses were performed using the online GEO2R suite (http://www.ncbi.nlm.nih.gov/geo/geo2r). The GEO2R enables the comparison of samples in a GEO dataset and the identification of differentially expressed genes (DEGs) under a particular experimental condition. We ignored the probe sets without a gene symbol. The GEO2R build-in R package Limma was used to identify DEGs (38). The raw expression data were corrected for background noise and normalized using the Robust Multi-array Average (RMA) algorithm, which takes into account data quantiles to correct for array biases (39). DEGs were identified by comparing normalized expression data from MCF-7 and MCF-7/ADR cell lines and looking for a minimum $|\log2 \text{ fold change (FC)}| > 1$ and a Bonferroni corrected P-value < 0.05. Correlations (the Pearson method) between gene expression data were calculated using the psych package in R (40). Only correlations with $|r| = 0.7$ and P-value < 0.05 were considered for network construction. The resulting correlation matrix was used for network construction using the R

TABLE 1 The detailed characteristics of the datasets included in this study.

Country	Cancer Type	Samples		Platform	Dataset	DEGs
		MCF-7/ADR	MCF-7			
USA	Breast cancer	2	2	Affymetrix HG-U133A_2	GSE24460	1108
China	Breast cancer	3	3	Affymetrix HG-U133_Plus_2	GSE76540	3207

package iGraph under the default settings (38). Gene clusters were generated using the clusterMaker plugin in Cytoscape based on the AutoSOME algorithm (41). Genes with the greatest betweenness and/or degree were chosen for further experimental validation, as previously described (42). Figure 1 shows the details of the bioinformatic workflow employed to identify DEGs and the final hub genes.

Functional annotation analysis

To assign specific functional roles to DEGs and to visualize them in the context of molecular pathways, we used a set of functional annotation and pathway inference tools. The Kyoto Encyclopedia of Genes and Genomes (KEGG) database was used for the functional annotation of DEGs. Gene ontology (GO) annotation allowed us to categorize DEGs into cellular components, molecular functions, and biological processes' functional ontologies. Protein-protein interactions were inferred by the Search Tool for the Retrieval of Interacting Genes/Proteins (STRING, www.string-db.org/cgi/input.pl) considering all interaction sources. Interactions with a combined score > 0.4 were used for network visualization, and those with a score > 0.7 were kept for further analysis.

Cell line characterization and authentication

The MCF-7 and MCF-7/ADR cell lines were obtained from the Iranian Biological Resources Center. The authenticity of cell lines was validated using Short Tandem Repeat (STR) DNA profiling. STR profiling was conducted using the AmpFlSTR Identifiler PCR Amplification Kit (Applied Biosystems, Foster City, CA, USA) according to the manufacturer's instructions. STR profiles were evaluated using the GeneMapper ID software. The MCF-7/ADR cell line was further characterized based on cell morphologies and IC_{50} drug dosage.

Cell culture

MCF-7 cells were cultured in Dulbecco's modified Eagle's medium (DMEM; Gibco source; DNA Biotech, Iran) supplemented with 100 units/mL penicillin-streptomycin and 10% FBS (BioIdea, Tehran, Iran) at 37 °C and 5% CO_2. MCF-7/ADR cells were cultured in RPMI 1640 medium (Gibco source) containing 10% FBS and 13 µg/mL doxorubicin. The drug was omitted from the culture medium 48 h before the experiment.

MTT assay to determine the lethal concentration (IC_{50}) of doxorubicin

Cells were seeded at a density of 2×10^4 cells/well in a 96-well culture plate and incubated at 37°C in a humidified environment containing 5% CO_2 for 16 hours. Subsequently, doxorubicin was added at concentrations of 0, 5, 10, and 15 µg/mL after cells fully adhered to the plate. The experiment was conducted in triplicate, with each drug concentration assayed in at least three independent wells. The MTT assay was performed by adding 20 µL of 3-(4,5-dimethylthiazol-2-yl)-2,5-diphenyltetrazolium bromide reagent (5 mg/mL) to each well and the cells were incubated for an additional 4 h. After incubation, 100 µL of dimethyl sulfoxide (DMSO) was added to each well and the plate was shaken for 15 min to ensure the complete dissolution of cells. The optical density (OD) was measured at 492 nm using a microplate reader. Cell growth inhibition was calculated using the formula: inhibitory rate (percentage) = (1 - mean OD value in the experimental group/ mean OD value in the control group) × 100. The IC_{50} value was estimated from the OD values and used to determine the doxorubicin cytostatic activity on MCF-7 and MCF-7/ADR cells.

Total RNA extraction and quantitative real-time PCR analysis

Total RNA was isolated from MCF-7 and MCF-7/ADR cell lines using the Roche High Pure RNA Isolation Kit (Roche GmbH, Mannheim, Germany) according to the manufacturer's instructions. The concentration and integrity of the extracted mRNAs were evaluated by a nanodrop spectrophotometer (Maestrogen, Taiwan) and agarose gel electrophoresis.

A total of 1 µg RNA was reverse transcribed in a 20 µL reaction mixture using the ExcelRT™ One-Step RT-qPCR Kit (SMOBIO, Taiwan) according to the manufacturer's protocol. qRT–PCR reactions were carried out under the following cycling conditions: a denaturation step at 95°C for 10 min, followed by 40 cycles of 95°C for 15 s and 60°C for 1 min in an ABI Step One Plus™ Real-Time PCR System (Applied Biosystems). RT–PCR reactions were performed in triplicate. The cycle threshold (Ct) values for the target gene and internal control gene (GAPDH)

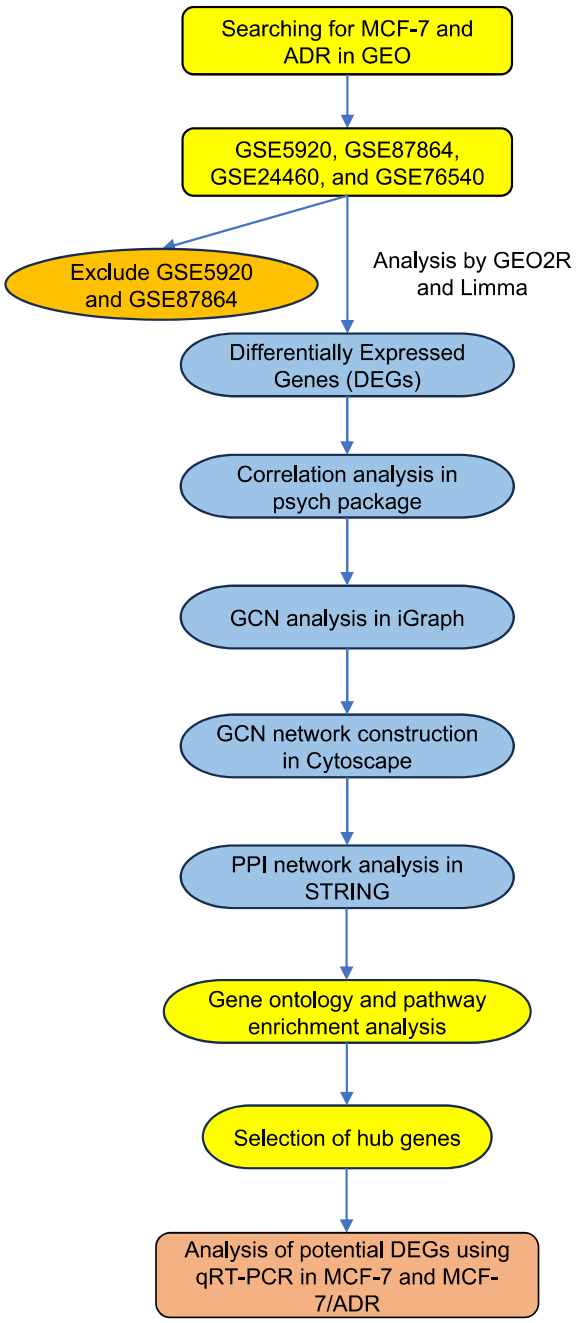

FIGURE 1
The diagram shows the overall analysis performed in this study. The mRNA expression datasets were retrieved from the GEO database by searching for the MCF-7 and ADR keywords. The candidate datasets were screened for the number of analyzed samples and the reproducibility of the expression data. Datasets with low sample numbers and inconsistent results were excluded from further analysis. DEGs, differentially expressed genes; PPI, Protein-Protein Interactions; GEO, Gene Expression Omnibus, GCN, Gene co-expression network.

were extracted and used to estimate gene expressions following the $2^{-\Delta\Delta Ct}$ method (43).

Primers used for qRT–PCR were designed using the Oligo7 software and searched against the human RefSeq database to verify their amplification specificities. Table 2 shows the sequence of primers used for qRT–PCR.

Statistical analysis

All statistical analyses were performed using GraphPad Prism (Version 9, San Diego, CA). Statistically significant differences between the treatment groups were identified using the student t-test. Statistical data are presented as mean ± sd. A P-value less than 0.05 was considered statistically significant.

Results

Comparing gene expression profiles between MCF-7 and MCF-7/ADR cell lines

To identify DEGs, the microarray gene expression profiles of MCF-7/ADR and its parent MCF-7 cell line were compared in two independent GSE datasets (GSE24460 and GSE76540), considering a minimum fold change in expression > 2 and an FDR-corrected P-value cutoff of 0.05 (Table 1; Supplementary Data 1). We identified 1,108 DEGs in GSE24460 (566 up-regulated and 542 down-regulated DEGs) and 3,207 in the GSE76540 dataset (1,835 up-regulated and 1,372 down-regulated DEGs), as shown by volcano plots in Figures 2A, B. Correlating gene expressions in each data set, considering a correlation coefficient > 0.7 and an adjusted P-value < 0.05, resulted in the identification of 36 strongly co-regulated genes in GSE24460 and 406 in GSE76540. GCN analysis resulted in the identification of 18 and 115 genes with the highest degree and/or betweenness for the GSE24460 and GSE76540 datasets, respectively (Figures 2C–E). Among the final list of candidate co-expressed genes, only nine were shared in the two data sets, some of which are already known to contribute to chemoresistance, including *ABCB1*, *LDHB*, and *ESR1*. We thus identified a total of 122 differentially expressed genes (two genes were excluded from further analysis due to a lack of gene symbols) between MCF-7/ADR and MCF-7 cells, including 86 upregulated and 36 downregulated genes. The expression patterns of the candidate DEGs in the two datasets are visualized in heatmaps (Figure 3).

Functional enrichment analysis of DEGs

To link the candidate DEGs to biological or molecular processes, a gene ontology enrichment analysis was performed. The gene enrichment analysis was conducted by the FunRich GO analysis software suite (44). Genes associated with all three functional categories, including biological processes (BP), molecular processes (MP), and cellular components (CC), were identified among the candidate DEGs. The genes categorized in the CC group mostly originate from the cytoplasm, nucleus, plasma membrane, and exosome. Genes associated with the MF category were mainly transcription factors, extracellular matrix structural constituents, cell adhesion molecules, and transcription regulators. Cell growth and/or maintenance, signal transduction, and cell communication were significantly enriched in the BP group (Figure 4).

TABLE 2 The sequence of primers used for quantitative real-time PCR (qRT-PCR) analysis of target genes.

Gene symbol	Primer sequence (5′ → 3′)
ABCB1	F: AACACCCGACTTACAGATGATG
	R: CTTCCAACCACGTGTAAATCCT
AKAP12	F: AAGTCATTGTCACAGAGGTTGGA
	R: CTCAGTGGGTTGTGTTAGCTCT
CNN3	F: CATCATCCTCTGCGAACTTATAAACA
	R: TTGCTTCGAATATGTCATGTGGC
ESR1	F: TGATGAAAGGTGGGATACGAAAAG
	R: GGTTGGCAGCTCTCATGTCT
FXYD3	F: TCCTTTCTACTATGACTGGCACA
	R: AGCTCCTCCACTCACTCATG
VIM	F: CCACGAAGAGGAAATCCAGGAG
	R: TACCATTCTTCTGCCTCCTGC
LDHB	F: GCGACTCAAGTGTGGCTGT
	R: GACTTCATAGGCACTTTCAACCAC
MMP1	F: GGACCAACAATTTCAGAGAGTACAA
	R: CCGATATCAGTAGAATGGGAGAGT
NEFH	F: GAGTGGTTCCGAGTGAGGC
	R: GCTCTGTGGTCCTGGCC
PLS3	F: TGGCAGCTGATGAGAAGATATACC
	R: TCCAGCTTCACTCAACGTTCT
TCEAL2	F: AGTCAGAGATGCAGGGAGGA
	R: TGCAGCCCTTGTTTCACTTTCT
CTGF	F: GTGTGCACCGCCAAAGATG
	R: GCTGGGCAGACGAACGT
GAPDH	F: GTATCGTGGAAGGACTCATGACC
	R: CAGTAGAGGCAGGGATGATGTTC

Most of the DEGs were enriched in pathways associated with insulin-like growth factor-2 mRNA binding proteins and epithelial-to-mesenchymal transition (Figure 5). KEGG pathway analysis also revealed that most of the DEGs are involved in propanoate and pyruvate metabolism, bladder cancer, and membrane transport (ABC transporters).

Establishing a PPI network for the candidate DEGs, cluster analysis, and selection of hub genes

The candidate co-expressed genes were searched for potential protein-protein interactions using STRING. The resulting PPI network included 122 nodes and 50 edges, with a PPI enrichment P-value of 1.3e-12 (Figure 6). Cluster analysis using Cytoscape revealed a critical module across the network with 10 essential co-regulated genes, including *EGFR*, *ESR1*, *FGF2*, *CDKN2A*, *KRT19*, *VIM*, *CTGF*, *CALD1*, *GJA1*, and *MMP1*. Particularly, *EGFR* and *ESR1* genes showed the highest degree of connectivity in the PPI network, suggesting their critical role in maintaining the integrity of the whole network. To confirm whether the changes in gene expression detected by microarray could be validated in the corresponding cell lines, the expression of these functionally significant genes was evaluated by qRT–PCR.

MCF-7/ADR cells showed resistance to doxorubicin-mediated apoptosis

To characterize whether MCF-7 and MCF-7/ADR cell lines have the same genetic origin, we performed STR profiling. Our results showed that MCF-7/ADR and its parent MCF-7 cell line have a shared STR profile, confirming their common origin. To test whether our MCF-7/ADR cell line has maintained its drug resistance phenotype, cell viability under an increasing concentration of doxorubicin was evaluated. Exposing MCF-7 cells to an increasing dose of doxorubicin for up to 48 h significantly decreased cell viability, while no significant change to the MCF-7/ADR cells was noted. MCF-7/ADR cells had a vitality almost three times higher than that of their parent MCF-7 cells. Doxorubicin treatment effectively suppressed the development of MCF-7 and MCF-7/ADR cells with an IC_{50} value of 3.09 ± 0.03 and 13.2 ± 0.2 μg/mL, respectively (Figure 7A). Doxorubicin at doses of 5, 10, and 15 μg/mL significantly inhibited the proliferation of MCF-7 cells ($P<0.05$). MCF-7/ADR cells treated with 5 and 10 μg/mL of doxorubicin for 7 days displayed a normal cell morphology with only minor swelling.

Evaluating the expression of the candidate DEGs in the MCF-7 and MCF-7/ADR cell lines

The qRT–PCR method was used to confirm the expression of ten candidate co-expressed genes, five of which were shared between the two datasets, namely *MMP1*, *ABCB1*, *AKAP12*, *PLS3*, and *CTGF*. Three genes were selected from the GSE76540 dataset, namely *VIM*, *TCEAL2*, and *NEFH*, while two genes were selected from the GSE24460 dataset, including *LDHB* and *CNN3* (Table 3). Two additional co-downregulated genes, ESR1 and FXYD3, were also included to further check for amplification biases. The expression of genes was compared between MCF-7 and MCF-7/ADR cell lines in the presence or absence of doxorubicin. In the absence of the drug, a low expression of *ESR1* and *FXYD3* mRNAs in MCF-7/ADR cells was noticeable. Their expressions increased steadily in the presence of the drug at concentrations greater than 5 μg/mL. A significant difference in *PLS3*, *CNN3*, and *NEFH* expression was also noted between MCF-7 and MCF-7/ADR cells, correlating with microarray data (Figure 7B). *CTGF* was the only gene for which no expression was detected by qRT–PCR.

Discussion

Doxorubicin is widely used as a first-line neoadjuvant chemotherapy medication to treat breast cancer (45). While

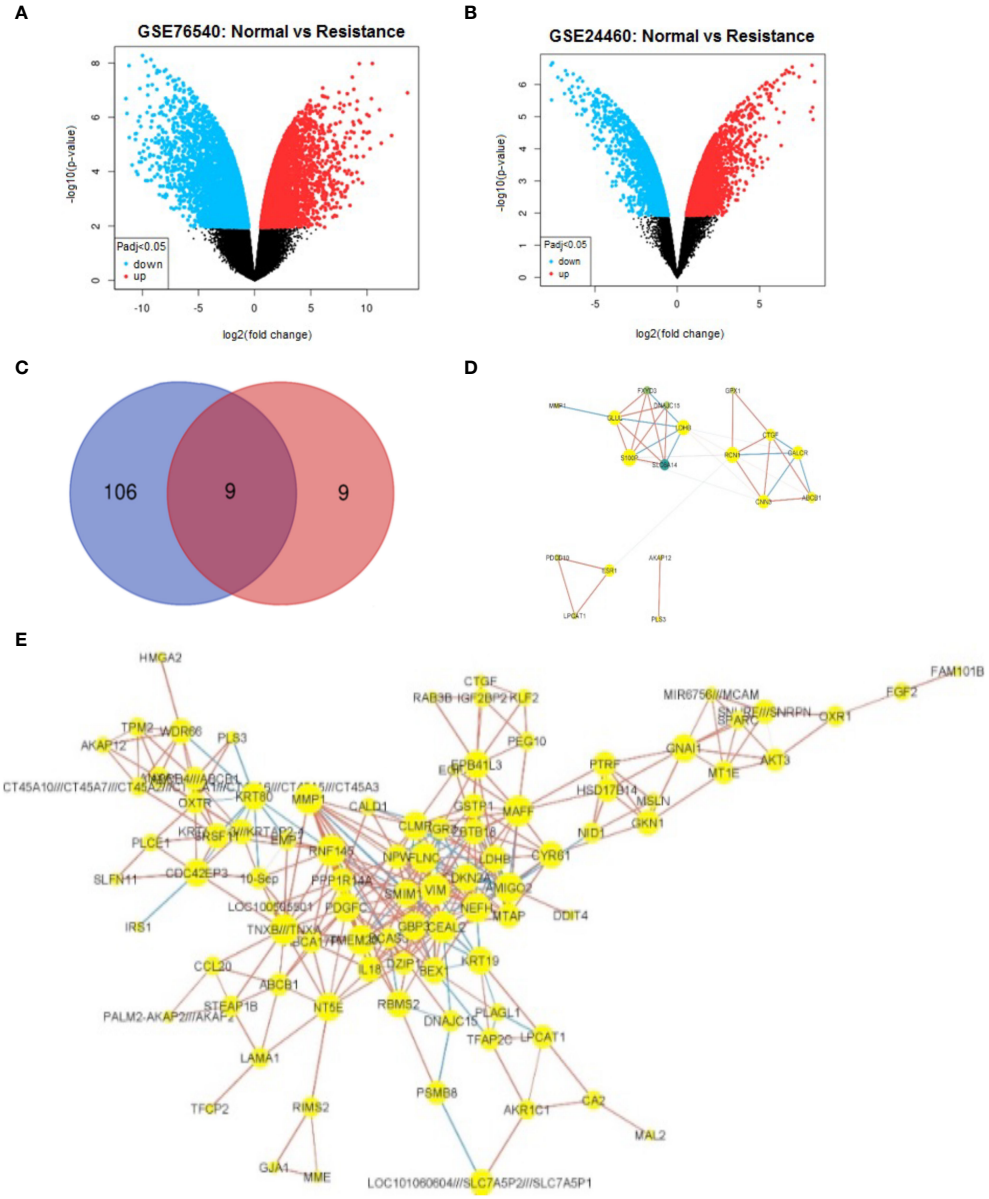

FIGURE 2
Identification and co-expression network visualization of DEGs between MCF-7 and MCF-7/ADR cell lines. Volcano plots show the overall changes in gene expression between MCF-7 and MCF-7/ADR cell lines analyzed in the GSE76540 **(A)** and GSE24460 **(B)** datasets. Among a final list of 124 DEGs, only nine were shared between the two datasets, as depicted in the Venn diagram **(C)**. One hundred and six DEGs were only detected in the GSE76540 dataset and nine in the GSE2446 dataset. The gene co-expression network of DEGs identified in the GSE24460 **(D)** and GSE76540 dataset **(E)**.

doxorubicin therapy proved to be extremely effective in the short-term treatments, long-term use may result in chemoresistance. Resistance to doxorubicin is a significant obstacle to the effectiveness of chemotherapy in patients with breast cancer. While the mechanism of chemoresistance is complex, identifying the critical genes and signaling pathways involved in the process is practically challenging. Large-scale analysis of gene expression in chemo-sensitive and chemo-resistant cells is a key approach to identifying genes or pathways associated with this phenomenon.

Here, we sought to explore the available microarray gene expression data sets to identify potentially important components of the chemoresistance mechanisms in MCF-7/ADR cells challenged with the chemotherapeutic agent doxorubicin. GCN analysis is commonly used to identify genes or molecular pathways in complex gene expression data (46–48). Using this approach, we identified several candidate DEGs that are known to implicate cell proliferation and/or maintenance, insulin-like growth factor 2 mRNA binding, and epithelial-to-mesenchymal transition (EMT). These include several potential hub genes in the PPI network, such as *EGFR*, *ESR1*, *FGF2*, *CDKN2A*, *VIM*, *CTGF*, *CALD1*, and *MMP1*. Only *ESR1* and *FXYD3* showed decreased expression

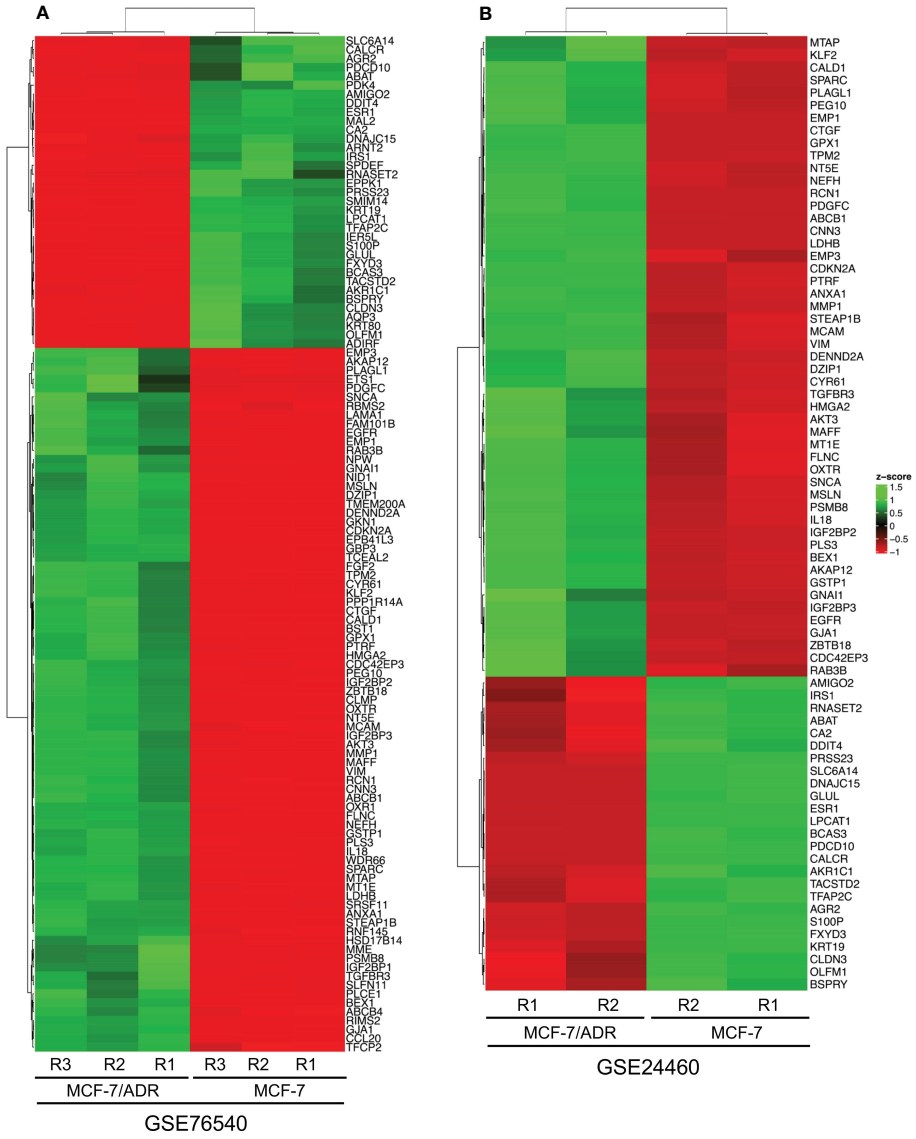

FIGURE 3
The heatmaps show the differentially expressed genes (DEGs) between the MCF-7 and MCF-7/ADR cell lines in the GSE76540 **(A)** and GSE24460 **(B)** datasets.

in the chemo-resistant cell line, whereas the remaining genes showed upregulation.

The most common mechanism for chemoresistance is the active efflux of the chemotherapeutic agent through the ABC transporters (28). ABC transporters are a large group of membrane proteins that mediate the import or export of diverse substrates across the cell membrane (49). Overexpression of cell surface efflux ABC transporters, including *ABCB1*, *ABCC1*, and *ABCG2*, was associated with chemoresistance in breast cancer (50, 51). Our analysis showed an increased expression of ABCB1, indicating its potential role in conferring resistance to doxorubicin.

Lactate dehydrogenase B (LDH-1) is a glycolytic enzyme linked to lysosomes and autophagy via the oxidative pathway (52, 53). Deacetylation of LDHB by SIRT5 promotes the development of autophagy vesicles and thus induces autophagy (54). Breast cancer cells expressing high levels of *LDHB* show basal-like and glycolytic phenotypes, whereas the suppression of its expression reduces their glycolytic dependence (55). The expression of *LDHB* is significantly increased in response to chemotherapy, suggesting a marker role for this gene in response to neoadjuvant chemotherapy in breast cancer (56). In line with our results, previous proteomic analysis of Adriamycin resistance in breast cancer also suggested a role for *LDHB* in drug resistance (57).

PLS3 encodes a protein called plastin-3 that is found in cancer cells. It promotes apoptosis via the TRAIL pathway, which is accomplished by expanding the death pathway of the mitochondrial arm (58). However, *PLS3* has been identified as a putative target for increasing p38 MAPK-mediated apoptosis triggered by drug resistance, suggesting that targeting this enzyme could be an effective strategy for overcoming drug resistance (59). We identified *AKAP12* as a key component of chemoresistance in the MCF-7/ADR cell line. In ovarian cancer, *AKAP12* has been

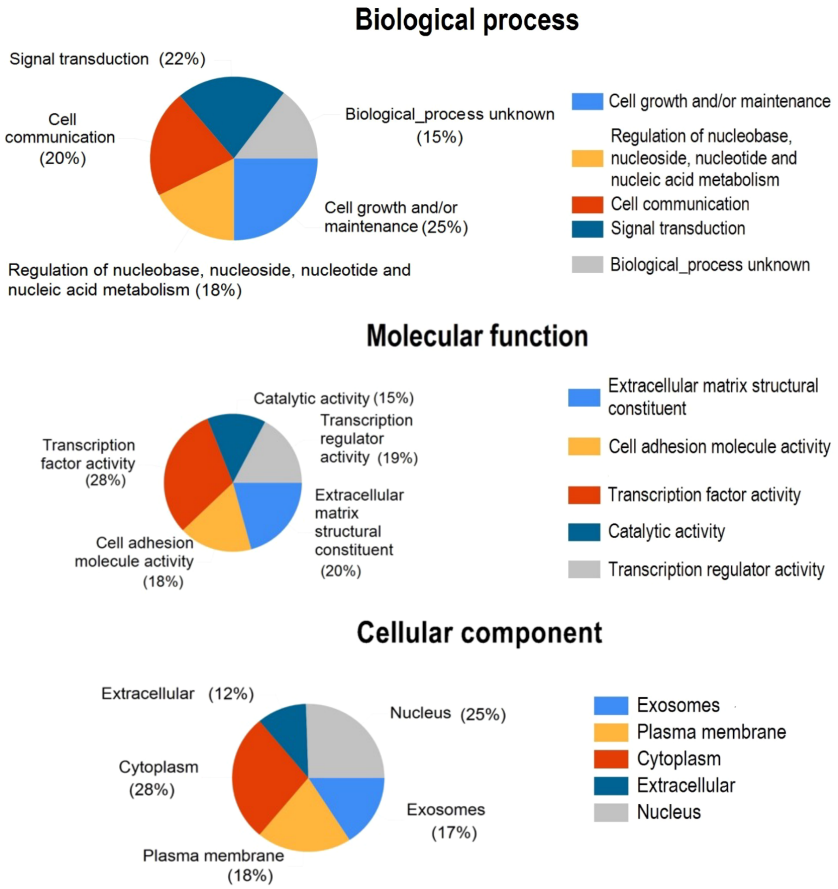

FIGURE 4
Pie charts show the gene ontology annotations for the DEGs discovered by GCN analysis. DEGs were classified as cellular components, molecular functions, and biological processes.

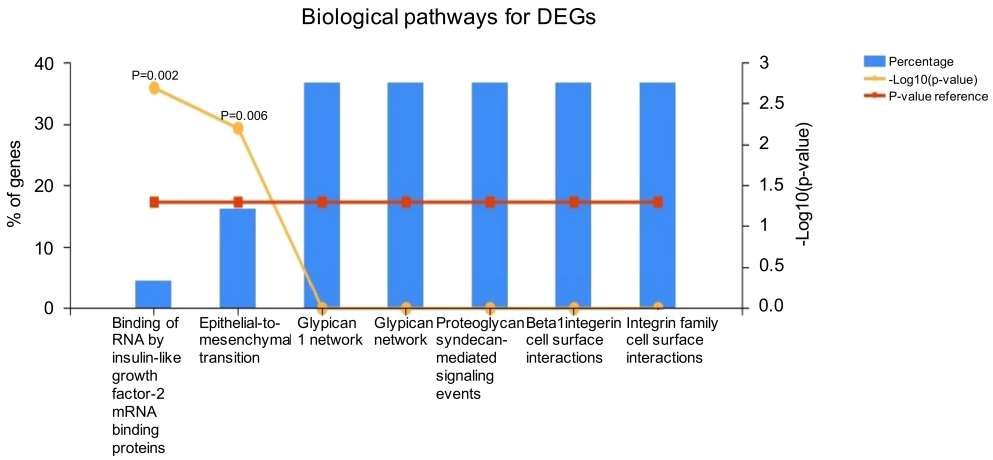

FIGURE 5
Functional enrichment analysis using the Kyoto Encyclopedia of Genes and Genomes (KEGG) database.

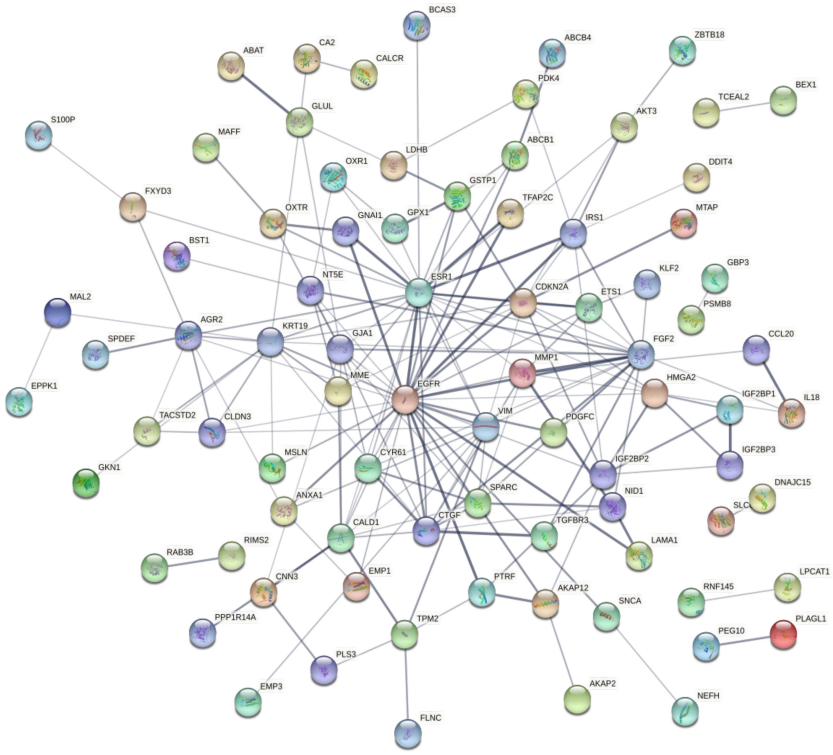

FIGURE 6
The network shows the protein-protein interactions between the candidate DEGs identified by comparing the transcriptomes of the MCF-7/ADR and MCF-7 cell lines. Proteins are represented by circles. Significant associations between proteins are shown by lines.

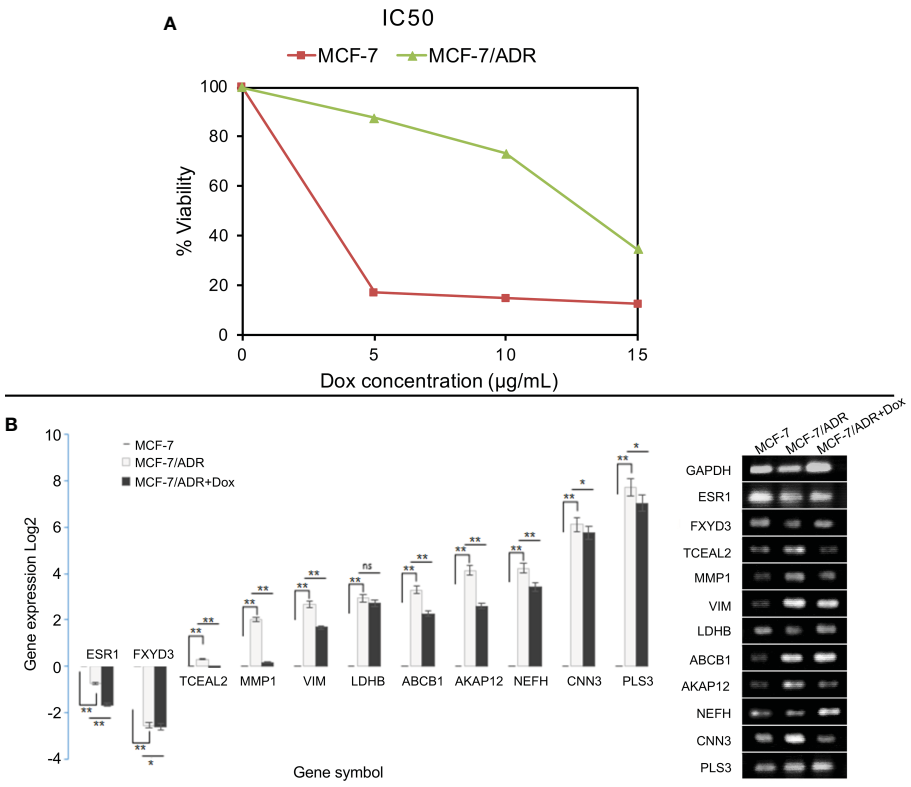

FIGURE 7
Cell viability and gene expression in the presence of doxorubicin in MCF-7/ADR and its parent cell line MCF-7. MCF-7 and MCF-7/ADR cells were treated with doxorubicin at concentrations of 0, 5, 10, and 15 μg/mL for 48 hours, and cell viability was determined using the MTT assay **(A)**. qRT–PCR analysis of the expression of candidate DEGs in MCF-7 and MCF-7/ADR in the presence or absence of doxorubicin **(B)**. The genes were selected from the GCN network based on their degree or betweenness. *CTGF* failed to amplify in both cell lines. *P-value < 0.05 and **P-value <0.01.

TABLE 3 The list of the candidate up/down-regulated genes selected for qRT-PCR analysis following GCN analysis in the MCF-7/ADR and MCF-7 cell lines.

Data Set	Name	Rank_stat	Degree	Betweenness
GSE76540	*VIM*	111.0	22	408.1
	TCEAL2	112.0	21	549.4
	NEFH	103.25	18	289.2
GSE24460	*LDHB*	15.5	7	10.9
	CNN3	13.5	6	5.8
GSE76540 and GSE24460	*MMP1*	107.75	18	391.8
	LDHB	15.5	7	10.9
	ABCB1	70.25	7	70.9
	AKAP12	43.25	4	0.4
	PLS3	27.25	3	0.0
	CTGF	11.25	5	3.8

associated with paclitaxel resistance by modulating signaling pathways related to cell survival and drug efflux (60). The role of this protein in doxorubicin tolerance is not well understood.

MMP-1 is a gene that encodes a zinc-dependent matrix-metalloprotease involved in the activation of EMT, the Akt signaling pathway (61), and angiogenesis through various mechanisms (62). Snail, Slug, and Twist are EMT-promoting transcription factors that directly induce *MMP-1* transcription in chemo-resistant cells (63). By inactivating the Fas receptor, *MMP-1* suppresses apoptosis and increases chemoresistance (64). In addition, other members of the MMP family proteases, including MMP-2 (65), MMP-7 (66), and MMP-9 (67), also contribute to metastasis and multidrug resistance by degrading extracellular matrix components in multiple types of cancer. MMP-1 expression has been linked to increased cell proliferation, tumor development, metastasis, and resistance to chemotherapy in various tumors (68, 69). Several studies have shown that overexpression of *MMP-1* significantly reduced drug sensitivity in MCF-7 cells, whereas *MMP-1* knockdown considerably increased drug sensitivity in MCF-7/ADR cells (63, 70). Another candidate DEG that is known to be involved in EMT is vimentin (VIM). The contribution of VIM to EMT is mediated by activating the Akt signaling pathway (71). CNN3 (calponin-3) expression is altered in colorectal and breast carcinomas (72, 73). It has been linked to EMT via β-Catenin, ERK1/2, c-Jun, heat shock protein 60, and mutant p53 pathways (74).

Our results suggest that gene co-expression network analysis can be used to identify genes that contribute to doxorubicin resistance in breast cancer. Several of these genes have been associated with cancer development, progression, metastasis, and resistance to chemotherapy based on previous studies. In many cases, potential inhibitors have been identified that could be used to overcome drug resistance (75, 76). This research included some limitations. For instance, it took advantage of microarray data; however, the results can be further complemented by additional analyses using mRNA sequencing and proteomics data to characterize changes in protein abundances, post-translational modifications, and protein localizations. Additional functional analyses, including gene knockout and/or overexpression, can help provide a mechanistic understanding of the role of these genes in the development of chemoresistance in breast cancer.

Conclusion

In this study, we analyzed microarray data sets from chemo-resistant and chemo-sensitive breast cancer cell lines using GCNs. Our results suggest a key role for certain extracellular matrix component proteins in the development of chemoresistance in the MCF-7/ADR breast cancer cell line. The results of the bioinformatics analysis were confirmed by qRT–PCR analyses of specific DEGs. These findings could pave the way for the identification of genes linked to molecular mechanisms governing chemotherapy resistance in breast cancer.

Data availability statement

The datasets presented in this study can be found in online repositories. The names of the repository/repositories and accession number(s) can be found in the article/Supplementary Material.

Author contributions

AM performed the experiments, analyzed the data, and drafted the manuscript. JG contributed to the writing and revision of the manuscript. ISM conducted the analysis of gene expression data. KS and VJ conceived and designed the study, and contributed to the writing of the manuscript. All authors reviewed and approved the final version of the manuscript.

Conflict of interest

The authors declare that the research was conducted in the absence of any commercial or financial relationships that could be construed as a potential conflict of interest.

Publisher's note

All claims expressed in this article are solely those of the authors and do not necessarily represent those of their affiliated organizations, or those of the publisher, the editors and the reviewers. Any product that may be evaluated in this article, or claim that may be made by its manufacturer, is not guaranteed or endorsed by the publisher.

Supplementary material

The Supplementary Material for this article can be found online at: https://www.frontiersin.org/articles/10.3389/fonc.2023.1135836/full#supplementary-material

SUPPLEMENTARY DATA SHEET 1

The complete list of all differentially expressed genes (DEGs) in GSE76540 and GSE24460, as determined by contrasting the MCF-7/ADR and MCF-7 cell lines. Statistically significant expression was defined as having a LogFC > 1 and an adjusted P-value cutoff of 0.05.

References

1. Siegel RL, Miller KD, Jemal A. Cancer statistics, 2016. *CA Cancer J Clin* (2016) 66 (1):7–30. doi: 10.3322/caac.21332

2. Gradishar WJ, Anderson BO, Balassanian R, Blair SL, Burstein HJ, Cyr A, et al. Breast cancer, version 4.2017, NCCN clinical practice guidelines in oncology. *J Natl Compr Canc Netw* (2018) 16(3):310–20. doi: 10.6004/jnccn.2018.0012

3. Miri A, Kiani E, Habibi S, Khafaei M. Triple-negative breast cancer: biology, pathology, and treatment. *CAJMPSI* (2021) 1(2):81–96. doi: 10.22034/CAJMPSI.2021.02.05

4. Stark A, Kleer CG, Martin I, Awuah B, Nsiah-Asare A, Takyi V, et al. African Ancestry and higher prevalence of triple-negative breast cancer: findings from an international study. *Cancer* (2010) 116(21):4926–32. doi: 10.1002/cncr.25276

5. Tsang JYS, Tse GM. Molecular classification of breast cancer. *Adv Anat Pathol* (2020) 27(1):27–35. doi: 10.1097/PAP.0000000000000232

6. Perou CM, Sorlie T, Eisen MB, van de Rijn M, Jeffrey SS, Rees CA, et al. Molecular portraits of human breast tumours. *Nature* (2000) 406(6797):747–52. doi: 10.1038/35021093

7. Johnson KS, Conant EF, Soo MS. Molecular subtypes of breast cancer: a review for breast radiologists. *J Breast Imaging* (2021) 3(1):12–24. doi: 10.1093/jbi/wbaa110

8. Prat A, Pineda E, Adamo B, Galvan P, Fernandez A, Gaba L, et al. Clinical implications of the intrinsic molecular subtypes of breast cancer. *Breast* (2015) 24 (Suppl 2):S26–35. doi: 10.1016/j.breast.2015.07.008

9. Sorlie T. Molecular portraits of breast cancer: tumour subtypes as distinct disease entities. *Eur J Cancer* (2004) 40(18):2667–75. doi: 10.1016/j.ejca.2004.08.021

10. Tang P, Tse GM. Immunohistochemical surrogates for molecular classification of breast carcinoma: a 2015 update. *Arch Pathol Lab Med* (2016) 140(8):806–14. doi: 10.5858/arpa.2015-0133-RA

11. Lehmann BD, Bauer JA, Chen X, Sanders ME, Chakravarthy AB, Shyr Y, et al. Identification of human triple-negative breast cancer subtypes and preclinical models for selection of targeted therapies. *J Clin Invest* (2011) 121(7):2750–67. doi: 10.1172/JCI45014

12. Shagufta, Ahmad I, Mathew S, Rahman S. Recent progress in selective estrogen receptor downregulators (SERDs) for the treatment of breast cancer. *RSC Med Chem* (2020) 11(4):438–54. doi: 10.1039/c9md00570f

13. Waks AG, Winer EP. Breast cancer treatment: a review. *JAMA* (2019) 321 (3):288–300. doi: 10.1001/jama.2018.19323

14. Yin L, Duan JJ, Bian XW, Yu SC. Triple-negative breast cancer molecular subtyping and treatment progress. *Breast Cancer Res* (2020) 22(1):61. doi: 10.1186/s13058-020-01296-5

15. Muley H, Fado R, Rodriguez-Rodriguez R, Casals N. Drug uptake-based chemoresistance in breast cancer treatment. *Biochem Pharmacol* (2020) 177:113959. doi: 10.1016/j.bcp.2020.113959

16. Lei J, Wang H, Zhu D, Wan Y, Yin L. Combined effects of avasimibe immunotherapy, doxorubicin chemotherapy, and metal-organic frameworks nanoparticles on breast cancer. *J Cell Physiol* (2020) 235(5):4814–23. doi: 10.1002/jcp.29358

17. Fraguas-Sánchez A, Fernández-Carballido A, Simancas-Herbada R, Martin-Sabroso C, Torres-Suárez A. CBD loaded microparticles as a potential formulation to improve paclitaxel and doxorubicin-based chemotherapy in breast cancer. *Int J Pharm* (2020) 574:118916. doi: 10.1016/j.ijpharm.2019.118916

18. Caparica R, Bruzzone M, Poggio F, Ceppi M, de Azambuja E, Lambertini M. Anthracycline and taxane-based chemotherapy versus docetaxel and cyclophosphamide in the adjuvant treatment of HER2-negative breast cancer patients: a systematic review and meta-analysis of randomized controlled trials. *Breast Cancer Res Treat* (2019) 174(1):27–37. doi: 10.1007/s10549-018-5055-9

19. Vidra R, Nemes A, Vidrean A, Pintea S, Tintari S, Deac A, et al. Pathological complete response following cisplatin or carboplatin-based neoadjuvant chemotherapy for triple-negative breast cancer: a systematic review and meta-analysis. *Exp Ther Med* (2022) 23(1):91. doi: 10.3892/etm.2021.11014

20. Korde LA, Somerfield MR, Carey LA, Crews JR, Denduluri N, Hwang ES, et al. Neoadjuvant chemotherapy, endocrine therapy, and targeted therapy for breast cancer: ASCO guideline. *J Clin Oncol* (2021) 39(13):1485–505. doi: 10.1200/JCO.20.03399

21. Zhao M, Ding XF, Shen JY, Zhang XP, Ding XW, Xu B. Use of liposomal doxorubicin for adjuvant chemotherapy of breast cancer in clinical practice. *J Zhejiang Univ Sci B* (2017) 18(1):15–26. doi: 10.1631/jzus.B1600303

22. Sokolova E, Kutova O, Grishina A, Pospelov A, Guryev E, Schulga A, et al. Penetration efficiency of antitumor agents in ovarian cancer spheroids: the case of recombinant targeted toxin DARPin-LoPE and the chemotherapy drug, doxorubicin. *Pharmaceutics* (2019) 11(5):219. doi: 10.3390/pharmaceutics11050219

23. Evens AM, Advani RH, Helenowski IB, Fanale M, Smith SM, Jovanovic BD, et al. Multicenter phase ii study of sequential brentuximab vedotin and doxorubicin, vinblastine, and dacarbazine chemotherapy for older patients with untreated classical Hodgkin lymphoma. *J Clin Oncol* (2018) 36(30):3015–22. doi: 10.1200/JCO.2018.79.0139

24. Trucco M, Barredo JC, Goldberg J, Leclerc GM, Hale GA, Gill J, et al. A phase I window, dose escalating and safety trial of metformin in combination with induction chemotherapy in relapsed refractory acute lymphoblastic leukemia: metformin with induction chemotherapy of vincristine, dexamethasone, PEG-asparaginase, and doxorubicin. *Pediatr Blood Cancer* (2018) 65(9):e27224. doi: 10.1002/pbc.27224

25. Guo B, Tam A, Santi SA, Parissenti AM. Role of autophagy and lysosomal drug sequestration in acquired resistance to doxorubicin in MCF-7 cells. *BMC Cancer* (2016) 16(1):762. doi: 10.1186/s12885-016-2790-3

26. Zhitomirsky B, Assaraf YG. Lysosomal accumulation of anticancer drugs triggers lysosomal exocytosis. *Oncotarget* (2017) 8(28):45117–32. doi: 10.18632/oncotarget.15155

27. Cao J, Zhang M, Wang B, Zhang L, Zhou F, Fang M. Chemoresistance and metastasis in breast cancer molecular mechanisms and novel clinical strategies. *Front Oncol* (2021) 11:658552. doi: 10.3389/fonc.2021.658552

28. Li W, Zhang H, Assaraf YG, Zhao K, Xu X, Xie J, et al. Overcoming ABC transporter-mediated multidrug resistance: molecular mechanisms and novel therapeutic drug strategies. *Drug Resist Update* (2016) 27:14–29. doi: 10.1016/j.drup.2016.05.001

29. Fultang N, Illendula A, Lin J, Pandey MK, Klase Z, Peethambaran B. ROR1 regulates chemoresistance in breast cancer via modulation of drug efflux pump ABCB1. *Sci Rep* (2020) 10(1):1821. doi: 10.1038/s41598-020-58864-0

30. Li Z, Chen C, Chen L, Hu D, Yang X, Zhuo W, et al. STAT5a confers doxorubicin resistance to breast cancer by regulating ABCB1. *Front Oncol* (2021) 11:697950. doi: 10.3389/fonc.2021.697950

31. McGuirk S, Audet-Delage Y, Annis MG, Xue Y, Vernier M, Zhao K, et al. Resistance to different anthracycline chemotherapeutics elicits distinct and actionable primary metabolic dependencies in breast cancer. *Elife* (2021) 10. doi: 10.7554/eLife.65150

32. Smith L, Watson MB, O'Kane SL, Drew PJ, Lind MJ, Cawkwell L. The analysis of doxorubicin resistance in human breast cancer cells using antibody microarrays. *Mol Cancer Ther* (2006) 5(8):2115–20. doi: 10.1158/1535-7163.MCT-06-0190

33. Zheng H-C. The molecular mechanisms of chemoresistance in cancers. *Oncotarget* (2017) 8(35):59950–64. doi: 10.18632/oncotarget.19048

34. Zhang H, Qiu C, Zhu W. Identification of forward regulated hub genes and pathways for cancer stem cell characteristics in African American breast cancer by the network analysis. *J Xiangya Med* (2020) 5(35). doi: 10.21037/jxym-20-81

35. Tang J, Kong D, Cui Q, Wang K, Zhang D, Gong Y, et al. Prognostic genes of breast cancer identified by gene co-expression network analysis. *Front Oncol* (2018) 8:374. doi: 10.3389/fonc.2018.00374

36. Shi W, Zou R, Yang M, Mai L, Ren J, Wen J, et al. Analysis of genes involved in ulcerative colitis activity and tumorigenesis through systematic mining of gene co-expression networks. *Front Physiol* (2019) 10:662. doi: 10.3389/fphys.2019.00662

37. Contreras-Lopez O, Moyano TC, Soto DC, Gutiérrez RA. Step-by-step construction of gene co-expression networks from high-throughput arabidopsis RNA sequencing data. In: *Root development*. New York, NY: Humana Press (2018).

38. Smyth GK, Ritchie M, Thorne N, Wettenhall J. LIMMA: linear models for microarray data. In: *Bioinformatics and computational biology solutions using r and bioconductor*. Statistics for Biology and Health (2005).

39. Irizarry RA, Hobbs B, Collin F, Beazer-Barclay YD, Antonellis KJ, Scherf U, et al. Exploration, normalization, and summaries of high density oligonucleotide array probe level data. *Biostatistics* (2003) 4(2):249–64. doi: 10.1093/biostatistics/4.2.249

40. Revelle WR. psych: Procedures for personality and psychological research. (2017)

41. Morris JH, Apeltsin L, Newman AM, Baumbach J, Wittkop T, Su G, et al. clusterMaker: a multi-algorithm clustering plugin for cytoscape. *BMC Bioinform* (2011) 12(1):436. doi: 10.1186/1471-2105-12-436

42. Delgado-Chaves FM, Gomez-Vela F, Garcia-Torres M, Divina F, Vazquez Noguera JL. Computational inference of gene co-expression networks for the identification of lung carcinoma biomarkers: an ensemble approach. *Genes (Basel)* (2019) 10(12):962. doi: 10.3390/genes10120962

43. Livak KJ, Schmittgen TD. Analysis of relative gene expression data using real-time quantitative PCR and the 2– ΔΔCT method. *methods* (2001) 25(4):402–8. doi: 10.1006/meth.2001.1262

44. Fonseka P, Pathan M, Chitti SV, Kang T, Mathivanan S. FunRich enables enrichment analysis of OMICs datasets. *J Mol Biol* (2021) 433(11):166747. doi: 10.1016/j.jmb.2020.166747

45. Zhang P, He D, Chen Z, Pan Q, Du F, Zang X, et al. Chemotherapy enhances tumor vascularization via notch signaling-mediated formation of tumor-derived endothelium in breast cancer. *Biochem Pharmacol* (2016) 118:18–30. doi: 10.1016/j.bcp.2016.08.008

46. Zhang L, Zhang X, Fan S, Zhang Z. Identification of modules and hub genes associated with platinum-based chemotherapy resistance and treatment response in ovarian cancer by weighted gene co-expression network analysis. *Med (Baltimore)* (2019) 98(44):e17803. doi: 10.1097/MD.0000000000017803

47. Xu Y, Zhang Z, Zhang L, Zhang C. Novel module and hub genes of distinctive breast cancer associated fibroblasts identified by weighted gene co-expression network analysis. *Breast Cancer* (2020) 27(5):1017–28. doi: 10.1007/s12282-020-01101-3

48. Zhang Y, Sun L, Wang X, Sun Y, Chen Y, Xu M, et al. FBXW4 acts as a protector of FOLFOX-based chemotherapy in metastatic colorectal cancer identified by co-expression network analysis. *Front Genet* (2020) 11:113. doi: 10.3389/fgene.2020.00113

49. Thomas C, Tampe R. Structural and mechanistic principles of ABC transporters. *Annu Rev Biochem* (2020) 89:605–36. doi: 10.1146/annurev-biochem-011520-105201

50. Modi A, Roy D, Sharma S, Vishnoi JR, Pareek P, Elhence P, et al. ABC transporters in breast cancer: their roles in multidrug resistance and beyond. *J Drug Targeting* (2022) 30(9):927–47. doi: 10.1080/1061186X.2022.2091578

51. Amawi H, Sim HM, Tiwari AK, Ambudkar SV, Shukla S. ABC transporter-mediated multidrug-resistant cancer. *Adv Exp Med Biol* (2019) 1141:549–80. doi: 10.1007/978-981-13-7647-4_12

52. McCleland ML, Adler AS, Shang Y, Hunsaker T, Truong T, Peterson D, et al. An integrated genomic screen identifies LDHB as an essential gene for triple-negative breast cancer. *Cancer Res* (2012) 72(22):5812–23. doi: 10.1158/0008-5472.CAN-12-1098

53. Shibata S, Sogabe S, Miwa M, Fujimoto T, Takakura N, Naotsuka A, et al. Identification of the first highly selective inhibitor of human lactate dehydrogenase b. *Sci Rep* (2021) 11(1):21353. doi: 10.1038/s41598-021-00820-7

54. Urbanska K, Orzechowski A. Unappreciated role of LDHA and LDHB to control apoptosis and autophagy in tumor cells. *Int J Mol Sci* (2019) 20(9):2085. doi: 10.3390/ijms20092085

55. Mishra D, Banerjee D. Lactate dehydrogenases as metabolic links between tumor and stroma in the tumor microenvironment. *Cancers (Basel)* (2019) 11(6). doi: 10.3390/cancers11060750

56. Wise-Draper TM, Gulati S, Palackdharry S, Hinrichs BH, Worden FP, Old MO, et al. Phase II clinical trial of neoadjuvant and adjuvant pembrolizumab in resectable local-regionally advanced head and neck squamous cell carcinoma. *Clin Cancer Res* (2022) 28(7):1345–52. doi: 10.1158/1078-0432.CCR-21-3351

57. Wang Z, Liang S, Lian X, Liu L, Zhao S, Xuan Q, et al. Identification of proteins responsible for adriamycin resistance in breast cancer cells using proteomics analysis. *Sci Rep* (2015) 5(1):9301. doi: 10.1038/srep09301

58. Ndebele K, Gona P, Jin T-G, Benhaga N, Chalah A, Degli-Esposti M, et al. Tumor necrosis factor (TNF)-related apoptosis-inducing ligand (TRAIL) induced mitochondrial pathway to apoptosis and caspase activation is potentiated by phospholipid scramblase-3. *Apoptosis* (2008) 13(7):845–56. doi: 10.1007/s10495-008-0219-4

59. Ma Y, Lai W, Zhao M, Yue C, Shi F, Li R, et al. Plastin 3 down-regulation augments the sensitivity of MDA-MB-231 cells to paclitaxel via the p38 MAPK signalling pathway. *Artif Cells Nanomed Biotechnol* (2019) 47(1):685–95. doi: 10.1080/21691401.2019.1576707

60. Bateman NW, Jaworski E, Ao W, Wang G, Litzi T, Dubil E, et al. Elevated AKAP12 in paclitaxel-resistant serous ovarian cancer cells is prognostic and predictive of poor survival in patients. *J Proteome Res* (2015) 14(4):1900–10. doi: 10.1021/pr5012894

61. Wang K, Zheng J, Yu J, Wu Y, Guo J, Xu Z, et al. Knockdown of MMP−1 inhibits the progression of colorectal cancer by suppressing the PI3K/Akt/c−myc signaling pathway and EMT. *Oncol Rep* (2020) 43(4):1103–12. doi: 10.3892/or.2020.7490

62. Winer A, Adams S, Mignatti P. Matrix metalloproteinase inhibitors in cancer therapy: turning past failures into future successes. *Mol Cancer Ther* (2018) 17(6):1147–55. doi: 10.1158/1535-7163.MCT-17-0646

63. Shen C-J, Kuo Y-L, Chen C-C, Chen M-J, Cheng Y-M. MMP1 expression is activated by slug and enhances multi-drug resistance (MDR) in breast cancer. *PloS One* (2017) 12(3):e0174487. doi: 10.1371/journal.pone.0174487

64. Gialeli C, Theocharis AD, Karamanos NK. Roles of matrix metalloproteinases in cancer progression and their pharmacological targeting. *FEBS J* (2011) 278(1):16–27. doi: 10.1111/j.1742-4658.2010.07919.x

65. Song JH, Kim SH, Cho D, Lee IK, Kim HJ, Kim TS. Enhanced invasiveness of drug-resistant acute myeloid leukemia cells through increased expression of matrix metalloproteinase-2. *Int J Cancer* (2009) 125(5):1074–81. doi: 10.1002/ijc.24386

66. Almendro V, Ametller E, Garcia-Recio S, Collazo O, Casas I, Auge JM, et al. The role of MMP7 and its cross-talk with the FAS/FASL system during the acquisition of chemoresistance to oxaliplatin. *PloS One* (2009) 4(3):e4728. doi: 10.1371/journal.pone.0004728

67. Fukuyama R, Ng KP, Cicek M, Kelleher C, Niculaita R, Casey G, et al. Role of IKK and oscillatory NFkappaB kinetics in MMP-9 gene expression and chemoresistance to 5-fluorouracil in RKO colorectal cancer cells. *Mol Carcinog* (2007) 46(5):402–13. doi: 10.1002/mc.20288

68. Wang K, Zheng J, Yu J, Wu Y, Guo J, Xu Z, et al. Knockdown of MMP1 inhibits the progression of colorectal cancer by suppressing the PI3K/Akt/cmyc signaling pathway and EMT. *Oncol Rep* (2020) 43(4):1103–12. doi: 10.3892/or.2020.7490

69. Dong F, Eibach M, Bartsch JW, Dolga AM, Schlomann U, Conrad C, et al. The metalloprotease-disintegrin ADAM8 contributes to temozolomide chemoresistance and enhanced invasiveness of human glioblastoma cells. *Neuro Oncol* (2015) 17(11):1474–85. doi: 10.1093/neuonc/nov042

70. Wang QM, Lv L, Tang Y, Zhang L, Wang LF. MMP−1 is overexpressed in triple −negative breast cancer tissues and the knockdown of MMP−1 expression inhibits tumor cell malignant behaviors. *vitro Oncol Lett* (2019) 17(2):1732–40. doi: 10.3892/ol.2018.9779

71. Tezcan O, Gunduz U. Vimentin silencing effect on invasive and migration characteristics of doxorubicin resistant MCF-7 cells. *BioMed Pharmacother* (2014) 68(3):357–64. doi: 10.1016/j.biopha.2014.01.006

72. Bing F, Zhao Y. Screening of biomarkers for prediction of response to and prognosis after chemotherapy for breast cancers. *Onco Targets Ther* (2016) 9:2593–600. doi: 10.2147/OTT.S92350

73. Nakarai C, Osawa K, Akiyama M, Matsubara N, Ikeuchi H, Yamano T, et al. Expression of AKR1C3 and CNN3 as markers for detection of lymph node metastases in colorectal cancer. *Clin Exp Med* (2015) 15(3):333–41. doi: 10.1007/s10238-014-0298-1

74. Nair VA, Al-Khayyal NA, Sivaperumal S, Abdel-Rahman WM. Calponin 3 promotes invasion and drug resistance of colon cancer cells. *World J Gastrointest Oncol* (2019) 11(11):971–82. doi: 10.4251/wjgo.v11.i11.971

75. Zhou H-H, Chen X, Cai L-Y, Nan X-W, Chen J-H, Chen X-X, et al. Erastin reverses ABCB1-mediated docetaxel resistance in ovarian cancer. *Front Oncol* (2019) 9:1398. doi: 10.3389/fonc.2019.01398

76. Zhang Y, Vagiannis D, Budagaga Y, Sabet Z, Hanke I, Rozkoš T, et al. Encorafenib acts as a dual-activity chemosensitizer through its inhibitory effect on ABCC1 transporter *in vitro* and ex vivo. *Pharmaceutics* (2022) 14(12). doi: 10.3390/pharmaceutics14122595

frontiers | Frontiers in Oncology

TYPE Review
PUBLISHED 16 June 2023
DOI 10.3389/fonc.2023.1155254

OPEN ACCESS

EDITED BY
Zhi-Gang Zhuang,
Shanghai First Maternity and Infant Hospital, China

REVIEWED BY
Macrina Beatriz Silva Cázares,
Autonomous University of San Luis Potosí, Mexico
Bruce Alan Bunnell,
University of North Texas Health Science Center, United States
Subhayan Das,
Indian Institute of Technology Kharagpur, India

*CORRESPONDENCE
Richa Tripathi
richa.trpths@gmail.com

RECEIVED 31 January 2023
ACCEPTED 05 June 2023
PUBLISHED 16 June 2023

CITATION
Singh S, Saini H, Sharma A, Gupta S, Huddar VG and Tripathi R (2023) Breast cancer: miRNAs monitoring chemoresistance and systemic therapy. *Front. Oncol.* 13:1155254. doi: 10.3389/fonc.2023.1155254

Breast cancer: miRNAs monitoring chemoresistance and systemic therapy

Shivam Singh[1], Heena Saini[2], Ashok Sharma[3], Subhash Gupta[1], V. G. Huddar[4] and Richa Tripathi[2*]

[1]Department of Radiation Oncology, Dr. B. R. Ambedkar Institute Rotary Cancer Hospital, All India Institute of Medical Sciences, New Delhi, India, [2]Integrated translational Molecular Biology laboratory, Department of Rog Nidan and Vikriti vigyan (Pathology), All India Institute of Ayurveda (AIIA), New Delhi, India, [3]Department of Biochemistry, All India Institute of Medical Sciences, New Delhi, India, [4]Department of Kaya Chikitsa (Internal Medicine), All India Institute of Ayurveda (AIIA), New Delhi, India

With a high mortality rate that accounts for millions of cancer-related deaths each year, breast cancer is the second most common malignancy in women. Chemotherapy has significant potential in the prevention and spreading of breast cancer; however, drug resistance often hinders therapy in breast cancer patients. The identification and the use of novel molecular biomarkers, which can predict response to chemotherapy, might lead to tailoring breast cancer treatment. In this context, accumulating research has reported microRNAs (miRNAs) as potential biomarkers for early cancer detection, and are conducive to designing a more specific treatment plan by helping analyze drug resistance and sensitivity in breast cancer treatment. In this review, miRNAs are discussed in two alternative ways-as tumor suppressors to be used in miRNA replacement therapy to reduce oncogenesis and as oncomirs to lessen the translation of the target miRNA. Different miRNAs like miR-638, miR-17, miR-20b, miR-342, miR-484, miR-21, miR-24, miR-27, miR-23 and miR-200 are involved in the regulation of chemoresistance through diverse genetic targets. For instance, tumor-suppressing miRNAs like miR-342, miR-16, miR-214, and miR-128 and tumor-promoting miRNAs like miR101 and miR-106-25 cluster regulate the cell cycle, apoptosis, epithelial to mesenchymal transition and other pathways to impart breast cancer drug resistance. Hence, in this review, we have discussed the significance of miRNA biomarkers that could assist in providing novel therapeutic targets to overcome potential chemotherapy resistance to systemic therapy and further facilitate the design of tailored therapy for enhanced efficacy against breast cancer.

KEYWORDS

micro RNA, breast cancer, chemoresistance, neoadjuvant (chemo)radiotherapy, systemic therapies

Highlights

1. Drug resistance is the major obstacle in breast cancer chemotherapy
2. miRNA biomarkers could provide novel therapeutic targets to overcome potential chemotherapy resistance to systemic therapy in breast cancer.
3. Targeting miRNAs—either reducing or raising their expression—seems to be an attractive approach for designing novel, more effective, and personalized treatments for breast cancer.
4. A novel approach to treating breast cancer that combines miRNA therapies with conventional chemotherapeutic techniques and drug targets is possible.

1 Introduction

The most common malignancy worldwide is breast cancer (BC). According to the status update on the GLOBOCAN 2020 projections of cancer incidence and mortality, BC is the primary cause of cancer death in women and accounts for 1 in 4 cancer diagnoses among females (1). An estimated 684,996 people died from breast cancer in 2020, with low-resource areas accounting for a disproportionate share of these deaths. According to statistics, the prevalence of BC ranges from 2-6% in Western nations to 10-20% in Asian nations (2), indicating that BC is becoming a global health concern, even in nations with sizable young populations like India. Although breast cancer diagnoses have increased recently (3), the prognosis for the disease has significantly improved, with expected 5-year survival rates rising from 40% to approximately 90% over the last 50 years. With few exceptions, en-bloc radical resections in the form of Halstead mastectomy and axillary clearing were formerly thought to be essential for managing BC (4). Recent advancements in clinical trials have been brought about by a greater understanding of the molecular processes associated with the heterogeneity of breast tumors. This understanding has allowed for more conservative surgical procedures and the personalization of treatment plans to maximize sensitization to the tumor while minimizing unneeded morbidity to the patient. This includes the era of cancer diagnostics, which has recognized BC as a diverse disease and routinely subcategorized these cancers into four genetically distinct, integral subgroups - luminal A breast cancer (LABC), luminal B breast cancer (LBBC), human epidermal growth factor receptor-2 enriched breast cancer (HER2+) and triple-negative breast cancer (TNBC). These subgroups have different clinical behavior, prognosis, treatment approaches, and clinical outcomes in the known treatments (5).

For BC patients, chemotherapy is regarded as the most successful and crucial therapeutic approach. Anthracyclins, Tamoxifen, Taxane, 5-FU and trastuzumab are the major chemotherapeutic drugs which are administered to BC patients (6–12). Doxorubicin, daunorubicin, and epirubicin are some of the anthracycline antibiotics that are frequently used. Anthracyclines can be administered at all BC stages and have demonstrated a crucial function in treating BC (8). Tamoxifen is specifically used for the oestrogen receptor (ER) positive subtype of BC (9). Anthracyclines and taxanes are used as the predominant treatment for TNBC (10). The two most widely used taxanes are-paclitaxel and docetaxel, causing acute hypersensitivity responses (HSRs) in 5% to 10% of patients (11). The human epidermal growth factor receptor 2 (HER-2) is frequently used to categorize BC patients based on its overexpression (also known as HER-2 positive) or lack of expression (also known as HER-2 negative) (13). The likelihood of BC metastases and poor prognosis are strongly correlated with HER-2 overexpression (13). A targeted therapy for HER-2 is trastuzumab (TRS), a humanized monoclonal antibody (12). Despite our efforts to categorize tumors into prognostic categories, tumor behavior and prognosis remains unpredictable, which makes it challenging to develop strategies that would improve disease control while minimizing toxicities to patients. Although, a better understanding of the disease has led to advancements in treatment over the past few decades, but drug resistance remains a challenge and the underlying molecular causes are still largely undefined (14). Drug-resistant cancer cells multiply rapidly and grow more hostile, increasing the likelihood that the tumor may aggressively spread to other organs. Drug resistance can be categorized in two different ways. One is internal resistance or inherited resistance, which occurs when tumors are resistant to treatment even before receiving it, meaning that even early detection and treatment are ineffective. Another form of resistance is received resistance or acquired resistance which occurs following an initial positive response to the therapy (15). Here, the targets and processes associated are a focus of significant research, and the mechanisms of such drug resistance are largely still under investigation (16). For instance, Martz et al. (2014) demonstrated that stimulation of the Notch-1, mitogen-activated protein kinase (RAS-MAPK), phosphoinositide 3-kinase (PI3K) and mammalian target of rapamycin (mTOR), PI3K/AKT and estrogen receptor (ER) signaling pathways resulted in resistance to a variety of drugs (17). It was observed that when Notch-1 is activated, BRAF (V600E) melanoma cells develop acquired resistance to MAPK inhibitors and breast cancer cells also exhibit resistance to tamoxifen (17). Hence, the research group used a Notch-1 inhibitor to restore sensitivity, indicating that Notch-1 knockdown could be a therapeutic strategy in melanomas and drug-resistant breast malignancies (17). Likewise, it seems, resistance to chemotherapy is also related to the epidermal growth factor receptor (EGFR) pathway. Genetically modified murine model (GEMM), human cell lines, and a clinically applicable model of KRAS-mutant colorectal cancer (CRC) have all been used to study EGFR and PI3K/mTOR (18). According to the evidence, PI3K/mTOR and EGFR inhibition boost drug sensitivity and are increasingly used in cancer therapy to combat drug resistance. Additionally, the use of systemic drugs as neoadjuvant enables the production of *in-vivo* data on tumor sensitivity, which has been shown to have predictive importance for disease survival and recurrence. These contemporary aspects of traditional breast cancer management shed light on the potential value of emerging

biomarkers in advancing the current treatment model. There are currently few biomarkers that may reliably predict response and resistance to systemic and targeted therapy and attempts to use non-invasive approaches to collect such biomarkers have largely been ineffective (19). This highlights how important it is for researchers to find new biomarkers that can assess patient response to therapy, predict the prognosis of breast cancer patients, and offer clinicians cutting-edge oncogenesis-targeting therapeutic approaches. In the context of BC chemoresistance monitoring and systemic therapy, this study focuses on the function of microRNA (miRNA) as new clinical biomarkers.

miRNAs are small non-coding RNAs ranging from 19 to 25 nucleotides in size and are involved in a variety of biological activities, including cell cycle, apoptosis, survival, and gene control (20). miRNAs primarily bind to the 3′ or 5′ untranslated region (UTR) of their target mRNAs and, depending on the degree of binding, participate in controlling the translation of proteins or destruction of the mRNA itself (21). A single miRNA may target several mRNAs, while many miRNAs may target single mRNA with varying degrees of efficiency (22). Therefore, changes in miRNA expression levels and gene expression silencing by miRNAs have a significant impact on human health and the emergence of diseases such as cancer, diabetes, neurological disease, and cardiovascular disorders (23–25). In the context of cancer, miRNAs can function as both tumor suppressors and oncogenes/oncomirs (26). In contrast to their counterparts in normal tissue, many miRNAs are reported to be up-or down-regulated in cancer tissues. For instance, practically all cancer types have increased miR-21 expression (27). Numerous B-cell malignancies have been shown to express miR-155 at high levels (28). One of the first miRNAs to be found was let-7 which is essentially missing throughout embryonic stages or tissues, although it is highly expressed in the majority of differentiated tissues (29). Similar to the fall in let-7 expression during development, the decline in let-7 expression in malignancies is more pronounced in cancer cells that are more advanced, less differentiated and have mesenchymal features (29). The generation, biology and function of miRNAs in cancer have been discussed in detail in further sections.

This review focuses primarily on the latest findings about the involvement of miRNAs in breast tumor resistance to chemotherapeutic agents and in the development of systemic therapy. Targeting miRNAs—either reducing or raising their expression—seems to be an attractive approach for designing novel, more effective, and personalized treatments for BC. Boosting drug efficacy by examining the downstream targets/pathways influenced by miRNA targeting and predicting patient response to various therapies can lead to better treatment outcomes for BC patients.

2 Breast cancer chemotherapy

Breast cancer bears 7% of the total number of cancers related deaths in 2020. To date, many strategies have been adapted to combat this disease. Complete surgical removal has usually enabled efficient breast cancer disease management (30). Regardless of the severity of the disease, William Halstead's radical mastectomy (which required significant removal of all the breast parenchyma, local lymph nodes, and pectoralis major muscle) used to be the cornerstone of breast cancer treatment (4). Cyclophosphamide, methotrexate, and 5-fluorouracil (CMF), the first chemotherapeutic treatment prescribed by Bonadanno et al. in 1976 with the intention of curing breast cancer, significantly decreased breast cancer relapse (94.7% of 207 patients administered chemotherapy *vs* 76.0% of 179 patients constrained chemotherapy) (31). However, since 1950s, Bernard Fisher and the National Surgical Adjuvant Breast and Bowel Project (NSABP) have hypothesized that aggressive surgery for breast cancer has only limited scientific and biomolecular justification because it is frequently insufficient to achieve complete disease control (32). Fisher's theory that all breast cancer patients needed systemic therapy (especially with chemotherapy) has, however, been thoroughly refuted.

However, the inherent advantage of treating cancer patients with chemotherapy in the neoadjuvant setting has now been recognized as an oncological practice. Neoadjuvant chemotherapy (NAC) benefits comprised tumor downstaging, expanding patient suitability for breast conservation surgery (BCS), and producing *in vivo* data related to tumor resistance, which has been shown to hold predictive value for cancer recurrence and overall survival (OS) (33, 34). The Early Breast Cancer Triallist's Collaborative Group (EBCTCG) recently published data from a meta-analysis of randomized clinical trials showing that locoregional recurrence (LRR) rates are higher following neoadjuvant therapy (21.4% *vs.* 15.9%), despite the fact that disease-free survival (DFS) and overall survival (OS) results are parallel with those treated in the adjuvant setting (35). Additionally, there is growing proof that people who have a pathological complete response (pCR) with NAC have a higher chance of living longer than those who have a latent disease (34, 36). Nevertheless, the clinical usefulness of NAC has been integrated into best-practice guidelines for HER2+ and Triple-negative breast cancer (TNBC). HER2+ malignancies should be treated with NAC and trastuzumab, with the exception of T1a-T1b N0 disease (37). High-risk LN (lymph node)- patients and those with LN positivity should receive anthracycline- and taxane-based chemotherapy along with trastuzumab (37). Further, until TNBC is identified with cancer stages T1a-T1b N0, patients with TNBC should always be provided with an anthracycline and taxane-based treatment (37). American Society of Clinical Oncology (ASCO) also supports the inclusion of platinum-based chemotherapy in TNBC based on the results of a recent meta-analysis because of a higher likelihood to obtain pCR (52.1% versus 37.0%) (38). Pembrolizumab and NAC significantly increased the pCR rates in the KEYNOTE522 trial's preliminary findings (pembrolizumab and NAC: 64.8% versus placebo and NAC: 51.2%) (39).

3 Need for miRNA-based therapy

The idea of improving pCR rates, simplifying the de-escalation of adjuvant therapy post pCR, and minimising treatment-related toxicities for patients receiving these neoadjuvant medicines are the

main directions for translational research efforts in the future (40). Therefore, numerous clinical trials have focused on practices that improve pCR rates (40). To further improve the pCR, the idea of manipulating treatment with miRNA-based therapies may be helpful in boosting pCR rates to NAC in breast cancer is now popular, and the same has been discussed in depth in this review.

4 Chemoresistance in breast cancer

Various molecular aspects are known to be involved in inducing chemoresistance in cancer cells (Figure 1). Some of them have also been summarized below:

- Resistant genes:

4.1 Twist

Twist is a key player in the invasion and metastasis of tumors because it regulates the epithelial-mesenchymal transition (EMT) (41). It has been reported that NF-κB up-regulation of twist-1 is a factor in the chemoresistance (42). Through the downregulation of estrogen receptor alpha (ERα) activity, twist overexpression can also contribute to hormone resistance in breast tumors (43).

4.2 Multidrug resistance gene

MDR1 has a significant impact on breast cancer's chemoresistance. P-glyocoprotein (P-gp), glutathione S-transferase (GST-π), and P53 are only a few examples of MDR1-encoded proteins that are involved in the chemoresistance cascade (44). In fact, Chen et al., 2022 suggested the synergistic effect of 7-*O*-geranylquercetin and miR-451 on undoing MDR-1 and P-gp-mediated chemoresistance in breast cancer MCF-7/ADR (Adriamycin) cells (45).

- Efflux proteins: Another mechanism of resistance to chemotherapy is mediated by ATP-dependent efflux pumps, which decrease the intracellular concentration of drugs. By using the energy from ATP hydrolysis, or the MDR phenomenon, the ATP-dependent efflux transporters in cancer cells can actively transport a range of substrates outside the cell membrane (46). MDR-associated proteins, such as P-gp, multidrug resistance-associated protein (MRP), ABCC subfamily, and breast cancer resistance protein (BCRP) are examples of ATP-binding cassette (ABC) transporters (47). Downregulation of ABCC4 with miR-124-3p overexpression significantly enhanced the ADR sensitivity in MCF7/ADR cells (48), highlighting the importance of miRNA-based targeting of resistant proteins for improved treatment of breast tumors that are resistant to certain drugs.
- *Signaling pathways:* Resistance to endocrine therapy for breast cancers can be brought on by cell surface receptors like epidermal growth factor receptor (EGFR), human epidermal growth factor receptor-2 (HER-2), and insulin-like growth factor 1 receptor (IGF-1R), and their downstream signaling pathways like PI3K/AKT/mTOR, RAS/MAPK/ERK, and upstream signaling pathways (49). Also, tamoxifen resistance has been linked to EGFR, HER-2/nue, PI3K, and other growth factor signaling pathways (50). Additionally, one of the gefitinib resistance mechanisms in breast cancer may involve EGFR nuclear translocation (51).
- *Response to DNA damage:* Many chemotherapeutic medications work to treat cancer by causing DNA damage (52). Single and double-strand breaks, intra- and inter-strand DNA crosslinks, methylated and oxidized bases, mismatched and protein-DNA adducts are several types of DNA damage. Cancer stem cells (CSCs), in particular, stimulate DNA damage repair (DDR) pathways to counteract DNA damage, explaining why chemotherapy that damages DNA might cause drug resistance (53). The following DDR pathways are found in breast cancer cells: homologous recombination (HR) (54) and non-homologous end joining (NHEJ) (55), involved in the elimination of double-strand breaks;

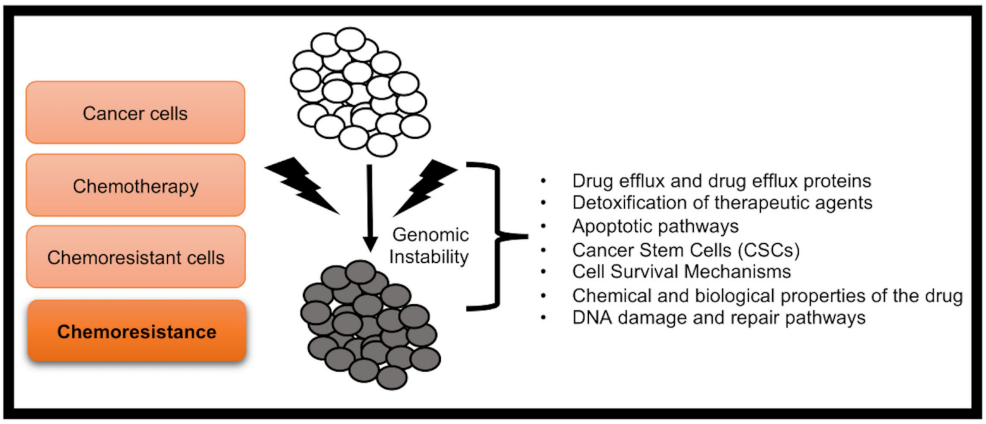

FIGURE 1
The major chemoresistance mechanisms of cancer cells.

mismatch repair (MMR), in charge of removing incorrect bases (56); nucleotide excision repair (NER) (57) and base excision repair (BER) (58), involved in the repair of single-strand breaks. In addition, these pathways contain a variety of components that are involved in the repair procedure, including the DNA repair genes - Excision Repair Cross-Complementation group (ERCC1/2/5) (59, 60), the BRCA1/2 (61), the Meiotic Recombination 11 (MRE11) and RAD50/51 (60, 62), and others. Understanding DNA repair mechanisms can aid in reversing breast cancer resistance to therapy.

- *Cancer Stem Cells (CSCs):* Chemoresistance in breast cancer is significantly influenced by cancer stem cells (63). CSCs overexpress several ABC transporters, such as ABCB5, ABCC1, ABCG2, and P-gp. Additionally, CSCs can cause drug resistance through increased anti-apoptotic levels and DNA repair activity (64). Another significant factor contributing to CSCs' drug resistance is Aldehyde dehydrogenase 1 (ALDH1) upregulation (65). Drug resistance of CSCs may also be influenced by signal transduction pathways such as Notch, Hedgehog, and Wnt/-catenin which are involved in the self-renewal and maintenance of stem cells (66). Expression of Let-7, a tumor suppressor miRNA, was shown to be considerably reduced in breast cancer stem cells compared to non-cancer stem cells. However, the upregulation of let-7 microRNA in breast cancer stem cells can encourage CSCs to enter the differentiation phase from the stationary phase, and hence increases the sensitivity of CSCs to the chemotherapeutics (67).
- *Drug detoxification:* Cell detoxification proteins such as ALDH, DNA topoisomerase, protein kinase C, dihydrofolate reductase, glutathione (68) and glutathione S-transferases (GST) are some of the key enzymes that contribute to MDR in cancer cells. These agents have the potential to enhance the transformation and catabolism of anti-neoplastic drugs, shorten the term of effective concentration of chemotherapeutic drugs in tumor cells, decrease drug accumulation in target areas, and ultimately limit drug efficacy (69). For example, GST-π can be employed as a separate index to direct a clinical treatment against BC as its expression in breast cancer patients was associated with the histological grade, the number of lymphatic metastases, and the age of the patients (70).

5 MicroRNAs

MicroRNAs are a class of small noncoding RNAs (ncRNAs), which function in post-transcriptional regulation of gene expression and are powerful regulators of various cellular activities and have been linked to many diseases (20). RNA polymerase II (Pol II), which produces the main transcripts, participates in several stages of microRNA synthesis (pri-miRNA). The pri-miRNA are split up into precursor miRNAs (pre-miRNAs) by the RNase III Drosha (71). The pre-miRNAs are subsequently moved from the nucleus into the cytoplasm by Exportin-5 (Exp5), where they are further split by Dicer into a mature single-stranded miRNA. The miRNA is induced to either degrade or suppress the translation of mRNA targets when the mature miRNA is removed from the pre-miRNA hairpin and attached to the RNA-induced silencing complex (RISC) (72). Figure 2 depicts a pictorial representation of miRNA biogenesis

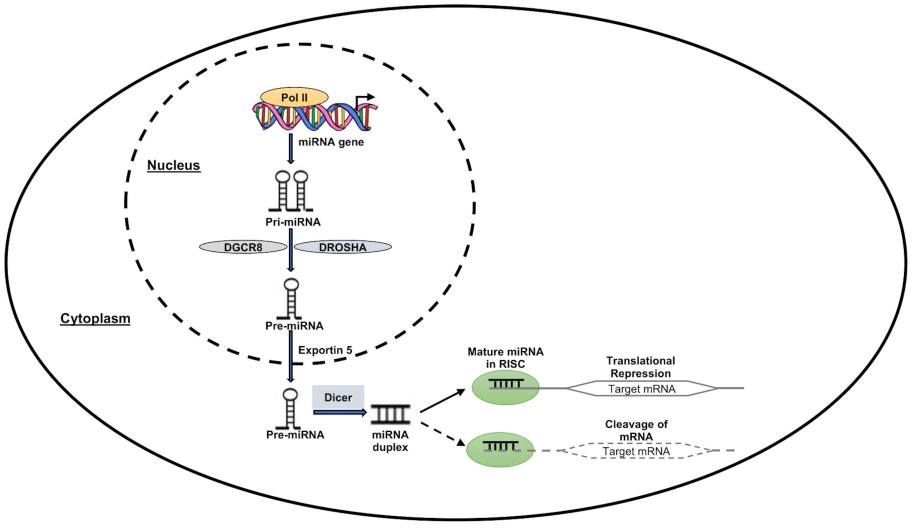

FIGURE 2
MiRNA expression and function. RNA polymerase II enzyme in the nucleus transcribes the miRNA-encoding genes, forming the "Pri-miRNA" hairpin-shaped molecule. DROSHA and DGCR8 molecules work together to transform the "Pri-miRNA" molecule into the "Pre-miRNA" precursor molecule. Pre-miRNA then travels to the nuclear export receptor "Exportin 5" and reaches the cytoplasm. This precursor is cleaved by Dicer complex in the cytoplasm to create a double-stranded molecule called "miRNA duplex." One of these two strands is left active after this process, and it has the ability to suppress or even activate the target downstream genes at the transcriptional or translational level.

and function. Besides miRNAs, other ncRNAs are long-chain non-coding RNAs (LncRNAs), piRNAs, and circle RNAs (circRNAs), which make up just 1% of the whole genome's RNA (73).

The molecular revolution enables us to design strategies to maximize patient outcomes, reduce toxicity, and control disease with less strenuous and more focused therapies. The development of chemotherapeutic response biomarkers is necessary in the future to speed up the removal of tumors and reduce the need for extended and excessive treatments. The utility of detecting miRNA expression (both in tumors and in the blood) is now being discussed in the scientific community. Doing so may help doctors prescribe medicines that are suitably targeted, address early relapse, or even enable miRNA-directed therapies. In general, miRNAs can be either tumor suppressors (tumor suppressor miRNA) or oncomirs, and they can affect the development of cancers in either way. Numerous miRNAs, along with their downstream targets, have been shown to be differentially expressed in breast cancer patients when compared to healthy controls (either circulating or in tumors) (Table 1).

6 miRNAs in BC subtyping

The three main subtypes of breast cancer that exist are (1) Positive ER and PR (2); HER-2 positive; and (3) (ER, PR, and HER-2 negative) Triple negative. However, this subtyping is expanded to a more precise one using the microarray approach for identifying miRNA profiles, including (1):Luminal A (ER-positive with low grade) (2); Luminal B (ER-positive with high grade) (3); HER-2 positive (4); Basal-like (Almost equal to triple-negative condition).

There are several miRNAs that are used for the breast cancer subgrouping as shown in Table 2 (87). Currently, it is possible to use miRNA profiling for the subgrouping of breast tumors. This capability can therefore aid in the selection of cancer patients who will get adjuvant therapy. In addition, miRNA profiling can be successful in identifying new therapeutic targets by revealing the genetic underpinnings of distinct subgroups of breast cancer.

7 Role of miRNA in BC drug resistance

It is well known that miRNAs can regulate drug resistance to traditional chemotherapeutic medicines, endocrine hormone treatments, and radiotherapies in cancer cells (90–93). It has been shown that miRNA expression can influence a breast cancer patient's ability to respond to or reject systemic treatment as shown in Table 3. The miRNAs along with other ncRNAs significantly reverse the BC cell drug resistance by suppressing signaling pathways such as Wnt/β-catenin, Hippo, AKT, TGF-β, or mTOR signaling pathways. A summary of molecules which can participate in target diversity in miRNA interactions leading to drug resistance using different chemotherapeutic drugs is mentioned in Table 3. According to various reports, there are scientific explanations and processes for chemotherapeutic resistance, including altered drug-target interactions, lower active drug doses, and increased tumor tissue survival (143). Numerous miRNA expression profiles have been linked to the prediction of

TABLE 1 miRNA targets and signaling pathways in Breast cancer.

miRNAs	Targets	Functional pathways	References
Tumor suppressor miRNAs			
miR-206	ESR1	ER signaling	(74)
miR-17-5p	AlB1,CCND1,E2F1	Proliferation	(75)
miR-125a,b	HER2,HER3	Anchorage-dependent growth	(76, 77)
miR-200c	BMl1,ZEB1,ZEB2	TGF-beta signaling	(78)
let-7	H-RAS, HMGA2, LIN28, PEBP1	Proliferation, differentiation	(79)
miR-34a	CCND1, CDK6, E2F3, MYC	DNA damage, proliferation	(80)
miR-31	FZD3, ITGA5, M-RIP, MMP16, RDX, RHOA	Metastasis	(81)
miR-335	SOX4, PTPRN2, MERTK, TNC	Metastasis	(82)
miR-27b	CYP1B1	Modulation of the response of tumor to anti-cancer drugs	(83)
Oncogenic miRNAs			
miR-21	BCL2, TPM1, PDCD4, PTEN, MASPIN	Apoptosis	(84)
miR-155	RHOA	TGF-beta signaling	(85)
miR-10b	HOXD10	Metastasis	(86)
miR-373/520c	CD44	Metastasis	(87)
miR-27a	Zinc finger ZBTB10, Myt-1	Cell cycle progression G2-M checkpoint regulation	(88)
miR221/222	p27/Kip1	Tamoxifen resistance	(89)

TABLE 2 MiRNAs used in breast cancer subtyping.

Breast cancer subtypes	miRNA changes
Luminal A	Overexpression of miR-126, miR-136, miR-100, miR-99a, miR-145, miR-10a, miR-199a/b, miR-130a, miR-30a-3p, miR-30a-5p, miR-224, miR-214, let-7a/b/c/f, miR-342
Luminal B	Overexpression of miR-106a/b, miR-93, miR-25, miR-10a, miR-30a-3p, miR-30a-5p, miR-224, let-7b/c/f, miR-342c
HER-2 positive	Overexpression of miR-150, miR-142-3p, miR-142-5p, miR-148a, miR-106b, miR-93, miR-155, miR-25, miR-187
TNBC	Downregulation of miR-139-5p, -10b-5p and -486-5p and up-regulation of miR-455-3p, miR-107, miR-146b-5p, miR-324-5p and miR-20a-5p

TABLE 3 ncRNAs related to drug resistance in Breast cancer.

ncRNA	Drugs	Function	Targets/mechanisms	References
miR-200b/c	Tamoxifen	Sensitivity	Activation of vimentin/ZEB/EMT	(94)
miR-186-3p	Tamoxifen	Resistance	Activation of EREG/EGFR	(95)
miR-221/222	Tamoxifen	Resistance	Inhibition of p27Kip1	(89)
miR-449a	Tamoxifen	Sensitivity	Inhibition of ADAM22	(96)
miR-451a	Tamoxifen	Sensitivity	Inhibition of MIF	(97)
lncRNA-ADAMTS9-AS2	Tamoxifen	Sensitivity	Inhibition of PTEN	(98)
lncRNA-ROR	Tamoxifen	Resistance	Inhibition of EMT	(99)
circRNA-0025202	Tamoxifen	Sensitivity	Inhibition of FOXA3a	(100)
miR-200c	Doxorubicin	Sensitivity	Inhibition P-gp	(101)
miR-34a	Adriamycin	Sensitivity	Inhibition Notch1	(102)
miR-302a/b/c/d	Adriamycin	Sensitivity	Activation P-gp MAPK/ERK	(103)
miR-148/152	Adriamycin	Resistance	Inhibition SPIN1	(103)
miR-124-3p	Adriamycin	Sensitivity	Inhibition ABCC4	(48)
miR-298	Adriamycin	Resistance	Inhibition P-gp	(104)
miR-29a	Adriamycin	Resistance	Inhibition PTEN/AKT/GSK3β	(105)
miR-130b	Adriamycin	Resistance	Inhibition PI3K/AKT	(106)
miR-222	Adriamycin	Resistance	Inhibition PTEN/AKT/p27 KIP1	(107)
miR-145	Doxorubicin	Sensitivity	Inhibition MRP1	(108)
miR-489	Adriamycin	Sensitivity	Inhibition EMT/Smad3	(109)
miR-760	Doxorubicin	Resistance	Inhibition EMT/Nanog	(110)
miR-192-5p	Doxorubicin	Sensitivity	Activation JNK/Bad/Caspase9, inhibition Bcl-2/PPIA	(111)
miR-221	Adriamycin	Sensitivity	Inhibition hormone receptor(HR)	(112)
LncRNA-00518	Adriamycin	Resistance	Inhibition miR-199a/MRP1 axis	(113)
Lin28	Paclitaxel	Resistance	Activation of p21 and Rb; inhibition of Let-7	(114)
Let-7a	Paclitaxel	Resistance	Inhibition of caspase-3	(115)
miR-125b	Paclitaxel	Resistance	Inhibition of BAK1	(76)
miR-520h	Paclitaxel	Resistance	Inhibition of DAPK2	(116)
miR-451	Paclitaxel	Resistance	Inhibition of Bcl-2	(117)
miR-100	Paclitaxel	Sensitivity	Inhibition of the Mtor signaling pathway	(118)

(Continued)

TABLE 3 Continued

ncRNA	Drugs	Function	Targets/mechanisms	References
miR-18a	Paclitaxel	Resistance	Inhibition of the mTOR signaling pathway	(119)
miR-101	Paclitaxel	Sensitivity	Inhibition of MCL-1	(120)
LncRNA-CASC2	Paclitaxel	Resistance	Inhibition miR-18a-5p/CDK19	(121)
miR-141	Docetaxel	Sensitivity	Activation of EIF4E/CP110	(122)
miR-129-3p	Docetaxel	Resistance	Inhibition of CP110	(123)
miR-3646	Docetaxel	Resistance	Activation of the GSK-3β/β-catenin signaling pathway	(124)
miR-452	Docetaxel	Resistance	Inhibition of APC4	(125)
miR-663	Docetaxel	Resistance	Inhibition of HSPG2	(126)
miR-139-5p	Docetaxel	Resistance	Inhibition of Notch1	(127)
miR-125a-3p	Docetaxel	Sensitivity	Inhibition of BRCA1	(77)
miR-222/29a	Docetaxel	Resistance	Activation of Akt/mTOR	(128)
LncRNA-EPB41L4A-AS2	Docetaxel	Sensitivity	Activation of ABCB1	(129)
miR-125a	Fluorouracil	Resistance	Inhibition LIF/Hippo signaling pathway	(130)
miR-508-5p	Fluorouracil	Resistance	Inhibition P-gp or ZNRD1	(131)
miR-200/203	Fluorouracil	Sensitivity	Inhibition P53/Bmi1	(132)
miR-448	Fluorouracil	Resistance	Inhibition EMT/NFkB	(133)
LncRNA-NEAT1	Fluorouracil	Resistance	Inhibition miR-211/HMGA2	(134)
Circ-CDR1as	Fluorouracil	Resistance	Inhibition miR-7/CCNE1	(135)
miR-21	Trastuzumab	Resistance	Inhibition of AKT and NF-κB	(84)
miR-221	Trastuzumab	Resistance	Inhibition of PTEN	(136)
miR-200c	Trastuzumab	Resistance	Inhibition of ZNF217/ZEB1/TGF-β signaling pathway	(137)
miR-375	Trastuzumab	Sensitivity	Inhibition of IGF1R	(138)
miR-542-3p	Trastuzumab	Sensitivity	Activation of PI3K/AKT	(139)
miR-630	Trastuzumab	Sensitivity	Inhibition of IGF1R	(140)
miR-16	Trastuzumab	Sensitivity	Inhibition of CCNJ and FUBP1	(141)
miR-7	Trastuzumab	Resistance	Inhibition of EGFR	(142)

chemoresistance and their regulatory role in influencing chemoresistance to chemotherapeutics. For example, reduced expression of miR-18a, miR-1207-5p, and miR-5195-3p in TNBC has recently been linked to translational research studies that predict resistance to paclitaxel or docetaxel in TNBC (144, 145). Similarly, Wu et al., 2019 discovered that by downregulating the expression of dCMP deaminase (DCTD) in TNBC, upregulation of miR-620 improves tumor resistance to gemcitabine-based chemotherapies (146). Further, finding higher levels of circulating miR-125b in 56 patients with invasive ductal carcinoma receiving curative treatment was associated with chemoresistance ($p = 0.008$) (147). Hypoxia-inducible factor-1 (HIF-1) pathway-dependent upregulation of cell resilience to hypoxia and inhibition of chemotherapy-induced apoptosis are two mechanisms through which miR-24 has been demonstrated to promote chemoresistance in early breast cancer (148). miR-155 has shown to be linked to drug resistance and cancer development (149) via modulation of FOXO3a signaling, the interruption of TGF-beta, and the induction of drug resistance through RhoA signaling. Likewise, in 25 breast cancer samples, miR-221 has been shown to alter the PTEN/Akt/mTOR signaling pathway, which promotes breast cancer resistance to Adriamycin (150).

The role of miRNAs in BC chemoresistance has been attributed to some of the following molecular mechanisms (Figure 3):

- *miRNAs and cell cycle:* Cell cycle deregulation is an established hallmark of cancer, and it has been linked to both drug resistance and poor prognosis when it is aberrantly activated. Various miRNAs have been reported to target genes linked to cell cycle regulation, resulting in either drug sensitivity or resistance such as miR-93, involved in G1/S phase arrest, was reported to be downregulated in paclitaxel-resistant BC samples compared to responder patients (Figure 3A) (151). Direct

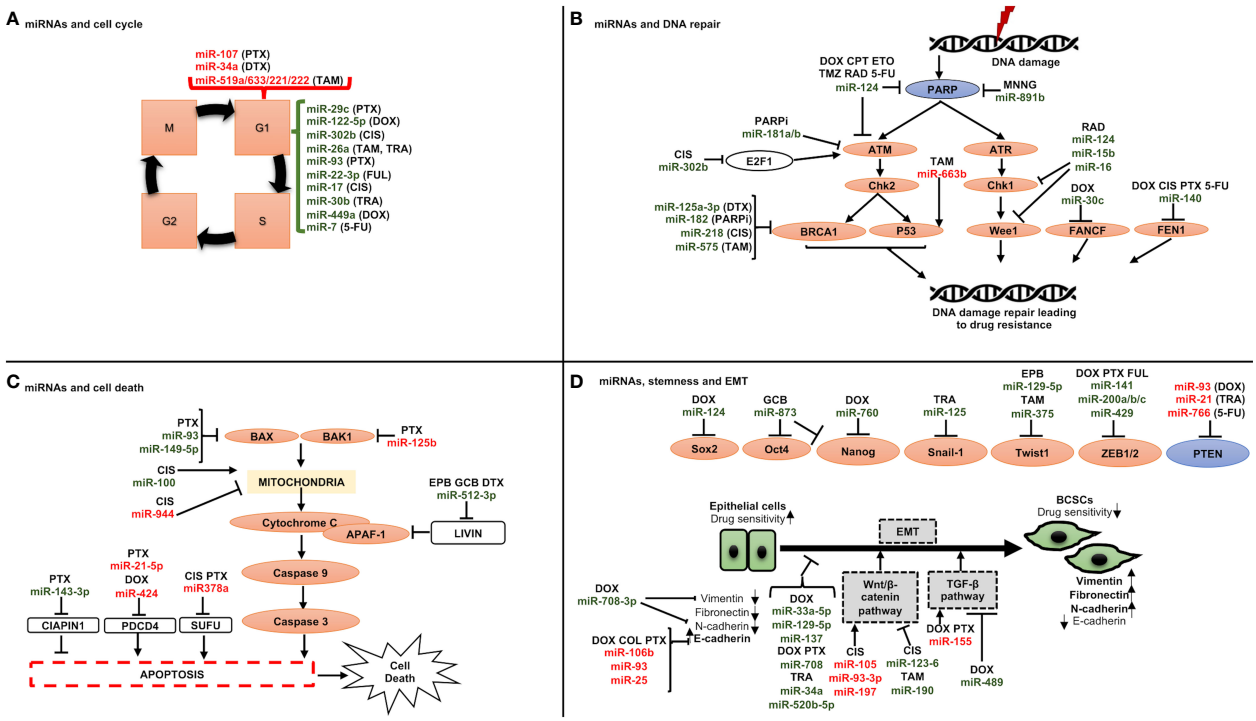

FIGURE 3
Schematic representation of miRNAs involved in drug resistance through regulating **(A)** cell cycle, **(B)** DNA repair checkpoints, **(C)** cell death, and **(D)** stemness and epithelial to mesenchymal transition. A line with a perpendicular line at the end designates inhibition and arrows designate activation. miRNAs increasing drug resistance are shown in red, and miRNAs increasing drug sensitivity are shown in green. CIS, cisplatin; DOX, doxorubicin; DTX, docetaxel; FUL, fulvestrant; PTX, paclitaxel; TAM, tamoxifen; TRA, trastuzumab; 5-FU, 5-fuorouracil; CPT, camptothecin; ETO, etoposide; MNNG, N-methylN′-nitro-N-nitrosoguanidine; PARPi, PARP inhibitors; RAD, radiation; TMZ, temozolomide; EPB, epirubicin; GCB, gemcitabine.

targets of this miRNA were discovered to include CCND1 and the E2F transcription factor 1 (E2F1), which upon downregulation resulted in cell cycle arrest in G1 phase and increased apoptosis *via* inhibiting AKT phosphorylation (p-AKT), and BCL-2 expression, and increasing the expression levels of BCL-2-associated X, apoptosis regulator (BAX), which could increase the paclitaxel sensitivity.

- *miRNAs and DNA repair machinery*: As mentioned above, most chemotherapy drugs used today to treat breast cancer cause either direct or indirect DNA damage. To counteract DNA damage, however, CSCs activate DDR pathways, explaining why chemotherapy that destroys DNA could result in drug resistance (Figure 3B). One such DDR pathway involves BRCA1 which is engaged in different cellular processes that maintain genomic stability like DNA damage repair, DNA damage-induced cell cycle checkpoint activation, chromatin remodelling, protein ubiquitination, transcriptional control, and cell death [43]. Drug sensitivity is thus impacted by its miRNA influenced control, for instance miR-182 inhibits BRCA1 expression to induce drug sensitization. Furthermore, it has been shown that overexpressing miR-182 makes BC cells more susceptible to PARPi (PADP-ribose polymerase 1 inhibitor). In contrast, miR-182 suppression raises BRCA1 levels and results in PARPi resistance (152).
- *miRNAs and cell death:* The interests of investigators are growing in drug-miRNA combination anticancer therapy since miRNAs can influence cell death (Figure 3C). Examples include miR-125b, which confers paclitaxel resistance by inhibiting the expression of BAK1 (BAX and/or BCL-2 Antagonist/Killer 1), which causes the release of cytochrome C from mitochondria to the cytoplasm, where it binds Apoptotic peptidase Activating Factor 1 (APAF-1) and triggers caspase activation (76). Similar findings were also made from miR-149-5p, whose overexpression was shown to boost BAX expression (153), and from miR-663b, which imparts tamoxifen resistance by indirectly upregulating BAX (154).
- *miRNAs, CSCs and epithelial to mesenchymal transition (EMT):* Breast cancer stem cells (BCSCs) are a small population of cells with a high ability for tumorigenesis and are involved in therapy resistance (155). The modulation of BCSCs' phenotype is mediated by several molecular mechanisms, the most significant of which is EMT. This process takes place as cancer develops, and it involves a decrease in the expression of molecules associated with epithelial growth, such as E-cadherin, and a rise in molecules associated with mesenchymal development, such as N-cadherin, vimentin (VIM), and fibronectin (FN1) (156). Thus, the cells become more capable of invasion and migration (155) and can nest in

various tissues where they can multiply and create new tumors through a process called metastasis (155). In this context, miRNAs play a significant role in controlling stemness and EMT by targeting a few genes implicated in these two pathways (Figure 3D). Among those engaged in the control of EMT, the miR-200 family has received the greatest research attention. Five different miRNAs make up this family: miR-141, miR200a, miR200b, miR200c, and miR-429 (157), which can inhibit the expression of ZEB1 and ZEB2 (Zinc finger E-Box-binding homeobox genes) (157). As a result, it has been demonstrated that overexpressing miR-200 in many cancer cell lines can reverse EMT (158). Another factor contributing to stemness in BC is the Wnt/-catenin signaling pathway. It has been shown that several miRNAs, including miR-105 and miR-93-3p, regulate this pathway. The Wnt/-catenin signaling pathway suppressor Secreted Frizzled Related Protein 1 (SPFR1) is the target of those miRNAs. This led Li et al. to show that those miRNAs encourage cisplatin resistance (159).

Four circulating miRNA patterns linked to pCR were recently identified using profiling of circulating miRNA (ct miRNA detected in plasma) to categorize NAC responders (from non-responders) in Her2+ patients (160). These results demonstrate the potential of miRNA signatures as prognostic and predictive biomarkers that could individualize breast cancer treatments and enhance patient sampling techniques for current therapies, including traditional cytotoxic chemotherapies. The following is a discussion of a few of them:

- *miR-638* – miR-638 was shown to be downregulated in cases with BC chemoresistance in a microarray analysis (161). A minimal patient-derived xenograft (MiniPDXTM) was also developed by the researchers to assess the chemosensitivity of various drugs. The results of this study demonstrated that in patients, who received 5-FU, miR-638 levels were relatively low in the 5-FU-resistant group compared to the 5-FU-sensitive group. So, according to the MiniPDX™ model, MDA-MB-231 BC cells overexpressing miR-638 were more susceptible to 5-FU treatment *in vivo*.
- *miR-17/20* – The serine-threonine kinase Akt1 has been linked to the regulation of cellular homeostasis, proliferation, and growth as well as hyperactivation in human malignancies (162). It is known that the miR-17/20 cluster blocks the proliferation of breast cancer cells by causing the G1/S cell cycle arrest by anchoring to the 3'UTR of cyclin D1 (163). Yu et al., 2014 demonstrated a unique mechanism by which miR17/20 controls p53 and Akt, which further control breast cancer cell apoptosis (163). Additionally, they have demonstrated that miR-17/20 overexpression, *via* Akt1, makes MCF-7 cells more susceptible to apoptosis brought on by either doxorubicin or UV irradiation. In brief, the apoptosis-inducing miR-17/20 increases Akt breakdown by upregulating p53 expression.
- *miR-342* – The mesenchymal stem cell-derived exosome (MSCs-Exo) carrying microRNAs has been proven to regulate tumor biological activities (164, 165). Yu et al., 2022 demonstrated the regulatory function of miR-342-3p in MSCs-Exo on the BC (166). They revealed considerably decreased levels of miR-342-3p in patients with metastatic illnesses (166). Additionally, miR-342-3p was found to target the Inhibitor of Differentiation 4 (ID4) and operate as a possible tumor suppressor by preventing the metastasis and chemoresistance of breast cancer cells (166).
- *miR-484* –By controlling cyclin E-CDK2 signaling, cytosine deaminase (CDA), a crucial chemoresistance axis, inhibits the advancement of the cell cycle (167). In a breast cancer model that is resistant to gemcitabine, miR-484 controls the CDA (167). CDA expression was found to be downregulated and inversely linked with miR-484 expression in clinical samples of BC (167). Additionally, in the same cohort, greater expression of CDA was linked to extended disease-free survival. Collectively, the findings of Ye et al., 2015 established that miR-484-modulated CDA promotes chemoresistance while inhibiting cell proliferation in breast cancer, highlighting the pathophysiological exchange that arises because of chemoresistance in this cancerous condition (167).
- *miR-451* – Gu et al. (2016) looked at the possible use of miR-451, which is prevalent in the serum of BC patients, to forecast NAC resistance (168). Here, qRT-PCR was used to determine the expression levels of miR-451 in the MCF-7 BC cell line, the docetaxel-resistant MCF-7 BC cell line (MCF-7/DTX), the epirubicin-resistant MCF-7 BC cell line (MCF-7/EPB), normal controls, NAC-sensitive group, and NAC-resistant group. The findings of this investigation confirmed the hypothesis that miR-451 expression was differentially expressed between NAC-sensitive and -resistant BC patients. Additionally, the research team noticed that miR-451 expression was much lower in the MCF-7/EPB and MCF-7/DTX cell lines than it was in the MCF-7 cell lines, indicating that miR-451 may be functionally crucial in predicting NAC resistance in breast cancer patients.
- *miR-222 and miR-29a* – In a 2013 study by Zhong et al., it was discovered that the changed expression pattern of miR-222 and miR-29a contributed to the development of DTX and adriamycin (ADR) resistance in breast cancer MCF-7 cells (128). The research team found that targeting Phosphatase and TENsin homolog (PTEN) with miR-222 and miR-29a mimics and inhibitors partially altered the treatment resistance of breast cancer cells.
- *miR-141* – About 50% of patients develop resistance to the chemotherapeutic medication docetaxel used to treat BC. The role of miR-141 expression in BC cells with acquired docetaxel resistance was studied by Yao et al., 2015 (122). Docetaxel-resistant cells (MCF-7/DTX and MDA-MB-231/

DTX, respectively) were more responsive to the drug when miR-141 was inhibited, but docetaxel-sensitive cells were more resistant when miR-141 was overexpressed (MCF-7 and MDA-MB-231, respectively). This research team showed that miR-141 operates on genes required for drug-induced apoptosis, leaving the cells drug resistant, through direct interaction with eukaryotic translation initiation factor 4E (EIF4E).

- *miR-140-5p* – In a training set, conducted by Di et al., 2019, starting from 51 circulating (ct)-miRNAs linked with pCR, four signatures were validated in the testing set: lapatinib at T0 and T1 [AUC 0.86; 95% confidence interval (CI), 0.73–0.98 and 0.71 (0.55–0.86)], respectively; trastuzumab at T1 (0.81; 0.70–0.92); lapatinib + trastuzumab at T1 (0.67; 0.51–0.83) (160). Although the levels of ct-miR-140-5p, which is a component of the trastuzumab signature, were linked to EFS (HR 0.43; 95% CI, 0.22-0.84), ct-miRNA signatures could not predict event-free survival (EFS). Patients with and without pCR after neoadjuvant lapatinib- and/or trastuzumab-based therapy can be distinguished by ct-miRNAs. To help to de-escalate treatment plans, ct-miRNAs at week two may be useful in identifying individuals who respond to trastuzumab and preventing needless combinations with other anti-HER2 medications.
- *miR-34a* – A link between enhanced miR-34a expression and docetaxel resistance has also been established (80). Kastl et al., 2012 confirmed that B-cell leukemia/lymphoma 2 protein (BCL-2) and cyclin D1 protein (CCND1), both of which are targeted by miR-34a, were shown to be expressed at lower levels in docetaxel-resistant cells (80). It was found that overexpressing miR-34a resulted in resistance in MCF-7 docetaxel-sensitive cells, but miR-34a inhibition improved responsiveness to docetaxel in MCF-7 docetaxel-resistant cells. To propose a prospective therapeutic target for the treatment of docetaxel-resistant breast cancer, this work described a pathway of acquired docetaxel resistance in these cells, presumably involving direct interactions with BCL-2 and CCND1.
- *miR-23, 24 and 27* – Recent research has shown that the extracted exosomes (D/exo) from the docetaxel-resistant breast cancer cells MCF-7 (MCF-7/Doc) were linked to the genetic cargo's contribution to resistance transmission (169, 170). The significance of D/exo during exposure to DRβ-H (d Rhamnose -hederin), an active ingredient obtained from the traditional Chinese medicine plant *Clematis ganpiniana*, was discovered by Chen et al., 2018, in MCF-7/DTX cells (171). Herein, the investigators have found that DRβ-H could reduce the expression of a few of the most common miRNAs (*miR-23a, miR-24*, and *miR-27a*) transported by D/exo. Target gene prediction and pathway analysis showed the relevance of these selected miRNAs in pathways related to disease relapse.
- *miR-200* –The miR-200 family of microRNAs have recently been revealed to be dysregulated in a variety of malignancies, and it has been shown that this family of miRNAs is crucial for tumor development, maintenance, tumor metastasis, and chemotherapy tolerance (172). MiR-200s are currently recognized as master EMT regulators, inhibiting cancer invasion and metastasis by focusing on a number of key inducers of the EMT, such as ZEB1, ZEB2, and SLUG (172). By playing critical and pleiotropic roles in malignancies, miR-200s are promising targets for cancer therapy. However, a recent study revealed that miR-200s play a role in breast cancer metastasis promotion, hence cautious evaluation should be done prior to treatment modalities using miR-200s as therapeutic targets (172).

8 miRNAs in neoadjuvant chemotherapies: predicting response

As already said, breast oncology research has advanced recently to realize that treating patients with chemotherapy in the neoadjuvant setting is both rational and beneficial (173, 174). Although conventional clinicopathological traits have been shown to correlate with response to NAC (33), it is still difficult for oncologists to identify patients who are likely to experience such reactions since success rates are frequently unpredictable. The latest research has linked miRNA expression profiles with breast cancer patients' responses to NAC therapy. For example, Xing et al., 2021 found that decreased expression of miR-638 and miR-451a and elevated expression of miR-200c-3p, miR-23a-3p and miR-214-3p correlated to chemoresistance (Miller–Payne grade 1) (175). In their analysis of 114 breast cancer patients participating in the Clinical Trials Ireland All-Ireland Cooperative Oncology Research Group (CTRIAL-IE ICORG) 10/11 prospective, multicenter translational trial, McGuire et al., 2020 emphasize the innate value of miR-21 expression as a factor associated to response to conventional NAC (176). Further, a study conducted by Liu et al., 2019 supported the findings of the CTRIAL-IE ICORG 10/11 trial by showing decreased miR-21 expression levels in responders (*vs* non-responders) following cycle 2 of NAC (177). Di Cosimo et al., 2020 described the clinical utility of venous sampling for miR-140a-5p, miR-148a-3p, and miR-374a-5p, and their predictive value in determining response to subsequent neoadjuvant therapy, with an enhanced combined predictive capability of 54% in determining pCR to trastuzumab in HER2+ illness, compared with 0% in cases of poor expression (178). In their series of 435 patients with either early-stage HER2+ or TNBC illness, Stevic et al. (2018) explained how the overexpression of miR-199a in patient plasma was indicative of pCR to NAC in the GeparSixto study (179). MiR-34a expression levels were shown to accurately distinguish between responders and non-responders in 39 patients receiving treatment for locally advanced breast cancer according to promising findings from Kassem et al., 2019 (area under the curve (AUC): 0.995, sensitivity: 97.4%, specificity: 100%) (180). In patients who successfully achieved a pCR to NAC, Garcia et al., 2019 showed lower miR-145-5p expression levels (AUC: 0.790, p = 0.003) (181). Table 4 shows systematic trials examining the function of miRNAs

TABLE 4 Table illustrating prospective trials evaluating the role of miRNAs in predicting response to neoadjuvant therapies.

Author	Year	Trial Phase	Trial Number/ Link	N	Treatment Arms	Findings	References
Jung	2012	Prospective (II)	N.A.	72	5-FU, EC and trastuzumab	Lower miR-210 expression levels predicted pCR in HER2+ cancers.	(182)
Muller	2014	Prospective phase II Geparquinto Trial	NCT:00567554	127	NAC with trastuzumab or lapatinib	Increased miR-21, miR-210, and miR-373 in patient's serum following treatment with NAC correlated to response to treatment.	(183)
Xue	2016	Prospective phase II clinical trial	N.A.	50	Carboplatin and Paclitaxel	Increased miR-621 expression profiles predicted pCR to NAC	(184)
Al-Khanbashi	2016	Prospective (II)	N.A.	36	DXR, cyclophosphamide and DTX	Serum miR-451 expression levels decreased during NAC in clinical responders.	(185)
Stevic	2018	Prospective phase II clinical trial GeparSixto Trial	NCT:01426880	211	Docetaxel or Paclitaxel +/− Carboplatin	Aberrant miR-199a expression correlates to pCR following neoadjuvant therapies	(179)
Zhu	2018	Prospective phase II clinical trial	NCT:02041338	24	Epirubicin and Docetaxel	After the second cycle of NAC, reduced miR-34a expression was correlated with patients who did not respond to treatment	(186)
Kahraman	2018	Prospective, case–control study (MODE-B study)	N.A.	42	Carboplatin and Paclitaxel	Identification of 74 miRNAs which predicted pCR based on changes in expression profiles pre- and post-NAC.	(187)
Di Cosimo	2019	NeoALLTO Phase III RCT	NCT:00553358	455	Neoadjuvant lapatinib, trastuzumab, or combined lapatinib and trastuzumab	Increased circulating plasma levels of miR-140a-5p, miR-148a-3p and 374a-5p were associated with pCR and miR-140a-5p predicted enhanced EFS	(160)
Lindholm	2019	Randomised, phase II clinical trial	NCT:00773695	132	FEC-T or FEC-P, +/− Bevacizumab	Hierarchical clustering of 627 miRNAs with response at 12 and 25 weeks to neoadjuvant treatment with NAC or NAC combined with Bevacizumab; of these, 217 had differential expression profiles (71 upregulated and 146 downregulated) between responders and non-responders.	(188)
Rodriguez-Martinez	2019	Prospective clinical trial	N.A.	53	AC	Exosomal expression of miR-21 correlated in a stepwise fashion with patients achieving a CR having significantly reduced miR-21 *vs.* patients with PR and SD, respectively	(189)
Di Cosimo	2020	NeoALLTO Phase III RCT	NCT:00553358	455	Neoadjuvant lapatinib, trastuzumab, or combined lapatinib and trastuzumab	After 2 weeks of neoadjuvant treatment, increased expression of miR-15a-5p, miR-140-3p, miR-320a, miR-320b, miR-363-3p, miR-378a-3p, miR-486-5p and miR-660-5p and decreased miR-30d-5p correlated with pCR to lapatinib. At 2 weeks of therapy, increased expression of miR-26a-5p and miR-374b-5p correlated with pCR to trastuzumab. Increased let-7g-5p and miR-191-5p and reduced miR-195-5p correlated with pCR to combined trastuzumab and lapatinib.	(178)
McGuire	2020	Prospective phase II clinical trial [CTRIAL-IE	NCT:00553358	114	Various NAC regimens	Responders had reduced miR-21 and miR-195 *vs.* non-responders in all breast cancer subtypes. MiR-21 independent predicted response (OR 0.538, 95% CI 0.308–0.943). In luminal cancers, reduced expression of miR-145 and miR-21 correlated with response to NAC.	(176)

(Continued)

TABLE 4 Continued

Author	Year	Trial Phase	Trial Number/ Link	N	Treatment Arms	Findings	References
		ICORG] 10/ 11					
Zhang	2020	Prospective phase II trials	SHPD001 NCT:02199418 and SHPH02	65	Paclitaxel, Cisplatin and trastuzumab	Low miR-222-3p expression was predictive of achieving pCR (OR: 0.258, 95% confidence interval: 0.070–0.958, p = 0.043) and favourable DFS and survival	(190)

N.A., Trial number/link not available; N, number; HER2-+ human epidermal growth factor receptor-2 positive NAC, neoadjuvant chemotherapy; pCR, pathological complete response; TNBC, triple-negative breast cancer; EFS, event-free survival; HER2-, human epidermal growth factor receptor-2 negative; FEC-T, 5-fluorouracil; epirubicin; and cyclophosphamide followed by docetaxel; FEC-P, 5-fluorouracil; epirubicin; and cyclophosphamide followed by paclitaxel; AC, doxorubicin and cyclophosphamide; CR, complete response; PR, partial response; SD, stable disease; OR, odds ratio; DFS, disease-free survival; NCT, national clinical trial identifier; TAN, tumor-associated normal; DTX, docetaxel; DXR, doxorubicin.

in determining how patients would respond to neoadjuvant therapy and lists the miRNAs that are important in this setting (160, 176, 178, 179, 183, 184, 186–190). Using miRNA expression profiles to assess response to adjuvant chemotherapy is substantially more difficult. It is quite challenging to measure whether medication improved oncological outcomes for patients who were most likely to succumb to recurrence, estimate the timing of miRNA sampling, and analyze treatment response rates in a crude way. Therefore, it is not surprising that most research evaluates miRNA expression patterns using metrics that indicate response to NAC rather than adjuvant chemotherapy (e.g., RECIST, Miller-Payne grade, Sataloff score, etc.).

9 MicroRNAs for therapeutic use in breast cancer

The use of miRNAs for the development of novel treatment approaches has been made easier by the current molecular technology. These entail the administration of carefully chosen miRNAs into the tumor microenvironment for therapeutic purposes or to improve the efficacy of currently available therapeutic modalities employed in standard clinical practice, such as systemic chemotherapy (143, 191). miRNAs can act as tumor suppressors or oncomirs, so there are two possible methods for using them as therapeutics (1): miRNA replacement therapy, which involves inducing and overexpressing specific miRNA to reduce oncogenesis or increasing sensitivity to systemic treatment, or (2) oncomir inhibition, which involves lowering targeted miRNA expression characteristics (i.e., miRNA silencing) by incorporating inhibitory miRNA to lessen the translation of the target miRNA (Figure 4).

- *miRNA Replacement Therapy* – By inhibiting oncogenes and the genes that regulate cell proliferation and death, tumor suppressor miRNAs can prevent the development of cancer (192). MiRNA replacement treatment includes reintroducing tumor-suppressing miRNA (or mimics) into the tumor microenvironment in order to inhibit tumor growth and restrain the spread of malignancy (193). They might be delivered into the cytoplasm of cancer cells through a variety of transporters, such as chemicals, electroporation, and modelling of the endogenous miRNA (192). Park et al., 2014 discussed the possible significance of overexpression of miR-34a in MCF7 cells in reducing cancer stem cell characteristics and increasing sensitivity to doxorubicin treatment by specifically targeting NOTCH1 (194). In studies involving animals and MDA-MB-231 and MDA-MB-549 chemoresistant breast cancer cell lines, Yu et al., 2007 and 2010 and Cochrane et al., 2009 show the value of gradually introducing and increasing the expression levels of let-7a, miR-30, and miR-200c to minimize oncogenesis and increase therapeutic index (195–197). Additionally, Kalinowski et al. (2014) analyzed how miR-7 replacement therapy can improve the efficacy of the traditional breast cancer chemotherapy currently being used to treat breast cancer (198).
- *Oncomir Inhibition* – Generally, oncomirs are elevated in the cancer (191). Anti-miRNA oligonucleotides, targeted miRNA silencing agents (antagomirs), and locked nucleic acids (LNA) can all be used to limit the action of oncogenic miRNAs (199). In various pre-clinical studies, such inhibitor mechanisms have been shown to increase the sensitivity of breast cancer cells to chemotherapeutic agents: For example, in MCF-7/ADR cell lines, miR-3609 was successfully transfected to increase the tumor cells' susceptibility to adriamycin-based chemotherapy (200). Similarly, Lin et al., 2021 successfully enhanced cell sensitivity to chemotherapy in 65 BC patients by inducing miR-133 into cisplatin-resistant TNBC cells from these patients (201). Li et al., 2021 also successfully overcome paclitaxel resistance in previously resistant breast cancer cells by transfecting miR-155-5p into tumor cells (85). Finally, Mei et al., 2010 report that downregulating miR-21 increased the susceptibility of MCF-7 BC cell lines to docetaxel treatment (202).

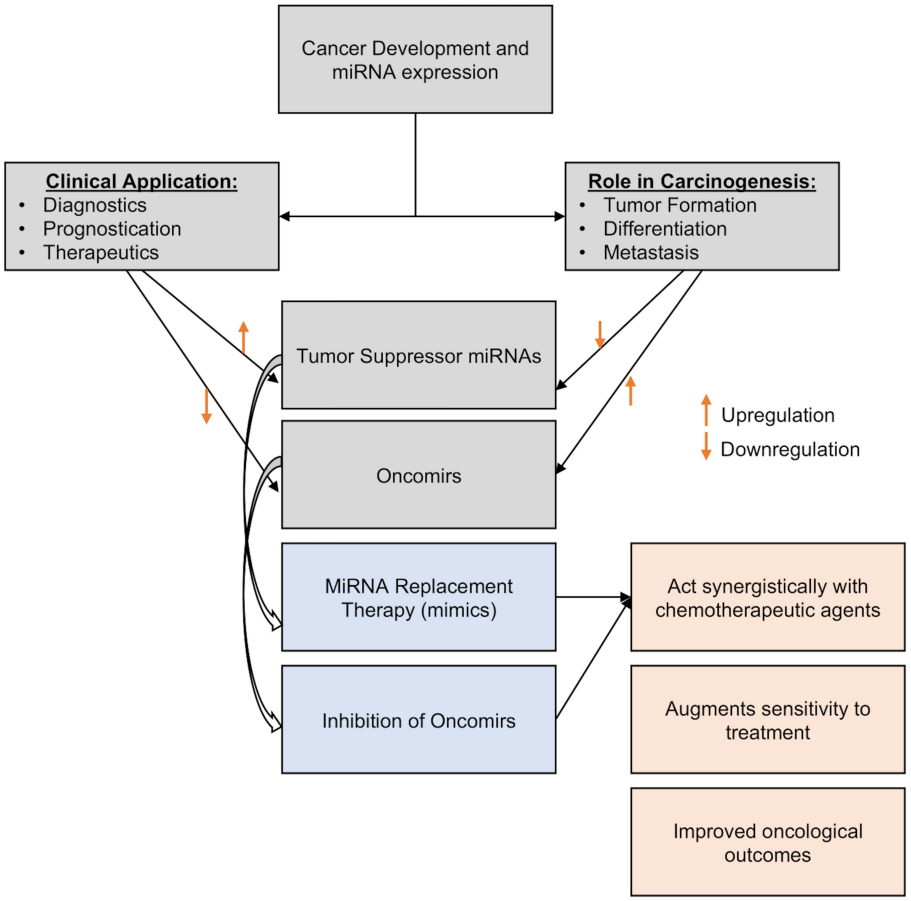

FIGURE 4
Figure showing how miRNA expression profiles can be altered for cancer treatment.

9.1 miRNA delivery strategies used for cancer therapy

miRNAs can be introduced therapeutically into cancer cells through a variety of methods. These approaches are typically divided into two categories of local and systemic delivery, which are thoroughly discussed below and in Figure 5:

Local delivery of miRNAs: Target gene suppression with less toxicity may result from the local delivery of miRNAs as opposed to the systemic delivery of miRNAs. According to Møller et al., 2013, the aforementioned strategy has been examined mainly for primary tumors including melanoma, breast, and cervical cancers (203). Recently, different local delivery techniques, such as the direct injection of miRNA vectors into the tumor site and the nanoparticles (NP) formulation with surface modifications, have been devised. For instance, glioblastoma multiform was treated using the intracranial miRNA delivery approach (203). In a study by Trang et al., 2010, let-7 was introduced into non-small-cell lung cancer using viral vectors, which inhibited the growth of KRAS-dependent tumors (204). The topical distribution approach is an additional technique for treating skin conditions. The target region is more accessible with fewer adverse effects when topical administration is used (205). Moreover, the local delivery system makes the use of modified miRNAs. For instance, astro-cyte elevated gene-1 (AEG-1) was the target of intratumoral miR-375 mimics in cholesterol-conjugated 2′-O-methyl modified form, which significantly suppressed tumor growth in *in-vivo* models of hepatoma xenograft (206).

However, as the local delivery system employs direct injection or local application of miRNAs with or without carriers, it cannot be recommended as a good strategy for treating late-stage metastatic disease. Therefore, developing a systemic delivery strategy is essential to provide efficient miRNA cancer therapy.

Systemic delivery of miRNAs: The systemic miRNA delivery technique represents a significant advancement in the effort to increase the effectiveness of cancer therapy and get over the drawback of miRNA delivery *in vivo*. Different systemic delivery strategies have been devised up until this point. A few of them are covered below:

- *Modification-based delivery* - Systemic distribution of miRNAs into tumor cells was mostly accomplished through chemical alterations (207). The altered oligonucleotides show a stronger propensity for the target molecule. However, there are some restrictions in this regard. For instance, a targeting moiety is necessary for

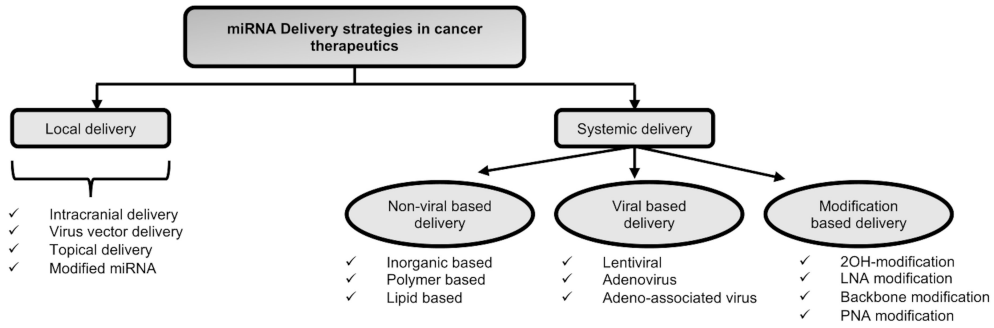

FIGURE 5
Types of microRNA delivery techniques employed in cancer therapy.

the intracellular uptake of modified miRNAs. Additionally, there might be a sign of short half-lives and uneven biodistribution because of quick renal and hepatic clearance. The stability of miRNA modulators and their resistance to nuclease degradation inside the blood circulation may both be improved by increasing the systemic delivery effect with various chemical modifications (208). These changes lessen the off-target effects of miRNAs and aid to overcome immune responses and low miRNA stability (207). The typical chemical modifications are 2′-OH group modification, LNA modifications, passenger strand modifications, Phosphorothioate modification and peptide nucleic acid (PNA) modifications.

- *Viral delivery of miRNAs* – miRNAs can be transmitted by being encoded in several types of vectors, including viral and non-viral vectors. In this regard, viral delivery is an advantageous strategy. One of its benefits include low off-target rate, resulting from given miRNAs being translated by tumor cells. Lentiviruses, adenoviruses, and adenoassociated viruses (AAVs) are among the viruses that have been identified as delivery vectors for miRNAs. As a result, targeting components were added to the viral capsid to strengthen the affinity between viral vectors and cancer-specific receptors, allowing for better transportation into tumors (209). However, due to the immunological reaction they cause and the difficulty of scaling up the production process in comparison to nonviral delivery systems, there are still some significant challenges to overcome. Additionally, the potential for a virus with replication competence may raise the risk of the pathogenic condition. For instance, some retroviruses can cause the start of a CNS illness as a result of their active reproduction (210).
- *Non-viral delivery of miRNAs* – The use of non-viral vectors is a beneficial strategy for miRNA delivery. In this approach, site-specific delivery, system optimization, or polyethylene glycol (PEG) molecule augmentation could be employed to achieve targeted ligands or lengthen circulation times. Additionally, nanocarriers are produced in a secure and straightforward manner, and they are distinguished by their affordability, minimal immunogenicity, and adaptability. Non-viral delivery vectors can be divided into three primary categories: inorganic materials, lipid-based carriers, and polymeric carriers (211, 212).

  However, non-viral-based approaches to miRNA delivery have their own shortcomings such as lower loading efficiency, lack of cargo protection, lower endosomal escape, nonspecific interaction with target cells and nucleic acids, etc (193).

10 Discussion

Considering that drug resistance continues to be a major obstacle in the clinical context, causing relapse and metastatic spread in many cancer types, novel treatment approaches are of the utmost importance. The discovery of miRNAs has provided a novel perspective on the molecular processes behind cancer, increasing the possibility of creating novel and more potent therapeutic approaches. This review is centered on new findings pertaining to the significance of miRNAs in breast cancer chemoresistance. miRNAs regulate numerous signaling pathways and regulatory networks, therefore even little changes in miRNA expression can have a big impact on the development and the progression of the disease. Targeting miRNAs—either reducing or enhancing their expression—seems promising to develop novel, more effective, and customized treatments, boost therapeutic efficacy, and predict patient response to various treatments. However, to fully explain all the miRNAs that are altered in tumors based on profiling data would be beyond the scope of this review. Numerous organizations are exploring the use of microRNAs as potential therapeutics. *In vivo* and translational investigations are currently the focus of increased research. Evidence exists that points to miRNAs as possible therapeutic agents, particularly when used in conjunction with anti-cancer chemotherapeutics. This could take the form of mimics that support miRNA function and expression or antagonists that block miRNA expression. By affecting the expression of endogenous microRNAs in cancer cells, miRNA mimics or anti-miRNAs can potentially change chemotherapy's efficacy. Two

clinical investigations have shown the potential therapeutic impact of miRNAs in the future. Among these is a phase 2a clinical trial with Miravirsen in 26 patients who had chronic hepatitis C virus (HCV) genotype 1 infection. Miravirsen is a nucleic acid–modified DNA phosphorothioate antisense oligonucleotide that encases mature miR-122 in a heteroduplex and inhibits its function. No side effects related to the experiment have been reported yet (213). Another phase 1 clinical trial including individuals with liver cancer or metastatic cancer with liver problems is MRX34 (a mimic of the tumor suppressor miR-34). Healthy volunteers and patients with advanced or metastatic liver cancer (hepatocellular carcinoma) are being tested for the safety and effectiveness of MRX34 in this study (214). Future possibilities for these novel medicines are encouraging given the encouraging preliminary findings from both trials.

Challenges in the field of miRNA therapy-As mentioned above, the miRNAs can be delivered by either local or systemic approaches. It might not be a suitable strategy, for advanced cancer. However, miRNA cancer therapy works well with systemic delivery. Figure 6 summarizes the various constraints to miRNA delivery. For instance, poor miRNA penetration is caused by the leaky nature of aberrant tumor vasculature (215). The rapid cleavage of naked miRNAs by serum nucleases of the RNase A type poses another challenge (216). Additionally, there is a rapid renal clearance, notably for naked miRNA (217). When utilizing big NPs (>100 nm), reticuloendothelial system (RES) clearance would rise in the liver, spleen, lung, and bone marrow, leading to nonspecific absorption by innate immune cells such monocytes and macrophages (218).

Additionally, the systemic miRNA distribution triggered the innate immune system, as with other nucleic acid types, which resulted in undesired toxicities. Immune system activation includes the release of inflammatory cytokines and Type I IFNs *via* Toll-like receptors (TLRs) (219). Anti-inflammatory miRNA treatment, however, may prevent the activation of inflammatory pathways (220). On the other hand, some miRNAs work through TLRs to trigger neurodegeneration. For instance, Lehmann et al. (2012) demonstrated that miRNA let7b can cause neurotoxicity by activating TLR7 signaling in neurons (221). Therefore, a significant issue for miRNA systemic cancer therapy is the incidence of miRNA-related neurotoxicity. Additionally, increased miRNA uptake in cancer cells is a problem, and methods to address this issue include increasing endosomal escape and releasing miRNA payloads into the cytoplasm.

Off-target effects brought on by the miRNA mode of action are yet another challenge for miRNA delivery systems. These compounds may have undesirable side effects since they may bind to the 3′-UTR of a number of genes and decrease their expression (222). A developed method to lessen these adverse effects is the use of multifunctional co-delivering systems (223). Furthermore, it was demonstrated that under specific circumstances, such as hypoxia, the activity of miRNA processing enzymes such RISC reduces, which lowers the expression of tumor suppressor miRNAs (224). De Carvalho Vicentini et al. (2013) suggest that altering the expression or activity of these enzymes is another method for suppressing miRNA (225).

11 Conclusion

The discovery, development, and enhancement of miRNAs as potential medicines for the treatment of breast cancer patients have received significant funding, yet this branch of translational research is still in its infancy. Numerous attempts have been made to tailor cancer therapies using miRNA, but little progress has been made in improving clinic-oncological outcomes using miRNA targeting. miRNA therapies are now facing several developmental obstacles. This study is constrained by the fact that most of the research done thus far provides information about *in-vitro* trials, with very few studies coming from sources other than animal or breast cancer cell lines. Clinical trials assessing the clinical

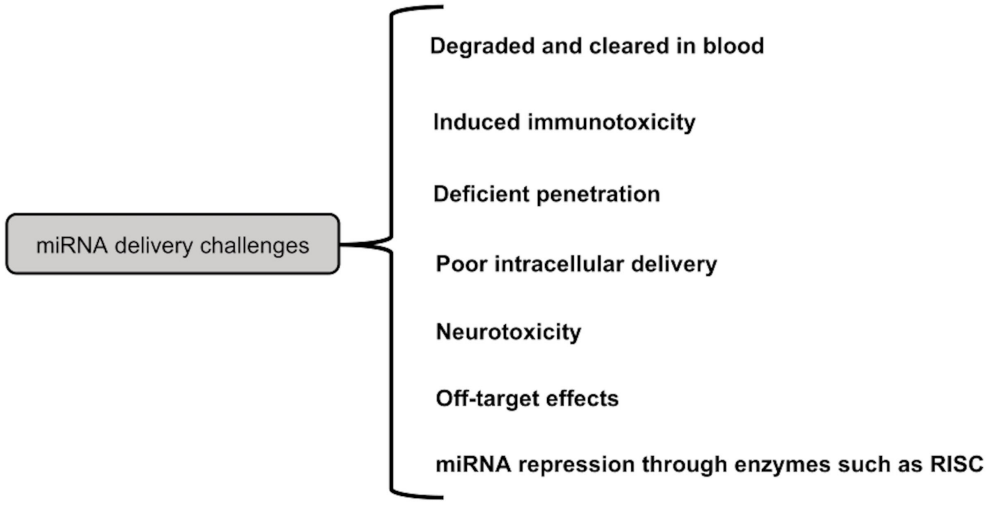

FIGURE 6
Challenges in miRNA delivery.

effectiveness, risk profiles, and premium benefit are necessary for addition to the generally accepted scientific technique to support the initial findings of these recent investigations. An in-depth discussion of how clinical trial research has transformed BC patient care over the last four decades is provided in the current review. This research has produced novel, individualized therapeutic approaches, minimally invasive surgical techniques for the breast and axilla, and improved clinico-oncological results for patients who might otherwise have died from their disease in earlier times. The personalization of BC patient care appears to be closer than ever thanks to ongoing trials evaluating cutting-edge targeted therapies like immune checkpoint modulation (39, 226) and the use of poly(adenosine diphosphate-ribose) polymerase inhibitors (or PARP inhibitors) in the treatment of early-stage breast cancer in BRCA mutation carriers (227).

Hence, before we can use miRNAs in the therapeutic setting, numerous obstacles remain to be overcome. The delivery method is the key impediment. We might be able to get over this obstacle with the use of chemical alterations, viral vectors, or nanoparticles. Despite these delivery issues, it is possible that miRNAs will play a significant role in cancer therapy, including BC, in the future. A novel approach to treating breast cancer that combines miRNA therapies with conventional chemotherapeutic techniques and drug targets is possible, but further study is needed before this promising paradigm can be implemented in the clinic. Thus, this review emphasizes how important it is to prioritize clinical trials and therapeutic interventions to advance the precision oncology movement's goal of "curing" breast cancer.

Author contributions

SS, RT conceived the study. SS drafted the manuscript. SS, HS, AS, SG, VH, RT revised the manuscript critically for important intellectual content. RT, HS provided important comments on the manuscript. All authors approved the final manuscript. All authors contributed to the article and approved the submitted version.

Funding

This review was supported by the Indian Council of Medical Research (ICMR) project (5/13/58/2020/NCD-III)

Acknowledgments

SS thanks ICMR project (5/13/58/2020/NCD-III) for providing Research Associate fellowship.

Conflict of interest

The authors declare that the research was conducted in the absence of any commercial or financial relationships that could be construed as a potential conflict of interest.

Publisher's note

References

1. Sung H, Ferlay J, Siegel RL, Laversanne M, Soerjomataram I, Jemal A, et al. Global cancer statistics 2020: GLOBOCAN estimates of incidence and mortality worldwide for 36 cancers in 185 countries. *CA Cancer J Clin* (2021) 71(3):209–49. doi: 10.3322/caac.21660

2. Bajpai J, Ventrapati P, Joshi S, Wadasadawala T, Rath S, Pathak R, et al. Unique challenges and outcomes of young women with breast cancers from a tertiary care cancer centre in India. *Breast* (2021) 60:177–84. doi: 10.1016/j.breast.2021.09.008

3. DeSantis CE, Ma J, Gaudet MM, Newman LA, Miller KD, Goding Sauer A, et al. Breast cancer statistics, 2019. *CA Cancer J Clin* (2019) 69(6):438–51. doi: 10.3322/caac.21583

4. Sakorafas GH, Safioleas M. Breast cancer surgery: an historical narrative. part II. 18th and 19th centuries. *Eur J Cancer Care (Engl)* (2010) 19(1):6–29. doi: 10.1111/j.1365-2354.2008.01060.x

5. Goldhirsch A, Winer EP, Coates AS, Gelber RD, Piccart-Gebhart M, Thürlimann B, et al. Personalizing the treatment of women with early breast cancer: highlights of the St gallen international expert consensus on the primary therapy of early breast cancer 2013. *Ann Oncol* (2013) 24(9):2206–23. doi: 10.1093/annonc/mdt303

6. Chen F, Chen J, Yang L, Liu J, Zhang X, Zhang Y, et al. Extracellular vesicle-packaged HIF-1α-stabilizing lncRNA from tumour-associated macrophages regulates aerobic glycolysis of breast cancer cells. *Nat Cell Biol* (2019) 21(4):498–510. doi: 10.1038/s41556-019-0299-0

7. Wei Y, Yang P, Cao S, Zhao L. The combination of curcumin and 5-fluorouracil in cancer therapy. *Arch Pharm Res* (2018) 41(1):1–13. doi: 10.1007/s12272-017-0979-x

8. Shah AN, Gradishar WJ. Adjuvant anthracyclines in breast cancer: what is their role? *Oncologist* (2018) 23(10):1153–61. doi: 10.1634/theoncologist.2017-0672

9. Chang M. Tamoxifen resistance in breast cancer. *Biomol Ther (Seoul)* (2012) 20(3):256–67. doi: 10.4062/biomolther.2012.20.3.256

10. Prat A, Parker JS, Karginova O, Fan C, Livasy C, Herschkowitz JI, et al. Phenotypic and molecular characterization of the claudin-low intrinsic subtype of breast cancer. *Breast Cancer Res* (2010) 12(5):R68. doi: 10.1186/bcr2635

11. Picard M. Management of hypersensitivity reactions to taxanes. *Immunol Allergy Clin North Am* (2017) 37(4):679–93. doi: 10.1016/j.iac.2017.07.004

12. Slamon D, Eiermann W, Robert N, Pienkowski T, Martin M, Press M, et al. Adjuvant trastuzumab in HER2-positive breast cancer. *N Engl J Med* (2011) 365(14):1273–83. doi: 10.1056/NEJMoa0910383

13. Łukasiewicz S, Czeczelewski M, Forma A, Baj J, Sitarz R, Stanisławek A. Breast cancer-epidemiology, risk factors, classification, prognostic markers, and current treatment strategies-an updated review. *Cancers (Basel)* (2021) 13(17). doi: 10.3390/cancers13174287

14. Nwabo Kamdje AH, Seke Etet PF, Vecchio L, Muller JM, Krampera M, Lukong KE. Signaling pathways in breast cancer: therapeutic targeting of the microenvironment. *Cell Signal* (2014) 26(12):2843–56. doi: 10.1016/j.cellsig.2014.07.034

15. Rebucci M, Michiels C. Molecular aspects of cancer cell resistance to chemotherapy. *Biochem Pharmacol* (2013) 85(9):1219–26. doi: 10.1016/j.bcp.2013.02.017

16. Haider T, Pandey V, Banjare N, Gupta PN, Soni V. Drug resistance in cancer: mechanisms and tackling strategies. *Pharmacol Rep* (2020) 72(5):1125–51. doi: 10.1007/s43440-020-00138-7

17. Martz CA, Ottina KA, Singleton KR, Jasper JS, Wardell SE, Peraza-Penton A, et al. Systematic identification of signaling pathways with potential to confer anticancer drug resistance. *Sci Signal* (2014) 7(357):ra121. doi: 10.1126/scisignal.aaa1877

18. Belmont PJ, Jiang P, McKee TD, Xie T, Isaacson J, Baryla NE, et al. Resistance to dual blockade of the kinases PI3K and mTOR in KRAS-mutant colorectal cancer models results in combined sensitivity to inhibition of the receptor tyrosine kinase EGFR. *Sci Signal* (2014) 7(351):ra107. doi: 10.1126/scisignal.2005516

19. Toss A, Venturelli M, Peterle C, Piacentini F, Cascinu S, Cortesi L. Molecular biomarkers for prediction of targeted therapy response in metastatic breast cancer: trick or treat? *Int J Mol Sci* (2017) 18(1). doi: 10.3390/ijms18010085

20. Hill M, Tran N. miRNA interplay: mechanisms and consequences in cancer. *Dis Model Mech* (2021) 14(4). doi: 10.1242/dmm.047662

21. Deng X, Liu Y, Luo M, Wu J, Ma R, Wan Q. Circulating miRNA-24 and its target YKL-40 as potential biomarkers in patients with coronary heart disease and type 2 diabetes mellitus. *Oncotarget* (2017) 8(38):63038–46. doi: 10.18632/oncotarget.18593

22. Ni WJ, Leng XM. Dynamic miRNA-mRNA paradigms: new faces of miRNAs. *Biochem Biophys Rep* (2015) 4:337–41. doi: 10.1016/j.bbrep.2015.10.011

23. Teng M, Yu ZH, Zhao P, Zhuang GQ, Wu ZX, Dang L, et al. Putative roles as oncogene or tumour suppressor of the mid-clustered microRNAs in gallid alphaherpesvirus 2 (GaHV2) induced marek's disease lymphomagenesis. *J Gen Virol* (2017) 98(5):1097–112. doi: 10.1099/jgv.0.000786

24. Snowhite IV, Allende G, Sosenko J, Pastori RL, Messinger Cayetano S, Pugliese A. Association of serum microRNAs with islet autoimmunity, disease progression and metabolic impairment in relatives at risk of type 1 diabetes. *Diabetologia* (2017) 60 (8):1409–22. doi: 10.1007/s00125-017-4294-3

25. Mellis D, Caporali A. MicroRNA-based therapeutics in cardiovascular disease: screening and delivery to the target. *Biochem Soc Trans* (2018) 46(1):11–21. doi: 10.1042/BST20170037

26. Ali Syeda Z, Langden SSS, Munkhzul C, Lee M, Song SJ. Regulatory mechanism of MicroRNA expression in cancer. *Int J Mol Sci* (2020) 21(5). doi: 10.3390/ijms21051723

27. Singh A, Singh AK, Giri R, Kumar D, Sharma R, Valis M, et al. The role of microRNA-21 in the onset and progression of cancer. *Future Med Chem* (2021) 13 (21):1885–906. doi: 10.4155/fmc-2021-0096

28. Due H, Svendsen P, Bødker JS, Schmitz A, Bøgsted M, Johnsen HE, et al. miR-155 as a biomarker in b-cell malignancies. *BioMed Res Int* (2016) 2016:9513037. doi: 10.1155/2016/9513037

29. Ma Y, Shen N, Wicha MS, Luo M. The roles of the let-7 family of MicroRNAs in the regulation of cancer stemness. *Cells* (2021) 10(9). doi: 10.3390/cells10092415

30. McVeigh TP, Boland MR, Lowery AJ. The impact of the biomolecular era on breast cancer surgery. *Surgeon* (2017) 15(3):169–81. doi: 10.1016/j.surge.2016.09.007

31. Bonadonna G, Brusamolino E, Valagussa P, Rossi A, Brugnatelli L, Brambilla C, et al. Combination chemotherapy as an adjuvant treatment in operable breast cancer. *N Engl J Med* (1976) 294(8):405–10. doi: 10.1056/NEJM197602192940801

32. Fisher B. Biological research in the evolution of cancer surgery: a personal perspective. *Cancer Res* (2008) 68(24):10007–20. doi: 10.1158/0008-5472.CAN-08-0186

33. Davey MG, Kerin E, O'Flaherty C, Maher E, Richard V, McAnena P, et al. Clinicopathological response to neoadjuvant therapies and pathological complete response as a biomarker of survival in human epidermal growth factor receptor-2 enriched breast cancer - a retrospective cohort study. *Breast* (2021) 59:67–75. doi: 10.1016/j.breast.2021.06.005

34. Spring LM, Fell G, Arfe A, Sharma C, Greenup R, Reynolds KL, et al. Pathologic complete response after neoadjuvant chemotherapy and impact on breast cancer recurrence and survival: a comprehensive meta-analysis. *Clin Cancer Res* (2020) 26 (12):2838–48. doi: 10.1158/1078-0432.CCR-19-3492

35. (EBCTCG) EBCTCG. Long-term outcomes for neoadjuvant versus adjuvant chemotherapy in early breast cancer: meta-analysis of individual patient data from ten randomised trials. *Lancet Oncol* (2018) 19(1):27–39. doi: 10.1016/S1470-2045(17)30777-5

36. Boughey JC, Ballman KV, McCall LM, Mittendorf EA, Symmans WF, Julian TB, et al. Tumor biology and response to chemotherapy impact breast cancer-specific survival in node-positive breast cancer patients treated with neoadjuvant chemotherapy: long-term follow-up from ACOSOG Z1071 (Alliance). *Ann Surg* (2017) 266(4):667–76. doi: 10.1097/SLA.0000000000002373

37. Korde LA, Somerfield MR, Carey LA, Crews JR, Denduluri N, Hwang ES, et al. Neoadjuvant chemotherapy, endocrine therapy, and targeted therapy for breast cancer: ASCO guideline. *J Clin Oncol* (2021) 39(13):1485–505. doi: 10.1200/JCO.20.03399

38. Li ZY, Zhang Z, Cao XZ, Feng Y, Ren SS. Platinum-based neoadjuvant chemotherapy for triple-negative breast cancer: a systematic review and meta-analysis. *J Int Med Res* (2020) 48(10):300060520964340. doi: 10.1177/0300060520964340

39. Schmid P, Cortes J, Pusztai L, McArthur H, Kümmel S, Bergh J, et al. Pembrolizumab for early triple-negative breast cancer. *N Engl J Med* (2020) 382 (9):810–21. doi: 10.1056/NEJMoa1910549

40. Bartsch R, Bergen E, Galid A. Current concepts and future directions in neoadjuvant chemotherapy of breast cancer. *Memo* (2018) 11(3):199–203. doi: 10.1007/s12254-018-0421-1

41. Zheng X, Carstens JL, Kim J, Scheible M, Kaye J, Sugimoto H, et al. Epithelial-to-mesenchymal transition is dispensable for metastasis but induces chemoresistance in pancreatic cancer. *Nature* (2015) 527(7579):525–30. doi: 10.1038/nature16064

42. Pham CG, Bubici C, Zazzeroni F, Knabb JR, Papa S, Kuntzen C, et al. Upregulation of twist-1 by NF-kappaB blocks cytotoxicity induced by chemotherapeutic drugs. *Mol Cell Biol* (2007) 27(11):3920–35. doi: 10.1128/MCB.01219-06

43. Vesuna F, Lisok A, Kimble B, Domek J, Kato Y, van der Groep P, et al. Twist contributes to hormone resistance in breast cancer by downregulating estrogen receptor-α. *Oncogene* (2012) 31(27):3223–34. doi: 10.1038/onc.2011.483

44. Gao L, Yang Y, Song S, Hong H, Zhao X, Li D. The association between genetic variant of MDR1 gene and breast cancer risk factors in Chinese women. *Int Immunopharmacol* (2013) 17(1):88–91. doi: 10.1016/j.intimp.2013.05.025

45. Chen Y, Li X, Shi L, Ma P, Wang W, Wu N, et al. Combination of 7-. *Aging (Albany NY)* (2022) 14(17):7156–69. doi: 10.18632/aging.204287

46. Ajith AK, Subramani S, Manickam AH, Ramasamy S. Chemotherapeutic resistance genes of breast cancer patients - an overview. *Adv Pharm Bull* (2022) 12 (4):649–57. doi: 10.34172/apb.2022.048

47. Kort A, Durmus S, Sparidans RW, Wagenaar E, Beijnen JH, Schinkel AH. Brain and testis accumulation of regorafenib is restricted by breast cancer resistance protein (BCRP/ABCG2) and p-glycoprotein (P-GP/ABCB1). *Pharm Res* (2015) 32(7):2205–16. doi: 10.1007/s11095-014-1609-7

48. Hu D, Li M, Su J, Miao K, Qiu X. Dual-targeting of miR-124-3p and ABCC4 promotes sensitivity to adriamycin in breast cancer cells. *Genet Test Mol Biomarkers* (2019) 23(3):156–65. doi: 10.1089/gtmb.2018.0259

49. Levin ER. Extranuclear estrogen receptor's roles in physiology: lessons from mouse models. *Am J Physiol Endocrinol Metab* (2014) 307(2):E133–40. doi: 10.1152/ajpendo.00626.2013

50. Ziauddin MF, Hua D, Tang SC. Emerging strategies to overcome resistance to endocrine therapy for breast cancer. *Cancer Metastasis Rev* (2014) 33(2-3):791–807. doi: 10.1007/s10555-014-9504-6

51. Huang WC, Chen YJ, Li LY, Wei YL, Hsu SC, Tsai SL, et al. Nuclear translocation of epidermal growth factor receptor by akt-dependent phosphorylation enhances breast cancer-resistant protein expression in gefitinib-resistant cells. *J Biol Chem* (2011) 286(23):20558–68. doi: 10.1074/jbc.M111.240796

52. Kitao H, Iimori M, Kataoka Y, Wakasa T, Tokunaga E, Saeki H, et al. DNA Replication stress and cancer chemotherapy. *Cancer Sci* (2018) 109(2):264–71. doi: 10.1111/cas.13455

53. Nikitaki Z, Michalopoulos I, Georgakilas AG. Molecular inhibitors of DNA repair: searching for the ultimate tumor killing weapon. *Future Med Chem* (2015) 7 (12):1543–58. doi: 10.4155/fmc.15.95

54. Prakash R, Zhang Y, Feng W, Jasin M. Homologous recombination and human health: the roles of BRCA1, BRCA2, and associated proteins. *Cold Spring Harb Perspect Biol* (2015) 7(4):a016600. doi: 10.1101/cshperspect.a016600

55. Martin JH, Bromfield EG, Aitken RJ, Lord T, Nixon B. Double strand break DNA repair occurs *via* non-homologous end-joining in mouse MII oocytes. *Sci Rep* (2018) 8(1):9685. doi: 10.1038/s41598-018-27892-2

56. Dietlein F, Thelen L, Reinhardt HC. Cancer-specific defects in DNA repair pathways as targets for personalized therapeutic approaches. *Trends Genet* (2014) 30 (8):326–39. doi: 10.1016/j.tig.2014.06.003

57. Marteijn JA, Lans H, Vermeulen W, Hoeijmakers JH. Understanding nucleotide excision repair and its roles in cancer and ageing. *Nat Rev Mol Cell Biol* (2014) 15 (7):465–81. doi: 10.1038/nrm3822

58. Krokan HE, Bjørås M. Base excision repair. *Cold Spring Harb Perspect Biol* (2013) 5(4):a012583. doi: 10.1101/cshperspect.a012583

59. Li W, Melton DW. Cisplatin regulates the MAPK kinase pathway to induce increased expression of DNA repair gene ERCC1 and increase melanoma chemoresistance. *Oncogene* (2012) 31(19):2412–22. doi: 10.1038/onc.2011.426

60. Silva SN, Tomar M, Paulo C, Gomes BC, Azevedo AP, Teixeira V, et al. Breast cancer risk and common single nucleotide polymorphisms in homologous recombination DNA repair pathway genes XRCC2, XRCC3, NBS1 and RAD51. *Cancer Epidemiol* (2010) 34(1):85–92. doi: 10.1016/j.canep.2009.11.002

61. Aleskandarany M, Caracappa D, Nolan CC, Macmillan RD, Ellis IO, Rakha EA, et al. DNA Damage response markers are differentially expressed in BRCA-mutated breast cancers. *Breast Cancer Res Treat* (2015) 150(1):81–90. doi: 10.1007/s10549-015-3306-6

62. Altan B, Yokobori T, Ide M, Bai T, Yanoma T, Kimura A, et al. High expression of MRE11-RAD50-NBS1 is associated with poor prognosis and chemoresistance in gastric cancer. *Anticancer Res* (2016) 36(10):5237–47. doi: 10.21873/anticanres.11094

63. Pavlopoulou A, Oktay Y, Vougas K, Louka M, Vorgias CE, Georgakilas AG. Determinants of resistance to chemotherapy and ionizing radiation in breast cancer stem cells. *Cancer Lett* (2016) 380(2):485–93. doi: 10.1016/j.canlet.2016.07.018

64. Zhou ZY, Wan LL, Yang QJ, Han YL, Li D, Lu J, et al. Nilotinib reverses ABCB1/P-glycoprotein-mediated multidrug resistance but increases cardiotoxicity of doxorubicin in a MDR xenograft model. *Toxicol Lett* (2016) 259:124–32. doi: 10.1016/j.toxlet.2016.07.710

65. Attia YM, El-Kersh DM, Ammar RA, Adel A, Khalil A, Walid H, et al. Inhibition of aldehyde dehydrogenase-1 and p-glycoprotein-mediated multidrug resistance by

curcumin and vitamin D3 increases sensitivity to paclitaxel in breast cancer. *Chem Biol Interact* (2020) 315:108865. doi: 10.1016/j.cbi.2019.108865

66. Angius A, Scanu AM, Arru C, Muroni MR, Rallo V, Deiana G, et al. Portrait of cancer stem cells on colorectal cancer: molecular biomarkers, signaling pathways and miRNAome. *Int J Mol Sci* (2021) 22(4). doi: 10.3390/ijms22041603

67. Sun X, Qin S, Fan C, Xu C, Du N, Ren H. Let-7: a regulator of the ERα signaling pathway in human breast tumors and breast cancer stem cells. *Oncol Rep* (2013) 29 (5):2079–87. doi: 10.3892/or.2013.2330

68. Hazarika M, Chuk MK, Theoret MR, Mushti S, He K, Weis SL, et al. U.S. FDA approval summary: nivolumab for treatment of unresectable or metastatic melanoma following progression on ipilimumab. *Clin Cancer Res* (2017) 23(14):3484–8. doi: 10.1158/1078-0432.CCR-16-0712

69. Al-Harras MF, Houssen ME, Shaker ME, Farag K, Farouk O, Monir R, et al. Polymorphisms of glutathione s-transferase π 1 and toll-like receptors 2 and 9: association with breast cancer susceptibility. *Oncol Lett* (2016) 11(3):2182–8. doi: 10.3892/ol.2016.4159

70. Fan L, Strasser-Weippl K, Li JJ, St Louis J, Finkelstein DM, Yu KD, et al. Breast cancer in China. *Lancet Oncol* (2014) 15(7):e279–89. doi: 10.1016/S1470-2045(13) 70567-9

71. Lee Y, Ahn C, Han J, Choi H, Kim J, Yim J, et al. The nuclear RNase III drosha initiates microRNA processing. *Nature* (2003) 425(6956):415–9. doi: 10.1038/nature01957

72. Bartel DP. MicroRNAs: genomics, biogenesis, mechanism, and function. *Cell* (2004) 116(2):281–97. doi: 10.1016/S0092-8674(04)00045-5

73. Slack FJ, Chinnaiyan AM. The role of non-coding RNAs in oncology. *Cell* (2019) 179(5):1033–55. doi: 10.1016/j.cell.2019.10.017

74. Adams BD, Furneaux H, White BA. The micro-ribonucleic acid (miRNA) miR-206 targets the human estrogen receptor-alpha (ERalpha) and represses ERalpha messenger RNA and protein expression in breast cancer cell lines. *Mol Endocrinol* (2007) 21(5):1132–47. doi: 10.1210/me.2007-0022

75. Hossain A, Kuo MT, Saunders GF. Mir-17-5p regulates breast cancer cell proliferation by inhibiting translation of AIB1 mRNA. *Mol Cell Biol* (2006) 26 (21):8191–201. doi: 10.1128/MCB.00242-06

76. Zhou M, Liu Z, Zhao Y, Ding Y, Liu H, Xi Y, et al. MicroRNA-125b confers the resistance of breast cancer cells to paclitaxel through suppression of pro-apoptotic bcl-2 antagonist killer 1 (Bak1) expression. *J Biol Chem* (2010) 285(28):21496–507. doi: 10.1074/jbc.M109.083337

77. Xu X, Lv YG, Yan CY, Yi J, Ling R. Enforced expression of hsa-miR-125a-3p in breast cancer cells potentiates docetaxel sensitivity *via* modulation of BRCA1 signaling. *Biochem Biophys Res Commun* (2016) 479(4):893–900. doi: 10.1016/j.bbrc.2016.09.087

78. Cochrane DR, Spoelstra NS, Howe EN, Nordeen SK, Richer JK. MicroRNA-200c mitigates invasiveness and restores sensitivity to microtubule-targeting chemotherapeutic agents. *Mol Cancer Ther* (2009) 8(5):1055–66. doi: 10.1158/1535-7163.MCT-08-1046

79. Yu F, Yao H, Zhu P, Zhang X, Pan Q, Gong C, et al. Let-7 regulates self renewal and tumorigenicity of breast cancer cells. *Cell* (2007) 131(6):1109–23. doi: 10.1016/j.cell.2007.10.054

80. Kastl L, Brown I, Schofield AC. miRNA-34a is associated with docetaxel resistance in human breast cancer cells. *Breast Cancer Res Treat* (2012) 131(2):445–54. doi: 10.1007/s10549-011-1424-3

81. Schmittgen TD. miR-31: a master regulator of metastasis? *Future Oncol* (2010) 6 (1):17–20. doi: 10.2217/fon.09.150

82. Tavazoie SF, Alarcón C, Oskarsson T, Padua D, Wang Q, Bos PD, et al. Endogenous human microRNAs that suppress breast cancer metastasis. *Nature* (2008) 451(7175):147–52. doi: 10.1038/nature06487

83. Tsuchiya Y, Nakajima M, Takagi S, Taniya T, Yokoi T. MicroRNA regulates the expression of human cytochrome P450 1B1. *Cancer Res* (2006) 66(18):9090–8. doi: 10.1158/0008-5472.CAN-06-1403

84. Gong C, Yao Y, Wang Y, Liu B, Wu W, Chen J, et al. Up-regulation of miR-21 mediates resistance to trastuzumab therapy for breast cancer. *J Biol Chem* (2011) 286 (21):19127–37. doi: 10.1074/jbc.M110.216887

85. Li Y, Zhang L, Dong Z, Xu H, Yan L, Wang W, et al. MicroRNA-155-5p promotes tumor progression and contributes to paclitaxel resistance *via* TP53INP1 in human breast cancer. *Pathol Res Pract* (2021) 220:153405. doi: 10.1016/j.prp.2021.153405

86. Ma L, Teruya-Feldstein J, Weinberg RA. Tumour invasion and metastasis initiated by microRNA-10b in breast cancer. *Nature* (2007) 449(7163):682–8. doi: 10.1038/nature06174

87. Huang Q, Gumireddy K, Schrier M, le Sage C, Nagel R, Nair S, et al. The microRNAs miR-373 and miR-520c promote tumour invasion and metastasis. *Nat Cell Biol* (2008) 10(2):202–10. doi: 10.1038/ncb1681

88. Mertens-Talcott SU, Chintharlapalli S, Li X, Safe S. The oncogenic microRNA-27a targets genes that regulate specificity protein transcription factors and the G2-m checkpoint in MDA-MB-231 breast cancer cells. *Cancer Res* (2007) 67(22):11001–11. doi: 10.1158/0008-5472.CAN-07-2416

89. Miller TE, Ghoshal K, Ramaswamy B, Roy S, Datta J, Shapiro CL, et al. MicroRNA-221/222 confers tamoxifen resistance in breast cancer by targeting p27Kip1. *J Biol Chem* (2008) 283(44):29897–903. doi: 10.1074/jbc.M804612200

90. Li H, Yang BB. Friend or foe: the role of microRNA in chemotherapy resistance. *Acta Pharmacol Sin* (2013) 34(7):870–9. doi: 10.1038/aps.2013.35

91. Magee P, Shi L, Garofalo M. Role of microRNAs in chemoresistance. *Ann Transl Med* (2015) 3(21):332. doi: 10.3978/j.issn.2305-5839.2015.11.32

92. Griñán-Lisón C, Olivares-Urbano MA, Jiménez G, López-Ruiz E, Del Val C, Morata-Tarifa C, et al. miRNAs as radio-response biomarkers for breast cancer stem cells. *Mol Oncol* (2020) 14(3):556–70. doi: 10.1002/1878-0261.12635

93. Muluhngwi P, Klinge CM. Roles for miRNAs in endocrine resistance in breast cancer. *Endocr Relat Cancer* (2015) 22(5):R279–300. doi: 10.1530/ERC-15-0355

94. Gao Y, Zhang W, Liu C, Li G. miR-200 affects tamoxifen resistance in breast cancer cells through regulation of MYB. *Sci Rep* (2019) 9(1):18844. doi: 10.1038/s41598-019-54289-6

95. He M, Jin Q, Chen C, Liu Y, Ye X, Jiang Y, et al. The miR-186-3p/EREG axis orchestrates tamoxifen resistance and aerobic glycolysis in breast cancer cells. *Oncogene* (2019) 38(28):5551–65. doi: 10.1038/s41388-019-0817-3

96. Li J, Lu M, Jin J, Lu X, Xu T, Jin S. miR-449a suppresses tamoxifen resistance in human breast cancer cells by targeting ADAM22. *Cell Physiol Biochem* (2018) 50 (1):136–49. doi: 10.1159/000493964

97. Liu ZR, Song Y, Wan LH, Zhang YY, Zhou LM. Over-expression of miR-451a can enhance the sensitivity of breast cancer cells to tamoxifen by regulating 14-3-3ζ, estrogen receptor α, and autophagy. *Life Sci* (2016) 149:104–13. doi: 10.1016/j.lfs.2016.02.059

98. Shi YF, Lu H, Wang HB. Downregulated lncRNA ADAMTS9-AS2 in breast cancer enhances tamoxifen resistance by activating microRNA-130a-5p. *Eur Rev Med Pharmacol Sci* (2019) 23(4):1563–73. doi: 10.26355/eurrev_201902_17115

99. Zhang HY, Liang F, Zhang JW, Wang F, Wang L, Kang XG. Effects of long noncoding RNA-ROR on tamoxifen resistance of breast cancer cells by regulating microRNA-205. *Cancer Chemother Pharmacol* (2017) 79(2):327–37. doi: 10.1007/s00280-016-3208-2

100. Sang Y, Chen B, Song X, Li Y, Liang Y, Han D, et al. circRNA_0025202 regulates tamoxifen sensitivity and tumor progression *via* regulating the miR-182-5p/FOXO3a axis in breast cancer. *Mol Ther* (2019) 27(9):1638–52. doi: 10.1016/j.ymthe.2019.05.011

101. Kopp F, Oak PS, Wagner E, Roidl A. miR-200c sensitizes breast cancer cells to doxorubicin treatment by decreasing TrkB and Bmi1 expression. *PloS One* (2012) 7 (11):e50469. doi: 10.1371/journal.pone.0050469

102. Li XJ, Ji MH, Zhong SL, Zha QB, Xu JJ, Zhao JH, et al. MicroRNA-34a modulates chemosensitivity of breast cancer cells to adriamycin by targeting Notch1. *Arch Med Res* (2012) 43(7):514–21. doi: 10.1016/j.arcmed.2012.09.007

103. Zhao L, Wang Y, Jiang L, He M, Bai X, Yu L, et al. MiR-302a/b/c/d cooperatively sensitizes breast cancer cells to adriamycin *via* suppressing p-glycoprotein(P-gp) by targeting MAP/ERK kinase kinase 1 (MEKK1). *J Exp Clin Cancer Res* (2016) 35:25. doi: 10.1186/s13046-016-0300-8

104. Bao L, Hazari S, Mehra S, Kaushal D, Moroz K, Dash S. Increased expression of p-glycoprotein and doxorubicin chemoresistance of metastatic breast cancer is regulated by miR-298. *Am J Pathol* (2012) 180(6):2490–503. doi: 10.1016/j.ajpath.2012.02.024

105. Shen H, Li L, Yang S, Wang D, Zhong S, Zhao J, et al. MicroRNA-29a contributes to drug-resistance of breast cancer cells to adriamycin through PTEN/AKT/GSK3β signaling pathway. *Gene* (2016) 593(1):84–90. doi: 10.1016/j.gene.2016.08.016

106. Miao Y, Zheng W, Li N, Su Z, Zhao L, Zhou H, et al. MicroRNA-130b targets PTEN to mediate drug resistance and proliferation of breast cancer cells *via* the PI3K/Akt signaling pathway. *Sci Rep* (2017) 7:41942. doi: 10.1038/srep41942

107. Wang DD, Yang SJ, Chen X, Shen HY, Luo LJ, Zhang XH, et al. miR-222 induces adriamycin resistance in breast cancer through PTEN/Akt/p27. *Tumour Biol* (2016) 37(11):15315–24. doi: 10.1007/s13277-016-5341-2

108. Gao M, Miao L, Liu M, Li C, Yu C, Yan H, et al. miR-145 sensitizes breast cancer to doxorubicin by targeting multidrug resistance-associated protein-1. *Oncotarget* (2016) 7(37):59714–26. doi: 10.18632/oncotarget.10845

109. Jiang L, He D, Yang D, Chen Z, Pan Q, Mao A, et al. MiR-489 regulates chemoresistance in breast cancer *via* epithelial mesenchymal transition pathway. *FEBS Lett* (2014) 588(11):2009–15. doi: 10.1016/j.febslet.2014.04.024

110. Hu SH, Wang CH, Huang ZJ, Liu F, Xu CW, Li XL, et al. miR-760 mediates chemoresistance through inhibition of epithelial mesenchymal transition in breast cancer cells. *Eur Rev Med Pharmacol Sci* (2016) 20(23):5002–8.

111. Zhang Y, He Y, Lu LL, Zhou ZY, Wan NB, Li GP, et al. miRNA-192-5p impacts the sensitivity of breast cancer cells to doxorubicin *via* targeting peptidylprolyl isomerase a. *Kaohsiung J Med Sci* (2019) 35(1):17–23. doi: 10.1002/kjm2.12004

112. Zhao R, Wu J, Jia W, Gong C, Yu F, Ren Z, et al. Plasma miR-221 as a predictive biomarker for chemoresistance in breast cancer patients who previously received neoadjuvant chemotherapy. *Onkologie* (2011) 34(12):675–80. doi: 10.1159/000334552

113. Chang L, Hu Z, Zhou Z, Zhang H. Linc00518 contributes to multidrug resistance through regulating the MiR-199a/MRP1 axis in breast cancer. *Cell Physiol Biochem* (2018) 48(1):16–28. doi: 10.1159/000491659

114. Lv K, Liu L, Wang L, Yu J, Liu X, Cheng Y, et al. Lin28 mediates paclitaxel resistance by modulating p21, Rb and let-7a miRNA in breast cancer cells. *PloS One* (2012) 7(7):e40008. doi: 10.1371/journal.pone.0040008

115. Tsang WP, Kwok TT. Let-7a microRNA suppresses therapeutics-induced cancer cell death by targeting caspase-3. *Apoptosis* (2008) 13(10):1215–22. doi: 10.1007/s10495-008-0256-z

116. Su CM, Wang MY, Hong CC, Chen HA, Su YH, Wu CH, et al. miR-520h is crucial for DAPK2 regulation and breast cancer progression. *Oncogene* (2016) 35 (9):1134–42. doi: 10.1038/onc.2015.168

117. Gu X, Li JY, Guo J, Li PS, Zhang WH. Influence of MiR-451 on drug resistances of paclitaxel-resistant breast cancer cell line. *Med Sci Monit* (2015) 21:3291–7. doi: 10.12659/MSM.894475

118. Zhang B, Zhao R, He Y, Fu X, Fu L, Zhu Z, et al. MicroRNA 100 sensitizes luminal a breast cancer cells to paclitaxel treatment in part by targeting mTOR. *Oncotarget* (2016) 7(5):5702–14. doi: 10.18632/oncotarget.6790

119. Sha LY, Zhang Y, Wang W, Sui X, Liu SK, Wang T, et al. MiR-18a upregulation decreases dicer expression and confers paclitaxel resistance in triple negative breast cancer. *Eur Rev Med Pharmacol Sci* (2016) 20(11):2201–8.

120. Liu X, Tang H, Chen J, Song C, Yang L, Liu P, et al. MicroRNA-101 inhibits cell progression and increases paclitaxel sensitivity by suppressing MCL-1 expression in human triple-negative breast cancer. *Oncotarget* (2015) 6(24):20070–83. doi: 10.18632/oncotarget.4039

121. Zheng P, Dong L, Zhang B, Dai J, Zhang Y, Wang Y, et al. Long noncoding RNA CASC2 promotes paclitaxel resistance in breast cancer through regulation of miR-18a-5p/CDK19. *Histochem Cell Biol* (2019) 152(4):281–91. doi: 10.1007/s00418-019-01794-4

122. Yao YS, Qiu WS, Yao RY, Zhang Q, Zhuang LK, Zhou F, et al. miR-141 confers docetaxel chemoresistance of breast cancer cells *via* regulation of EIF4E expression. *Oncol Rep* (2015) 33(5):2504–12. doi: 10.3892/or.2015.3866

123. Zhang Y, Wang Y, Wei Y, Li M, Yu S, Ye M, et al. MiR-129-3p promotes docetaxel resistance of breast cancer cells *via* CP110 inhibition. *Sci Rep* (2015) 5:15424. doi: 10.1038/srep15424

124. Zhang X, Zhong S, Xu Y, Yu D, Ma T, Chen L, et al. MicroRNA-3646 contributes to docetaxel resistance in human breast cancer cells by GSK-3β/β-Catenin signaling pathway. *PloS One* (2016) 11(4):e0153194. doi: 10.1371/journal.pone.0153194

125. Hu Q, Chen WX, Zhong SL, Zhang JY, Ma TF, Ji H, et al. MicroRNA-452 contributes to the docetaxel resistance of breast cancer cells. *Tumour Biol* (2014) 35 (7):6327–34. doi: 10.1007/s13277-014-1834-z

126. Hu H, Li S, Cui X, Lv X, Jiao Y, Yu F, et al. The overexpression of hypomethylated miR-663 induces chemotherapy resistance in human breast cancer cells by targeting heparin sulfate proteoglycan 2 (HSPG2). *J Biol Chem* (2013) 288 (16):10973–85. doi: 10.1074/jbc.M112.434340

127. Zhang HD, Sun DW, Mao L, Zhang J, Jiang LH, Li J, et al. MiR-139-5p inhibits the biological function of breast cancer cells by targeting Notch1 and mediates chemosensitivity to docetaxel. *Biochem Biophys Res Commun* (2015) 465(4):702–13. doi: 10.1016/j.bbrc.2015.08.053

128. Zhong S, Li W, Chen Z, Xu J, Zhao J. MiR-222 and miR-29a contribute to the drug-resistance of breast cancer cells. *Gene* (2013) 531(1):8–14. doi: 10.1016/j.gene.2013.08.062

129. Huang P, Li F, Li L, You Y, Luo S, Dong Z, et al. lncRNA profile study reveals the mRNAs and lncRNAs associated with docetaxel resistance in breast cancer cells. *Sci Rep* (2018) 8(1):17970. doi: 10.1038/s41598-018-36231-4

130. Nandy SB, Arumugam A, Subramani R, Pedroza D, Hernandez K, Saltzstein E, et al. MicroRNA-125a influences breast cancer stem cells by targeting leukemia inhibitory factor receptor which regulates the hippo signaling pathway. *Oncotarget* (2015) 6(19):17366–78. doi: 10.18632/oncotarget.3953

131. Zhang Y, Qu X, Teng Y, Li Z, Xu L, Liu J, et al. Cbl-b inhibits p-gp transporter function by preventing its translocation into caveolae in multiple drug-resistant gastric and breast cancers. *Oncotarget* (2015) 6(9):6737–48. doi: 10.18632/oncotarget.3253

132. Yin J, Zheng G, Jia X, Zhang Z, Zhang W, Song Y, et al. A Bmi1-miRNAs cross-talk modulates chemotherapy response to 5-fluorouracil in breast cancer cells. *PloS One* (2013) 8(9):e73268. doi: 10.1371/journal.pone.0073268

133. Li QQ, Chen ZQ, Cao XX, Xu JD, Xu JW, Chen YY, et al. Involvement of NF-κB/miR-448 regulatory feedback loop in chemotherapy-induced epithelial-mesenchymal transition of breast cancer cells. *Cell Death Differ* (2011) 18(1):16–25. doi: 10.1038/cdd.2010.103

134. Li X, Wang S, Li Z, Long X, Guo Z, Zhang G, et al. The lncRNA NEAT1 facilitates cell growth and invasion via the miR-211/HMGA2 axis in breast cancer. *Int J Biol Macromol* (2017) 105(Pt 1):346–53. doi: 10.1016/j.ijbiomac.2017.07.053

135. Yang W, Gu J, Wang X, Wang Y, Feng M, Zhou D, et al. Inhibition of circular RNA CDR1as increases chemosensitivity of 5-FU-resistant BC cells through up-regulating miR-7. *J Cell Mol Med* (2019) 23(5):3166–77. doi: 10.1111/jcmm.14171

136. Ye X, Bai W, Zhu H, Zhang X, Chen Y, Wang L, et al. MiR-221 promotes trastuzumab-resistance and metastasis in HER2-positive breast cancers by targeting PTEN. *BMB Rep* (2014) 47(5):268–73. doi: 10.5483/BMBRep.2014.47.5.165

137. Bai WD, Ye XM, Zhang MY, Zhu HY, Xi WJ, Huang X, et al. MiR-200c suppresses TGF-β signaling and counteracts trastuzumab resistance and metastasis by targeting ZNF217 and ZEB1 in breast cancer. *Int J Cancer* (2014) 135(6):1356–68. doi: 10.1002/ijc.28782

138. Ye XM, Zhu HY, Bai WD, Wang T, Wang L, Chen Y, et al. Epigenetic silencing of miR-375 induces trastuzumab resistance in HER2-positive breast cancer by targeting IGF1R. *BMC Cancer* (2014) 14:134. doi: 10.1186/1471-2407-14-134

139. Ma T, Yang L, Zhang J. MiRNA−542−3p downregulation promotes trastuzumab resistance in breast cancer cells *via* AKT activation. *Oncol Rep* (2015) 33(3):1215–20. doi: 10.3892/or.2015.3713

140. Corcoran C, Rani S, Breslin S, Gogarty M, Ghobrial IM, Crown J, et al. miR-630 targets IGF1R to regulate response to HER-targeting drugs and overall cancer cell progression in HER2 over-expressing breast cancer. *Mol Cancer* (2014) 13:71. doi: 10.1186/1476-4598-13-71

141. Venturutti L, Cordo Russo RI, Rivas MA, Mercogliano MF, Izzo F, Oakley RH, et al. MiR-16 mediates trastuzumab and lapatinib response in ErbB-2-positive breast and gastric cancer *via* its novel targets CCNJ and FUBP1. *Oncogene* (2016) 35 (48):6189–202. doi: 10.1038/onc.2016.151

142. Huynh FC, Jones FE. MicroRNA-7 inhibits multiple oncogenic pathways to suppress HER2Δ16 mediated breast tumorigenesis and reverse trastuzumab resistance. *PloS One* (2014) 9(12):e114419. doi: 10.1371/journal.pone.0114419

143. Casey MC, Sweeney KJ, Brown JA, Kerin MJ. Exploring circulating micro-RNA in the neoadjuvant treatment of breast cancer. *Int J Cancer* (2016) 139(1):12–22. doi: 10.1002/ijc.29985

144. Liu M, Gong C, Xu R, Chen Y, Wang X. MicroRNA-5195-3p enhances the chemosensitivity of triple-negative breast cancer to paclitaxel by downregulating EIF4A2. *Cell Mol Biol Lett* (2019) 24:47. doi: 10.1186/s11658-019-0168-7

145. Hou X, Niu Z, Liu L, Guo Q, Li H, Yang X, et al. miR-1207-5p regulates the sensitivity of triple-negative breast cancer cells to taxol treatment *via* the suppression of LZTS1 expression. *Oncol Lett* (2019) 17(1):990–8. doi: 10.3892/ol.2018.9687

146. Wu C, Zhao A, Tan T, Wang Y, Shen Z. Overexpression of microRNA-620 facilitates the resistance of triple negative breast cancer cells to gemcitabine treatment by targeting DCTD. *Exp Ther Med* (2019) 18(1):550–8. doi: 10.3892/etm.2019.7601

147. Wang H, Tan G, Dong L, Cheng L, Li K, Wang Z, et al. Circulating MiR-125b as a marker predicting chemoresistance in breast cancer. *PloS One* (2012) 7(4):e34210. doi: 10.1371/journal.pone.0034210

148. Roscigno G, Puoti I, Giordano I, Donnarumma E, Russo V, Affinito A, et al. MiR-24 induces chemotherapy resistance and hypoxic advantage in breast cancer. *Oncotarget* (2017) 8(12):19507–21. doi: 10.18632/oncotarget.14470

149. Yu DD, Lv MM, Chen WX, Zhong SL, Zhang XH, Chen L, et al. Role of miR-155 in drug resistance of breast cancer. *Tumour Biol* (2015) 36(3):1395–401. doi: 10.1007/s13277-015-3263-z

150. Yin Y, Wang X, Li T, Ren Q, Li L, Sun X, et al. MicroRNA-221 promotes breast cancer resistance to adriamycin *via* modulation of PTEN/Akt/mTOR signaling. *Cancer Med* (2020) 9(4):1544–52. doi: 10.1002/cam4.2817

151. Bao C, Chen J, Chen D, Lu Y, Lou W, Ding B, et al. MiR-93 suppresses tumorigenesis and enhances chemosensitivity of breast cancer *via* dual targeting E2F1 and CCND1. *Cell Death Dis* (2020) 11(8):618. doi: 10.1038/s41419-020-02855-6

152. Moskwa P, Buffa FM, Pan Y, Panchakshari R, Gottipati P, Muschel RJ, et al. miR-182-mediated downregulation of BRCA1 impacts DNA repair and sensitivity to PARP inhibitors. *Mol Cell* (2011) 41(2):210–20. doi: 10.1016/j.molcel.2010.12.005

153. Xiang F, Fan Y, Ni Z, Liu Q, Zhu Z, Chen Z, et al. Ursolic acid reverses the chemoresistance of breast cancer cells to paclitaxel by targeting MiRNA-149-5p/MyD88. *Front Oncol* (2019) 9:501. doi: 10.3389/fonc.2019.00501

154. Jiang H, Cheng L, Hu P, Liu R. MicroRNA−663b mediates TAM resistance in breast cancer by modulating TP73 expression. *Mol Med Rep* (2018) 18(1):1120–6. doi: 10.3892/mmr.2018.9064

155. Dave B, Mittal V, Tan NM, Chang JC. Epithelial-mesenchymal transition, cancer stem cells and treatment resistance. *Breast Cancer Res* (2012) 14(1):202. doi: 10.1186/bcr2938

156. Pinto CA, Widodo E, Waltham M, Thompson EW. Breast cancer stem cells and epithelial mesenchymal plasticity - implications for chemoresistance. *Cancer Lett* (2013) 341(1):56–62. doi: 10.1016/j.canlet.2013.06.003

157. Brabletz S, Bajdak K, Meidhof S, Burk U, Niedermann G, Firat E, et al. The ZEB1/miR-200 feedback loop controls notch signalling in cancer cells. *EMBO J* (2011) 30(4):770–82. doi: 10.1038/emboj.2010.349

158. Zhao N, Powell RT, Yuan X, Bae G, Roarty KP, Stossi F, et al. Morphological screening of mesenchymal mammary tumor organoids to identify drugs that reverse epithelial-mesenchymal transition. *Nat Commun* (2021) 12(1):4262. doi: 10.1038/s41467-021-24545-3

159. Li HY, Liang JL, Kuo YL, Lee HH, Calkins MJ, Chang HT, et al. miR-105/93-3p promotes chemoresistance and circulating miR-105/93-3p acts as a diagnostic biomarker for triple negative breast cancer. *Breast Cancer Res* (2017) 19(1):133. doi: 10.1186/s13058-017-0918-2

160. Di Cosimo S, Appierto V, Pizzamiglio S, Tiberio P, Iorio MV, Hilbers F, et al. Plasma miRNA levels for predicting therapeutic response to neoadjuvant treatment in HER2-positive breast cancer: results from the NeoALTTO trial. *Clin Cancer Res* (2019) 25(13):3887–95. doi: 10.1158/1078-0432.CCR-18-2507

161. Wang B, Wang K, Yu J, Hao XM, Liu YL, Xing AY. miR-638 serves as a biomarker of 5-fluorouracil sensitivity to neoadjuvant chemotherapy in breast cancer. *J Breast Cancer* (2022) 25(3):193–206. doi: 10.4048/jbc.2022.25.e24

162. Choi JS, Cho YY. Novel wiring of the AKT-RSK2 signaling pathway plays an essential role in cancer cell proliferation *via* a G. *Biochem Biophys Res Commun* (2023) 642:66–74. doi: 10.1016/j.bbrc.2022.12.048

163. Yu Z, Xu Z, Disante G, Wright J, Wang M, Li Y, et al. miR-17/20 sensitization of breast cancer cells to chemotherapy-induced apoptosis requires Akt1. *Oncotarget* (2014) 5(4):1083–90. doi: 10.18632/oncotarget.1804

164. Zhang F, Lu Y, Wang M, Zhu J, Li J, Zhang P, et al. Exosomes derived from human bone marrow mesenchymal stem cells transfer miR-222-3p to suppress acute myeloid leukemia cell proliferation by targeting IRF2/INPP4B. *Mol Cell Probes* (2020) 51:101513. doi: 10.1016/j.mcp.2020.101513

165. Naseri Z, Oskuee RK, Jaafari MR, Forouzandeh Moghadam M. Exosome-mediated delivery of functionally active miRNA-142-3p inhibitor reduces tumorigenicity of breast cancer *in vitro* and in vivo. *Int J Nanomed* (2018) 13:7727–47. doi: 10.2147/IJN.S182384

166. Yu S, Zhou Y, Niu L, Qiao Y, Yan Y. Mesenchymal stem cell-derived exosome mir-342-3p inhibits metastasis and chemo-resistance of breast cancer through regulating ID4. *Genes Genomics* (2022) 44(5):539–50. doi: 10.1007/s13258-021-01200-1

167. Ye FG, Song CG, Cao ZG, Xia C, Chen DN, Chen L, et al. Cytidine deaminase axis modulated by miR-484 differentially regulates cell proliferation and chemoresistance in breast cancer. *Cancer Res* (2015) 75(7):1504–15. doi: 10.1158/0008-5472.CAN-14-2341

168. Gu X, Xue JQ, Han SJ, Qian SY, Zhang WH. Circulating microRNA-451 as a predictor of resistance to neoadjuvant chemotherapy in breast cancer. *Cancer biomark* (2016) 16(3):395–403. doi: 10.3233/CBM-160578

169. Chin AR, Wang SE. Cancer-derived extracellular vesicles: the 'soil conditioner' in breast cancer metastasis? *Cancer Metastasis Rev* (2016) 35(4):669–76. doi: 10.1007/s10555-016-9639-8

170. Kourembanas S. Exosomes: vehicles of intercellular signaling, biomarkers, and vectors of cell therapy. *Annu Rev Physiol* (2015) 77:13–27. doi: 10.1146/annurev-physiol-021014-071641

171. Chen WX, Xu LY, Qian Q, He X, Peng WT, Fan WQ, et al. D rhamnose β-hederin reverses chemoresistance of breast cancer cells by regulating exosome-mediated resistance transmission. *Biosci Rep* (2018) 38(5). doi: 10.1042/BSR20180110

172. Zhang HF, Xu LY, Li EM. A family of pleiotropically acting microRNAs in cancer progression, miR-200: potential cancer therapeutic targets. *Curr Pharm Des* (2014) 20(11):1896–903. doi: 10.2174/13816128113199990519

173. Yau C, Osdoit M, van der Noordaa M, Shad S, Wei J, de Croze D, et al. Residual cancer burden after neoadjuvant chemotherapy and long-term survival outcomes in breast cancer: a multicentre pooled analysis of 5161 patients. *Lancet Oncol* (2022) 23(1):149–60. doi: 10.1016/S1470-2045(21)00589-1

174. Provenzano E. Neoadjuvant chemotherapy for breast cancer: moving beyond pathological complete response in the molecular age. *Acta Med Acad* (2021) 50(1):88–109. doi: 10.5644/ama2006-124.328

175. Xing AY, Wang B, Li YH, Chen X, Wang YW, Liu HT, et al. Identification of miRNA signature in breast cancer to predict neoadjuvant chemotherapy response. *Pathol Oncol Res* (2021) 27:1609753. doi: 10.3389/pore.2021.1609753

176. McGuire A, Casey MC, Waldron RM, Heneghan H, Kalinina O, Holian E, et al. Prospective assessment of systemic MicroRNAs as markers of response to neoadjuvant chemotherapy in breast cancer. *Cancers (Basel)* (2020) 12(7). doi: 10.3390/cancers12071820

177. Liu B, Su F, Lv X, Zhang W, Shang X, Zhang Y, et al. Serum microRNA-21 predicted treatment outcome and survival in HER2-positive breast cancer patients receiving neoadjuvant chemotherapy combined with trastuzumab. *Cancer Chemother Pharmacol* (2019) 84(5):1039–49. doi: 10.1007/s00280-019-03937-9

178. Di Cosimo S, Appierto V, Pizzamiglio S, Silvestri M, Baselga J, Piccart M, et al. Early modulation of circulating MicroRNAs levels in HER2-positive breast cancer patients treated with trastuzumab-based neoadjuvant therapy. *Int J Mol Sci* (2020) 21(4). doi: 10.3390/ijms21041386

179. Stevic I, Müller V, Weber K, Fasching PA, Karn T, Marmé F, et al. Specific microRNA signatures in exosomes of triple-negative and HER2-positive breast cancer patients undergoing neoadjuvant therapy within the GeparSixto trial. *BMC Med* (2018) 16(1):179. doi: 10.1186/s12916-018-1163-y

180. Kassem NM, Makar WS, Kassem HA, Talima S, Tarek M, Hesham H, et al. Circulating miR-34a and miR-125b as promising non invasive biomarkers in Egyptian locally advanced breast cancer patients. *Asian Pac J Cancer Prev* (2019) 20(9):2749–55. doi: 10.31557/APJCP.2019.20.9.2749

181. García-García F, Salinas-Vera YM, García-Vázquez R, Marchat LA, Rodríguez-Cuevas S, López-González JS, et al. miR–145–5p is associated with pathological complete response to neoadjuvant chemotherapy and impairs cell proliferation by targeting TGFβR2 in breast cancer. *Oncol Rep* (2019) 41(6):3527–34. doi: 10.3892/or.2019.7102

182. Jung EJ, Santarpia L, Kim J, Esteva FJ, Moretti E, Buzdar AU, et al. Plasma microRNA 210 levels correlate with sensitivity to trastuzumab and tumor presence in breast cancer patients. *Cancer* (2012) 118(10):2603–14. doi: 10.1002/cncr.26565

183. Müller V, Gade S, Steinbach B, Loibl S, von Minckwitz G, Untch M, et al. Changes in serum levels of miR-21, miR-210, and miR-373 in HER2-positive breast cancer patients undergoing neoadjuvant therapy: a translational research project within the geparquinto trial. *Breast Cancer Res Treat* (2014) 147(1):61–8. doi: 10.1007/s10549-014-3079-3

184. Xue J, Chi Y, Chen Y, Huang S, Ye X, Niu J, et al. MiRNA-621 sensitizes breast cancer to chemotherapy by suppressing FBXO11 and enhancing p53 activity. *Oncogene* (2016) 35(4):448–58. doi: 10.1038/onc.2015.96

185. Al-Khanbashi M, Caramuta S, Alajmi AM, Al-Haddabi I, Al-Riyami M, Lui WO, et al. Tissue and serum miRNA profile in locally advanced breast cancer (LABC) in response to neo-adjuvant chemotherapy (NAC) treatment. *PloS One* (2016) 11(4):e0152032. doi: 10.1371/journal.pone.0152032

186. Zhu W, Liu M, Fan Y, Ma F, Xu N, Xu B. Dynamics of circulating microRNAs as a novel indicator of clinical response to neoadjuvant chemotherapy in breast cancer. *Cancer Med* (2018) 7(9):4420–33. doi: 10.1002/cam4.1723

187. Kahraman M, Röske A, Laufer T, Fehlmann T, Backes C, Kern F, et al. MicroRNA in diagnosis and therapy monitoring of early-stage triple-negative breast cancer. *Sci Rep* (2018) 8(1):11584. doi: 10.1038/s41598-018-29917-2

188. Lindholm EM, Ragle Aure M, Haugen MH, Kleivi Sahlberg K, Kristensen VN, Nebdal D, et al. miRNA expression changes during the course of neoadjuvant bevacizumab and chemotherapy treatment in breast cancer. *Mol Oncol* (2019) 13(10):2278–96. doi: 10.1002/1878-0261.12561

189. Rodríguez-Martínez A, de Miguel-Pérez D, Ortega FG, García-Puche JL, Robles-Fernández I, Exposito J, et al. Exosomal miRNA profile as complementary tool in the diagnostic and prediction of treatment response in localized breast cancer under neoadjuvant chemotherapy. *Breast Cancer Res* (2019) 21(1):21. doi: 10.1186/s13058-019-1109-0

190. Zhang S, Wang Y, Peng J, Yuan C, Zhou L, Xu S, et al. Serum miR-222-3p as a double-edged sword in predicting efficacy and trastuzumab-induced cardiotoxicity for HER2-positive breast cancer patients receiving neoadjuvant target therapy. *Front Oncol* (2020) 10:631. doi: 10.3389/fonc.2020.00631

191. Svoronos AA, Engelman DM, Slack FJ. OncomiR or tumor suppressor? the duplicity of MicroRNAs in cancer. *Cancer Res* (2016) 76(13):3666–70. doi: 10.1158/0008-5472.CAN-16-0359

192. Menon A, Abd-Aziz N, Khalid K, Poh CL, Naidu R. miRNA: a promising therapeutic target in cancer. *Int J Mol Sci* (2022) 23(19). doi: 10.3390/ijms231911502

193. Mollaei H, Safaralizadeh R, Rostami Z. MicroRNA replacement therapy in cancer. *J Cell Physiol* (2019) 234(8):12369–84. doi: 10.1002/jcp.28058

194. Park EY, Chang E, Lee EJ, Lee HW, Kang HG, Chun KH, et al. Targeting of miR34a-NOTCH1 axis reduced breast cancer stemness and chemoresistance. *Cancer Res* (2014) 74(24):7573–82. doi: 10.1158/0008-5472.CAN-14-1140

195. Elghoroury EA, ElDine HG, Kamel SA, Abdelrahman AH, Mohammed A, Kamel MM, et al. Evaluation of miRNA-21 and miRNA let-7 as prognostic markers in patients with breast cancer. *Clin Breast Cancer* (2018) 18(4):e721–e6. doi: 10.1016/j.clbc.2017.11.022

196. Yu F, Deng H, Yao H, Liu Q, Su F, Song E. Mir-30 reduction maintains self-renewal and inhibits apoptosis in breast tumor-initiating cells. *Oncogene* (2010) 29(29):4194–204. doi: 10.1038/onc.2010.167

197. Mutlu M, Raza U, Saatci Ö, Eyüpoğlu E, Yurdusev E, Şahin Ö. miR-200c: a versatile watchdog in cancer progression, EMT, and drug resistance. *J Mol Med (Berl)* (2016) 94(6):629–44. doi: 10.1007/s00109-016-1420-5

198. Kalinowski FC, Brown RA, Ganda C, Giles KM, Epis MR, Horsham J, et al. microRNA-7: a tumor suppressor miRNA with therapeutic potential. *Int J Biochem Cell Biol* (2014) 54:312–7. doi: 10.1016/j.biocel.2014.05.040

199. Langer C, Rücker FG, Buske C, Döhner H, Kuchenbauer F. Targeted therapies through microRNAs: pulp or fiction? *Ther Adv Hematol* (2012) 3(2):97–104. doi: 10.1177/2040620711432582

200. Li D, Wang X, Yang M, Kan Q, Duan Z. miR3609 sensitizes breast cancer cells to adriamycin by blocking the programmed death-ligand 1 immune checkpoint. *Exp Cell Res* (2019) 380(1):20–8. doi: 10.1016/j.yexcr.2019.03.025

201. Lin Y, Lin F, Anuchapreeda S, Chaiwongsa R, Duangmano S, Ran B, et al. Effect of miR-133b on progression and cisplatin resistance of triple-negative breast cancer through FGFR1-wnt-β-catenin axis. *Am J Transl Res* (2021) 13(6):5969–84.

202. Mei M, Ren Y, Zhou X, Yuan XB, Han L, Wang GX, et al. Downregulation of miR-21 enhances chemotherapeutic effect of taxol in breast carcinoma cells. *Technol Cancer Res Treat* (2010) 9(1):77–86. doi: 10.1177/153303461000900109

203. Møller HG, Rasmussen AP, Andersen HH, Johnsen KB, Henriksen M, Duroux M. A systematic review of microRNA in glioblastoma multiforme: micro-modulators in the mesenchymal mode of migration and invasion. *Mol Neurobiol* (2013) 47(1):131–44. doi: 10.1007/s12035-012-8349-7

204. Trang P, Wiggins JF, Daige CL, Cho C, Omotola M, Brown D, et al. Systemic delivery of tumor suppressor microRNA mimics using a neutral lipid emulsion inhibits lung tumors in mice. *Mol Ther* (2011) 19(6):1116–22. doi: 10.1038/mt.2011.48

205. Schneider MR. MicroRNAs as novel players in skin development, homeostasis and disease. *Br J Dermatol* (2012) 166(1):22–8. doi: 10.1111/j.1365-2133.2011.10568.x

206. He XX, Chang Y, Meng FY, Wang MY, Xie QH, Tang F, et al. MicroRNA-375 targets AEG-1 in hepatocellular carcinoma and suppresses liver cancer cell growth *in vitro* and in vivo. *Oncogene* (2012) 31(28):3357–69. doi: 10.1038/onc.2011.500

207. Lennox KA, Behlke MA. Chemical modification and design of anti-miRNA oligonucleotides. *Gene Ther* (2011) 18(12):1111–20. doi: 10.1038/gt.2011.100

208. Zhou LY, Qin Z, Zhu YH, He ZY, Xu T. Current RNA-based therapeutics in clinical trials. *Curr Gene Ther* (2019) 19(3):172–96. doi: 10.2174/1566523219666190719100526

209. Kasar S, Salerno E, Yuan Y, Underbayev C, Vollenweider D, Laurindo MF, et al. Systemic *in vivo* lentiviral delivery of miR-15a/16 reduces malignancy in the NZB *de*

novo mouse model of chronic lymphocytic leukemia. *Genes Immun* (2012) 13(2):109–19. doi: 10.1038/gene.2011.58

210. Yin H, Kanasty RL, Eltoukhy AA, Vegas AJ, Dorkin JR, Anderson DG. Non-viral vectors for gene-based therapy. *Nat Rev Genet* (2014) 15(8):541–55. doi: 10.1038/nrg3763

211. Fernandez-Piñeiro I, Badiola I, Sanchez A. Nanocarriers for microRNA delivery in cancer medicine. *Biotechnol Adv* (2017) 35(3):350–60. doi: 10.1016/j.biotechadv.2017.03.002

212. Jones CH, Chen CK, Ravikrishnan A, Rane S, Pfeifer BA. Overcoming nonviral gene delivery barriers: perspective and future. *Mol Pharm* (2013) 10(11):4082–98. doi: 10.1021/mp400467x

213. Janssen HL, Reesink HW, Lawitz EJ, Zeuzem S, Rodriguez-Torres M, Patel K, et al. Treatment of HCV infection by targeting microRNA. *N Engl J Med* (2013) 368(18):1685–94. doi: 10.1056/NEJMoa1209026

214. Ling H, Fabbri M, Calin GA. MicroRNAs and other non-coding RNAs as targets for anticancer drug development. *Nat Rev Drug Discovery* (2013) 12(11):847–65. doi: 10.1038/nrd4140

215. Stylianopoulos T, Jain RK. Combining two strategies to improve perfusion and drug delivery in solid tumors. *Proc Natl Acad Sci U S A* (2013) 110(46):18632–7. doi: 10.1073/pnas.1318415110

216. Raemdonck K, Vandenbroucke RE, Demeester J, Sanders NN, De Smedt SC. Maintaining the silence: reflections on long-term RNAi. *Drug Discovery Today* (2008) 13(21-22):917–31. doi: 10.1016/j.drudis.2008.06.008

217. Yu B, Zhao X, Lee LJ, Lee RJ. Targeted delivery systems for oligonucleotide therapeutics. *AAPS J* (2009) 11(1):195–203. doi: 10.1208/s12248-009-9096-1

218. Garzon R, Marcucci G, Croce CM. Targeting microRNAs in cancer: rationale, strategies and challenges. *Nat Rev Drug Discovery* (2010) 9(10):775–89. doi: 10.1038/nrd3179

219. Judge AD, Sood V, Shaw JR, Fang D, McClintock K, MacLachlan I. Sequence-dependent stimulation of the mammalian innate immune response by synthetic siRNA. *Nat Biotechnol* (2005) 23(4):457–62. doi: 10.1038/nbt1081

220. Ceppi M, Pereira PM, Dunand-Sauthier I, Barras E, Reith W, Santos MA, et al. MicroRNA-155 modulates the interleukin-1 signaling pathway in activated human monocyte-derived dendritic cells. *Proc Natl Acad Sci U S A* (2009) 106(8):2735–40. doi: 10.1073/pnas.0811073106

221. Lehmann SM, Krüger C, Park B, Derkow K, Rosenberger K, Baumgart J, et al. An unconventional role for miRNA: let-7 activates toll-like receptor 7 and causes neurodegeneration. *Nat Neurosci* (2012) 15(6):827–35. doi: 10.1038/nn.3113

222. van Dongen S, Abreu-Goodger C, Enright AJ. Detecting microRNA binding and siRNA off-target effects from expression data. *Nat Methods* (2008) 5(12):1023–5. doi: 10.1038/nmeth.1267

223. Macfarlane LA, Murphy PR. MicroRNA: biogenesis, function and role in cancer. *Curr Genomics* (2010) 11(7):537–61. doi: 10.2174/138920210793175895

224. Ho JJ, Metcalf JL, Yan MS, Turgeon PJ, Wang JJ, Chalsev M, et al. Functional importance of dicer protein in the adaptive cellular response to hypoxia. *J Biol Chem* (2012) 287(34):29003–20. doi: 10.1074/jbc.M112.373365

225. Vicentini FT, Borgheti-Cardoso LN, Depieri LV, de Macedo Mano D, Abelha TF, Petrilli R, et al. Delivery systems and local administration routes for therapeutic siRNA. *Pharm Res* (2013) 30(4):915–31. doi: 10.1007/s11095-013-0971-1

226. Schmid P, Adams S, Rugo HS, Schneeweiss A, Barrios CH, Iwata H, et al. Atezolizumab and nab-paclitaxel in advanced triple-negative breast cancer. *N Engl J Med* (2018) 379(22):2108–21. doi: 10.1056/NEJMoa1809615

227. Tutt ANJ, Garber JE, Kaufman B, Viale G, Fumagalli D, Rastogi P, et al. Adjuvant olaparib for patients with. *N Engl J Med* (2021) 384(25):2394–405. doi: 10.1056/NEJMoa2105215

Glossary

miRNAs	MicroRNAs
BC	breast cancer
LABC	Luminal A Breast Cancer
LBBC	Luminal B Breast Cancer
HER2+	Human Epidermal Growth Factor Receptor-2 Enriched Breast Cancer
TNBC	Triple-Negative Breast Cancer
MAPK	mitogen-activated protein kinase
PI3K	Phosphoinositide 3-Kinase
mTOR	Mammalian Target of Rapamycin
ER	Estrogen Receptor
Pol II	RNA polymerase II
pre-miRNAs	Precursor miRNAs
Exp5	Exportin-5
RISC	RNA-induced silencing complex
CMF	Cyclophosphamide
methotrexate	and 5-fluorouracil
NAC	Neoadjuvant chemotherapy
BCS	Breast Conservation Surgery
EBCTCG	The Early Breast Cancer Triallist's Collaborative Group
LRR	Locoregional Recurrence
DFS	Disease-Free Survival
OS	Overall Survival
pCR	Pathological Complete Response
LN	Lymph node
ASCO	American Society of Clinical Oncology
EMT	Epithelial-Mesenchymal Transition
MiniPDXTM	Minimal Patient-Derived Xenograft
PTEN	Phosphatase and TENsin homolog
5-FU	5-fluorouracil
MSCs-Exo	Mesenchymal Stem Cell-Derived Exosome
ID4	Inhibitor of Differentiation 4
CDA	Cytosine Deaminase
MCF-7/DTX	Docetaxel-Resistant MCF-7 BC cell line
DOX	Doxorubicin
MCF-7/EPB	Epirubicin-Resistant MCF-7 BC cell line
ADR	Adriamycin
EIF4E	Eukaryotic Translation Initiation Factor 4E
EFS	Event-Free Survival
BCL-2	B-cell Leukemia/Lymphoma 2 Protein
CCND1	Cyclin D1 protein
DCTD	dCMP Deaminase
HIF-1	Hypoxia-inducible factor-1
DTX	Docetaxel
EPB	Epirubicin
GCB	Gemcitabine
ct-miRNA	circulating miRNA
EMT	epithelial-mesenchymal transition
MDR1	Multidrug Resistance gene
P-gp	P-glyocoprotein
GST-π	glutathione S-transferase
MRP	multidrug resistance-associated protein
ABC	ATP-binding cassette transporters
BCRP	breast cancer resistance protein
EGFR	epidermal growth factor receptor
CSCs	Cancer stem cells
DDR	DNA damage repair

frontiers | Frontiers in Oncology

TYPE Original Research
PUBLISHED 19 June 2023
DOI 10.3389/fonc.2023.1136380

OPEN ACCESS

EDITED BY
Chunyan Dong,
Tongji University, China

REVIEWED BY
Marzia Locatelli,
European Institute of Oncology (IEO), Italy
Pablo Mandó,
Norberto Quirno Medical Education and Clinical Research Center (CEMIC), Argentina

*CORRESPONDENCE
Zhiyong Yu
zyyu@sdfmu.edu.cn
Xinzhao Wang
08wangxinzhao@163.com

†These authors share first authorship

RECEIVED 03 January 2023
ACCEPTED 05 June 2023
PUBLISHED 19 June 2023

CITATION
Liu X, Zhang P, Li C, Song X, Liu Z, Shao W, Li S, Wang X and Yu Z (2023) Efficacy and safety of inetetamab-containing regimens in patients with HER2-positive metastatic breast cancer: a real-world retrospective study in China.
Front. Oncol. 13:1136380.
doi: 10.3389/fonc.2023.1136380

Efficacy and safety of inetetamab-containing regimens in patients with HER2-positive metastatic breast cancer: a real-world retrospective study in China

Xiaoyu Liu[1†], Peng Zhang[2†], Chao Li[3], Xiang Song[1,3], Zhaoyun Liu[3], Wenna Shao[1], Sumei Li[4], Xinzhao Wang[3,5*] and Zhiyong Yu[1,3*]

[1]First Clinical Medical College, Shandong University of Traditional Chinese Medicine, Jinan, China, [2]Department of General Surgery, Zouping People's Hospital, Binzhou, China, [3]Breast Cancer Center, Shandong Cancer Hospital and Institute, Shandong First Medical University and Shandong Academy of Medical Sciences, Jinan, China, [4]College of Traditional Chinese Medicine, Shandong University of Traditional Chinese Medicine, Jinan, China, [5]REMEGEN, LTD, Yantai Economic & Technological Development Area, Yantai, China

Background: Inetetamab (cipterbin) is an innovative anti-HER2 humanized monoclonal antibody. The efficacy and safety of a combination of inetetamab and vinorelbine in the first-line treatment of human epidermal receptor positive (HER2+) metastatic breast cancer (MBC) have been confirmed. We aimed to investigate real-world data of inetetamab in complex clinical practice.

Methods: We retrospectively reviewed the medical records of patients who received inetetamab as a salvage treatment at any line setting from July 2020 to June 2022. The main endpoint was progression-free survival (PFS).

Results: A total of 64 patients were included in this analysis. The median progression-free survival (mPFS) was 5.6 (4.6–6.6) months. Of the patients, 62.5% received two or more lines of therapy before treatment with inetetamab. The most common chemotherapy and anti-HER2 regimens combined with inetetamab were vinorelbine (60.9%) and pyrotinib (62.5%), respectively. Patients treated with inetetamab plus pyrotinib plus vinorelbine benefited the most (p=0.048), with the mPFS of 9.3 (3.1–15.5) months and an objective response rate of 35.5%. For patients with pyrotinib pretreatment, inetetamab plus vinorelbine plus pyrotinib agents resulted in mPFS of 10.3 (5.2–15.4) months. Regimens (inetetamab plus vinorelbine plus pyrotinib vs. other therapeutic agents) and visceral metastases (yes vs. no) were independent predictors of PFS. Patients with visceral metastases treated with inetetamab plus vinorelbine plus pyrotinib had a mPFS of 6.1(5.1–7.1) months. The toxicity of inetetamab was tolerable, with the most common grade 3/4 adverse event being leukopenia (4.7%).

Conclusions: HER2+ MBC patients pretreated with multiple-line therapies still respond to inetetamab-based treatment. Inetetamab combined with vinorelbine and pyrotinib may be the most effective treatment regimen, with a controllable and tolerable safety profile.

KEYWORDS

breast cancer, inetetamab, human epidermal receptor 2 positive, monoclonal antibody, real-word data

1 Introduction

Breast cancer(BC) is the most common cancer and a leading cause of death among women worldwide (1). There are three major breast cancer subtypes: hormone receptor positive(estrogen receptor (ER) positive or progesterone receptor(PR) positive), human epidermal receptor 2 (HER2) positive (HER2+) and triple negative breast cancer (ER negative, PR negative, HER2 negative) (2). HER2 is a transmembrane receptor tyrosine kinase in the epidermal growth factor receptor family that is amplified or overexpressed in approximately 20% of breast cancers, and is associated with poor prognosis in the absence of systemic therapy (3). HER2+ ductal tumors are associated with the presence of calcifications, as well as high tumor grade and increased likelihood of spread to the lymph nodes (4, 5). Without the development and widespread use of anti-HER2-targeted drugs, HER2+ BC is an aggressive disease and has poor prognosis (6). Although huge progresses have been achieved in the last few years in understanding and treating HER2+ breast cancer, they remain a disproportionate health burden to patients and huge unmet need (7). Especially, HER2+ metastatic breast cancer(MBC) remains incurable, and novel treatment options are needed. Many anti-HER2-targeted drugs have been applied successfully in clinical or currently under review in recent years. Antibody–drug conjugates (ADC) drugs are on rise and provides novel therapeutic advancements in the management of HER2+ MBC (8). But in China, they are expensive and not included in medical insurance which limited their usage.

The innovative drug of recombinant anti-HER2 humanized monoclonal antibody (inetetamab, Cipterbin) for injection independently researched and developed in China is a non-biological analog drug produced by Sansheng Guojian Pharmaceutical (Shanghai) Co., Ltd. (formerly CITIC Guojian Pharmaceutical Co., Ltd.) and approved by the State Food and Drug Administration of China for clinical research on July 2, 2004 (Approval No. 2004L02352). Inetetamab is a monoclonal antibody binding to domain IV of HER2 receptor. The Fab domain of inetetamab is identical with trastuzumab, but whose amino acid sequence at positions 359 (D359, aspartic acid) and 361 (L361, leucine) is different from trastuzumab (E359 (glutamate) and M361 (methionine), respectively) in the constant region of the heavy chain of the Fc domain (9). Previous study confirmed the significant efficacy and good safety of the combination of cipterbin and vinorelbine in the first-line treatment of HER2 positive advanced breast cancer patients who had not received anti-HER2-targeted therapy after previous taxus treatment (10).

Based on the current situation of clinical treatment and needs, we conducted a retrospective study to fill a knowledge gap by investigating the efficacy of inetetamab for HER2+ recurrent and metastatic breast cancer patients pretreated with multi-lines treatment.

2 Material and methods

2.1 Subjects and study design

This retrospective, single-center study enrolled patients with HER2+ MBC treated with inetetamab at Shandong Frist Medical University and Shandong Academy of Medical Sciences between July 2020 and June 2022. The Ethics Committee and Institutional Review Board of Shandong First Medical University and Shandong Academy of Medical Sciences approved this study (SDTHEC2022012020). All investigations were conducted in accordance with the Declaration of Helsinki.

2.2 Patients

The inclusion criteria for participants were as follows: female sex, age ≥18 years, histologically or cytologically confirmed MBC with documentation of HER2 overexpression, prior trastuzumab therapy with or without other HER2-targeted treatment, at least one cycle of inetetamab, and complete medical records. The exclusion criteria were non-measurable or non-evaluable lesions and those lost to follow-up. There were no limits to the number of prior cytotoxic regimens for metastatic diseases. The last follow-up was conducted in November 2022. Until the last follow-up date, patients who were lost to follow-up were considered as censored data. All data were retrospectively collected from medical records and laboratory results. Patients or their family members (for patients who already died at the study initiation) provided signed informed consent or oral agreement with tape recording.

2.3 Assessments

The characteristics of the patients at the time of initial diagnosis (including age, ECOG performance status, and menstrual status),

tumor characteristics (including tumor size, lymph node involvement, grade, histology, and receptor status), treatment regimen in the (neo)adjuvant and metastatic settings (including chemotherapy, anti-HER2, endocrine regimen, surgery, radiotherapy, dose reductions or delays, etc.) were extracted from electronic medical records. Hormone receptor (HR) was defined as estrogen receptor (ER) and/or progesterone receptor (PR) positivity (ER and PR were determined by at least 10% of positively stained nuclei). HER2 positivity was defined as an immunohistochemistry (IHC) score of 3+ or 2+ together with HER2 gene amplification verified by fluorescence *in situ* hybridization(FISH+). Disease-free interval (DFI) was defined as the time from surgery to diagnosis of metastasis.

Clinical response was evaluated using computed tomography, magnetic resonance imaging, and physical examination according to the Response Evaluation Criteria in Solid Tumors, version 1.1. The main endpoint was progression-free survival (PFS), defined as the time from treatment initiation until disease progression or death. Other endpoints included the objective response rate (ORR), clinical benefit rate (CBR), and safety. ORR was defined as the proportion of patients who achieved a complete response (CR) or partial response (PR). CBR was defined as the proportion of patients who achieved CR, PR, or stable disease (SD). Adverse events (AEs) were graded based on the National Cancer Institute Common Terminology Criteria for AEs, version 4.0.

2.4 Statistical analyses

The median (range) or percentage of patients was used to represent the clinicopathological characteristics. Continuous variables were analyzed by One-way ANOVA. Categorical variables were assessed by the Pearson's chi-squared test or Fisher's exact test. The Kaplan–Meier method was used to estimate PFS. Additionally, Cox univariable model was employed to assess the covariate effects on PFS, and then Cox multivariate models were used to assess the factors with relative significant p-values($p \leq 0.1$) in univariate analysis to PFS with hazard ratios(HR.) and corresponding 95% confidence intervals (CIs). Statistical significance for all analyses was set at $p<0.05$. GraphPad Prism 9.3.1 software was used to perform all statistical analyses.

3 Results

3.1 Patients and treatments

A total of 69 patients with HER2+ MBC treated with inetetamab were recruited. After considering the exclusion criteria, 64 (92.8%) patients were included in the study (Figure 1).

The baseline characteristics are presented in Table 1. The median age of the patients at diagnosis was 46 years (range: 27–67 years), 54 (84.4%) underwent surgery, 14 patients (21.9%) had stage IV BC as their first diagnosis. Moreover, 53.1% of the patients had more than two metastatic sites, with the four most common metastatic sites being the lymph node (48.4%), local sites (35.9%), bone (32.8%), and liver (32.8%). Half of the patients had visceral metastases, whereas 13 (20.3%) had brain metastases. All patients had been exposed to anti-HER2 therapy, with 64.1% prescribed pyrotinib and 18.8% with lapatinib. More than four-fifths of the patients received trastuzumab during salvage treatment. Furthermore, 62.5% of patients received two or more lines of systemic therapy before inetetamab. These results suggest that, in a real-world setting, patients receiving inetetamab are more likely to be heavily pretreated.

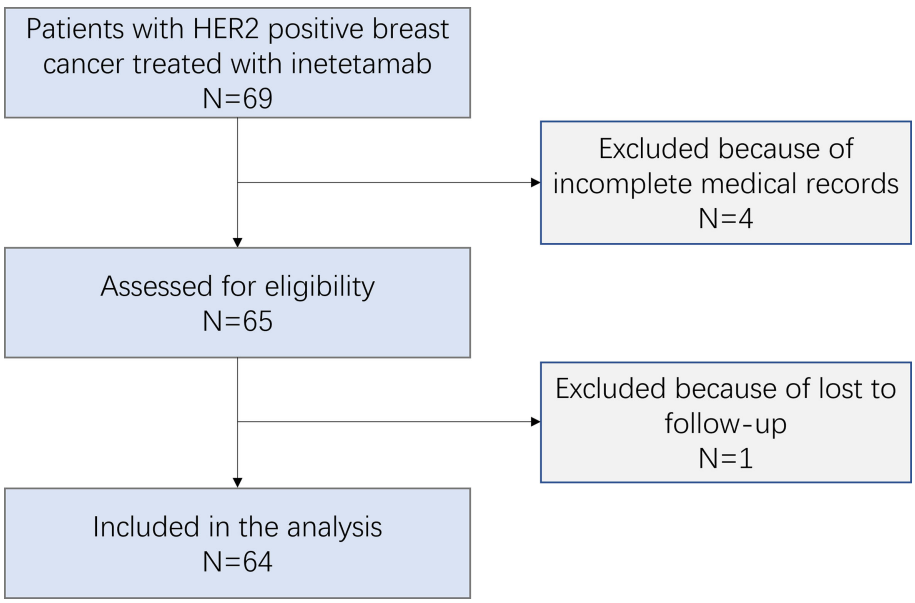

FIGURE 1
Patient's profile.

TABLE 1 Baseline characteristics of patients.

Characteristics	Patients, No (%) N = 64
Age, median (range years)	46 (27-67)
Menstrual status	
pre	38 (59.4)
post	26 (40.6)
ECOG performance status	
0-1	52 (81.3)
≥2	12 (18.8)
Pathological type	
Invasive ductal cancer	62 (96.9)
Invasive lobular cancer	2 (3.1)
HER2 expression	
IHC2+ and FISH+	13 (20.3)
IHC3+	51 (79.7)
HR status at metastatic setting	
Positive	29 (45.3)
Negative	35 (54.7)
Surgery	
No	10 (15.6)
Yes	54 (84.4)
Radiotherapy	
No	35 (54.7)
Yes	29 (45.3)
Endocrine therapy	
No	41 (64.1)
Yes	23 (35.9)
DFI (month)	
≤12	16 (25.0)
>12	34 (53.1)
De novo IV stage	14 (21.9)
Previous trastuzumab treatment	
Neoadjuvant setting	5 (7.8)
Adjuvant setting	22 (34.4)
Metastatic setting	52 (81.3)
Previous anti-HER2 drugs	
Pyrotinib	41 (64.1)
Pertuzumab	10 (15.6)
TDM-1	2 (3.1)
Aptinib	2 (3.1)
Lapatinib	12 (18.8)
Anlotinib	1 (1.6)
Number of sites in primary recurrence	
1	34 (53.1)
>1	30 (46.9)
Lines of inetetamab in metastatic setting	
1	3 (4.7)
2	21 (32.8)
≥3	40 (62.5)
Number of sites before inetetamab	
1	21 (32.8)
2	9 (14.1)
≥3	34 (53.1)
Metastatic sites before inetetamab	
Local sites	23 (35.9)
Lymph node	31 (48.4)
Bone	21 (32.8)
Brain	13 (20.3)
Lung	15 (23.4)
Liver	21 (32.8)
Others	11 (17.2)
Visceral metastases	
Yes	32 (50.0)
No	32 (50.0)

3.2 Treatment administration

The treatment regimens are shown in Table 2. Most patients were treated with inetetamab in combination with chemotherapy and/or other HER2-targeted therapies. The most common chemotherapy regimens were vinorelbine (n = 39, 60.9%) and abraxane (n = 15, 23.4%). Pyrotinib and inetetamab in combination were administered to 40 (62.5%) patients. Meanwhile, three (3.1%) patients received inetetamab and brain radiotherapy but did not receive any other anti-cancer drugs.

3.3 Treatment efficacy in overall patients

All patients were evaluated for PFS. The median follow-up time was 14.3(12.7–15.9) months. The median progression-free survival (mPFS) was 5.6 (4.6–6.6) months and the ORR was 26.6% (Figure 2A).

TABLE 2 Treatment administration.

Treatment administration	Patients, No (%) N = 64
Combined regimens with inetetamab	
Vinorelbine	39 (60.9)
Abraxane	15 (23.4)
Other	7 (10.9)
No	3 (3.1)
Target regimens with inetetamab	
Pyrotinib	40 (62.5)
Pertuzumab	6 (9.4)
Alone	18 (28.1)

Patients who received inetetamab-based therapy as first and later lines of metastatic treatment had a median PFS of 5.7 (1.9–9.5) and 5.3 (3.8–6.8) months, respectively (Figure 2B). Thirty-two patients with visceral metastases showed a median PFS of 5.3 (3.9–6.7) months. A total of 31 patients with lymph node metastases, 23 patients with local metastases, 21 patients with bone metastases and 13 patients with brain metastases had median PFS of 5.7 (0.5–10.9) months, 7.0 (0.8–13.2) months, 4.1(3.4–4.8) months and 4.2 (2.0–6.4) months, respectively (Figure 2C).

To determine the best combination for inetetamab, we firstly investigated the anti-HER2 treatment in the overall cohort. Baseline characteristics were analyzed in Supplementary Tables 1-3. The median PFSs among inetetamab plus pyrotinib, inetetamab plus pertuzumab and inetetamab alone were 6.1 (2.5–9.7) months, 2.5 (1.9–3.1) months, and 5.3 (4.6–6.6) months, respectively. Inetetamab plus pyrotinib was the best combination among the three groups (p=0.005) (Figure 3A). However, the age of patients treated with inetetamab plus pertuzumab is relatively old than other two cohorts(p=0.001) and 6 patients(100%) received at least 3 lines of rescue treatment(p=0.016), which led to the unbalanced baseline characteristics among three cohorts. As vinorelbine and abraxane were the most common combined cytotoxic drugs, we compared the PFS of different chemotherapies. The median PFSs among inetetamab plus vinorelbine, inetetamab plus abraxane and inetetamab plus other therapeutic agents were 5.7 (3.7-7.7) months, 5.7 (4.4–7.0) months, and 4.0 (1.4–6.6) months, respectively (Figure 3B). Furthermore, we compared the efficacy of the combination treatments. The median PFS of inetetamab plus pyrotinib plus vinorelbine was 9.3 (3.1–15.5) months; inetetamab plus pyrotinib plus abraxane, 5.6(0-13.6) months; and inetetamab plus other therapeutic agents, 4.1 (3.0–5.2) months. There were statistically significant differences among the three groups (p = 0.048) (Figure 3C). These findings indicate that inetetamab plus pyrotinib plus vinorelbine may be the most effective inetetamab-based regimen. Thirty-one (48.4%) patients received inetetamab plus pyrotinib plus vinorelbine. The subgroup of patients achieved an ORR of 35.5% and CBR of 48.4%, with CR achieved in three patients, PR achieved in eight patients, and SD achieved in four patients (Figure 3C).

3.4 Efficacy of inetetamab-based therapy in certain drugs pretreated patients

Thirty-five patients received vinorelbine before inetetamab-based therapy. The mPFS of patients with versus without vinorelbine pretreatment was 5.7 (4.0–7.4) months versus 5.6 (3.5–7.7) months, respectively (p=0.750) (Figure 4A). Forty-one patients received pyrotinib before inetetamab-based therapy. The mPFS of patients with versus without pyrotinib pretreatment was 5.7 (3.5–7.9) months versus 5.3 (3.3–7.3) months, respectively (p=0.988) (Figure 4B). These results indicate that the medication history of vinorelbine and/or pyrotinib had no influence on the efficacy of the drug.

We also analyzed the PFS of the patients pretreated with pyrotinib (Figure 4C). A total of 41 patients were included in this subgroup analysis, with an ORR of 29.3%. Two patients achieved CR and 10 patients achieved PR. Patients exposed to inetetamab plus vinorelbine plus pyrotinib agent had significantly longer PFS (10.3 (5.2–15.4) months) than those exposed to other therapeutic agents (4.0 (2.0–6.0) months) (p=0.018).

3.5 Efficacy in patients with visceral metastasis

The univariate analysis indicated that age group (<40 vs. ≥40 years), menstrual status (pre vs. post), hormone receptor status (negative vs. positive), and regimens (inetetamab plus vinorelbine

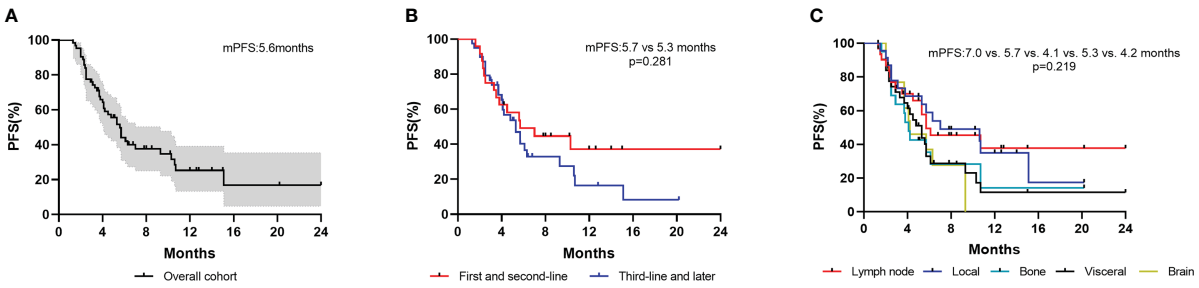

FIGURE 2
Kaplan–Meier curves of PFS for patients. **(A)** Overall cohort; **(B)** Patients stratified by treatment lines; **(C)** Patients with different metastatic sites.

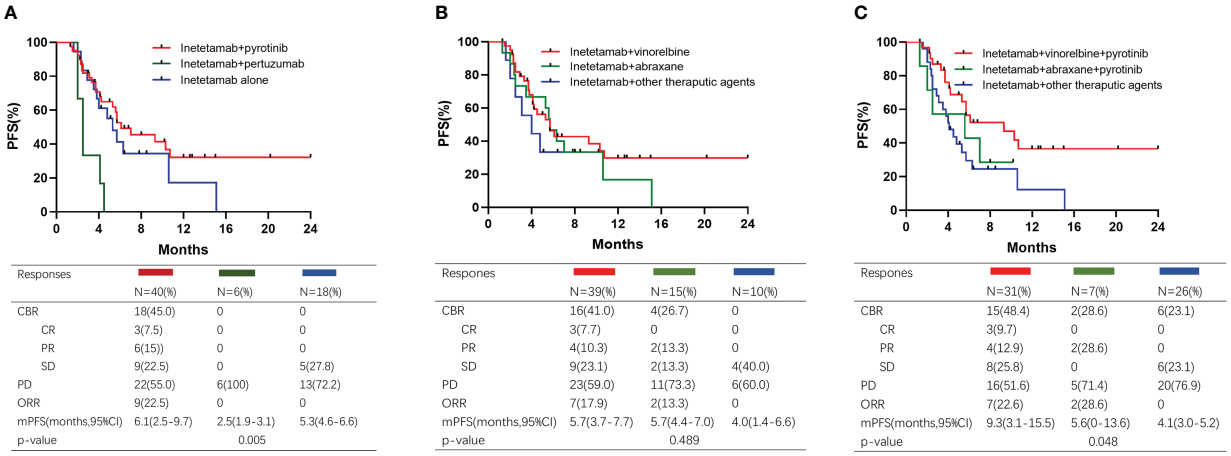

Responses	N=40(%)	N=6(%)	N=18(%)
CBR	18(45.0)	0	0
CR	3(7.5)	0	0
PR	6(15))	0	0
SD	9(22.5)	0	5(27.8)
PD	22(55.0)	6(100)	13(72.2)
ORR	9(22.5)	0	0
mPFS(months,95%CI)	6.1(2.5-9.7)	2.5(1.9-3.1)	5.3(4.6-6.6)
p-value		0.005	

Respones	N=39(%)	N=15(%)	N=10(%)
CBR	16(41.0)	4(26.7)	0
CR	3(7.7)	0	0
PR	4(10.3)	2(13.3)	0
SD	9(23.1)	2(13.3)	4(40.0)
PD	23(59.0)	11(73.3)	6(60.0)
ORR	7(17.9)	2(13.3)	0
mPFS(months,95%CI)	5.7(3.7-7.7)	5.7(4.4-7.0)	4.0(1.4-6.6)
p-value		0.489	

Respones	N=31(%)	N=7(%)	N=26(%)
CBR	15(48.4)	2(28.6)	6(23.1)
CR	3(9.7)	0	0
PR	4(12.9)	2(28.6)	0
SD	8(25.8)	0	6(23.1)
PD	16(51.6)	5(71.4)	20(76.9)
ORR	7(22.6)	2(28.6)	0
mPFS(months,95%CI)	9.3(3.1-15.5)	5.6(0-13.6)	4.1(3.0-5.2)
p-value		0.048	

FIGURE 3
Kaplan–Meier curves of PFS and responses for different treatment. **(A)** Patients treated with different dual anti-HER2 therapy; **(B)** Patients treated with different chemotherapy; **(C)** Patients treated with different combined regimens.

plus pyrotinib vs. other therapeutic agents) were correlated with PFS ($p<0.05$). Next, we constructed a multivariate model with the above factors, ECOG performance status(0-1 vs ≥2) and visceral metastasis (yes vs. no) as covariates for PFS (Table 3). After adjustment, Cox multivariate regression analysis showed that the regimens (inetetamab plus vinorelbine plus pyrotinib vs. other therapeutic agents) and visceral metastasis (yes vs. no) were independent predictors of PFS (Table 3).

Thirty-two patients (50.0%) exhibited visceral metastasis. Patients with and without visceral metastases had PFS times of 5.3 months and 7.0 months, respectively (Figure 5A). Of the 32 patients, 18 received inetetamab plus vinorelbine plus pyrotinib treatment, with an ORR of 27.8% and a CBR of 33.3%. One patient achieved CR, four achieved PR, and one achieved SD. The median PFS was significantly different for patients who underwent inetetamab plus vinorelbine plus pyrotinib or other therapeutic agents (6.1 (5.1–7.1) vs. 2.9-(0.9–4.9) months, p=0.002; Figure 5B).

3.6 Safety assessment

The safety assessments of etamab-based therapy are listed in Table 4. After the initial etamab-based therapy, 10 (15.6%) patients in the inetetamab group experienced a dose reduction, and two (3.1%) patients interrupted the treatment. The most common grade 3/4 AEs were leukopenia (4.7%) and neutropenia (3.1%). No treatment-related deaths were reported. Overall, the results show that the safety of etamab-based therapy is controllable and tolerable.

4 Discussion

This study revealed the real-world clinical practice of inetetamab in HER2+ MBC patients after trastuzumab-based treatment. Previously, the efficacy and safety of inetetamab in combination with chemotherapy as first-line treatment of HER2+ MBC was evaluated (9). But the above study of inetetamab was designed for patients who did not receive any anti-HER2 drugs. Therefore, the role of inetetamab in more heavily treated patients needs further study. To the best of our knowledge, this is the first investigation of the effectiveness of inetetamab in HER2+ MBC patients pretreated with multiline anti-HER2 treatment. Our cohort represented the general population of patients with HER2+ MBC who were usually heavily treated with multiple anti-HER2 agents. Yet, our cohort included a low percentage of patients receiving TDM1(3.1%) and no patient receiving new drugs such as

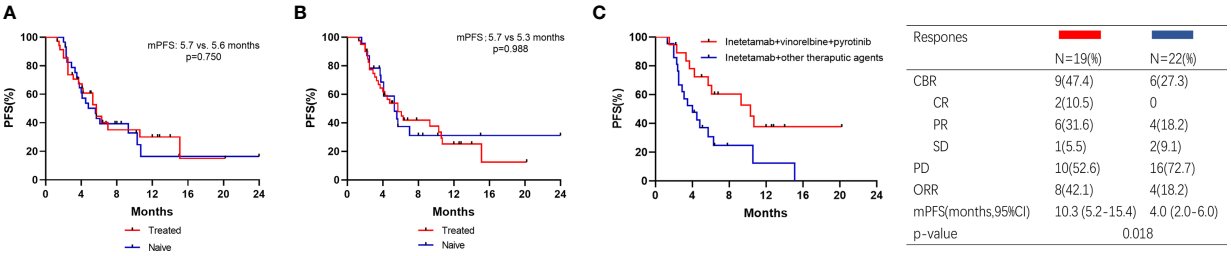

Respones	N=19(%)	N=22(%)
CBR	9(47.4)	6(27.3)
CR	2(10.5)	0
PR	6(31.6)	4(18.2)
SD	1(5.5)	2(9.1)
PD	10(52.6)	16(72.7)
ORR	8(42.1)	4(18.2)
mPFS(months,95%CI)	10.3 (5.2-15.4)	4.0 (2.0-6.0)
p-value	0.018	

FIGURE 4
Kaplan–Meier curves of PFS for patients and responses. **(A)** Patients with vinorelbine-treated or vinorelbine-naive; **(B)** Patients with pyrotinib-treated or pyrotinib-naive; **(C)** Patients who were pyrotinib-treated received inetetamab + vinorelbine + pyrotinib or other therapeutic agents.

TABLE 3 Univariate and multivariate analysis of factors associated with progression-free survival.

Characteristic	HR. (95% CI)	Univariate analysis p-value	HR. (95% CI)	Multivariate analysis p-value
Age group (<40 vs. ≥40)	0.433 (0.224-0.839)	0.013	0.528 (0.238-1.174)	0.117
ECOG performance status (0-1 vs ≥2)	0.419 (0.162-1.088)	0.074	0.440 (0.150-1.295)	0.136
Menstrual status (pre vs. post)	0.454 (0.230-0.896)	0.023	1.156 (0.468-2.860)	0.753
Hormone receptor status (negative vs. positive)	1.982 (1.064-3.692)	0.031	1.426 (0.704-2.885)	0.324
DFI (≤12 months vs.>12 months vs. *de novo* IV stage)	1.375 (0.564-3.353)	0.484	N/A*	N/A
Number of sites in primary recurrence (1 vs. >1)	1.350 (0.729-2.498)	0.340	N/A	N/A
Number of metastatic sites before inetetamab (1 vs. ≥2)	0.838 (0.447-1.573)	0.583	N/A	N/A
Brain metastasis (no vs. yes)	1.516 (0.731-3.145)	0.263	N/A	N/A
Visceral metastasis (no vs. yes)	1.735 (0.928-3.244)	0.084	2.444 (1.095-5.457)	0.029
Regimens (other therapeutic agents vs. inetetamab + vinorelbine + pyrotinib)	2.167 (1.140-4.119)	0.018	3.543 (1.680-7.471)	0.001

*N/A, Not applicable.

Trastuzumab Deruxtecan (T-DXd) or Tucatinib, which limited our research.

The combination of inetetamab, pyrotinib and vinorelbine, as evidence-based, trustworthy and promising drugs, play a synergistic role in efficacy. Pyrotinib, a small-molecule irreversible tyrosine kinase inhibitor(TKI), has attracted much attention due to its unique properties in recent years. According to the National Comprehensive Cancer Network guidelines, pyrotinib is a valid treatment option. A number of reports have verified the therapeutic efficacy of pyrotinib in HER2+ MBC. Several multicenter analyses showed that pyrotinib treatment led to a mPFS time of about 8 months (11, 12) the ORR of 17.1% in two or later line therapy (13). Besides, the clinical benefits and safety of dual HER2 blockade by anti-HER2 monoclonal antibody plus TKI for patients that had progressed during trastuzumab-based treatment regimens were confirmed (14–16). Thus, inetetamab, as an identical monoclonal antibody with trastuzumab, combined with pyrotinib led to a satisfactory efficacy. On the other hand, vinorelbine is a semi-synthetic, antimitotic, microtubule destabilizing drug that has been shown to be effective and well-tolerated for the treatment of MBC (17). It is noteworthy that compared with other chemotherapy drugs, the combined index CI of vinorelbine and trastuzumab was only 0.34 (18–20). It is suggested that the combination of vinorelbine and anti-HER2 monoclonal antibody has the best

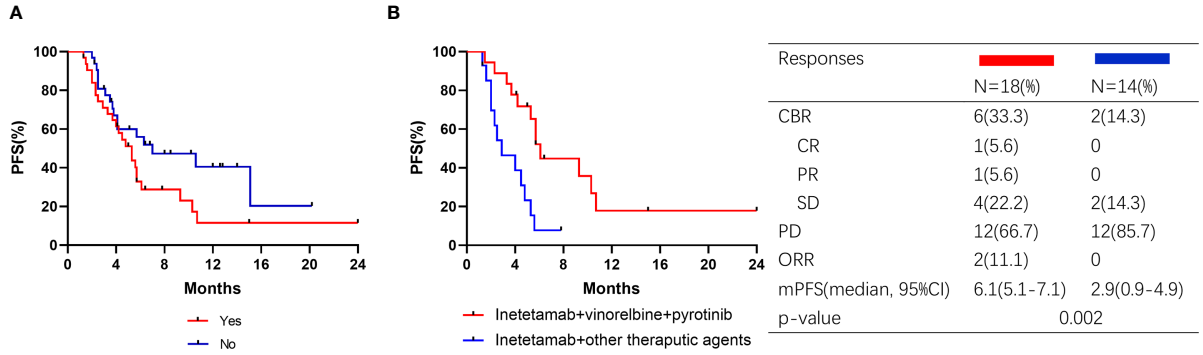

Responses	N=18(%)	N=14(%)
CBR	6(33.3)	2(14.3)
CR	1(5.6)	0
PR	1(5.6)	0
SD	4(22.2)	2(14.3)
PD	12(66.7)	12(85.7)
ORR	2(11.1)	0
mPFS(median, 95%CI)	6.1(5.1-7.1)	2.9(0.9-4.9)
p-value	0.002	

FIGURE 5
Kaplan–Meier curves of PFS for patients and responses in subgroup. **(A)** Patients with visceral metastasis or not; **(B)** Visceral metastasis patients treated with pyrotinib or pyrotinib + trastuzumab.

TABLE 4 Safety assessment.

Safety assessment	Patients, No (%) N = 64
Dose reduction of inetetamab treatment due to AEs	10 (15.6)
Interruption of inetetamab treatment due to AEs	2 (3.1)
Adverse events (grade 3/4)	
Neutropenia	2 (3.1)
Leukopenia	3 (4.7)
Thrombocytopenia	1 (1.6)
Anemia	1 (1.6)
Aminotransferase increased	1 (1.6)
Hand-foot syndrome	1 (1.6)

synergistic effect. In first-line treatment, the combination of vinorelbine with trastuzumab and pertuzumab reached the mPFS of 14.2 months, indicated that vinorelbine plus dual anti-HER2 therapy showed successful anti-tumor activity and few adverse effects (21, 22).. A retrospective study reported that the mPFS of patients treated with metronomic vinorelbine and triweekly trastuzumab was 8.9 months (23). Two multicenter retrospective studies showed pyrotinib plus vinorelbine therapy had promising efficacy and tolerable toxicity in HER2+ MBC, with mPFS of 7.8 and 8.3 months, respectively (24, 25). In addition, pyrotinib combined with vinorelbine in HER2+ MBC was effective regardless of resistant status of trastuzumab (24, 25).

Considering that inetetamab is similar to trastuzumab (9), the combination of inetetamab and trastuzumab should have a good efficacy in metastatic setting. But the small sample data resulted in some analysis biases and the inability to conduct depth analysis. Despite the combination of inetetamab plus pyrotinib plus vinorelbine showed satisfactory outcomes, which was comparable to the mPFS of 9.6 months in the EMILIA study (26), there is a significant gap compared to T-DXd(mPFS=28.8 months) according to the updated results from DESTINY-Breast03 trial (27). Notwithstanding, high prices of TDM1 and T-DXd results in limitations in the ability to use in clinical practice. Whereas, inetetamab plus pyrotinib plus vinorelbine can be considered as an alternative treatment option.

Brain and visceral metastases have poor prognosis and limit treatment for HER2+ MBC (3, 28). For patients with visceral metastasis, the outcomes of the combination regimen are inferior to that reported for pyrotinib-based regimens in the previous multicenter retrospective study (24, 29–32). The reason might be in our study, patients were less sensitive to anti-HER2 treatment after multi-lines treatment, especially after pyrotinib-based treatment. Despite mounting evidence verified that pyrotinib-based combination therapy was efficient to treat HER2+ brain metastasis (11, 33–37), brain metastasis was not a significant factor affecting the efficacy of inetetamab in our study and the recruited patients with brain metastasis was too little for further analysis.

In terms of toxicity, the published results of the large clinical trials indicated that there were no significant change in grades and incidences of AEs, showing that inetetamab and trastuzumab are equivalently safe (9). Inetetamab-based therapy was also tolerated in our study. Yet, the medical records might omit important information about AEs even though we have thoroughly reviewed the patient's examination results and medical records, which resulted in deviations in our results.

In conclusion, major populations of HER2+ MBC patients previously treated with multiple anti-HER2 therapies including trastuzumab still responded to inetetamab-based treatment in clinical practice. Inetetamab combined vinorelbine and pyrotinib might be the most effective inetetamab-based regimen. And the safety of inetetamab was controllable and tolerable. Notwithstanding the efficacy and safety of clinical trials are applicable for two or later-line inetetamab-based therapy remains questionable, our study of a series of patients provides real-world data to further explore inetetamab-based treatment patterns and more experience outside the clinical trials for clinicians in treating general HER2+ MBC patients.

Data availability statement

The raw data supporting the conclusions of this article will be made available by the authors, without undue reservation.

Ethics statement

The studies involving human participants were reviewed and approved by The Ethics Committee and Institutional Review Board of Shandong First Medical University and Shandong Academy of Medical Sciences (SDTHEC2022012020). The patients/participants provided their written informed consent to participate in this study.

Author contributions

XL and PZ collected the data. XL analyzed data and wrote the manuscript. CL, XS, ZL, WS and SL revised the manuscript. ZY and XW played a role in developing the idea. All authors contributed to manuscript revision, read, and approved the submitted version.

Funding

The article was funded by Youth Science Fund Cultivation Program of Shandong First Medical University and Shandong Academy of Medical Sciences(202201-115).

Acknowledgments

The authors thank the patients, doctors, and nurses for their supports to our study.

Conflict of interest

XW was employed by REMEGEN, LTD.

The remaining authors declare that the research was conducted in the absence of any commercial or financial relationships that could be construed as a potential conflict of interest.

Publisher's note

All claims expressed in this article are solely those of the authors and do not necessarily represent those of their affiliated organizations, or those of the publisher, the editors and the reviewers. Any product that may be evaluated in this article, or claim that may be made by its manufacturer, is not guaranteed or endorsed by the publisher.

Supplementary material

The Supplementary Material for this article can be found online at: https://www.frontiersin.org/articles/10.3389/fonc.2023.1136380/full#supplementary-material

References

1. Sung H, Ferlay J, Siegel RL, Laversanne M, Soerjomataram I, Jemal A, et al. Global cancer statistics 2020: GLOBOCAN estimates of incidence and mortality worldwide for 36 cancers in 185 countries. *CA Cancer J Clin* (2021) 71:209–49. doi: 10.3322/caac.21660

2. Barzaman K, Karami J, Zarei Z, Hosseinzadeh A, Kazemi MH, Moradi-Kalbolandi S, et al. Breast cancer: biology, biomarkers, and treatments. *Int Immunopharmacol* (2020) 84:106535. doi: 10.1016/j.intimp.2020.106535

3. Waks AG, Winer EP. Breast cancer treatment: a review. *JAMA* (2019) 321:288–300. doi: 10.1001/jama.2018.19323

4. Radenkovic S, Konjevic G, Isakovic A, Stevanovic P, Gopcevic K, Jurisic V. HER2-positive breast cancer patients: correlation between mammographic and pathological findings. *Radiat Prot Dosimetry* (2014) 162:125–8. doi: 10.1093/rpd/ncu243

5. O'Grady S, Morgan MP. Microcalcifications in breast cancer: from pathophysiology to diagnosis and prognosis. *Biochim Biophys Acta Rev Cancer* (2018) 1869:310–20. doi: 10.1016/j.bbcan.2018.04.006

6. Slamon DJ, Godolphin W, Jones LA, Holt JA, Wong SG, Keith DE, et al. Studies of the HER-2/neu proto-oncogene in human breast and ovarian cancer. *Science* (1989) 244:707–12. doi: 10.1126/science.2470152

7. Society CSoCOCAACoBC. Expert consensus on diagnosis and management of human epidermal growth factor receptor 2 positive breast cancer (version 2021). *Natl Med J China* (2021) 101:6. doi: 10.21037/tbcr-21-42

8. Najjar MK, Manore SG, Regua AT, Lo HW. Antibody-drug conjugates for the treatment of HER2-positive breast cancer. *Genes (Basel)* (2022) 13(11):2065. doi: 10.3390/genes13112065

9. Wang T, Zhang P, Di L, Wang X, Yang J, Tong Z, et al. Efficacy and safety of inetetamab in combination with chemotherapy as first-line treatment of HER2-positive metastatic breast cancer: a subgroup analysis in the HOPES study. *Trans Breast Cancer Res* (2022) 3:15–5. doi: 10.21037/tbcr-21-42

10. Bian L, Xu BH, Di LJ, Wang T, Wang XJ, Jiao SC, et al. Phase III randomized controlled, multicenter, prospective study of recombinant anti-HER2 humanized monoclonal antibody (Cipterbin) combined with vinorelbine in patients with HER2 positive metastatic breast cancer: the HOPES study. *Zhonghua Yi Xue Za Zhi* (2020) 100:2351–57. doi: 10.3760/cma.j.cn112137-20200116-00105

11. Anwar M, Chen Q, Ouyang D, Wang S, Xie N, Ouyang Q, et al. Pyrotinib treatment in patients with HER2-positive metastatic breast cancer and brain metastasis: exploratory final analysis of real-world, multicenter data. *Clin Cancer Res* (2021) 27:4634–41. doi: 10.1158/1078-0432.CCR-21-0474

12. Zhang L, Wu X, Zhou J, Zhu M, Yu H, Zhang Y, et al. Pyrotinib in the treatment of women with HER2-positive advanced breast cancer: a multicenter, prospective, real-world study. *Front Oncol* (2021) 11:699323. doi: 10.3389/fonc.2021.699323

13. Hua Y, Li W, Jin N, Cai D, Sun J, Sun C, et al. Treatment with pyrotinib-based therapy in lapatinib-resistant HER2-positive metastatic breast cancer: a multicenter real-world study. *Ther Adv Med Oncol* (2022) 14:17588359221085232. doi: 10.1177/17588359221085232

14. Blackwell KL, Burstein HJ, Storniolo AM, Rugo H, Sledge G, Koehler M, et al. Randomized study of lapatinib alone or in combination with trastuzumab in women with ErbB2-positive, trastuzumab-refractory metastatic breast cancer. *J Clin Oncol* (2010) 28:1124–30. doi: 10.1200/JCO.2008.21.4437

15. Han Y, Wang J, Liu W, Yuan P, Li Q, Zhang P, et al. Trastuzumab treatment after progression in HER2-positive metastatic breast cancer following relapse of trastuzumab-based regimens: a meta-analysis. *Cancer Manag Res* (2019) 11:4699–706. doi: 10.2147/CMAR.S198962

16. Xie XF, Zhang QY, Huang JY, Chen LP, Lan XF, Bai X, et al. Pyrotinib combined with trastuzumab and chemotherapy for the treatment of human epidermal growth factor receptor 2-positive metastatic breast cancer: a single-arm exploratory phase II trial. *Breast Cancer Res Treat* (2022) 197(1):93–101. doi: 10.21203/rs.3.rs-1752120/v1

17. Romero A, Rabinovich MG, Vallejo CT, Perez JE, Rodriguez R, Cuevas MA, et al. Vinorelbine as first-line chemotherapy for metastatic breast carcinoma. *J Clin Oncol* (1994) 12:336–41. doi: 10.1200/JCO.1994.12.2.336

18. Foucquier J, Guedj M. Analysis of drug combinations: current methodological landscape. *Pharmacol Res Perspect* (2015) 3:e00149. doi: 10.1002/prp2.149

19. Pegram MD, Konecny GE, O'Callaghan C, Beryt M, Pietras R, Slamon DJ. Rational combinations of trastuzumab with chemotherapeutic drugs used in the treatment of breast cancer. *J Natl Cancer Inst* (2004) 96:739–49. doi: 10.1093/jnci/djh131

20. Pegram M, Hsu S, Lewis G, Pietras R, Beryt M, Sliwkowski M, et al. Inhibitory effects of combinations of HER-2/neu antibody and chemotherapeutic agents used for treatment of human breast cancers. *Oncogene* (1999) 18:2241–51. doi: 10.1038/sj.onc.1202526

21. Andersson M, Lidbrink E, Bjerre K, Wist E, Enevoldsen K, Jensen AB, et al. Phase III randomized study comparing docetaxel plus trastuzumab with vinorelbine plus trastuzumab as first-line therapy of metastatic or locally advanced human epidermal growth factor receptor 2-positive breast cancer: the HERNATA study. *J Clin Oncol* (2011) 29:264–71. doi: 10.1200/JCO.2010.30.8213

22. Reinhorn D, Kuchuk I, Shochat T, Nisenbaum B, Sulkes A, Hendler D, et al. Taxane versus vinorelbine in combination with trastuzumab and pertuzumab for first-line treatment of metastatic HER2-positive breast cancer: a retrospective two-center study. *Breast Cancer Res Treat* (2021) 188:379–87. doi: 10.1007/s10549-021-06198-4

23. Liu CT, Hsieh MC, Su YL, Hung CM, Pei SN, Liao CK, et al. Metronomic vinorelbine is an excellent and safe treatment for advanced breast cancer: a retrospective, observational study. *J Cancer* (2021) 12:5355–64. doi: 10.7150/jca.60682

24. Li Y, Qiu Y, Li H, Luo T, Li W, Wang H, et al. Pyrotinib combined with vinorelbine in HER2-positive metastatic breast cancer: a multicenter retrospective study. *Front Oncol* (2021) 11:664429. doi: 10.3389/fonc.2021.664429

25. Xie Y, Li Y, Ting L, Sang D, Yuan P, Li W, et al. Pyrotinib plus vinorelbine versus lapatinib plus capecitabine in patients with previously treated HER2-positive metastatic breast cancer: a multicenter, retrospective study. *Front Oncol* (2021) 11:699333. doi: 10.3389/fonc.2021.699333

26. Verma S, Miles D, Gianni L, Krop IE, Welslau M, Baselga J, et al. Trastuzumab emtansine for HER2-positive advanced breast cancer. *N Engl J Med* (2012) 367:1783–91. doi: 10.1056/NEJMoa1209124

27. Hurvitz SA, Hegg R, Chung WP, Im SA, Jacot W, Ganju V, et al. Trastuzumab deruxtecan versus trastuzumab emtansine in patients with HER2-positive metastatic breast cancer: updated results from DESTINY-Breast03, a randomised, open-label, phase 3 trial. *Lancet* (2023) 401:105–17. doi: 10.1016/S0140-6736(22)02420-5

28. Deluche E, Antoine A, Bachelot T, Lardy-Cleaud A, Dieras V, Brain E, et al. Contemporary outcomes of metastatic breast cancer among 22,000 women from the multicentre ESME cohort 2008-2016. *Eur J Cancer* (2020) 129:60–70. doi: 10.1016/j.ejca.2020.01.016

29. Sun Y, Chen B, Li J, Peng L, Li S, Yu X, et al. Real-world analysis of the efficacy and safety of a novel irreversible HER2 tyrosine kinase inhibitor pyrotinib in patients with HER2-positive metastatic breast cancer. *Cancer Manag Res* (2021) 13:7165–74. doi: 10.2147/CMAR.S321428

30. Yin S, Chi Y, Du Y, Wang J, Shan C, Yi W, et al. Efficacy and safety of pyrotinib-containing regimen in the patients with HER2-positive metastatic breast cancer: a multicenter real-world study. *Cancer Med* (2022) 12(3):2333–44. doi: 10.1002/cam4.5056

31. Li C, Bian X, Liu Z, Wang X, Song X, Zhao W, et al. Effectiveness and safety of pyrotinib-based therapy in patients with HER2-positive metastatic breast cancer: a real-world retrospective study. *Cancer Med* (2021) 10:8352–64. doi: 10.1002/cam4.4335

32. Lin Y, Lin M, Zhang J, Wang B, Tao Z, Du Y, et al. Real-world data of pyrotinib-based therapy in metastatic HER2-positive breast cancer: promising efficacy in lapatinib-treated patients and in brain metastasis. *Cancer Res Treat* (2020) 52:1059–66. doi: 10.4143/crt.2019.633

33. Ma X, Li Y, Li L, Gao C, Liu D, Li H, et al. Pyrotinib-based treatments in HER2-positive breast cancer patients with brain metastases. *Ann Med* (2022) 54:3085–95. doi: 10.1080/07853890.2022.2139411

34. Nader-Marta G, Martins-Branco D, Agostinetto E, Bruzzone M, Ceppi M, Danielli L, et al. Efficacy of tyrosine kinase inhibitors for the treatment of patients with HER2-positive breast cancer with brain metastases: a systematic review and meta-analysis. *ESMO Open* (2022) 7:100501. doi: 10.1016/j.esmoop.2022.100501

35. Gao M, Fu C, Li S, Chen F, Yang Y, Wang C, et al. The efficacy and safety of pyrotinib in treating HER2-positive breast cancer patients with brain metastasis: a multicenter study. *Cancer Med* (2022) 11:735–42. doi: 10.1002/cam4.4481

36. Yao JH, Xie ZY, Li M, Zhang ML, Ci HF, Yang Y. Metastatic brain tumors respond favorably to pyrotinib in a HER2-positive breast cancer following failure using trastuzumab. *Am J Transl Res* (2020) 12:5874–81.

37. Chen Q, Ouyang D, Anwar M, Xie N, Wang S, Fan P, et al. Effectiveness and safety of pyrotinib, and association of biomarker with progression-free survival in patients with HER2-positive metastatic breast cancer: a real-world, multicentre analysis. *Front Oncol* (2020) 10:811. doi: 10.3389/fonc.2020.00811

frontiers | Frontiers in Oncology

TYPE Review
PUBLISHED 11 July 2023
DOI 10.3389/fonc.2023.1194835

OPEN ACCESS

EDITED BY
Helena Chang,
UCLA Health System, United States

REVIEWED BY
Marco Franchi,
University of Bologna, Italy
Claudia Angélica Garay-Canales,
National Autonomous University of Mexico, Mexico

*CORRESPONDENCE
Bole Tian
hxtbl0338@163.com
Xijie Yu
xijieyu@hotmail.com

†These authors have contributed equally to this work

RECEIVED 27 March 2023
ACCEPTED 26 June 2023
PUBLISHED 11 July 2023

CITATION
Li Y, Wang C, Huang T, Yu X and Tian B (2023) The role of cancer-associated fibroblasts in breast cancer metastasis. *Front. Oncol.* 13:1194835. doi: 10.3389/fonc.2023.1194835

The role of cancer-associated fibroblasts in breast cancer metastasis

Yi Li[1†], Changyuan Wang[2,3†], Ting Huang[1], Xijie Yu[4*] and Bole Tian[2*]

[1]Department of Breast Surgery, Sichuan Provincial People's Hospital, University of Electronic Science and Technology of China, Chengdu, China, [2]Department of Pancreatic Surgery, West China Hospital, Sichuan University, Chengdu, China, [3]Hepatobiliary Surgery Department II, Guizhou Provincial People's Hospital, Guiyang, China, [4]Department of Endocrinology and Metabolism, Laboratory of Endocrinology and Metabolism, National Clinical Research Center for Geriatrics, West China Hospital, Sichuan University, Chengdu, China

Breast cancer deaths are primarily caused by metastasis. There are several treatment options that can be used to treat breast cancer. There are, however, a limited number of treatments that can either prevent or inhibit the spread of breast tumor metastases. Thus, novel therapeutic strategies are needed. Studies have increasingly focused on the importance of the tumor microenvironment (TME) in metastasis of breast cancer. As the most abundant cells in the TME, cancer-associated fibroblasts (CAFs) play important roles in cancer pathogenesis. They can remodel the structure of the extracellular matrix (ECM) and engage in crosstalk with cancer cells or other stroma cells by secreting growth factors, cytokines, and chemokines, as well as components of the ECM, which assist the tumor cells to invade through the TME and cause distant metastasis. Clinically, CAFs not only foster the initiation, growth, angiogenesis, invasion, and metastasis of breast cancer but also serve as biomarkers for diagnosis, therapy, and prediction of prognosis. In this review, we summarize the biological characteristics and subtypes of CAFs and their functions in breast cancer metastasis, focusing on their important roles in the diagnosis, prognosis, and treatment of breast cancer. Recent studies suggest that CAFs are vital partners of breast cancer cells that assist metastasis and may represent ideal targets for prevention and treatment of breast cancer metastasis.

KEYWORDS

breast cancer, metastasis, cancer-associated fibroblasts (CAFs), tumor microenvironment (TME), extracellular matrix (ECM)

1 Introduction

According to the cancer statistics released by the World Health Organization in 2020, breast cancer surpassed lung cancer to become the disease with the highest incidence worldwide and the leading cause of cancer-related deaths in women (1). It is a heterogeneous disease with several known subtypes, which can be classified as luminal (hormone receptor positive), HER2 overexpressing, and triple negative. These types exhibit

different biological and molecular features, leading to a requirement for different treatment modalities, as well as different response patterns and characteristic differences across clinical outcomes (2). Breast cancer deaths are primarily caused by metastasis, which accounts for 90% of all cancer-associated deaths. The 5-year survival rate for patients with localized breast cancer is 99%, but for those with metastatic breast cancer it is 28% (3). The most common sites of breast cancer metastasis are bone, liver, lung, and brain, among which bone is the most common site of breast cancer metastasis, with 70% of metastatic breast cancers involving bone metastasis (4). To suppress this fatal biological behavior, many researchers have investigated its mechanisms and attempted to identify more molecular targets and relevant treatment approaches.

Tumor metastasis relies on multiple steps. Tumor cells first grow at the primary site, invade the ECM and then the systemic circulation, extravasate into the target organ, and finally grow at the metastatic site (5). Steven Paget (6) proposed the "seed and soil" theory, where the "soil" is the tumor microenvironment (TME). Cancer cells received more attention in earlier studies (7), but recently there has been an increased focus on the importance of TME in breast cancer metastasis (8–10). The development of cancer, including metastasis, depends not only on the tumor cells themselves but also, significantly, on the TME (11, 12). The dynamic TME of the primary tumor is involved in the development and invasion of tumor cells, whereas the metastatic TME play a role in the colonization and growth of tumor cells (13).

The TME consists of numerous components, including stromal cells and non-cellular components, with complex interactions between the tumor and stroma. In breast TME, cellular components include cancer-associated fibroblasts (CAFs), immune cells, inflammatory cells, endothelial cells, pericytes, adipocytes, and bone-marrow-derived cells (14–16). The non-cellular components include soluble factors such as chemokines, cytokines, growth factors, and metalloproteinases (MMPs), as well as insoluble factors such as exosomes and extracellular matrix (ECM) (17). CAFs are the most abundant cells in the TME and have important roles in cancer pathogenesis. They can remodel the structure of the ECM and engage in crosstalk with cancer cells or other stroma cells by secreting growth factors, cytokines, and chemokines, which assist the tumor cells to invade through the TME and achieve distant metastasis (18). Clinically, CAFs not only foster the initiation, growth, angiogenesis, invasion, and metastasis of breast cancer but also serve as biomarkers for diagnosis, therapy, and prognostic prediction (19).

Given the importance of CAFs in breast cancer, we undertook this review to discuss current information about the origins, biomarkers, and subtypes of CAFs, as well as their functions, mainly in breast cancer. We focus particularly on their contributions to breast tumor metastasis and the possible implications for cancer therapy.

2 Biological characteristics of CAFs

2.1 Biological features

CAFs are special fibroblasts in the stroma surrounding the tumor mass. They are also known as activated fibroblasts, myofibroblasts, peri-tumoral fibroblasts, reactive fibroblasts, or tumor-associated fibroblasts (TAFs) (20).They produce ECM components (including collagens, elastin, proteoglycans, glycosaminoglycans and glycoproteins) (21), hormones, cytokines, proteases, and growth factors. Early in 1971, Gabbiani et al. first reported that myofibroblasts could be seen in granulation tissue during wound healing (22). Then, in 1986, Dvorak proposed the concept of cancer as a wound that does not heal (23). Therefore, myofibroblasts exist not only in wounds but also in the stroma of malignant tumors (24). CAFs or activated fibroblasts, also called myofibroblasts, acquire higher abilities of proliferation and migration compared with normal fibroblasts (NFs) (25).

2.2 Biomarkers

Various proteins have been reported to show higher expression in CAFs, including alpha smooth muscle actin (α-SMA) (26), tenascin-C (27), chondroitin sulfate proteoglycan (NG2) (28), fibroblast-specific protein (FSP)-1/S100A4 (28), platelet-derived growth factor receptors (PDGFR)α/β (29), fibroblast activation protein (FAP) (30), and podoplanin (31). These are classic biomarkers of CAFs because of their wide application. Different molecular markers, however, have been identified in different CAF subtypes, demonstrating that CAFs represent heterogeneous populations of cells with distinct roles in regulating cancer progression and metastasis (28). Moreover, the expression of these markers in CAFs varies at different metastasis sites. Kim et al. analyzed 132 specimens of breast cancer metastases by immunohistochemistry and found that the expression of CAF-related proteins in the stroma varies with the location of breast cancer metastasis: in lung metastasis, PDGFRα is highly expressed; in liver metastasis, S100A4 and PDGFRα have low expression; and in bone metastasis, podoplanin, S100A4, and PDGFRα are highly expressed (32). Using immunofluorescence, Jaroslaw S. et al. observed that PDPN-positive CAFs colocalized with blood vessels stained with anti-CD34 antibodies in tumor stroma of IDC patients (33). It was Yamazaki and Eyden who first described CD34+ fibroblasts in mammary stroma and intralobular fibroblasts in the breast. But the majority of tumor stroma in ductal carcinoma in situ (DCIS) and invasive breast cancer of no special type (IBC-NST) were characterized by α-SMA positive myofibroblasts rather than CD34+ fibroblasts, several CD34+ fibroblasts are preserved in invasive lobular carcinomas (ILC) (34). In mouse triple-negative breast cancer (TNBC), multiple CAF subpopulations coexist, and the abundance and dynamics of each marker depend on the tumor type and time (35).

In addition to these classic markers, many other markers have been identified. Recently, studies have reported other molecules with higher expression in breast CAFs, including FGF2 (36) and EZH2 (37). One study used bioinformatics analysis to identify a CAF subtype based on gene expression profiles (COL10A1, COL11A1, CXCL11, CXCR6, ADAMTS12, AEBP1, EDNRA, EPPK1, and WNT7B), which was associated with significantly different overall survival rates, proportions of immune cells, and immunotherapy response rates in TNBC (38). In both mouse models and in patients, interleukin (IL)-33 is upregulated in

fibroblasts associated with breast cancer metastases, especially lung metastases (39). IL-33 can activate type 2 inflammation in the metastatic microenvironment and facilitate enrollment of eosinophils, neutrophils, and inflammatory monocytes to metastasis sites (39). Integrin α11 is a cell-surface receptor that binds to collagen and other ECM molecules. When it is expressed in CAFs, it helps them to remodel collagen in the TME, allowing them to migrate and contribute to tumor progression (40). CAFs and breast cancer patients' stroma express high levels of PYCR1, which plays a key part in proline synthesis. *In vivo* and *in vitro*, reducing PYCR1 levels in CAFs reduces tumor collagen production, tumor growth, and metastatic spread (41).

2.3 Cellular origins and activation pathways

CAFs comprise a complex and heterogeneous group of cells (42). Their characteristics and molecular markers differ, possibly because of their different cellular origins, which are presumed to form six dominant categories. The majority are NFs, followed by human mesenchymal stem cells (hMSCs) (43–46), and other transdifferentiated cells including endothelial cells, epithelial cells, adipocytes, and pericytes (47–52). Especially in invasive lobular carcinoma of the breast, resident CD34+stromal cells/Telocytes provide a significant proportion of CAFs (53). Compared with these cells of different origin, the process of converting CAF deserves more attention. Multiple pathways have been reported, predominantly involving induction by tumor cells.

2.3.1 Induction by tumor cells

NFs are typical tumor suppressor cells (54), but they are turned into "friends" by tumor cells to assist proliferation, migration, and invasion. Much evidence indicates that this transition is induced by secretion of cytokines by tumor cells. Some cytokines, including IL-6, basic fibroblast growth factor and PDGF-α/β, activate NFs through paracrine effects (55–59). In addition, the miR-9/EFEMP1 axis is crucial for activation (60). Another study demonstrated that as well as IL-6, breast cancer secretes TNF-α to stimulate KDM2A expression in normal mammary fibroblasts and transform them into CAFs (61). Butti et al. reported that tumor-derived osteopontin (OPN) engages CD44 and αvβ3 integrins on the fibroblast surface to induce myofibroblast differentiation and CXCL12 expression (62). These cytokines also take part in tumor metabolism. For instance, HMGB1 secreted by breast cancer cells promotes fibroblast activation via RAGE/aerobic glycolysis, and activated fibroblasts enhance breast cancer cell metastasis through increased lactate levels (63). Cancer cells also produce extracellular vesicles (EVs) that participate in this transition. Molecules including miR-370-3p, miR-125b, and miR-9 are carried by EVs to facilitate activation of NFs (64–66). The effects of cancer-cell-derived micro vesicles on fibroblast activation are regulated by the physical properties of the microenvironment (67). A joint medical-industrial study showed that pre-metastatic breast cancer cells could align ECM fibrils in a force-dependent manner, thereby allowing tumor-derived exosomes to reach the stroma more easily and convert NFs to CAFs (68) (Figure 1).

Mishra observed that both *in vitro* and *in vivo*, long-term co-culture of breast cancer cell condition medium and hMSCs led to differentiation of hMSCs into a myofibroblast phenotype, with upregulation of α-SMA, vimentin, fibroblast surface protein, and stromal derived factor 1 (SDF-1) (43). Another study showed that tumor-derived OPN transferred hMSC-to-CAF though the OPN-MZF1-TGF-β1 pathway (44). Moreover, Strong reported that co-culture of breast cancer cells and obese adipose derived stem cells (obASCs) also led to an increase in CAF biomarkers of obASCs (69). In tumors, bone mesenchymal stem cells (BMSCs) are recruited to tumor sites, resulting in their conversion into CAFs that aid tumor growth (70).

2.3.2 Other pathways

As well as breast tumor cells, normal breast epithelial cells can induce the transition. De Vincenzo reported that c-Myc-expressing mammary epithelial cells could mobilize and activate NFs through the IGFs/IGF-IR axis, thereby establishing an environment for malignant transformation (71). Previous studies have reported that deletion of certain tumor suppressor genes in NFs, such as p53, p21, Pten and caveolin-1 (Cav-1), could activate oncogenic effects (72–75). Cav-1 downregulation may play a critical part in maintaining the aberrant status of breast-cancer-associated fibroblasts (76). Subsequently, a study reported that downregulation of p53 could transform NFs to CAFs, in a manner dependent on c-Ski-induced upregulation of SDF-1 (77). In low-stiffness stroma, loss of SPIN90-mediated microtubule acetylation was involved in CAF activation, which was associated with breast cancer progression (78).

Epithelial and endothelial cells become CAFs via epithelial–mesenchymal transition (EMT) and endothelial–mesenchymal transition, respectively (24, 79–81). A study showed that FOXF2-deficient breast cancer epithelial cells adopted a CAF-like phenotype (82). These cells are more likely to migrate to visceral organs by increasing autocrine TGF-β expression and enhancing aggressiveness of neighboring cells through increased paracrine TGF-β expression (82). The differentiation of CAFs gradually increases during tumor progression and may depend on the combined stimulation of TGF-β and SDF-1/CXCR4 autocrine signaling loops in CAFs to maintain stable differentiation (83, 84). TGF-β also plays this part through autophagy under oxidative stress in the TME (85, 86). Exhaustion of USP27X could inhibit TGFβ-induced fibroblast activation (87).

OPN could facilitate the transformation of mesenchymal stromal cells into CAFs, as well as increasing levels of CAF markers such as α-SMA, CXCL12, FSP-1, and tenascin-c specifically at tumor metastatic sites (88). Overexpression of miR-222 or knockdown of the LBR gene is enough to induce NFs to show CAF characteristics such as enhanced migration, invasion, and senescence; furthermore, conditioned medium from these cells increased migration and invasion of breast cancer cells (89). Chronic inflammation can induce the conversion of BMSCs to CAFs, leading to the production of pro-tumor inflammatory CAFs (90), a subtype of CAFs.

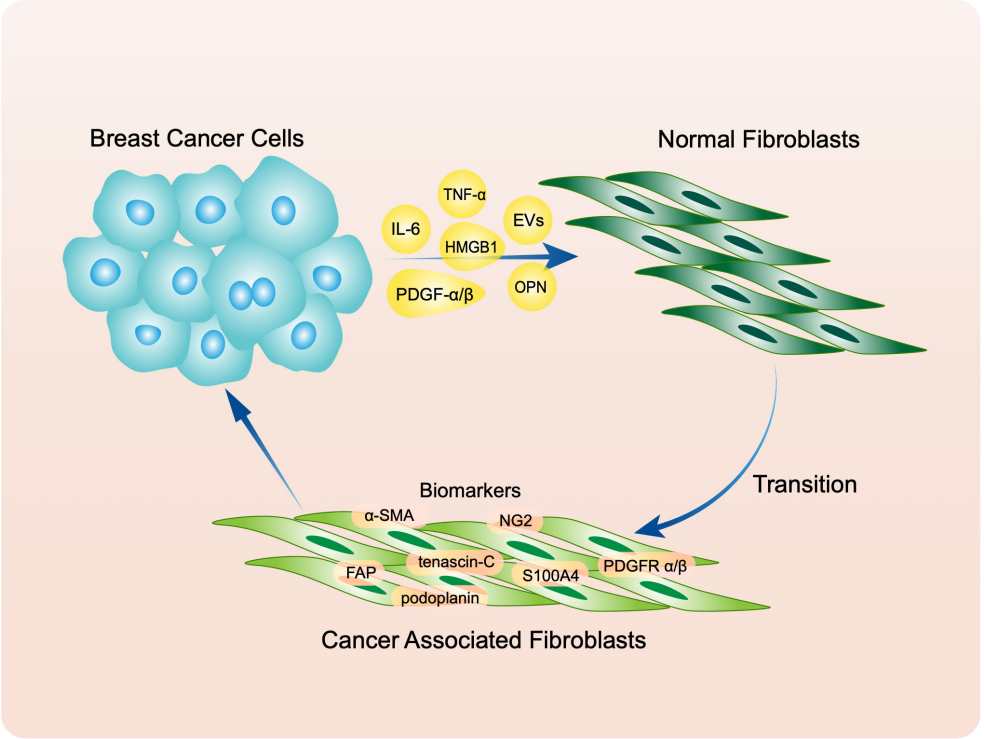

FIGURE 1
Breast cancer transfer normal fibroblasts (NFs) to cancer associated fibroblasts (CAFs) through secreting molecules including IL-6, TNF-α, PDGF α/β, OPN, HMGB1 and extracellular vesicles (EVs). Activated CAFs express classic biomarkers like α-SMA, tenascin-C, NG2, S100A4, PDGFR α/β, FAP and podoplanin.

3 Subtypes of breast-CAFs

As mentioned above, CAFs are not a single cell type but comprise many subtypes, possibly owing to their various origins. Different methods are used to identify CAFs in breast cancer TME, results in different subtypes according to variety biomarkers (Tables 1, 2). The subtypes of breast-CAFs, are supposed to play the same role in promoting breast cancer aggression via distinguished pathways, however, several CAFs can bring benefit for breast cancer treatment.

3.1 Identified by immunohistochemical (IHC) staining

In an earlier publication, breast CAFs were described as two types by IHC staining, depending on whether they were positive or negative for CD146, and this description was used to evaluate their role in estrogen receptor (ER)-dependent proliferation and tamoxifen sensitivity (91). The results showed that tamoxifen sensitivity of tamoxifen-resistant breast cancer cells could be restored after co-culture with CD146-positive CAFs. On the other hand, CD146 negativity was correlated with inferior clinical response to tamoxifen and worse patient outcomes (91). Recently, the same research team reported that CD146-negative CAFs could promoted tumor metastasis and predict the possibility of lymph node metastasis in small primary tumors (92). These findings provide an experimental basis for clinical precision therapy.

3.2 Identified by multicolor flow cytometry

Mechta-Grigoriou et al. characterized four CAF subsets, CAF-S1, S2, S3, and S4, using multicolor flow cytometry (fluorescence-activated cell sorting) and found that the CAF-S1 subset had a key role in the immunosuppressive milieu of breast cancer (93). Two years later, they confirmed the presence of these four subpopulations in metastatic lymph nodes and described their biomarkers and functions (94).

3.3 Identified by single-cell sequencing

Single-cell sequencing has been a hot topic in recent years. Wu SZ el al. used this technique to divide CAFs into myofibroblast-like CAFs (myCAFs) and inflammatory CAFs (iCAFs) in TNBC (95). The biomarkers of myCAFs are ACTA2, FAP, PDPN, COL1A1, and COL1A2; and CXCL12 (SDF-1) is a biomarker of iCAFs (95). Another study showed that iCAFs were from CD26 positive NFs and myCAFs were from CD26 negative NFs (97). Bartoschek et al. also used it to distinguish four subtypes of breast-cancer-associated fibroblasts: vascular CAFs (vCAFs), matrix CAFs (mCAFs), developmental CAFs (dCAFs), and cycling CAFs (cCAFs) (96). The terms are relatively clear and easy to understand. This description is more detailed than previous ones and includes origin, significantly differentially expressed genes, gene ontology (GO) sets, markers, and functions. The team validated expression

TABLE 1 Breast-CAFs identified by IHC or flow cytometry.

Subtypes	Biomarkers					Function
Brechbuhl HM et al. (91, 92)						
CD146 associated CAFs	CD146 positive					Reversal of tamoxifen resistance in ER positive breast cancer (91)
	CD146 negative					Enhance the drug resistance to tamoxifen (91) Promoted cancer metastasis and indicate poor prognosis of breast cancer patients (92)
Costa A et al. (93, 94)						
	FAP	CD29	αSMA	PDPN	PDGFRβ	
CAF-S1	High	Med-High	High	High	High	Play an important role in the immunosuppressive environment of breast cancer (93) Stimulate cancer cell migration and initiate EMT through CXCL12 and TGF-β pathways (94)
CAF-S2	Neg	Low	Neg-Low	Low	Low	Unknown
CAF-S3	Neg-Low	Med	Neg-Low	Low	Low-Med	Unknown
CAF-S4	Low-Med	High	High	Low	Med	Induce cancer cell invasion in three dimensions via NOTCH signaling (94)

TABLE 2 Breast-CAFs identified by single-cell sequencing.

Subtypes	DEGs/SDE genes	GO sets	Origin	Markers	Functions
Wu SZ et al. (95)					
myCAFs	MMP2/MMP11/FN1/LOX/PDPN/FAP/COL1A1/COL8A1/COL11A1/COL12A1	Collagen biosynthesis and ECM regulatory pathways	Unknown	ACTA2/FAP/PDPN/COL1A1/COL1A2	Elevated capabilities for collagen secretion and alignment
iCAFs	IGF1/FIGF/CXCL12/DLK1/CXCL13/CXCL1/IGF2/PDGFD/ALDH1A1/ID2/EGFR/FGF10	Developmental signaling pathways and chemotactic regulation	Unknown	CXCL12	Associated with cytotoxic T-lymphocyte dysfunction
Bartoschek et al. (96)					
vCAFs	**Vascular regulators:** Notch3/Epas1/Col18a1/Nr2f2	Vascular development and angiogenesis	Perivascular location	Nidogen-2	Associated with blood vessels in early stages of tumor development
mCAFs	**Glycoproteins:** Dcn/Lum/Vcan **Structural proteins:** Col14a1 **Matricellular proteins:** Fbln1/Fbln2/Smoc **Matrix-modifying enzymes:** Lox/Loxl1 **Immune-cell-attracting factor:** CXCL14	Related to the ECM and EMT	Descendants of resident fibroblasts	Fibulin-1/PDGFRα	Regulation of the tumor immune response
cCAFs	**Vascular regulators:** Notch3/Epas1/Col18a1/Nr2f2 **Cell cycle genes:** Nuf2/Mki67/Ccna2/Top2a/Cep55	Related to the cell cycle	Proliferating segment of vCAFs	Unknown	Represent the proliferative segment of vCAFs
dCAFs	**Various stem cell types:** Scrg1/Sox9/Sox10	Connected to differentiation of cells and development of tissues	Tumor cells that have undergone EMT	SCRG1	Tissue development

DEGs, differentially expressed genes; SDE, significantly differentially expressed; GO, gene ontology.

profiles in clinical samples (96). Experiments *in vitro* showed that both vCAFs and mCAFs could promote tumor invasion and may represent potential targets for clinical therapies (96). Sebastian et al. also used single-cell sequencing to identify six CAF subsets in BALB/c-derived 4T1 mammary tumors with distinct gene expression profiles (98).

4 Functions of CAFs in breast cancer metastasis

As mentioned in the introduction, cancer metastasis relies on multiple steps, including growth at the primary site, EMT, invasion into the systemic circulation, dissemination via circulation, extravasation into the target organ, and finally growth at the metastatic site (5). CAFs participate in all these steps. Most previous reviews have summarized the roles of CAFs at different stages. Our review, however, focuses on the ways in which CAFs function and the results achieved.

4.1 Secret molecules to assist cancer metastasis

Many of studies have demonstrated that CAFs assist the progression of breast cancer cells though paracrine signaling by various molecules, including biological macromolecules, cytokines, and enzymes, as well as exosomes (99) (Figure 2).

4.1.1 Chemokines

SDF-1, currently known as CXCL12, directly binds to its receptor CXCR4, a G-protein-coupled receptor, to induce tumor angiogenesis, thereby promoting breast cancer growth (100). OPN-driven CAFs release CXCL12 to initiate EMT in tumor cells (62). CAF-enriched primary tumor stroma can mimic the CXCL12-rich bone metastatic niche and can thus be used to help identify potentially metastatic cancer cells (101). CXCL12 stimulates the proliferation of CD44-positive and CD24-negative breast cancer stem cells (102). The diabetes drug metformin can prevent the production of CXCL12 and IL-8 by CAFs, which is associated with increased phospho-AMP kinase levels. Therefore, metformin can be used to interrupt HIF-1α-driven SDF-1 signaling in CAFs to decrease breast cancer invasion (103). The same family member CXCL14 can promote tumor growth by stimulating angiogenesis and recruiting macrophages through nitric oxide synthase 1 (NOS1) (104). CXCL14-induced NOS1 or ACKR2 downregulation attenuates EMT and migration (105). IL-32, also known as NK4, secreted by CAFs stimulates the invasion and metastatic potential of breast cancer cells via activation of integrin β3-p38 MAPK (106). IL-6 produced by CAFs stimulates the signal transducer and activator of transcription 3 (STAT3) pathway, promoting breast cancer cell growth and radioresistance (107).

4.1.2 Growth factors

Growth factors are known to have significant effects on mammary cells. Studies have shown that breast stromal fibroblasts produce FGF7, which has profound effects on epithelial and myoepithelial cells. For instance, Palmieri et al.

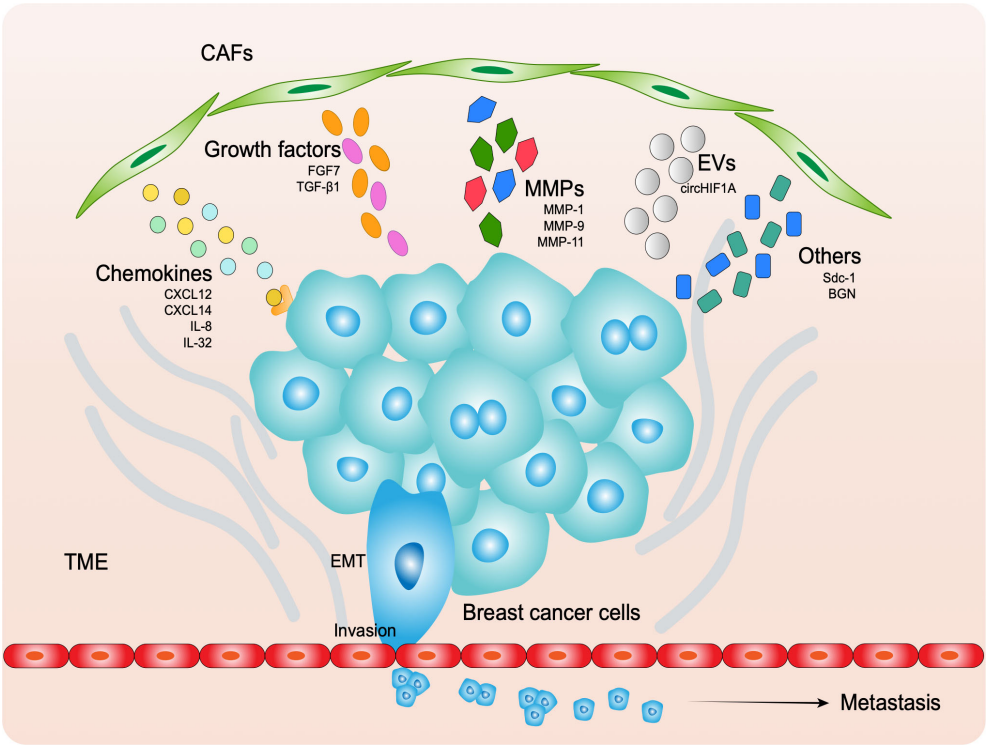

FIGURE 2
CAFs secret molecules to assist cancer EMT, invasion and metastasis, including chemokines, growth factors, MMPs, EVs and others.

used immunohistochemistry to demonstrate FGF7 expression in stroma of lobular carcinomas and invasive ductal carcinomas, and illustrated with Matrigel-embedded organoids that FGF7 increases cell proliferation (108). By secreting another growth factor, TGF-β1, CAFs activate the TGF-β/Smad signaling pathway in breast cancer cells, promoting their aggressive phenotype, which involves enhanced cell–ECM adhesion, migration, invasion, and EMT (109).

4.1.3 MMPs

There are 26 human MMPs, which can be classified into six groups according to their substrate specificity and homology. During tumor invasion and metastasis, MMPs are essential for the degradation of stromal connective tissue and basement membrane components. During ECM remodeling, MMPs contribute to tumor progression primarily by degrading ECM (110). Studies have shown that CAF-derived MMP-1 and MMP-9 promote the invasion of breast cancer cells (111, 112). Another study showed that MMP-11 (stromelysin-3) was preferentially expressed in the stroma of tumors and was associated with poor prognosis (113–115).

4.1.4 EVs

EVs are membrane-bound vesicles released into the extracellular microenvironment by both prokaryotic and eukaryotic cells. They are composed of several lipid-bilayer nanosized vesicles. In a recent study, Luga et al. (116) reported that CAFs secrete exosomes that activate Wnt-planar cell polarity signaling in breast cancer cells, promoting cell motility and metastasis. Moreover, in breast cancer stem cells, hypoxic CAFs release exosomes to transfer circHIF1A, which regulates miR-580-5p by sponging CD44 expression (117).

4.1.5 Others

CAF-derived Sdc1 is associated with significantly higher microvascular density and larger vessel area, which stimulate breast carcinoma growth and angiogenesis (118). Furthermore, another secretory protein, biglycan (BGN) was found to be upregulated in CAFs compared with normal cancer-adjacent fibroblasts. Notably, BGN expression was negatively correlated with CD8+ T cells and was associated with poor prognoses, possibly because of the immunosuppressive TME (119).

4.2 Functions through other molecules

Some molecules are not secreted by CAFs but interact with them to promote the progression of breast cancer. Some regulate CAFs to assist cancer metastasis, whereas others are affected by CAFs. Gene regulation techniques can be used to investigate the function of CAFs.

Protein-kinase-R-like endoplasmic reticulum kinase (PERK), which is selectively activated by Rho-associated kinase (ROCK) in mammary tumor epithelium, recruits and persists cancer-promoting CAFs (120). A CAF phenotype is generated by myeloid zinc finger-1 phosphorylation in mesenchymal stem cells, which leads to an increase in the stemness of cancer cells (121). Autophagy and survival are enhanced by Nox4 and Nrf2 pathway activation in CAFs during tumorigenesis and metastasis of breast cancers (122). In a mixed xenograft and indirect co-culture model, estrogen was shown to induce CAFs to activate FGF2/FGFR1 paracrine signaling and trigger expression of connective tissue growth factor (CTGF), leading to migration and invasion of breast cancer cells (123). Conversely, CAF-conditioned media induced ER ubiquitination and proteasomal degradation of MCF7 and T47D cells (124). The activation of PI3K-AKT signaling by C3a-C3aR enhances pro-metastatic cytokine secretion and expression of ECM components by CAFs. In mouse models of breast cancer, treating mice with genetic or pharmacological inhibitors of C3aR signaling effectively inhibits lung metastasis (125). It has been shown that Gremlin1 (GREM1), which has high expression in CAFs, abrogates bone morphogenetic protein (BMP)/SMAD signaling and promotes the mesenchymal phenotype, stemness, and invasion of breast cancer cells, which are associated with poor prognosis regardless of molecular subtype (126). Phosphodiesterase 5 (PDE5) is highly expressed in CAFs and also contributes to the progression of breast cancer and affects clinical outcomes (127). Furthermore, CAFs enhanced GPNMB expression in breast cancer cells in an organotypic model of tumor-stroma interactions (128); however, its mechanism is unclear. According to Soon et al. (129), CAFs induce significantly more EMT molecular markers in MCF7 cells than NFs, as manifested by increased vimentin expression, whereas E-cadherin expression was decreased in MCF7 cells.

The role of some molecules in CAF can be better understood through gene regulation techniques. Overexpression of mitochondrial uncoupling proteins (UCP-1) in CAFs can induce mitochondrial dysfunction by enhancing β-oxidation to produce ketone bodies and vesicles enriched with ATP, acting as fuel for tumor growth (130). Knockout of adhesion kinase (FAK) in CAFs did not affect primary tumor growth and proliferation but significantly limited breast cancer metastasis via exosomal microRNA-mediated intercellular communication (131). In addition, STAT1 depletion in CAFs reduced periductal reactive fibrosis and retarded the progression of early breast cancer *in vivo*, suggesting that STAT1 contributes to tumorigenesis from the stroma (132).

4.4 Function as a bodyguard for breast cancer cells

4.4.1 Co-metastasis with cancer cells

When tumors invade blood vessels or lymphatic vessels, CAFs form clusters with cancer cells. The CAFs protect the cancer cells from immune attack, enable them to endure fluid mechanical force, and reduce their apoptosis, as well as improving vessel invasion. Metastatic lung cancer cells that co-metastasized with their own CAFs from the primary site were found to grow more rapidly than those that did not in a tumor metastasis mouse model (133). Alternatively, removing cancer-associated factors results in a significant reduction in metastatic cancer cells. Cancer cells and

CAFs extravasate through blood vessels or lymphatic vessels, resulting in metastatic lesions in the appropriate organs. In the new environment, CAFs can survive and continuously secrete growth factors and cytokines to stimulate the growth of metastatic cancer cells. These findings warrant further investigation into which subgroups of CAFs co-metastasize with tumor cells and to find biomarkers that distinguish them and may provide new targets for tumor therapy.

4.4.2 Suppressing immunity

There is evidence that tumors with CAF-rich microenvironments exhibit immunologically cold environments, suggesting that therapeutically targeting a specific CAF subpopulation in breast could improve clinical outcomes (134). In addition, an animal study demonstrated that CAFs impaired the function of tumor-infiltrated immune cells *in vivo* and significantly promoted breast tumor progression (135). The IL6-adenosine positive feedback loop is mediated by CD73+ gamma delta regulatory T cells (Tregs), which further promote IL6 secretion by CAFs via adenosine/A2BR/p38MAPK signaling. The infiltration of CD73+ gamma delta Tregs also impaired the tumoricidal activities of CD8+ T cells, and this effect was associated with significantly worse patient prognosis. It appears that IL6-adenosine loops between CD73+ gamma delta Tregs and CAFs play a critical part in promoting tumor progression and immunosuppression in breast cancer (136). Timperi E et al. suggests that lipid-associated macrophages (LAM) recruited via the CAF-driven CXCL12-CXCR4 axis support an immunosuppressive microenvironment by acquiring protumorigenic functions (137).

4.4.3 Assisting tumor metabolism

In the TME, stromal cells cooperate with cancer cells metabolically. Tumor cells can utilize CAF metabolic byproducts to feed anabolic metabolism and proliferation, indicating that metabolic symbiosis has an important role in tumor growth (138). Some studies have helped to elucidate the metabolic dynamics between cancer cells and CAFs. For example, FATP1, which is relatively highly expressed in CAFs, has been proposed as a potential target for disrupting breast cancer cell lipid transfer (139). Another study showed that extracellular ATP promotes interactions between breast cancer cells and fibroblasts, where S100A4 is produced in collaboration with breast cancer cells to exacerbate breast cancer metastasis (140). Aspartate derived from CAFs sustains cancer cell proliferation, whereas glutamate derived from CAFs promotes remodeling of the ECM (141).

4.5 Other findings

The authors recently proposed a novel tumor invasion mechanism based on invasive cancer cells migrating independently on elongated CAFs (CAF fibers) embedded in a three-dimensional collagen matrix. This mechanism involves cancer cells interacting with fibronectin fibrils assembled on CAFs primarily through integrin-α5β1 (142). A study by Gao et al. (143) demonstrated that CAFs located within human breast cancer interface zones have a significant role in inducing EMT. The same results can be obtained by artificially altering the expression of certain molecules in CAFs. In cancer tissue, mechanical pressure is also believed to play a part in the mechanisms (144, 145). In cancer cells expressing the matrix-remodeling CAF receptor Endo180 (MRC2), genetic deletion profoundly limits tumor growth and metastasis (146). MDA-MB-231 cells are accelerated (1) by direct physical interactions, where activated fibroblasts penetrate the matrix and act as scaffolds for coalescence and aggregation; and (2) through release of soluble accelerating factors such as MMPs or, in the case of activated normal human dermal fibroblasts (NHDFs), SDF-1α/CXCL12 (147).

5 Clinical value of CAFs in breast cancer

CAFs have an important role in the development of breast cancer and are involved in tumor cell occurrence, growth, angiogenesis, cell invasion, and metastasis. Some of these molecular markers can provide a data basis for the determination of breast cancer types, the choice of treatment, and prediction of patient prognosis. CAFs secrete products that regulate tumor cells and have a positive impact on clinical outcomes. Therefore, the clinical application value of CAFs for breast cancer has attracted the attention of many researchers worldwide.

5.1 Relationship of CAF-associated molecules with clinical diagnosis and prognosis

CAF-associated molecules are related to the clinical outcomes of breast tumors and metastasis, and survival of patients. They are important indicators of prognosis and can enable early intervention for breast cancer patients, as well as helping to provide new strategies (148).

5.1.1 CAF biomarkers

After α-SMA was stained in 60 invasive breast cancer patients, computer-aided image analysis showed that the expression of α-SMA significantly differed between the metastasis group and the non-metastasis group. The metastasis group showed high α-SMA expression and a significantly lower overall survival rate (149). α-SMA can cause cancer cell metastasis and reduce overall survival, because α-SMA-positive CAFs can promote tumor growth through OPN secretion (150).

PDGF receptor expression is associated with unfavorable prognosis in breast cancer when the PDGF pathway is dysregulated. High PDGFRα expression has been linked to aggressive subtypes of breast cancer including TNBC, and high PDGF-CC expression increases the risk of 5-year distant recurrence. Moreover, PDGFR expression in tumor cells has been reported to be significantly elevated in lymph node metastases and asynchronous recurrences (151). Another study used double immunostaining of α11 integrin and PDGFRβ in human breast

cancer samples and associated normal tissues of DCIS patients (152). The results showed that invasive ductal cancer (IDC) had higher densities of integrin-11 or PDGFR than DCIS tumors, which suggested that integrin α11 is mainly expressed by a subset of PDGFRβ-positive CAFs in human breast cancer. Furthermore, patient outcomes were analyzed with respect to the integrin α11/PDGFRβ+ CAF subgroup, showing that an increase in stromal density of integrin α11/PDGFR was associated with higher tumor grade, metastasis, and patient mortality. Recently, Akanda, M. R. et al. reported that in breast cancer brain metastasis patients, expression of PDGFR-β in the stroma of metastasis site was associated with recurrence free survival (153).

In addition, FAP expressed by CAFs is an independent factor predicting the prognosis of breast cancer patients, and the expression of FAP is correlated with cancer cell metastasis and survival (154). An IHC study of 449 patients with DCIS who had undergone extensive resection and did not receive radiotherapy and chemotherapy concluded that FAP-α and GOLPH3 overexpression were highly specific for the recurrence and progression of DCIS and may thus represent novel tumor markers for progression of DCIS to invasive breast cancer (IDC) (155). In breast tumors with a high stromal content, radiolabeled FAP-specific enzyme inhibitor (FAPIs) may offer high contrast for fast imaging and could serve as anti-tumor agents (156). In 68Ga-FAPI positron emission tomography/computed tomography, remarkably high uptake and image contrast were observed for several widely prevalent cancers. These findings could lead to new applications such as noninvasive tumor identification, staging examinations, or the use of radioligand therapy (157).

5.1.2 MMPs

Immunohistochemical analysis of 154 breast cancer patients and 42 women without tumor disease revealed that postmenopausal patients, hormone-receptor-positive patients, and histological ductal carcinoma patients had higher MMP-1 staining intensity and higher MMP3 staining percentages and intensities (158). A clinical study of 48 patients with breast cancer and 13 patients with benign breast disease found that expression levels of MMP-9 mRNA were significantly increased in breast cancer patients compared with patients with benign breast disease. In addition, plasma MMP-2 and MMP-9 were significantly reduced in breast cancer patients after surgery, so both MMP-2 and MMP-9 could be used as markers of breast cancer disease response to therapy (159). On the other hand, MMP-2 expression was correlated with tumor size and neovascularization, MMP-9 expression was correlated with hormone receptor status, and stromal cell co-expression of MMP-2 and MMP-9 was significantly associated with tumor size. Therefore, these markers could be used in combination to assess the prognosis of breast cancer patients (160). MMP-9, MMP-11, and TIMP-2 expression by CAFs were also significantly associated with poor prognosis in luminal A tumors (161).

5.1.3 CAV-1

CAV-1 is a structural protein involved in the trafficking of vesicles and signaling in caveolae, which are sphingolipid-rich invaginations of the plasma membrane. Cell lines and primary breast cancers from humans contain negative CAV-1 RNA and protein levels, and CAV-1 reintroduced *in vitro* inhibits many tumorigenic properties, including anchorage independent growth (162). A study analyzed 669 tumor specimens with TNBC by immunohistochemistry, showing that lack of stromal CAV-1 expression in TNBC was significantly associated with worse overall survival; conversely, increased mRNA levels of CAV-1 in 141 tumor samples were associated with better overall survival (163). Another study showed that low expression of CAV-1 in breast cancer stroma was associated with early recurrence, progression, tamoxifen resistance, and 5-year survival, especially in invasive micropapillary carcinoma, whereas CAV-1 gene expression promoted EGFR signal transduction, which mediates tyrosine kinase activity and was found to be an effective marker for breast cancer diagnosis and prognosis (164).

5.1.4 Others

It has been demonstrated that tumor grade is significantly related to a high level of immunostaining for AUF1 in both cancer cells and adjacent CAFs (165). Locally advanced breast cancer patients with high levels of DNMT1 in breast stromal fibroblasts have poor survival, because DNMT1 promotes angiogenesis through IL-8/VEGF-A upregulation (166). In TNBC patients, increased CAF activation was linked to increased infiltration of polarized CD163-positive tumor-associated macrophages (TAMs), as well as lymph node metastasis. CAF activation, TAM infiltration, and lymph node metastasis were shown to be independent prognostic factors for disease-free survival in TNBC patients (167). Din contrast to factors with high expression, depletion of FAK in CAFs prompts its activation of protein kinase A via CCR1/CCR2 on cancer cells, leading to increased glycolysis in malignant cells, which mediates the metabolism of malignant cells, reduces overall patient survival, and leads to poor prognosis of breast cancer patients (168). There has been evidence that the five-gene prognostic CAF signature (RIN2, THBS1, IL1R1, RAB31, and COL11A1) is not only effective for predicting prognosis, but also for estimating clinical immunotherapy response (169).

To sum up, substances related to CAFs, transformation of CAFs by deletion of molecular markers, and derivatives of CAFs and tumor suppressor genes have clinical applications in the diagnosis, prognosis, and treatment of breast cancer. They can also be used to provide data and information for precision treatment of breast cancer patients and speed up the process of breast cancer treatment.

5.2 Relationship of CAF-associated molecules with treatment

As mentioned above, CAFs and related molecules have an important impact on the prognosis of breast cancer and can thus be explored as targets for the treatment of breast cancer. Treatment plans for breast cancer include vaccines, reducing drug resistance, and mediating the radiation resistance of CAFs.

5.2.1 Anti-FAP vaccines

FAP is one of the most important biomarkers of CAFs and is primarily expressed on the CAF surface. Many anti-tumor therapies focus on FAP. It is possible to increase the potency of T-cell-mediated anti-tumor effects by targeting FAPα, and combination of a dual-targeting vaccine with doxorubicin effectively increased the anti-tumor activity of the vaccine by decreasing immunosuppressive factors and promoting the infiltration of tumor cells by lymphocytes; this finding may provide useful guidance for clinical research on the combination of DNA vaccination with low-dose chemotherapy (170). Another chemotherapy drug, cyclophosphamide, together with FAPα-targeted modified vaccinia Ankara, have been shown to be effective in overcoming immunosuppression and improving specific anti-tumor immune responses (171). Importantly, mice vaccinated with FAP and given cyclophosphamide chemotherapy showed significant tumor growth suppression (inhibition ratio: 80%) and longer survival times (172). Another vaccine reduced the growth of 4T1 tumors by promoting production of cytotoxic T lymphocytes that killed CAFs, and the decrease in FAPα-expressing CAFs markedly decreased collagen I and other stromal factors, resulting in a marked attenuation of tumor progression (173). Another study developed a tumor vaccine prepared from tumor-cell-derived exosome-like nanovesicles (eNVs-FAP), which demonstrated excellent anti-tumor effects in a variety of tumor-bearing mouse models. According to mechanistic analysis, eNVs-FAP stimulated dendritic cell maturation, increased infiltration of effector T cells into tumor cells and FAP+ CAFs and decreased the number of immunosuppressive cells such as M2-like TAMs, myeloid-derived suppressor cells, and Tregs in the TME. In addition, FAP+ CAF clearance enhanced ferroptosis via interferon-gamma (174). Another drug delivery agent, functionalized nanocaged HFn-FAP, could specifically enhance targeted therapy for CAFs when administered intravenously in TNBC (175).

5.2.2 Reversal of drug resistance

Antitumor drug resistance is among the main culprits in breast cancer recurrence and metastasis. Recent studies on drug resistance involving CAFs have mainly focused on tamoxifen, anti-HER2 drugs, and chemotherapy. Drug resistance to breast cancer can be reversed through treatments that reduce CAF activity, thereby reducing recurrence and metastasis. Tamoxifen is an ER modulator used for endocrine therapy in patients with ER-positive breast cancer. According to a study, tamoxifen resistance in breast cancer may be caused by CD63+ CAFs via exosomal miR-22 (176). CAFs with upregulation of HMGB1 expression and secretion via GPR30/PI3K/AKT signaling enhanced MCF-7 cell resistance to TAM by increasing autophagy dependent on ERK activity (177). The TAF/FGF5/FGFR2/c-Src/HER2 axis is responsible for HER2-targeted therapy resistance in breast cancer, which can be reversed by FGFR inhibitors (178). In patients with HER2-positive breast cancer, CAF-derived NRG1 contributes to trastuzumab resistance through high expression of HER3/AKT, but combination with pertuzumab may reverse resistance (179). Cancer-derived xenografts engraft successfully when CD10 +GPR77+ CAFs are present, and treating these CAFs with an anti-GPR77 antibody eliminates tumor formation and restores tumor chemosensitivity (180). Claudin-low TNBCs are resistant to chemotherapy when CAF activates IFN signaling. Inhibition of this pathway could improve breast cancer outcomes in a novel way (181). A study showed that gMG treatment significantly retards tumor growth, reduces CAF production, and improves DOX sensitivity in a DOX-resistant TNBC tumoroid-bearing mouse model, because it was found that INFG/STAT1/NOTCH3 is a molecular link between breast cancer stem cells and CAFs, and it's expression was increased in DOX-resistant TNBC cell lines, as well as CAF-transformation and self-renewal ability (182).

5.2.3 Reversal of radiation resistance

CAFs have been shown to be radioresistant and to undergo significant changes in oxidative metabolism indices. It is likely that CAFs that survive radiation treatment influence the fate of associated cancer cells. Identifying these CAFs, determining their mode of communication with cancer cells, and eradicating them, especially when they exist at the margins of a radiotherapy target volume, may improve cancer treatment effectiveness (183). Dendrigraft poly-L-lysine (DGL)/gemcitabine (GEM)@PP/GA nanoparticles for TAF-targeted regulation and deep tumor penetration have been reported. When MMP-2 was overexpressed in the TME, GEM-conjugated small nanoparticles (DGL/GEM) are released from DGL/GEM@PP/GA, causing the large nanoparticles (PP/GA) loaded with 18beta-glycyrrhetinic acid (GA) to accumulate at the tumor site. The released DGL/GEM can penetrate deep into the tumor to release GEM intracellularly and kill tumor cells. It is also possible that residual GA-loaded nanoparticles may accumulate around tumor vessels and be absorbed more efficiently by TAFs, which regulate the secretion of Wnt16, an essential damage response program (DRP) molecule, around tumor vessels. When DGL/GEM@PP/GA was applied to breast cancer models with stroma-rich stroma, significant and long-term anti-tumor effects were observed (184).

6 Conclusions and prospecs

CAFs, the most abundant cells in breast cancer stroma, secrete various ECM components, growth factors, cytokines, proteins, enzymes, and hormones. CAFs participate in the development and progression of breast cancer by stimulating epithelial cell malignant transformation, tumor initiation, tumor growth, ECM degradation, tumor angiogenesis, and cancer cell invasion and metastasis. Furthermore, CAFs are valuable in the clinical diagnosis of breast cancer, as well as in therapy and prediction of prognosis. However, many aspects remain unclear, including the relationship between CAFs and other mesenchymal cells or stroma structures, such as tunneling nanotubes, which are made by exosomes derived from breast cancer cells but not CAFs (185), the precise mechanism of their escape from immune attack, and whether other valuable molecular markers of CAFs exist. The breast cancer immune-microenvironment with tumor-associated tertiary lymphoid structure (TA-TLS) usually have a higher representation of tumor-infiltrating lymphocytes (TIL) and show a better response

to chemotherapy and immunotherapy (186). A study showed that TA-TLS could be coordinated by FAP^{neg} CAFs that exhibit characteristics like lymphoid tissue organizers and their roles are to facilitate anti-tumor immunity and immune response to checkpoint immunotherapy (187). Unfortunately, this study was done in melanoma, not breast cancer. In conclusion, the role of CAFs in breast cancer warrant further investigation.

Author contributions

YL conceptualized the manuscript, YL and CW did literature search and wrote it. TH designed the figures. XY and BT critically reviewed it. All authors contributed to the article and approved the submitted version.

Funding

This work was supported by grants from the University of Electronic Science and Technology of China (ZYGX2021YGLH205).

Acknowledgments

The authors thank Pro. Jingping Liu from department of breast surgery, Sichuan Provincial People's Hospital for his great support in the writing of this paper.

Conflict of interest

The authors declare that the research was conducted in the absence of any commercial or financial relationships that could be construed as a potential conflict of interest.

Publisher's note

References

1. Sung H, Ferlay J, Siegel RL, Laversanne M, Soerjomataram I, Jemal A, et al. Global cancer statistics 2020: GLOBOCAN estimates of incidence and mortality worldwide for 36 cancers in 185 countries. *CA Cancer J Clin* (2021) 71(3):209–49. doi: 10.3322/caac.21660

2. Kwa M, Makris A, Esteva FJ. Clinical utility of gene-expression signatures in early stage breast cancer. *Nat Rev Clin Oncol* (2017) 14(10):595–610. doi: 10.1038/nrclinonc.2017.74

3. Siegel RL, Miller KD, Fuchs HE, Jemal A. Cancer statistics, 2021. *CA Cancer J Clin* (2021) 71(1):7–33. doi: 10.3322/caac.21654

4. Hernandez RK, Wade SW, Reich A, Pirolli M, Liede A, Lyman GH. Incidence of bone metastases in patients with solid tumors analysis of oncology electronic medical records in the United States. *BMC Cancer* (2018) 18(44). doi: 10.1186/s12885-017-3922-0

5. Talmadge JE, Fidler IJ. AACR centennial series: the biology of cancer metastasis: historical perspective. *Cancer Res* (2010) 70(14):5649–69. doi: 10.1158/0008-5472.CAN-10-1040

6. Paget S. The distribution of secondary growths in cancer of the breast. *Lancet* (1889) 8(2):98–101. doi: 10.1016/S0140-6736(00)49915-0

7. Hanahan D, Weinberg RA. The hallmarks of cancer. *Cell* (2000) 100(1):57–70. doi: 10.1016/S0092-8674(00)81683-9

8. Allinen M, Beroukhim R, Cai L, Brennan C, Lahti-Domenici J, Huang H, et al. Molecular characterization of the tumor microenvironment in breast cancer. *Cancer Cell* (2004) 6(1):17–32. doi: 10.1016/j.ccr.2004.06.010

9. Luo H, Tu G, Liu Z, Liu M. Cancer-associated fibroblasts: a multifaceted driver of breast cancer progression. *Cancer Lett* (2015) 361(2):155–63. doi: 10.1016/j.canlet.2015.02.018

10. Houthuijzen JM, Jonkers J. Cancer-associated fibroblasts as key regulators of the breast cancer tumor microenvironment. *Cancer Metastasis Rev* (2018) 37(4):577–97. doi: 10.1007/s10555-018-9768-3

11. Lorusso G, Ruegg C. The tumor microenvironment and its contribution to tumor evolution toward metastasis. *Histochem Cell Biol* (2008) 130(6):1091–103. doi: 10.1007/s00418-008-0530-8

12. Bissell MJ, Radisky DC, Rizki A, Weaver VM, Petersen OW. The organizing principle: microenvironmental influences in the normal and malignant breast. *Differentiation* (2002) 70(9-10):537–46. doi: 10.1046/j.1432-0436.2002.700907.x

13. Guo M, Li W, Li B, Zou B, Wang S, Fan B, et al. Multiple immune features-based signature for predicting recurrence and survival of inoperable LA-NSCLC patients. *Front Oncol* (2020) 10:571380. doi: 10.3389/fonc.2020.571380

14. Yan X, Xie Y, Yang F, Hua Y, Zeng T, Sun C, et al. Comprehensive description of the current breast cancer microenvironment advancements via single-cell analysis. *J Exp Clin Cancer Res* (2021) 40(1):142. doi: 10.1186/s13046-021-01949-z

15. Pietras K, Ostman A. Hallmarks of cancer: interactions with the tumor stroma. *Exp Cell Res* (2010) 316(8):1324–31. doi: 10.1016/j.yexcr.2010.02.045

16. Arendt LM, Rudnick JA, Keller PJ, Kuperwasser C. Stroma in breast development and disease. *Semin Cell Dev Biol* (2010) 21(1):11–8. doi: 10.1016/j.semcdb.2009.10.003

17. Kaushik N, Kim S, Suh Y, Lee SJ. Proinvasive extracellular matrix remodeling for tumor progression. *Arch Pharm Res* (2019) 42(1):40–7. doi: 10.1007/s12272-018-1097-0

18. Gaggioli C, Hooper S, Hidalgo-Carcedo C, Grosse R, Marshall JF, Harrington K, et al. Fibroblast-led collective invasion of carcinoma cells with differing roles for RhoGTPases in leading and following cells. *Nat Cell Biol* (2007) 9(12):1392–400. doi: 10.1038/ncb1658

19. Franco OE, Shaw AK, Strand DW, Hayward SW. Cancer associated fibroblasts in cancer pathogenesis. *Semin Cell Dev Biol* (2010) 21(1):33–9. doi: 10.1016/j.semcdb.2009.10.010

20. Kalluri R. The biology and function of fibroblasts in cancer. *Nat Rev Cancer.* (2016) 16(9):582–98. doi: 10.1038/nrc.2016.73

21. Naba A, Clauser KR, Hoersch S, Liu H, Carr SA, Hynes RO. The matrisome: *in silico* definition and *in vivo* characterization by proteomics of normal and tumor extracellular matrices. *Mol Cell Proteomics* (2012) 11(4). doi: 10.1074/mcp.M111.014647

22. Gabbiani G, Ryan GB, Majne G. Presence of modified fibroblasts in granulation tissue and their possible role in wound contraction. *Experientia* (1971) 27(5):549–50. doi: 10.1007/BF02147594

23. Dvorak HF. Tumors: wounds that do not heal. similarities between tumor stroma generation and wound healing. *N Engl J Med* (1986) 315(26):1650–9. doi: 10.1056/NEJM198612253152606

24. Kalluri R, Zeisberg M. Fibroblasts in cancer. *Nat Rev Cancer.* (2006) 6(5):392–401. doi: 10.1038/nrc1877

25. Polyak K, Kalluri R. The role of the microenvironment in mammary gland development and cancer. *Cold Spring Harb Perspect Biol* (2010) 2(11):a003244. doi: 10.1101/cshperspect.a003244

26. Desmouliere A, Guyot C, Gabbiani G. The stroma reaction myofibroblast: a key player in the control of tumor cell behavior. *Int J Dev Biol* (2004) 48(5-6):509–17. doi: 10.1387/ijdb.041802ad

27. De Wever O, Nguyen QD, Van Hoorde L, Bracke M, Bruyneel E, Gespach C, et al. Tenascin-c and SF/HGF produced by myofibroblasts *in vitro* provide convergent pro-invasive signals to human colon cancer cells through RhoA and rac. *FASEB J* (2004) 18(9):1016–8. doi: 10.1096/fj.03-1110fje

28. Sugimoto H, Mundel TM, Kieran MW, Kalluri R. Identification of fibroblast heterogeneity in the tumor microenvironment. *Cancer Biol Ther* (2006) 5(12):1640–6. doi: 10.4161/cbt.5.12.3354

29. Pietras K, Sjöblom T, Rubin K, Heldin C-H, Ostman A. PDGF receptors as cancer drug targets. *Cancer Cell* (2003) 3(5):439–43. doi: 10.1016/S1535-6108(03)00089-8

30. Strell C, Paulsson J, Jin SB, Tobin NP, Mezheyeuski A, Roswall P, et al. Impact of epithelial-stromal interactions on peritumoral fibroblasts in ductal carcinoma in situ. *J Natl Cancer Inst* (2019) 111(9):983–95. doi: 10.1093/jnci/djy234

31. Kawase A, Ishii G, Nagai K, Ito T, Nagano T, Murata Y, et al. Podoplanin expression by cancer associated fibroblasts predicts poor prognosis of lung adenocarcinoma. *Int J Cancer.* (2008) 123(5):1053–9. doi: 10.1002/ijc.23611

32. Kim HM, Jung WH, Koo JS. Expression of cancer-associated fibroblast related proteins in metastatic breast cancer: an immunohistochemical analysis. *J Transl Med* (2015) 13:222. doi: 10.1186/s12967-015-0587-9

33. Suchanski J, Tejchman A, Zacharski M, Piotrowska A, Grzegrzolka J, Chodaczek G, et al. Podoplanin increases the migration of human fibroblasts and affects the endothelial cell network formation: a possible role for cancer-associated fibroblasts in breast cancer progression. *PloS One* (2017) 12(9):e0184970. doi: 10.1371/journal.pone.0184970

34. Barth PJ, Ebrahimsade S, Ramaswamy A, Moll R. CD34+ fibrocytes in invasive ductal carcinoma, ductal carcinoma in situ, and benign breast lesions. *Virchows Arch* (2002) 440(3):298–303. doi: 10.1007/s004280100530

35. Venning FA, Zornhagen KW, Wullkopf L, Sjolund J, Rodriguez-Cupello C, Kjellman P, et al. Deciphering the temporal heterogeneity of cancer-associated fibroblast subpopulations in breast cancer. *J Exp Clin Cancer Res* (2021) 40(1):175. doi: 10.1186/s13046-021-01944-4

36. Suh J, Kim DH, Lee YH, Jang JH, Surh YJ. Fibroblast growth factor-2, derived from cancer-associated fibroblasts, stimulates growth and progression of human breast cancer cells via FGFR1 signaling. *Mol Carcinog.* (2020) 59(9):1028–40. doi: 10.1002/mc.23233

37. Kang Y, Zhang Y, Sun Y. Comprehensive analysis of the expression characteristics of the enhancer of the zeste homolog 2 gene in pan-cancer. *Front Genet* (2021) 12:658241. doi: 10.3389/fgene.2021.658241

38. Wang M, Feng R, Chen Z, Shi W, Li C, Liu H, et al. Identification of cancer-associated fibroblast subtype of triple-negative breast cancer. *J Oncol* (2022) 2022:1–14. doi: 10.1155/2022/6452636

39. Shani O, Vorobyov T, Monteran L, Lavie D, Cohen N, Raz Y, et al. Fibroblast-derived IL33 facilitates breast cancer metastasis by modifying the immune microenvironment and driving type 2 immunity. *Cancer Res* (2020) 80(23):5317–29. doi: 10.1158/0008-5472.CAN-20-2116

40. Zeltz C, Alam J, Liu H, Erusappan PM, Hoschuetzky H, Molven A, et al. alpha11beta1 integrin is induced in a subset of cancer-associated fibroblasts in desmoplastic tumor stroma and mediates *In vitro* cell migration. *Cancers (Basel)* (2019) 11(6):765. doi: 10.3390/cancers11060765

41. Kay EJ, Paterson K, Riero-Domingo C, Sumpton D, Dabritz JHM, Tardito S, et al. Cancer-associated fibroblasts require proline synthesis by PYCR1 for the deposition of pro-tumorigenic extracellular matrix. *Nat Metab* (2022) 4(6):693–710. doi: 10.1038/s42255-022-00582-0

42. Ohlund D, Handly-Santana A, Biffi G, Elyada E, Almeida AS, Ponz-Sarvise M, et al. Distinct populations of inflammatory fibroblasts and myofibroblasts in pancreatic cancer. *J Exp Med* (2017) 214(3):579–96. doi: 10.1084/jem.20162024

43. Mishra PJ, Mishra PJ, Humeniuk R, Medina DJ, Alexe G, Mesirov JP, et al. Carcinoma-associated fibroblast-like differentiation of human mesenchymal stem cells. *Cancer Res* (2008) 68(11):4331–9. doi: 10.1158/0008-5472.CAN-08-0943

44. Weber CE, Kothari AN, Wai PY, Li NY, Driver J, Zapf MA, et al. Osteopontin mediates an MZF1-TGF-β1-dependent transformation of mesenchymal stem cells into cancer-associated fibroblasts in breast cancer. *Oncogene* (2015) 34(37):4821–33. doi: 10.1038/onc.2014.410

45. Jeon ES, Moon HJ, Lee MJ, Song HY, Kim YM, Cho M, et al. Cancer-derived lysophosphatidic acid stimulates differentiation of human mesenchymal stem cells to myofibroblast-like cells. *Stem Cells* (2008) 26(3):789–97. doi: 10.1634/stemcells.2007-0742

46. Spaeth EL, Dembinski JL, Sasser AK, Watson K, Klopp A, Hall B, et al. Mesenchymal stem cell transition to tumor-associated fibroblasts contributes to fibrovascular network expansion and tumor progression. *PloS One* (2009) 4(4):e4992. doi: 10.1371/journal.pone.0004992

47. Giorello MB, Borzone FR, Labovsky V, Piccioni FV, Chasseing NA. Cancer-associated fibroblasts in the breast tumor microenvironment. *J Mammary Gland Biol Neoplasia.* (2021) 26(2):135–55. doi: 10.1007/s10911-020-09475-y

48. Arina A, Idel C, Hyjek EM, Alegre ML, Wang Y, Bindokas VP, et al. Tumor-associated fibroblasts predominantly come from local and not circulating precursors. *Proc Natl Acad Sci U S A.* (2016) 113(27):7551–6. doi: 10.1073/pnas.1600363113

49. LeBleu VS, Kalluri R. A peek into cancer-associated fibroblasts: origins, functions and translational impact. *Dis Model Mech* (2018) 11(4). doi: 10.1242/dmm.029447

50. Bu L, Baba H, Yoshida N, Miyake K, Yasuda T, Uchihara T, et al. Biological heterogeneity and versatility of cancer-associated fibroblasts in the tumor microenvironment. *Oncogene* (2019) 38(25):4887–901. doi: 10.1038/s41388-019-0765-y

51. Kwa MQ, Herum KM, Brakebusch C. Cancer-associated fibroblasts: how do they contribute to metastasis? *Clin Exp Metastasis* (2019) 36(2):71–86. doi: 10.1007/s10585-019-09959-0

52. Ronnov-Jessen L, Petersen OW, Koteliansky VE, Bissell MJ. The origin of the myofibroblasts in breast cancer. recapitulation of tumor environment in culture unravels diversity and implicates converted fibroblasts and recruited smooth muscle cells. *J Clin Invest.* (1995) 95(2):859–73. doi: 10.1172/JCI117736.

53. Díaz-Flores L, Gutiérrez R, González-Gómez M, García MP, Díaz-Flores LJr., Carrasco JL, et al. CD34+ stromal Cells/Telocytes as a source of cancer-associated fibroblasts (CAFs) in invasive lobular carcinoma of the breast. *Int J Mol Sci* (2021) 22(7):3686. doi: 10.3390/ijms22073686

54. Quail DF, Joyce JA. Microenvironmental regulation of tumor progression and metastasis. *Nat Med* (2013) 19(11):1423–37. doi: 10.1038/nm.3394

55. Bronzert DA, Pantazis P, Antoniades HN, Kasid A, Davidson N, Dickson RB, et al. Synthesis and secretion of platelet-derived growth factor by human breast cancer cell lines. *Proc Natl Acad Sci U S A.* (1987) 84(16):5763–7. doi: 10.1073/pnas.84.16.5763

56. Shao ZM, Nguyen M, Barsky SH. Human breast carcinoma desmoplasia is PDGF initiated. *Oncogene* (2000) 19(38):4337–45. doi: 10.1038/sj.onc.1203785

57. Strutz F, Zeisberg M, Hemmerlein B, Sattler B, Hummel K, Becker V, et al. Basic fibroblast growth factor expression is increased in human renal fibrogenesis and may mediate autocrine fibroblast proliferation. *Kidney Int* (2000) 57(4):1521–38. doi: 10.1046/j.1523-1755.2000.00997.x

58. Giannoni E, Bianchini F, Masieri L, Serni S, Torre E, Calorini L, et al. Reciprocal activation of prostate cancer cells and cancer-associated fibroblasts stimulates epithelial-mesenchymal transition and cancer stemness. *Cancer Res* (2010) 70(17):6945–56. doi: 10.1158/0008-5472.CAN-10-0785

59. Hendrayani SF, Al-Khalaf HH, Aboussekhra A. The cytokine IL-6 reactivates breast stromal fibroblasts through transcription factor STAT3-dependent up-regulation of the RNA-binding protein AUF1. *J Biol Chem* (2014) 289(45):30962–76. doi: 10.1074/jbc.M114.594044

60. Cosentino G, Romero-Cordoba S, Plantamura I, Cataldo A, Iorio MV. miR-9-Mediated inhibition of EFEMP1 contributes to the acquisition of pro-tumoral properties in normal fibroblasts. *Cells* (2020) 9(9):2143. doi: 10.3390/cells9092143

61. Chen JY, Li CF, Lai YS, Hung WC. Lysine demethylase 2A expression in cancer-associated fibroblasts promotes breast tumour growth. *Br J Cancer.* (2021) 124(2):484–93. doi: 10.1038/s41416-020-01112-z

62. Butti R, Nimma R, Kundu G, Bulbule A, Kumar TVS, Gunasekaran VP, et al. Tumor-derived osteopontin drives the resident fibroblast to myofibroblast differentiation through Twist1 to promote breast cancer progression. *Oncogene* (2021) 40(11):2002–17. doi: 10.1038/s41388-021-01663-2

63. Chen Y, Cai L, Guo X, Li Z, Liao X, Zhang X, et al. HMGB1-activated fibroblasts promote breast cancer cells metastasis via RAGE/aerobic glycolysis. *Neoplasma* (2021) 68(1):71–8. doi: 10.4149/neo_2020_200610N620

64. Ren Z, Lv M, Yu Q, Bao J, Lou K, Li X. MicroRNA-370-3p shuttled by breast cancer cell-derived extracellular vesicles induces fibroblast activation through the CYLD/Nf-kappaB axis to promote breast cancer progression. *FASEB J* (2021) 35(3):e21383. doi: 10.1096/fj.202001430RR

65. Vu LT, Peng B, Zhang DX, Ma V, Mathey-Andrews CA, Lam CK, et al. Tumor-secreted extracellular vesicles promote the activation of cancer-associated fibroblasts via the transfer of microRNA-125b. *J Extracell Vesicles.* (2019) 8(1):1599680. doi: 10.1080/20013078.2019.1599680

66. Baroni S, Romero-Cordoba S, Plantamura I, Dugo M, D'Ippolito E, Cataldo A, et al. Exosome-mediated delivery of miR-9 induces cancer-associated fibroblast-like properties in human breast fibroblasts. *Cell Death Dis* (2016) 7(7):e2312. doi: 10.1038/cddis.2016.224

67. Schwager SC, Bordeleau F, Zhang J, Antonyak MA, Cerione RA, Reinhart-King CA. Matrix stiffness regulates microvesicle-induced fibroblast activation. *Am J Physiol Cell Physiol* (2019) 317(1):C82–92. doi: 10.1152/ajpcell.00418.2018

68. Jung WH, Yam N, Chen CC, Elawad K, Hu B, Chen Y. Force-dependent extracellular matrix remodeling by early-stage cancer cells alters diffusion and induces carcinoma-associated fibroblasts. *Biomaterials* (2020) 234:119756. doi: 10.1016/j.biomaterials.2020.119756

69. Strong AL, Pei DT, Hurst CG, Gimble JM, Burow ME, Bunnell BA. Obesity enhances the conversion of adipose-derived Stromal/Stem cells into carcinoma-associated fibroblast leading to cancer cell proliferation and progression to an invasive phenotype. *Stem Cells Int* (2017) 2017:9216502. doi: 10.1155/2017/9216502

70. Yang X, Hao J, Mao Y, Jin ZQ, Cao R, Zhu CH, et al. bFGF promotes migration and induces cancer-associated fibroblast differentiation of mouse bone mesenchymal stem cells to promote tumor growth. *Stem Cells Dev* (2016) 25(21):1629–39. doi: 10.1089/scd.2016.0217

71. De Vincenzo A, Belli S, Franco P, Telesca M, Iaccarino I, Botti G, et al. Paracrine recruitment and activation of fibroblasts by c-myc expressing breast epithelial cells through the IGFs/IGF-1R axis. *Int J Cancer.* (2019) 145(10):2827–39. doi: 10.1002/ijc.32613

72. Kiaris H, Chatzistamou I, Trimis G, Frangou-Plemmenou M, Pafiti-Kondi A, Kalofoutis A. Evidence for nonautonomous effect of p53 tumor suppressor in carcinogenesis. *Cancer Res* (2005) 65(5):1627–30. doi: 10.1158/0008-5472.CAN-04-3791

73. Trimis G, Chatzistamou I, Politi K, Kiaris H, Papavassiliou AG. Expression of p21waf1/Cip1 in stromal fibroblasts of primary breast tumors. *Hum Mol Genet* (2008) 17(22):3596–600. doi: 10.1093/hmg/ddn252

74. Trimboli AJ, Cantemir-Stone CZ, Li F, Wallace JA, Merchant A, Creasap N, et al. Pten in stromal fibroblasts suppresses mammary epithelial tumours. *Nature* (2009) 461(7267):1084–91. doi: 10.1038/nature08486

75. Trimmer C, Sotgia F, Whitaker-Menezes D, Balliet RM, Eaton G, Martinez-Outschoorn UE, et al. Caveolin-1 and mitochondrial SOD2 (MnSOD) function as tumor suppressors in the stromal microenvironment: a new genetically tractable model for human cancer associated fibroblasts. *Cancer Biol Ther* (2011) 11(4):383–94. doi: 10.4161/cbt.11.4.14101

76. Mercier I, Casimiro MC, Wang C, Rosenberg AL, Quong J, Minkeu A, et al. Human breast cancer-associated fibroblasts (CAFs) show caveolin-1 downregulation and RB tumor suppressor functional inactivation: implications for the response to hormonal therapy. *Cancer Biol Ther* (2008) 7(8):1212–25. doi: 10.4161/cbt.7.8.6220

77. Wang L, Hou Y, Sun Y, Zhao L, Tang X, Hu P, et al. C-ski activates cancer-associated fibroblasts to regulate breast cancer cell invasion. *Mol Oncol* (2013) 7 (6):1116–28. doi: 10.1016/j.molonc.2013.08.007

78. You E, Huh YH, Kwon A, Kim SH, Chae IH, Lee OJ, et al. SPIN90 depletion and microtubule acetylation mediate stromal fibroblast activation in breast cancer progression. *Cancer Res* (2017) 77(17):4710–22. doi: 10.1158/0008-5472.CAN-17-0657

79. Polyak K, Weinberg RA. Transitions between epithelial and mesenchymal states: acquisition of malignant and stem cell traits. *Nat Rev Cancer*. (2009) 9(4):265–73. doi: 10.1038/nrc2620

80. Potenta S, Zeisberg E, Kalluri R. The role of endothelial-to-mesenchymal transition in cancer progression. *Br J Cancer*. (2008) 99(9):1375–9. doi: 10.1038/sj.bjc.6604662

81. Zeisberg EM, Potenta S, Xie L, Zeisberg M, Kalluri R. Discovery of endothelial to mesenchymal transition as a source for carcinoma-associated fibroblasts. *Cancer Res* (2007) 67(21):10123–8. doi: 10.1158/0008-5472.CAN-07-3127

82. Lu JT, Tan CC, Wu XR, He R, Zhang X, Wang QS, et al. FOXF2 deficiency accelerates the visceral metastasis of basal-like breast cancer by unrestrictedly increasing TGF-beta and miR-182-5p. *Cell Death Differ* (2020) 27(10):2973–87. doi: 10.1038/s41418-020-0555-7

83. Kojima Y, Acar A, Eaton EN, Mellody KT, Scheel C, Ben-Porath I, et al. Autocrine TGF-beta and stromal cell-derived factor-1 (SDF-1) signaling drives the evolution of tumor-promoting mammary stromal myofibroblasts. *Proc Natl Acad Sci U S A*. (2010) 107(46):20009–14. doi: 10.1073/pnas.1013805107

84. Stuelten CH, Busch JI, Tang B, Flanders KC, Oshima A, Sutton E, et al. Transient tumor-fibroblast interactions increase tumor cell malignancy by a TGF-beta mediated mechanism in a mouse xenograft model of breast cancer. *PloS One* (2010) 5(3):e9832. doi: 10.1371/journal.pone.0009832

85. Huang M, Fu M, Wang J, Xia C, Zhang H, Xiong Y, et al. TGF-beta1-activated cancer-associated fibroblasts promote breast cancer invasion, metastasis and epithelial-mesenchymal transition by autophagy or overexpression of FAP-alpha. *Biochem Pharmacol* (2021) 188:114527. doi: 10.1016/j.bcp.2021.114527

86. Jezierska-Drutel A, Rosenzweig SA, Neumann CA. Role of oxidative stress and the microenvironment in breast cancer development and progression. *Adv Cancer Res* (2013) 119:107–25. doi: 10.1016/B978-0-12-407190-2.00003-4

87. Lambies G, Miceli M, Martinez-Guillamon C, Olivera-Salguero R, Pena R, Frias CP, et al. TGFbeta-activated USP27X deubiquitinase regulates cell migration and chemoresistance via stabilization of Snail1. *Cancer Res* (2019) 79(1):33–46. doi: 10.1158/0008-5472.CAN-18-0753

88. Mi Z, Bhattacharya SD, Kim VM, Guo H, Talbot LJ, Kuo PC. Osteopontin promotes CCL5-mesenchymal stromal cell-mediated breast cancer metastasis. *Carcinogenesis* (2011) 32(4):477–87. doi: 10.1093/carcin/bgr009

89. Chatterjee A, Jana S, Chatterjee S, Wastall LM, Mandal G, Nargis N, et al. MicroRNA-222 reprogrammed cancer-associated fibroblasts enhance growth and metastasis of breast cancer. *Br J Cancer*. (2019) 121(8):679–89. doi: 10.1038/s41416-019-0566-7

90. Rubinstein-Achiasaf L, Morein D, Ben-Yaakov H, Liubomirski Y, Meshel T, Elbaz E, et al. Persistent inflammatory stimulation drives the conversion of MSCs to inflammatory CAFs that promote pro-metastatic characteristics in breast cancer cells. *Cancers (Basel)* (2021) 13(6):1472. doi: 10.3390/cancers13061472

91. Brechbuhl HM, Finlay-Schultz J, Yamamoto TM, Gillen AE, Cittelly DM, Tan AC, et al. Fibroblast subtypes regulate responsiveness of luminal breast cancer to estrogen. *Clin Cancer Res* (2017) 23(7):1710–21. doi: 10.1158/1078-0432.CCR-15-2851

92. Brechbuhl HM, Barrett AS, Kopin E, Hagen JC, Han AL, Gillen AE, et al. Fibroblast subtypes define a metastatic matrisome in breast cancer. *JCI Insight* (2020) 5 (4):e130751. doi: 10.1172/jci.insight.130751

93. Costa A, Kieffer Y, Scholer-Dahirel A, Pelon F, Bourachot B, Cardon M, et al. Fibroblast heterogeneity and immunosuppressive environment in human breast cancer. *Cancer Cell* (2018) 33(3):463–79 e10. doi: 10.1016/j.ccell.2018.01.011

94. Pelon F, Bourachot B, Kieffer Y, Magagna I, Mermet-Meillon F, Bonnet I, et al. Cancer-associated fibroblast heterogeneity in axillary lymph nodes drives metastases in breast cancer through complementary mechanisms. *Nat Commun* (2020) 11(1):404. doi: 10.1038/s41467-019-14134-w

95. Wu SZ, Roden DL, Wang C, Holliday H, Harvey K, Cazet AS, et al. Stromal cell diversity associated with immune evasion in human triple-negative breast cancer. *EMBO J* (2020) 39(19):e104063. doi: 10.15252/embj.2019104063

96. Bartoschek M, Oskolkov N, Bocci M, Lovrot J, Larsson C, Sommarin M, et al. Spatially and functionally distinct subclasses of breast cancer-associated fibroblasts revealed by single cell RNA sequencing. *Nat Commun* (2018) 9(1):5150. doi: 10.1038/s41467-018-07582-3

97. Houthuijzen JM, de Bruijn R, van der Burg E, Drenth AP, Wientjens E, Filipovic T, et al. CD26-negative and CD26-positive tissue-resident fibroblasts contribute to functionally distinct CAF subpopulations in breast cancer. *Nat Commun* (2023) 14 (1):183. doi: 10.1038/s41467-023-35793-w

98. Sebastian A, Hum NR, Martin KA, Gilmore SF, Peran I, Byers SW, et al. Single-cell transcriptomic analysis of tumor-derived fibroblasts and normal tissue-resident fibroblasts reveals fibroblast heterogeneity in breast cancer. *Cancers (Basel)* (2020) 12 (5):1307. doi: 10.3390/cancers12051307

99. Vokurka M, Lacina L, Brabek J, Kolar M, Ng YZ, Smetana KJr. Cancer-associated fibroblasts influence the biological properties of malignant tumours via paracrine secretion and exosome production. *Int J Mol Sci* (2022) 23(2):964. doi: 10.3390/ijms23020964

100. Orimo A, Gupta PB, Sgroi DC, Arenzana-Seisdedos F, Delaunay T, Naeem R, et al. Stromal fibroblasts present in invasive human breast carcinomas promote tumor growth and angiogenesis through elevated SDF-1/CXCL12 secretion. *Cell* (2005) 121 (3):335–48. doi: 10.1016/j.cell.2005.02.034

101. Zhang XH, Jin X, Malladi S, Zou Y, Wen YH, Brogi E, et al. Selection of bone metastasis seeds by mesenchymal signals in the primary tumor stroma. *Cell* (2013) 154 (5):1060–73. doi: 10.1016/j.cell.2013.07.036

102. Huang M, Li Y, Zhang H, Nan F. Breast cancer stromal fibroblasts promote the generation of CD44+CD24- cells through SDF-1/CXCR4 interaction. *J Exp Clin Cancer Res* (2010) 29:80. doi: 10.1186/1756-9966-29-80

103. Shao S, Zhao L, An G, Zhang L, Jing X, Luo M, et al. Metformin suppresses HIF-1alpha expression in cancer-associated fibroblasts to prevent tumor-stromal cross talk in breast cancer. *FASEB J* (2020) 34(8):10860–70. doi: 10.1096/fj.202000951RR

104. Augsten M, Sjöberg E, Frings O, Vorrink SU, Frijhoff J, Olsson E, et al. Cancer-associated fibroblasts expressing CXCL14 rely upon NOS1-derived nitric oxide signaling for their tumor-supporting properties. *Cancer Res* (2014) 74(11):2999–3010. doi: 10.1158/0008-5472.CAN-13-2740

105. Sjoberg E, Meyrath M, Milde L, Herrera M, Lovrot J, Hagerstrand D, et al. A novel ACKR2-dependent role of fibroblast-derived CXCL14 in epithelial-to-Mesenchymal transition and metastasis of breast cancer. *Clin Cancer Res* (2019) 25 (12):3702–17. doi: 10.1158/1078-0432.CCR-18-1294

106. Wen S, Hou Y, Fu L, Xi L, Yang D, Zhao M, et al. Cancer-associated fibroblast (CAF)-derived IL32 promotes breast cancer cell invasion and metastasis via integrin beta3-p38 MAPK signalling. *Cancer Lett* (2019) 442:320–32. doi: 10.1016/j.canlet.2018.10.015

107. Guo Z, Zhang H, Fu Y, Kuang J, Zhao B, Zhang L, et al. Cancer-associated fibroblasts induce growth and radioresistance of breast cancer cells through paracrine IL-6. *Cell Death Discovery* (2023) 9(1):6. doi: 10.1038/s41420-023-01306-3

108. Palmieri C, Roberts-Clark D, Assadi-Sabet A, Coope RC, O'Hare M, Sunters A, et al. Fibroblast growth factor 7, secreted by breast fibroblasts, is an interleukin-1beta-induced paracrine growth factor for human breast cells. *J Endocrinol* (2003) 177(1):65–81. doi: 10.1677/joe.0.1770065

109. Yu Y, Xiao CH, Tan LD, Wang QS, Li XQ, Feng YM. Cancer-associated fibroblasts induce epithelial-mesenchymal transition of breast cancer cells through paracrine TGF-beta signalling. *Br J Cancer*. (2014) 110(3):724–32. doi: 10.1038/bjc.2013.768

110. Kessenbrock K, Plaks V, Werb Z. Matrix metalloproteinases: regulators of the tumor microenvironment. *Cell* (2010) 141(1):52–67. doi: 10.1016/j.cell.2010.03.015

111. Wang TN, Albo D, Tuszynski GP. Fibroblasts promote breast cancer cell invasion by upregulating tumor matrix metalloproteinase-9 production. *Surgery* (2002) 132(2):220–5. doi: 10.1067/msy.2002.125353

112. Eck SM, Côté AL, Winkelman WD, Brinckerhoff CE. CXCR4 and matrix metalloproteinase-1 are elevated in breast carcinoma-associated fibroblasts and in normal mammary fibroblasts exposed to factors secreted by breast cancer cells. *Mol Cancer Res* (2009) 7(7):1033–44. doi: 10.1158/1541-7786.MCR-09-0015

113. Nakopoulou L, Panayotopoulou EG, Giannopoulou I, Alexandrou P, Katsarou S, Athanassiadou P, et al. Stromelysin-3 protein expression in invasive breast cancer: relation to proliferation, cell survival and patients' outcome. *Mod Pathol* (2002) 15 (11):1154–61. doi: 10.1097/01.MP.0000037317.84782.CD

114. Vizoso FJ, González LO, Corte MD, Rodríguez JC, Vázquez J, Lamelas ML, et al. Study of matrix metalloproteinases and their inhibitors in breast cancer. *Br J Cancer*. (2007) 96(6):903–11. doi: 10.1038/sj.bjc.6603666

115. Eiro N, Fernandez-Garcia B, Vazquez J, Del Casar JM, Gonzalez LO, Vizoso FJ. A phenotype from tumor stroma based on the expression of metalloproteases and their inhibitors, associated with prognosis in breast cancer. *Oncoimmunology* (2015) 4(7): e992222. doi: 10.4161/2162402X.2014.992222

116. Luga V, Wrana JL. Tumor-stroma interaction: revealing fibroblast-secreted exosomes as potent regulators of wnt-planar cell polarity signaling in cancer metastasis. *Cancer Res* (2013) 73(23):6843–7. doi: 10.1158/0008-5472.CAN-13-1791

117. Zhan Y, Du J, Min Z, Ma L, Zhang W, Zhu W, et al. Carcinoma-associated fibroblasts derived exosomes modulate breast cancer cell stemness through exonic circHIF1A by miR-580-5p in hypoxic stress. *Cell Death Discovery* (2021) 7(1):141. doi: 10.1038/s41420-021-00506-z

118. Maeda T, Desouky J, Friedl A. Syndecan-1 expression by stromal fibroblasts promotes breast carcinoma growth *in vivo* and stimulates tumor angiogenesis. *Oncogene* (2006) 25(9):1408–12. doi: 10.1038/sj.onc.1209168

119. Zheng S, Zou Y, Tang Y, Yang A, Liang JY, Wu L, et al. Landscape of cancer-associated fibroblasts identifies the secreted biglycan as a protumor and immunosuppressive factor in triple-negative breast cancer. *Oncoimmunology* (2022) 11(1):2020984. doi: 10.1080/2162402X.2021.2020984

120. Boyle ST, Poltavets V, Kular J, Pyne NT, Sandow JJ, Lewis AC, et al. ROCK-mediated selective activation of PERK signalling causes fibroblast reprogramming and tumour progression through a CRELD2-dependent mechanism. *Nat Cell Biol* (2020) 22 (7):882–95. doi: 10.1038/s41556-020-0523-y

121. Kuo MC, Kuo PC, Mi Z. Myeloid zinc finger-1 regulates expression of cancer-associated fibroblast and cancer stemness profiles in breast cancer. *Surgery* (2019) 166 (4):515–23. doi: 10.1016/j.surg.2019.05.042

122. Mir S, Golden BDO, Griess BJ, Vengoji R, Tom E, Kosmacek EA, et al. Upregulation of Nox4 induces a pro-survival Nrf2 response in cancer-associated fibroblasts that promotes tumorigenesis and metastasis, in part via Birc5 induction. *Breast Cancer Res* (2022) 24(1):48. doi: 10.1186/s13058-022-01548-6

123. Santolla MF, Vivacqua A, Lappano R, Rigiracciolo DC, Cirillo F, Galli GR, et al. GPER mediates a feedforward FGF2/FGFR1 paracrine activation coupling CAFs to cancer cells toward breast tumor progression. *Cells* (2019) 8(3):233. doi: 10.3390/cells8030223

124. Piasecka D, Braun M, Kitowska K, Mieczkowski K, Kordek R, Sadej R, et al. FGFs/FGFRs-dependent signalling in regulation of steroid hormone receptors - implications for therapy of luminal breast cancer. *J Exp Clin Cancer Res* (2019) 38 (1):230. doi: 10.1186/s13046-019-1236-6

125. Shu C, Zha H, Long H, Wang X, Yang F, Gao J, et al. C3a-C3aR signaling promotes breast cancer lung metastasis via modulating carcinoma associated fibroblasts. *J Exp Clin Cancer Res* (2020) 39(1):11. doi: 10.1186/s13046-019-1515-2

126. Ren J, Smid M, Iaria J, Salvatori DCF, van Dam H, Zhu HJ, et al. Cancer-associated fibroblast-derived gremlin 1 promotes breast cancer progression. *Breast Cancer Res* (2019) 21(1):109. doi: 10.1186/s13058-019-1194-0

127. Catalano S, Panza S, Augimeri G, Giordano C, Malivindi R, Gelsomino L, et al. Phosphodiesterase 5 (PDE5) is highly expressed in cancer-associated fibroblasts and enhances breast tumor progression. *Cancers (Basel)* (2019) 11(11):1740. doi: 10.3390/cancers11111740

128. Truong DD, Kratz A, Park JG, Barrientos ES, Saini H, Nguyen T, et al. A human organotypic microfluidic tumor model permits investigation of the interplay between patient-derived fibroblasts and breast cancer cells. *Cancer Res* (2019) 79 (12):3139–51. doi: 10.1158/0008-5472.CAN-18-2293

129. Soon PS, Kim E, Pon CK, Gill AJ, Moore K, Spillane AJ, et al. Breast cancer-associated fibroblasts induce epithelial-to-mesenchymal transition in breast cancer cells. *Endocr Relat Cancer.* (2013) 20(1):1–12. doi: 10.1530/ERC-12-0227

130. Sanchez-Alvarez R, Martinez-Outschoorn UE, Lamb R, Hulit J, Howell A, Gandara R, et al. Mitochondrial dysfunction in breast cancer cells prevents tumor growth: understanding chemoprevention with metformin. *Cell Cycle* (2013) 12(1):172–82. doi: 10.4161/cc.23058

131. Wu HJ, Hao M, Yeo SK, Guan JL. FAK signaling in cancer-associated fibroblasts promotes breast cancer cell migration and metastasis by exosomal miRNAs-mediated intercellular communication. *Oncogene* (2020) 39(12):2539–49. doi: 10.1038/s41388-020-1162-2

132. Zellmer VR, Schnepp PM, Fracci SL, Tan X, Howe EN, Zhang S. Tumor-induced stromal STAT1 accelerates breast cancer via deregulating tissue homeostasis. *Mol Cancer Res* (2017) 15(5):585–97. doi: 10.1158/1541-7786.MCR-16-0312

133. Duda DG, Duyverman AM, Kohno M, Snuderl M, Steller EJ, Fukumura D, et al. Malignant cells facilitate lung metastasis by bringing their own soil. *Proc Natl Acad Sci U S A.* (2010) 107(50):21677–82. doi: 10.1073/pnas.1016234107

134. Jenkins L, Jungwirth U, Avgustinova A, Iravani M, Mills A, Haider S, et al. Cancer-associated fibroblasts suppress CD8+ T-cell infiltration and confer resistance to immune-checkpoint blockade. *Cancer Res* (2022) 82(16):2904–17. doi: 10.1158/0008-5472.CAN-21-4141

135. Dou D, Ren X, Han M, Xu X, Ge X, Gu Y, et al. Cancer-associated fibroblasts-derived exosomes suppress immune cell function in breast cancer via the miR-92/PD-L1 pathway. *Front Immunol* (2020) 11:2026. doi: 10.3389/fimmu.2020.02026

136. Hu G, Cheng P, Pan J, Wang S, Ding Q, Jiang Z, et al. An IL6-adenosine positive feedback loop between CD73(+) gammadeltaTregs and CAFs promotes tumor progression in human breast cancer. *Cancer Immunol Res* (2020) 8(10):1273–86. doi: 10.1158/2326-6066.CIR-19-0923

137. Timperi E, Gueguen P, Molgora M, Magagna I, Kieffer Y, Lopez-Lastra S, et al. Lipid-associated macrophages are induced by cancer-associated fibroblasts and mediate immune suppression in breast cancer. *Cancer Res* (2022) 82(18):3291–306. doi: 10.1158/0008-5472.CAN-22-1427

138. Lyssiotis CA, Kimmelman AC. Metabolic interactions in the tumor microenvironment. *Trends Cell Biol* (2017) 27(11):863–75. doi: 10.1016/j.tcb.2017.06.003

139. Lopes-Coelho F, Andre S, Felix A, Serpa J. Breast cancer metabolic cross-talk: fibroblasts are hubs and breast cancer cells are gatherers of lipids. *Mol Cell Endocrinol* (2018) 462(Pt B):93–106. doi: 10.1016/j.mce.2017.01.031

140. Liu Y, Geng YH, Yang H, Yang H, Zhou YT, Zhang HQ, et al. Extracellular ATP drives breast cancer cell migration and metastasis via S100A4 production by cancer cells and fibroblasts. *Cancer Lett* (2018) 430:1–10. doi: 10.1016/j.canlet.2018.04.043

141. Bertero T, Oldham WM, Grasset EM, Bourget I, Boulter E, Pisano S, et al. Tumor-stroma mechanics coordinate amino acid availability to sustain tumor growth and malignancy. *Cell Metab* (2019) 29(1):124–40 e10. doi: 10.1016/j.cmet.2018.09.012

142. Miyazaki K, Togo S, Okamoto R, Idiris A, Kumagai H, Miyagi Y. Collective cancer cell invasion in contact with fibroblasts through integrin-alpha5beta1/fibronectin interaction in collagen matrix. *Cancer Sci* (2020) 111(12):4381–92. doi: 10.1111/cas.14664

143. Gao MQ, Kim BG, Kang S, Choi YP, Park H, Kang KS, et al. Stromal fibroblasts from the interface zone of human breast carcinomas induce an epithelial-mesenchymal transition-like state in breast cancer cells in vitro. *J Cell Sci* (2010) Pt 20):3507–14. doi: 10.1242/jcs.072900

144. Jain RK, Martin JD, Stylianopoulos T. The role of mechanical forces in tumor growth and therapy. *Annu Rev BioMed Eng.* (2014) 16:321–46. doi: 10.1146/annurev-bioeng-071813-105259

145. Karagiannis GS, Poutahidis T, Erdman SE, Kirsch R, Riddell RH, Diamandis EP. Cancer-associated fibroblasts drive the progression of metastasis through both paracrine and mechanical pressure on cancer tissue. *Mol Cancer Res* (2012) 10 (11):1403–18. doi: 10.1158/1541-7786.MCR-12-0307

146. Jungwirth U, van Weverwijk A, Evans RJ, Jenkins L, Vicente D, Alexander J, et al. Impairment of a distinct cancer-associated fibroblast population limits tumour growth and metastasis. *Nat Commun* (2021) 12(1):3516. doi: 10.1038/s41467-021-23583-1

147. Wessels DJ, Pradhan N, Park YN, Klepitsch MA, Lusche DF, Daniels KJ, et al. Reciprocal signaling and direct physical interactions between fibroblasts and breast cancer cells in a 3D environment. *PloS One* (2019) 14(6):e0218854. doi: 10.1371/journal.pone.0218854

148. Sun C, Wang S, Zhang Y, Yang F, Zeng T, Meng F, et al. Risk signature of cancer-associated fibroblast-secreted cytokines associates with clinical outcomes of breast cancer. *Front Oncol* (2021) 11:628677. doi: 10.3389/fonc.2021.628677

149. Yamashita M, Ogawa T, Zhang X, Hanamura N, Kashikura Y, Takamura M, et al. Role of stromal myofibroblasts in invasive breast cancer: stromal expression of alpha-smooth muscle actin correlates with worse clinical outcome. *Breast Cancer.* (2012) 19(2):170–6. doi: 10.1007/s12282-010-0234-5

150. Muchlinska A, Nagel A, Popeda M, Szade J, Niemira M, Zielinski J, et al. Alpha-smooth muscle actin-positive cancer-associated fibroblasts secreting osteopontin promote growth of luminal breast cancer. *Cell Mol Biol Lett* (2022) 27 (1):45. doi: 10.1186/s11658-022-00351-7

151. Jansson S, Aaltonen K, Bendahl PO, Falck AK, Karlsson M, Pietras K, et al. The PDGF pathway in breast cancer is linked to tumour aggressiveness, triple-negative subtype and early recurrence. *Breast Cancer Res Treat* (2018) 169(2):231–41. doi: 10.1007/s10549-018-4664-7

152. Primac I, Maquoi E, Blacher S, Heljasvaara R, Van Deun J, Smeland HY, et al. Stromal integrin alpha11 regulates PDGFR-beta signaling and promotes breast cancer progression. *J Clin Invest.* (2019) 129(11):4609–28. doi: 10.1172/JCI125890

153. Akanda MR, Ahn EJ, Kim YJ, Salam SMA, Noh MG, Lee TK, et al. Analysis of stromal PDGFR-β and α-SMA expression and their clinical relevance in brain metastases of breast cancer patients. *BMC Cancer.* (2023) 23(1):468. doi: 10.1186/s12885-023-10957-5

154. Kieffer Y, Hocine HR, Gentric G, Pelon F, Bernard C, Bourachot B, et al. Single-cell analysis reveals fibroblast clusters linked to immunotherapy resistance in cancer. *Cancer Discovery* (2020) 10(9):1330–51. doi: 10.1158/2159-8290.CD-19-1384

155. Yu LN, Liu Z, Tian Y, Zhao PP, Hua X. FAP-a and GOLPH3 are hallmarks of DCIS progression to invasive breast cancer. *Front Oncol* (2019) 9:1424. doi: 10.3389/fonc.2019.01424

156. Loktev A, Lindner T, Mier W, Debus J, Altmann A, Jager D, et al. A tumor-imaging method targeting cancer-associated fibroblasts. *J Nucl Med* (2018) 59(9):1423–9. doi: 10.2967/jnumed.118.210435

157. Kratochwil C, Flechsig P, Lindner T, Abderrahim L, Altmann A, Mier W, et al. (68)Ga-FAPI PET/CT: tracer uptake in 28 different kinds of cancer. *J Nucl Med* (2019) 60(6):801–5. doi: 10.2967/jnumed.119.227967

158. Argote Camacho AX, Gonzalez Ramirez AR, Perez Alonso AJ, Rejon Garcia JD, Olivares Urbano MA, Torne Poyatos P, et al. Metalloproteinases 1 and 3 as potential biomarkers in breast cancer development. *Int J Mol Sci* (2021) 22(16):9012. doi: 10.3390/ijms22169012

159. Alrehaili AA, Gharib AF, Karam RA, Alhakami RA, El Sawy WH, Abd Elrahman TM. Clinical significance of plasma MMP-2 and MMP-9 levels as biomarkers for tumor expression in breast cancer patients in Egypt. *Mol Biol Rep* (2020) 47(2):1153–60. doi: 10.1007/s11033-019-05216-5

160. Majumder A, Ray S, Banerji A. Epidermal growth factor receptor-mediated regulation of matrix metalloproteinase-2 and matrix metalloproteinase-9 in MCF-7 breast cancer cells. *Mol Cell Biochem* (2019) 452(1-2):111–21. doi: 10.1007/s11010-018-3417-6

161. Cid S, Eiro N, Fernandez B, Sanchez R, Andicoechea A, Fernandez-Muniz PI, et al. Prognostic influence of tumor stroma on breast cancer subtypes. *Clin Breast Cancer.* (2018) 18(1):e123–e33. doi: 10.1016/j.clbc.2017.08.008

162. Bouras T, Lisanti MP, Pestell RG. Caveolin-1 in breast cancer. *Cancer Biol Ther* (2004) 3(10):931–41. doi: 10.4161/cbt.3.10.1147

163. Yeong J, Thike AA, Ikeda M, Lim JCT, Lee B, Nakamura S, et al. Caveolin-1 expression as a prognostic marker in triple negative breast cancers of Asian women. *J Clin Pathol* (2018) 71(2):161–7. doi: 10.1136/jclinpath-2017-204495

164. Liang YN, Liu Y, Wang L, Yao G, Li X, Meng X, et al. Combined caveolin-1 and epidermal growth factor receptor expression as a prognostic marker for breast cancer. *Oncol Lett* (2018) 15(6):9271–82. doi: 10.3892/ol.2018.8533

165. Al-Tweigeri T, AlRaouji NN, Tulbah A, Arafah M, Aboussekhra M, Al-Mohanna F, et al. High AUF1 level in stromal fibroblasts promotes carcinogenesis and chemoresistance and predicts unfavorable prognosis among locally advanced breast cancer patients. *Breast Cancer Res* (2022) 24(1):46. doi: 10.1186/s13058-022-01543-x

166. Al-Kharashi LA, Tulbah A, Arafah M, Eldali AM, Al-Tweigeri T, Aboussekhra A. High DNMT1 expression in stromal fibroblasts promotes angiogenesis and unfavorable outcome in locally advanced breast cancer patients. *Front Oncol* (2022) 12:877219. doi: 10.3389/fonc.2022.877219

167. Zhou J, Wang XH, Zhao YX, Chen C, Xu XY, Sun Q, et al. Cancer-associated fibroblasts correlate with tumor-associated macrophages infiltration and lymphatic metastasis in triple negative breast cancer patients. *J Cancer*. (2018) 9(24):4635–41. doi: 10.7150/jca.28583

168. Demircioglu F, Wang J, Candido J, Costa ASH, Casado P, de Luxan Delgado B, et al. Cancer associated fibroblast FAK regulates malignant cell metabolism. *Nat Commun* (2020) 11(1):1290. doi: 10.1038/s41467-020-15104-3

169. Xu A, Xu XN, Luo Z, Huang X, Gong RQ, Fu DY. Identification of prognostic cancer-associated fibroblast markers in luminal breast cancer using weighted gene co-expression network analysis. *Front Oncol* (2023) 13:1191660. doi: 10.3389/fonc.2023.1191660

170. Geng F, Bao X, Dong L, Guo QQ, Guo J, Xie Y, et al. Doxorubicin pretreatment enhances FAPalpha/survivin co-targeting DNA vaccine anti-tumor activity primarily through decreasing peripheral MDSCs in the 4T1 murine breast cancer model. *Oncoimmunology* (2020) 9(1):1747350. doi: 10.1080/2162402X.2020.1747350

171. Xia Q, Zhang FF, Geng F, Liu CL, Wang YQ, Xu P, et al. Improvement of anti-tumor immunity of fibroblast activation protein alpha based vaccines by combination with cyclophosphamide in a murine model of breast cancer. *Cell Immunol* (2016) 310:89–98. doi: 10.1016/j.cellimm.2016.08.006

172. Xia Q, Geng F, Zhang FF, Liu CL, Xu P, Lu ZZ, et al. Cyclophosphamide enhances anti-tumor effects of a fibroblast activation protein alpha-based DNA vaccine in tumor-bearing mice with murine breast carcinoma. *Immunopharmacol Immunotoxicol*. (2017) 39(1):37–44. doi: 10.1080/08923973.2016.1269337

173. Xia Q, Zhang FF, Geng F, Liu CL, Xu P, Lu ZZ, et al. Anti-tumor effects of DNA vaccine targeting human fibroblast activation protein alpha by producing specific immune responses and altering tumor microenvironment in the 4T1 murine breast cancer model. *Cancer Immunol Immunother*. (2016) 65(5):613–24. doi: 10.1007/s00262-016-1827-4

174. Hu S, Ma J, Su C, Chen Y, Shu Y, Qi Z, et al. Engineered exosome-like nanovesicles suppress tumor growth by reprogramming tumor microenvironment and promoting tumor ferroptosis. *Acta Biomater* (2021) 135:567–81. doi: 10.1016/j.actbio.2021.09.003

175. Sitia L, Bonizzi A, Mazzucchelli S, Negri S, Sottani C, Grignani E, et al. Selective targeting of cancer-associated fibroblasts by engineered h-ferritin nanocages loaded with navitoclax. *Cells* (2021) 10(2):328. doi: 10.3390/cells10020328

176. Gao Y, Li X, Zeng C, Liu C, Hao Q, Li W, et al. CD63(+) cancer-associated fibroblasts confer tamoxifen resistance to breast cancer cells through exosomal miR-22. *Adv Sci (Weinh)*. (2020) 7(21):2002518. doi: 10.1002/advs.202002518

177. Liu L, Liu S, Luo H, Chen C, Zhang X, He L, et al. GPR30-mediated HMGB1 upregulation in CAFs induces autophagy and tamoxifen resistance in ERalpha-positive breast cancer cells. *Aging (Albany NY)*. (2021) 13(12):16178–97. doi: 10.18632/aging.203145

178. Fernandez-Nogueira P, Mancino M, Fuster G, Lopez-Plana A, Jauregui P, Almendro V, et al. Tumor-associated fibroblasts promote HER2-targeted therapy resistance through FGFR2 activation. *Clin Cancer Res* (2020) 26(6):1432–48. doi: 10.1158/1078-0432.CCR-19-0353

179. Guardia C, Bianchini G, Arpi LO, Menendez S, Casadevall D, Galbardi B, et al. Preclinical and clinical characterization of fibroblast-derived neuregulin-1 on trastuzumab and pertuzumab activity in HER2-positive breast cancer. *Clin Cancer Res* (2021) 27(18):5096–108. doi: 10.1158/1078-0432.CCR-20-2915

180. Su S, Chen J, Yao H, Liu J, Yu S, Lao L, et al. CD10(+)GPR77(+) cancer-associated fibroblasts promote cancer formation and chemoresistance by sustaining cancer stemness. *Cell* (2018) 172(4):841–56 e16. doi: 10.1016/j.cell.2018.01.009

181. Broad RV, Jones SJ, Teske MC, Wastall LM, Hanby AM, Thorne JL, et al. Inhibition of interferon-signalling halts cancer-associated fibroblast-dependent protection of breast cancer cells from chemotherapy. *Br J Cancer*. (2021) 124(6):1110–20. doi: 10.1038/s41416-020-01226-4

182. Lawal B, Wu AT, Chen CH, TA G, Wu SY. Identification of INFG/STAT1/NOTCH3 as γ-mangostin's potential targets for overcoming doxorubicin resistance and reducing cancer-associated fibroblasts in triple-negative breast cancer. *BioMed Pharmacother*. (2023) 163:114800. doi: 10.1016/j.biopha.2023.114800

183. Domogauer JD, de Toledo SM, Howell RW, Azzam EI. Acquired radioresistance in cancer associated fibroblasts is concomitant with enhanced antioxidant potential and DNA repair capacity. *Cell Commun Signal* (2021) 19(1):30. doi: 10.1186/s12964-021-00711-4

184. Cun X, Chen J, Li M, He X, Tang X, Guo R, et al. Tumor-associated fibroblast-targeted regulation and deep tumor delivery of chemotherapeutic drugs with a multifunctional size-switchable nanoparticle. *ACS Appl Mater Interfaces*. (2019) 11(43):39545–59. doi: 10.1021/acsami.9b13957

185. Mahadik P, Patwardhan S. ECM stiffness-regulated exosomal thrombospondin-1 promotes tunneling nanotubes-based cellular networking in breast cancer cells. *Arch Biochem Biophys* (2023) 742:109624. doi: 10.1016/j.abb.2023.109624

186. Rodriguez AB, Engelhard VH. Insights into tumor-associated tertiary lymphoid structures: novel targets for antitumor immunity and cancer immunotherapy. *Cancer Immunol Res* (2020) 8(11):1338–45. doi: 10.1158/2326-6066.CIR-20-0432

187. Rodriguez AB, Peske JD, Woods AN, Leick KM, Mauldin IS, Meneveau MO, et al. Immune mechanisms orchestrate tertiary lymphoid structures in tumors via cancer-associated fibroblasts. *Cell Rep* (2021) 36(3):109422. doi: 10.1016/j.celrep.2021.109422

frontiers | Frontiers in Oncology

TYPE Original Research
PUBLISHED 11 August 2023
DOI 10.3389/fonc.2023.1207867

OPEN ACCESS

EDITED BY
Zhi-Gang Zhuang,
Shanghai First Maternity and Infant Hospital, China

REVIEWED BY
Marcos Lopez,
University of Puerto Rico, Puerto Rico
Dipendra Khadka,
Wonkwang University School of Medicine, Republic of Korea

*CORRESPONDENCE
Wanju Wang
Wangwanju0417@163.com

RECEIVED 18 April 2023
ACCEPTED 21 July 2023
PUBLISHED 11 August 2023

CITATION
Gui Z, Liu P, Zhang D and Wang W (2023) Clinical implications and immune implications features of TARS1 in breast cancer. *Front. Oncol.* 13:1207867. doi: 10.3389/fonc.2023.1207867

Clinical implications and immune implications features of TARS1 in breast cancer

Zhengwei Gui[1,2], Piao Liu[3], Dong Zhang[3] and Wanju Wang[3]*

[1]Tongji Hospital, Tongji Medical College, Huazhong University of Science and Technology, Wuhan, China, [2]Department of Breast and Thyroid Surgery, Tongji Hospital, Wuhan, Hubei, China, [3]Department of General Surgery, Hubei Provincial Hospital of Integrated Traditional Chinese and Western Medicine, Wuhan, Hubei, China

Background: There has been an increase in the number of women suffering from breast cancer in recent years, and discovering new therapeutic targets and efficacy predictive markers is critical for comprehensive breast cancer treatment.

Methods: First, we used bioinformatics methods to analyze TARS1(encoding cytoplasmicthreonyl-tRNA synthetase) expression, prognosis, and clinicopathological characteristics in TCGA database breast cancers, and then we collected breast cancer specimens from our center for validation. TARS1 was then subjected to GSEA (Gene Set Enrichment Analysis) enrichment analysis, GO/KEGG pathway enrichment analysis, and breast cancer immune infiltration characterization. As a last step, we examined TARS1's effects on breast cancer cell behavior with cellular assays.

Results: The overexpression of TARS1 has been found in several malignant tumors, including breast cancer, and has been linked to poor prognoses. Breast cancers with large primary tumors and negative hormone receptors are more likely to overexpress TARS1. Overexpression of TARS1 promotes the infiltration of T cells, such as Tregs and Th2s, while inhibiting the infiltration of NK cells and CD8+ T cells, which are anticancer cells in breast cancer. TARS1 was also found to be co-expressed with the majority of immune checkpoint-related genes, and breast cancer with TARS1 overexpression responded better to immunotherapy. By knocking down TARS1, breast cancer cells were prevented from proliferating and invading, as well as exhibiting other malignant biological properties.

Conclusion: According to our study, TARS1 may be an oncogene in breast cancer and may be a biomarker of efficacy or a target of immunotherapy in breast cancer.

KEYWORDS

TARS1, breast cancer, cell proliferation, immune infiltration, clinical feature

Introduction

Globally, breast cancer (BC) is the most common malignancy among women, threatening the health of more and more individuals every day (1). The promotion of comprehensive breast cancer treatment, which includes surgical treatment, chemotherapy, radiotherapy, endocrine therapy, and targeted therapy, has considerably improved the prognosis of BC patients (2). In particular, there is still no effective treatment available for triple negative breast cancer, which is a pathological form of breast cancer (3). Therefore, discovering new breast cancer oncogenes and developing new therapeutic targets are critical for improving the prognosis of breast cancer. The efficacy of various therapy regimens for different forms of breast cancer varies substantially (4). As a result, distinguishing between the major breast cancer pathological stages and other clinicopathological aspects impacted by the causal genes is critical for accurate breast cancer treatment (5, 6).

Immunotherapy is regarded as the new treatment with the greatest potential to cure cancer at its source (7); nonetheless, its efficacy in breast cancer needs to be improved. Discovering novel immunotherapy efficacy prediction biomarkers will allow for focused immunotherapy for breast cancer. Precision therapy could lower national health care investment, which is especially essential for many developing countries, according to health economists (8).

The threonine-tRNA synthetase (TARS) is an aminoacyl-tRNA synthetase that plays a key role in protein synthesis. Aminoacyl-tRNA synthetases (aaRS) are housekeeping proteins that catalyze the attachment of tRNAs to homologous amino acids, hence providing aminoacyl-tRNA building blocks for ribosomal protein synthesis (9). Mammalian cytoplasmic and mitochondrial protein synthesis each have their own set of aaRSs, whereas TARS1 and TARS2 encode eukaryotic cytoplasmic and mitochondrial threonine-tRNA synthetases (ThrRSs) (10, 11). TARS1 has been demonstrated to be important in muscle development and is released during inflammation to enhance endothelial cell migration and angiogenesis (12). TARS1 is also involved in the regulation of translation initiation, which helps to positively regulate vertebrate mRNA translation (13).There is evidence that TARS is upregulated in gastric cancer and is associated with poor outcome and metastasis (14), in endometrial cancer, TARS1 was associated with poor outcomes (15). As of yet, no clear understanding of TARS1's role in breast cancer has been established.

Initially, we examined the expression of TARS1 in various cancers, including breast cancer, the impact of TARS1 on breast cancer prognosis and its association with clinicopathological characteristics of breast cancer patients using data from the TCGA database and GTEx database, and collected breast cancer specimens from our center for quantitative analysis and validation. Then, using GSEA analysis, GO/KEGG pathway enrichment analysis, and breast cancer immune infiltration analysis, the potential benefit of TARS1 for breast cancer treatment was investigated. As a final step, we assessed TARS1's potential to predict immunotherapy effectiveness using TIDE (Tumor Immune Dysfunction and Exclusion), by analyzing its co-expression with immune checkpoint-related genes.

Breast cancer treatment is entering the precision therapy era, with several studies leading to new personalized medicines and biomarkers. Traditional indicators such as ER, PR, and Her-2 have improved the prognosis of breast cancer patients dramatically (16–19). When chemotherapy is used, commercial gene expression combinations like OncotypeDX and Mammaprint are the best prognostic predictors for ER-positive, HER2-negative, lymph node-negative breast cancer (20, 21). New prognostic indicators are also indicated in specific metastatic breast cancer scenarios. The NCCN advises testing for BRCA1/2 germline mutation status in each metastatic patient to anticipate the potential benefit of PARP inhibitor therapy (22, 23). For targeted therapy, they may additionally include MSI/MMR, TMB, and NTRK (24, 25). The discovery of novel biomarkers is critical for improving prognosis and lowering healthcare costs for breast cancer patients (26, 27).

Materials and methods

The collection and processing of data

We used R and Graphpad Prism version 8.0 to conduct all statistical analyses and visualizations. Data from the GTEx and TCGA databases were used to analyze breast cancer patients' mRNA expression profiles. We have removed duplicate samples and those lacking clinical information. In total, there were 179 paracancerous tissues and 1065 breast cancer tissues. The survival curve data were obtained from the KM plotter website (28).

Correlation and enrichment analyses

The TCGA-BRCA database was analyzed for gene co-expression, the FoldChange was arranged in descending order, the genes with $P>0.05$ were removed, and the top 300 genes were selected for GSEA enrichment analysis. The 324 genes with absolute FoldChange values greater than 1.5 and $P<0.05$ were selected for GO/KEGG analysis.

Pathological sample collection and processing

We collected 76 breast cancer specimens from Tongji Hospital between September 2021 and February 2023. There were 24 pairs of fresh frozen tissues matched with paracancer, 21 pairs of paired paraffin-embedded tissues, and 32 cancer tissue specimens. A protocol for this study has been approved by the Ethics Committee of Tongji Hospital in accordance with the Helsinki Declaration (approval number TJIRB20221218). Fixation of tissues in 10% formalin, paraffin embedding, serial sectioning into 5 mm layers, dewaxing, rehydration, and microwave antigen repair were all carried out on the tissues. At 1 degree Celsius, the slides were incubated overnight with 1:200 dilutions of TARS1 antibody (AFFINITY, df2315). The secondary antibodies were incubated for 30 minutes at room temperature before being stained with the

DAB substrate and then re-stained with hematoxylin. The quantitative immunohistochemical analysis was carried out using ImageJ and AI tools.

extraction and quantitative real-time PCR: RNA

According to the manufacturer's instructions, total RNA was extracted using the TRIzol reagent (Invitrogen, USA). DynaScience Biotechnology in China provided qRT-PCR primers, including those for TARS1 and GAPDH. The primer sequences: TARS1: forward - TGTGCCATTGAATAAGGA, reverse - CACCTTCA TTATCAAGATAC (5'-3'). GAPDH forward - GGAGCGAGAT CCCTCCAAAAT, reverse -GGCTGTTGTCATACTTCTCATGG. The PCR conditions were as follows: 95°C for 5 minutes; (95°C for 5 seconds, 60°C for 30 seconds) 40 amplification cycles. Relative expression levels were standardized to the internal control and computed according to the 2-ΔΔCT technique.

Cell culture and treatment

Shanghai Institute of Cell Biology provided the MCF7, MDA-MB-231, MDA-MB-468, and SKBR3 human breast cancer cell lines. MDA-MB-468 cells were cultivated in RPMI-1640 media (Gibco, USA), whereas MCF7, MDA-MB-231, and SKBR3 cells were grown in DMEM medium (Gibco, USA). All media are supplemented with 10% fetal bovine serum. All cell lines were cultured at 37°C in a ThermoFisher incubator with 5% CO2. By employing STR to identify and compare all bought cell lines to reputable databases.

CCK8 assay

Cells from each experimental group that were in the logarithmic growth phase and under good growth conditions were digested and resuspended in full culture medium. Proliferation of cells was determined according to the manufacturer's instructions using the Cell Counting Kit-8 (Invitrogen, USA). A marker enzyme was used to measure the optical density at 450 nm.

Colony-formation assay

During the 14-day culture period, 1000 breast cancer cells were injected into six-well plates. The medium was replaced every three days and the medium utilized for each of the cells was as previously described. We stained the cell colonies with crystal violet after they had been fixated in 4% polyacetal for 10 minutes, photographed, and counted.

Transwell assay

Transwell chambers in 24-well plates are filled with 20,000 breast cancer cells each. Various cells were resuspended in serum-free medium, uniformly added to the upper chamber, and the lower well was filled with medium containing 10% fetal bovine serum. We wiped the top surface of the chamber after incubating the cells at 37° C for 24 hours. A 10-minute fixation process with 4% paraformaldehyde was followed by a 10-minute staining process with crystal violet on the bottom surface of the chambers. Counting and photographing migratory cells was done.

Scratch test

Breast cancer cells in the log phase of growth were inserted in 24-well plates with IBIDI two-well culture inserts and incubated for 24 hours. Forceps were utilized to carefully remove the culture implants from the immaculate table. Each well received 1 mL of low-serum medium, upon removal of the inserts, the migration rate of cells was determined under a light microscope at 0 and 24 hours.

Immune cell infiltration

Using the GSVA package [version 1.34.0] of R, immune cell infiltration in BC was examined (version 3.6.3). On ssGSEA, the outcomes were based. The classification of immune cells and references to earlier studies' markers were made. According to the median TARS1 expression in TCGA BC samples, two groups were identified (high and low), This dataset includes RNAseq data (level 3) as well as clinical information on 1101 breast tumors. TIDE was used to predict likely immunotherapeutic responses. Removal of duplicate samples and removal of samples that do not contain clinical information.

Results

TARS1 expression analysis

TARS1 was overexpressed in 15 cancers according to a pan-cancer study (Figure 1A). Contrarily, TARS1 was significantly overexpressed in breast cancer samples from both paired and unpaired individuals (Figures 1B, C).

TARS1 expression and prognosis in breast cancer patients

KM plotter data showed that breast cancer groups with high TARS1 had significantly lower overall survival rates (HR=1.71, P=0.001), progress-free interval (HR=1.82, P=0.001), and disease-specific survival (HR=1.86, P=0.006). DSS (disease specific survival) decreased considerably (HR=1.86, P=0.006) (Figures 2A–C). TARS1-based ROC had an AUC of 0.800, CI: 0.771-0.828. (Figure 2D)

Clinicopathological variables and TARS1 expression

Bioinformatics analysis suggested that TARS1 overexpression was associated with T stage (T1 < T2), ER(Estrogen receptor)

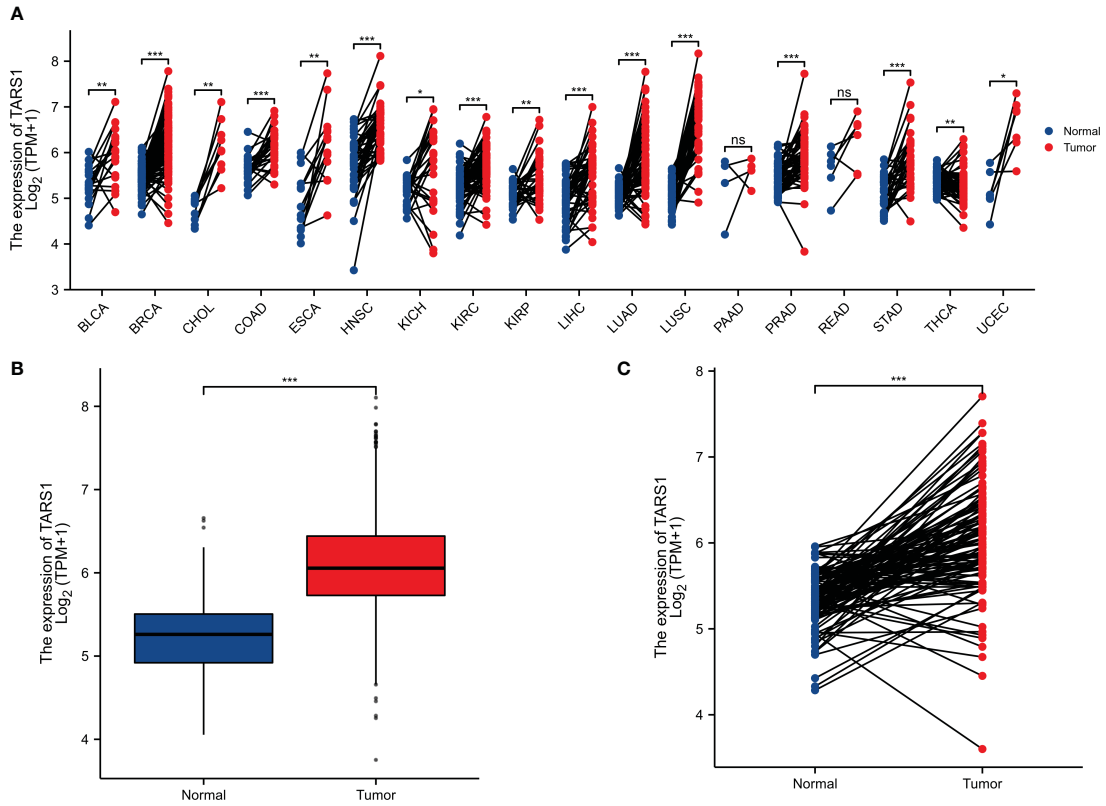

FIGURE 1
The expression difference of TARS1 in cancer tissue and normal tissue. **(A)** Expression of TARS1 in pan-cancer and adjacent normal tissues in TCGA and GTEx databases. **(B)** Expression of TARS1 in unpaired breast cancer samples in TCGA-BRCA database. **(C)** Expression of TARS1 in paired breast cancer samples in TCGA-BRCA database. Data were shown as mean ± SD. *p < 0.05, **p < 0.01, ***p < 0.001.

status (positive < negative), PR (Progesterone receptors) status (positive < negative), HER-2 (Human epidermal growth factor receptor 2) status (positive > negative) in breast cancer patients, PAM50 (LumA < LumB, HER-2, Basal) and Histological type (infiltrating ductal carcinoma > infiltrating lobular carcinoma), but not N stage, M stage and Pathological stage was not relevant (Figure 3, Supplementary Table 1). Breast cancer specimens collected in our center were processed and statistically analyzed, and typical IHC images are shown in Figure 4. TARS1 overexpression in breast cancer was demonstrated at the mRNA and protein levels in fresh frozen tissue and paraffin-embedded tissue, respectively (Figure 5). <The relationship between TARS overexpression and T stage, ER status, PR status, PAM50 and Pathological stage was consistent with the raw signal results, while the relationship with N stage (N0, N2) and HER-2 status was different.

Correlation and enrichment analyses

GSEA analysis of TARS1 includes GPCR ligand binding, signaling by RHO GTPases, M phase, Class A1 rhodopsin-like receptors and DNA repair (Figure 6A). In Figures 6B, C, the GO/KEGG enrichment study is displayed.

TARS1 expression and immune cell infiltration

Based on the median expression of TARS1, breast cancers from TCGA-BRCA Database (removed duplicate samples and those lacking clinical information) were divided into low and high expression groups and immune cell infiltration was separately analyzed. Figure 7 shows the comparison of 24 immune cell pairs. A significant number of anti-tumor cells, such as CD8+ T cells and NK cells, were found in the TARS1 high expression group, as opposed to pro-tumor cells, such as Tregs and Th2 cells (Figure 8). The RNA-sequencing expression (level 3) profiles and corresponding clinical information for breast cancer (BC) were obtained from the TCGA dataset. In order to evaluate the credibility of immune score assessment, the immuneeconv R software package was utilized. This package incorporates six contemporary algorithms, namely TIMER, xCell, MCP-counter, CIBERSORT, EPIC, and quanTIseq, all of which have been benchmarked and possess distinctive strengths. In an investigation of the coexpression of TARS1 with 47 immune checkpoint-related genes, 30 were found to coexpress with TARS1. The 47 immune checkpoint-related genes frequently identified in prior studies were chosen.

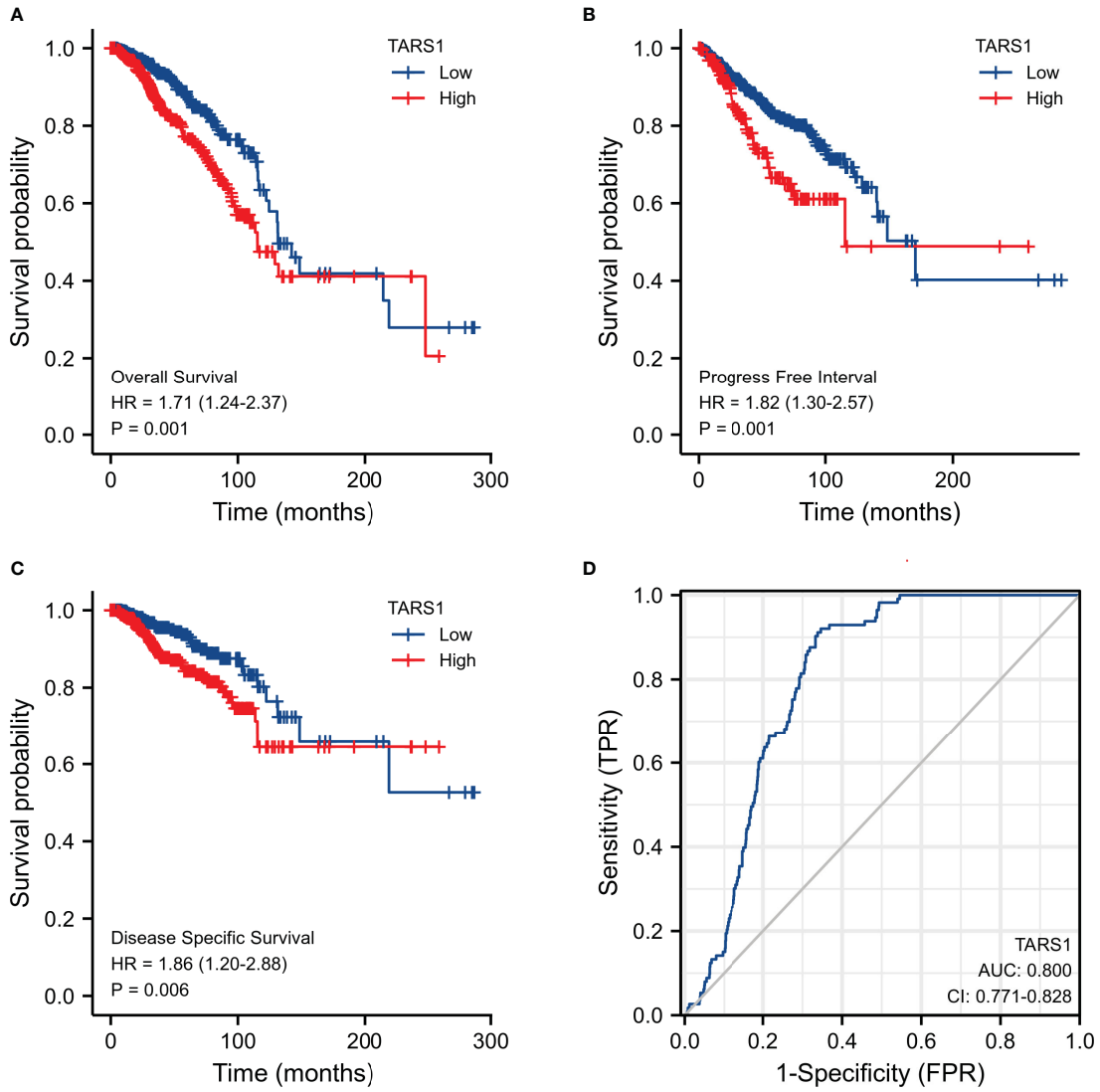

FIGURE 2
Expression of TARS1 and prognosis of breast cancer patients. **(A)** OS of breast cancer patients based on TARS1 expression level. **(B)** RFS of breast cancer patients based on TARS1 expression level. **(C)** DMFS of breast cancer patients based on TARS1 expression level. **(D)** ROC curve of TARS1.

(Figure 9). The TIDE algorithm (29) additionally revealed that breast cancers with higher TARS1 expression responded better to immunotherapy with checkpoint inhibitors. (Figure 10).

Breast cancer cells with TARS1 knockdown displayed reduced malignant behavior:

A significant increase in TARS1 expression was observed in MDA-MB-231, MDA-MB-468, SKBR3 and MCF-7 cells in comparison with normal mammary cells, MCF-10A (Figure 11A). The initial four cell lines represent three types of breast cancer: triple negative, HER-2 positive, and hormone receptor positive, while the MCF-10A cell line represents normal breast cells. TARS1 was successfully knocked down in MDA-MB-231, SKBR3 and MCF-7 cells using siRNA (Figures 11B–D), and CCK8 (Figures 12A–C) and clone formation (Figures 12D, E) assays revealed that breast cancer cell proliferation was significantly reduced. The Transwell assay (Figures 12F, G) and the scratch assay (Figures 12H, I), in contrast, demonstrated that the ability of breast cancer cells to invade was greatly diminished. Using ImageJ and AI software, statistically significant results were obtained from the clone formation assay, Transwell assay, and scratch assay. (Figures 12D–F).

Discussion

Throughout the past four decades, breast cancer incidence has been increasing. From 2010 to 2019, the incidence of breast cancer increased on average by 0.5% each year (30). Biomarkers like ER, PR, and HER-2 play a crucial role in the diagnosis and management of breast cancer (31). However, there is still no effective treatment for triple-negative breast cancer, and hormone receptor-positive and HER-2-positive cancers also experience drug resistance (32). It is vital to discover new causative genes or therapeutic targets in order to treat breast cancer.

10.3389/fonc.2023.1207867

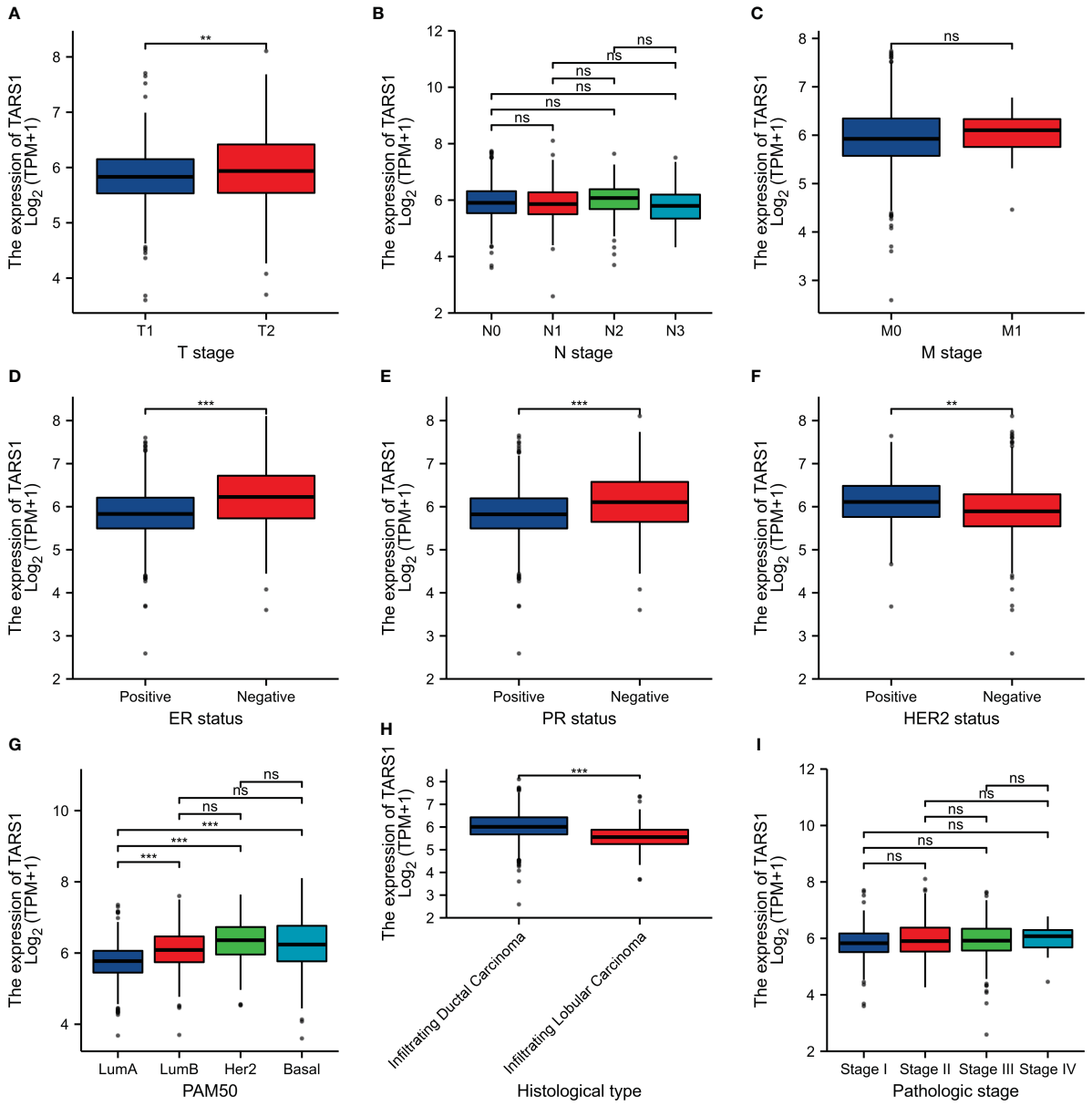

FIGURE 3
Relationship between TARS1 expression and clinicopathologic features of breast cancer patients in TCGA. Data are shown for **(A)** T stage; **(B)** N stage; **(C)** M stage; **(D)** ER status; **(E)** PR status; **(F)** HER-2 stage; **(G)** PAM50; **(H)** Histological type; **(I)** Pathologic type; *p < 0.05, **p < 0.01, ***p < 0.001. LumA, Luminal A; LumB, Luminal B; ER, estrogen receptor; PR, progesterone receptor; HER2, human epidermal growth factor receptor 2.

TARS1 is significantly expressed in a number of malignancies, including breast cancer, and is associated with poor prognoses TARS1 overexpression was linked to bigger primary tumor size, hormone receptor negativity, and HER-2 receptor positivity, according to further study of the clinicopathological characteristics of BC patients. TARS1 is overexpressed in breast cancer at both the transcriptional and translational levels, according to quantitative analysis of breast cancer specimens obtained at our center. TARS1 is a crucial constituent of mRNA translation in vertebrates and serves a significant function in protein synthesis. Previous research has shown that TARS1 is secreted in inflammatory states and stimulates endothelial cell migration and angiogenesis, and given the hypermetabolic state of tumors and their reliance on neovascularisation, researchers believe this is one of the reasons why it promotes the development of breast cancer (12).Breast cancer cells exhibit a swift metabolism and abbreviated proliferation cycle in contrast to normal breast cells, resulting in more robust protein synthesis, particularly during cellular metamorphosis and migration. Consequently, TARS1 overexpression aligns with the heightened metabolic state of cancer cells, potentially contributing to the promotion of breast cancer proliferation and migration. Breast cancer patient clinicopathological characteristics were quantified using immunohistochemistry, and it was discovered that overexpression of

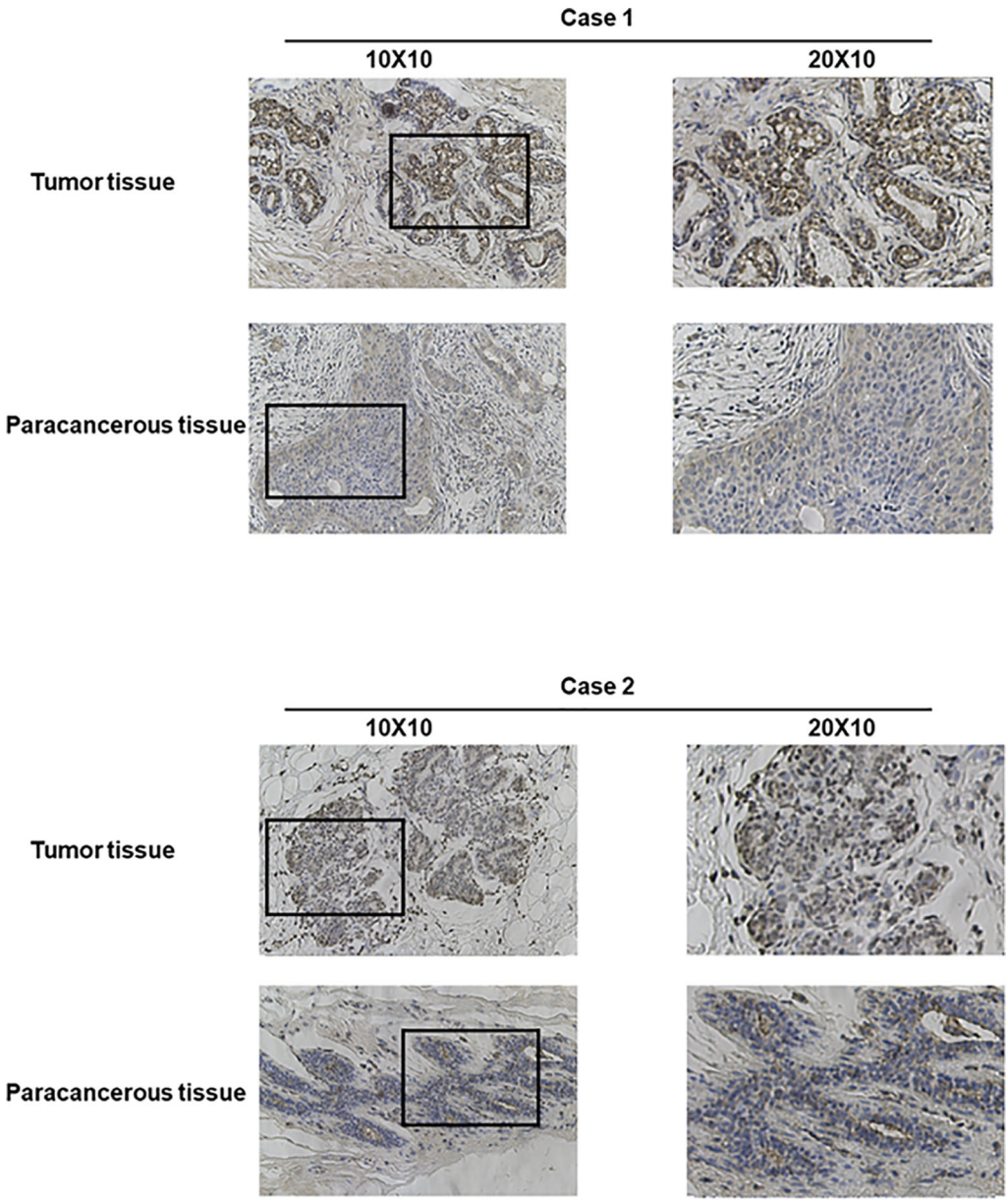

FIGURE 4
Representative images of TARS1 expression in breast cancer tissues and their matched paracancerous tissues. Original magnifications 40× and 100× (inset panels).

TARS1 was linked to higher initial tumor sizes and hormone receptor negativity. According to bioinformatic study, this is accurate. However, our results suggest that TARS1 overexpression is more pronounced in patients with lymph node metastases, independent of HER-2 expression, which is different from the bioinformatic results and requires further validation with larger volume samples. In conclusion, the association of TARS1 overexpression and clinicopathological features of breast cancer targets a possible beneficiary population for its clinical translation.

Immunotherapy brings a new light to cancer patients. It is important for stromal cells in the tumor microenvironment, particularly immune cells, to regulate tumor cell malignancy (33). They are clinically important for assessing cancer patients' prognosis and treatment outcomes, according to a growing body of research (34, 35). In our study, we discovered that TARS1 overexpression inhibited the infiltration of anti-cancer immune cells like CD8+ T cells and NK cells while promoting the infiltration of oncogenic immune cells like Treg and Th2 in breast cancer. A drop in anti-tumor cells promotes breast cancer cell proliferation, but an increase in pro-tumor cell infiltration generates an immunological milieu more suitable for breast cancer cell migration. This could be one of

10.3389/fonc.2023.1207867

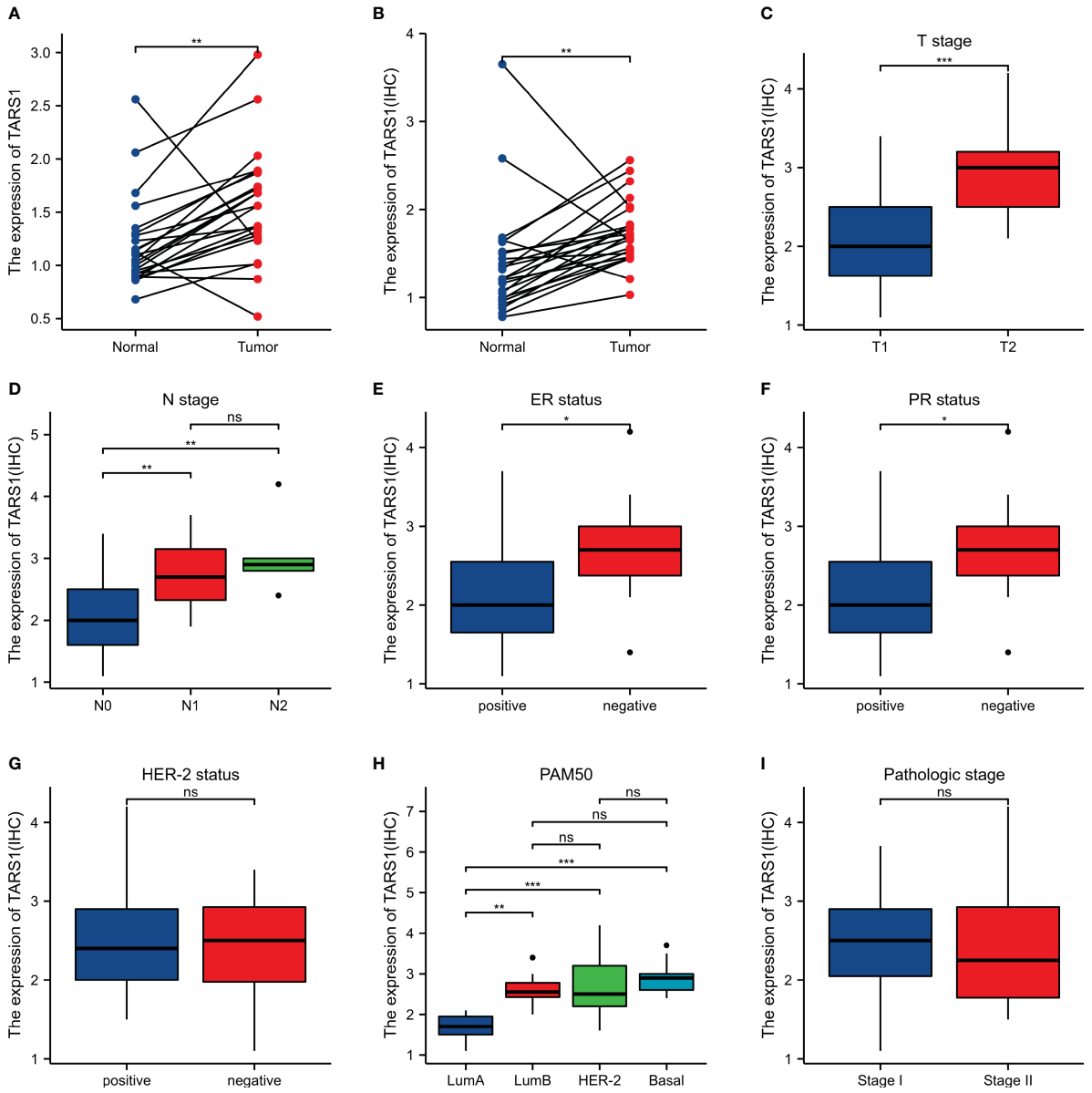

FIGURE 5
Expression and the relationship between TARS1 and breast cancer clinicopathologic features in our center. **(A)** mRNA levels of TARS1 in 24 pairs of fresh frozen specimens **(B)** Protein levels of TARS1 in 21 pairs of paraffin sections **(C)** T stage; **(D)** N stage; **(E)** ER status; **(F)** PR status; **(G)** HER-2 status; **(H)** PM50; **(I)** Pathologic stage; *p < 0.05, **p < 0.01, ***p < 0.001.

the reasons why TARS1 overexpression enhances breast cancer cell proliferation and migration, ultimately leading to a poor prognosis for patients with breast cancer. KEYNOTE-086 study (36) demonstrates the safety and antitumor activity of pablizumab monotherapy in metastatic TNBC, suggesting its use as first-line treatment for mTNBC. On the basis of this, KEYNOTE-355 study (37) further demonstrate that for metastatic TNBC with CPS ≥10, pablizumab in combination with chemotherapy improved progression-free survival significantly more than placebo in combination with chemotherapy suggests that adding pablizumab to standard chemotherapy in the first-line treatment of metastatic triple-negative breast cancer is important. As the indications for immune checkpoint inhibitors expand, the question of how to find the patients most likely to benefit and accurately predict efficacy has become a concern. A majority of immune checkpoint-associated genes are co-expressed with TARS1, implying that it may be inter-regulated with multiple targets in the immune checkpoint-associated pathway and could be a predictive biomarker of efficacy or a novel therapeutic target for ICI in the treatment of BC. In the TIDE algorithm, which assesses tumor immune escape by using several gene expression markers, two mechanisms are assessed, A number of immunosuppressive

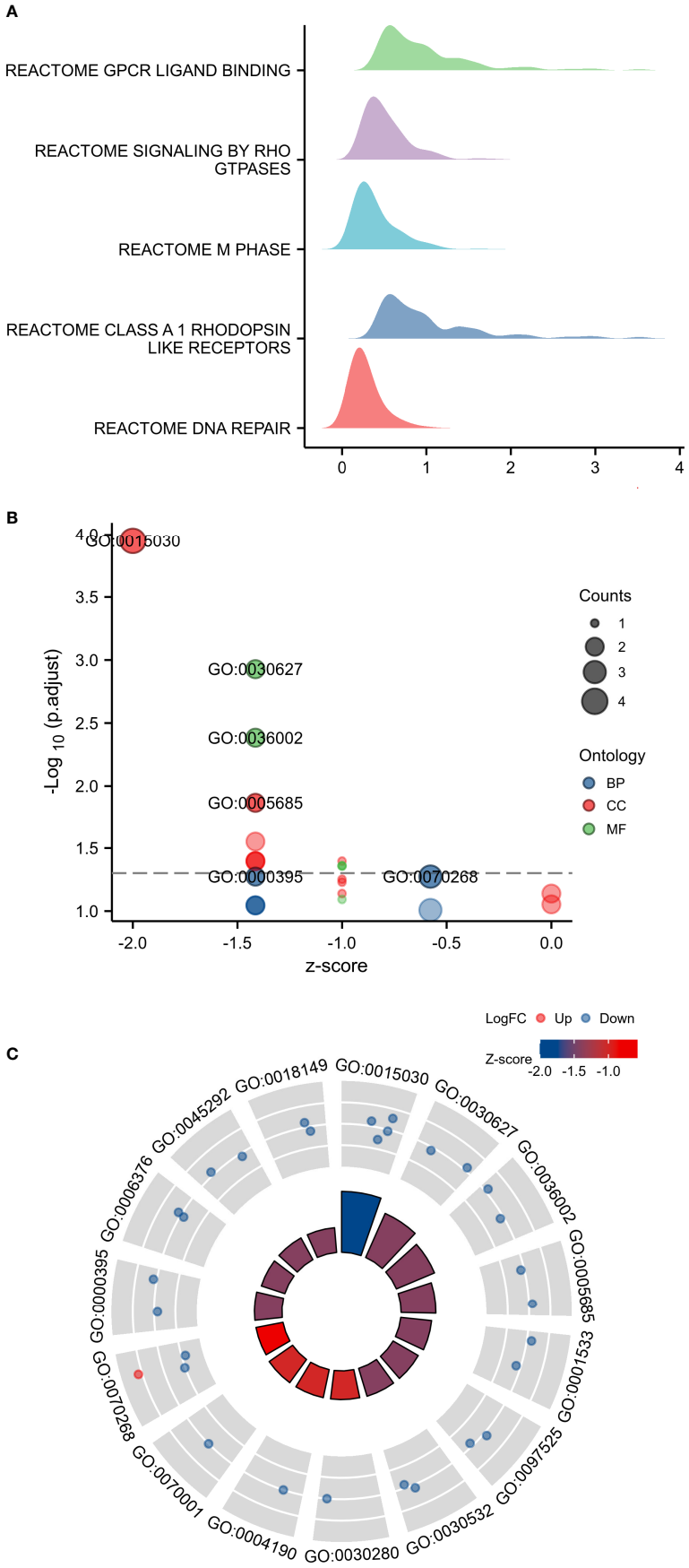

FIGURE 6
GSEA and GO/KEGG enrichment analysis of TARS1. **(A)** GSEA analysis of TARS1 **(B, C)** GO/KEGG enrichment of TARS1.

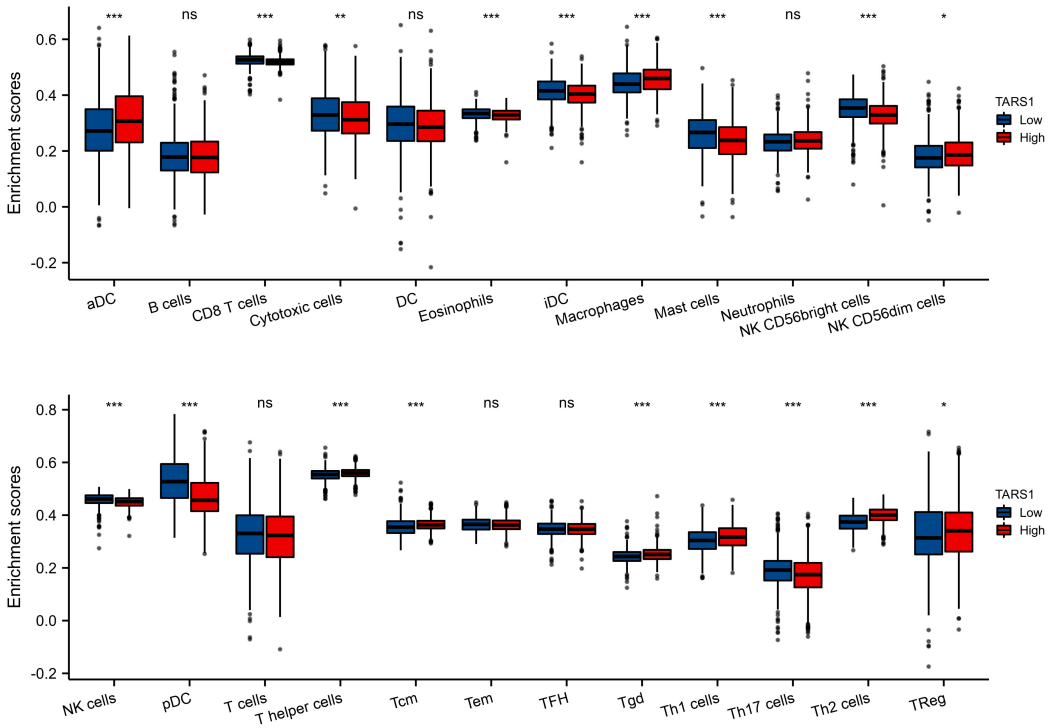

FIGURE 7
The expression level various immune cell infiltration in High and low TARS1 breast cancer. *p < 0.05, **p < 0.01, ***p < 0.001. ns, not significant.

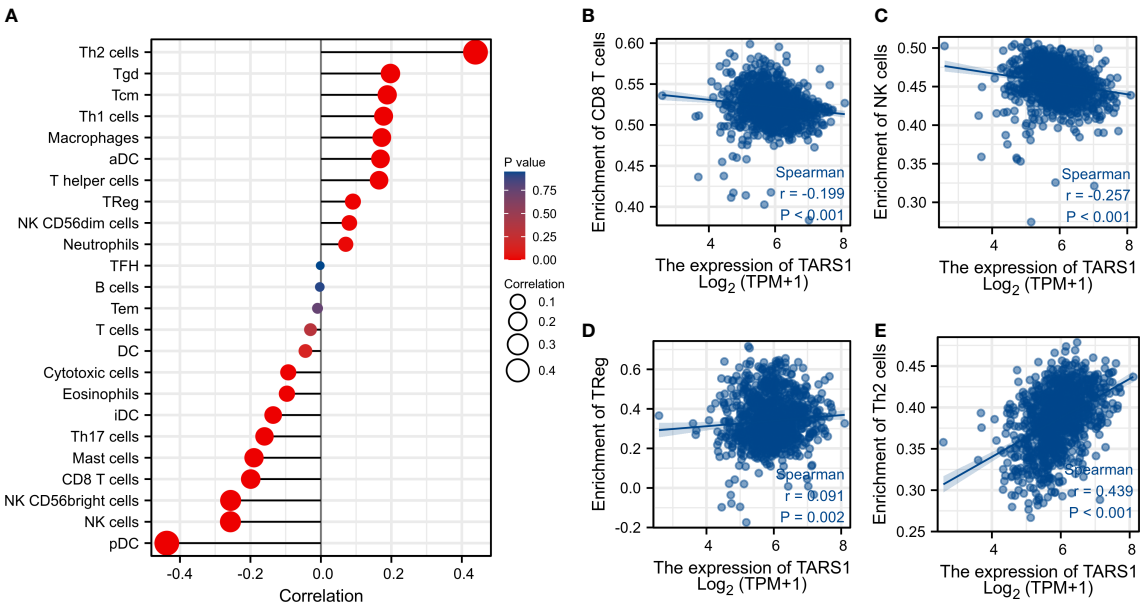

FIGURE 8
Associated between TARS1 with immune cell infiltration. **(A)** Correlation between the expression level of TARS1 and various immune cell infiltration. **(B)** Correlation between TARS1 expression and CD8+T cells. **(C)** Correlation between TARS1 expression and NK cells. **(D)** Correlation between TARS1 expression and Treg cells. **(E)** correlation between TARS1 expression and Th2 cells.

10.3389/fonc.2023.1207867

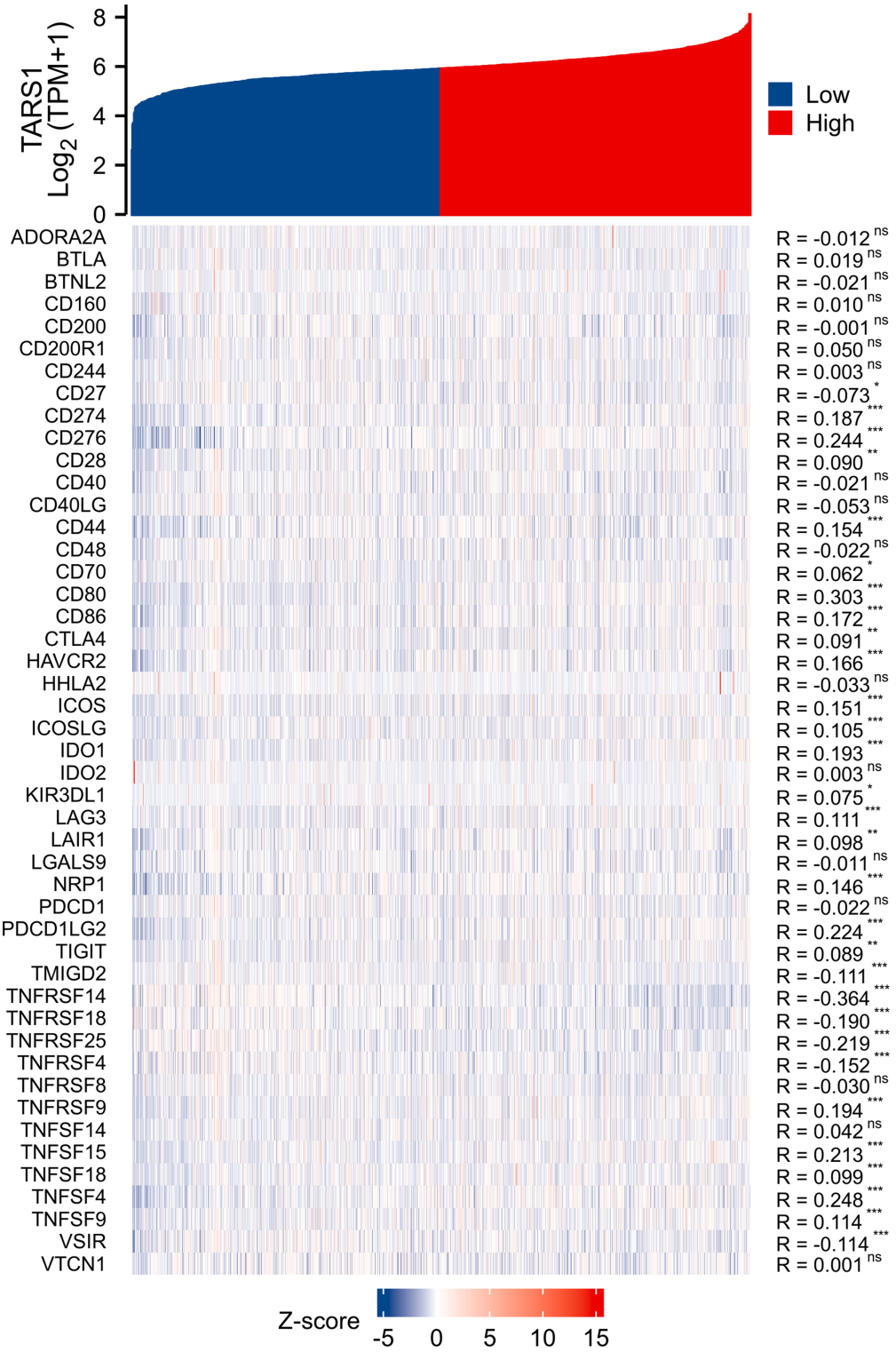

FIGURE 9
Co-expression of TARS1 and immune checkpoint related genes. *p < 0.05, **p < 0.01, ***p < 0.001. ns, not significant.

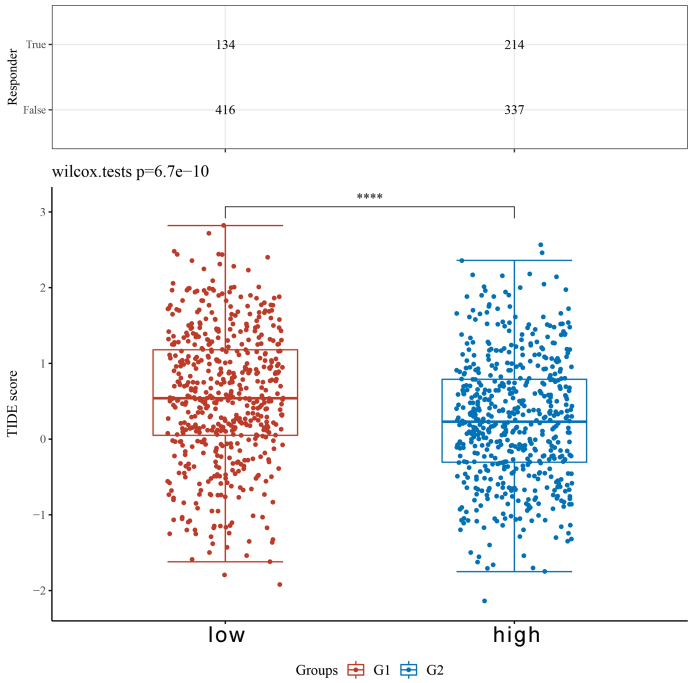

FIGURE 10
TIDE based on the expression level of TARS1. ****p < 0.0001.

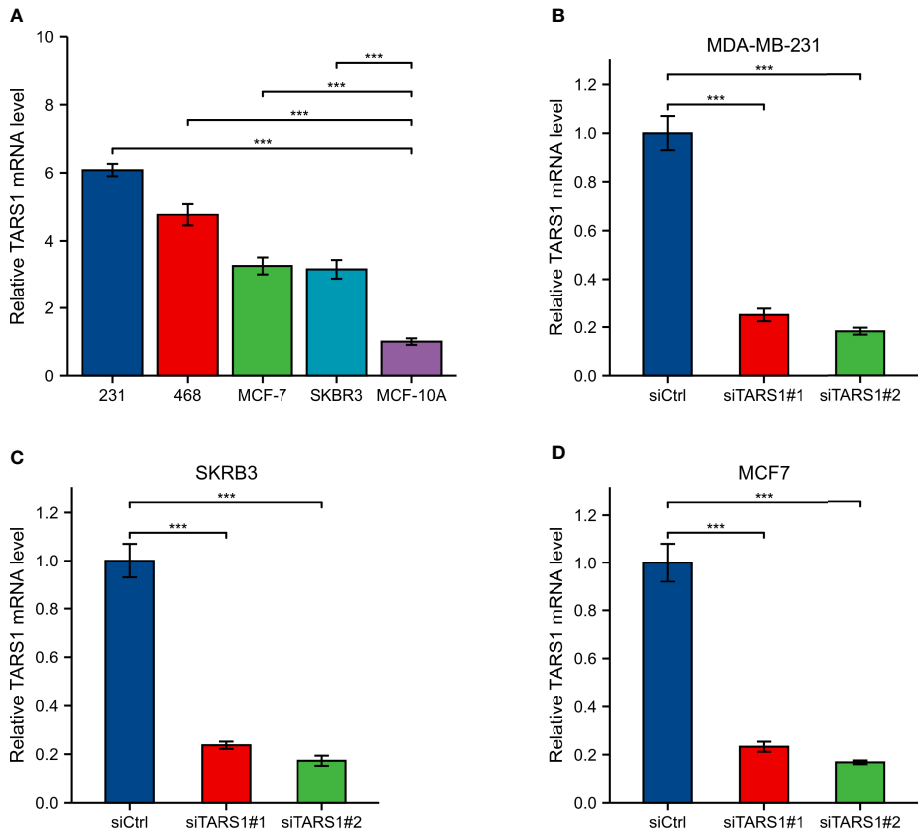

FIGURE 11
Expression and knockdown of TARS1 in various cell lines **(A)** TARS1 expression in MDA-MB-231, MDA-MB-468, MCF7, SKBRE3, and MCF10A cell lines. **(B-D)** TARS1 knockdown efficiency of two siRNA in MDA-MB-231, SKBR3, MCF7 cell lines. ***p < 0.001.

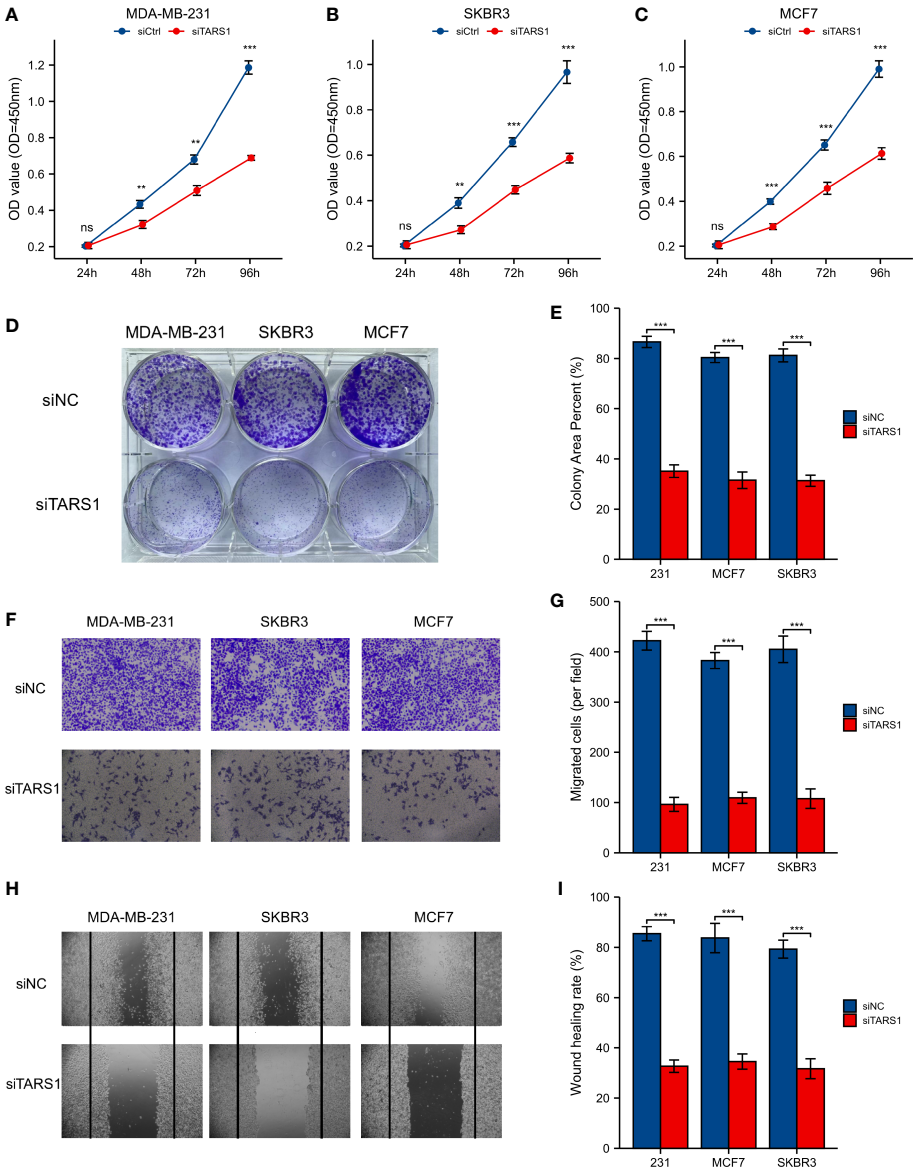

FIGURE 12
CCK8 experiment, Clone formation experiment, Transwell experiment and scratch experiment. **(A-C)** CCK-8 experiment in MDA-MB-231, SKBR3, MCF7 cell lines. **(D, E)** Clone formation of control group and two siRNA knockout groups in MDA-MB-231, SKBR3, MCF7 cell lines and quantitative analysis **(F, G)** Transwell images of control group and two siRNA knockout groups in MDA-MB-231, SKBR3, MCF7 cell lines and quantitative analysis. **(H, I)** Scratch test images of control group and two siRNA knockout groups in MDA-MB-231, SKBR3, MCF7 cell lines and quantitative analysis. All assays were independently repeated at least three times. Data are presented as the mean ± SD. **p < 0.01, ***p < 0.001, **** p < 0.0001. ns, not significant.

factors, as well as dysfunction of tumor-infiltrating cytotoxic T lymphocytes (CTL), were used as a means of testing our suspicions (38). It has been shown that the higher the TIDE score, the less effective immune checkpoint blockade therapy (ICB) is and the shorter the survival after ICB. TARS1 high expression groups were found to be more responsive to ICB.

Overall, our study found that TARS1 may be a causative gene in breast cancer and is more significantly overexpressed in breast cancers with specific clinicopathological features. TARS1 overexpression leads to a suppressed state of immune infiltration within breast cancer and may be a predictive biomarker for the efficacy of immunotherapy in breast cancer.

Data availability statement

The original contributions presented in the study are included in the article/Supplementary Material. Further inquiries can be directed to the corresponding author.

Ethics statement

A protocol for this study has been approved by the Ethics Committee of Tongji Hospital in accordance with the Helsinki Declaration (approval number TJIRB20221218).

Author contributions

ZG and PL obtained clinical specimens; PL performed the data analysis; DZ performed the formal analysis; ZG and DZ performed immunohistochemical analysis; WW and PL wrote the manuscript. All authors contributed to the article and approved the submitted version.

Funding

This research was funded by National Natural Science Foundation of China (Grant No 21834002).

Conflict of interest

The authors declare that the research was conducted in the absence of any commercial or financial relationships that could be construed as a potential conflict of interest.

Publisher's note

Supplementary material

The Supplementary Material for this article can be found online at: https://www.frontiersin.org/articles/10.3389/fonc.2023.1207867/full#supplementary-material

References

1. Sung H, Ferlay J, Siegel RL, Laversanne M, Soerjomataram I, Jemal A, et al. Global cancer statistics 2020: GLOBOCAN estimates of incidence and mortality worldwide for 36 cancers in 185 countries. *CA Cancer J Clin* (2021) 71(3):209–49. doi: 10.3322/caac.21660

2. Gradishar WJ, Moran MS, Abraham J, Aft R, Agnese D, Allison KH, et al. Breast cancer, version 3.2022, NCCN clinical practice guidelines in oncology. *J Natl Compr Canc Netw* (2022) 20(6):691–722. doi: 10.6004/jnccn.2022.0030

3. Diana A, Carlino F, Franzese E, Oikonomidou O, Criscitiello C, De Vita F, et al. Early triple negative breast cancer: Conventional treatment and emerging therapeutic landscapes. *Cancers (Basel)* (2020) 12(4). doi: 10.3390/cancers12040819

4. Prat A, Pineda E, Adamo B, Galvan P, Fernandez A, Gaba L, et al. Clinical implications of the intrinsic molecular subtypes of breast cancer. *Breast.* (2015) 24 Suppl 2:S26–35. doi: 10.1016/j.breast.2015.07.008

5. Pareja F, Weigelt B, Reis-Filho JS. Problematic breast tumors reassessed in light of novel molecular data. *Mod Pathol* (2021) 34(Suppl 1):38–47. doi: 10.1038/s41379-020-00693-7

6. Denkert C, von Minckwitz G, Darb-Esfahani S, Lederer B, Heppner BI, Weber KE, et al. Tumour-infiltrating lymphocytes and prognosis in different subtypes of breast cancer: a pooled analysis of 3771 patients treated with neoadjuvant therapy. *Lancet Oncol* (2018) 19(1):40–50. doi: 10.1016/S1470-2045(17)30904-X

7. Basu A, Ramamoorthi G, Jia Y, Faughn J, Wiener D, Awshah S, et al. Immunotherapy in breast cancer: Current status and future directions. *Adv Cancer Res* (2019) 143:295–349. doi: 10.1016/bs.acr.2019.03.006

8. Al-Ziftawi NH, Shafie AA, Mohamed Ibrahim MI. Cost-effectiveness analyses of breast cancer medications use in developing countries: a systematic review. *Expert Rev Pharmacoecon Outcomes Res* (2021) 21(4):655–66. doi: 10.1080/14737167.2020.1794826

9. Guo M, Schimmel P. Essential nontranslational functions of tRNA synthetases. *Nat Chem Biol* (2013) 9(3):145–53. doi: 10.1038/nchembio.1158

10. Peng GX, Mao XL, Cao Y, Yao SY, Li QR, Chen X, et al. RNA granule-clustered mitochondrial aminoacyl-tRNA synthetases form multiple complexes with the potential to fine-tune tRNA aminoacylation. *Nucleic Acids Res* (2022) 50(22):12951–68. doi: 10.1093/nar/gkac1141

11. Antonellis A, Green ED. The role of aminoacyl-tRNA synthetases in genetic diseases. *Annu Rev Genomics Hum Genet* (2008) 9:87–107. doi: 10.1146/annurev.genom.9.081307.164204

12. Williams TF, MIrando AC, Wilkinson B, Francklyn CS, Lounsbury KM. Secreted Threonyl-tRNA synthetase stimulates endothelial cell migration and angiogenesis. *Sci Rep* (2013) 3:1317. doi: 10.1038/srep01317

13. Jeong SJ, Park S, Nguyen LT, Hwang J, Lee EY, Giong HK, et al. A threonyl-tRNA synthetase-mediated translation initiation machinery. *Nat Commun* (2019) 10 (1):1357. doi: 10.1038/s41467-019-09086-0

14. Gao X, Guo R, Li Y, Kang G, Wu Y, Cheng J, et al. Contribution of upregulated aminoacyl-tRNA biosynthesis to metabolic dysregulation in gastric cancer. *J Gastroenterol Hepatol* (2021) 36(11):3113–26. doi: 10.1111/jgh.15592

15. Si L, Liu L, Yang R, Li W, Xu X. High expression of TARS is associated with poor prognosis of endometrial cancer. *Aging (Albany NY)* (2023) 15. doi: 10.18632/aging.204558

16. Wolff AC, Hammond ME, Hicks DG, Dowsett M, McShane LM, Allison KH, et al. Recommendations for human epidermal growth factor receptor 2 testing in breast cancer: American Society of Clinical Oncology/College of American Pathologists clinical practice guideline update. *J Clin Oncol* (2013) 31(31):3997–4013. doi: 10.1200/JCO.2013.50.9984

17. Allison KH, Hammond MEH, Dowsett M, McKernin SE, Carey LA, Fitzgibbons PL, et al. Estrogen and progesterone receptor testing in breast cancer: American society of clinical oncology/college of american pathologists guideline update. *Arch Pathol Lab Med* (2020) 144(5):545–63. doi: 10.5858/arpa.2019-0904-SA

18. Allison KH, Hammond MEH, Dowsett M, McKernin SE, Carey LA, Fitzgibbons PL, et al. Estrogen and progesterone receptor testing in breast cancer: ASCO/CAP guideline update. *J Clin Oncol* (2020) 38(12):1346–66. doi: 10.1200/JCO.19.02309

19. Wolff AC, Hammond ME, Schwartz JN, Hagerty KL, Allred DC, Cote RJ, et al. American Society of Clinical Oncology/College of American Pathologists guideline recommendations for human epidermal growth factor receptor 2 testing in breast cancer. *Arch Pathol Lab Med* (2007) 131(1):18–43. doi: 10.5858/2007-131-18-ASOCCO

20. Piccart M, van 't Veer LJ, Poncet C, Lopes Cardozo JMN, Delaloge S, Pierga JY, et al. 70-gene signature as an aid for treatment decisions in early breast cancer: updated results of the phase 3 randomised MINDACT trial with an exploratory analysis by age. *Lancet Oncol* (2021) 22(4):476–88. doi: 10.1016/S1470-2045(21)00007-3

21. Sestak I, Filipits M, Buus R, Rudas M, Balic M, Knauer M, et al. Prognostic value of endoPredict in women with hormone receptor-positive, HER2-negative invasive lobular breast cancer. *Clin Cancer Res* (2020) 26(17):4682–7. doi: 10.1158/1078-0432.CCR-20-0260

22. Robson M, Im SA, Senkus E, Xu B, Domchek SM, Masuda N, et al. Olaparib for metastatic breast cancer in patients with a germline BRCA mutation. *N Engl J Med* (2017) 377(6):523–33. doi: 10.1056/NEJMoa1706450

23. Litton JK, Rugo HS, Ettl J, Hurvitz SA, Goncalves A, Lee KH, et al. Talazoparib in patients with advanced breast cancer and a germline BRCA mutation. *N Engl J Med* (2018) 379(8):753–63. doi: 10.1056/NEJMoa1802905

24. Sukumar J, Gast K, Quiroga D, Lustberg M, Williams N. Triple-negative breast cancer: promising prognostic biomarkers currently in development. *Expert Rev Anticancer Ther* (2021) 21(2):135–48. doi: 10.1080/14737140.2021.1840984

25. Zhu Y, Zhu X, Tang C, Guan X, Zhang W. Progress and challenges of immunotherapy in triple-negative breast cancer. *Biochim Biophys Acta Rev Cancer* (2021) 1876(2):188593. doi: 10.1016/j.bbcan.2021.188593

26. Pritzker KP. Predictive and prognostic cancer biomarkers revisited. *Expert Rev Mol Diagn* (2015) 15(8):971–4. doi: 10.1586/14737159.2015.1063421

27. Clark GM, Zborowski DM, Culbertson JL, Whitehead M, Savoie M, Seymour L, et al. Clinical utility of epidermal growth factor receptor expression for selecting patients with advanced non-small cell lung cancer for treatment with erlotinib. *J Thorac Oncol* (2006) 1(8):837–46. doi: 10.1016/S1556-0864(15)30414-7

28. Liu J, Lichtenberg T, Hoadley KA, Poisson LM, Lazar AJ, Cherniack AD, et al. An integrated TCGA pan-cancer clinical data resource to drive high-quality survival outcome analytics. *Cell.* (2018) 173(2):400–16 e11. doi: 10.1016/j.cell.2018.02.052

29. Jiang P, Gu S, Pan D, Fu J, Sahu A, Hu X, et al. Signatures of T cell dysfunction and exclusion predict cancer immunotherapy response. *Nat Med* (2018) 24(10):1550–8. doi: 10.1038/s41591-018-0136-1

30. Giaquinto AN, Sung H, Miller KD, Kramer JL, Newman LA, Minihan A, et al. Breast cancer statistics, 2022. *CA Cancer J Clin* (2022) 72(6):524–41. doi: 10.3322/caac.21754

31. Onitilo AA, Engel JM, Greenlee RT, Mukesh BN. Breast cancer subtypes based on ER/PR and Her2 expression: comparison of clinicopathologic features and survival. *Clin Med Res* (2009) 7(1-2):4–13. doi: 10.3121/cmr.2008.825

32. de Melo Gagliato D, Jardim DL, Marchesi MS, Hortobagyi GN. Mechanisms of resistance and sensitivity to anti-HER2 therapies in HER2+ breast cancer. *Oncotarget.* (2016) 7(39):64431–46. doi: 10.18632/oncotarget.7043

33. Binnewies M, Roberts EW, Kersten K, Chan V, Fearon DF, Merad M, et al. Understanding the tumor immune microenvironment (TIME) for effective therapy. *Nat Med* (2018) 24(5):541–50. doi: 10.1038/s41591-018-0014-x

34. Sahin Ozkan H, Ugurlu MU, Yumuk PF, Kaya H. Prognostic role of immune markers in triple negative breast carcinoma. *Pathol Oncol Res* (2020) 26(4):2733–45. doi: 10.1007/s12253-020-00874-4

35. Oliver AJ, Lau PKH, Unsworth AS, Loi S, Darcy PK, Kershaw MH, et al. Tissue-dependent tumor microenvironments and their impact on immunotherapy responses. *Front Immunol* (2018) 9:70. doi: 10.3389/fimmu.2018.00070

36. Adams S, Schmid P, Rugo HS, Winer EP, Loirat D, Awada A, et al. Pembrolizumab monotherapy for previously treated metastatic triple-negative breast cancer: cohort A of the phase II KEYNOTE-086 study. *Ann Oncol* (2019) 30(3):397–404. doi: 10.1093/annonc/mdy517

37. Cortes J, Cescon DW, Rugo HS, Nowecki Z, Im SA, Yusof MM, et al. Pembrolizumab plus chemotherapy versus placebo plus chemotherapy for previously untreated locally recurrent inoperable or metastatic triple-negative breast cancer (KEYNOTE-355): a randomised, placebo-controlled, double-blind, phase 3 clinical trial. *Lancet.* (2020) 396(10265):1817–28. doi: 10.1016/S0140-6736(20)32531-9

38. Wang Q, Li M, Yang M, Yang Y, Song F, Zhang W, et al. Analysis of immune-related signatures of lung adenocarcinoma identified two distinct subtypes: implications for immune checkpoint blockade therapy. *Aging (Albany NY)* (2020) 12(4):3312–39. doi: 10.18632/aging.102814

frontiers | Frontiers in Oncology

TYPE Review
PUBLISHED 22 August 2023
DOI 10.3389/fonc.2023.1221773

OPEN ACCESS

EDITED BY
Zhi-Gang Zhuang,
Shanghai First Maternity and Infant Hospital, China

REVIEWED BY
Huiping Li,
Peking University, China
Elisa Frullanti,
University of Siena, Italy

*CORRESPONDENCE
Omar Najim
omar.najim@azr.be

RECEIVED 12 May 2023
ACCEPTED 28 July 2023
PUBLISHED 22 August 2023

CITATION
Najim O, Papadimitriou K, Broeckx G, Huizing M and Tjalma W (2023) Validation of liquid biopsy for ESR1-mutation analysis in hormone-sensitive breast cancer: a pooled meta-analysis.
Front. Oncol. 13:1221773.
doi: 10.3389/fonc.2023.1221773

Validation of liquid biopsy for ESR1-mutation analysis in hormone-sensitive breast cancer: a pooled meta-analysis

Omar Najim[1,2]*, Konstantinos Papadimitriou[1,2,3], Glenn Broeckx[1,2,4], Manon Huizing[2,5] and Wiebren Tjalma[1,2,6]

[1]Multidisciplinary Breast Clinic Antwerp University Hospital, University of Antwerp, Edegem, Belgium, [2]Faculty of Medicine, University of Antwerp, Edegem, Belgium, [3]Department of Medical Oncology, Antwerp University Hospital, Edegem, Belgium, [4]Department of Pathology, Antwerp University Hospital, Edegem, Belgium, [5]Biobank, Antwerp University Hospital, Edegem, Belgium, [6]Unit of Gynecologic Oncology, Department of Obstetrics and Gynecology, Antwerp University Hospital, University of Antwerp, Edegem, Belgium

Several retrospective and prospective studies have shown that genomic alterations in Estrogen-receptor one (ESR1) can be characterized not only in tissue samples but also by sequencing circulating tumor DNA (ctDNA) in liquid biopsy. Therefore, liquid biopsy is a potential noninvasive surrogate for tissue biopsy. This meta-analysis was designed to compare the prevalence of ESR 1 mutation detected with liquid biopsy and tissue biopsy. A pooled meta-analysis of studies published between 1 January 2007 and 1 March 2021 was conducted regarding the methodologies used for ESR1 mutation analysis. Liquid biopsy is a valid, inexpensive, and attractive noninvasive alternative to tumor biopsies for the identification of ESR1 mutations. Liquid biopsy for ESR 1 analysis would facilitate regular testing, allowing monitoring of the sensitivity to ET and guiding treatment strategies.

KEYWORDS

ESR1, liquid biopsy, next-generation sequencing, digital PCR, metastasized breast cancer

Introduction

Our understanding of cancer biology using minimally invasive techniques to collect circulating tumor DNA (ctDNA) from body fluids is rapidly evolving. The fragmented DNA segments found in blood samples of cancer patients could be used to validate the presence of tumor specific mutations (1–3).

Breast tumors commonly express hormone receptors (HR), including the estrogen receptor (ER) and/or progesterone receptor (PR) (4). Endocrine therapy (ET), which targets the ER pathway, is a major treatment modality for HR-positive cancers. At diagnosis, ER positivity is a favorable prognostic factor for breast cancer (BC). However,

this positive prognostic effect degrades over time (5). Resistance to ET is considered an important step in the natural evolution of HR-positive BC and is related to a higher risk of recurrence and increased mortality (6). In the last decade, several clinical trials have assessed the incidence of ESR1 mutations in BC based on liquid biopsies. This knowledge is likely to encompass important information on the development of resistance to ET in real time, and is eventually applied for patient/treatment selection and monitoring of ET efficacy (7, 8).

Currently, the detection and molecular characterization of ctDNA represents one of the most active fields of translational cancer research. The recent development of NGS has expanded the monitoring of ctDNA with a range of diagnostic clinical applications. However, there are several limitations, including difficulties in interpreting novel or rare mutations and cost issues (9). On the other hand, the newly developed digital polymerase chain reaction (dPCR) has the potential to detect rare mutants, in which a variant of a single-nucleotide polymorphism is predominantly present among wild-type sequences (10). Droplet digital polymerase chain reaction (ddPCR), which can perform thousands of PCRs on a nanoliter scale simultaneously, would be an attractive method for massive parallel sequencing to identify the significance of low-frequency rare mutations. ddPCR is the most appropriate method for detecting known hotspot mutations, but is not the most appropriate approach for detecting unknown and 'not-targeted' mutations (11). Compared with singleplex reactions, multiplexing ddPCR not only increases the number of targets measured in a single reaction but also reduces the amount of clinical material required to analyze multiple single-nucleotide polymorphisms by measuring >1 target in a single reaction (12).

In BC, as in other solid tumors, the genomic alterations found within a given tumor biopsy may differ depending on the region sampled, as between the primary tumor and metastatic deposits, and even between different metastatic deposits (13). Genomic analyses of BC have provided direct evidence of spatial and temporal intratumoral heterogeneity (14, 15). Currently, clinical and therapeutic decisions are based on individual tissue biopsies that may not be representative of the entire tumor burden or on real-time assessments of the tumor genotype (16). This practical limitation could be overcome by the use of liquid biopsies, which represent a promising technique for decoding tumor heterogeneity.

In this review, we compare the prevalence ESR1 mutations for female patients with ER+ recurrent/metastasized BC pretreated with ET as detected by liquid biopsy versus standard tissue biopsy. This review discusses and summarizes the techniques of DNA sequencing, including ddPCR and NGS, which are used by several laboratories to address the potential clinical needs of ESR1 mutation-specific BC. A thorough understanding of these applications may provide useful information for ESR1 testing, ensure reliable test results for use in clinical practice, and eventually advance personalized therapeutic strategies. Aromatase Inhibitors (AIs) reduce circulating estrogen by inhibiting estrogen synthesis in peripheral tissues by 90% or more, but do not affect estrogen production in the ovaries. ESR1 mutations allow ERα to be activated in the absence of estradiol, eliminating AIs activity and making ESR1 a potential predictive factor.

Materials and methods

A literature search was conducted using two databases: PubMed and Thomson Reuters Web of Science. The following search terms were used: [('liquid biopsy' OR 'tissue sample') AND ('ESR1 mutation' OR 'ESR mutation') AND ('next generation sequencing' OR ' digital PCR) AND ('breast cancer')]. The reviewers performed the procedure of study selection by: (1) assessment of each clinical trial independently in an unblended standardized manner; (2) duplicates were removed afterwards; (3) only full-text English articles were included; (4) after the independent screening, all the results were compared and the articles with conflict were discussed until agreement was established; (5) the article should refer to an interventional trial; reviews, lectures and book sections were excluded; and (6) the final decision for study selection of the remaining articles were treated separately; studies that did not meet the inclusion criteria or did not contain useful information for this systematic review were excluded after consensus.

The included articles were published between 1 January 2007 and 1 March 2021. The extracted data included the type of clinical trial (RCT or non-RCT), characteristics of the study population, number of participants, exclusion of primary disease, nature of biopsy samples (plasma or tissue), and method of mutation analysis (ddPCR or NGS). The selected patients met the following inclusion criteria: 1. Female aged >18 years, 2. ER+ breast cancer cells pre-treated with endocrine therapy, and 3. Disease recurrence and metastases. Patients with primary breast cancer were excluded from this study. Overall incidence of ESR1 mutation was assessed using a meta analysis for proportions. Because of high diversity in type of studies, patients and therapies, a random effects model is used. Heterogeneity is judged by forest plot, Cochran Q and I-squared. Results are presented in a forest plot for proportions. Incidence of ESR1 mutation was compared between plasma versus tissue samples and between ddPCR versus NGS. Subgroup differences are evaluated by the between subgroups heterogeneity statistic in the random effects meta-analysis. P-values were considered statistically significant if it was < 0,05.

Results

A literature search fulfilling the previously explained search criteria and taking place in the proposed time interval resulted in a collection of 153 articles in PubMed and 204 articles in Web of Science. A total of 231 articles were evaluated after excluding duplicates. Articles that did not meet the inclusion criteria or that did not contain useful information for this systematic review, were discarded after consensus. Thereafter, 16 articles, four multicenter double-blinded RCTs, and 12 cohort trials were obtained for this meta-analysis (Figure 1).

From the reviewed studies, we included 2,744 pooled tissues and plasma samples for this analysis. Plasma samples were used in 57.1% (1,568/2,744) of the study population, tissue samples in 37.7% (1,033/2,744), and tissue-plasma pairs in 5.2% (143/2,744).

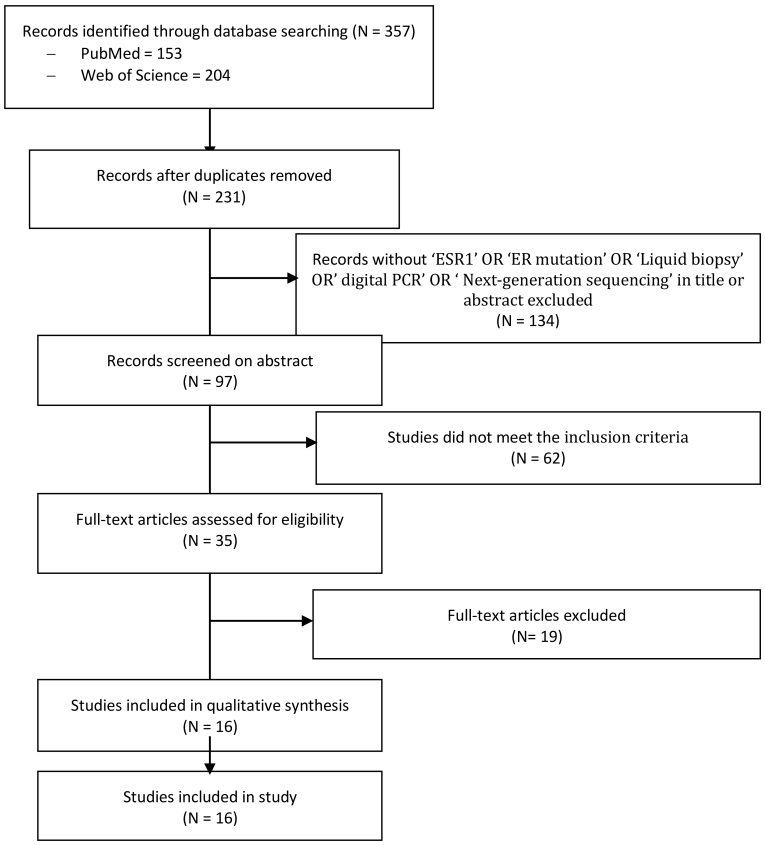

FIGURE 1
PRISMA flow diagram and the process of data selection. Selection of studies was performed using predefined data fields, taking study quality indicators into consideration. Eligibility criteria included terms with 'ESR1', 'ESR mutation' and 'liquid biopsy' or 'tissue sample', and/or 'next generation sequencing' and/or 'ddPCR' in the abstract or title by using the endnote library search option.

Tissue samples were obtained from loco regional or distant metastatic sites in four and six studies, respectively. Both archived and recent plasma samples were used for ESR1 analysis in four and two studies, respectively. ESR1 analysis was performed using ddPCR in 61.3% (1,684/2,744) of the study population and NGS in 38.7% (1,060/2,744).

Of the 2,744 samples pooled for this study, the overall incidence of ESR1 mutation is 23% (95 CI 18%–28%) (Figure 2). However, the

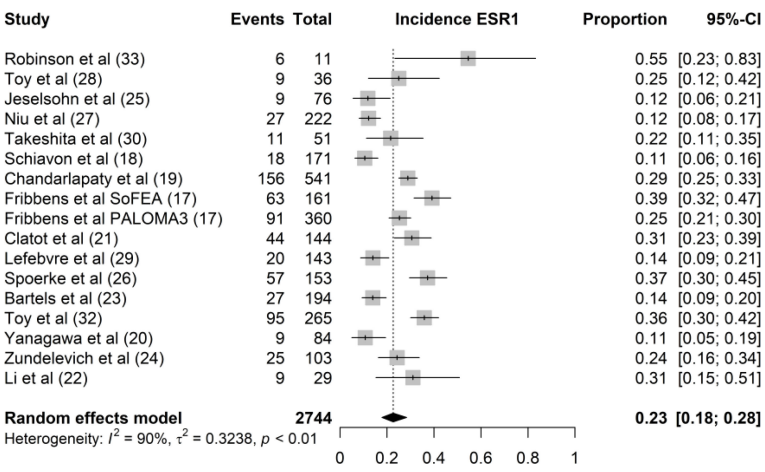

FIGURE 2
Forest plot of the overall incidence rate of ESR1 mutation. The proportion of ESR1 mutation per study is displayed with a grey box, with the 95%-CI visualized by horizontal lines. The overall frequency of ESR1 mutations was 0.23 (95%-CI: 0.18 0.28), as indicated by the black diamond at the bottom of the forest plot.

different studies demonstrated a considerable variability in the prevalence of ESR1 mutations ranged from 11% in Schiavon et al. (17) and Yanagawa et al. (18) to 55% in Robinson et al. (19) The wide range in incidence rate of ESR1 mutation could be attributed to heterogeneity in the study populations.

In the articles under review, nine studies used tissue biopsy while five studies used plasma biopsy. In a trial by Yanagawa et al. (18), whole-exon sequencing of the ESR1 gene was performed separately in tissue and plasma samples. In 15 of the 16 studies included, the incidence rates of ESR1 mutations in plasma and tissue samples were 26% (95% CI, 18%–35%) and 21% (95% CI, 15%–28%), respectively (Figure 3). We found no significant difference in ESR1 mutation incidence between plasma and tissue samples (P = 0.34). The samples from Lefebvre et al. (20) were excluded from the comparative analysis between liquid and tissue biopsies because ESR1 sequencing was performed in tissue-blood pairs. In this study, the mutational profiles of 143 tissue-blood pairs from patients with hormone receptor-positive (HR+) metastatic BC were analyzed. Twelve genes (TP53, PIK3CA, GATA3, ESR1, MAP3K1, CDH1, AKT1, MAP2K4, RB1, PTEN, CBFB, and CDKN2A) were significantly mutated in MBC. This study concluded that ESR1 mutation was the most frequent mutation in the HR+ MBC subgroup (n = 143). In total, 22 mutations were identified in 20 of 143 patients with HR+/HER2− BC (14%). Li et al. demonstrated that ESR1 mutations could be detected by serial monitoring of ctDNA. In this study, mutation profiles, including ESR1, were highly concordant between plasma and paired tissue samples from 45 patients with MBC (20).

Both ddPCR and NGS were used to determine ESR1 mutations in the tissue and plasma samples. ddPCR was used in seven studies and NGS was used in nine studies. ddPCR is the standard method for ESR1 testing in liquid biopsies, except in the study by Yanagawa et al. NGS was used to analyze both tissue and plasma samples. However, both NGS and ddPCR have been used for ESR1 testing of tissue biopsies. The incidence rates of ESR1 mutations using ddPCR and NGS were 26% (95% CI, 20%–33%) and 19% (95% CI, 13%–27%), respectively (Figure 4). We found no significant difference in ESR1 mutation incidence between ddPCR and NGS techniques (P = 0.15).

All studies on both plasma and tissue samples have described their methodology regarding collection, processing, and analysis in a more or less complete manner, despite some missing pre-analytical aspects (17–19, 21–32). Of the six studies researching plasma samples, only one used NGS (18), while the other studies used ddPCR (17, 21–24). Two of the 10 studies used ddPCR (29, 32), while eight other studies used NGS (18, 19, 25–28, 30, 31). Remarkably, all studies performing ddPCR, whether on tissue samples or plasma samples, used the same platform (Bio-Rad QX200 ddPCR system) and more or less the same pre-analytical and DNA-quantification steps; however, the hotspot mutation panel might differ according to the respective study (17, 21–24, 29, 32). In contrast, many different NGS platforms are used, with many different library preparation kits and quantification tools. Some of the NGS platforms used are the Illumina HiSeq 2000 series and the Ion Torrent platform (18, 19, 25–27, 30, 31). Additionally and important to note, genomic profiling was performed by Foundation Medicine on the Foundation One platform in one study on tissue samples (28). As this study did not aim to investigate the different aspects of the ESR1 analysis methodology, we will not go into detail in the different preanalytical, DNA-quantification, and mutation analysis steps. Nonetheless, these data can be found in the schematic overview of the available

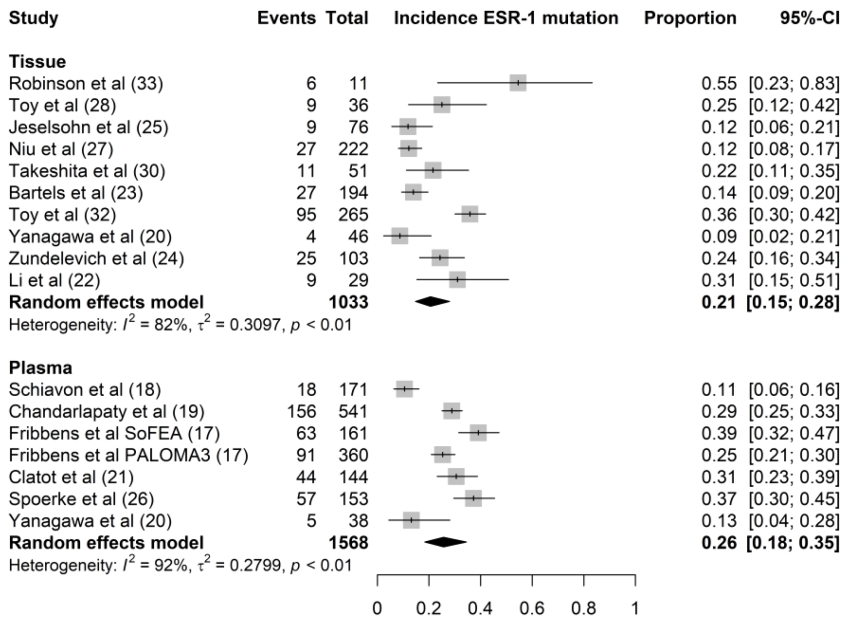

FIGURE 3
Forest plot of the comparison of ESR1 mutation in tissue versus plasma samples. Grey boxes indicate the proportion of ESR1 mutations in each study, with a horizontal line representing the 95% CI. Overall proportion and 95% CI in tissue and plasma subgroup is displayed with a black diamond. We found no significant difference in ESR1 mutation incidence between plasma and tissue samples (P=0.34).

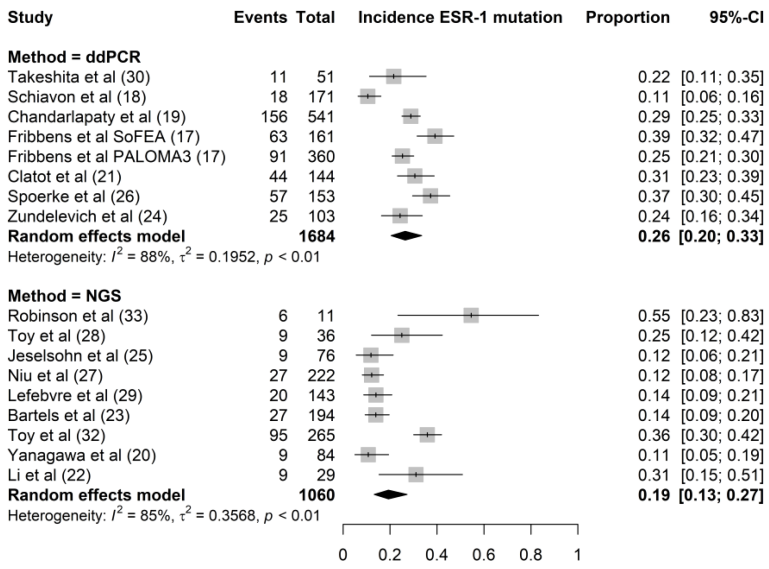

FIGURE 4
Forest plot of the comparison of the proportion of ESR1 mutation using NGS versus ddPCR techniques. Grey boxes indicate the proportion of ESR1 mutations in each study, with a horizontal line representing the 95% CI. Overall proportion and 95% CI in NGS and ddPCR subgroup is displayed with a black diamond. We found no significant difference in ESR1 mutation incidence between the two techniques (P=0.15).

preanalytical and analytical parameters provided in Tables 1, 2. We previously published in an earlier review a detailed ESR1 specific mutational profile analysis, including D538G, Y537S, and Y537N as the most prevalent mutations (33).

Discussion

A growing body of clinical trials on ER+ BC strongly supports the use of ESR1 as a valid predictor of response to ET. Understanding the mechanisms of acquired resistance to ET can impact therapeutic strategies to overcome the effects of mutant genes responsible for ET failure. Analysis of ESR1 mutations conferring resistance to ET has already been demonstrated in patients with ER+ advanced stage BC (31, 33). Furthermore, *in vitro* studies have shown that ESR1 mutations are likely to be acquired because of ET deprivation (34). However, ESR1 mutations are rare in endocrine therapy-naive ER+/HER2− BC, and the frequency is even lower if an AI has not been administered in the adjuvant setting: 3%–6% (17, 35). In contrast, studies that enrolled patients after first-line AI therapy found that approximately 30% of patients have ESR1mutated (17, 21, 36–41). In the current meta-analysis, the incidence rate of ESR1 was 23%, which was consistent with the results of previous trials.

To date, screening for ESR1 in ER+ BC is not considered the standard of care; tumor tissue sampling remains the standard method for addressing tumor biology, despite issues in terms of acquisition and utility; tissue biopsies are invasive and do not have potential complications, and sample preservation may hamper the use of tumor tissue for cancer sequencing (42). Intra/inter-tumor heterogeneity, mostly observed in advanced cancers, is also a major limitation of tumor biopsy (13, 43). This heterogeneity is partially attributed to dynamic genetic changes that occur after therapeutic selective pressure (44). Therefore, tissue biopsy may not be the most appropriate method for mutational analysis of metastatic BC, especially when looking for rare point mutations in a background of wild-type sequences, as in the case of ESR1.

Liquid biopsy is a rapid, cost-effective, and noninvasive technique, capable of capturing molecular heterogeneity during disease evolution and potentially overcoming the aforementioned issues (44, 45). Cell-free DNA (cfDNA) is a potential surrogate for the entire tumor genome (46). The cfDNA fragments provide a representative reflection of genomic alterations of the original tumor because cfDNA fragments are derived from all tumor sites in a patient's body circulation (45, 47). Acquired resistance to endocrine therapy prior to disease progression could also be monitored by longitudinally analysis of ESR1 mutations (33). ctDNA analyses are highly sensitive because DNA is abundant in most advanced malignancies, allowing the successful tracking of ESR1 mutations (44). Therefore, liquid biopsy is widely available and easier to perform than standard tumor biopsies (48). Recent improvements in PCR techniques for analyzing cfDNA provide a potential alternative to tumor biopsies, provide information on tumor genetic alterations, and have been used as diagnostic, prognostic, or even predictive tools (49). Our results showed no statistical difference in ESR1 incidence for plasma-tissue comparison (21% vs. 26%; P = 0.34), in accordance with the results of previous reports (21, 23, 29, 30, 32).

At present, ddPCR represents a low-cost and effective technique that has been recently commercialized to detect and quantify small amounts of genetic material (50, 51). ddPCR is a potential alternative to next-generation sequencing (NGS); however, it is only suitable for testing known mutations. Recently, PCR-based digital investigations have been coupled with techniques that use

TABLE 1 Overview of the collection, processing and ESR1 mutation analysis in all studies concerning the analysis of plasma samples.

Study	Collection	TTP	Centrifugation		Volume cleared plasma	Storage	DNA extraction kit	DNA quantification				Analysis	Comments
			Speed	Time				Method	Reference gene	Mass	Concentration		
Fribbens et al. 2016 (17) **SoFEA trial**	EDTA tubes	0-9 days	1600 g	20 minutes	/	-80°C	QIAamp Circulating Nucleic Acid Kit (Qiagen, Hilden, Germany)	ddPCR (Bio-Rad QX200 system)	RNase P		10^2-10^7copies/mL	Multiplex ddPCR and characterization on uniplex ddPCR (Bio-Rad QX200 system)	Multiplex 1: c.1138G.C(E380Q), c.1607T.G(L536R), c.1610A.G(Y537C), c.1613A.G(D538G) Multiplex 2: c.1387T.C(S463P), c.1609T.A(Y537N), c.1610A.C(Y537S)
Fribbens et al. 2016 (17) **PALOMA3 study**	EDTA tubes	0-30 minutes	1500-2000 g	10 minutes	/	-80°C	QIAamp Circulating Nucleic Acid Kit (Qiagen, Hilden, Germany)	ddPCR (Bio-Rad QX200 system)	RNase P		10^2-10^7copies/mL	Multiplex ddPCR and characterization on uniplex ddPCR (Bio-Rad QX200 system)	Multiplex 1: c.1138G.C(E380Q), c.1607T.G(L536R), c.1610A.G(Y537C), c.1613A.G(D538G) Multiplex 2: c.1387T.C(S463P), c.1609T.A(Y537N), c.1610A.C(Y537S)
Schiavon et al. 2015 (18)	EDTA tubes	0-2 hours	1600 g	20 minutes	/	-20°C	QIAamp Circulating Nucleic Acid Kit (Qiagen, Hilden, Germany)	ddPCR (Bio-Rad QX200 system)	RNase P			Multiplex ddPCR and characterization on uniplex ddPCR (Bio-Rad QX200 system)	Multiplex 1: c.1607T.G(L536R), c.1610A.G(Y537C), c.1609T.A(Y537N) Multiplex 2: c.1610A.C(Y537S) c.1613A.G(D538G)
Chandarlapaty et al. 2016 (19)	EDTA tubes	0-30 minutes	1100-1300 g	/	0.3-3.3 mL (median 1.8 mL)	-70°C	QIAamp Circulating Nucleic Acid Kit (Qiagen, Hilden, Germany)	qPCR (KAPA Human Genomic DNA Quantification and QC kit)	/			Uniplex ddPCR (Bio-Rad QX200 system)	Uniplex: c.1610A.C(Y537S) c.1613A.G(D538G)
Yanagawa et al. 2017 (20)	/	/	3000 g	10 minutes	/	-80°C	QIAamp Circulating Nucleic Acid Kit (Qiagen, Hilden, Germany)					NGS (Thermo Fisher Ion Torrent PGM)	Primer design: Ion Ampliseq™ Custom DNA Panels Library preparation: Ion Ampliseq Library Kit 2.0 MAF cut off 3.0%

(Continued)

10.3389/fonc.2023.1221773

TABLE 1 Continued

Study	Collection	TTP	Centrifugation		Volume cleared plasma	Storage	DNA extraction kit	DNA quantification				Analysis	Comments
			Speed	Time				Method	Reference gene	Mass	Concentration		
Clatot et al. 2016 (21)	Heparinized tubes	0-2 hours	2000 g	10 min		4-20°C*	QIAamp Circulating Nucleic Acid Kit (Qiagen, Hilden, Germany)	Fluorometry (Invitrogen Quanti-IT^{TM} PicoGreen® dsDNA Assay Kit)			200-2000 copies/mL	Multiplex ddPCR (Bio-Rad QX200 system)	Multiplex: c.1609T.A(Y537N), c.1610A.C(Y537S), c.1610A.G(Y537C), c.1613A.G(D538G)
Spoerke et al. 2016 (26)	EDTA	0-1 hour	820 g 16000 g	10 min 10 min		-80°C		qPCR (LINE-1) quantitative real-time PCR assay)		3-1500 ng		ddPCR OncoBEAM BC1 BEAMing Digital PCR panel	Panel: c.1138G.C(E380Q), c.1387T.C(S463P), c.1604C.A(P535H), c.1607T.A(L536H), c.1607T.C(L536P), c.1607_1608delTCinsAG (L536Q), c.1607T.G(L536R), c.1610A.G(Y537C) c.1609T.A(Y537N), c.1610A.C(Y537S), c.1613A.G(D538G)

TTP, time to preparation; EDTA. ddPCR, droplet digital polymerase chain reaction; qPCR, quantifying polymerase chain reaction; NGS, next generation sequencing; MAF, mutant allelic frequency.

10.3389/fonc.2023.1221773

TABLE 2 Overview of the collection, processing and ESR1 mutation analysis in all studies concerning the analysis of Tissue samples.

Study	Biopsy site	Preparation			DNA extraction	DNA Quantification	Analysis					Comments
		Medium	Slides				Type	Panel primer design	Library preparation	Quantification libraries	Instrument	
			Number	Thickness								
Bartels et al. 2018 (23)	Bone marrow	FFPE	2-6 slides	10µm	Maxwell RSC DNA FFPE Kit Maxwell RSC instrument	Fluorometry Qubit 2.0 Fluorometer dsDNA high sensitivity Assay Kit	NGS	Ion Ampliseq Designer	Ion Ampliseq Library kit 2.0	qPCR Ion Library Quantification Kit	Ion PGM Hi-Q Kit v2	
Jeselsohn et al. 2014 (25)	Primary site Metastatic sites	FFPE	/	40µm	Maxwell 16 FFPE Plus LEV DNA Purification Kit	Fluorometry PicoGreen fluorescence assay	NGS	/	RNA based baits hybridization	/	Illumina HiSeq2000	
Li et al. 2020 (22)	Metastatic sites Liquor	FFPE	/	/	/	Fluorometry PicoGreen fluorescence assay	NGS	/	KAPA Hyper DNA Library Prep Kit	/	Illumina HiSeq	
Niu et al. 2015 (27)	Primary site Metastatic site	/	/	/	/	/	NGS	/	/	/	/	Genomic profiling by Foundation Medicine on Foundation One platform
Yanagawa et al. 2017 (20)	Recurrent site Metastatic site	FFPE	3	10µm	QIAamp DNA FFPE Tissue Kit	/	NGS	Ion AmpliSeq Custom DNA Panels	Ion Ampliseq Library kit 2.0	/	Ion Torrent PGM	
Robinson et al. 2013 (33)	/	/	/	/	/	/	NGS	/	/	/	/	
Takeshita et al. 2015 (30)	Primary site Metastatic site	FFPE	/	/	AllPrep DNA/RNA Mini Kit PicoPure DNA Extraction Kit	Spectrophotometry NanoDrop 2000 Spectrometer	ddPCR	NA	NA	NA	Bio-Rad QX200 Droplet Digital PCR System	Uniplex ddPCR: c.1610A.C (Y537S), c.1609T.A (Y537N), c.1610A.G (Y537C), c.1613A.G (D538G)

(Continued)

10.3389/fonc.2023.1221773

TABLE 2 Continued

Study	Biopsy site	Preparation			DNA extraction	DNA Quantification	Analysis					Comments
		Medium	Slides				Type	Panel primer design	Library preparation	Quantification libraries	Instrument	
			Number	Thickness								
Toy et al. 2013 (28)	Primary site Metastatic site	FFPE Fresh frozen	/	/	QuickGeneTM DNA tissue Kit	Fluorometry Nanodrop Fluorospectrometer	NGS	Agilent SureSelect Nimblegen SeqCap	Illumina TruSeq NEBNext DNA Library Prep Kit	Nimblegen SeqCap	Illumina HiSeq 2000	
Toy et al. 2017 (32)	Metastatic site	FFPE	15-20	10µm	QIAamp DNA Micro Kit	/	NGS	/	Nimblegen SeqCap	Nimblegen SeqCap	Illumina HiSeq 2500	
Zundelevich et al. 2020 (24)	Primary site Metastatic site	FFPE	1-10	10µm	All Prep DNA/RNA FFPE Kit	Fluorometry Qubit 2.0 Fluorometer dsDNA high sensitivity Assay kit	ddPCR	NA	NA	NA	Bio-Rad QX100 Droplet Digital PCR System Bio-Rad QX200 Droplet Digital PCR System	Uniplex ddPCR: c.1613A.G (D538G), c.1607T.G (L536R), c.1610A.C (Y537S), c.1609T.A (Y537N), c.1610A.G (Y537C)
Schiavon et al. 2015 (18)	Recurrent site Metastatic site	FFPE	4-8	4µm	QIAamp DNA FFPE Tissue Kit All Prep DNA/RNA FFPE Kit	ddPCR Bio-Rad QX200 Digital Droplet PCR Reference gene: RNase P	ddPCR	NA	NA	NA	Bio-Rad QX200 Droplet Digital PCR System	Multiplex ddPCR 1: c.1607T.G (L536R), c.1610A.G (Y537C), c.1609T.A (Y537N) Multiplex ddPCR 2: c.1610A.C (Y537S) c.1613A.G (D538G)

TTP, time to preparation;. ddPCR, droplet digital polymerase chain reaction; qPCR, quantifying polymerase chain reaction; NGS, next generation sequencing; NA, not applicable.

10.3389/fonc.2023.1221773

NGS to enumerate rare mutant variants in complex DNA mixtures (52). Both techniques support the screening and clinical validity of genomic alterations in ctDNA as a 'liquid biopsy' in breast cancer, including ESR1 mutants (53, 54). ddPCR is particularly useful for the detection of rare mutant DNA sequences in large quantities of background wild-type sequences. Our results showed no statistical difference in ESR1 incidence between the ddPCR-NGS comparisons (26% vs. 19%; P = 0.15).

Although the analysis of cfDNA is a truly growing field, liquid biopsy is not yet routinely used in clinical practice to decode the tumor genome, despite the fact that acquiring plasma samples is more accessible and minimally invasive compared to tissue samples. Furthermore, when comparing the cost-effectiveness of ddPCR and NGS, there was no clear winner. It is generally accepted that ddPCR is a low-cost, time-saving, and effective method for genomic analyses (55, 56). Moreover, ddPCR is designed highly sensitive detection of hotspot mutations, making it more suitable for the detection of low concentrations of cfDNA in plasma samples. NGS relies on different reagents but is capable of testing multiple samples for multiple genes simultaneously. This process is, of course, more time-consuming (7–10 days) and less cost-effective (55, 56). However, assuming a fair number of samples to be tested in routine practice, ddPCR may be a cost-effective and time-sparing method, on the condition that hotspot mutations of interest are known, as is the case for ESR1. In this case, ddPCR may require as little as half the cost of NGS. In our opinion, the analysis of liquid biopsy using ddPCR is the most favorable combination for ESR1 testing in terms of sample feasibility, time, and cost. Table 3 shows the potential advantages of liquid biopsy compared to tissue biopsy.

To our knowledge, this is the largest meta-analysis to carry out a comparative analysis between liquid and tissue biopsies, and between ddPCR and NGS. The results of this review show no significant difference in prevalence of ESR1 mutation detected with liquid biopsy or tissue biopsy. Different studies show a large variability in the prevalence of ESR1 mutations (11% to 55%). The wide range in the incidence rates of ESR1 mutations could be attributed to heterogeneity in the study populations and inter-laboratory findings. A recent review on the progress in detecting ESR1 mutations based on liquid biopsy and different sequencing technologies in ER+ MBC also highlights its potential clinical impacts and prospects in accordance with these conclusions (57).

According to the hypothesis of this review, there was a risk of selection bias because the selected patients had progressive and recurrent BC. Furthermore, meta-analyses on their own may suffer from several sources of bias in individuals and across studies. First, not all trials lead to publication, which induces publication bias for positive findings, and the language of the original publication might have resulted in a selection bias. For some research questions, only a small number of studies were included in the meta-analysis. The quality of the studies varied. Due to the broad scope of our research questions, not only randomized controlled trials, but also case–control and uncontrolled cohort trials were eligible for inclusion in the review. Confounding and baseline differences may be more pronounced in non-randomized or uncontrolled studies than in randomized controlled trials. Furthermore, paired tissue plasma samples were available for only 5.2% of samples. Taken together, these limitations discourage the difficulty of obtaining evidence that plasma is non-inferior to tissue, since both have been measured in different patients and in different studies; solid proof for such a conclusion could only be derived from a large-scale prospective study comparing tissue and plasma samples from the same patients.

This meta-analysis demonstrates that ESR1 mutations are found at high frequency in liquid biopsies of ER+ recurrent/metastasized BC and could be tracked relatively simply and inexpensively using both ddPCR and NGS technologies. Both technologies are equally effective for the identification of ESR1 mutations in tissue and plasma samples; however, ddPCR is inexpensive. Regular ESR1 mutation analysis is needed during

TABLE 3 The comparison of liquid versus tissue samples for DNA analysis.

	Liquid biopsy	Tissue biopsy	In favor of
Invasive method	Minimally	More invasive Might require surgical intervention	Liquid biopsy
Longitudinal monitoring	Easy	Difficult	Liquid biopsy
Accessibility	Easy	More challenging	Liquid biopsy
Tumor heterogeneity	Covered	Minimally covered	Liquid biopsy
Tumor material	Less	More	Tissue biopsy
DNA concentrations	Low	High	Tissue biopsy
Complications	Low morbidity: Phlebitis	Higher morbidity: More risk of bleeding, infection and surgical complications	Liquid biopsy
Cost	ddPCR: Low NGS: High	ddPCR: Moderate NGS: Moderate	*Liquid biopsy if ddPCR
Sample processing and preservation	Easy: EDTA-tubes Centrifugation Freezing	Difficult & time-consuming More expensive Formalin fixation Paraffin embedding Large storage rooms	Liquid biopsy

*Assuming routine practice with fair amount of samples.

endocrine treatment before disease recurrence or progression. The incorporation of cfDNA-based ESR1 analysis is the current challenge for clinicians to ensure that ESR1 testing can be integrated into routine clinical care; however, widespread diagnostic application requires for rigorous studies to demonstrate not only clinical validity but also clinical utility. Recent data from a small cohort of patients suggest that liquid biopsy can reveal the presence of minimal residual disease several years before the appearance of clinically detectable metastatic disease, demonstrating that comprehensive liquid biopsy analysis provides important information for the therapeutic management of breast cancer patients (58). However, the clinical utility of ESR1 analysis as an early predictor needs to be proven in a randomized prospective clinical setting to guide therapeutic decisions on liquid biopsy analysis and on established endpoints (59). Ongoing trials in this setting, such as the SERENA 6, have already addressed the efficacy and safety of switching the ET partner of first-line CDK4/6i therapy at the earliest time point when ESR1m is detected in ctDNA, and before clinical disease progression (60).

In conclusion, the present pooled meta-analysis only provides additional evidence that liquid biopsies can replace tumor tissue biopsies in molecular screening programs for ESR1 mutations in a potentially easier and cost-effective approach. However, the key question of whether changing therapy based on ESR1 mutations before radiologic progression will improve long-term disease control and OS compared to therapy changes based on radiologic progression is yet to be answered.

Author contributions

Study design, analysis, and interpretation of data: ON. Acquisition of data, technical laboratory support: GB. Statistical analysis: ON, KP, and WT. Study supervision: MH, KP, and WT. ON wrote the manuscript. The final manuscript was edited, reviewed and approved by MH, KP, GB, and WT.

Funding

The Ladies Circle Dendermonde, located in Sint-Gillislaan 47,9200 Dendermonde, Belgium, funded this study.

Acknowledgments

This work is dedicated to the spirit of Mme. Frija De Bock, a member of Ladies Circle Dendermonde, who died at the age of 41 years because of breast cancer.

Conflict of interest

The authors declare that the research was conducted in the absence of any commercial or financial relationships that could be construed as a potential conflict of interest.

Publisher's note

References

1. Guttery DS, Page K, Hills A, Woodley L, Marchese SD, Rghebi B, Shaw JA. Noninvasive detection of activating estrogen receptor 1 (ESR1) mutations in estrogen receptor-positive metastatic breast cancer. *Clin Chem* (2015) 61(7):974–82. doi: 10.1373/clinchem.2015.238717

2. Norton SE, Norton SE, Lechner JM, Williams T, Fernando MR. A stabilizing reagent prevents cell-free DNA contamination by cellular DNA in plasma during blood sample storage and shipping as determined by digital PCR. *Clin Biochem* (2013) 46(15):1561–5. doi: 10.1016/j.clinbiochem.2013.06.002

3. Najim O, Huizing M, Papadimitriou K, Trinh XB, Pauwels P, Goethals S, Tjalma W. The prevalence of estrogen receptor-1 mutation in advanced breast cancer: The estrogen receptor one study (EROS1). *Cancer Treat Res Commun* (2019) 19:100123. doi: 10.1016/j.ctarc.2019.100123

4. Lim E, Metzger-Filho O, Winer EP. The natural history of hormone receptor-positive breast cancer. *Oncol (Williston Park)* (2012) 26(8):688–94, 696.

5. Bentzon N, Düring M, Rasmussen BB, Mouridsen H, Kroman N. Prognostic effect of estrogen receptor status across age in primary breast cancer. *Int J Cancer* (2008) 122(5):1089–94. doi: 10.1002/ijc.22892

6. Clarke R, Tyson JJ, Dixon JM. Endocrine resistance in breast cancer - An overview and update. *Mol Cell Endocrinol* (2015) 418:220–34. doi: 10.1016/j.mce.2015.09.035

7. Tabarestani S, Motallebi M, Akbari ME. Are estrogen receptor genomic aberrations predictive of hormone therapy response in breast cancer? *Iran J Cancer Prev* (2016) 9(4):e6565. doi: 10.17795/ijcp-6565

8. Alix-Panabieres C, Pantel K. Circulating tumor cells: liquid biopsy of cancer. *Clin Chem* (2013) 59(1):110–8. doi: 10.1373/clinchem.2012.194258

9. Yohe S, Thyagarajan B. Review of clinical next-generation sequencing. *Arch Pathol Lab Med* (2017) 141(11):1544–57. doi: 10.5858/arpa.2016-0501-RA

10. Vogelstein B, Kinzler KW. Digital PCR. *Proc Natl Acad Sci U.S.A.* (1999) 96 (16):9236–41. doi: 10.1073/pnas.96.16.9236

11. Angus L, Beije N, Jager A, Martens JW, Sleijfer S. ESR1 mutations: Moving towards guiding treatment decision-making in metastatic breast cancer patients. *Cancer Treat Rev* (2017) 52:33–40. doi: 10.1016/j.ctrv.2016.11.001

12. Huggett JF, Whale A. Digital PCR as a novel technology and its potential implications for molecular diagnostics. *Clin Chem* (2013) 59(12):1691–3. doi: 10.1373/clinchem.2013.214742

13. Gerlinger M, Rowan AJ, Horswell S, Larkin J, Endesfelder D, Gronroos E, Swanton C. Intratumor heterogeneity and branched evolution revealed by multiregion sequencing. *N Engl J Med* (2012) 366(10):883–92. doi: 10.1056/NEJMoa1113205

14. Nik-Zainal S, Van Loo P, Wedge DC, Alexandrov LB, Greenman CD, Lau KW, et al. The life history of 21 breast cancers. *Cell* (2012) 149(5):994–1007. doi: 10.1016/j.cell.2012.04.023

15. Yates LR, Gerstung M, Knappskog S, Desmedt C, Gundem G, Van Loo P, Campbell PJ. Subclonal diversification of primary breast cancer revealed by multiregion sequencing. *Nat Med* (2015) 21(7):751–9. doi: 10.1038/nm.3886

16. De Mattos-Arruda L, Caldas C. Cell-free circulating tumour DNA as a liquid biopsy in breast cancer. *Mol Oncol* (2016) 10(3):464–74. doi: 10.1016/j.molonc.2015.12.001

17. Schiavon G, Hrebien S, Garcia-Murillas I, Cutts RJ, Pearson A, Tarazona N, Turner NC. Analysis of ESR1 mutation in circulating tumor DNA demonstrates evolution during therapy for metastatic breast cancer. *Sci Transl Med* (2015) 7 (313):313ra182. doi: 10.1126/scitranslmed.aac7551

18. Yanagawa T, Kagara N, Miyake T, Tanei T, Naoi Y, Shimoda M, et al. Detection of ESR1 mutations in plasma and tumors from metastatic breast cancer patients using next-generation sequencing. *Breast Cancer Res Treat* (2017) 163(2):231–40. doi: 10.1007/s10549-017-4190-z

19. Robinson DR, Wu YM, Vats P, Su F, Lonigro RJ, Cao X, et al. Activating ESR1 mutations in hormone-resistant metastatic breast cancer. *Nat Genet* (2013) 45 (12):1446–51. doi: 10.1038/ng.2823

20. Lefebvre C, Bachelot T, Filleron T, Pedrero M, Campone M, Soria JC, et al. Mutational profile of metastatic breast cancers: A retrospective analysis. *PloS Med* (2016) 13(12):e1002201. doi: 10.1371/journal.pmed.1002201

21. Chandarlapaty S, Chen D, He W, Sung P, Samoila A, You D, et al. Prevalence of ESR1 mutations in cell-free DNA and outcomes in metastatic breast cancer: A secondary analysis of the BOLERO-2 clinical trial. *JAMA Oncol* (2016) 2(10):1310–5. doi: 10.1001/jamaoncol.2016.1279

22. Clatot F, Perdrix A, Augusto L, Beaussire L, Delacour J, Calbrix C, et al. Kinetics, prognostic and predictive values of ESR1 circulating mutations in metastatic breast cancer patients progressing on aromatase inhibitor. *Oncotarget* (2016) 7(46):74448–59. doi: 10.18632/oncotarget.12950

23. Fribbens C, O'Leary B, Kilburn L, Hrebien S, Garcia-Murillas I, Beaney M, et al. Plasma ESR1 mutations and the treatment of estrogen receptor-positive advanced breast cancer. *J Clin Oncol* (2016) 34(25):2961–8. doi: 10.1200/JCO.2016.67.3061

24. Spoerke JM, Gendreau S, Walter K, Qiu J, Wilson TR, Savage H, et al. Heterogeneity and clinical significance of ESR1 mutations in ER-positive metastatic breast cancer patients receiving fulvestrant. *Nat Commun* (2016) 7:11579. doi: 10.1038/ncomms11579

25. Bartels S, Christgen M, Luft A, Persing S, Jödecke K, Lehmann U, et al. Estrogen receptor (ESR1) mutation in bone metastases from breast cancer. *Mod Pathol* (2018) 31 (1):56–61. doi: 10.1038/modpathol.2017.95

26. Jeselsohn R, Yelensky R, Buchwalter G, Frampton G, Meric-Bernstam F, Gonzalez-Angulo AM, et al. Emergence of constitutively active estrogen receptor-alpha mutations in pretreated advanced estrogen receptor-positive breast cancer. *Clin Cancer Res* (2014) 20(7):1757–67. doi: 10.1158/1078-0432.CCR-13-2332

27. Li X, Lu J, Zhang L, Luo Y, Zhao Z, Li M. Clinical implications of monitoring ESR1 mutations by circulating tumor DNA in estrogen receptor positive metastatic breast cancer: A pilot study. *Transl Oncol* (2020) 13(2):321–8. doi: 10.1016/j.tranon.2019.11.007

28. Niu J, Andres G, Kramer K, Kundranda MN, Alvarez RH, Klimant E, et al. Incidence and clinical significance of ESR1 mutations in heavily pretreated metastatic breast cancer patients. *Onco Targets Ther* (2015) 8:3323–8. doi: 10.2147/OTT.S92443

29. Takeshita T, Yamamoto Y, Yamamoto-Ibusuki M, Inao T, Sueta A, Fujiwara S, et al. Droplet digital polymerase chain reaction assay for screening of ESR1 mutations in 325 breast cancer specimens. *Transl Res* (2015) 166(6):540–553 e2. doi: 10.1016/j.trsl.2015.09.003

30. Toy W, Shen Y, Won H, Green B, Sakr RA, Will M, et al. ESR1 ligand-binding domain mutations in hormone-resistant breast cancer. *Nat Genet* (2013) 45(12):1439–45. doi: 10.1038/ng.2822

31. Toy W, Weir H, Razavi P, Lawson M, Goeppert AU, Mazzola AM, et al. Activating ESR1 mutations differentially affect the efficacy of ER antagonists. *Cancer Discovery* (2017) 7 (3):277–87. doi: 10.1158/2159-8290.CD-15-1523

32. Zundelevich A, Dadiani M, Kahana-Edwin S, Itay A, Sella T, Gadot M, et al. ESR1 mutations are frequent in newly diagnosed metastatic and loco-regional recurrence of endocrine-treated breast cancer and carry worse prognosis. *Breast Cancer Res* (2020) 22(1):16. doi: 10.1186/s13058-020-1246-5

33. Najim O, Seghers S, Sergoynne L, Van Gaver H, Papadimitriou K, Wouters K, Tjalma W. The association between type of endocrine therapy and development of estrogen receptor-1 mutation(s) in patients with hormone-sensitive advanced breast cancer: A systematic review and meta-analysis of randomized and non-randomized trials. *Biochim Biophys Acta Rev Cancer* (2019) 1872(2):188315.

34. Dustin D, Gu G, Fuqua SAW. ESR1 mutations in breast cancer. *Cancer* (2019) 125(21):3714–28. doi: 10.1002/cncr.32345

35. Bidard FC, Callens C, Dalenc F, Pistilli B, De La Motte Rouge T, Clatot F, Bachelot T. Prognostic impact of ESR1 mutations in ER+ HER2-MBC patients prior treated with first line AI and palbociclib: An exploratory analysis of the PADA-1 trial. (2020), 1010–0. doi: 10.1200/JCO.2020.38.15_suppl.1010

36. Bidard F-C, Kaklamani VG, Neven P, Streich G, Montero AJ, Forget F, et al. Elacestrant (oral selective estrogen receptor degrader) versus standard endocrine therapy for estrogen receptor–positive, human epidermal growth factor receptor 2–negative advanced breast cancer: results from the randomized phase III EMERALD trial. *J Clin Oncol* (2022) 40(28):3246. doi: 10.1200/JCO.22.00338

37. O'Leary B, Hrebien S, Morden JP, Beaney M, Fribbens C, Huang X, et al. Early circulating tumor DNA dynamics and clonal selection with palbociclib and fulvestrant for breast cancer. *Nat Commun* (2018) 9:896. doi: 10.1038/s41467-018-03215-x

38. Turner NC, Swift C, Kilburn L, Fribbens C, Beaney M, Garcia-Murillas I, et al. ESR1 mutations and overall survival on fulvestrant versus exemestane in advanced hormone receptor–positive breast cancer: a combined analysis of the phase III SoFEA and efect trials. *Clin Cancer Res* (2020) 26(19):5172–7. doi: 10.1158/1078-0432.CCR-20-0224

39. Goetz MP, Hamilton EP, Campone M, Hurvitz SA, Cortes J, Johnston SR, et al. Acquired genomic alterations in circulating tumor DNA from patients receiving abemaciclib alone or in combination with endocrine therapy. (2020), 3519–9. doi: 10.1200/JCO.2020.38.15_suppl.3519

40. Hanna D, Hutchins J, Yu J, Marino E, Kumar N, Kucharlapati R, et al. Abstract PS18-15: Real-world clinical-genomic data identifies the ESR1 clonal and subclonal circulating tumor DNA (ctDNA) landscape and provides insight into clinical outcomes. *Cancer Res* (2021) 81(4_Supplement):PS18–15. doi: 10.1158/1538-7445.SABCS20-PS18-15

41. Martin M, Zielinski C, Ruiz-Borrego M, Carrasco E, Turner N, Ciruelos EM, Gil-Gil M. Palbociclib in combination with endocrine therapy versus capecitabine in hormonal receptor-positive, human epidermal growth factor 2-negative, aromatase inhibitor-resistant metastatic breast cancer: A phase III randomised controlled trial—PEARL. *Ann Oncol* (2021) 32(4):488–99. doi: 10.1016/j.annonc.2020.12.013

42. Aparicio S, Caldas C. The implications of clonal genome evolution for cancer medicine. *N Engl J Med* (2013) 368(9):842–51. doi: 10.1056/NEJMra1204892

43. Holdhoff M, Schmidt K, Donehower R, Diaz LA. Analysis of circulating tumor DNA to confirm somatic KRAS mutations. *J Natl Cancer Inst* (2009) 101(18):1284–5. doi: 10.1093/jnci/djp240

44. Diaz LA Jr., Bardelli A. Liquid biopsies: genotyping circulating tumor DNA. *J Clin Oncol* (2014) 32(6):579–86. doi: 10.1200/JCO.2012.45.2011

45. Murtaza M, Dawson SJ, Tsui DW, Gale D, Forshew T, Piskorz AM, Rosenfeld N. Non-invasive analysis of acquired resistance to cancer therapy by sequencing of plasma DNA. *Nature* (2013) 497(7447):108–12. doi: 10.1038/nature12065

46. Heitzer E, Ulz P, Geigl JB. Circulating tumor DNA as a liquid biopsy for cancer. *Clin Chem* (2015) 61(1):112–23. doi: 10.1373/clinchem.2014.222679

47. Diaz LA Jr., Williams RT, Wu J, Kinde I, Hecht JR, Berlin J, Vogelstein B. The molecular evolution of acquired resistance to targeted EGFR blockade in colorectal cancers. *Nature* (2012) 486(7404):537–40. doi: 10.1038/nature11219

48. Misale S, Yaeger R, Hobor S, Scala E, Janakiraman M, Liska D, et al. Emergence of KRAS mutations and acquired resistance to anti-EGFR therapy in colorectal cancer. *Nature* (2012) 486(7404):532–6. doi: 10.1038/nature11156

49. Iwahashi N, Sakai K, Noguchi T, Yahata T, Matsukawa H, Toujima S, Ino K. Liquid biopsy-based comprehensive gene mutation profiling for gynecological cancer using CAncer Personalized Profiling by deep Sequencing. *Sci Rep* (2019) 9(1):10426. doi: 10.1038/s41598-019-47030-w

50. Hudecova I. Digital PCR analysis of circulating nucleic acids. *Clin Biochem* (2015) 48(15):948–56. doi: 10.1016/j.clinbiochem.2015.03.015

51. Pinheiro LB, Coleman VA, Hindson CM, Herrmann J, Hindson BJ, Bhat S, et al. Evaluation of a droplet digital polymerase chain reaction format for DNA copy number quantification. *Anal Chem* (2012) 84(2):1003–11. doi: 10.1021/ac202578x

52. Forshew T, Murtaza M, Parkinson C, Gale D, Tsui DW, Kaper F, et al. Noninvasive identification and monitoring of cancer mutations by targeted deep sequencing of plasma DNA. *Sci Transl Med* (2012) 4(136):136ra68. doi: 10.1126/scitranslmed.3003726

53. Board RE, Wardley AM, Dixon JM, Armstrong AC, Howell S, Renshaw L, et al. Detection of PIK3CA mutations in circulating free DNA in patients with breast cancer. *Breast Cancer Res Treat* (2010) 120(2):461–7. doi: 10.1007/s10549-010-0747-9

54. Beaver JA, Jelovac D, Balukrishna S, Cochran RL, Croessmann S, Zabransky DJ, et al. Detection of cancer DNA in plasma of patients with early-stage breast cancer. *Clin Cancer Res* (2014) 20(10):2643–50. doi: 10.1158/1078-0432.CCR-13-2933

55. Ding PN, Becker T, Bray V, Chua W, Ma Y, Xu B, et al. Plasma next generation sequencing and droplet digital PCR-based detection of epidermal growth factor receptor (EGFR) mutations in patients with advanced lung cancer treated with subsequent-line osimertinib. *Thorac Cancer* (2019) 10(10):1879–84. doi: 10.1111/1759-7714.13154

56. Garcia J, Forestier J, Dusserre E, Wozny AS, Geiguer F, Merle P, et al. Cross-platform comparison for the detection of RAS mutations in cfDNA (ddPCR Biorad detection assay, BEAMing assay, and NGS strategy). *Oncotarget* (2018) 9(30):21122–31. doi: 10.18632/oncotarget.24950

57. Liao H, Huang W, Pei W, Li H. Detection of ESR1 mutations based on liquid biopsy in estrogen receptor-positive metastatic breast cancer: clinical impacts and prospects. *Front Oncol* (2020) 10:5876715. doi: 10.3389/fonc.2020.587671

58. Stergiopoulou D, Markou A, Strati A, Zavridou M, Tzanikou E, Mastoraki S, et al. Comprehensive liquid biopsy analysis as a tool for the early detection of minimal residual disease in breast cancer. *Sci Rep* (2023) 13(1):1258. doi: 10.1038/s41598-022-25400-1

59. Brett JO, Spring LM, Bardia A, Wander SA. ESR1 mutation as an emerging clinical biomarker in metastatic hormone receptor-positive breast cancer. *Breast Cancer Res* (2021) 23:1–155. doi: 10.1186/s13058-021-01462-3

60. Turner N, Huang-Bartlett C, Kalinsky K, Cristofanilli M, Bianchini G, Chia S, et al. Design of SERENA-6, a phase III switching trial of camizestrant in ESR1-mutant breast cancer during first-line treatment. *Future Oncol* (2023) 19(8):559–73. doi: 10.2217/fon-2022-1196

frontiers | Frontiers in Oncology

TYPE Review
PUBLISHED 13 September 2023
DOI 10.3389/fonc.2023.1187477

OPEN ACCESS

EDITED BY
Sharon R. Pine,
University of Colorado Anschutz Medical Campus, United States

REVIEWED BY
Prem Prakash Kushwaha,
Case Western Reserve University, United States
Yu-Feng Wang,
Zhejiang Chinese Medical University, China

*CORRESPONDENCE
Huaidong Cheng
chd1975ay@126.com

†These authors have contributed equally to this work

RECEIVED 16 March 2023
ACCEPTED 29 August 2023
PUBLISHED 13 September 2023

CITATION
Liu S, Huang R, Li A, Yu S, Yao S, Xu J, Tang L, Li W, Gan C and Cheng H (2023) The role of the oxytocin system in the resilience of patients with breast cancer. *Front. Oncol.* 13:1187477. doi: 10.3389/fonc.2023.1187477

The role of the oxytocin system in the resilience of patients with breast cancer

Shaochun Liu[1†], Runze Huang[1†], Anlong Li[1†], Sheng Yu[1], Senbang Yao[1], Jian Xu[1], Lingxue Tang[1], Wen Li[1], Chen Gan[1] and Huaidong Cheng[1,2,3*]

[1]Department of Oncology, The Second Hospital of Anhui Medical University, Hefei, Anhui, China, [2]Shenzhen Clinical Medical School of Southern Medical University, Guangzhou, China, [3]Department of Oncology, Shenzhen Hospital of Southern Medical University, Shenzhen, Guangdong, China

Breast cancer is a grave traumatic experience that can profoundly compromise patients' psychological resilience, impacting their overall quality of life. The oxytocin system represents one of the essential neurobiological bases of psychological resilience and plays a critical role in regulating resilience in response to social or traumatic events during adulthood. Oxytocin, through its direct interaction with peripheral or central oxytocin receptors, has been found to have a significant impact on regulating social behavior. However, the precise mechanism by which the activation of peripheral oxytocin receptors leads to improved social is still not completely comprehended and requires additional research. Its activation can modulate psychological resilience by influencing estrogen and its receptors, the hypothalamic-pituitary-adrenal axis, thyroid function, 5-hydroxytryptamine metabolism levels, and arginine pressure release in breast cancer patients. Various interventions, including psychotherapy and behavioral measures, have been employed to improve the psychological resilience of breast cancer patients. The potential effectiveness of such interventions may be underpinned by their ability to modulate oxytocin release levels. This review provides an overview of the oxytocin system and resilience in breast cancer patients and identifies possible future research directions and interventions.

KEYWORDS

breast cancer, resilience, oxytocin system, behavioral interventions, psychotherapy

1 Introduction

1.1 Development of the concept of resilience

In 1974, Anthony introduced the concept of psychological resilience based on child psychological development, which arises from successful adaptation to adversity (1). Masten et al. argue that this concept persists throughout life and is a dynamic psychological process that constantly adjusts to the internal and external environment

(2); similarly, Bonanno et al. suggest that resilience represents a stable trajectory for individuals to maintain healthy functioning after experiencing highly adverse events (3). In 2014, Southwick et al. summarized that resilience should be defined according to the individual's stage and environment and the types of traumatic events encountered (4). Continued advancements in life sciences and biomedical engineering have provided researchers with additional means to investigate the biological processes that shape and develop this concept (5). It has been demonstrated that psychological resilience is closely linked to rehabilitating malignant tumors and chronic diseases and that good psychological resilience can prevent disease onset and effectively maintain a sense of well-being in life (6). Thus, these findings have shown that good psychological resilience protects against diseases and supports overall well-being.

1.2 Involvement of the oxytocin system in shaping resilience

In 2020, Feldman and colleagues proposed a neurobiological model of resilience based on the oxytocin system, the affiliative brain, and biobehavioral synchrony from an evolutionary and sociological perspective (7). This model identifies plasticity, sociality, and meaning as the three key features of resilience, which provide theoretical possibilities for improving resilience. The oxytocin system, one of the three bases of resilience, is interconnected with the affiliative brain and biobehavioral synchrony and is involved in shaping psychological resilience. Oxytocin, as the endogenous core substance of this system, is a multi-potent peptide hormone with unique chemical properties that can act as an anti-inflammatory and antioxidant molecule in response to stress caused by adversity and trauma (8, 9). Oxytocin receptors belong to the group of seven transmembrane G-protein-coupled receptors, consisting of 389 amino acid residues and belonging to the class I G protein-coupled receptor family (10); the distribution of oxytocin receptors in the brain may be the histological basis for the involvement of the oxytocin system in shaping psychological resilience. These properties may help explain the benefits of positive social experiences and have drawn attention to this system as a possible treatment for various disorders. Of particular interest, the oxytocin system regulates resilience throughout a woman's life, from brain maturation in the mother's womb through pregnancy, childbirth, breastfeeding, and various social behaviors and connections (11).

1.3 Distribution and expression of central and peripheral oxytocin receptors

Oxytocin is primarily synthesized in the paraventricular nucleus (PVN) and supraoptic nucleus (SON) of the hypothalamus, specifically in large and small cell neurons (12). Magnocellular oxytocin neurons release oxytocin into the peripheral blood through the posterior pituitary gland. These neurons also have significant central projections that innervate nerves in the forebrain, contributing to regulating various behaviors. On the other hand, parvocellular neurons, which are smaller in size, mainly project to the posterior brain and spinal cord. They are thought to regulate functions like cardiovascular function, breathing, feeding behavior, and nociception (13).

Furthermore, studies have indicated that Magnocellular oxytocin neurons may incidentally project to more than 50 different brain regions, including the caudate Putnam (14). This extensive investigation suggests that these neurons play a crucial role in central activities mediated by oxytocin, such as fear attenuation, social interaction, and movement. In summary, the oxytocin system is a complex network of peripheral and central activity regulated by diverse neuronal populations and pathways, serving a wide range of physiological and behavioral functions.

In animal experiments, oxytocin injection into different brain regions produced other physiological or social behavioral effects. In primate experiments, blood pressure decreased with intracerebroventricular oxytocin administration (15). Social interactions can promote oxytocin production, and oxytocin can promote bonding or attachment between individuals (e.g., mother-infant and sexual partners) (16). Oxytocin may also have other effects (17). For example, naloxone antagonizes the persistent effects of oxytocin in the tail-flick test, suggesting that oxytocin may increase the activity of endogenous opioids (18). Oxytocin receptor gene-negative mice have a lower proportion of hippocampal neurons expressing GABAergic synapses, an imbalance in glutamate-GABA transmission, and an upregulated number of V1a receptors in the hippocampus, showing abnormal social skills, impaired cognitive flexibility (associated with hippocampal function) and reduced distress at separation from the mother. Oxytocin restores symptoms such as cognitive flexibility and seizure susceptibility in mice (19). Injecting oxytocin into the hippocampus or intraperitoneally in rats stimulates cell proliferation in the dentate gyrus of the hippocampus. The oxytocin-induced increase in newborn neurons in the DG may help reduce anxiety and enhance learning ability (20).

The distribution of oxytocin receptors in the brain also affects psychological resilience. It has been shown that the expression of distributed oxytocin receptors in the ACC (anterior cingulate area) regulates anxious behavior. Microinjection of oxytocin in mice's ACC significantly increased the threshold of mechanical foot contraction response and reduced chronic pain-induced anxiety in neurologically injured mice by selectively blocking the maintenance of presynaptic long-duration enhancement (21). In clinical studies, transnasal administration of oxytocin to healthy female youths activated the ACC and attenuated the neurological effects of subthreshold threat stimuli, acting as an anxiolytic (22). In addition, transnasal administration of oxytocin has been used in randomized controlled trials in various neuropsychiatric disorders, such as Autism Spectrum Disorder, Generalized/Social Anxiety Disorder, and Posttraumatic Stress Disorder; some of these studies are listed in Table 1. In most studies, transnasal administration of oxytocin produced beneficial effects for the patients. However, some studies did not find significant efficacy with intranasal oxytocin administration. For example, the benefit of

TABLE 1 Use of intranasal oxytocin in selected neuropsychiatric disorders.

Types of disease	Source of drugs	Dose of the drug administered	Time of administration	Sample Size	Subjects	Effect	Reference
ASD	Tergus Pharma	4-8IU/day	Once daily for 24 weeks	355	3 to 17 patients with ASD children and adolescents	Social or cognitive functioning—	(23)
	Novartis, Switzerland	48IU per dose	Once a day for 6 weeks	106	People aged 18-48 years with autistic disorder, Asperger's disorder or pervasive developmental disorder	Autism Diagnostic Observation Schedule (ADOS) reciprocity↓	(24)
	F.Hoffmann-La Roche Ltd, Basel, Switzerland	10-mg balovaptan adult-equivalent dose per dose	Once daily for 24 weeks	599	Between the ages of 5 and 17 years, patients diagnosed with ASD	The efficacy of social interaction and communication in the population —	(25)
	–	18 or 24 IU per dose	The treatment was given once daily for 8 weeks	16	Young men aged 12 to 19 years diagnosed with autism or Asperger's syndrome	Emotion recognition ability ↑	(26)
	Farma Holding, Oslo, Norway	8 or 24 IU per dose	Treatment 3 times, each time intervals of 1 ~ 72 hours	17	Adult men with ASD	emotion salience↑	(27)
GSAD	··	24 IU per dose	Two treatments, The interval between each treatment was 1 week	36	Male patients with GSAD aged 19 to 55 years	The severity of social anxiety ↓ Integration and regulation of social responses ↑ Amygdala response to fear ↓	(28–30)
PTSD	Defiante Farmaceutica, S.A., Funchal Portugal	40 IU per dose	1 treatment	40	Police officers diagnosed with PTSD	sensitivity for social support and therapeutic alliance↑↑	(31)
	Defiante Farmaceutica, Funchal, Portugal	40 IU per dose	Twice a day for 8 days	1107	Adults with more than moderate acute distress	The severity of acute PTSD symptoms ↓	(32)
	Novartis, Brazil	24 IU per dose	It was received twice in a week	35	Adult female patients with PTSD	the intensity of provoked PTSD symptoms↓↓	(33)
SZ	Novartis, Basel Switzerland	40 IU per dose	Once daily for 1 week and twice daily after that	20	Patients with SCID-confirmed DSM-IV diagnosis of schizophrenia	verbal memory↑↑ scores on the Positive and Negative Symptom Scale↓	(34, 35)
	Novartis	24IU per dose	The treatment was given twice daily for 14 days	23	Patients 18 to 55 years of age with a DSM-IV diagnosis of paranoid or undifferentiated schizophrenia	Social Cognitive deficits ↓	(36)
	Seoul National University Hospital	40IU per dose	The drugs were administered twice at an interval of one week	32	Male patients with schizophrenia	activity for happy faces↑	(37)
FTD	Novartis	24IU per dose	The drug was administered once	20	Patients who met the consensus criteria for FTD	Patients who met the consensus criteria for FTD ↑	(38)
	Novartis, Bern, Switzerland	24IU per session	Three doses were administered every 10 minutes	51	Patients who met the consensus criteria for FTD	Activity in limbic regions associated with the processing of emotional expressions ↑	(39)

ASD, Autism Spectrum Disorder; GSAD, Generalized/Social Anxiety Disorder; PTSD, Post-traumatic Stress Disorder; SZ, Schizophrenia; FTD, Frontotemporal Dementia; DSM, The Diagnostic and Statistical Manual of Mental Disorders.
Based on a review of the literature, the effects are listed as follows in clinical randomized controlled trials of different designs: ↑= improved; ↓ = reduced; —= no significant change.

oxytocin for social functioning in patients with autism spectrum disorders was not superior to the placebo (25). Thus, in breast cancer patients, changes in plasma oxytocin levels and peripheral oxytocin receptor distribution may influence psychological resilience and the ability to mentally cope with a crisis or quickly return to pre-crisis status. However, it's important to note that the central effects of oxytocin, although potentially significant, are less understood due to limited studies on primary oxytocin levels and receptor distribution. This area could be a valuable avenue for future investigation, even though intranasal oxytocin does not always function as expected.

1.4 Low level of resilience in breast cancer patients

Breast cancer is the most commonly diagnosed cancer among women, accounting for 11.7% of all cases, and one in six women with cancer dies from breast cancer (40). Breast cancer presents a clinical challenge with up to ten different molecular subtypes, including ductal A, ductal B, her2-enriched, and basal-like. Insulin-regulated aminopeptidase (IRAP), the only enzyme that cleaves oxytocin, is correlated with circulating levels of oxytocin and may affect mammary breast tumor tissue metabolism by modulating GLUT4 and angiotensin II (ATII) levels (41–43). In the context of breast cancer treatment, the American Society of Clinical Oncology (ASCO) guidelines emphasize using neoadjuvant systemic therapy, including chemotherapy, endocrine therapy, and targeted therapy, to improve outcomes in patients with invasive breast cancer (44). Diagnosis, symptoms, treatment, surgery, and the impact of breast cancer on patients' lives can all induce significant stress, leading to higher rates of anxiety and depression in breast cancer patients compared to non-cancerous women (45). These factors contribute to the lower level of resilience commonly observed in breast cancer patients.

1.5 Relationship between changes in the oxytocin system and resilience regulation in breast cancer patients

In breast cancer patients, alterations in the oxytocin system are associated with the regulation of resilience. The development of breast cancer significantly impacts the oxytocin system, and studies have shown that the level of resilience in these patients may be related to the severity of anxiety or depressive symptoms (46). Interestingly, not all women with breast cancer experience severe psychological distress and those with higher levels of resilience exhibit lower probabilities or degrees of such symptoms (47). Resilience in breast cancer patients is both a state and a trait, as demonstrated by a study investigating resilience's role in these patients (48). In the context of the COVID-19 pandemic, it was found that breast cancer patients with higher levels of resilience had fewer concerns about tumor progression due to COVID-19 infection (49). Resilience, therefore, plays a crucial role in the quality of life of breast cancer patients and their ability to cope with diagnosis, treatment, and recovery.

Notably, the level of psychological resilience in breast cancer patients is influenced by various factors such as disease stage, treatment duration, social support, and level of education. Patients with early clinical stages, short treatment courses, high social support, and education tend to have higher resilience (50–52). Conversely, more treatment courses and faster disease progression are associated with lower resilience (53). Improving the resilience of breast cancer patients is crucial for enhancing their quality of life, independent of their survival. To enhance resilience, non-pharmacological interventions based on behavioral and sociological theories have been explored, including spirituality, supportive-expressive group therapy, art and movement therapies, nursing interventions, and educational components (54–56). Interestingly, a study of depressed patients using psychodynamics demonstrated that the more significant the change in oxytocin response during treatment, the more influential the improvement in depressive symptoms (57), similar to another study suggesting that resilience may be a preventive factor for depression (58). Therefore, it is plausible to hypothesize that changes in the oxytocin system are one of the pathways through which resilience is modulated in breast cancer patients.

1.6 Methodology and purpose

This article aims to analyze the interaction of the oxytocin system with social, genetic, physiological, and pathological factors in breast cancer resilience and propose a theoretical regulatory model. We conducted a systematic literature search from January 1990 to May 2023 using specific MESH terms and key terms. The data source was PubMed. The search terms were ((“oxytocin”[MeSH Terms] OR “oxytocin”[All Fields]) OR (“breast neoplasms”[MeSH Terms] OR (“breast”[All Fields] AND) “neoplasms”[All Fields]) OR “breast neoplasms”[All Fields] OR (“breast”[All Fields] AND “cancer”[All Fields]) OR “breast cancer”[All Fields])) AND (“resilience, psychological”[MeSH Terms] OR (“resilience”[All Fields] AND “psychological”[All Fields]) OR “psychological resilience”[All Fields] OR “resilience”[All Fields]). We focused on original research articles and reviews in English and excluded non-English studies.

2 The oxytocin system and the mammary gland

2.1 The impact of oxytocin on mammary tissue during pregnancy and lactation

The oxytocin system has been demonstrated to affect women's mammary tissue during pregnancy or lactation (41, 59, 60). Medications administered during pregnancy or delivery may impact oxytocin secretion, leading to impaired milk production or delayed lactation initiation (61). However, there is a paucity of

research on the non-lactating period (46). Several studies have reported that stimuli such as mechanical pumps and tactile sensations can promote elevated plasma oxytocin levels (62). The activated noradrenergic, histaminergic, and glutamatergic receptor systems may stimulate central oxytocin release during lactation. For example, norepinephrine has been shown to stimulate central oxytocin receptors during gestation (63). Breastfeeding mothers have been observed to exhibit higher plasma and salivary oxytocin levels (64).

2.2 Oxytocin's protective role against breast cancer development

The predominant viewpoint suggests that oxytocin functions as a preventive factor for breast cancer by acting on myoepithelial cells, which relieves the expansion of secretory vesicles and facilitates the elimination of carcinogenic substances, ultimately decreasing the risk of breast tumor development (65, 66). Downregulation of oxytocin-related genes FOS, ITPR1, RCAN1, CAMK2D, and CACNA2D was observed in breast cancer samples, implying a correlation between the expression of this endogenous molecule and breast tumor malignancy (67). Additionally, oxytocin inhibited estrogen-induced cell growth and enhanced tamoxifen's inhibitory effect on cell proliferation (10). Intranasal administration of oxytocin has been proposed as a breast cancer prevention strategy, where nipple fluid samples collected for testing by intranasal Oxytocin injection can be utilized as a screening tool for individuals at high risk of breast cancer (68).

2.3 Oxytocin receptors in breast cancer: implications for estrogen receptors and metastasis

While oxytocin receptors are expressed in various human breast cancer cell lines, their significance in developing and diagnosing breast cancer remains unclear. Some researchers have proposed that the distribution of oxytocin receptors in breast tumor tissue correlates with the expression of estrogen receptors (ER) (46, 69, 70). In a study on triple-negative breast cancer tissues, researchers found that MDA-MB-231 cells overexpressing oxytocin receptors were more sensitive to Epidermal Growth Factor (EGF) and demonstrated enhanced migration. The study suggested that high oxytocin receptor levels are associated with increased EGF sensitivity and that oxytocin receptors promote EGF-stimulated RSK activation via the mTOR pathway, leading to downstream rpS6 activation and enhanced migration of breast cancer cells. The researchers also found that rapamycin, a selective inhibitor of mTOR, reduced the migration of oxytocin receptor overexpressing cells (71). However, this study was only conducted on cellular models; additional clinical or animal studies have yet to support this finding. Contrastingly, one study found higher oxytocin receptor levels in healthy breast tissue compared to cancerous tissue. This suggests that reduced oxytocin receptor expression in breast tissue may promote carcinogenesis (72). This study did not investigate triple-negative breast cancer tissue, so it could not refute the earlier study's findings. Although oxytocin receptor signaling may stimulate some aspects of breast cancer progression *in vitro*, oxytocin's net impact *in vivo* seems to inhibit cancer, hinting at complex context-dependent effects. Further research must elucidate how oxytocin signaling differentially affects healthy versus malignant breast tissue through changes in oxytocin receptor levels, downstream pathways, and interacting factors.

3 The oxytocin system and resilience

3.1 The role of oxytocin system in maternal depression and neonatal resilience formation

Maternal depression can negatively affect children's mental health, increasing the risk of developing mental illness later in life (73, 74). The oxytocin system may be involved in the transmission of depression from mother to child and the establishment of neonatal resilience. During the early sensitive period of maternal care, the infant's oxytocin system is formed and highly influenced by epigenetics. The intergenerational transmission of the oxytocin system suggests that maternal oxytocin levels may influence maternal care and shape the infant's oxytocin system (74, 75). Social synchronization, the mutual adaptation between parent and child, is one of the bases of resilience formation. A long-term follow-up study found that when a mother experiences depression, high salivary oxytocin levels in the child suggest higher synchronization and a lower likelihood of developing mood or psychiatric disorders, indicating resilience (74).

3.2 Oxytocin receptors as predictors of psychological resilience: implications for breast cancer patients

Oxytocin receptors have been linked to differences in personal psychological resources such as self-esteem, optimism, and mastery, considered protective factors for developing resilient functioning. Furthermore, attachment and relationship quality, critical components of resilient functioning, have also been shown to be associated with oxytocin receptors. For instance, non-maltreated children with AA or AG genotypes of the oxytocin receptor have been found to exhibit higher levels of psychological resilience compared to maltreated children with identical genotypes (76). The impact of the oxytocin system on cognitive and social functioning has been widely discussed, although discrepancies in findings across studies have been observed. This may be related to variations in oxytocin receptor genotypes. The effect of oxytocin receptor variants on social functioning in individuals is mainly derived from two single nucleotide polymorphisms located in the third intron, rs53576 and rs2254298 (77). The association between childhood family environment and psychological resilience varies depending on the oxytocin receptor rs53576 genotype, with a

stronger correlation observed in individuals with the AG genotype (78). In a healthy Korean population, psychological resilience scores were strongly correlated with the oxytocin receptor SNP rs53576 genotype, with GG carriers exhibiting the highest level of resilience and each additional copy of the A allele resulting in a 3.84 decrease in CD-RISC score (79).

Conversely, veterans with insecure attachment and the A allele of the oxytocin receptor SNP rs53576 were found to be at a higher risk of PTSD (76). The diverse roles of psychological resilience in different domains have been proposed, with some studies suggesting that oxytocin receptor DNA methylation in children can predict (80). Hence, the oxytocin receptor genotype holds promise as a predictor of resilience in breast cancer patients.

3.3 Insights from prairie vole model: unraveling the oxytocin system's influence on psychological resilience and social behavior

The prairie vole model with standard monogamy is highly informative in revealing individual differences in the effects and mechanisms of the oxytocin system on psychological resilience (81). Notably, studies have demonstrated the crucial role of the oxytocin system in regulating the social behavior of steppe voles. Prairie voles deficient in the oxytocin receptor gene exhibit reduced empathic responses and helpful behavior compared to controls (82). Numerous studies have investigated the pathways by which the oxytocin system is involved in the social behavior of steppe voles. For instance, in neonatally isolated female prairie voles, the distribution of oxytocin receptors in the nucleus ambiguous (NAcc) is significantly correlated with partner preference (PP) behavior, and those females with high oxytocin receptor densities in the NAcc demonstrate resilience to the effects of neonatal social isolation on later PP behavior. Oxytocin activity in the NAcc may mediate the response to adverse life events, vulnerability, or toughness (83). In contrast, early social deprivation in prairie voles impairs the formation of social connections and increases anxiety in adulthood, while touch stimulation restores some of these functions (increasing EGR-1 gene immunoreactivity in hypothalamic oxytocin neurons and inducing oxytocin signaling).

Furthermore, using the MC3/4R (Melanocortin 3/4 Receptors) agonist MTII has been found to activate oxytocin neurons and enhance stimulus-induced oxytocin release in the brains of adult prairie voles, which could potentially mitigate the negative impact of isolation on adult relationships. In particular, MTII has been shown to stimulate EGR-1 immunoreactivity in oxytocin neurons and increase hypertonic saline-induced oxytocin release to the NAcc (65). In contrast, the administration of oxytocin A, an oxytocin receptor antagonist, to male voles has been found to increase the binding of Arginine vasopressin (AVP) pressor to V1aR in the ventral pallidum, a region where dopamine also binds. This finding suggests that oxytocin may affect dopamine metabolic processes, potentially explaining its association with negative coping behaviors (84).

4 Pathways involved in the regulation of resilience in breast cancer patients by the oxytocin system

Oxytocin is a neuropeptide that plays a crucial role in regulating mood, behavior, and cardiovascular function by increasing serotonin activity in the brain (85). It also interacts with other body systems, such as the *AVP* system, which is responsible for cardiovascular regulation, and the thyroid system, which is required for metabolism and mood (86, 87). Due to changes in estrogen levels, breast cancer patients may experience decreased oxytocin activity, leading to thyroid dysfunction, decreased psychological tolerance, and symptoms such as cognitive changes, fatigue, and appetite disturbances (88). Breast cancer cells may also aberrantly express *AVP*, affecting cardiovascular function and emotional behavior (89). Because these systems are interdependent, changes in one system can significantly impact the others. Understanding these interactions is critical for effective treatment and improving the quality of life of breast cancer patients.

4.1 Regulation of resilience in breast cancer patients by influencing psychological and physiological phenomena

Oxytocin facilitates social behavior and adaptive responses to threats by activating the vagus nerve and reducing fear and immobility, while abnormal oxytocin levels in trauma can lead to dissociation and impaired health. Oxytocin regulates social and emotional responses through effects on the vagus nerve, enabling adaptive coping in stress, while dysfunction may contribute to trauma-related psychological conditions (8). Oxytocin regulates social behavior and emotional functioning by acting on brain regions and neurotransmitter systems to reduce stress and fear, though abnormalities in oxytocin are linked to mental health conditions. By modulating the amygdala, prefrontal cortex, and neurotransmitter systems, oxytocin facilitates social behaviors and emotions by reducing stress and anxiety but dysfunction may contribute to psychiatric disorders (17).

4.1.1 Oxytocin and fear

The oxytocin system may play a role in buffering the fear of cancer recurrence (FCR) that often plagues breast cancer patients, potentially enhancing psychological resilience. FCR, defined as "fear, worry, or concern about the recurrence or progression of cancer," affects over 20% of cancer survivors, with women being more susceptible to it than men (90). Some studies have found that breast cancer patients with higher levels of psychological resilience are less likely to experience FCR (91). Oxytocin acts on various brain regions to regulate the fear response. The mesogenic oxytocin system in the hypothalamus is activated during fear learning.

In contrast, oxytocin in the central nucleus of the amygdala reduces contextual fear responses, and oxytocin receptor activation

in the nucleus accumbens promotes suggestive fear (92). In an animal experiment, mice lacking oxytocin receptors in the forebrain after weaning exhibited reduced freezing behavior and abnormal fear learning (93). Injecting synthetic or selective oxytocin receptor agonists in the basolateral area suppresses the expression of contextually conditioned fear in rats (94).

4.1.2 Oxytocin and exercise

Exercise can play a significant role in promoting resilience in breast cancer patients by enhancing the oxytocin system. Exercise has been shown to improve cellular bioenergetics, regulate cellular metabolism, and reduce the inflammatory response, thereby supporting and protecting the central nervous system (95). An active lifestyle can enhance an individual's resistance to stress, thus promoting resilience. Studies in mouse models have shown that exercise can contribute to symptom relief in various neurological disorders such as Huntington's chorea, Parkinson's disease, and Alzheimer's disease and can also reduce the risk of recurrence of colon and breast cancer (96).

A retrospective study has shown that moderate physical activity can enhance resilience in postoperative breast cancer patients, although the underlying biological mechanism remains unclear (97). In a study involving mice with breast cancer, exercise training increased oxytocin secretion and decreased the activity of the PI3K/AKT axes (Phosphatidylinositol 3-Kinase/Protein Kinase B axes) and ERK axes(Extracellular Signal-Regulated Kinase axes), inhibiting tumor cell proliferation (98). Hence, exercise may promote resilience in breast cancer patients by stimulating oxytocin secretion and altering tumor cell metabolism to reduce growth and metastasis.

4.1.3 Oxytocin and tissue regeneration

Oxytocin has been found to have the potential to promote wound healing by reducing leukocyte infiltration in granulation tissue, decreasing inflammatory cytokine release, and promoting vascular remodeling and maturation. Such an effect may suggest an improvement in resilience. Moderate inflammatory responses are necessary for resilience in the face of stress or injury, whereas an excessive inflammatory response is detrimental to resilience (99). Hence, the oxytocin system may regulate extreme inflammatory responses by promoting wound healing, clearing damaged cells or tissues of the organism, and enhancing the ability to adapt to traumatic events, promoting resilience. However, an animal experiment using male SKH-1-h pure-hybrid hairless mice did not observe an increase in the rate of wound healing in mice injected with oxytocin compared to the control group (100). Therefore, further investigations are necessary to verify whether oxytocin can promote tissue regeneration.

4.1.4 Oxytocin and pain adaptation

In breast cancer patients, persistent pain is a common treatment-related side effect, affecting more than 10% of patients (101). However, the oxytocin system may play a role in promoting pain adaptation and psychological resilience. Studies have shown that breast cancer patients with high resilience levels have lower pain interference levels (102). In particular, patients with higher psychological well-being and resilience may exhibit more excellent pain adaptation. Oxytocin may contribute to this effect, as evidenced by its analgesic properties in neonates following delivery. Animal experiments suggest that this may be due to oxytocin's ability to reduce the GABA-evoked calcium response and depolarize GABA drive in trigeminal neurons, thus increasing the pain threshold of neonates (103).

4.2 Regulation of resilience in breast cancer patients by modulating neuroendocrine function

Oxytocin is a neuropeptide that bidirectionally communicates between the neuroendocrine and immune systems to regulate acute inflammatory responses and chronic immune surveillance, though aberrant oxytocin signaling suppresses and enhances cancer progression depending on the specific tumor context. Targeting the oxytocin-mediated interface between the nervous and immune systems may provide opportunities to therapeutically modulate inflammation and immunity in various diseases (9). Multidirectional oxytocin signaling provides delicate neuroendocrine control over immune homeostasis, though dysregulation can contribute to immunopathology, highlighting the oxytocinergic system as a potential therapeutic target (104).

4.2.1 The oxytocin system and the hypothalamic-pituitary-adrenal axis

In response to environmental threats, the HPA axis is activated and primarily mediates the central stress response system (105). Breast cancer diagnosis, a disease with a high mortality rate, is a severe traumatic event that can be very stressful for women. This intense stress can modulate changes in multiple pro-inflammatory cytokines, including interleukin-6 (IL-6) and tumor necrosis factor-α (TNF-α), leading to the appearance of depressive symptoms, such as sadness, lethargy, and lack of pleasure, and even to depression (106, 107). C-reactive protein is a biomarker of inflammation that lacks specificity. According to a small clinical study, high concentrations of C-reactive protein in plasma were associated with decreased levels of resilience in breast cancer patients. In contrast, patients with high levels of resilience tended to have higher progesterone levels, suggesting that high inflammatory levels are linked to low resilience (108). Another review suggests that activating pro-inflammatory transcriptional control pathways increases susceptibility to depression (109). The review proposes that the HPA axis modulates inflammation by upregulating or suppressing it in response to stress. When the HPA axis is activated by cancer as a stressor, it increases glucocorticoid release, which blocks the inflammatory cascade initiated by pro-inflammatory transcription factors and pathways such as the NF-kB pathway, thus suppressing the inflammatory response. This mechanism allows for a level of inflammatory activity that does not surpass the individual's tolerance level. However, continuous activation of the HPA axis may lead to the emergence of glucocorticoid tolerance,

where immune cells become insensitive to glucocorticoids (110). This could be why cancer patients experience anxiety and depressive symptoms despite elevated glucocorticoid levels. In contrast, resilience may mitigate the effects of stress on inflammation-related depressive symptoms by improving sleep quality and enhancing physical activity (111).

In rats treated with glucocorticoids or exposed to stress, oxytocin has been shown to have a stimulatory effect on cell proliferation, which suggests that oxytocin may protect hippocampal sites from the adverse effects of elevated glucocorticoids (20). The oxytocin system and the HPA axis have been found to regulate each other mutually, and some researchers suggest that dysregulation of oxytocin and cortisol release levels could predict susceptibility to PTSD. When a stressor is encountered, the activity of the HPA axis is activated, and cortisol is produced in response. However, central oxytocin can inhibit the secretion of adrenocorticotropic hormone (ACTH), thus reducing the production and release of cortisol, which is involved in the neuroendocrine stress response (112). Following a traumatic event, individuals can fine-tune HPA axis activity by modulating multiple brain pathways, including the prefrontal cortex, amygdala, and PVN, thereby altering the level of glucocorticoid release from the adrenal cortex. Glucocorticoids regulate an individual's physiological and psychological state in response to a traumatic or stressful event through various physiological pathways that affect neurological activity, immunity, and metabolism. When individuals show resilience by actively coping with stress or difficulties, glucocorticoid levels are better regulated (113).

In an animal experiment, the researchers observed that unpredictable maternal separation (UMS) of rats led to reduced time spent in the central area of an open field compared to the standard feeding group, indicating increased anxiety levels in these rats. In contrast, rats subjected to predictable maternal separation (PMS) showed lower anxiety levels than the standard feeding group. Oxytocin and OXTR mRNA levels were significantly higher in the medial prefrontal cortex (mPFC) of rats in the PMS group (114). These findings are consistent with another study, where mPFC produced anxiolytic effects by engaging the corticotropin-releasing hormone binding protein (CRHBP), enhancing the activity of male postsynaptic layer 2/3 pyramidal cells through antagonism of CRH (corticotropin-releasing hormone). In this pathway, mPFC regulates oxytocin response to CR (115), suggesting that blocking the oxytocin pathway from the paraventricular nucleus of the hypothalamus (PVN) to the mPFC could increase the risk of anxiety in rats.

However, an animal experiment revealed contradictory results when researchers administered oxytocin receptor antagonists into the third ventricle of adult Wistar rats. These rats exhibited significantly higher plasma ACTH concentrations than controls 2 days after the end of stress, which recovered to control levels by day 20. This suggests that endogenous brain oxytocin prolongs the duration of the response to stress in rats (116). It is noteworthy that oxytocin has also been shown to increase anxiety. Research has identified crfr2α as an essential regulator of anxiety. In a separate animal experiment, long-term oxytocin administration resulted in selective splicing of hypothalamic adrenocorticotropic hormone-releasing factor receptor 2α (Crfr2α) in rats, leading to anxiety-like behavior in rats (117). Therefore, further research is necessary to explore the relationship between oxytocin and the HPA axis more deeply.

4.2.2 The oxytocin system and estrogen

The oxytocin system may promote resilience by increasing estrogen receptor (ER) expression in the brain to counteract anxiety behavior or decreasing ER expression in breast cancer tissue to reduce tumor load and improve symptoms in breast cancer patients. Increased endogenous estrogen levels and exposure to exogenous estrogens through hormone replacement therapy and oral contraceptives are critical high-risk factors for breast cancer. Estrogen metabolites and estrogen receptors play a role in all stages of the estrogen-promoting carcinogenic process (118). Hypothalamic oxytocin expression is demonstrated to be estrogen-dependent (119). There are also various associations between estrogen and its receptors and the oxytocin system. For instance, administering oxytocin to newborn female prairie voles increases ER mRNA expression in the hypothalamus and hippocampus (84). However, after intraperitoneal oxytocin administration to mammary carcinoma mice (MC4-L2), the mRNA expression of miR-195 and its associated signaling pathways, such as dephosphorylated Akt and ERK, the oxytocin receptor, and Bax genes, was significantly increased.

Atosiban reversed decreased mRNA expression of ERα, PI3K, NF-κB, cyclin D1, and Bcl-2 genes. Although commonly considered an oxytocin antagonist, some evidence indicates that atosiban may act as a biased agonist (120). The oxytocin receptor is a G protein-coupled receptor that interacts with Gq and Gi proteins. Typically oxytocin binds the receptor and activates Gq proteins, but atosiban may preferentially activate Gi proteins instead. By shifting signaling to Gi pathways, atosiban could inhibit adenylate cyclase and block oxytocin's activation of Gq cascades, antagonizing oxytocin's effects (121). Another study showed that oxytocin could downregulate ERα mRNA levels and reduce ERα protein expression in MCF-7 cells (122). These studies suggest a direct anti-estrogen-dependent mitogenic effect of oxytocin.

The oxytocin system regulates breast cancer patient's physiological and pathological processes through NF-κB. Studies have shown that oxytocin can reduce tumor volume in a mouse model of breast cancer by downregulating NF-κB and upregulating miR-195 expression (120). Additionally, NF-κB activity is downregulated by increased expression of oxytocin receptors, leading to a decrease in the inflammatory response (123). Inflammatory and autoimmune pathologies are often associated with aberrant NF-κB activity, which the ER mediates the inhibition of at various levels. The interaction between these regulators may be harnessed to treat cancer (124, 125). Furthermore, nuclear NF-κB transcriptional machinery is disrupted in breast tumors resistant to SERM after estrogen treatment, potentially indicating that inhibition of NF-κB may be one of the pathways by which estrogen promotes apoptosis in breast tumor cells (126).

Endocrine therapy targeting ER+ is a necessary treatment for breast cancer, with evidence suggesting that estradiol acting in the brain distributing ER can modulate anxiety and depressive behavior

(69). For instance, the administration of ER antagonists into the hippocampus of female rats resulted in increased anxiety behaviors (127). The distribution of oxytocin receptors is also linked to the ER. Specifically, compared to tissues with low oxytocin receptor expression, more ER-positive tissues have a diffuse distribution of oxytocin receptors (128). Estradiol has been shown to upregulate oxytocin receptor expression in breast malignancy tissues (MCF-7), while progesterone has the opposite effect (129). Moreover, oxytocin receptor gene expression was increased up to 8.6-fold in the corresponding tissues of ER-positive patients compared to those of ER-negative patients (72). The complex interactions between the oxytocin system and estrogen signaling pathways highlight oxytocin's multifaceted roles in both breast cancer progression and patient resilience, underscoring the need for additional research to unravel the nuances of oxytocin signaling in cancer.

4.2.3 The oxytocin system and 5-hydroxytryptamine

In addition to its anxiolytic effects, oxytocin has been shown to play a crucial role in social behavior, stress reduction, and interaction with the 5-Hydroxytryptamine (5-HT) system. The relationship between oxytocin and the 5-HT system has been studied extensively, with findings suggesting that oxytocin promotes resilience in breast cancer patients by increasing 5-HT activity (130). A recent study used Venus cDNA to investigate the role of oxytocin in the 5-HT system. The researchers observed that around 50% of tryptophan hydroxylase immunoreactive neurons in the nucleus accumbens were positive for Venus after placing the cDNA variant of yellow fluorescent protein into the regulatory region of the mouse encoding the OXT-R gene. In addition, the injection of oxytocin in the septum of mice increased the release of 5-HT in this region. However, this effect was blocked by 5-HT2A/2C receptor antagonists (131). These results highlight the intricate relationship between oxytocin and the 5-HT system and provide new insights into how oxytocin may promote resilience and reduce anxiety and depression in breast cancer patients.

4.2.4 Oxytocin and AVP

The intricate relationship between AVP and oxytocin and their roles in breast cancer patients are emerging areas of increasing research interest. AVP is produced constitutively by the hypothalamus and primarily acts on renal collecting duct cells, while oxytocin, structurally similar to AVP, is involved in cardiovascular regulation (132). Studies have shown that low social support, reduced touch with loved ones, or behavioral stress can negatively impact vascular endothelial function, increase the rate of coronary atherosclerosis formation, and decrease oxytocin release (133). The balance between oxytocin and AVP release is also associated with altered mood behavior in individuals (134). Both oxytocin and AVP can act on oxytocin receptors in the lateral ventricles of mice to enhance social recognition (135).

Interestingly, various breast cancer cell lines, including MCF-7 and Skbr3, aberrantly express AVP and its receptor, which may produce anti-apoptotic effects (89). Therefore, the abnormal release of AVP from these breast cancer cells may, in conjunction with oxytocin, participate in the regulation of the cardiovascular system while also affecting the emotional behavior of individuals and playing a role in the regulation of resilience. Further research is needed to fully understand the relationship between oxytocin and AVP in breast cancer patients and their potential implications for treatment.

4.2.5 The oxytocin system and thyroid function

Decreased oxytocin levels in the hypothalamic circulation may contribute to thyroid dysfunction and decreased psychological resilience in breast cancer patients. Some researchers suggest that alterations in estrogen levels, often in breast cancer patients, may lead to decreased IRAP activity and reduced oxytocin metabolism in the hypothalamus. As a result, circulating oxytocin levels increase, leading to decreased release of thyroid-stimulating hormone (TSH) from the pituitary gland and ultimately causing thyroid dysfunction (136). This thyroid dysfunction may result in psychological symptoms, such as psychomotor retardation, pleasure deficits, loss of libido, cognitive changes, and appetite disorders. These symptoms can lead to attention and executive impairment, fatigue, reduced quality of life, and increased risk of anxiety or depression (137, 138).

Moreover, breast cancer patients have a higher prevalence of thyroid peroxidase autoantibodies, likely due to the co-expression of thyroid peroxidase in both the thyroid and some breast tissues. Lactoperoxidase, structurally similar to thyroid peroxidase, is expressed in breast tumor cells, leading to immune responses to common thyroid/mammary antigens (139). Breast cancer patients who undergo chemotherapy, radiation, and immunotherapy may also damage the thyroid, further contributing to thyroid dysfunction. Thus, diminished oxytocin activity in the hypothalamic circulation may lead to thyroid dysfunction and psychological difficulties in breast cancer patients, resulting in decreased mental and physical health resilience. The complex interactions between the oxytocin system and estrogen signaling pathways highlight oxytocin's multifaceted roles in both breast cancer progression and patient resilience, underscoring the need for additional research to unravel the nuances of oxytocin signaling in cancer.

4.2.6 Balancing oxytocin signaling in breast cancer: implications for progression and resilience

Oxytocin interacts complexly with the HPA axis, estrogen signaling, the serotonin system, vasopressin, and thyroid function to impact breast cancer progression. It may counteract cancer-induced inflammation and glucocorticoid resistance by dampening HPA axis hyperactivity. However, prolonged oxytocin could also extend stress responses. Oxytocin exhibits anti-estrogenic properties by downregulating breast tumors' estrogen receptors while activating estrogen receptors in healthy tissues. The balance between oxytocin and vasopressin signaling impacts mood and cardiovascular function in cancer patients. Decreased oxytocin may contribute to thyroid dysfunction and psychological symptoms. Overall, oxytocin plays multifaceted modulatory and compensatory roles, potentially inhibiting and promoting breast cancer depending

on the physiological context. Further research is needed to elucidate the precise mechanisms by which oxytocin interfaces with other hormones to influence tumor development and patient resilience. As shown in Figure 1, oxytocin regulates breast cancer patients' psychological resilience by controlling the nervous system and endocrine function.

5 Conclusion

Resilience formation and change mechanisms are complex and involve various biological and social factors. These mechanisms can be traced back to the evolution of mammals. The oxytocin system is a critical component of the neurobiological model of resilience and is involved in shaping resilience during fetal development and regulating resilience in response to social or traumatic events in adulthood. To illustrate the relationship between the oxytocin system and resilience, we propose a theoretical model shown in Figure 2.

Breast cancer is a traumatic event that can significantly affect a patient's quality of life, and the level of resilience plays a critical role in how well a patient copes with the disease. Breast cancer patients often exhibit lower resilience levels than individuals without cancer, suggesting that the disease can negatively impact resilience. The oxytocin system regulates resilience in breast cancer patients in several ways. On the one hand, oxytocin acts directly on peripheral or central oxytocin receptors to regulate social behavior. On the other hand, oxytocin system activation can regulate psychological resilience by affecting estrogen and its receptors, the hypothalamic-pituitary-adrenal axis, thyroid function, metabolic levels of 5-HT, and the release of AVP in breast cancer patients. Additionally, oxytocin can indirectly affect resilience by influencing an individual's ability to adapt to stressful situations, suppressing excessive inflammatory responses, and reducing pain.

Overall, the oxytocin system plays a significant role in regulating resilience in breast cancer patients. It is essential to consider the implications of these findings in clinical practice, particularly when diagnosing and treating breast cancer.

Currently, various measures are used to improve the resilience of breast cancer patients, mainly involving behavioral interventions or psychotherapy. Adjusting the release level of oxytocin may be the basis for the effectiveness of these interventions. In addition, moderate physical exercise also plays a vital role in improving resilience. In animal experiments, exercise can promote the release of oxytocin in mice, which may be one of the pathways through which exercise improves resilience. Intranasal administration of oxytocin has been shown to improve social communication deficits in disorders such as autism, which may be related to oxytocin's direct action on central nervous system oxytocin receptors. In the future, plasma or salivary oxytocin levels and oxytocin genotypes could be used as predictive resilience indicators in breast cancer patients. Intranasal administration of oxytocin can be considered a pharmacological intervention pathway to improve the resilience of breast cancer women under the premise of strict adherence to safe doses.

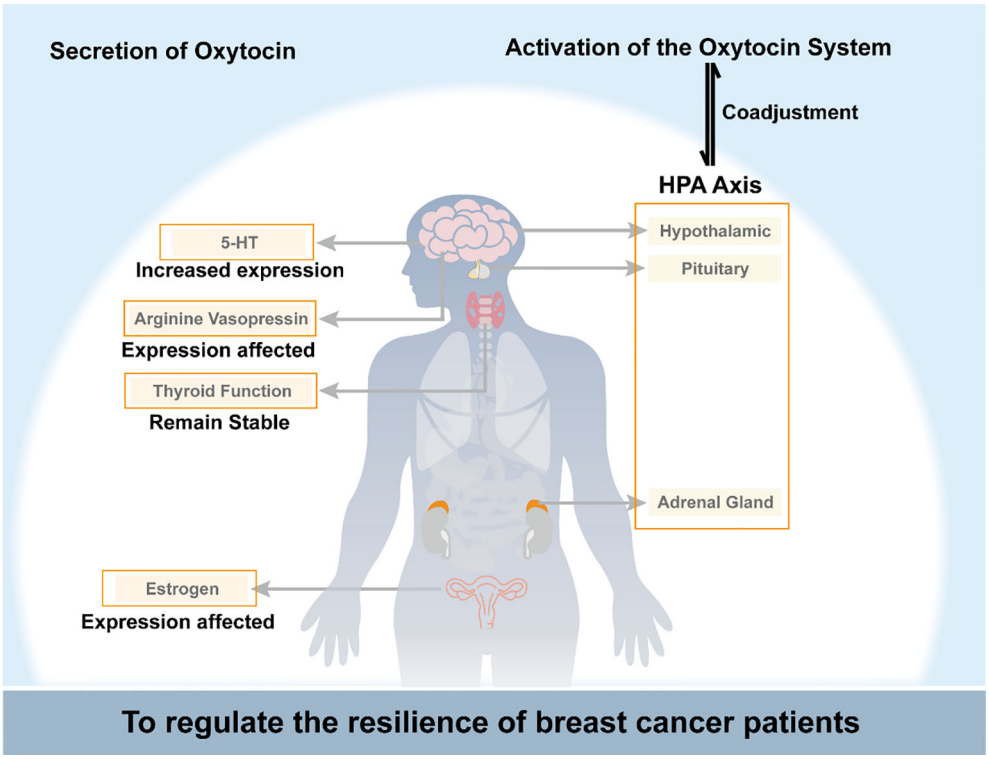

FIGURE 1
Schematic diagram of oxytocin regulating breast cancer patients' psychological resilience by controlling the nervous system and endocrine function. HPA axis, the hypothalamic-pituitary-adrenal axis; 5-HT, 5-hydroxytryptamine.

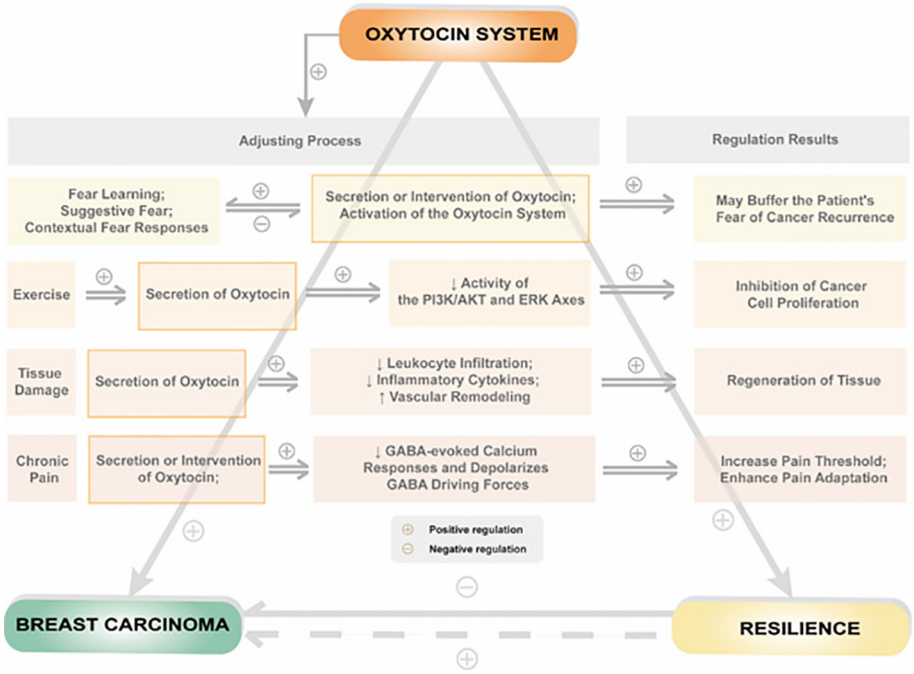

FIGURE 2
Relationship between psychological or physiological influences by regulation of the oxytocin system and resilience in patients with breast cancer.

Unfortunately, there is still no research on using oxytocin to improve resilience in breast cancer patients. Considering that oxytocin is involved in various functions of the female reproductive system and social behavior, oxytocin acting on the central nervous system is more likely to cause abnormal social behavior (140). Therefore, relevant research can be conducted, but the safe dosage of intranasal oxytocin administration for female patients must be determined.

Author contributions

All authors proposed this manuscript's concept, indicating a collective effort toward its development. To ensure the manuscript's comprehensiveness, SL and RH conducted a comprehensive literature search. All authors collaborated in writing the first draft and continued to review and edit subsequent drafts until reaching a satisfactory final version. Finally, all authors participated in reading and approving the final version, which attests to the manuscript's quality and accuracy. The dedication and collaboration of the authors highlight the importance of this topic, and their work will undoubtedly contribute to advancing the field's knowledge on this matter. All authors contributed to the article and approved the submitted version.

Funding

This research was supported by the Postgraduate Innovation Research and Practice Program of Anhui Medical University (No. YJS20230086).

Conflict of interest

The authors declare that the research was conducted in the absence of any commercial or financial relationships that could be construed as a potential conflict of interest.

Publisher's note

All claims expressed in this article are solely those of the authors and do not necessarily represent those of their affiliated organizations, or those of the publisher, the editors and the reviewers. Any product that may be evaluated in this article, or claim that may be made by its manufacturer, is not guaranteed or endorsed by the publisher.

References

1. Anthony EJ. *The syndrome of the psychologically vulnerable child, The child in his family: Children at psychiatric risk*. Oxford, England: John Wiley & Sons (1974).

2. Masten AS, Cicchetti D. Risk and resilience in development and psychopathology: the legacy of Norman Garmezy. *Dev Psychopathol* (2012) 24:333–4. doi: 10.1017/S0954579412000016

3. Bonanno GA. Loss, trauma, and human resilience: have we underestimated the human capacity to thrive after extremely aversive events? *Am Psychol* (2004) 59:20–8. doi: 10.1037/0003-066X.59.1.20

4. Southwick SM, Bonanno GA, Masten AS, Panter-Brick C, Yehuda R. Resilience definitions, theory, and challenges: interdisciplinary perspectives. *Eur J Psychotraumatol* (2014) 5. doi: 10.3402/ejpt.v5.25338

5. Cicchetti D, Rogosch FA. Gene × Environment interaction and resilience: effects of child maltreatment and serotonin, corticotropin releasing hormone, dopamine, and oxytocin genes. *Dev Psychopathol* (2012) 24:411–27. doi: 10.1017/S0954579412000077

6. Babić R, Babić M, Rastović P, Ćurlin M, Šimić J, Mandić K, et al. Resilience in health and illness. *Psychiatr Danub* (2020) 32:226–32.

7. Feldman R. What is resilience: an affiliative neuroscience approach. *World Psychiatry* (2020) 19:132–50. doi: 10.1002/wps.20729

8. Carter CS, Kenkel WM, MacLean EL, Wilson SR, Perkeybile AM, Yee JR, et al. Is oxytocin "Nature's medicine"? *Pharmacol Rev* (2020) 72:829–61. doi: 10.1124/pr.120.019398

9. Wang P, Yang HP, Tian S, Wang L, Wang SC, Zhang F, et al. Oxytocin-secreting system: A major part of the neuroendocrine center regulating immunologic activity. *J neuroimmunol* (2015) 289:152–61. doi: 10.1016/j.jneuroim.2015.11.001

10. Gimpl G, Fahrenholz F. The oxytocin receptor system: structure, function, and regulation. *Physiol Rev* (2001) 81:629–83. doi: 10.1152/physrev.2001.81.2.629

11. Liu N, Yang H, Han L, Ma M. Oxytocin in women's health and disease. *Front Endocrinol* (2022) 13:786271. doi: 10.3389/fendo.2022.786271

12. Carcea I, Caraballo NL, Marlin BJ, Ooyama R, Riceberg JS, Mendoza Navarro JM, et al. Oxytocin neurons enable social transmission of maternal behavior. *Nature* (2021) 596:553–7. doi: 10.1038/s41586-021-03814-7

13. Eliava M, Melchior M, Knobloch-Bollmann HS, Wahis J, da Silva Gouveia M, Tang Y, et al. A new population of parvocellular oxytocin neurons controlling magnocellular neuron activity and inflammatory pain processing. *Neuron* (2016) 89:1291–304. doi: 10.1016/j.neuron.2016.01.041

14. Zhang B, Qiu L, Xiao W, Ni H, Chen L, Wang F, et al. Reconstruction of the hypothalamo-neurohypophysial system and functional dissection of magnocellular oxytocin neurons in the brain. *Neuron* (2021) 109:331–346.e7. doi: 10.1016/j.neuron.2020.10.032

15. Richard P, Moos F, Freund-Mercier MJ. Central effects of oxytocin. *Physiol Rev* (1991) 71:331–70. doi: 10.1152/physrev.1991.71.2.331

16. Uvnäs-Moberg K. Antistress pattern induced by oxytocin. *News Physiol Sci* (1998) 13:22–5. doi: 10.1152/physiologyonline1998.13.1.22

17. Wang P, Wang SC, Liu X, Jia S, Wang X, Li T, et al. Neural functions of hypothalamic oxytocin and its regulation. *ASN Neuro* (2022) 14:17590914221100706. doi: 10.1177/17590914221100706

18. Uvnäs-Moberg K. Oxytocin may mediate the benefits of positive social interaction and emotions. *Psychoneuroendocrinology* (1998) 23:819–35. doi: 10.1016/S0306-4530(98)00056-0

19. Sala M, Braida D, Lentini D, Busnelli M, Bulgheroni E, Capurro V, et al. Pharmacologic rescue of impaired cognitive flexibility, social deficits, increased aggression, and seizure susceptibility in oxytocin receptor null mice: a neurobehavioral model of autism. *Biol Psychiatry* (2011) 69:875–82. doi: 10.1016/j.biopsych.2010.12.022

20. Leuner B, Caponiti JM, Gould E. Oxytocin stimulates adult neurogenesis even under conditions of stress and elevated glucocorticoids. *Hippocampus* (2012) 22:861–8. doi: 10.1002/hipo.20947

21. Li XH, Matsuura T, Xue M, Chen QY, Liu RH, Lu JS, et al. Oxytocin in the anterior cingulate cortex attenuates neuropathic pain and emotional anxiety by inhibiting presynaptic long-term potentiation. *Cell Rep* (2021) 36:109411. doi: 10.1016/j.celrep.2021.109411

22. Luo L, Becker B, Geng Y, Zhao Z, Gao S, Zhao W, et al. Sex-dependent neural effect of oxytocin during subliminal processing of negative emotion faces. *NeuroImage* (2017) 162:127–37. doi: 10.1016/j.neuroimage.2017.08.079

23. Sikich L, Kolevzon A, King BH, McDougle CJ, Sanders KB, Kim SJ, et al. Intranasal oxytocin in children and adolescents with autism spectrum disorder. *New Engl J Med* (2021) 385:1462–73. doi: 10.1056/NEJMoa2103583

24. Yamasue H, Okada T, Munesue T, Kuroda M, Fujioka T, Uno Y, et al. Effect of intranasal oxytocin on the core social symptoms of autism spectrum disorder: a randomized clinical trial. *Mol Psychiatry* (2020) 25:1849–58. doi: 10.1038/s41380-018-0097-2

25. Hollander E, Jacob S, Jou R, McNamara N, Sikich L, Tobe R, et al. Balovaptan vs placebo for social communication in childhood autism spectrum disorder: A randomized clinical trial. *JAMA Psychiatry* (2022) 79:760–9. doi: 10.1001/jamapsychiatry.2022.1717

26. Guastella AJ, Einfeld SL, Gray KM, Rinehart NJ, Tonge BJ, Lambert TJ, et al. Intranasal oxytocin improves emotion recognition for youth with autism spectrum disorders. *Biol Psychiatry* (2010) 67:692–4. doi: 10.1016/j.biopsych.2009.09.020

27. Quintana DS, Westlye LT, Hope S, Nærland T, Elvsåshagen T, Dørum E, et al. Dose-dependent social-cognitive effects of intranasal oxytocin delivered with novel Breath Powered device in adults with autism spectrum disorder: a randomized placebo-controlled double-blind crossover trial. *Trans Psychiatry* (2017) 7:e1136. doi: 10.1038/tp.2017.103

28. Dodhia S, Hosanagar A, Fitzgerald DA, Labuschagne I, Wood AG, Nathan PJ, et al. Modulation of resting-state amygdala-frontal functional connectivity by oxytocin in generalized social anxiety disorder. *Neuropsychopharmacology* (2014) 39(9):2061–9. doi: 0.1038/npp.2014.53

29. Gorka SM, Fitzgerald DA, Labuschagne I, Hosanagar A, Wood AG, Nathan PJ, et al. Oxytocin modulation of amygdala functional connectivity to fearful faces in generalized social anxiety disorder. *Neuropsychopharmacology* (2015) 40:278–86. doi: 10.1038/npp.2014.168

30. Labuschagne I, Phan KL, Wood A, Angstadt M, Chua P, Heinrichs M, et al. Oxytocin attenuates amygdala reactivity to fear in generalized social anxiety disorder. *Neuropsychopharmacology* (2010) 35:2403–13. doi: 10.1038/npp.2010.123

31. Nawijn L, van Zuiden M, Koch SB, Frijling JL, Veltman DJ, Olff M. Intranasal oxytocin increases neural responses to social reward in post-traumatic stress disorder. *Soc Cogn Affect Neurosci* (2017) 12:212–23. doi: 10.1093/scan/nsw123

32. van Zuiden M, Frijling JL, Nawijn L, Koch SBJ, Goslings JC, Luitse JS, et al. Intranasal oxytocin to prevent posttraumatic stress disorder symptoms: A randomized controlled trial in emergency department patients. *Biol Psychiatry* (2017) 81:1030–40. doi: 10.1016/j.biopsych.2016.11.012

33. Sack M, Spieler D, Wizelman L, Epple G, Stich J, Zaba M, et al. Intranasal oxytocin reduces provoked symptoms in female patients with posttraumatic stress disorder despite exerting sympathomimetic and positive chronotropic effects in a randomized controlled trial. *BMC Med* (2017) 15:40. doi: 10.1186/s12916-017-0801-0

34. Feifel D, Macdonald K, Cobb P, Minassian A. Adjunctive intranasal oxytocin improves verbal memory in people with schizophrenia. *Schizophr Res* (2012) 139:207–10. doi: 10.1016/j.schres.2012.05.018

35. Feifel D, Macdonald K, Nguyen A, Cobb P, Warlan H, Galangue B, et al. Adjunctive intranasal oxytocin reduces symptoms in schizophrenia patients. *Biol Psychiatry* (2010) 68:678–80. doi: 10.1016/j.biopsych.2010.04.039

36. Pedersen CA, Gibson CM, Rau SW, Salimi K, Smedley KL, Casey RL, et al. Intranasal oxytocin reduces psychotic symptoms and improves Theory of Mind and social perception in schizophrenia. *Schizophr Res* (2011) 132:50–3. doi: 10.1016/j.schres.2011.07.027

37. Shin NY, Park HY, Jung WH, Park JW, Yun JY, Jang JH, et al. Effects of oxytocin on neural response to facial expressions in patients with schizophrenia. *Neuropsychopharmacology* (2015) 40:1919–27. doi: 10.1038/npp.2015.41

38. Jesso S, Morlog D, Ross S, Pell MD, Pasternak SH, Mitchell DG, et al. The effects of oxytocin on social cognition and behavior in frontotemporal dementia. *Brain J Neurol* (2011) 134:2493–501. doi: 10.1093/brain/awr171

39. Oliver LD, Stewart C, Coleman K, Kryklywy JH, Bartha R, Mitchell DGV, et al. Neural effects of oxytocin and mimicry in frontotemporal dementia: A randomized crossover study. *Neurology* (2020) 95:e2635–47. doi: 10.1212/WNL.0000000000010933

40. Sung H, Ferlay J, Siegel RL, Laversanne M, Soerjomataram I, Jemal A, et al. Global cancer statistics 2020: GLOBOCAN estimates of incidence and mortality worldwide for 36 cancers in 185 countries. *CA: Cancer J Clin* (2021) 71:209–49. doi: 10.3322/caac.21660

41. Harbeck N, Gnant M. Breast cancer. *Lancet (London England)* (2017) 389:1134–50. doi: 10.1016/S0140-6736(16)31891-8

42. Li DT, Habtemichael EN, Bogan JS. Vasopressin inactivation: Role of insulin-regulated aminopeptidase. *Vitamins hormones* (2020) 113:101–28. doi: 10.1016/bs.vh.2019.08.017

43. Ramirez-Exposito MJ, Duenas-Rodriguez B, Carrera-Gonzalez MP, Navarro-Cecilia J, Martinez-Martos JM. Insulin-regulated aminopeptidase in women with breast cancer: A role beyond the regulation of oxytocin and vasopressin. *Cancers (Basel)* (2020) 12. doi: 10.3390/cancers12113252

44. Korde LA, Somerfield MR, Carey LA, Crews JR, Denduluri N, Hwang ES, et al. Neoadjuvant chemotherapy, endocrine therapy, and targeted therapy for breast cancer: ASCO guideline. *J Clin Oncol* (2021) 39:1485–505. doi: 10.1200/JCO.20.03399

45. Perez-Tejada J, Labaka A, Vegas O, Larraioz A, Pescador A, Arregi A. Anxiety and depression after breast cancer: The predictive role of monoamine levels. *Eur J Oncol Nurs* (2021) 52:101953. doi: 10.1016/j.ejon.2021.101953

46. Liu H, Gruber CW, Alewood PF, Moller A, Muttenthaler M. The oxytocin receptor signalingsystem and breast cancer: a critical review. *Oncogene* (2020) 39:5917–32. doi: 10.1038/s41388-020-01415-8

47. Tu PC. The effects of trait resilience and rumination on psychological adaptation to breast cancer. *Health Psychol Open* (2022) 9:20551029221140765. doi: 10.1177/20551029221140765

48. Ye ZJ, Zhang Z, Zhang XY, Tang Y, Chen P, Liang MZ, et al. State or trait? Measuring resilience by generalisability theory in breast cancer. *Eur J Oncol Nurs* (2020) 46:101727. doi: 10.1016/j.ejon.2020.101727

49. Schwab R, Droste A, Stewen K, Elger T, Theis S, Heimes AS, et al. Resilience as a source of easement to health-related worries in women at increased risk for breast or ovarian cancer during the COVID-19 pandemic. *Int J Gen Med* (2022) 15:7039–52. doi: 10.2147/IJGM.S373191

50. Yan Z, Zhang Q, Chang L, Liu Y, Li Y. Dyadic effects of family resilience on post-traumatic stress symptoms among breast cancer patients and their primary family caregivers: A cross-sectional study. *Eur J Oncol Nurs* (2021) 53:101998. doi: 10.1016/j.ejon.2021.101998

51. Kourou K, Manikis G, Poikonen-Saksela P, Mazzocco K, Pat-Horenczyk R, Sousa B, et al. A machine learning-based pipeline for modeling medical, socio-demographic, lifestyle and self-reported psychological traits as predictors of mental health outcomes after breast cancer diagnosis: An initial effort to define resilience effects. *Comput Biol Med* (2021) 131:104266. doi: 10.1016/j.compbiomed.2021.104266

52. Padilla-Ruiz M, Ruiz-Román C, Pérez-Ruiz E, Rueda A, Redondo M, Rivas-Ruiz F. Clinical and sociodemographic factors that may influence the resilience of women surviving breast cancer: cross-sectional study. *Support Care Cancer* (2019) 27:1279–86. doi: 10.1007/s00520-018-4612-4

53. Liesto S, Sipilä R, Hietanen M, Kalso E. Cognitive function is well preserved in a cohort of breast cancer survivors: Roles of cognitive reserve, resilience, and general health. *Breast (Edinburgh Scotland)* (2022) 65:157–63. doi: 10.1016/j.breast.2022.07.013

54. Zhou K, Ning F, Wang W, Li X. The mediator role of resilience between psychological predictors and health-related quality of life in breast cancer survivors: a cross-sectional study. *BMC Cancer* (2022) 22:57. doi: 10.1186/s12885-022-09177-0

55. Oei SL, Thronicke A, Matthes H, SChad F. Evaluation of the effects of integrative non-pharmacological interventions on the internal coherence and resilience of breast cancer patients. *Support Care Cancer* (2021) 29:1413–21. doi: 10.1007/s00520-020-05617-4

56. Ye ZJ, Zhang Z, Tang Y, Liang J, Sun Z, Hu GY, et al. Resilience patterns and transitions in the Be Resilient To Breast Cancer trial: an exploratory latent profile transition analysis. *Psycho-oncology* (2021) 30:901–9. doi: 10.1002/pon.5668

57. Atzil-Slonim D, Stolowicz-Melman D, Bar-Kalifa E, Gilboa-Schechtman E, Paz A, Wolff M, et al. Oxytocin reactivity to the therapeutic encounter as a biomarker of change in the treatment of depression. *J Couns Psychol* (2022) 69:755–60. doi: 10.1037/cou0000617

58. Southwick SM, Vythilingam M, Charney DS. The psychobiology of depression and resilience to stress: implications for prevention and treatment. *Annu Rev Clin Psychol* (2005) 1:255–91. doi: 10.1146/annurev.clinpsy.1.102803.143948

59. Dashtinejad E, Abedi P, Afshari P. Comparison of the effect of breast pump stimulation and oxytocin administration on the length of the third stage of labor, postpartum hemorrhage, and anemia: a randomized controlled trial. *BMC Pregnancy Childbirth* (2018) 18:293. doi: 10.1186/s12884-018-1832-z

60. Triansyah A, Stang, Indar, Indarty A, Tahir M, Sabir M, et al. The effect of oxytocin massage and breast care on the increased production of breast milk of breastfeeding mothers in the working area of the public health center of Lawanga of Poso District. *Gac Sanit* (2021) 35 Suppl 2:S168–s170. doi: 10.1016/j.gaceta.2021.10.017

61. Hannan FM, Elajnaf T, Vandenberg LN, Kennedy SH, Thakker RV. Hormonal regulation of mammary gland development and lactation. *Nat Rev Endocrinol* (2023) 19:46–61. doi: 10.1038/s41574-022-00742-y

62. Amico JA, Finley BE. Breast stimulation in cycling women, pregnant women and a wOman with induced lactation: pattern of release of oxytocin, prolactin and luteinizing hormone. *Clin Endocrinol* (1986) 25:97–106. doi: 10.1111/j.1365-2265.1986.tb01670.x

63. Bealer SL, Armstrong WE, Crowley WR. Oxytocin release in magnocellular nuclei: neurochemical mediators and functional significance during gestation. *Am J Physiol Regulatory Integr Comp Physiol* (2010) 299:R452–8. doi: 10.1152/ajpregu.00217.2010

64. Grewen KM, Davenport RE, Light KC. An investigation of plasma and salivary oxytocin responses in breast- and formula-feeding mothers of infants. *Psychophysiology* (2010) 47:625–32. doi: 10.1111/j.1469-8986.2009.00968.x

65. Murrell TG. The potential for oxytocin (OT) to prevent breast cancer: a hypothesis. *Breast Cancer Res Treat* (1995) 35:225–9. doi: 10.1007/BF00668213

66. Liu X, Jia S, Zhang Y, Wang Y-F. Pulsatile but not tonic secretion of oxytocin plays the role of anti-precancerous lesions of the mammary glands in rat dams separated from the pups during lactation. *M.J.o.N* (2016) 1:1–9.

67. Behtaji S, Ghafouri-Fard S, Sayad A, Sattari A, Rederstorff M, Taheri M. Identification of oxytocin-related lncRNAs and assessment of their expression in breast cancer. *Sci Rep* (2021) 11:6471. doi: 10.1038/s41598-021-86097-2

68. Suijkerbuijk KP, van der Wall E, Meijrink H, Pan X, Borel Rinkes IH, Ausems MG, et al. Successful oxytocin-assisted nipple aspiration in women at increased risk for breast cancer. *Fam Cancer* (2010) 9:321–5. doi: 10.1007/s10689-010-9344-7

69. Kalinina TS, Kononchuk VV, Sidorov SV, Obukhova DA, Abdullin GR, Gulyaeva LF. Oxytocin receptor expression is associated with estrogen receptor status in breast tumors. *BioMed Khim* (2021) 67:360–5. doi: 10.18097/pbmc20216704360

70. Vasudevan N, Davidkova G, Zhu YS, Koibuchi N, Chin WW, Pfaff D. Differential interaction of estrogen receptor and thyroid hormone receptor isoforms on the rat oxytocin receptor promoter leads to differences in transcriptional regulation. *Neuroendocrinology* (2001) 74:309–24. doi: 10.1159/000054698

71. Liu H, Muttenthaler M. High oxytocin receptor expression linked to increased cell migration and reduced survival in patients with triple-negative breast cancer. *Biomedicines* (2022) 10. doi: 10.3390/biomedicines10071595

72. Ariana M, Pornour M, Mehr SS, Vaseghi H, Ganji SM, Alivand MR, et al. Preventive effects of oxytocin and oxytocin receptor in breast cancer pathogenesis. *Personalized Med* (2019) 16:25–34. doi: 10.2217/pme-2018-0009

73. Bouvette-Turcot AA, Fleming AS, Unternaehrer E, Gonzalez A, Atkinson L, Gaudreau H, et al. Maternal symptoms of depression and sensitivity mediate the relation between maternal history of early adversity and her child temperament: The inheritance of circumstance. *Dev Psychopathol* (2020) 32:605–13. doi: 10.1017/S0954579419000488

74. Priel A, Djalovski A, Zagoory-Sharon O, Feldman R. Maternal depression impacts child psychopathology across the first decade of life: Oxytocin and synchrony as markers of resilience. *J Child Psychol psychiatry Allied disciplines* (2019) 60:30–42. doi: 10.1111/jcpp.12880

75. Uvnäs-Moberg K, Gross MM, Agius A, Downe S, Calleja-Agius J. Are there epigenetic oxytocin-mediated effects on the mother and infant during physiological childbirth? *Int J Mol Sci* (2020) 21. doi: 10.3390/ijms21249503

76. Sippel LM, Han S, Watkins LE, Harpaz-Rotem I, Southwick SM, Krystal JH, et al. Oxytocin receptor gene polymorphisms, attachment, and PTSD: Results from the National Health and Resilience in Veterans Study. *J Psychiatr Res* (2017) 94:139–47. doi: 10.1016/j.jpsychires.2017.07.008

77. McDonald NM, Baker JK, Messinger DS. Oxytocin and parent-child interaction in the development of empathy among children at risk for autism. *Dev Psychol* (2016) 52:735–45. doi: 10.1037/dev0000104

78. Bradley B, Davis TA, Wingo AP, Mercer KB, Ressler KJ. Family environment and adult resilience: contributions of positive parenting and the oxytocin receptor gene. *Eur J Psychotraumatol* (2013) 4. doi: 10.3402/ejpt.v4i0.21659

79. Kim HW, Kang JI, An SK, Kim SJ. Oxytocin receptor gene variants are associated with emotion recognition and resilience, but not with false-belief reasoning performance in healthy young Korean volunteers. *CNS Neurosci Ther* (2019) 25:519–26. doi: 10.1111/cns.13075

80. Milaniak I, Cecil CAM, Barker ED, Relton CL, Gaunt TR, McArdle W, et al. Variation in DNA methylation of the oxytocin receptor gene predicts children's resilience to prenatal stress. *Dev Psychopathol* (2017) 29:1663–74. doi: 10.1017/S0954579417001316

81. Ryabinin AE, Hostetler CM. Prairie voles as a model to screen medications for the treatment of alcoholism and addictions. *Int Rev Neurobiol* (2016) 126:403–21. doi: 10.1016/bs.irn.2016.02.019

82. Kitano K, Yamagishi A, Horie K, Nishimori K, Sato N. Helping behavior in prairie voles: A model of empathy and the importance of oxytocin. *iScience* (2022) 25:103991. doi: 10.1016/j.isci.2022.103991

83. Barrett CE, Arambula SE, Young LJ. The oxytocin system promotes resilience to the effects of neonatal isolation on adult social attachment in female prairie voles. *Transl Psychiatry* (2015) 5:e606. doi: 10.1038/tp.2015.73

84. Carter CS, Boone EM, Pournajafi-Nazarloo H, Bales KL. Consequences of early experiences and exposure to oxytocin and vasopressin are sexually dimorphic. *Dev Neurosci* (2009) 31:332–41. doi: 10.1159/000216544

85. Yoon S, Kim YK. The role of the oxytocin system in anxiety disorders. *Adv Exp Med Biol* (2020) 1191:103–20. doi: 10.1007/978-981-32-9705-0_7

86. Cilz NI, Cymerblit-Sabba A, Young WS. Oxytocin and vasopressin in the rodent hippocampus. *Genes brain Behav* (2019) 18:e12535. doi: 10.1111/gbb.12535

87. Wang SC, Zhang F, Zhu H, Yang H, Liu Y, Wang P, et al. Potential of endogenous oxytocin in endocrine treatment and prevention of COVID-19. *Front Endocrinol* (2022) 13:799521. doi: 10.3389/fendo.2022.799521

88. Rajoria S, Suriano R, George AL, Shanmugam A, Jussim C, Shin EJ, et al. Estrogen activity as a preventive and therapeutic target in thyroid cancer. *Biomed pharmacother = Biomed pharmacotherapie* (2012) 66:151–8. doi: 10.1016/j.biopha.2011.11.010

89. Alkafaas SS, Loutfy SA, Diab T, Hessien M. Vasopressin induces apoptosis but does not enhance the antiproliferative effect of dynamin 2 or PI3K/Akt inhibition in luminal A breast cancer cells. *Med Oncol (Northwood London England)* (2022) 40:35. doi: 10.1007/s12032-022-01889-4

90. Schapira L, Zheng Y, Gelber SI, Poorvu P, Ruddy KJ, Tamimi RM, et al. Trajectories of fear of cancer recurrence in young breast cancer survivors. *Cancer* (2022) 128:335–43. doi: 10.1002/cncr.33921

91. Koral L, Cirak Y. The relationships between fear of cancer recurrence, spiritual well-being and psychological resilience in non-metastatic breast cancer survivors during the COVID-19 outbreak. *Psycho-oncology* (2021) 30:1765–72. doi: 10.1002/pon.5727

92. Olivera-Pasilio V, Dabrowska J. Oxytocin promotes accurate fear discrimination and adaptive defensive behaviors. *Front Neurosci* (2020) 14:583878. doi: 10.3389/fnins.2020.583878

93. Pagani JH, Lee HJ, Young WS. 3rd, Postweaning, forebrain-specific perturbation of the oxytocin system impairs fear conditioning. *Genes brain Behav* (2011) 10:710–9. doi: 10.1111/j.1601-183X.2011.00709.x

94. Campbell-Smith EJ, Holmes NM, Lingawi NW, Panayi MC, Westbrook RF. Oxytocin signaling in basolateral and central amygdala nuclei differentially regulates the acquisition, expression, and extinction of context-conditioned fear in rats. *Learn Memory (Cold Spring Harbor N.Y.)* (2015) 22:247–57. doi: 10.1101/lm.036962.114

95. Nowacka-Chmielewska M, Grabowska K, Grabowski M, Meybohm P, Burek M, Małecki A. Running from stress: neurobiological mechanisms of exercise-induced stress resilience. *Int J Mol Sci* (2022) 23. doi: 10.3390/ijms232113348

96. Guo S, Huang Y, Zhang Y, Huang H, Hong S, Liu T. Impacts of exercise interventions on different diseases and organ functions in mice. *J sport Health Sci* (2020) 9:53–73. doi: 10.1016/j.jshs.2019.07.004

97. Huang Y, Huang Y, Bao M, Zheng S, Du T, Wu K. Psychological resilience of women after breast cancer surgery: a cross-sectional study of associated influencing factors. *Psychol Health Med* (2019) 24:866–78. doi: 10.1080/13548506.2019.1574353

98. Alizadeh AM, Heydari Z, Rahimi M, Bazgir B, Shirvani H, Alipour S, et al. Oxytocin mediates the beneficial effects of the exercise training on breast cancer. *Exp Physiol* (2018) 103:222–35. doi: 10.1113/EP086463

99. Vodovotz Y. Computational modelling of the inflammatory response in trauma, sepsis and wound healing: implications for modelling resilience. *Interface Focus* (2014) 4:20140004. doi: 10.1098/rsfs.2014.0004

100. Sorg H, Grambow E, Eckl E, Vollmar B. Oxytocin effects on experimental skin wound healing. *Innovative Surg Sci* (2017) 2:219–32. doi: 10.1515/iss-2017-0033

101. Sipilä R, Kalso E, Lötsch J. Machine-learned identification of psychological subgroups with relation to pain interference in patients after breast cancer treatments. *Breast (Edinburgh Scotland)* (2020) 50:71–80. doi: 10.1016/j.breast.2020.01.042

102. Liesto S, Sipilä R, Aho T, Harno H, Hietanen M, Kalso E. Psychological resilience associates with pain experience in women treated for breast cancer. *Scandinavian J Pain* (2020) 20:545–53. doi: 10.1515/sjpain-2019-0137

103. Mazzuca M, Minlebaev M, Shakirzyanova A, Tyzio R, Taccola G, Janackova S, et al. Newborn analgesia mediated by oxytocin during delivery. *Front Cell Neurosci* (2011) 5:3. doi: 10.3389/fncel.2011.00003

104. Li T, Wang P, Wang SC, Wang YF. Approaches mediating oxytocin regulation of the immune system. *Front Immunol* (2016) 7:693. doi: 10.3389/fimmu.2016.00693

105. Joseph DN, Whirledge S. Stress and the HPA axis: balancing homeostasis and fertility. *Int J Mol Sci* (2017) 18. doi: 10.3390/ijms18102224

106. Slavich GM, Irwin MR. From stress to inflammation and major depressive disorder: a social signal transduction theory of depression. *psychol Bull* (2014) 140:774–815. doi: 10.1037/a0035302

107. Goldsmith DR, Rapaport MH, Miller BJ. A meta-analysis of blood cytokine network alterations in psychiatric patients: comparisons between schizophrenia, bipolar disorder and depression. *Mol Psychiatry* (2016) 21:1696–709. doi: 10.1038/mp.2016.3

108. Gundogmus AG, Sezer Katar K, Orsel S, Ozturk G, Yilmaz KB. The relationship of potential biomarkers with psychological resilience and post-traumatic growth in female patients with breast cancer. *PloS One* (2022) 17:e0277119. doi: 10.1371/journal.pone.0277119

109. Irwin MR, Cole S, Olmstead R, Breen EC, Cho JJ, Moieni M, et al. Moderators for depressed mood and systemic and transcriptional inflammatory responses: a randomized controlled trial of endotoxin. *Neuropsychopharmacology* (2019) 44:635–41. doi: 10.1038/s41386-018-0259-6

110. Huang H, Wang W. Molecular mechanisms of glucocorticoid resistance. *Eur J Clin Invest* (2023) 53:e13901. doi: 10.1111/eci.13901

111. Manigault AW, Kuhlman KR, Irwin MR, Cole SW, Ganz PA, Crespi CM, et al. Psychosocial resilience to inflammation-associated depression: A prospective study of breast-cancer survivors. *psychol Sci* (2022) 33:1328–39. doi: 10.1177/09567976221079633

112. Li Y, Hassett AL, Seng JS. Exploring the mutual regulation between oxytocin and cortisol as a marker of resilience. *Arch Psychiatr Nurs* (2019) 33:164–73. doi: 10.1016/j.apnu.2018.11.008

113. Sharma SR, Gonda X, Dome P, Tarazi FI. What's Love Got to do with it: Role of oxytocin in trauma, attachment and resilience. *Pharmacol Ther* (2020) 214:107602. doi: 10.1016/j.pharmthera.2020.107602

114. Shi DD, Zhang YD, Ren YY, Peng SY, Yuan TF, Wang Z. Predictable maternal separation confers adult stress resilience *via* the medial prefrontal cortex oxytocin signaling pathway in rats. *Mol Psychiatry* (2021) 26:7296–307. doi: 10.1038/s41380-021-01293-w

115. Li K, Nakajima M, Ibañez-Tallon I, Heintz N. A cortical circuit for sexually dimorphic oxytocin-dependent anxiety behaviors. *Cell* (2016) 167:60–72.e11. doi: 10.1016/j.cell.2016.08.067

116. Nakashima T, Noguchi T, Furukawa T, Yamasaki M, Makino S, Miyata S, et al. Brain oxytocin augments stress-induced long-lasting plasma adrenocorticotropic hormone elevation in rats. *Neurosci Lett* (2002) 321:161–4. doi: 10.1016/S0304-3940(01)02548-4

117. Winter J, Meyer M, Berger I, Royer M, Bianchi M, Kuffner K, et al. Chronic oxytocin-driven alternative splicing of Crfr2α induces anxiety. *Mol Psychiatry* (2021). doi: 10.1038/s41380-021-01141-x

118. Yager JD, Davidson NE. Estrogen carcinogenesis in breast cancer. *New Engl J Med* (2006) 354:270–82. doi: 10.1056/NEJMra050776

119. Nishimura K, Yoshino K, Ikeda N, Baba K, Sanada K, Akiyama Y, et al. Oestrogen-dependent hypothalamic oxytocin expression with changes in feeding and body weight in female rats. *Commun Biol* (2022) 5:912. doi: 10.1038/s42003-022-03889-6

120. Khori V, Alizadeh AM, Khalighfard S, Heidarian Y, Khodayari H. Oxytocin effects on the inhibition of the NF-κB/miR195 pathway in mice breast cancer. *Peptides* (2018) 107:54–60. doi: 10.1016/j.peptides.2018.07.007

121. Busnelli M, Saulière A, Manning M, Bouvier M, Galés C, Chini B. Functional selective oxytocin-derived agonists discriminate between individual G protein family subtypes. *J Biol Chem* (2012) 287:3617–29. doi: 10.1074/jbc.M111.277178

122. Cassoni P, Catalano MG, Sapino A, Marrocco T, Fazzari A, Bussolati G, et al. Oxytocin modulates estrogen receptor alpha expression and function in MCF7 human breast cancer cells. *Int J Oncol* (2002) 21:375–8.

123. Szeto A, Sun-Suslow N, Mendez AJ, Hernandez RI, Wagner KV, McCabe PM. Regulation of the macrophage oxytocin receptor in response to inflammation. *Am J Physiol Endocrinol Metab* (2017) 312:E183–e189. doi: 10.1152/ajpendo.00346.2016

124. Kalaitzidis D, Gilmore TD. Transcription factor cross-talk: the estrogen receptor and NF-kappaB. *Trends Endocrinol metabolism: TEM* (2005) 16:46–52. doi: 10.1016/j.tem.2005.01.004

125. Hinohara K, Kobayashi S, Kanauchi H, Shimizu S, Nishioka K, Tsuji E, et al. ErbB receptor tyrosine kinase/NF-κB signaling controls mammosphere formation in human breast cancer. *Proc Natl Acad Sci United States America* (2012) 109:6584–9. doi: 10.1073/pnas.1113271109

126. Jordan VC. Selective estrogen receptor modulation: concept and consequences in cancer. *Cancer Cell* (2004) 5:207–13. doi: 10.1016/S1535-6108(04)00059-5

127. Walf AA, Frye CA. A review and update of mechanisms of estrogen in the hippocampus and amygdala for anxiety and depression behavior. *Neuropsychopharmacology* (2006) 31:1097–111. doi: 10.1038/sj.npp.1301067

128. Ito Y, Kobayashi T, Kimura T, Matsuura N, Wakasugi E, Takeda T, et al. Investigation of the oxytocin receptor expression in human breast cancer tissue using newly established monoclonal antibodies. *Endocrinology* (1996) 137:773–9. doi: 10.1210/endo.137.2.8593829

129. Amico JA, Rauk PN, Cai HM. Estradiol and progesterone regulate oxytocin receptor binding and expression in human breast cancer cell lines. *Endocrine* (2002) 18:79–84. doi: 10.1385/ENDO:18:1:79

130. Slattery DA, Neumann ID. Oxytocin and major depressive disorder: experimental and clinical evidence for links to aetiology and possible treatment. *Pharm (Basel Switzerland)* (2010) 3:702–24. doi: 10.3390/ph3030702

131. Yoshida M, Takayanagi Y, Inoue K, Kimura T, Young LJ, Onaka T, et al. Evidence that oxytocin exerts anxiolytic effects *via* oxytocin receptor expressed in serotonergic neurons in mice. *J Neurosci* (2009) 29:2259–71. doi: 10.1523/JNEUROSCI.5593-08.2009

132. Lieberwirth C, Wang Z. Social bonding: regulation by neuropeptides. *Front Neurosci* (2014) 8:171. doi: 10.3389/fnins.2014.00171

133. Knox SS, Uvnäs-Moberg K. Social isolation and cardiovascular disease: an atherosclerotic pathway? *Psychoneuroendocrinology* (1998) 23:877–90. doi: 10.1016/S0306-4530(98)00061-4

134. Neumann ID, Landgraf R. Balance of brain oxytocin and vasopressin: implications for anxiety, depression, and social behaviors. *Trends Neurosci* (2012) 35:649–59. doi: 10.1016/j.tins.2012.08.004

135. Song Z, Larkin TE, Malley MO, Albers HE. Oxytocin (OT) and arginine-vasopressin (AVP) act on OT receptors and not AVP V1a receptors to enhance social recognition in adult Syrian hamsters (Mesocricetus auratus). *Hormones Behav* (2016) 81:20–7. doi: 10.1016/j.yhbeh.2016.02.004

136. Carrera-González MP, Ramírez-Expósito MJ, de Saavedra JM, Sánchez-Agesta R, Mayas MD, Martínez-Martos JM. Hypothalamus-pituitary-thyroid axis disruption in rats with breast cancer is related to an altered endogenous oxytocin/insulin-regulated aminopeptidase (IRAP) system. *Tumor Biol* (2011) 32:543–9. doi: 10.1007/s13277-010-0149-y

137. Siegmann EM, Müller HHO, Luecke C, Philipsen A, Kornhuber J, Grömer TW. Association of depression and anxiety disorders with autoimmune thyroiditis: A systematic review and meta-analysis. *JAMA Psychiatry* (2018) 75:577–84. doi: 10.1001/jamapsychiatry.2018.0190

138. Zach J, Ackerman SH. Thyroid function, metabolic regulation, and depression. *Psychosomatic Med* (1988) 50:454–68. doi: 10.1097/00006842-198809000-00002

139. Muller I, Barrett-Lee PJ. The antigenic link between thyroid autoimmunity and breast cancer. *Semin Cancer Biol* (2020) 64:122–34. doi: 10.1016/j.semcancer.2019.05.013

140. Bales KL, Perkeybile AM, Conley OG, Lee MH, Guoynes CD, Downing GM, et al. Chronic intranasal oxytocin causes long-term impairments in partner preference formation in male prairie voles. *Biol Psychiatry* (2013) 74:180–8. doi: 10.1016/j.biopsych.2012.08.025

Frontiers in Oncology

Advances knowledge of carcinogenesis and tumor progression for better treatment and management

The third most-cited oncology journal, which highlights research in carcinogenesis and tumor progression, bridging the gap between basic research and applications to imrpove diagnosis, therapeutics and management strategies.

Discover the latest Research Topics

See more →

Frontiers

Avenue du Tribunal-Fédéral 34
1005 Lausanne, Switzerland
frontiersin.org

Contact us

+41 (0)21 510 17 00
frontiersin.org/about/contact